Fig.1

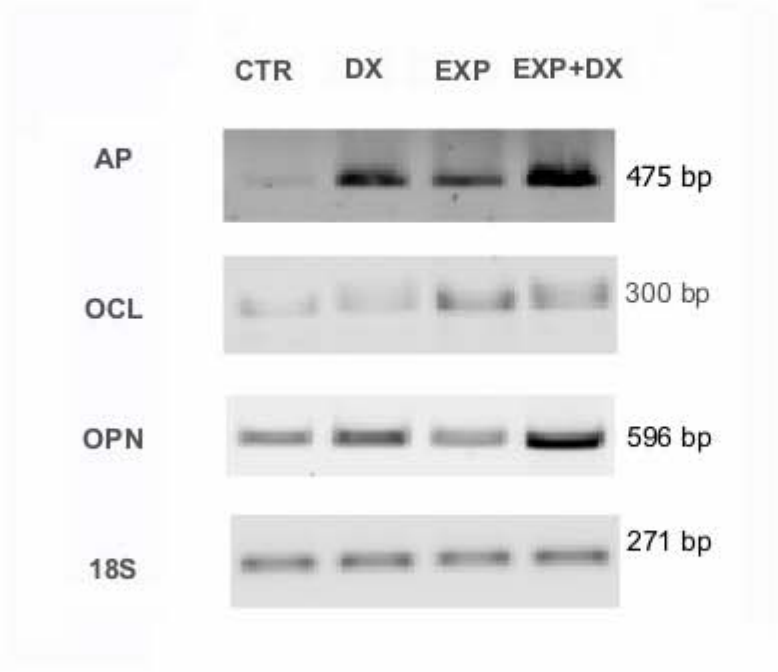


Fig. 1 - RT-PCR analysis. Total mRNA was extracted from Control (CTR), Dexamethasone (DX), Exposed (EXP) and Exposed+Dexamethasone-treated stem cells (EXP-DX). RT-PCR analysis was used for osteoblast differentiation markers detection with specific primers: Alkaline Phosfatase (AP), Osteocalcin (OCL) and Osteopontin (OPN). Dexamethasone treatment is the positive control. The amount of template and the number of amplification cycles were preliminarily optimized for each PCR reaction to avoid conditions of saturation.

Fig.2

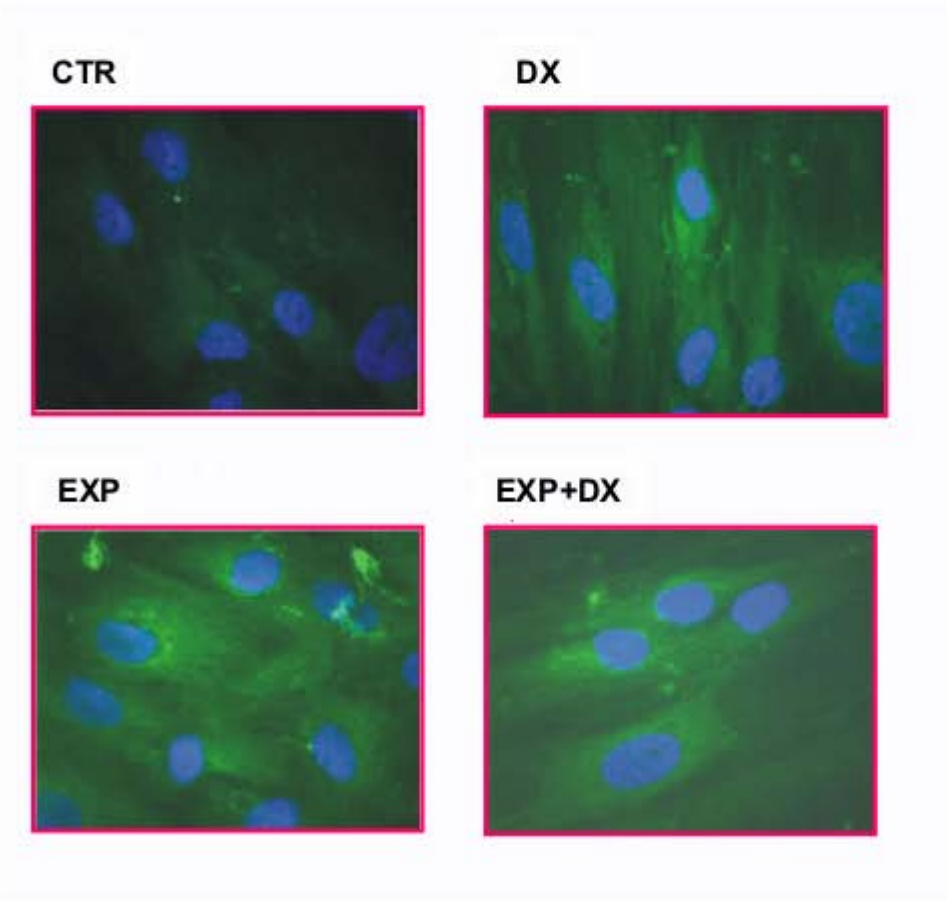


Fig. 2 ELF-MF (50Hz) modulation Osteopontin
differentiation marker expression see by indirect immunofluorescence microscopy.
Images show modulation of Osteopontin expression in control (CTR), Dexamethasone (DX), Exposed (EX) and Exposed+ Dexamethasone-trated (EXP+DX) stem cells. Figures were executed with 100x objective.

THE NATIONAL REGISTER OF RF WORKERS (UK): A LONG-TERM FOLLOW-UP STUDY

Ian Litchfield, Tom Sorahan.

The Institute of Occupational and Environmental Health, The University of Birmingham, Edgbaston, Birmingham, England B15 2TT

AIMS AND OBJECTIVES: In 1999, the Minister of Public Health asked the Radiation Protection Division of the Health Protection Agency (formerly the National Radiological Protection Board (NRPB)) to set up an independent expert group to examine the possible effects on health from the use of mobile phone telecommunication technologies. The group, under the chairmanship of Sir William Stewart, published its report in May 2000 [1]. One of the main conclusions was that there was no evidence to suggest that exposures to radiofrequency (RF) radiation below the guidelines of the NRPB and the International Commission on Non-Ionising Radiation Protection (ICNIRP) cause adverse health effects. Nevertheless, a key recommendation was that a register of occupationally exposed workers be established to facilitate studies into cancer incidence, mortality or other potentially harmful effects.

The Health and Safety Executive (HSE) responded to this recommendation by holding a consultation meeting on 9 January 2001 in Birmingham to which independent experts and those with an interest in telecommunications were invited. At this meeting, a decision was made to establish a Working Group to discuss how the recommendation should be implemented. In an attempt to ensure involvement across the whole industrial sector, representatives from the broadcast companies, mobile phone operators (FEI), contractors, the Ministry of Defence, National Grid, Trade Unions, and HSE were included.

The Working Group agreed to set up a register of exposed workers with a potential for exposure to radio-frequency radiation, and that the register would be confined to people whose work brings them in close proximity to transmitting antennas on telecommunication, broadcasting masts or other similar structures. Information about the workers would be retained and maintained in a centralised database or register. The Institute of Occupational and Environmental Medicine (IOEM) was contracted to administer the database. Now in its second phase, the register is guided by a Steering Group consisting of representatives from the HSE, the Institute of Occupational and Environmental Medicine and industry.

The study described here seeks to obtain important new information on the topic of long-term health effects of occupational RF exposure by examining data from the on-going National Register of RF workers.

MATERIALS AND METHODS: Analyses will be based on data from the on-going National Register of RF workers. The Register was first supported by the Health and Safety Executive (HSE) for the two-year period 2003-2004. It was always the intention of the HSE to support the start-up costs but then seek industry support for later years of data collection and analysis. Industry support is currently in place for the three-year period 2005-2007.

STUDY POPULATION

The cohort available for analysis currently comprises 604 male employees. All employees have some period of employment working in close proximity to transmitting antennas on telecommunication, broadcasting masts or other similar structures in the period 1961-2004. Work continues on increasing the size of the Register and in the next twelve months it is estimated that the Register will comprise some 2000 employees.

In order to account for the variation in exposure between different occupationally exposed jobs the participants are asked to supply their job title. This is then placed in one of five job categories (Antenna Support, General Maintenance Worker, Occasional Climber, Rigger and Satellite Support). The level of exposure typically experienced by each job category is informed by the five-year study carried out

by the Institute of Occupational and Environmental Medicine in conjunction with the Radiation Protection Division of the Health Protection Agency. This work, titled 'A Feasibility Study for an Epidemiological Investigation into the Health Effects of Radiofrequency Fields and Radiation' [2] produced a job exposure matrix for job titles relevant to the Register.

The National Register of RF Workers follow-up study will seek the approval of the Office for National Statistics (ONS) to receive follow-up particulars (copies of death certificates and cancer registration (incidence) details from the National Health Service Central Register (NHSCR) of the ONS). Underlying cause and multiple-cause coding will be supplied by the ONS for all deaths according to the tenth revision of the International Classification of Diseases (ICD-10).

STANDARDISED MORTALITY RATIOS AND STANDARDISED REGISTRATION RATIOS

The mortality experience of the cohort will be compared with that which might have been expected to occur if rates of mortality for the general population of England and Wales had been operating on the study cohort, having due regard to the composition of the study cohort by sex, age (five-year age groups), and calendar year (five-year calendar periods). Expectations based on person-years-at-risk (pyr) will be calculated using the PERSONYEARS computer program.[3] Individuals enter the pyr on the date of consenting to join the National Register. Individuals leave the pyr on the date of death, date of emigration, date last known alive or the closing date of the study, whichever is the earlier. Individuals will be "censored" on reaching their 85th birthday - that is, they will make no further contributions to expected or observed numbers past this age. Standardised mortality ratios (SMRs) will be calculated as the ratio of observed to expected numbers of deaths expressed as a percentage. In calculating P-values and confidence intervals, it will be assumed that deaths occur as a Poisson process [4]. Any significance tests will be two-tailed. Similar analyses will be performed on the cancer registration data to calculate standardized registration ratios (SRRs). Overall SMRs and SRRs will be calculated for individual sites of cancer (3-digit IICD codes) as well as SMRs for broader non-cancer causes (ICD chapters). Causes of special interest will be selected on the basis of significantly elevated SMRs or SRRs obtained either from this study or from similar studies of RF workers in other parts of the world. For causes of special interest, SMRs and SRRs will also be calculated by industry sector (telecommunications or broadcast), job type (1-5 names) and period from first RF work (ten-year intervals). In addition SMRs and SRRs for causes of special interest will also be calculated separately for workers reporting any high exposure incidents.

COLLABORATION: The National Register of RF Workers seeks to collaborate with international bodies undertaking similar research with the aim of contributing data and expertise and increasing understanding of the issue for the benefit of those occupationally exposed to RF radiation.

REFERENCES

1. Independent Expert Group on Mobile Phones; Mobile Phones and Health, 2000 (IEGMP pub)

2. A Feasibility Study for an Epidemiological Investigation into the Health Effects of Radiofrequency Fields and Radiation (University of Birmingham, unpublished)

3. Coleman M, Douglas A, Hermon C, Peto J. Cohort study analysis with a Fortran computer program. *Int J Epidemiol* 1986;**15**:134-7.

4. Breslow NE, Day NE. *Statistical methods in cancer research. Vol II - The design and analysis of cohort studies.* Lyon: International Agency for Research on Cancer, 1987. (IARC sci pub No 82.)

NUMERICAL CHARACTERIZATION OF AN EXPOSURE SET UP FOR 900 MHz AND 1800 MHz *in vitro* EXPERIMENTS

ROSARIA FALSAPERLA, SERGIO LO MEO, PAOLO ROSSI

National Institute of Occupational Safety and Prevention - Occupational Hygiene Dept. (ISPESL) Rome, Italy
Via Fontana Candida, 1 - 00040 Monte Porzio Catone (Rome)
Tel. +39 0694181440 - Fax +39 0694181419
E-mail: rosaria.falsaperla@ispesl.it, sergio.lomeo@ispesl.it, paolo.rossi@ispesl.it

Abstract

The aim of this study is to evaluate the efficiency of two exposure set up realized for *in vitro* experiments purposes. Maximum dimensions of these systems are 198x99x27 mm, with an exposure zone of 80x99x27 mm in order to allow the simultaneous insertion of four Petri dishes 35 mm of diameter, or other shape flasks. The set up efficiency was been evaluated at the frequency of 900 MHz and 1820 MHz by means of SAR calculations (local and average) on cell cultures. To this scope a commercial software package (CST Microwave Studio) based on Finite Integration Technique (FIT) was used. Cad drawing tools allowed the parameterization of the structure made up of culture medium thickness contained in plexiglas dishes or flasks inserted between two metallic plates fed by 1 W power.

All materials employed were electromagnetically characterized by appropriate values of dielectric permittivity and conductivity. SAR calculation accuracy was improved by defining a refining mesh in the cell culture volume. SAR distributions on the exposed samples were investigated, and several SAR calculations were made employing flasks of various forms and with different quantity of culture medium.

The study was developed in the frame of activities referring to the European Project EMF-NET, Main Task 2, Work Package 12 (focused on numerical calculations for occupational exposure).

I. Introduction

The study of the effects of radio frequency radiation on biological systems is a topic of great concern due to the rapid spreading of mobile communication systems in the recent years and the identification of the mobile phone as a potential source of risk for people. Then a wide number of research has been and is presently carried out with particular reference to the frequencies employed by the Global System for Mobile Communications (GSM) standard, that is frequencies near 900 MHz and 1800 MHz.

This paper presents a numerical efficiency evaluation of two exposure set up designed in such scenario for *in vitro* experiments purposes.
The efficiency of the systems was investigated through numerical SAR evaluation inside cell cultures, performing *in vitro* tests based on the employ of flasks and dishes of different size and culture medium content. The effects of the number of samples exposed at the same time on SAR were also investigated.
Basing on the equipment present in our laboratory, an experimental characterization of the efficiency of the two set up were also performed by means of the ratio between direct and reflected power. The results of measurements indicated that the frequencies giving the best performance of the two systems (minimum reflected power) are centred respectively at 900 MHz and 1820 MHz.
These frequencies were then selected for the simulations.
Both experimental and numerical characterization was carried out at the ISPESL Research Centre in Monte Porzio Catone (Rome).

II. Exposure set up

The exposure set up under test consisted of two parallel metallic plates T-modelled as shown in Figure 1.



Figure 1 – Exposure set up operating near 1800 MHz

Both set up were designed to generate an RF electric field, one at 900 MHz and the other one at 1800 MHz, as much as possible uniform between the two metallic plates and orthogonal to them.
To this aim the systems consisted of two contiguous zones. The first one (the basis of the T), the so called adaptive section, was designed in order to maximize the power transfer from the feed to the exposure zone by means of a gradual change of the wave impedance. A coaxial connection allowed to feed the systems.
The second zone (the head of the T), the so called exposure zone, was the volume available for the exposure of the biological samples. In this regard the final part of this zone was open (see Figure 1), while the side walls were closed by two layers of absorbing material covered by thin plastic sheets.

The dimensions of the exposure zone were the same for both set up, that is about 80×99×27 mm, inside of which 80×80×27 mm were available for exposure (between the two panels of absorbing material). On the opposite, due to the different working frequencies, the dimensions of the adaptive sections were different for the two systems and are the following:

- 118×69×27 mm for 900 MHz set up
- 80×99×27 mm for 1800 MHz set up

III. Numerical method and SAR evaluation

Computational simulations have been carried out by employing the electromagnetic commercial simulator Microwave Studio (MWS) by CST-Germany [1], based on the Finite Integration Technique (FIT) [2]. This numerical method, developed by Weiland in 1977, provides a discrete reformulation of Maxwell's equations in their integral form suitable for computers and it allows simulating real-world electromagnetic field problems with complex geometry. In order to numerically solve Maxwell's equations, a finite calculation domain is defined. By creating a suitable mesh system, this domain is split up into small cubes, so-called grid cells.
In combination with the FIT, MWS employs the Perfect Boundary Approximation (PBA) for the spatial discretization of the simulated structure that allows an accurate modelling of bend-shaped structures also [3].

In order to simulate *in vitro* tests, the exposure set up were simplified. In fact in the numerical model only the exposure zone of the two set up was modelled, presuming that the detailed description of the adaptive section was not relevant for SAR evaluation purposes. Each exposure set up was then represented as two parallel metallic plates of (80 × 99) mm size, at 27 mm of distance.

Figures 2 show the various simulations performed inserting different Petri dishes or flasks between the plates. In particular Figure 2 a) refers to exposure to 900 MHz electromagnetic field of one plexiglas dish of 54 mm diameter, height of 11 mm and of 1 mm of thickness. Culture medium was then parameterized as dish of 52 mm of diameter, height of 2.4 mm for a total liquid volume of 5 ml.
Figure 2 b) refers to simultaneous exposure to 900 MHz electromagnetic field of four plexiglas dishes of 35 mm of diameter, height of 8 mm and 1 mm of thickness. Each culture medium was then parameterized as dish of 33 mm of diameter and 3.5 mm of height for a total liquid volume of 3 ml.
Figure 2 c) refers to simultaneous exposure to 1820 MHz electromagnetic field of two plexiglas flasks. Each flask was represented by means of a plexiglas parallelepiped of (35 x 35 x 20) mm size and of 1 mm thickness for each wall. Consequently each culture medium was parameterized as a parallelepiped of (33 x 33 x 3.7) mm size, for a total liquid volume of 5 ml.

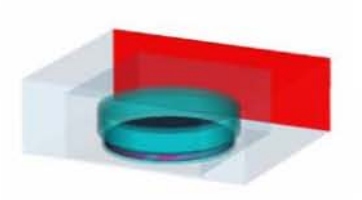


Fig 2 a



Fig 2 b

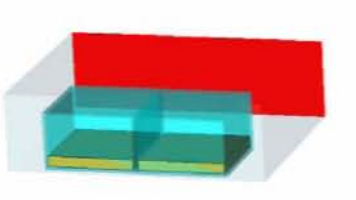


Fig 2 c

All simulations have been carried out feeding exposure systems through an electromagnetic pulse of 1 W.
All materials were characterized, on the basis of data literature, with their particular values of dielectric permittivity (ε_r), conductivity (σ) and density (ρ) at the frequency of 900 MHz and 1820 MHz as shown in Table 1.

Table 1 - Properties of materials used in the simulations

Materials	ε_r	ρ [kg/m^3]	σ [S/m]
	frequency 900 MHz		
Plexiglas	2.6	1200	neglectable
Cell Culture (culture medium)	80.5	1000	1.55
	frequency 1820 MHz		
Plexiglas	2.6	1200	neglectable
Cell Culture (culture medium)	76.8	1000	2.21

To perform dosimetric evaluation with better accuracy, a refined mesh in the culture medium volume was adopted. This involved a not uniform spatial discretization of the calculation domain ensuring a good compromise between the need of accuracy in the volume of interest and the simulation time.

As MWS evaluates both local and total average SAR through closed routines, in order to be sure regarding the mass involved in the calculation, we adopted a suitable numerical procedure made up of two steps [4].
The first one was aimed to produce electric field peak values on the whole domain by MWS, with higher accuracy in the sample volume. As second step, a mesh refinement limited in the cell cultures volumes was carried out, and the electric field values were recalculated. In this way the volume of each culture medium was discretized with spatial resolution of about (0.5 x 0.05 x 0.5) mm corresponding to 157248 mesh nodes. Finally, the electric field values were exported to commercial SW and post-processed to compute local spatial SAR (W/kg) values according to the relation**:**

$$SAR = \frac{\sigma E_{(i)}^2}{2\rho} \qquad \text{(Eq. 1)}$$

where:

- $E_{(i)}$: internal electric field in an elementary volume of the cell culture (peak value) [V/m]
- σ : conductivity of culture medium [S/m]
- ρ : density of culture medium [kg/m^3]

The total average SAR was evaluated by summing every SAR spatial contribution on the basis of relation:

$$\langle SAR \rangle = \frac{1}{N} \frac{\sigma}{2\rho} \sum_{k=1}^{N} E_{(i)k}^2 \qquad \text{(Eq. 2)}$$

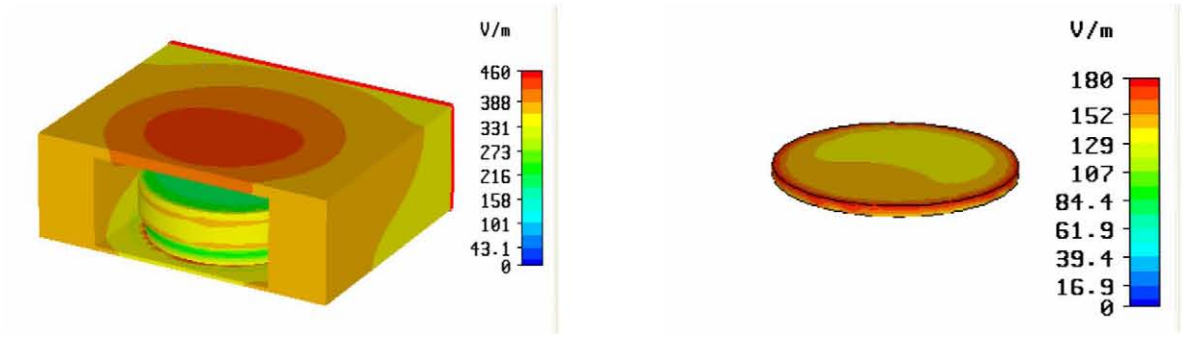
where:

- $E_{(i)k}$: internal electric field in an elementary volume (k-elementary cell) of the cell culture (peak value) [V/m]
- σ : conductivity of culture medium [S/m]
- ρ : density of culture medium [kg/m^3]

IV Results

900 MHz

Figures show the most relevant results for electric field calculations. Figures 2 (a) e (b) show a chromatic 3D scalar representation of the absolute value of electric field distribution (peak values) in the exposure set-up and in the culture medium, as calculated by MWS.



(a) E field in exposure set-up (b) E field in culture medium

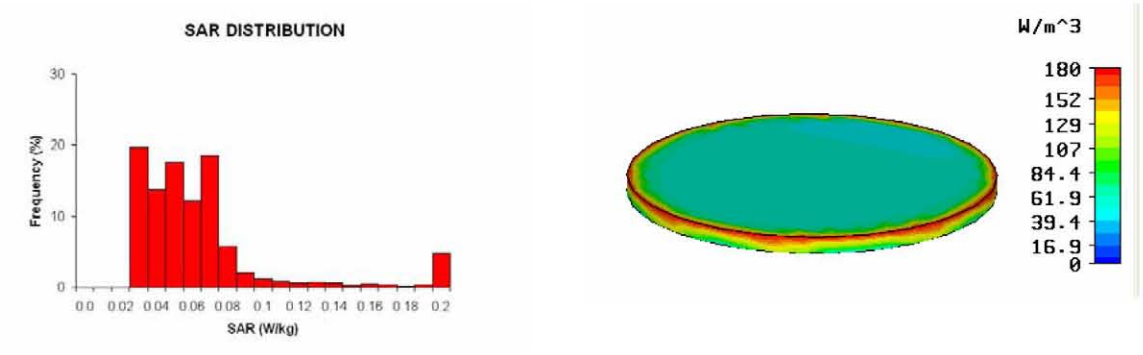
Fig.2 - 3D scalar representation of the electric field inside the structure (peak values)

Figures 3 show the SAR distribution histogram inside the culture medium and a chromatic power loss density (PLD) distribution inside the cell cultures. The local spatial SAR values inside the cell culture as calculated from our numerical procedure previously described. The total average SAR calculated from these distributions is 0.1 W/kg .

Power Loss Density is supplied by MWS and it is related to the electromagnetic power locally delivered into the sample. PLD is described by

$$PLD = \frac{d}{dt}\left(\frac{dU}{dV}\right) \qquad \text{(Eq. 3)}$$

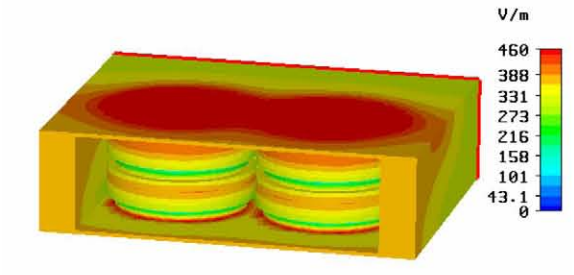
where dU is the incremental energy dissipated in an a volume element dV. The PLD values are expressed in units of W/m^3.



(a) – SAR (b) – Power Lost

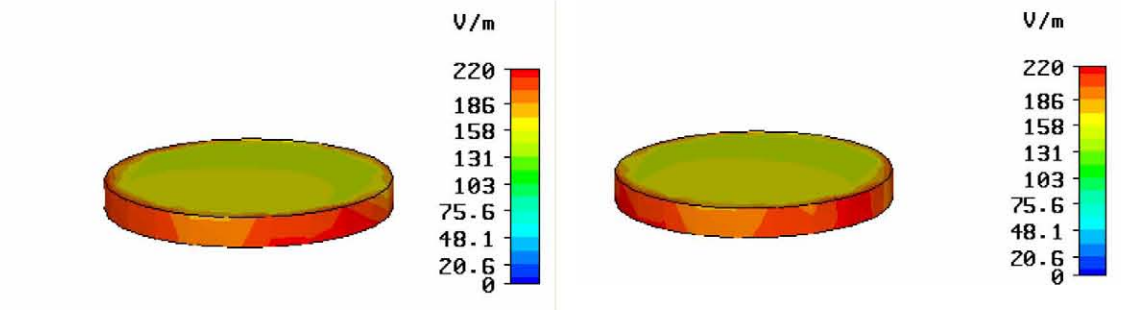
Fig. 3 -SAR and Power loss density distribution histogram in the culture medium

Figures from 4 to 7 show the most relevant results of the 4 disks case.

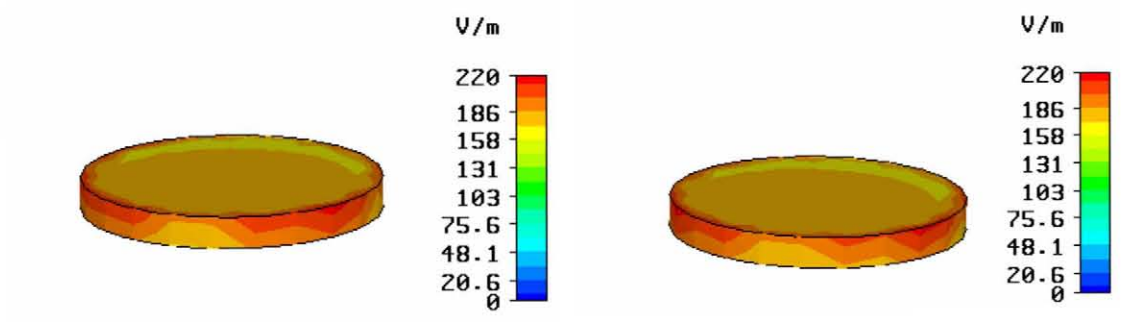


(a) E field in exposure set-up

Fig 4

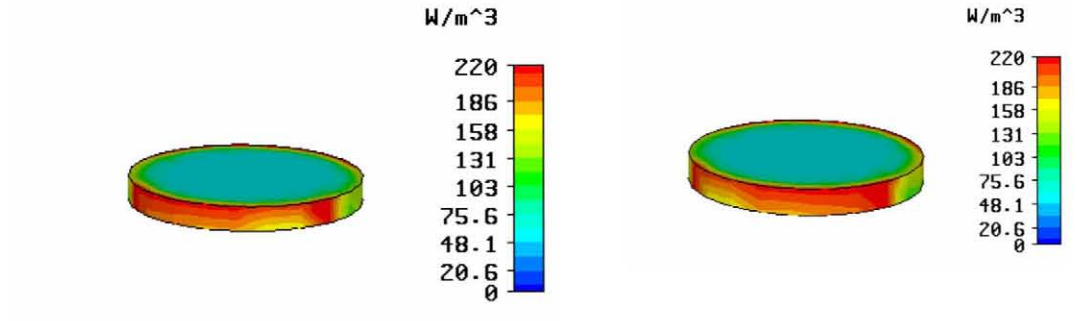


(a) – E field (up left culture) (b) E field (up right culture)

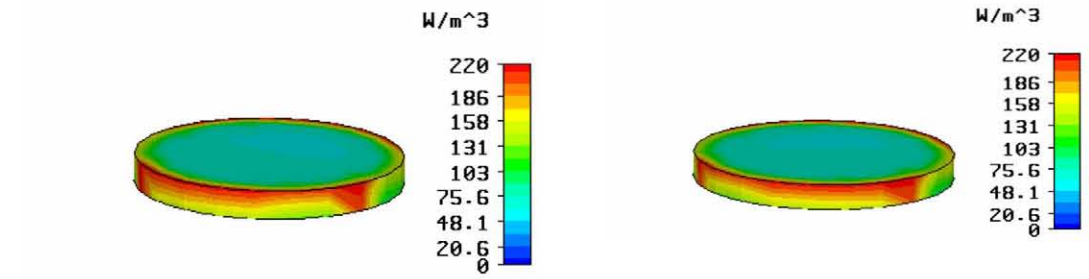


(c) –E field (down left culture) (d) E field (down right culture)

Fig 5

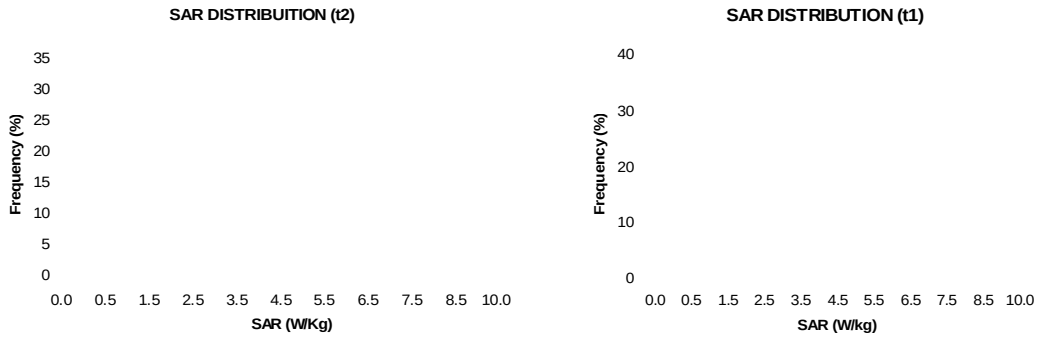


(a) – PLD (up left culture) (b) PLD (up right culture)

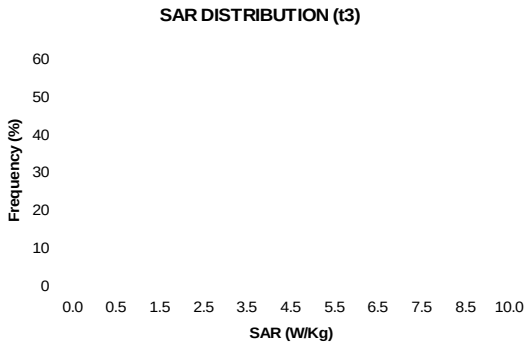


(c) –PLD (down left culture) (d) PLD (down right culture)

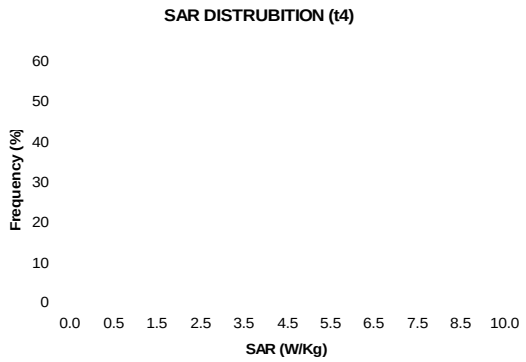
Fig 6



(a) – SAR histogram (up left culture) (b) SAR histogram (up right culture)



(c) – SAR histogram (down left culture)



(d) SAR histogram (down right culture)

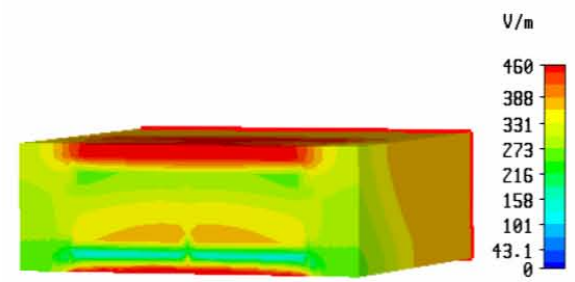
Fig 7

The total average SAR calculated from these distributions is:

CULTURE POSITION	SAR (W/kg)
up left	1.1
up right	1.1
down left	1.4
down right	1.4

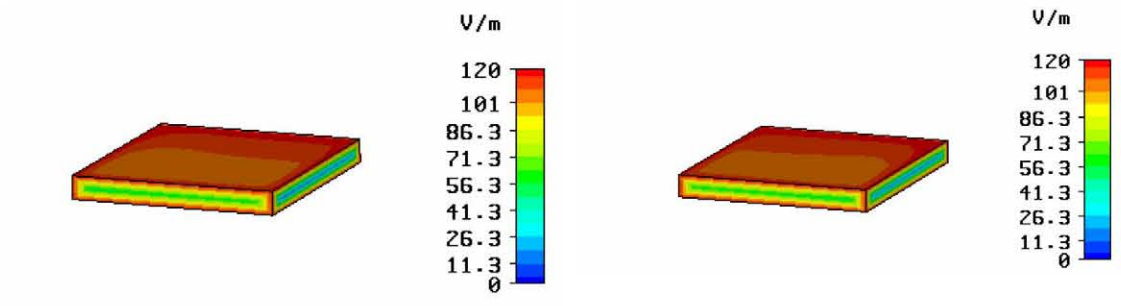
1820 MHz

Figures from 8 to 11 show the most relevant results, as calculated by MWS at the frequency of 1820 MHz. At this frequency, there are some modes of field propagation. For each mode, we have calculated SAR contribution. Only first an second mode have a significant value. However, in our calculations, we have considered ten modes.



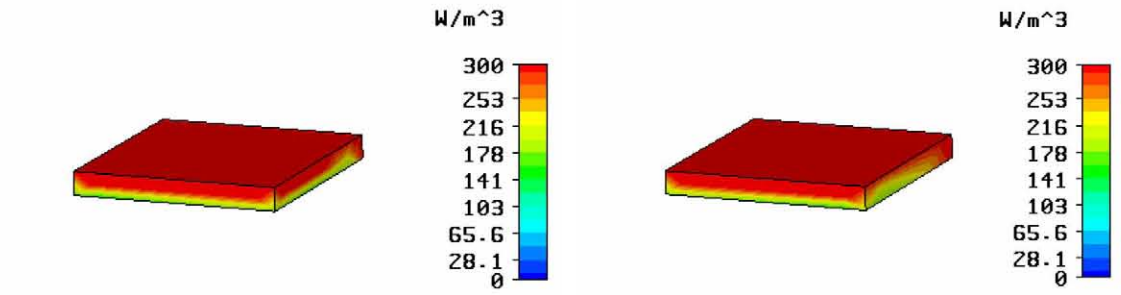
(a) E field in exposure set-up

Fig 8



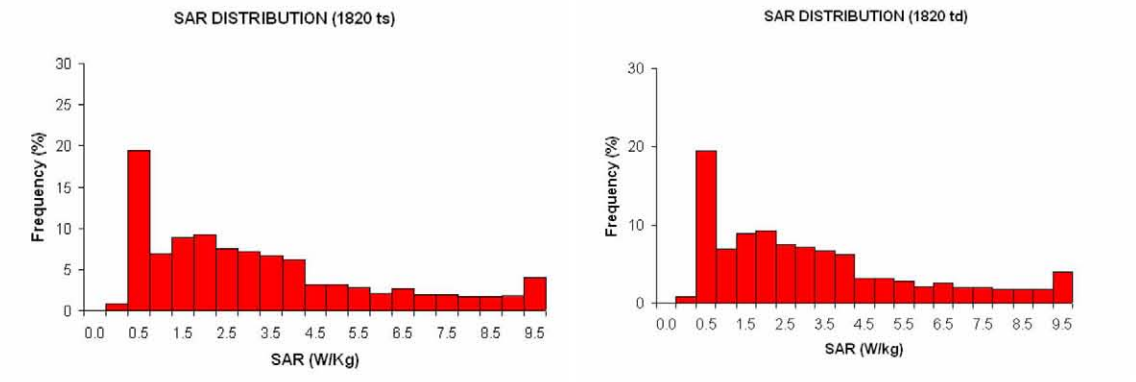
(a) – E field left culture (b) E field right culture

Fig 9



(a) – PLD left culture (b) PLD right culture

Fig 10



(a) – SAR histogram left culture (b) SAR histogram right culture

Fig 11

The total average SAR calculated is 3.5 W/Kg for the left culture and the right culture

V Concluding Remarks

This study was carried out in the frame of activities referring to the European Project EMF-NET, Main Task 2. In fact our group is leader of the Work Package 12 focused on numerical calculations for occupational exposure.

Variability of the efficiency depending of the shape of terrain culture container (flask o dish), number of samples exposed at the same time, their positions, has been investigated.

Separately, for the various numerical calculations performed, the results can be summarized as follows:

- 900 MHz average SAR and distribution depend on quantity of culture medium (3 o 5 ml) and depend on number of culture exposed.
- 900 MHz average SAR and distribution depend on positions of the culture medium
- 1820 MHz average SAR doesn't depend on positions, because we have a symmetry in our set up.
- All simulations show that the spatial distribution of SAR inside each sample is not homogeneous, and local SAR values may be highly variable

Acknowledgments

The authors would like to thank Vincenzo Brugaletta for his precious support in experimental characterization of the exposure set up.

References

[1]	Microwave Studio, User's Manuals 5.02 2004, CST Computer Simulation Technology, D-64289 Darmstadt, Germany.
[2]	T. Weiland, "A discretization method for the solution of Maxwell's equations for six-component field", *Electronics and Communications AEÜ*, vol.31, no.3, pp.116-120, 1977.
[3]	B. Krietenstein, R. Schuhmann, P. Thoma, T. Weiland, "The Perfect Boundary Approximation technique facing the challenge of high precision field computation", *Proc. of the XIX International Linear Accelerator Conference (LINAC '98)*, Chicago, USA, pp. 860-862, 1998.
[4]	Cannelli V., Falsaperla R., "Numerical SAR evaluation for cell culture exposed to 900 MHz continuous waves", Third International Workshop on ElectroMagnetic Fields; 4-8 October 2004,Kos, Greece.

EFFECT OF SIGNAL MODULATION ON THE LINEAR RESPONSE OF ELECTRIC FIELD PROBES USED TO DETERMINE SPECIFIC ABSORPTION RATE

BENJAMIN LOADER, DANIEL BOWNDS.
NATIONAL PHYSICAL LABORATORY,
HAMPTON ROAD, TEDDINGTON MIDDLESEX, UK, TW11 0LW

Abstract
Electric field probes used to assess the specific absorption rate (SAR) of energy in human tissues due to radio transmitters are largely based on diode detectors. To determine the accuracy of SAR measurements, it is necessary to characterise the effect of the signal modulation on the linear response of these probes. This paper describes the system developed at the National Physical Laboratory to assess the linearity of SAR probes to different signal modulations, and gives results for four commercially available SAR probes. There was a wide variation in the linearity of the probes to pulse modulated signals, and this highlights the need to assess the linearity to the signal modulation to be measured. The results show that the tests in the IEEE 1528-2003 [1] give a conservative estimate for the linearity error in most cases.

Introduction
SAR is the specific absorption rate of radio frequency energy in a material and has the unit watts per kilogram. SAR forms part of the basic restriction limiting exposure of humans to radio-frequency fields over the frequency range 100 kHz to 10 GHz. The SAR resulting from the use of mobile radio transmitters is assessed by measuring the electric field in a liquid phantom that approximates the electrical properties of the biological material of interest. For a dielectric, SAR is then calculated by

$$SAR = \frac{E^2 \sigma}{\rho} \tag{1}$$

where E is the electric field in the liquid, σ its conductivity and ρ its density. The electric field probes used to assess SAR contain three orthogonal electric field sensors, and these commonly use Schottky diode detectors. Below the diode compression point the output voltage from the diode is proportional to the average power during the measurement (square law region). At high powers the output voltage is proportional to the r.m.s voltage during the measurement period (linear region). There is a transition region between the linear and square law region. Since the diodes are operated beyond the square law region, the output voltage (V) must be corrected to obtain a linear response (V_{LIN}), using

$$V_{LIN} = V\left(1 + \frac{V}{DCP}\right) \tag{2}$$

where DCP is the diode compression point. For pulse-modulated signals, the sample rate of the probe may be too slow to correctly sample the modulation, and in this case the V_{LIN} is obtained using

$$V_{LIN} = V\left(1 + \frac{CF \times V}{DCP}\right) \tag{3}$$

where CF is the crest factor of the signal. Linearity is defined as the maximum deviation over the measurement range of the measured quantity from the closest linear reference curve defined over a given interval [2]. The linearity of each sensor in the probe must be assessed to determine the uncertainty for SAR measurements. This paper describes the system developed at NPL for testing the linearity of SAR probes, and gives the measurement results for probes from three manufacturers to a range of communications signals.

Description of the measurement system
Linearity is measured by placing the sensor in an electric field and recording the diode output voltage as a function of input power to the system used to generate the field. This can be done with the sensor in air or liquid, but air is preferable since the conductivity of liquids will change with temperature, introducing non-linearity to the field generating system. Figure 1 shows a schematic of the system used. The probe is placed into IEC-R22 (UK WG8) waveguide through an aperture in the broad-wall with its axis at an angle of 54.7° to the axis of the waveguide, so that rotation of the probe about its axis allows each sensor in turn to be aligned with the polarisation of the field. This is necessary to avoid over-range errors occurring. The signals were generated using an Agilent ESG vector signal generator, which can produce a wide range of communications signals. A 5 W low noise linear amplifier allowed sensors to be tested up to a sensor output voltage that is equivalent to 100 Wkg^{-1}.

A power sensor monitors the input power to the system via a high directivity coupler and step attenuator. The step attenuator was adjusted to keep the burst average power readings in the range –20 dBm to 0 dBm, as this limits the uncertainty due to the linearity of the power sensor. Note that changing the attenuation step does not alter the power transfer between the signal generator and the waveguide, and this is an important requirement for such a system.

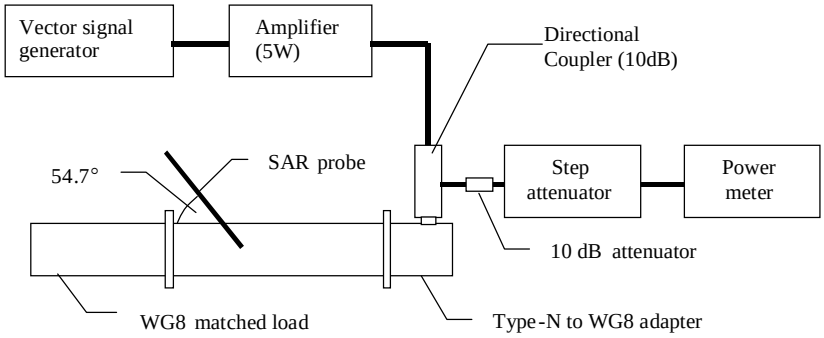


Figure 1: Schematic of linearity measurement system.

The linearity measurements were made at 1800 MHz. Table 1 lists the modulation frequency and crest factor for the signals used. UMTS 1 has a single carrier (5 MHz bandwidth), and UMTS 4 has four carriers (20 MHz bandwidth). Pulse 1 and Pulse 2 correspond to the linearity tests specified in [1].

Table 1. Signal characteristics

Signal type	Crest factor	Modulation frequency
CW	1	0 Hz
GSM	8	217 Hz
DECT	12	100 Hz
TETRA	4	17.6 Hz
Bluetooth	3.25	(625μs per slot)
WCDMA-1	1	0 Hz
WCDMA-4	1	0 Hz
Pulse 1	10	11 Hz
Pulse 2	25	1 kHz

Measurement results

The linearity of the probes was measured for peak SAR readings over the range 0.02 Wkg^{-1} to 100 Wkg^{-1}. Table 2 gives the maximum linearity error of the probes over this range. Figures 2 to 5 show the SAR reading against the ratio of average input power to the system. All of the probes over-read at high SAR levels when measuring pulse-modulated signals. The extent of the linearity error varies considerable between probes from different manufacturers. The linearity error for UMTS signals is similar to that for CW signals. Table 3 gives the maximum change in the relative sensitivity of the three sensors in each probe over the range 0.02 Wkg^{-1} to 100 Wkg^{-1}. This corresponds to the change in isotropy due to differences in linearity of the three sensors in the probe.

Table 2: Linearity over the peak SAR range 0.02 Wkg^{-1} to 100 Wkg^{-1}.

Signal type	Maximum linearity error (± dB)				
	Power sensor	Probe A	Probe B[1]	Probe C	Probe D
CW	0.05	0.12	0.51	0.82	0.93
GSM	0.07	0.68	1.71	4.39	1.45
DECT	0.06	0.51	1.98	4.00	2.80
TETRA	0.06	0.69	3.74	4.90	3.33
Bluetooth	0.07	1.04	0.52	4.60	1.13
WCDMA 1	0.05	0.12	0.25	0.55	0.91
WCDMA 4	0.05	0.20	0.18	0.41	1.31
Pulse 1	0.05	0.58	0.97	3.11	1.81
Pulse 2	0.25	1.81	0.57	4.76	2.41

[1] Quoted over the range 0.1 Wkg^{-1} to 100 Wkg^{-1}, as this probe has limited sensitivity.

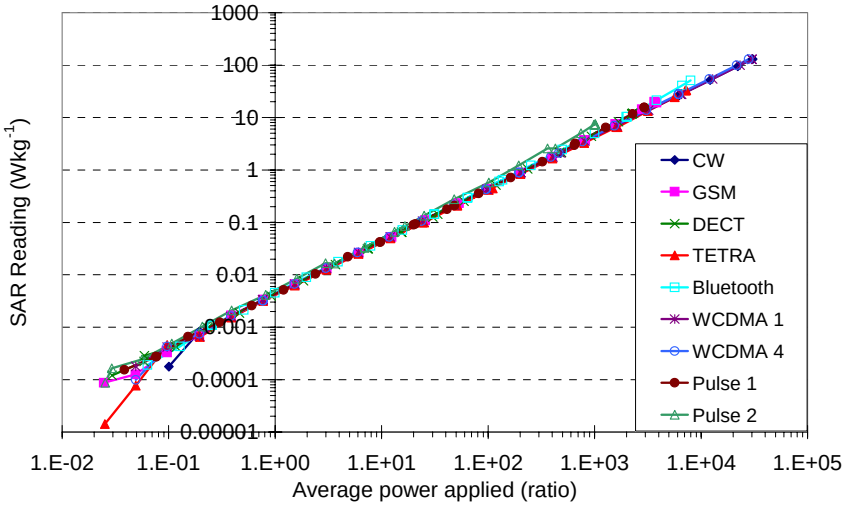


Figure 2. Probe A: SAR reading against average applied power.

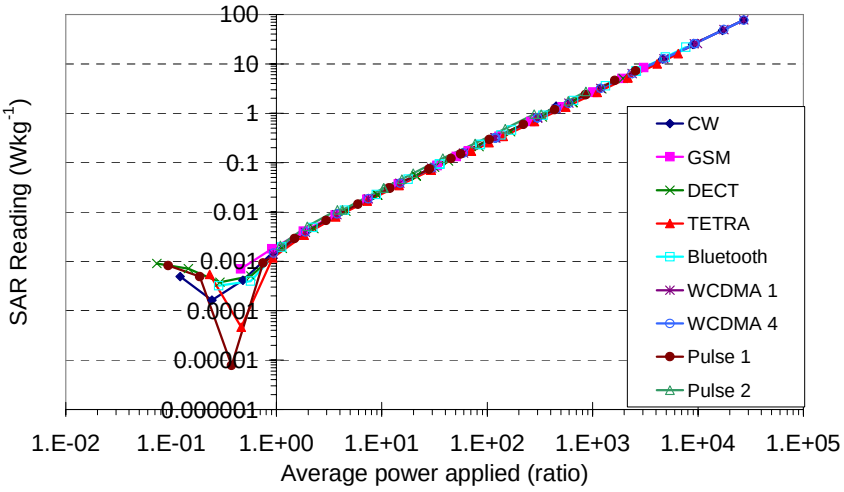


Figure 3. Probe B: SAR reading against average applied power.

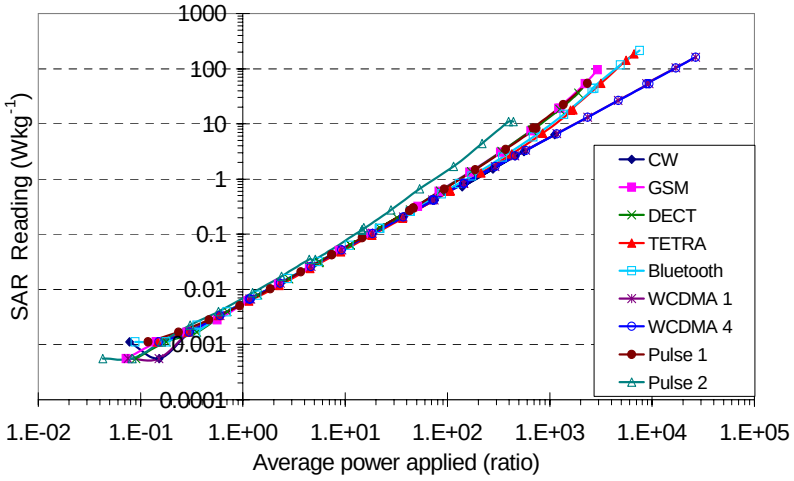


Figure 4. Probe C: SAR reading against average applied power.

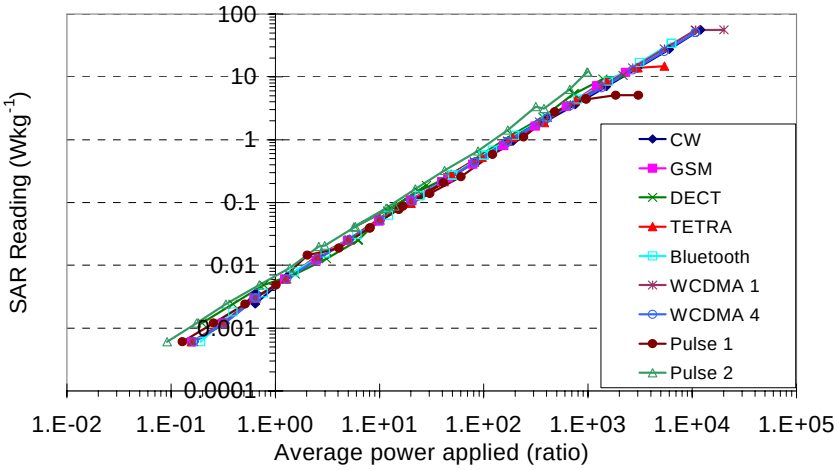


Figure 5. Probe D: SAR reading against average applied power.

Table 3: Change in isotropy over the peak SAR range 0.02 Wkg^{-1} to 100 Wkg^{-1}.

Signal Type	Maximum change in relative sensitivity of the three sensors (dB)			
	Probe A	Probe B	Probe C	Probe D
CW	0.30	0.30	0.39	0.25
GSM	0.16	0.57	0.39	0.31
DECT	0.24	0.68	2.13	0.76
TETRA	0.29	2.42	0.47	0.69
Bluetooth	0.05	0.22	0.59	0.23
WCDMA 1	0.03	0.03	0.24	0.27
WCDMA 4	0.03	0.06	0.02	0.31
Pulse 1	0.28	0.69	0.33	0.94
Pulse 2	0.14	0.44	2.53	1.21

Conclusions

The linearity performance of four commercially available probes for measuring SAR was tested for a variety of communications signals over the range 0.02 Wkg^{-1} to 100 Wkg^{-1}. The linearity performance of the probes to CW signals and UMTS signals was found to be good. The low-level detection limit of one probe was limited to around 0.05 Wkg^{-1}. For pulse-modulated signals, the equation used to compensate for diode compression (Eq 3) was found to cause the probes to over-read at high peak SAR levels. The extent of this error varied considerably between the probes tested. For one probe, this correction did not give a linear response for pulse-modulated signals. Differences between the linear responses of the three sensors in the probes were also observed. It is therefore essential to characterise the linear performance of SAR probes to determine the measurement uncertainty. Each sensor should be tested separately, as differences in linear response between the sensors change the isotropy of the probe. In most cases, the tests specified in the [1] gives a conservative estimate for the linearity error for the range of pulse modulation schemes, but will over-estimate the measurement uncertainty for many real signals. Ideally, the linearity should be tested to the actual signal modulation to be measured.

Acknowledgement.

The Department for Trade and Industry (DTI) funded this work for the National Measurement System (NMS) of the UK.

References

[1] IEEE Standard 1528-2003 "Recommended Practice for Determining the Peak Spatial-Averaged Specific Absorption Rate (SAR) in the Human Head from Wireless Communications Devices: Measurement Techniques".

[2] British Standard BS EN 503361:2001. “Basic standard for the measurement of specific absorption rate related to human exposure to electromagnetic fields from mobile phones (300 MHz – 3 GHz)”.

C-FOS EXPRESSION ON BRAIN AFTER ACUTE EXPOSURE TO 900 MHz GSM RADIATION OF PICROTOXIN MODEL OF EPILEPTIC RATS IS RECOVERING AFTER 3 DAYS.

LÓPEZ-MARTÍN E.[(1)], CARBALLO QUINTÁ M. [(1)], RELOVA QUINTEIRO JL[(2)], SEBASTIAN FRANCO JL[(3)], JORGE BARREIRO[(1)] ARES F.J [(4)]

[(1)] *MORPHOLOGICAL SCIENCES DEPARMENT, UNIVERSITY OF SANTIAGO DE COMPOSTELA, 15782 SANTIAGO DE COMPOSTELA, SPAIN.*
Emails: cmelena@usc.es (Lopez–Martin); cmjorge@usc.es (Jorge–Barreiro)

[(2)] *PHYSIOLOGY DEPARMENT, UNIVERSITY OF SANTIAGO DE COMPOSTELA, 15782 SANTIAGO DE COMPOSTELA, SPAIN.*
Email: fsrelova@usc.es (Relova–Quinteiro)

[(3)] *DEPARMENT OF APPLIED PHYSICS III, UNIVERSITY COMPLUTENSE OF MADRID, 28040, MADRID, SPAIN.*
Email: jlsf@fis.ucm.es (Sebastian–Franco)

[(4)] *RADIATING SYSTEM GROUP, APPLIED PHYSICS, UNIVERSITY OF SANTIAGO DE COMPOSTELA, 15782 SANTIAGO DE COMPOSTELA, SPAIN.*
Email: faares@usc.es (Ares–Pena)

Abstract

Acute effect of electromagnetic fields (EMFs) and induction of genes, with no thermal stress, have been reported but remain controversial. In previous studies we have found neuronal activation markers (c–fos) in the brain of rats pre–treated with subconvulsive doses of picrotoxin, after 2hs exposure to 900 MHz GSM radiation, at intensities similar to those emitted by mobile phones. In this study we analyzed in 50 adult male Sprague-Dawley rats the time course effects of induction of c–fos immunochemical testing of relevant anatomical areas with acute experimentally model induced by picrotoxin, after 60 minutes, 24 hours and 3 days of exposure to EMF radiation. C-Fos positives cells were counted in cortical and hippocampal areas, using a morphometric software, having expressed counts per field as means ± s.e m.. 60 m and 24 hs after the radiation (AR), the c-Fos positive cells were increase on cortical and hippocampal areas; after 3 days the counts were similar in the same areas of the exposed–and–treated and non–exposed–and–treated animals. After 3 days, none of them showed differences. The time course of the effects after the GSM radiation on the CNS showed to be recovered after 3 days.

1. Introduction

The modulation of gene expression can be initiated by external events, acting through intracellular signalling pathways triggers changes in differentiation of cells, cell growth and programmed cell death. It

is well know that the induction and up-regulation of immediate–early genes (IEGs) precede degenerative process of central nervous system (CNS). Induction of c-fos has been associated with cellular injury and even cellular death (1, 2) c-fos is also easly induced under non-pathogenic environmental conditions and can be used as a sensitive marker of neuronal activation (3, 4). The expression of genes called proto-oncogenes can be increased by tumor-promoting agents, ultraviolet radiation and X-rays.
In relation with gene activation by exposure to non-ionizing radiofrequency electromagnetic radiation on CNS is controversial topic that normally it is explain normally by thermal influence. The results of studies of gene expression in mammals have been variable and generally negative (5). Studies of changes in the expression of the early response gen c-fos (6, 7, 8, 9) in the brain of rats and mice exposed to RF radiation and in vitro exposure (10,11) generally find no effects following at thermally insignificant levels. In any case, c-fos expression is known to increase enter sham and exposure animals of the expression levels proto-oncogene c-fos after exposure to RF and suggest the acute genomic response detected was due to immobilisation (12) of an animal or to increase simply as a result of stress (13). In previous study in rats that have been made seizure-prone by subconvulsive doses of picrotoxin, GSM radiation can trigger seizures and induce changes in cerebral activity reflected by high levels of c-Fos-positive neurons in certain brain areas (14). The brain tissue of seizure proneness can be especially sensitive to the effects of mobile-phone type radiation (15).In this paper the time course of the effects of radiation were evaluated by immunochemical testing of relevant brain areas for a marker of neuronal activation c-Fos expression at 60m 24 hs and 3 days after 2h of GSM-modulated 900 MHz radiation at intensity similar to that emitted by mobile phones.

2. Material and Methods

2.1. Animals and experimental procedure

72 adult male Sprague-Dawley rats weighing 230-270 g were housed during exposure under standard environmental conditions (12:12 h light/dark cycle, 22°C) with food and water available *ad libitum*. Twelve groups of eight rats were given the following treatments:

EXPERIMENTAL GROUPS	
Group 1:	**Picrotoxin Treated (PT)+ irradiated (IR) studied to 60m**
Group 2:	**PT+ Non-Irradiated (NIR) studied to 60m**
Group 3:	**PT+ IR studied to 24hs**
Group 4:	**PT+ NIR studied to 24hs**
Group 5	**PT+ IR studied to 3 ds**
Group 6	**PT+ NIR studied to 3ds**
Group 7	**Non-Treated with Picrotoxin (NTP) + IR studied to 60m**
Group 8	**NTP + NIR studied to 60m**
Group 9	**NTP + IR studied to 24hs**
Group 10	**NTP + NIR studied to 24hs**
Group 11	**NTP + IR studied to 3 ds**
Group 12	**NTP + NIR studied to 3 ds**

Table 1. This table showed experimental groups used in this experiment

Immediately following intraperitoneal administration of 2 mg/kg of picrotoxin (Sigma), used in groups 1-6, each animal was immobilized in a methacrylate tube and placed in a $150 \times 46 \times 70\,cm^3$ radiation cage that had previously been calibrated to enable measurement of the radiation absorbed by the animal.

2.2. Determination of exposure

Animals belonging to groups 1 and 4 (2 and 5) were irradiated with GSM-modulated (non-modulated) 900 MHz radiation, and the power absorbed by the animal was correspondingly determined (see [14]). The irradiation power level ± 1000 MW, was chosen to be somewhat lower than the average power radiated by a GSM mobile phone. In the metallic cage all the animals were videotaped to record their behaviours while radiated; after 2 h they were removed from the cage and sedated with pentobarbital to transfer them to the histochemistry laboratory. In the radiation cage, the experimental animal in its methacrylate tube was located between a radiating antenna and a receiving antenna with its head at an electromagnetic field maximum (as calculated by finite-difference time domain (FTDT) calculations [16] for the cage plus radiating antenna set up).

2.3. Immunohistochemistry, quantification and statistical analysis of immunohistochemical findings

Approximately 1 h after removal from the radiation cage, the rats were given an overdose of pentobarbital, as said above, and prefixed by transcardial perfusion with physiological saline followed by formaldehyde in phosphate buffer (pH 7.4). Their brains were immediately removed and processed in sections of 40µ. The free-floating sections were used for polyclonal sheep anti-Fos antibody immunochemistry tests (from Cambridge Research Biochemicals, Billingham, UK).
For each rat, c-Fos positivity was evaluated in cerebral cortex (frontal motor, parietal motor, piriform olfactory and entorhinal olfactory areas), in hippocampal structures (dentate gyrus, CA1 and CA3). For each area, three or four sections were examined. c-Fos-positive cells were counted in a 0.30 mm^2 field magnified 20×. Counts per field were reported for each group of rats as means ± SEMs. The significance of between-group differences was estimated by two-way analysis of variance (*picrotoxin status*: PT *vs* NTP × *radiation status*: IGSM *vs* INM *vs* NI). *Post hoc* comparisons were made using Scheffé-type tests. Differences with $p > 0.05$ were considered not to be statistically significant.

3. Results and Discussion

3.1. SAR Results

The parameters of radiation absorbed power, incident power, for the calculus of average SAR $_{exp}$, Peak SAR values calculated for picrotoxin-treated and untreated irradiated rats are listed in Table 1. Every values are lower thermal level (5 W/kg)

	Absorbed Power (AP)	**Incident Power (IP)**	**Efficiency= Mean Abs. Power / Incident Power (η)**	**Mean Weight**	**Mean SAR (experim.) in Brain**	**Mean SAR (experim.) in Body**	**Peak SAR (experim.) averaged in 1g brain**	**Peak SAR (experim.) averaged in 1g body**
	(mW)		**(%)**	**(g)**	**(W/kg)**			
Group 1	178.37	956.72	19.00	209.95	1.32379	0.74551	1.48858	4.09329
Group 3	192.67	710.83	27.16	225.07	1.32961	0.74879	1.49512	4.11127
Group 5	186.17	717.50	26.10	199.98	1.44819	0.81556	1.62846	4.47793
Group 7	189.41	1060.64	17.84	211.83	1.38628	0.7807	1.55884	4.28651
Group 9	202.33	744.17	27.28	228.65	1.37498	0.77434	1.54613	4.25156
Group 11	201.60	801.88	25.10	230.66	1.35739	0.76443	1.52636	4.19719

Table1. SAR values (W/kg) of picrotoxin-treated and untreated rats during irradiation with GSM-modulated 900MHz radiation (means of 7 or 8 rats) Rat group whole body Brain Mean Peak 1-g-averaged Mean Peak 1-g

3.2. Morphological Results

In picrotoxin-treated animals, c-Fos-positive neurons appeared systematically in the thalamus and cortical areas, and some animals also showed more-or less scattered c-Fos positivity in the hippocampus, amygdale, or putamen–caudate complex, and/or in hypothalamic and pontomesencephalic nuclei c-Fos-positive neuron counts.

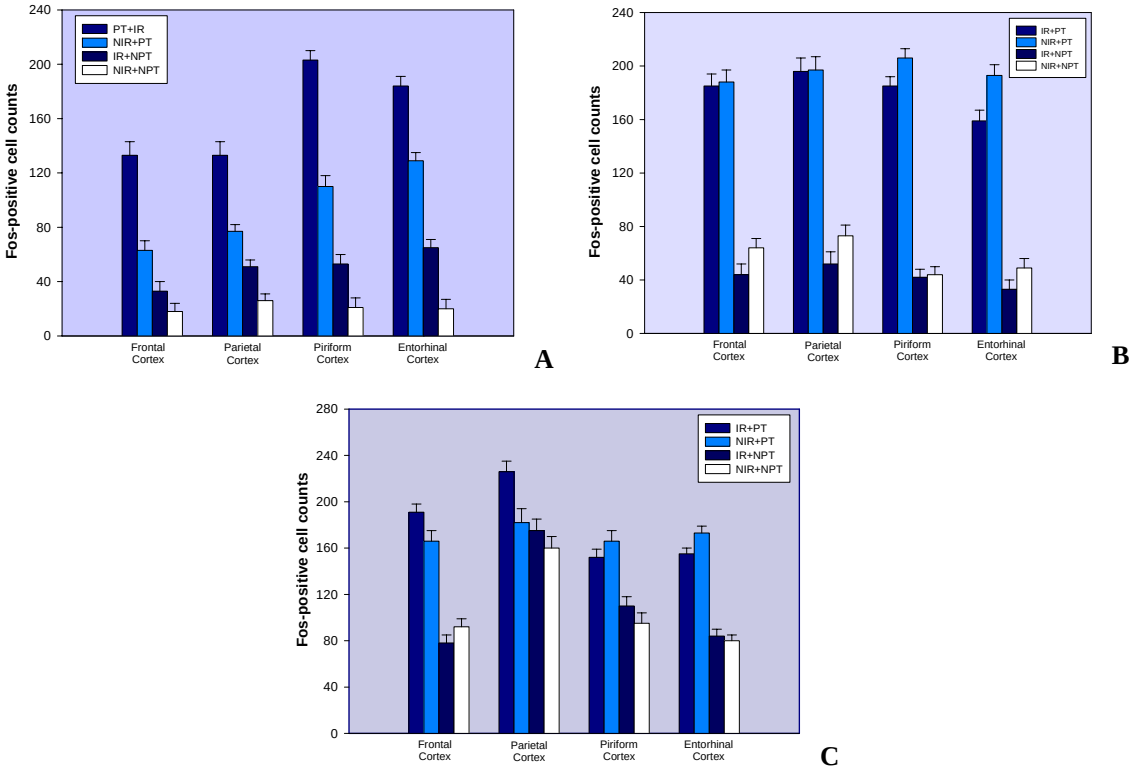


Figure 1. C-fos-positive cell counts in the frontal, parietal, piriform and entorhinal cortex (**A**) 60 minutes (**B**) 24 hours (**C**) 3 days after irradiation. (means of seven or eight rat groups; whiskers indicate SEMs).

3.2.1. Cortical Areas:

- Sixty minutes after radiation neuron counts in irradiated picrotoxin-treated rats were almost double those found in non-irradiated picrotoxin-treated rats. In rats without picrotoxin treatment, counts were lower than in picrotoxin-treated animals and may were in relation with cortical area. In almost all the areas examined analysis of variance showed that both picrotoxin and radiation had statistically significant effects on counts, and that the effect of each was significantly modified by the other.

Irradiated picrotoxin-treated animals had significantly higher counts than non-irradiated picrotoxin-treated animals in both the frontal cortex ($p < 0.001$) and the parietal cortex ($p < 0.004$). There were no significant differences for counts in frontal cortex but in parietal cortex we found significant differences ($p < 0.05$) between irradiated and non-irradiated rats that had not received picrotoxin. In the piriform cortex there is statistically significant difference in picrotoxin-treated irradiated and non irradiated ($p < 0.001$) and non treated irradiated and non irradiated animals ($p < 0.003$), in this area there is important interaction between radiation and treatment ($p= 0.002$). In entorhinal cortex did radiation per se have a statistically significant influence on counts ($p < 0.001$) and in this area it significantly modified the effect of picrotoxin ($p < 0.01$) but there is not a statistically significant interaction between both variables; In both areas there was a statistically significant difference in counts between irradiated and non-irradiated rats that had not received picrotoxin ($p < 0.05$).

Twenty-four hours after radiation neuron counts in irradiated picrotoxin-treated rats values were similar found in non-irradiated picrotoxin-treated rats. In cortical areas examined analysis of variance showed that picrotoxin had statistically significant effects on neuron counts. However both variables picrotoxin and radiation had statistically significant effects on counts alone in Entorhinal cortex ($p < 0.001$). In neither the frontal, parietal and piriform cortex did radiation per se have a statistically significant influence on counts, but in this areas the

counts it significantly modified for the effect of picrotoxin**.** In neither cortical area was there a statistically significant difference in counts between irradiated and non-irradiated rats that had not received picrotoxin.

Three days after radiation in cortical areas there are a statistically significant effects on counts in relation with treatment picrotoxin but the statistically significant interaction effects between radiation x picrotoxin it happen on frontal cortex alone. C–fos positive neurons in irradiated-treated rats showed statistically significant difference in non-irradiated picrotoxin-treated rats on frontal ($p < 0.026$) and parietal ($p < 0.05$) cortex. In neither cortical areas there were a statistically significant difference in counts between irradiated and non-irradiated rats that had not received picrotoxin.

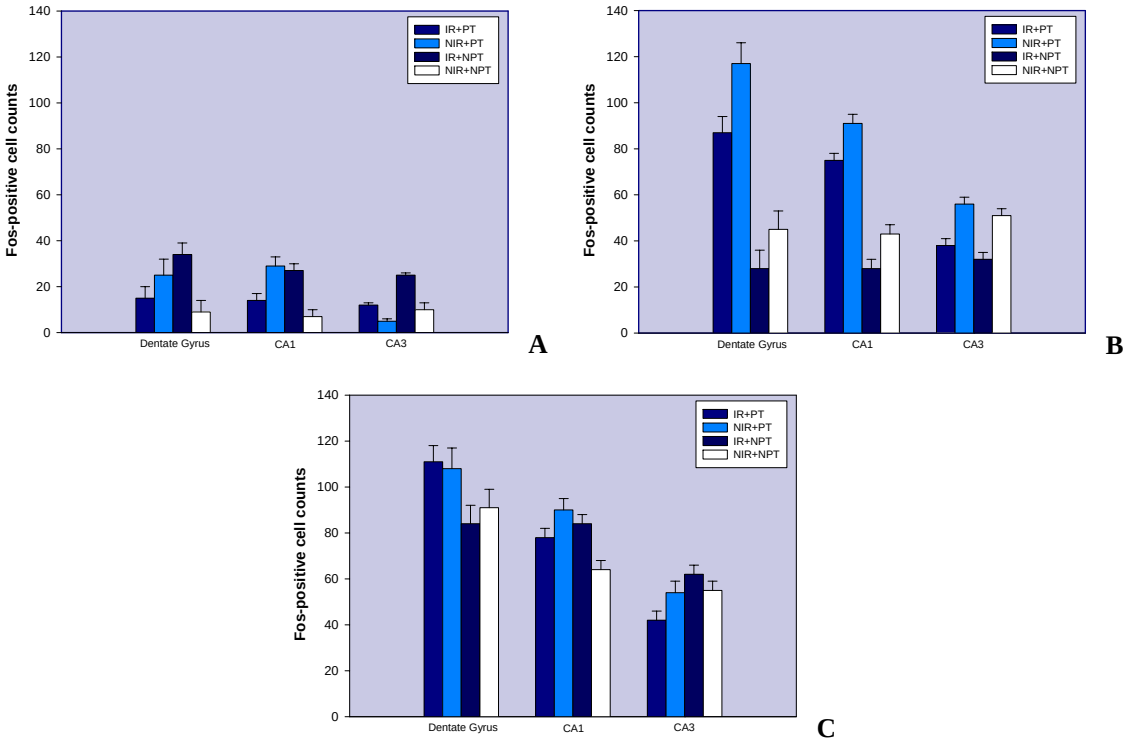


Figure 2. C-fos-positive cell counts in Gyrus dentate,CA1 and CA3 in Hippocampal areas (**A**) 60 minutes (**B**) 24hous (**C**) 3 days after irradiation. (means of seven or eight rat groups; whiskers indicate SEMs).

3.2.2. Hippocampal Areas:

-Sixty minutes after radiation neuron counts in hippocampal areas showed the highest levels c-Fos in rats without picrotoxin treatment and irradiated. The two way analysis of variance showed that there is a statistically significant interaction between radiation and treatment in hippocampal areas and generally a major effect of radiation in untreated animals. In Gyrus dentate untreated and radiated animals showed significance differences with treated and radiated animals ($p < 0.013$) and untreated and non radiated animals ($p < 0.002$). C-Fos positive neuron counts in non picrotoxin treated and irradiated animals had statistically significant difference with picrotoxin treated and irradiated animals in CA1 ($p < 0.009$) and CA3 ($p < 0.013$). Irradiated and untreated animals and non-irradiated and untreated animals showed significance differences in both areas CA1 ($p < 0.001$) and CA3 ($p < 0.001$).Treated animal irradiated and non irradiated showed significant differences in CA1 alone ($p < 0.012$).

- Twenty-four hours after radiation neuron counts in the most animals unirradiated showed higher levels of c-fos positives neurons than irradiated animals. The same way picrotoxin treatment animals showed important levels in the counts neurons respect to animals without treatment. Non-irradiated picrotoxin-treated animals had significantly higher counts than irradiated picrotoxin-treated animals in GD, CA1 and CA3 ($p < 0.05$, $p < 0.05$, $p < 0.001$). Non irradiated animals without picrotoxin showed significance differences with in irradiated animals in three cortical areas.

-Three days after radiation disappear the major differences in the counts in picrotoxin treated and irradiated animals and non picrotoxin treated and non-irradiated animals except in CA3 area where there is a significance differences in counts enter two groups ($p < 0.05$). The animals without picrotoxin treatment showed significant differences in irradiated and unradiated animals in CA1 hippocampal area alone.

3.3. Discussion

We have studied the time course of effects of RF radiation on the CNS in two relevant anatomical areas: cerebral cortex and hippocampal areas. Within the CNS, the cerebral cortex is the part of the brain that is most vulnerable to the electromagnetic field (EMF) [17] exposure as it is a peripheral anatomical structure that received most of SAR of microwave radiation at non thermal levels (see table). However, a very low level of radiation may produce effects due to the vulnerability of cerebral cortex, altering the activity of the nervous system [18]. Hippocampal areas are in the middle of the brain and the low level SAR did not explain the direct effect of GSM radiation in this area. The radiation seems to act as a periodic peripheral stimulus that increases the vulnerability of neuronal circuits that, in the case of GABA-ergic circuits, have already been weakened by picrotoxin [14]. Sixty minutes after radiation there is high expression of c-Fos in cortical areas. Neuronal changes are not persistent and 24 hs after irradiation both groups, picrotoxin-treated rat irradiated and picrotoxin-treated and non radiated, had similar levels. Finally 3days after irradiation there was a compensation in most of the groups. The progressive time course recovering of c-fos levels in this acute model of seizure-proneness indicate no altered functionally physiological normal mechanism after acute radiation.

4. Conclusions

The time course of the effects after the GSM radiation in rats that have been treated by subconvulsive doses of picrotoxin showed induced changes in cerebral activity. These are reflected by high levels of c-Fos-positive neurons in certain brain areas after 60m. The differences between the irradiated and non irradiated groups are shown to be minor after 24 hs from radiation and finally they be recovered after 3 days.

5. Acknowledgements

This work was supported by the Secretariat General for Research and Development of the Xunta de Galicia under project PGIDIT02BTF2060

6. References

[1] Smeyne R. J., Vendrell M., Hayward M., Baker S.J., Miao J., Schilling K., Robertson L.M., Curran T. and Morgan J.I. Continous c-fos expression precedes programmed cell death in vivo. *Nature*.363, 166-169. (1993).

[2] Schreiber S. S and Baudry M, Selective neuronal vulnerability in the hippocampus –a role for gene expression, Trends Neurosci.,18, (1995) 446-451.

[3] Morgan J.I. and Curran T. Stimulus-transcription coupling in the nervous system: involvement of the inducible proto-oncogenes fos and jun. *A. Rev. Neurosci.* 14, 421-451. (1991)

[4] J. I. Morgan and T. Curran, Proto-oncogene transcription factors and epilepsy, *Trends Pharmacology Science* 12 (9) 343-349. (1991)

[5] Whitehead TD, Brownstein BH, Parry JJ, Thompson D, Cha BA, Moros EG, Rogers BE, Roti Roti JL. Expression of proto-oncogene Fos after exposure to radiofrequency radiation relevant to wireless communications *Radiat Res* 164 (4 pt 1);420-30. (2005)

[6] Mickley G.A. Mickley, B.L. Cobb, P.A. Mason, S. Farrell, Disruption of putative working memory task and selective expression of brain c-fos following microwave-induced hyperthermia, *Physiol. Behav.* 55 1029 (1994).

[7] Walters TJ, Mason PA, Sherry CJ, Stevens C and Merritt JH, No detectable bioe-effects following acute exposure to high peak power ultra-wide band electromagnetic radiation in rats. *Aviat Space Environ Med* 66 (6), 562 (1995)

[8] K. Fritze, C. Wiessner, N. Kuster, C. Sommer, P. Gass, D.M. Hermann,M. Kiessling, K.A. Hossmann, Effect of global system for mobile communication microwave exposure on the genomic response of the rat brain, *Neuroscience* 81 (3) 627–63(1997)

[9] R.W. Morrissey, S. Raney, E. Heasley, P. Rathinavelu, M. Dauphinee, J.H. Fallon, IRIDIUM exposure increases c-fos expression in the brain only at levels which likely result in tissue heating, *Neuroscience* 92, 1539–1546 (1999).

[10] Oleg I. Ivaschuk, Robert A. Jones, Tamako Ishida-Jones, Wendy Haggren, W. Ross Adey and Jerry L. Phillips Exposure of nerve growth factor treated PC12 rat pheochro mocytoma cells a modulated radiofrequency field at 836.55 MHz: effects on c-jun and c-fos expression. *Bioelectromagnetics* 18: 223-229 (1997)

[11] Goswami PC, Albee L.D, Parsian A.J, Baty J.D, Moros E.G, Pickard W.F, Roti Roti JL, Hunt C.R, Proto-oncogene mRNA levels and activities of multiple transcription factors in C3H 10T ½ murine embryonic fibroblast exposed to 835.62 and 847.74 MHz cellular phone communications frequency radiation, *Rad Res* 151(3):300-9.(1999)

[12] w.E. Cullinan, J.P. Herman, D.F. Battaglia, H. Akil, S.J. Watson, Pattern and time course of immediate early gene expression in rat brain following acute stress, *Neuroscience* 64 (2) 477–505. (1995)

[13]Finnie JW, Expression of immediate early gene, c-fos, in mouse brain after acute global system for mobile communication microwave exposure, *Pathology* 37(3):231-3 (2005)

[14] López-Martín. E., Relova –Quinteiro José Gallego-Gómez Rosalía, Peleteiro-Fernández Manuel, Jorge-Barreiro Francisco J, Ares-Pena Francisco J, GSM radiation triggers seizures and increases cerebral c-Fos positivity in rats pretreated with subconvulsive doses of picrotoxin, *Neuroscience Letters*, 398, 139-144 (2006)

[15] K.A. Hossmann and Hermann, Effects of electromagnetic radiation of mobile phones on the central nervous system, *Bioelectromagnetics* 24:49-62 (2003).

[16] Schmid & Partner Engineering AG, Reference manual for the SEMCAD Simulation Platform for Electromagnetic Compatibility, Antenna Design and Dosimetry, vilable from: http://www.semcad.com.

[17] Huber R., Treyer V., Schuderer J., Berthold T., Buck A., Kuster N., Landolt H.P., Achermann P. 2002 Exposure to pulse-modulated radiofrequency electromagnetic fields affects regional cerebral blood flow *European Journal of Neuroscience* 21, 1000-1009

[18] James C. Lin, 2003. Cellular telephone radiation and electroencephalograms (EEG) of the human brain. *IEEE Antennas and Propagation Magazine*, 45 (5)150-153.

EXPOSURE OF RAT THYROID GLAND TO 2450 MHZ MICROWAVE INDUCES CHANGES IN EXPRESSION OF HSP-90.

MISA AGUSTIÑO M. J. [(1)], JORGE MORA M. T. [(1)], MORENO PIQUEIRO E. [(2)], ARES PENA F. J. [(2)], JORGE BARREIRO F. J. [(3)], LÓPEZ MARTÍN E. [(3)].

[(1)] PHYSICAL MEDICINE AND REHABILITATION, UNIVERSITY HOSPITAL COMPLEX OF SANTIAGO DE COMPOSTELA, SPAIN.
Email: mjmisa73@hotmail.com (Misa–Agustiño)

[(2)] RADIATING SYSTEMS GROUP, DEPARTMENT OF APPLIED PHYISCS, UNIVERSITY OF SANTIAGO DE COMPOSTELA, 15782, SANTIAGO DE COMPOSTELA, SPAIN.
Email: faares@usc.es (Ares–Pena)

[(3)] MORPHOLOGIC SCIENCE DEPARTMENT OF MEDICINE FACULTY OF SANTIAGO DE COMPOSTELA, SPAIN.
Email: cmelena@usc.es (López–Martín)

Abstract

Rat thyroid gland was exposed in vivo to 2.450 MHz microwave fields using a commercial set up (GTEM). Heat shock protein Hsp90 is constitutively expressed in most cells under normal physiological conditions and is induced in cells upon cellular stress. The purpose of this work is to explore the expression of chaperone Hsp-90 as a biological marker that determines the sensitivity of thyroid gland to whether acute or repeated microwave exposures.

Twenty-six female Sprague-Dawley rats were studied with an irradiating microwave experimental system subject to: 1) 30 minutes acute exposure to whether 1,5 or 3,0 W and 2) Repeated exposure of 30 minutes per day during 10 days to 3,0 W. Rats were perfused with 4% paraformaldehyde, and thyroid gland removed 90 min and 24 hours post-exposure. Finally the thyroid glands were studied with histochemestry techniques: Hematoxylin-Eosin and inmunocytochemical analysis of Hsp90

These results suggest that microwave radiation provokes a stress stimulus for thyroid gland with both thermal and non-thermal mechanisms. In acute exposures they showed response to functional activity changes, but with chronic exposure the physiological mechanism of the gland suffered a certain degree of adaptation to this type of stress.

1. Introduction

The heat shock proteins (Hsps) are a cytoprotective cellular system which has different physiologic functions for homeostatic cellular balance and in response to cellular stress. Hsps have been shown to function in protein maturation events such as protein folding, unfolding and translocation across membranes [1] [2]. There are two cytoplasmic isoforms mains: Hsp90α (inducible form/major form) and Hsp90ß (constitutive form/ minor form) [3][4].

Hsp90 is an abundant and highly conserved molecular chaperone that is essential for viability in eukaryotes [5], comprises as much as 1%-2% of total cellular protein under basal conditions and increase to 4%-6% of cellular

proteins under stress [4]. Therefore, it is constitutively expressed in most cells under normal physiological conditions and is induced in cells upon exposure to elevated temperatures or other forms of cellular stress [6] as hypoxic/anoxic injury, radiations, heavy metals, viral infections, drugs … Then Hsp90 is a main functional component of an important cytosol chaperone complex, and is involved in different cellular processes, such as cell proliferation, differentiation and apoptosis. It is also associated with various cellular proteins such as steroid-hormone receptors, aryl hydrocarbon receptor, MyoD, oncogen tyrosine kinases, haem-regulated aukariotic initiation factor 2α kinase, casein kinase II, actin and tubulin [7]. Hsp90 expression is higher in proliferative cellular process than in normal tissues [8] and allow tumor cells to tolerate alterations that would be lethal.
A lot of years before ionizing radiation has been proven to cause genetic damage, which can lead to cancer and thyroid gland is one of the organs most sensitive to radiation [9][10]. In the last years the investigation of anti-cancer therapy is direct to specific proteins as Hsp90 [11][12][13].
Heat shock protein is released after exposure to microwave at levels causing, or not, heating [14][15]. And thyroid gland function change in response to environmental temperature and can be directly stimulated by microwave heating changed the activity [15].
Although non-ionizing radiation like microwaves have not been established as a cancer-causing agent, we like to explore the expression of chaperone, Hsp90 as a biological marker that determines the sensitivity of thyroid gland to whether acute or repeated microwave exposures. And we like to check if existed differences between thyroid gland exposed to microwaves and non exposed (controls).

2. Material and Methods

2.1. Animal exposure

Twenty-six female Sprague-Dawley rats, weighting between 168,7 and 248,5 gr. were exposed in vivo to 2.450 MHz microwave fields using a commercial set up GTEM 250: twenty-two rats were exposed during 30 minutes one day, acute exposure to 1,5 or 3,0 W and four rats were exposed during 30 minutes/day for 10 days, chronic exposure to 3,0 W. Radiation was direct to left front leg. During exposure, rats were housed in transparent cylindrical perspex jigs that did not allow them to move.

GROUP	TIME EXPOSURE -MICROWAVE POWER - PERFUSION		
1	EXPOSURE 30´ ,	P= 1,5 w ,	PERFUSION 90´
2	EXPOSURE 30´ ,	P= 1,5 w ,	PERFUSION 24 h
3	EXPOSURE 30´,	P= 3 w,	PERFUSION 90´
4	EXPOSURE 30´,	P= 3 w,	PERFUSION 24 h
5	EXPOSURE 30´/10 days,	P=3 W,	PERFUSION 10 d

TABLE 1. Exposure groups relative to time of exposure, microwave power applied and time elapsed until perfusion with 4% paraformaldehyde.

2.2. Tissue processed

Rats were anesthetized with dose of pentobarbital 40 mg/Kg and sacrificed 90 minutes or 24 hours after exposure. Were perfused with 4% paraformaldehyde in phosphate buffer during 20 minutes through transcardiac cannula and thyroid glands removed 90 minutes and 24 hours post-exposure and were introduced in post-fixed (10% paraformaldehyde) during 12-24 hours.
The tissues were passed for different alcohols for dehydrate (OH 70º one hour, OH 96º two hours, OH 100º two hours, and finally Toluol two hours), following paraffin embedding during six hours and 4 µ sections were taken for Hematoxylin-Eosin and inmunocytochemical analysis of Hsp90.
The same process was realized regarding to control groups.
All tissues were observed with optical microscope for different magnification (20x, 40x and 100x) of the constitutive structures and a quantitative model was established between exposure rats and control rats.

3. Morphological Results

In thyroid glands the structures studied were: connective tissue of capsular membrane; interlobule connective tissue; follicular cell and parafollicular cell.
In acute microwave exposure of thyroid glands, Hsp90 proteins expressed increase at all structures respect to controls and this increase was greater with high potency. But this increase was lesser in thyroid removed 24 hours respect to 90 minutes post-exposure. In chronic microwave exposure we observed a decreased of Hsp90 expression respect to the control in all structures studied.
In table 2 we can see the representation of data. Results concerning SAR will be presented in the poster.

ACUTE EXPOSURE 1,5 W		**ACUTE EXPOSURE 3,0 W**		**CHRONIC EXPOSURE 3,0 W**	
PERFUSION		**PERFUSION**		**PERFUSION**	
90 minutes	**24 hours**	**90 minutes**	**24 hours**	**90 minutes**	
+ + +	+ + +	+ + +	+	+	**CONNECTIVE TISSUE CAPSULAR MEMBRANE**
+ +	+ +	+ + +	+ +	+	**CONNECTIVE TISSUE INTERLOBULE**
+	+	+ +	+	-	**FOLLICULAR CELL**
+	+	+ +	+	-	**PARAFOLLICULAR CELL**

TABLE 2. In this table we group the results about all types of radiation (acute and chronic) power, exposure time and perfusion time after radiation.

- - Without expression
- + Poor expression
- + + Moderate expression
- + + + High expression

The Hsp90 expression in different structures of thyroid gland respect corresponding controls:

- **Capsular membrane:** Hsp90 expression is high whether for 3.0W or 1.5W, for the animals sacrificed 90 minutes after exposure. But for animals sacrificed 24 hours after exposure there is a decrease in the Hsp90 expression, and such a decrease is more pronounced in animals exposed to 3.0W including expressed levels below the control group. For exposures chronics the Hsp90 expression were poor for all samples with respect to the control group.

- **Interlobule:** The levels Hsp90 expression are higher with 3.0W than with 1.5W for animals sacrificed 90 minutes after exposure. With 3.0W Hsp90 expression was higher than with 1.5W. But when animals were sacrificed 24 hours after exposure the expression is equal for both 1.5W and

3.0W. And for chronic exposed animals Hsp90 presented a decrease with respect to the control group with a poor expression at the same mode than capsular membrane.

- **Follicular cell:** Hsp90 expression was higher for groups exposed to 3.0W (moderate expression) than for groups exposed to 1.5W (poor expression), all of them sacrificed 90 minutes after exposure. The expression was very marked at the periphery follicular cells. 24 hours after exposure, to whether 3.0 W or 1.5W, a poor expression persisted (with respect to control group). And in the other hand in follicular cells of thyroid glands exposed with chronic radiation did not express Hsp90, while the control group presented a minimal expression.

- **Parafollicular cell:** The expression of these cells is similar to that of follicular cells. In thyroid gland removed 90 minutes after exposure, the group exposed to 3.0W presented a higher Hsp90 expression compared to the group exposed to 1.5W, respect to control group. When thyroid glands were removed 24 hours after exposure, Hsp90 expression was the same for two groups (3.0W and 1.5W). And in contrast to chronic exposure control (minimal expression of Hsp90) the chronic exposure group did not present Hsp90 expression.

PHOTOS

CONTROL **ACUTE EX. (3.0W)**

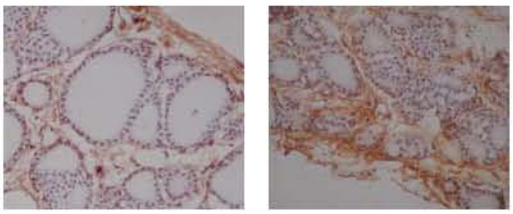


Figure 1. In thyroid glands exposed to acute radiation, the HSP90 expression increase in cellular membrane and intracellular structures with respect to control.

Figure 1. In thyroid glands exposed to acute radiation, the Hsp90 expression increase in cellular membrane and in intracellular structures respect your control.

CONTROL **CHRONIC EX. (3.0W)**

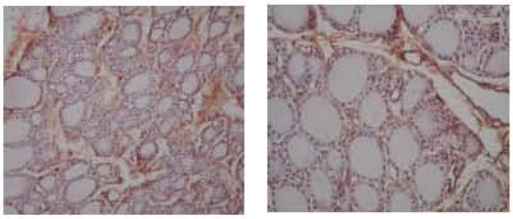


Figure 2. In thyroid glands exposed to chronic radiation the HSP90 expression in chronic exposure is is lower than in control.

Figure 2. In thyroid glands exposed to chronic radiation the Hsp90 expression is lower in chronic exposure than in control.

4. Discussion

With these results we can observe that the use of microwave power at whether 1.5w or 3.0W stimulated Hsp90 production, compared to control groups, because this radiation constitutes a stressing factor for thyroid gland, in acute exposure. In chronic exposure Hsp90 expression decreased, perhaps due to adaptation of the cells to this type of stress. M. Brennan and colleagues observed the effects of body temperature during exercise training on myocardial, and they described that Hsp90 increases with exercise in cold run; and at the end of 9 weeks training Hsp90 levels were no longer significantly increased, which may indicate that a certain degree of adaptation to this type of stress occurs [17]. By contrast, in animals adapted to some stressor, such as anoxia, Hsp90 expression does increase after acute stress exposure; and in chronic exposure Hsp90 experiment a rapid increase. It is possible that such an increase in the expression of stress proteins is part of a rescue mechanism, triggered at the survival limit, similar to a behaviour observed in the experiment with the western painted turtle Chrysemys picta belli, which is the most anoxia-tolerant vertebrate known [18].

5. Conclusions

These results suggest that microwave radiation is a stressful stimulus for thyroid gland in acute exposure with power of 1.5 and 3.0 watts. Nevertheless, with chronic exposure the gland suffers a certain degree of adaptation to this type of stress revealed by the Hsp90 expression decrease.

6. References

[1] J. Biochem (1994) 219: 11-23. Heat shock proteins as molecular chaperones. J. Becker, EA Craig.
[2] Cell prolif (2000) 33: 341-365. Chaperones in cell cycle regulation and mitogen signal transduction: a review. K. Helmbrecht, E. Zeise, L. Rensing.
[3] FEBS Letters (2004) 562 11-15. Hsp90 isoforms: functions, expression and clinical importance. Amere Subbarao Sreedhar, Eva Kalmar, Peter Csermeley Yu-Fei Shen.
[4] Pharmacol. Ther. (1998); 79: 129-68. The 90 Kda molecular chaperone family: structure, function and clinical applications. Csemeley P et al.
[5] Cell.Mol. Life Sci. (2002) 59 1640-1648.
Heat-shock protein 90, a chaperone for folding and regulation CMLS, D Picard. [7] Little JB. Ionizing Radiation. In: Kufe DF, Pollock RE, Weischelbaum RR, et al., eds. Cancer Medicine e. 6. Hamilton, London: B.C. Decker, Inc. 2003: 289-302.
[6] Cell Stress and Chaperones (1998) 3 (3), 188-199. Constitutive expression of heat shock proteins Hsp90, Hsc70, Hsp70 and Hsp60 in neural and non-neural tissues of the rat during postnatal development. Sandra M. D´Souza and Ian R. Brown.
[7] Biochem J. (1996) 314, 205-213. The 90 KDa heat-shock protein (hsp90) modulates the binding of the oestrogen receptor to its cognate DNA. Michèle Sabbah et al.
[8] Jpn J Cancer Res (1996) 87: 908-915. Expression and roles of heat shock proteins in human breast cancer. Yano M, Naito Z, Takana S, Asano G.
[9] Little JB. Ionizing Radiation. (2003): 289-302.
In: Kufe DF, Pollock RE, Weischelbaum RR, et al., eds. Cancer Medicine e. 6. Hamilton, London: B.C. Decker, Inc.
[10] j. Clin Endocrinol Metab (1950); 10: 1296-1308. Thyroid cancer in chilshood and adolescence. Report of 28 cases.Duffy BJ, Fitzgerald P.
[11]The Journal of Clinical Endocrinology and Metabolism (2003) 88 (7):3346-3353. The Heat Shock protein 90-Binding Geldanamycin Inhibits Cancer Cell Proliferation, Down-Regulates Oncoproteins, and Inhibits Epidermal Grow Factor-Induced Invasion in Thyroid Cancer Cell Lines. Jin-Woo Park et al.
[12] Molecular Cancer Therapeutics (2004); 3 (8) Minireview. Altered Hsp90 function in cancer: A unique therapeutic opportunity. Rouchelle Bagatell and Luke Whitesell.
[13]Annals of Oncology (2003) 14:1169-1176. The Hsp90 chaperone complex as a novel target for cancer therapy. M. P. Goetz, D. O. Toft, M. M. Ames and C. Erlichman.
[14] Generation of Heat shock proteins by EMF. Sianette Kwee. Institute of Medical Biochemistry Denmark, Helsinki 2004. AARHUS UNIVERSITY.
[15] Mutat. Research (1997) 399,55. Transgenic nematodes as biomotors of microwave–induced stress. Danniells J. A., Device I., Thomas D., Sewell P., Tatterstall J. and De Pomerai.
[16] IEEE Transaction on Biomedical Engineering, Vol BME-24, Nº 6, November 1977. Microwave Heating Effect on the Dog Thyroid Gland. Richard L Magin, Shin-Tsu Lu, Sol M. Michaelson.
[17] Am J Physios Heart Circ Physiol (2001) 280: H2271-H2280. Effects of body temperature during exercice training on myocardial adaptations. M. Brennan Harris and Joseph W. Starnes.
[18] The Journal of Experimental Biology (2004) 207, 3775-3784. Time-dependent expression of heat shock proteins 70 and 90 in tissues of the anoxic western painted turtle. Valeria Ramaglia and Leslie T. Buck.

MICROWAVE EXPOSURE OF RATS TO THERMAL AND NON-THERMAL 2450 MHz RADIATION PRODUCES CHANGES IN NEURONAL EXPRESSION OF HEAT SHOCK PROTEIN (HSP-90).

JORGE-MORA M. T. [(1)], MISA-AGUSTIÑO M. J. [(1)], BREGAINS J. C. [(2)], ARES-PENA F. J. [(2)], JORGE-BARREIRO F. J [(3)], LÓPEZ-MARTÍN E. [(3)]

[(1)] PHYSICAL MEDICINE AND REHABILITATION, UNIVERSITY HOSPITAL OF SANTIAGO DE COMPOSTELA. SPAIN.
Email: mjmisa73@hotmail.com (Misa–Agustiño)

[(2)] RADIATING SYSTEMS GROUP, APPLIED PHYSICS, UNIVERSITY OF SANTIAGO DE COMPOSTELA, 15782, SPAIN.
Emails: fares@usc.es (Ares–Pena); fajulio@usc.es (Brégains)

[(3)] DEPARTMENT OF MORPHOLOGIC SCIENCE, FACULTY OF MEDICINE, UNIVERSITY OF SANTIAGO DE COMPOSTELA, 15782, SPAIN.
Emails: cmelena@usc.es (Lopez–Martin); cmjorge@usc.es (Jorge–Barreiro)

Abstract

Microwave radiation can switch certain genes in response to stressful challenges to the cell. Heat shock protein 90 (HSP-90) are immediately expressed as marker of stress injury and play a protective role on central nervous system. Moreover, HSP-90 is preferentially expressed in neuronal cell populations in the unstressed mammalian brain. We explore the expression of molecular chaperone HSP-90 on brain neuronal circuits of rats using high-power microwaves with no-thermal or thermal radiation.
Twenty adult males Spragüe-Dawley were exposure to radiation (1.5 and 3 W at 2.45 GHz) using a commercial set up GTEM-250. (1) In acute exposures during 30´; (2) Repeated acute exposures (30´) during ten days. Control-rats were immobilized in set up considering the same elapse time but with no exposure to microwave.
Approximately 90´and 24 h after removal from the radiation cage, the rats were prefixed by transcardial perfusion saline followed by formaldehyde (4%). Their brains were cut with a vibrotome in transverse 40 µm sections. Finally, the sections were processed with blue toulidine and were tested with HSP-90 immunochemistry on hypothalamus, thalamus, hippocampus and cortical areas.
Acute exposure to microwave increases the HSP-90 expression in subregions of hypothalamus, thalamus, hippocampus and cortical areas; and these changes persist with repeated exposure.

1. Introduction

In the last years a great social and scientific concern has arisen for the possible adverse effects of the electromagnetic fields in the living organisms, in short of the radiofrequency, given the great technological advance of the last years, mainly in the field of the mobile telephones. However, already for many years that one comes applying the radiofrequency, in short the microwave, in the human being. A clear example is the medical-therapeutic application of high frequency radiation microwave (2,45 GHz)

in processes ostheoarticulars (diathermy for microwave) at different powers, usually between 25 and 200 watts (w). Microwave treatment is applying in humans directly over the anatomical treatment part about 15-30 minuts during 10-20 sessions. There is recently experimental evidence that the interaction of the radiofrequency with the living organism could produce effects not cause by heating biological tissue (D. Pomerai, 2003; E.Diem, 2005). There by, there are describe two types of biological effects: thermal and not thermal. Thermal effects make reference to secondary effects of energy deposited in the organism which cause an increase of temperature in the biological body and secondarily stimulates the thermoregulation mechanisms; and non-thermal effects are caused by the microwave radiation which does not increase the temperature in the organism (J. L. Franco and cols, 2006).

Heat shock proteins are constitutively expressed under normal conditions in cells and they intervene in a routine way in the metabolic processes essentials for the cell, like the "novo" proteins folding (D. Picard, 2002). But it is also known that under stressful conditions these proteins are overexpressed (induced HSP) to have a protective role in cells (D. S. Latchman, 2004), and even several studies showed that HSP synthesis is responsible for the protective effect of preconditioning by mild stressful stimuli (V. Amin et al, 1995). Recent studies have demonstrated than heat shock protein 90 (HSP-90) is expressed under physiologic conditions in more quantity in neural tissue that not neural (P. Gass, 1994; S. M. D´Souza and I. R. Brown, 1998), and that overexpression of HSP-90 plays an important role in the maintenance of the survival neuronal (G.S. Jeon and cols, 2004; R.G. Ahmed, 2005), for what we conclude that HSP-90 constitutes a biomarker that will help us to know the effects at level neuronal of different types of cellular stress, in this case of the radiation microwave.

The aim of this study was to explore the expression of molecular chaperone HSP-90 on brain neural circuits of rats, using whether thermal and non-thermal acute high-powered microwave (HPM) radiations (2,45 GHz) at 3.0 and 1.5 W respectively, and also after repeated-acute radiation exposure.

2. Material and Methods

2.1. Animals and Experimental Procedure

16 female Spragüe-Dawley rats were exposed to a HPM radiation (2.45 GHz) by using a GTEM250 commercial chamber. Rats were assigned to one of this two treatment groups: Acute and Chronic. "Acute group" rats were radiated, only one time, at 1.5 w or 3.0 w, for 30 minutes, and "Chronic group" rats were exposed to repeated acute HPM at 3.0 w for 30 minutes during 10 sessions (1 per/day) (see Table 1).

Table 1. Radiated Experimental Groups

Group	Microwave Power (watts)	Time Exposure (minuts)	Time Postradiation	Repeated Sesions (days)
Acute (n=16)	1,5 (n=8)	30	90 m	–
		30	24 h	–
	3 (n=8)	30	90 m	–
		30	24 h	–
Chronic (n=4)	3 (n=4)	30	90 m	10

The issuing field of the radiation was directed toward the upper left leg. Besides, control-rats were inmobilized during 30 minutes similar that radiation animals, but not exposured to radiation, in set up the same time (see Table 2).

Table 2. Non Radiated Control Groups

Group	Time post-inmovilization	N
Control Acute	90 m	5
	24 h	5
Control Chronic	90 m, 10 days	4

2.2- Tissue Preparation and Immunohistochemistry

Rats were deeply anesthetized with pentobarbital sodium and then, they were perfused transcardially with heparinized physiological saline followed by a solution of 4% parafolmaldehide in fosfate buffer, 90 minutes (m) and 24 hours (h) postradiation in acute group, and 90 m post radiation in chronic group. Following, rats were sacrificed, their brains were immediately removed and cryoprotected in sucrose for

approximately 24 hours. Subsequently, brains were frozen and cut into 40 µ coronal sections using a cryostat. These sections were processed using immunohystochemical techniques for demonstrating HSP-90 expression.

Finally, we evaluated HSP-90 positivity under an optic microscope Nikon Eclipse E2000 in 12 selected encephalic anatomical areas which nomenclature are from Paxinos and Watson: Hypothalamus (nucleus periventricular, PV; nucleus paraventricular, Pa; Lateral of Hypothalamus, LH and nucleus Arcuate, Arc), Hippocampus (Dentaty Gyrus, DG; CA1, CA2 and CA3) and Cortex (frontal, Fr; parietal, Parl; piriform, Pir and entorhinal, Ent). We compared acute and chronic radiated groups with their respective control-rats.

3. Results and Discussion

3.1 HSP-90 Expression in Acute 1.5 W Group

90 minutes after HPM exposure resulted in increases HSP-90 expression in all studies anatomical rat brain areas respect control, except PV of hypothalamus, where expression was similar to controls-rats. This expression still remained high after 24 hours microwave exposure in the same areas except in LH where the expression was similar to controls (see Table 3). HSP-90 expression was similar in hippocampus and cortex after 24 hours than after 90 minutes post radiation. Several studies have been observed that heat shock stress produced upregulation throughout the brain (Tynell M, 1993; Goldbaum O. & Ritchter-Landsberg, 2001), however, heat shock response depends on different factors, such as stress stimulus, and little is known about HSP-90 response to microwave at 2.45 GHz in the brain of rats, thereby we cannot compare our results.

3.2 HSP-90 Expression in Acute 3.0 W Group

HSP-90 expression in 90´postradiation group was greater than control-rats in subregions of hypothalamus (Pa and Arc) and hippocampus (CA1, CA2, CA3). The PV and LH expression were decrease and there were not different with controls in GD and cortex. After 24 hours, hsp-90 expression increase in more areas (nucleus arcuatus, hippocampus, and cortex), however, there were not significant changes in PV, Pa and LH (see Table 3).

Tabla 3. Expression of HSP-90 following exposure acute power (1.5 and 3 W) microwave radiations compared with control groups.

Anatomical Areas	1.5 W		3.0 W	
	Post–irradiation time		Post–irradiation time	
	90 m	24 h	90 m	24h
Hypothalamus				
PV	—	—/↑	↓	—
Pa	↑	↑	↑	—
LH	↑	—	↓	—
Arc	↑	↑	↑	↑
Hippocampus				
DG	↑↑	↑↑	—	↑
CA1	↑↑	↑↑	↑	↑
CA2	↑↑	↑↑	↑	↑
CA3	↑↑	↑↑	↑	↑
Cortex				
Fr	↑↑	↑↑	—	↑↑
Parl	↑↑	↑↑	—	↑↑
Pir	↑↑	↑↑	—	↑↑
Ent	↑↑	↑↑	—	↑↑

PV, periventricular nucleus; Pa, paraventricular hypothalamic nucleus; LH, lateral hypothalamus; Arc, arcuate nucleus; DG, dentate gyrus; Fr, frontal cortex; Par1, parietal cortex; Pir, piriform cortex; Ent, entorhinal cortex.

We observed than brain areas exposed to 3.0 W power microwave radiation are as much stimulated as brain areas exposed to 1.5 W; and HSP-90 expression at 3 W even was decreased with respect to 1.5 W acute group in some areas, such as hypothalamus and cortex.

3.3 HSP-90 Expression in Chronic Group

We observed that HSP-90 expression decreased in DG of hippocampus, hypothalamus (PV, Pa and LH) and piriform and entorhinal cortex (see Table 4). There were not differences in Arc, CA1, CA2, CA3 and frontal and parietal cortex.

Table 4. Expression of HSP-90 following repeated acute exposure to high-power microwave radiations (3 W, during 10 days) compare with controls.

Anatomical Areas	
Hypothalamus	
PV	↓↓
Pa	↓
LH	↓↓
Arc	–
Hippocampus	
DG	↓
CA1	–
CA2	–
CA3	–
Cortex	
Fr	–
Parl	–
Pir	↓
Ent	↓

PV, periventricular nucleus; Pa, paraventricular hypothalamic nucleus; LH, lateral hypothalamus; Arc, arcuate nucleus; DG, dentate gyrus; Fr, frontal cortex; Par1, parietal cortex; Pir, piriform cortex; Ent, entorhinal cortex.

We noted that the less stimulated area in all the groups corresponds to hypothalamus, and even in chronic group the expression in this area spreads to diminish. Loones and cols. (2000) have shown that HSP90 is most abundant in hypothalamus, preoptic areas, pons and medulla in the central nervous system of unstressed mouse.
Both the SAR values and the morphological thermal–SAR results will be presented on the poster, at the Symposium.

4. Conclusions

Acute high power (1.5 and 3.0 Watts) 2.45 GHz microwave radiation produces an upregulation heat shock response in subregions of central nervous system. Moreover, we observe that HSP–90 expression decrease when the delivered power increases in animals that are subject to acute exposure. Nevertheless, the repeated acute exposure causes decrease of the HSP–90 expression in hypothalamus and limbic areas, whereas keeps unchanged (compared to control groups) in several cortex and hyppocampal areas.

5. References

Ahmed R. G. *Heat stress induced histopathology and pathophysiology of the central nervous system.* Int. J. Devl. Neuroscience 23 (2005) 549-557.

Amin V, Cumming D , Coffin R, Latchman D. The degree of protection provided to neuronal cells by a pre-conditioning stress correlates with the amount of heat shock protein 70 it induces and not with the similarity of the subsequent stress. Neuroscience Letters 200 (1995) 85-88.

D´Souza S. M., Brown I. R. *Constitutive expression of heat shock proteins Hsp90, Hsc70 and Hsp60 in neural and non-neural tissues of the rat during postnatal development.* Cell stress and Chaperones (1998) 3 (3), 188-199.

Diem E., Schwarz C., Adlkofer F., Jahn O., Rüdiger H. Non-thermal DNA breakage bu mobile-phone radiation (1800 MHz) in human fibroblast and in transformed GFSH-R17 rat granulosa cells in vitro. Mutation Research 583 (2005) 178-183.

Gass P. , Schröder H. , Prior P., Kiessling M. Constitutive expression of heat shock protein 90 (HSP90) in neurons of the rat brain. Neuroscience Letters 182 (1994) 188-192.

Goldbaum O. and Richter-Landsberg. Stress proteins in oligodendrocytes: differential effects of heat shock and oxidative stress. Journal of Neurochemistry, 2001, 78, 1233-1242.

Jeon GS, Park SW, Kim DW, Seo JH, Cho J, Lim SY, Kim SD and Cho SS. Glial expression of the 90-kDa heat shock protein (HSP90) and the 94-kDa glucose-regulated protein (GRP94) following an excitotoxic lesion in the mouse hippocampus. Glia 48:250-258 (2004).

Latchman D. *Protective effect of heat shock proteins in the nervous system.* Current Neurovascular Research, 2004, 1, 21-27.

Loones MT, Chang Y, Morange M. The distribution of heat shock proteins in the nervous system of the unstressed mouse embryo suggest a role in neuronal and non-neuronal differenciation. Cell Stress & Chaperones (2000) 5 (4), 291-305.

Paxinos G., Watson C., The rat brain in steretaxic coordinates. 2nd ed. Sydney: Academic Press; 1986.
Picard D. *Heat-shock protein 90, a chaperone for folding and regulation*. CMLS Cellular and Molecular Life Science. 59 (2002) 1640-1648.

Pomerai D. Smith B. Dawe A., North K., Smith T., Archer D., Duce I. R., Jones D. and Candido P. M. Microwave radiation can alter protein conformation without bulk heating. FEBS Letter 543 (2003) 93-97.

Sebastian Franco JL, Muñoz San-Martín S, Sancho Ruíz M and Miranda Pantoja, JM. Medición de radiación en seres vivos. Investigación y Ciencia, Febrero, 2006, 46-55.

Tynell M., Barbe m. F. and Brown I. R. Stress (heat shock) protein accumulation in the central nervous system. Its relationship to cell stress and damage. Advances in Neurology. Vol 59

ANALYSIS OF MICROWAVE EXPOSURE TO A METEOROLOGICAL RADAR

C. MALACARNE, R. PONTALTI, A. VACCARI, L. CRISTOFORETTI

ITC-IRST - CENTRO PER LA RICERCA SCIENTIFICA E TECNOLOGICA

VIA SOMMARIVE, 18 - 38050 POVO, TRENTO – ITALY

Abstract

Exposure evaluation to radiofrequency and microwave non-ionizing radiation of both general public and workers is considered an emerging sector in environmental and safety work surveys. Nevertheless, radars are typically rarely analyzed, due to difficulties in measuring such kind of source, but also inaccessibility or even secrecy of some installations.

Aim of this study was to analyze the emissions of a meteorological doppler radar, placed in the Province of Trento (North Italy), working in C band, with a wavelength of about 5 cm and nominal peak power of 250 kW.

The survey involved: i) electric field monitoring around the radar, to assess the general public and operators exposure, and ii) test measurements on radar functioning, such as evaluation of the antenna's radiation pattern.

In the first case measurements were performed with electric field probe and spectrum analyzer, while in the second case only with spectrum analyzer in far field conditions. The signal was characterized both in frequency domain, to analyze operating frequency and frequency stability, and time domain, to acquire radiation patterns in the principal planes as well as pulse duration and duty cycle.

The obtained results are compared to standard limits, with particular reference to the EU Directive 2004/40/CE.

Introduction

Starting from the 1980s radar networks have become extensively used in meteorology for determining the location of rain and storm activity. The radar under analysis is one of the North–Italian network and consists of a DSWR-2500C (EEC) pulsed-doppler radar, which means that it is not only capable of detecting target's location (bearing, range, and altitude), but also measuring its velocity. In particular, velocity is determined by transmitting many radar pulses towards each target (hydrometeor in this specific case) over a very short period of time, and thus measuring relative target movement between each pulse. The frequency in which the pulses are emitted are usually referred to as Pulse Repetition Frequency (PRF). The radar operates at 5.8 GHz (C–band), with a wavelength of 5.5 cm; its nominal peak power is 250 kW, thus guaranteeing a coverage range of about 120 km.

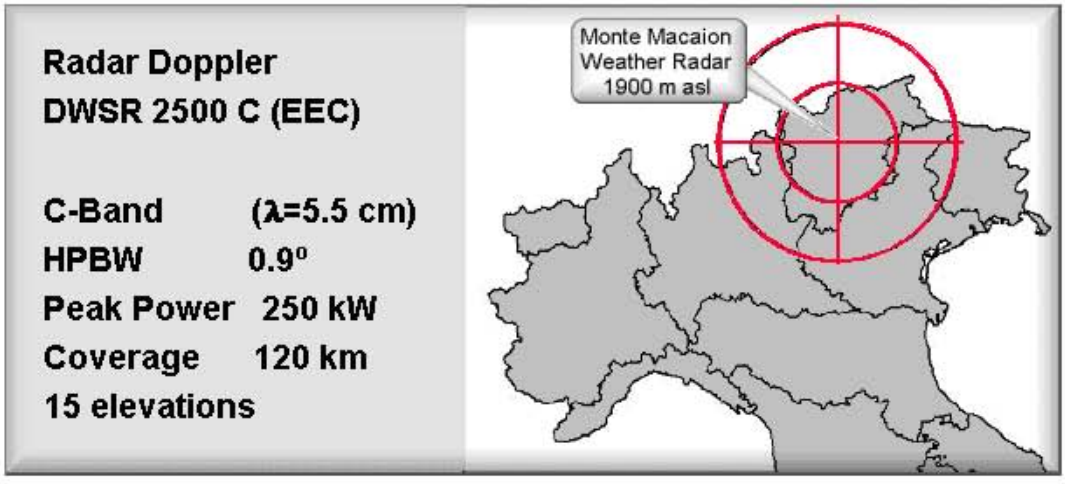


Figure 1: Location and main technical specifications of the weather radar system under analysis (Northern Italy).

The weather radar systems are generally designed and located to ensure that power densities that humans could be exposed to, fulfil the exposure limits. In order to assess this, measurements have to be carried out when the system is installed and operating in fully functioning conditions.
In particular, the two principal aspects investigated in this work were:

- the electric field values monitoring in the proximity of the radar (in near field conditions), in order to assess the exposure of both population and maintenance workers. Besides the radar personnel, exposed people could be only hikers, considering that in the area neither residential buildings nor commercial concerns are present.
- the measurement of the antenna's radiation pattern, being this latter crucial to predict the far field exposure. It is worth noting that the radar is located at a high altitude (1900 m a.s.l.), which permits a good extension of its horizons, otherwise limited by the mountainous orography. Therefore, the closest built-up areas are out of the radar's optical visibility, whilst those areas satisfying this condition are several kilometres far form the source, and at a significantly lower altitude.

In the first case, both the broadband electric field sensor and the spectrum analyser were used in proximity of the radar. Conversely, in the second case measurements were performed on a mountain 15 km south of the radar's location, since this ensured at the same time the fulfilling of the far field conditions (at a distance from the emitter larger than 700 meters), the good optical visibility, as well as a higher altitude (necessary for the characterisation of the antenna's lobe along the vertical direction). In this case only the spectrum analyser with the suitable antenna was used.
Afterwards, the results of the radioprotectional survey were compared to the limits provided by the EU Directive 2004/40/CE on workers' exposure to electromagnetic fields [1], to the thresholds reported by the ICNIRP [2] referred both to general public and workers, and also with the limits imposed by the national Italian law concerning general public exposure [3].

Site Description

The site housing the radar system lies on the top of a mountain (Monte Macaion, 1865.5 m a.s.l.; longitude WGS84: 11º12'32.6", latitude WGS84: 46º29'35.7"), characterised by a ridge gently descending towards west and by a rocky vertical front in east direction. The radar is mounted on a metallic tower 10 m high, with, at its bottom, two shelters housing the electronic equipment connected to the antenna. The radiating system consists of a 4.27 m diameter paraboloid antenna installed on a motorised pedestal, which enables orientations along whatever azimuth angles and elevations from -2º and 90º. Moreover, the antenna is covered by a 6.25 m diameter glass–reinforced plastic radome (Figure 2).

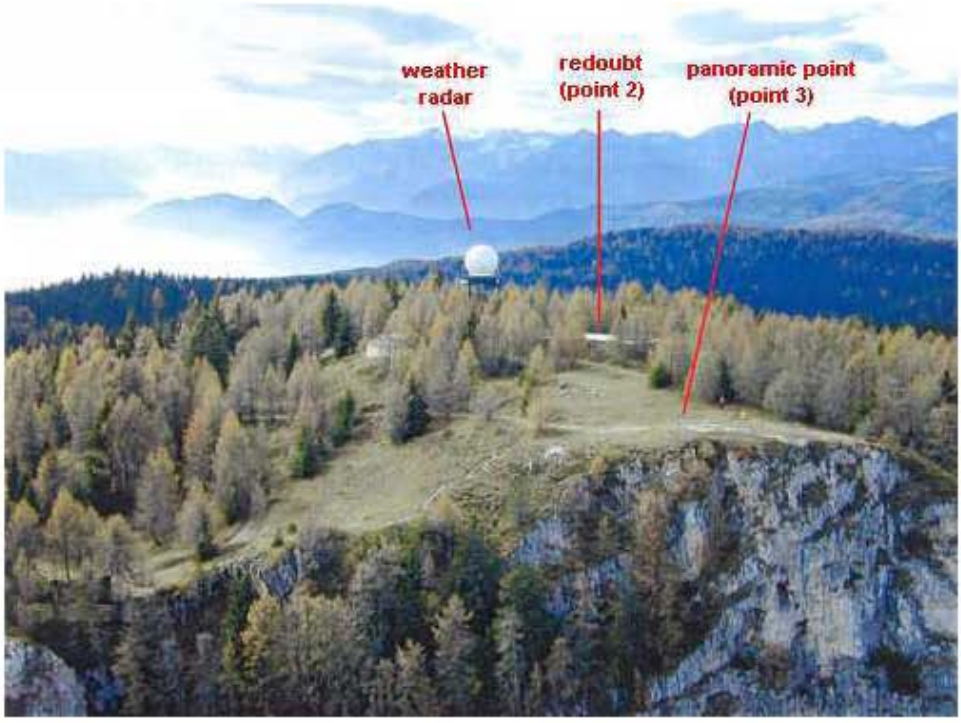


Figure 2: The Monte Macaion summit, housing the weather radar. Measurement points 2 and 3 are also indicated.

In east direction with respect to the radar's tower there are some ruins and a redoubt, whose roof represented the highest measurement point of the area. Proceeding a few tens of meters in north-east direction, the terrain is

gently descending and without trees, forming a panoramic site rather frequented by hikers, especially during the summertime. About 350 m in 160º north direction there is another hill, at the same level of Monte Macaion, housing several broadcast antennas which contribute to the overall RF exposure level in this area.

Measurement points, instruments and technique

The measurement points for radioprotectional purposes were chosen at ground level and providing that optical visibility of the source was satisfied. In the absence of such a condition–even when the sight was obstructed only by leafy branch–a so considerable attenuation of the field was indeed registered, that exposure levels became insignificant from a radioprotectional point of view. The reason of such behaviour could be easily found in the highly absorptive character of high water content media in the microwaves frequency range.
Four different measurement points were chosen:

1. The radar equipment room, where personnel stands occasionally. The measurements were carried out with the radar in operating conditions, in order to assess possible dispersions from the cases containing the generation apparatuses.
2. The roof of the redoubt visible in Figure 2, as it is an interesting and comfortable place to stay for hikers, which also corresponds to the closest approaching point to the emission beam of the paraboloid antenna. During the measurements the most conservative conditions for the exposure were reproduced, by choosing an elevation of -2º and keeping an azimuth angle fixed along the receiving antenna direction. It is worth mentioning that such angle choices are not likely in normal operating conditions. In particular, the chosen elevation value produces images highly disturbed by orography and the fix azimuth angle is meaningless for meteorological purposes, even though manually selectable. In correspondence of this point the difference in height between the electric centres of the antennas (receiving antenna and radar) was 7 m, their distance was 30 m in 30º north direction, and the radar observation angle was +10º.
3. The panoramic site (see Figure 2) in north-east direction from the radar. In this case the difference in height between the electric centres of the antennas was 13 m, their distance was about 80 m in 40º north direction, and the radar observation angle was +9º.
4. The summit of the mountain Monte Roen, 14.9 km far from the radar. Its altitude is 2065.5 m a.s.l., that is 200 m higher than the Monte Macaion; its longitude WGS84 is 11º11’12.6”, its latitude WGS84 46º21’41.8”. The receiving antenna was placed 3 m above the ground, thus resulting in a difference in height of about 195 m between the electric centres of the antennas. The radar could see this point setting a theoretical azimuth value of 185.1º north with an elevation equals to +0.75º.

The measurements were performed by using:

- a spectrum analyser Agilent Technologies ESA–E4407B, which operates in the frequency range 100 Hz–26 GHz;
- a doubled ridge horn antenna EMCO 3115, linearly polarised and operating in the frequency range 1–18 GHz;
- a power density sensor General Microwave RAHAM (RAdiation HAzard Meter), Model 495. It features a six minute power density averaging function which automatically computes and displays the average exposure measurement over the six minute period as required by safety standards;
- an isotropic E-field probe General Microwave Model 94, operating in the frequency range 200 kHz–40 GHz and characterised by a wide dynamic range of 46 dB (from 0.005 to 200 W/m^2, or correspondingly from 1.37 to 274 V/m).

Being the radar signal composed by a succession of pulses, each of which lasts about 1/1000 of the time occurring between one pulse and the successive, the linearity of the response of the broadband sensors was initially checked. This was performed at the ITC-irst laboratory, before any measurement on site. The instruments used in this case were:

- a pulse generator (Philips PM5705) 0.1 Hz–10 MHz;
- a voltage variable attenuator (Mini Circuits ZFAS–15);
- a synthesised RF generator (HP8660C) from 10 kHz to 2600 MHz;
- a high power RF amplifier (PST–BHE, 500W);
- a biconical antenna (EMCO 3109);

In particular, the attenuator received the signal from the two generators (RF and pulse), mixing them into a new “composed” signal which was then amplified and used to feed the biconical antenna, placed in an anechoic chamber (Siemens–Matsushita). In this way, in the proximity of the antenna, pulses with E–field peak values of hundreds of V/m and a duty cycle typical of the radar (1/1000) were obtained. In these conditions, the satisfactory linearity of the sensor RAHAM 495 with its probe 94 was verified, at least up to values of about 10 V/m, corresponding to E peak values of 320 V/m. This led to the conclusion that, in the aforesaid E field range, the displayed value actually corresponded to the time-averaged field and the sensor was hence suitable for on-site radar signal measurements.

The electric field measurements for radioprotectional purposes were generally performed by the only use of the broadband sensor, with the exception of point 2, which was analysed also in narrow band with spectrum analyser and horn antenna. In correspondence of point 4 (far field) the only narrow band characterisation was instead performed.
While operating with the broadband sensor, it was placed at the three different heights (1.1, 1.5 and 1.9 m above the ground) prescribed by the Italian CEI 211-7 guide [4]. Considering the fact that the radar was remotely controlled, pointing the antenna towards the measurement point and keeping constant the signal emission conditions, the results obtained with the two operational modes 'Normal' (for direct reading of power density) and 'Average' (for computing the average power density over a six minute period) were equivalent. In fact, this assumption neglected the possible magnetron power fluctuations, but these were found to be insignificant with respect to those characteristic of the measurement point itself, such as the unpredictable signal scattering due to the foliage waving in the breeze. Consequently, the 'Normal' mode was used, which refreshed the power density values every 1.5 s.
The measurements with spectrum analyser were carried out in time domain (zero span), in peak detection mode and selecting a resolution bandwidth of 5 MHz, in order to filter as little as possible the impulsive nature of the signal. Furthermore, the chosen sweep time (20 μs) was the shortest selectable for the acquired points number. The signal was acquired in max-hold mode, which provides the envelope of all the maxima observed during the acquisition time, so that the snapshot of each pulse was frozen on the display as soon as it appeared in the measurement time window.
The horn antenna was placed with its electric centre at 1.5 m above the ground, in conformity with the CEI 211-7 guide [4] prescriptions. The polarisation of the antenna was horizontal, like that of the radar. During the measurements, the neglectability of the vertical component of the signal was also assessed: while in optical visibility of the radar, it always remained 15–20 dB lower than the horizontal.
Finally, the measurements performed in correspondence of point 4 (Monte Roen, 14.9 km far from the radar) were carried out with the only use of the spectrum analyser, following the same set-up just described, with some variations/additions. In particular:

- the horn antenna was placed at the highest possible height (3 m) on the roof of an off-road vehicle, in order to minimise the contribution of signals scattered from the ground;
- measurements were carried out also in the frequency domain, setting a 10 MHz span, in order to characterise the magnetron frequency as well as the pulse duration;
- some measurements were devoted to the assessment of the PRF (Pulse Repetition Frequency), by using the same settings described before (zero span), but with longer sweep times (up to 10 ms);
- the radiation pattern measurements were performed with the same settings, but making use of much longer sweep times (up to 100 s), in order to cover the complete azimuth revolution time. Consequently, the number of acquired points per sweep was much higher than before (up to 3600 points), in order to obtain a good angular resolution;
- the radiation pattern in the vertical plane was determined in a similar way. In this case, the radar azimuth angle was set as that maximising the radiation in correspondence of the measurement point; afterwards, the radar was made scan vertically, covering an overall amplitude of 27º (from -1º to +26º).

Results

It is well known that regulations in general define different limit for general public and occupational exposure. Moreover, some of them refer explicitly to only one of these categories: either the general public (like for example the Italian law DPCM 8 July 2003 [3]) or the workers (like for example the European Directive 2004/40/EC [1]). Regarding the general population, both the Italian law and the ICNIRP [2] limits were taken into account in the present work. In the first case, the E-field limit imposed in the frequency range under analysis is 40 V/m, expressed as rms value, which must not be exceeded in any case. The same law, as a cautionary measure to protect against any possible long-term effects, adopts a more conservative 'attention value' of 6 V/m in correspondence of children's playgrounds, residential dwellings, school premises and in general in those areas where people could stay for 4 hours or more per day, as well as in outdoor annexes that may be used as residential environments, such as balconies, terraces, courtyards, but excluding roof pavings. Therefore, this second limit was suitable only for residential buildings, far from the radar source. Both these values must be averaged over any six-minute period in an area equivalent to the vertical cross-section of the human body
Yet while the Italian Law does not discriminate between pulsed and not-pulsed sources, the ICNIRP guide establishes a peak value limit for the pulse, which must not exceed–in the considered spectrum range–1000 times its average value in terms of density power (S). Another aspect, which is taken into account in the ICNIRP guide while is lacking in Italian regulation, concerns the safeguard from annoying auditory effects, possibly caused by a thermoelastic interaction in the auditory cortex of the brain [5, 6, 7]. In order to avoid the onset of such kind of effect, the ICNIRP guide fixes a limit on the Specific Absorption (SA–energy per mass unit), which is however impossible to assess directly, being it related to quantities internal to the body. In addition, the guide indicates a

threshold for perception of about 100–400 mJ m^{-2} for pulses of duration less than 30 μs at 2.45 GHz (corresponding to an SA of 4–16 mJ kg^{-1}). However, other publications identify more conservative values: a threshold of 20 mJ m^{-2}, always for pulses of duration less than 30 μs, is stated in [8], while in [9] RF hearing has been reported also for energy density per pulse values lower than 90 mJ m^{-2} for pulse widths from 3 to 5000 μs. Furthermore, the Australian Radiation Protection and Nuclear Safety Agency in its Standard [10] establishes, on the basis of the considerations exposed in [11], a limit for the spatial peak SA of 2 mJ kg^{-1} (for general public) and 10 mJ kg^{-1} (for workers) in the head within any 50 μs interval.
On the other side, regarding the occupational exposure, there is not a specific Italian regulation, so that the normative reference has been the European Directive 2004/40/EC, which assumes in its turn the same limits established by the ICNIRP guideline for the workers.
Summing it up, the limits taken into account in this work were:

- Electric field: 40 V/m (averaged) for the general public–DPCM 8 July 2003;
  1952 V/m (61 V/m × 32), as peak value, for the general public–ICNIRP;
  137 V/m (averaged), for the workers–ICNIRP and 2004/40/EC;
  4384 V/m (137 V/m × 32), as peak value, for the workers–ICNIRP and 2004/40/EC
- Energy density per pulse: 20 mJ m^{-2}

Finally, the compliance with the 'attention value' of 6 V/m of the DPCM 8 July 2003 were also verified, in correspondence of the residential places at far distance from the radar but in optical visibility of it. Considering the minimum elevation of the radar (equals to -2º), at least 10 km are necessary to the radar beam for reaching the altitude of the closest villages (1500 m a.s.l).

In evaluating the electric field values, conservative hypotheses were applied, in order to eventually overestimate the field. Similarly, during the measurements, conservative parameters were adopted. For instance, it is customary to estimate the electric field in the antenna boresight (which extends up to $0.2\ D^2/\lambda = 70$ m) with its time-averaged value, without taking count of its angular-averaged value due to its rotation. Assuming this, it is:

$$E = \sqrt{\frac{Z_0\ P\ dc}{\pi\ D^2/4}} = 78.6\ \text{V/m}$$

where Z_0 (377 Ω) is the free space characteristic impedance, *dc* is the duty cycle (conservatively chosen as 0.00094), D is the paraboloid diameter (4.27 m) and P is the nominal peak power (250 kW). This averaged E-field intensity corresponds to a peak value of 2563 V/m. The energy density per pulse values are equal to 6.9, 13.9 and 34.8 mJ/m^2 for the three considered kinds of pulses, corresponding to the 'velocity' mode the first two and to the 'intensity' mode the last one.
From these results it follows that in the antenna boresight (cylinder which base corresponds to the paraboloid aperture and with an height of 70 m) a worker could occasionally stay in safety conditions according to the Directive 2004/40/EC and the ICNIRP, but with a possible auditory effect (perceived as a noise at 250 Hz) in the 'intensity' mode. Furthermore, no site in the antenna boresight is accessible to the general public, whilst the only site accessible to the workers is the platform (with parapet) surrounding the antenna radome.
Considering the first kilometre from the radar, only the broadcast towers in south direction could be interested by considerable exposure levels. However, owing to the minimum elevation value of -2º, the radar beam could only approach them from above, so that only maintenance workers who should climb them could be exposed to the radar primary radiation lobe. In this condition, neglecting again the radar rotation (thus representing the conservative but unlikely condition of fixed azimuth at 160ºN and elevation of -2º), the electric field can be estimated as:

$$E = \frac{\sqrt{30\ P\ dc\ G_n}}{d} = 41.5\ \text{V/m}$$

where $30 = 377/(4\pi)$, G_n represents the numeric antenna gain that is about 30000, d is the distance (radar–broadcast towers) equals to 350 m. Should the angular average be taken into account, this would introduce a further multiplying factor of $360^{-1/2} = 0.053$, which would make decrease the obtained value to about 2.2 V/m.
Therefore, even maintenance personnel potentially working on the towers facing the radar would operate in safety conditions accordingly to ICNIRP and EU Directive.
While these exposure points were characterised only from a theoretical point of view, those accessible to general public, as well as the equipment room (as described in the third paragraph), were instead actually measured. In particular, Table 1 refers to the results obtained in correspondence of point 2, where measurements were carried out both in broad- and narrow-band. Taking into account the different measurement techniques (in the first case three values at different heights were acquired, each of which represented the 6-minute average value; in the

second case one only intermediate height was considered and the acquisition was detected in peak mode), the difference between the two obtained values (1.2 dB) is widely justified.

POINT 2 (broadband)

Height 110 cm: E = 8.68 V/m

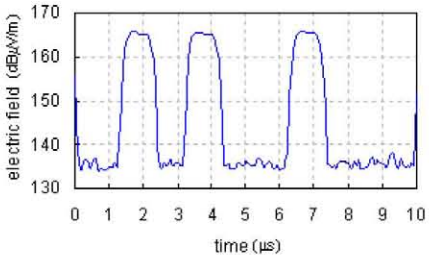
Height 150 cm: E = 5.12 V/m

Height 190 cm: E = 5.82 V/m

Spatial average:

$$E = \frac{8.68^2 + 5.12^2 + 5.82^2}{3} = 6.72\ \text{V/m}$$

POINT 2 (narrow band)



Height 150 cm:
E (peak value) = 165.65 dBμV/m

Mean value with duty cycle:

$$E = 10^{-6} \cdot 10^{\frac{165.65}{20}} \quad 9.4 \times 10^{-4} = 5.87\ \text{V/m}$$

Table 1: Electric field measurements in correspondence of point 2 (redoubt's roof). On the left the results obtained averaging the values acquired for the three heights, by using the broadband RAHAM sensor, are presented, while on the right, those obtained with the spectrum analyser. The picture in the middle displays the acquired spectrum: the three different peaks are due to the max-hold operating mode, and refer to different repetitions of the radar signal.

In correspondence of the remaining measurement points, the sensitivity limit (0.5 μW/cm^2) of the sensor was never reached, which means that the electric field kept lower than 1.37 V/m

The other set of measurements performed were devoted to the characterisation of the radar antenna radiation pattern in far field conditions. The horizontal plane pattern (alongside the azimuth angle) was acquired by making the antenna rotate with an angular velocity of 5º/s and by setting the spectrum analyser in zero span mode with a sweep time suitable to cover a complete turn. Figure 3 shows the part of the diagram concerning the angular range from -40º to +40º from the radiation maximum, acquired at 1.1º of elevation. In the remaining part of the diagram, the electric field level kept about 40 dB under the maximum and did not rise in correspondence of either the back lobe or possible spillovers.

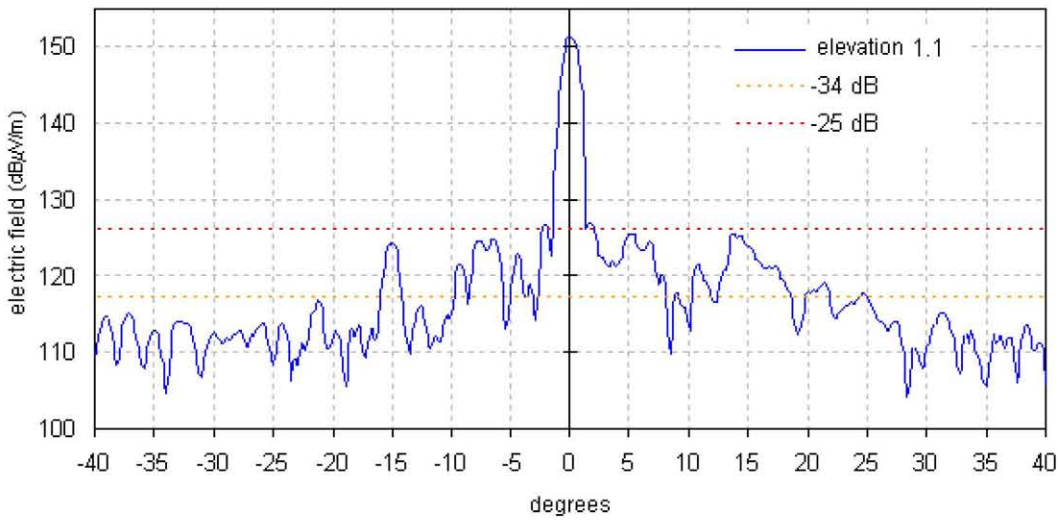


Figure 3: Electric field diagram by varying azimuth angle (horizontal plane), centred in the main lobe.

Finally, further measurements were carried out to better characterise the main lobe, in particular determining its amplitude in both the azimuth and elevation directions. The knowledge of these quantities (θ e φ, expressed in radiant and calculated at -3 dB from the maximum) enables to determine the antenna gain (Gn), on the basis of the formula:

$$Gn = \pi^2/(\theta\varphi)$$

which assumes a gaussian profile of the main lobe. The data acquired for different elevation values are shown in Figure 4 together with the parabola, which represents the fit using a quadratic regression. Being the ordinate axis in logarithmic scale, the curve would correspond to a gaussian trend in linear scale, thus confirming the suitability of the previous formula in determining the antenna gain.
The θ e φ angles obtained from the diagrams are 0.93º (azimuth) and 1.14º (elevation), thus giving a Gn=44.85 dB. This value is very close to that provided by the manufacturer: 45 dB.

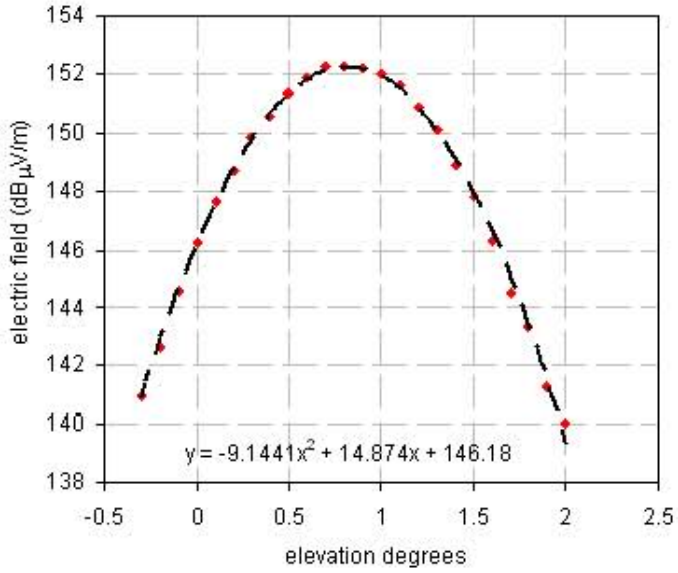


Figure 4:
Characterisation of the main lobe by varying the elevation (vertical plane). Points represent the acquired data, while the parabola is the fit obtained by using a quadratic regression.

Furthermore, the peak amplitude is verifiable by means of the following analytical formula, valid in far field condition:

$$E\,[\mathrm{dB\mu V/m}] = 120 + 20\log_{10}\frac{30\,P\,G_n}{d} = 150.28\ \mathrm{dB\mu V/m}$$

where P is the nominal peak power ($2.5\ 10^5$ W), G_n is the numerical gain of the antenna and d is the distance ($1.49\ 10^4$ m). The comparison between this result and the actually measured value (with spectrum analyser, in peak mode detection) shows a discrepancy of 2 dB, with measured values exceeding those estimated. However, some considerations have to be taken into account:

- the directivity of the radar antenna is so high that, even at a long distance, the electric field peak values are important. For instance, at 15 km distance E=30 V/m, which however corresponds to 1 V/m provided it is time-averaged;
- also in this case the radar beam was intentionally pointing the measuring point, without rotating. In realistic operating conditions, the radar is continuously rotating, so that further reduction factors representing its movement both in the horizontal and vertical planes should be added.

As a consequence, it is possible to confirm that, even in correspondence of the residential places satisfying the optical visibility requirement and considering direct pointing of the radar beam over them, also the 'attention value' (6 V/m) of the Italian law would be fulfilled.

Conclusions

Regarding both the measurements and the theoretical estimation of electric field for radioprotectional purposes, all sites taken into consideration in the present work met the requirements of the Italian law DPCM 8 July 2003 (only concerning the general public), even considering the unlikely and highly conservative operating conditions of the radar, directly and constantly pointing to the measurement point. Moreover, no significant RF dispersion was found inside the equipment room. Also the exposure conditions of the maintenance personnel who could

access on broadcast towers facing the radar were assessed–through theoretical estimations–to comply the safety standards for the workers (ICNIRP and Directive 2004/40/CE), even in case of direct pointing of the radar beam towards their direction. The peak exposure thresholds of the ICNIRP and Directive 2004/40/CE are fulfilled as well, as the multiplying factor to introduce for the continuous exposure corresponds to the inverse of the radar duty cycle. Even the possible access on the platform surrounding the radar radome would comply the occupational limits. The only effect which could be observed in such condition (within the antenna boresight), as reported in literature [8, 9], is the onset of annoying auditory effects, as long as the 'intensity' pulse mode had been used. The antenna boresight is reachable by workers in this only situation, while it is never accessible to the general public.

References

[1] Directive 2004/40/EC of the European Parliament and of the Council on the minimum health and safety requirements regarding the exposure of workers to the risks arising from physical agents (electromagnetic fields) (18th individual Directive within the meaning of Article 16(1) of Directive 89/391/EEC), 29 April 2004.

[2] International Commission on Non Ionizing Radiation Protection (ICNIRP), "Guidelines for Limiting Exposure to Time-varying Electric, Magnetic, and Electromagnetic Fields (up to 300 GHz)". Health Physics 74: 494-522, 1998.

[3] DPCM 8 luglio 2003, "Fissazione dei limiti di esposizione, dei valori di attenzione e degli obiettivi di qualità per la protezione della popolazione dalle esposizioni a campi elettrici, magnetici ed elettromagnetici generati a frequenze comprese tra 100 kHz e 300 GHz", GU n. 199 del 28 agosto 2003.

[4] CEI 211-7, Fascicolo 5909: "Guida per la misura e per la valutazione dei campi elettromagnetici nell'intervallo di frequenza 10 kHz – 300 GHz, con riferimento all'esposizione umana", 2001.
CEI (Comitato Elettrotecnico Italiano) is the Italian Electrotechnical Committee. CEI is member of CENELEC, and CEI Standards are often endorsement of CENELEC Standards, designated by the same number.

[5] JC Lin. "Hearing microwaves: The microwave auditory phenomenon." IEEE Antennas Propagation Mag 43:166–168, 2001.

[6] J.A. Elder and C.K. Chou. "Auditory Responses to Pulsed Radiofrequency Energy", Bioelectromagnetics Suppl 6: S162-73, 2003.

[7] Louis N. Heynick, Peter Polson, "Human Exposure to Radiofrequency Radiation: a Comprehensive Review of the Literature Pertinent to Air Force Operations", United States Air Force Research Laboratory Technical Report AL/OE-TR-1996-0035, Brooks Air Force Base, Texas USA, 1996.

[8] Martin Röösli, Regula Rapp and Ursula Ackermann-Liebrich, "Hochfrequente Strahlung und Gesundheit", Bundesamt für Umwelt, Wald and Landshaft (BUWAL), 2003.

[9] Röschmann P. "Human auditory system response to pulsed radiofrequency energy in RF coils for magnetic resonance at 2.4 to 179 MHz." Magn Reson Med 21:197–215, 1991.

[10] Australian Radiation Protection and Nuclear Safety Agency, "Radiation Protection Standard for Maximum exposure levels to radiofrequency fields - 3kHz to 300GHz", Radiation Protection Series No. 3, 8 May 2003.

[11] Australian Radiation Protection and Nuclear Safety Agency, "Human auditory perception resulting from exposure to high power pulsed or modulated microwave radiation–specification of appropriate safety limits", 10 December 2004 (http://www.arpansa.gov.au/aud_perc.htm)

EXTREMELY LOW FREQUENCY ELECTROMAGNETIC FIELDS AND OXIDATIVE STRESS IN EXCITABLE CELL LINES

MARIA A. MARIGGIÒ[▲●], FERNANDA AMICARELLI[*], MARIA R. GROSSI[*], STEFANO FALONE[*], CATERINA MORABITO[▲●], ENZO TETTAMANTI[■], GIORGIO FANÒ[▲●], FRANCO CUCCURULLO[▲], CARMINE DI ILIO[▲]

LAB. FISIOLOGIA -[•]ISTITUTO INTERUNIVERSITARIO DI MIOLOGIA (IIM), [▲]CENTRO DI STUDI DELL'INVECCHIAMENTO (CESI) – UNIVERSITÀ "G.D'ANNUNZIO" CHIETI-PESCARA ", VIA COLLE DELL'ARA, I-66013 CHIETI)
***LAB DI BIOLOGIA APPLICATA, DIP. BIOLOGIA DI BASE ED APPLICATA, UNIVERSITÀ DEGLI STUDI DELL'AQUILA VIA VETOIO, COPPITO, I-67100 L'AQUILA**
[■]*DIP. DI SCIENZE BIOMEDICHE COMPARATE – FACOLTÀ DI MEDICINA VETERINARIA - UNIVERSITÀ DI TERAMO*

Corresponding Author: Prof. Maria A. Mariggiò Lab Fisiologia, Centro di Studi dell'Invecchiamento – Università "G.d'Annunzio"-Chieti-Pescara
via Colle dell'Ara
Chieti 66013, Italy
Tel +39 0871 3554048 Fax +39 0871 3554043
e-mail: mariggio@unich.it

M.A. MARIGGIÒ, F. AMICARELLI, M.R. GROSSI, S. FALONE, C. MORABITO, E. TETTAMANTI, G. FANÒ, F. CUCCURULLO, C. DI ILIO

Abstract
Recently, epidemiological studies and researches have proposed a relation between exposure to electromagnetic fields (extremely low frequency, ELF) and the development of several neurodegenerative diseases (WHO and NRPT progress reports 12-4-2004). This has stimulated scientific interest to verify ELF effects on different life forms (Repacholi MH, 2003).
We have analysed the effects of ELF on neuron-like cell lines (PC12 and SH-SY5Y), glioblastoma GL15 as glial model and C2C12 myocytes as muscle model, focusing our attention on the cellular oxidative stress machinery.
We exposed cell cultures to 50Hz ELF (0-1mT) generated by a solenoid or Helmholtz coils adapted to a confocal microscope, and investigated cell proliferation, ROS production, mitochondrial membrane potential, antioxidant enzymatic activities (SOD, Catalase, GSH-Px, etc).
The growth curves of tested cells did not show any differences between ELF-treated cells towards controls. The presence of ELF influenced ROS production in dependence of cell phenotype and of field intensity. Also mitochondrial potential as well as antioxidant enzymatic activities were altered by ELF.
These results show that ELF modified oxidative stress status in excitable cells. These were able, in different way depending on their biological activity, to counteract ELF effects and to adapt themselves without altering their proliferation rate.

Introduction
In 1996, the World Health Organization (WHO) decided to start a world program named "International Electromagnetic Fields (EMF) Project" regarding potential dangerous health effects of the exposure to electric and magnetic fields at extremely low frequencies (ELF-EMF). Such exposures arise mainly from the transmission and use of electrical energy at power frequencies of 50/60 Hz. The International EMF Project is scheduled to complete its health risk assessments of EMF in 2007, since it is likely that current and proposed research should provide sufficient results within this time frame to allow more definitive health risk assessments.
While the enormous benefits of using electricity in every day life and health care are unquestioned, the presence of possible inappropriate effects, or health consequence, needs to be clearly identified. The results of research currently available are often contradictory and this adds to people confusion and lack of confidence that supportable conclusions about safety can be reached.
The biological effects in cell lines derived from different modalities of ELF-EMF exposures have been frequently noted but the basic interaction mechanism(s) between such fields and living matter is unknown (Kavet et al., 2001; Foster KR, 2003). Even if some hypotheses have been suggested, none of these is adequately supported by experimental data (Repacholi and Greenebaum, 1999; Preece et al., 2000). Various cellular components, processes, and systems can be affected by ELF-EMF exposure, e.g. cell membrane (both internal and external) and signal transduction pathways (Czyz et al., 2004), cell cycle regulation and cell proliferation and/or differentiation (Simko and Mattsson, 2004; Frahm et al., 2006). Also direct or indirect DNA damage can be measured in different substrates but this does not directly lead to genotoxic effects (Villarini et al., 2006; Stronati et al., 2004). If the biological effects induced by ELF-EMF exposures are not easy to understand, the possible physiological effect of power frequency fields is still a hotly debated issue. In living organisms, above all in vertebrates, some tissue constituted by excitable cells (neurons and muscle fibres) are more sensible to the presence of perturbation of electric fields present around their cell membranes (Sieron et al., 2004). Some recent papers seem to confirm this assumption, in fact short-time exposure (5 days) to ELF-EMF radiations showed, by the cytotoxic glutamate (Glu) pulse test, a 30% decrease of cell survival in primary neurons, prepared from newborn rat cerebellum (Nikolova et al., 2005) and ELF-EMF exposure of neural progenitor cells transiently affects the transcript level of genes related to apoptosis and cell cycle control (Blackman et al., 1993). Also "in vivo" experiments seem to confirm the peculiar responsiveness of this particular cell typology to ELF-EMF presence. It has been found, in fact, that ELF-EMF exposure for 14 days (1 h daily) did not influence the level of the biogenic amines and their metabolites, but increased the rate of synthesis of DA and 5-HT in rat frontal cortex as compared to control (Jenrow et al., 1998). Several investigations have revealed that electrical activity within the central nervous system (CNS) can be affected by exposure to ELF-EMF. Many of these studies have concerned CNS structures exhibiting endogenous oscillations and synchrony as optimal sites for field coupling. In this regard, a particularly well characterized structure is the rat hippocampus whose rhythmic slow activities (necessary to some pathways of memory procedures) are exclusively susceptible to field-mediated perturbation suggesting that the sensitivity of these networks to ELF-EMF exposure may be really significant (Wolf et al., 2005).
In conclusion, the various modifications measured in several laboratories utilizing different substrates showed the presence of real biological effects (acute and chronic) derived from ELF-EMF exposure even if not without troublesome questions, these responses can be associated with detectable changes in cell physiology. This last consideration suggests that somehow, compensatory mechanisms at the translational and posttranslational level could exist.
Also for this reason, it is necessary to suggest the hypothesis regarding a possible initial cellular event affected

by exposure to ELF-EMF, an event which is present in a large number of effects observed as consequence of ELF-EMF exposure. Based on an extensive reviewed literature, Simko and Mattsson (2004) recently suggested that ELF-EMF exposure is able to perform such activation by means of increasing levels of free radicals. Such a general activation is compatible with the diverse nature of observed effects. Free radicals are intermediates in natural processes and they could be the stimulus to induce an "activated state" of the cell which then enhances the release of free radicals, in turn leading to biological events such as, in the CNS, an inhibition of the effects of the melatonin release and, as consequence of this, an alteration of biological rhythms or the deregulation of the neurotransmitter synthesis. In general, reactions in which radicals are involved become more frequent, increasing the possibility of DNA damage and therefore, to an increased risk of tumour development.
The purpose of this paper is to provide information about the effects of ELF-EMF applied to excitable cell lines. In particular, we focused our attention on the generation of radical oxygen species (ROS) and on the antioxidant system correlated with “in vitro” cell exposure to ELF-EMF having different intensities and duration using pheocromocytoma- and neuroblastoma-derived cell lines (PC12 and SH-SY5Y respectively) as neuronal models, glioblastoma GL15 as glial model and C2C12 myocytes as muscle substrates.
Results. To verify if the “in vitro” cell exposure to ELF-EMF influences cell proliferation rate, the cells were grown for 4-7 days in absence (control) or in presence of ELF-EMF (0.1, 0.5, 1.0mT). In fig. 1 a representative proliferation curve of the muscle cell line C2C12 is shown. At every considered intensities the proliferation rate didn’t show any significant difference in regard to control cells.

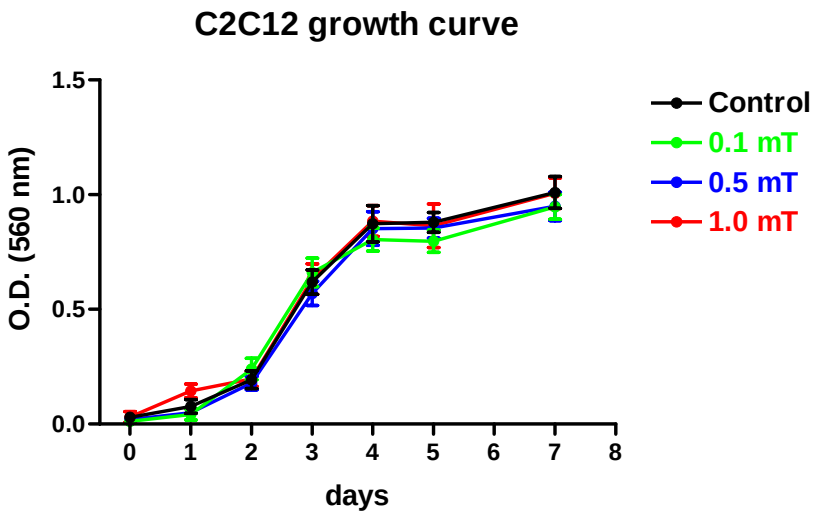


Fig. 1: Proliferation rate in C2C12 cell line exposed 0-7 days at different ELF-EMF intensities (0.1, 0.5 and 1 mT). The data are means±SEM, n=8.

In Tab.I we have reported the mean values of cell number/1000 ± SEM after 4 exposure days in the other tested cell lines. The PC12 cells showed a very slight dose-dependent increase of cell number (529.2±22.6 in the controls and 579.2±19.0 in the cell exposed to 1.0 mT), while the SH-SY5Y cell line didn't show any modification and the GL15 cells seemed to suffer a very slight decrease after 4 days at 1.0 mT ELF-EMF.

Proliferating cells (mean of the cell number/1000 ± SEM after 4 exposure days in growth medium, n=5)				
	Control	0.1 mT	0.5 mT	1.0 mT
PC12	529.2±22.6	547.2±25.6	569.0±27.6	579.2±19.0
SH-SY5Y	887.0±49.6	897.0±39.0	857.5±33.6	877.0±40.3
GL15	580.4±31.6	550.7±47.8	563.5±33.8	504.5±43.8

Tab. I: Cell proliferation of three cell lines (PC12, GL15 and SH-SY5Y) after 4 days exposure to ELF-EMF of different intensities (0.1, 0.5 and 1 mT).

To summarize, under these experimental conditions, the ELF-EMF exposure didn't show a single significant effect on cell proliferation rate.
A possible effect of the exposure to electric and magnetic fields at extremely low frequencies could be an

increase of ROS production and, as one consequence of this, a modification of mitochondrial membrane potential. To check if the exposure to ELF-EMF could induce ROS production, SH-SY5Y and GL15 cells were exposed to ELF-EMF (10-60 min) and ROS production was assayed (fig. 2). The data obtained show that in both cell lines and at each ELF-EMF intensity tested, there is a significant increase of ROS production at 20 min even with a quantitative and qualitative different time-course.

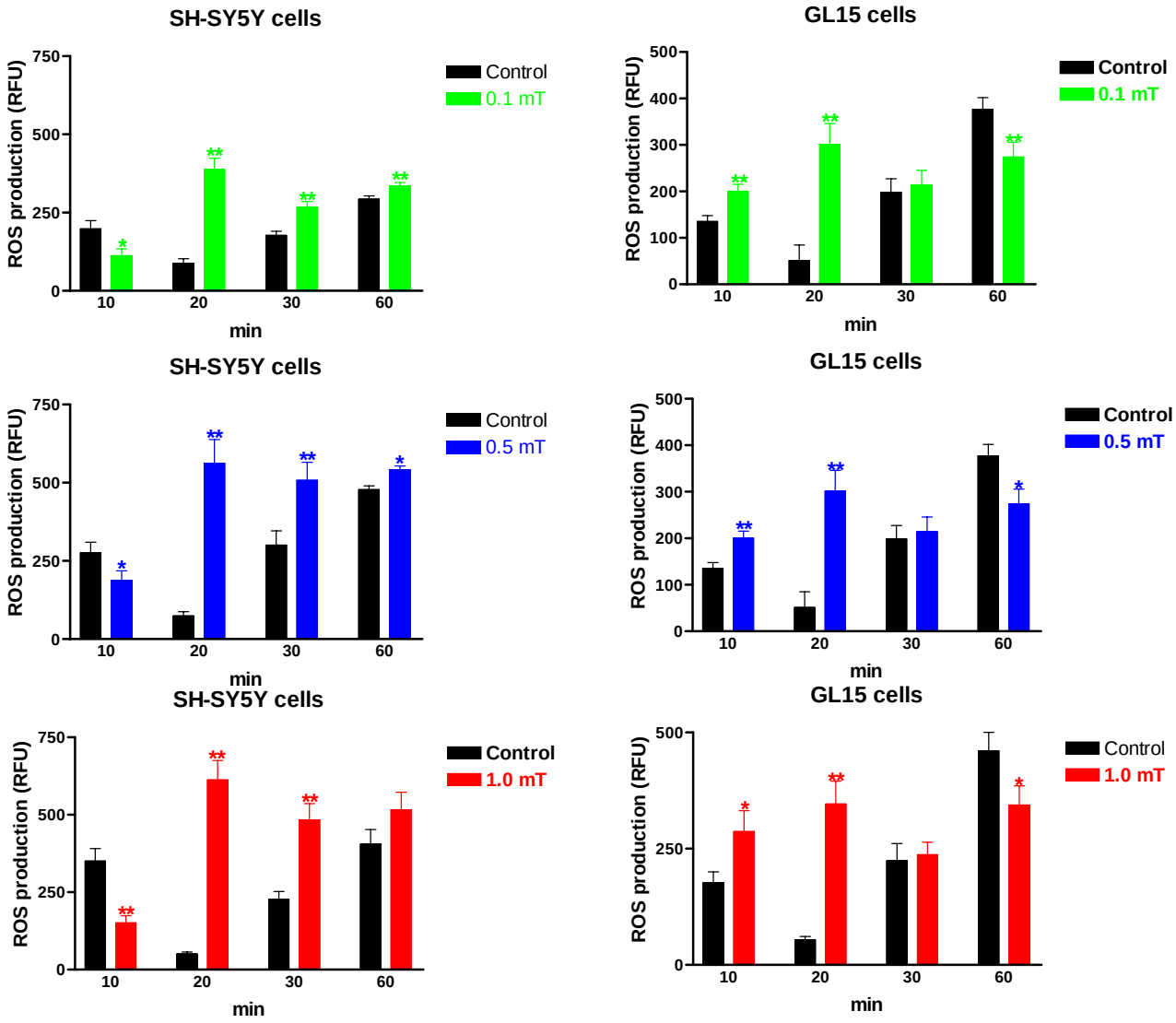


Fig. 2: ROS production analysed on cell populations. The ROS production was measured using DCF fluorescence emission assayed at different exposure times (10′, 20′, 30′, 60′) and different ELF-EMF intensities (0,1, 0,5 e 1mT). Data are mean ±SEM, n=4; *p<0.05, **p<0.01 vs control.

Using a single cell approach and a specific fluorescent dye (JC-1), we monitored mitochondrial membrane potential during ELF-EMF exposures utilizing a confocal microscope equipped by Helmholtz coils. Preliminary data suggested that mitochondrial membrane potential was affected by 1.0mT ELF-EMF on the cell lines tested. The undaubted increase of ROS production could induce, as response, an activation of endogenous antioxidant system. For this reason, in PC12 and GL15, we tested the antioxidant enzymatic activities (superoxide dismutase: SOD, glutathione reductase: GSSG-Rx, catalase: CAT, glutathione transferase: GST, glutathione peroxidase/Se-dependent: GSH-Px/Se^{+}, γ-glutamylcysteine synthetase: γGCS) after 3 days 1.0mT ELF-EMF exposure. As shown in Fig. 3, these activities varied depending on the cellular typology and on the considered enzyme. Each cell line showed a peculiar pattern of enzymatic activities probably depending on their biological activity.

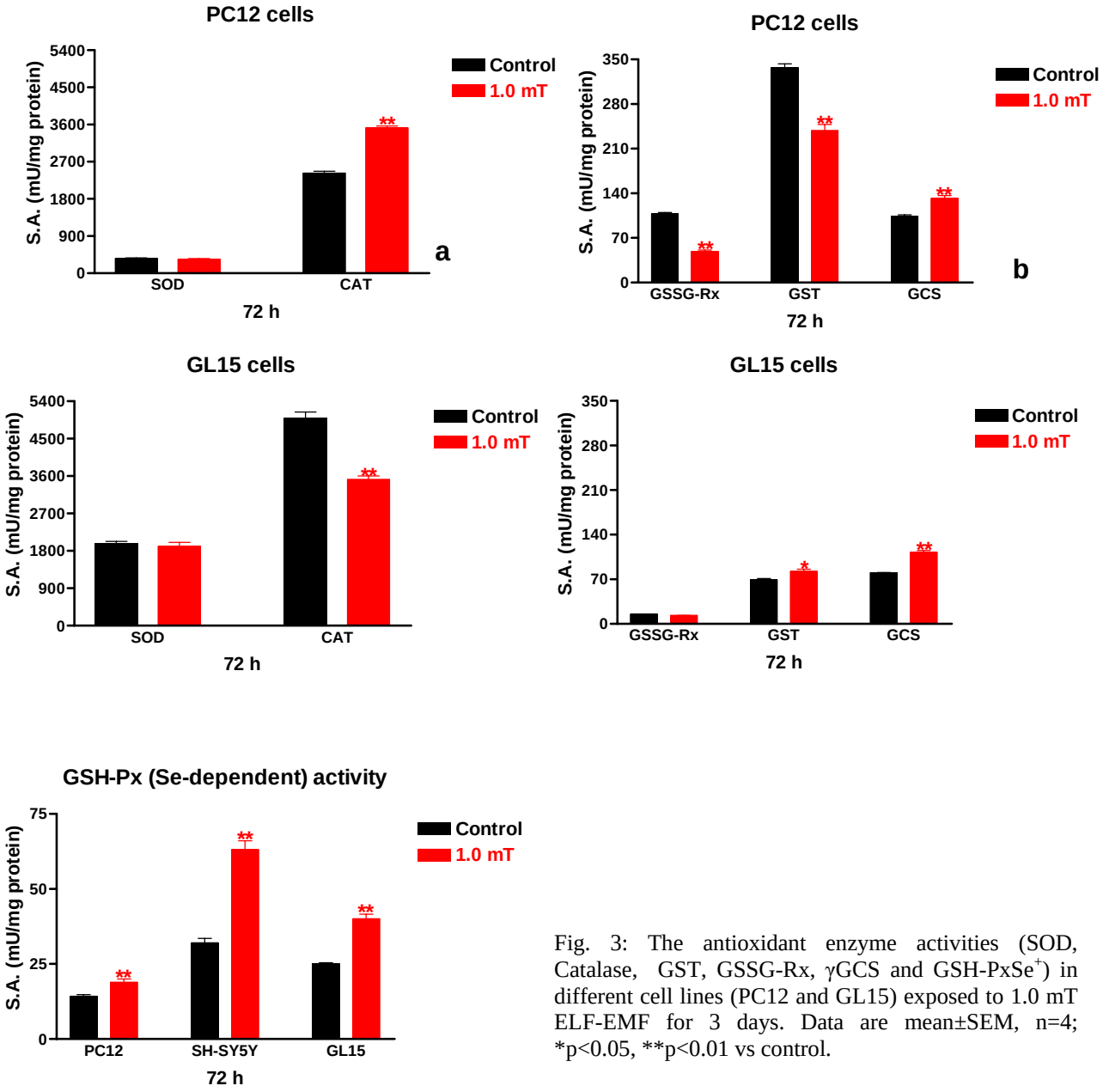


Fig. 3: The antioxidant enzyme activities (SOD, Catalase, GST, GSSG-Rx, γGCS and GSH-PxSe^{+}) in different cell lines (PC12 and GL15) exposed to 1.0 mT ELF-EMF for 3 days. Data are mean±SEM, n=4; *p<0.05, **p<0.01 vs control.

To complete the picture of the antioxidant system in GL15 cells, the levels of GSH, an endogenous antioxidant source, were measured. The levels of this molecule increased in GL15 cell line in the presence of ELF-EMF (fig. 4).

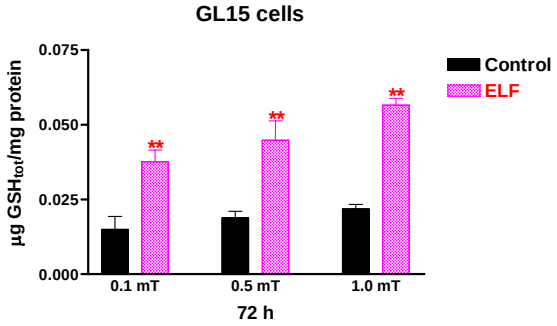


Fig. 4: The GSH total levels measured in GL15 cell line. Data are means±SEM, n=4; ** p<0,001.

In conclusion, depending on their intensity (mT), ELF-EMF affected the oxidative status, but the cells counteracted the induced increase of ROS production modifying their antioxidant ability.

Discussion. One mechanism through which ELF-EMF could influence neoplastic development is the deregulation of cancer-related genes and, in particular those related to different cyclins and cyclin-dependent kinases which are deputy to control cell cycle progression and cellular proliferation. The results of our experiments show that a slight, but dose-dependent, increase of proliferation rate was observed only in PC12 cells after exposure to ELF-EMF with graduated intensities (0.1-1.0 mT). This result is only apparently contradictory compared to those already published by McFarlane et al (2000) which reported no effect on cell proliferation of PC12 cells exposed to 4.5-15.8 microT ELF-EMF. In addition, during our experiments, if the intensity of ELF-EMF was lower than 0.5 mT, no modification in cell proliferation was noted. In the other cell types no variations (SH-5YSY) nor a significant slight decrease (GL15) after 4 days of exposure to the highest ELF-EMF intensity (1.0 mT) occurred. From these results, an initial consideration comes out: the effect of ELF-EMF on cell proliferation is dependent on the phenotype of cell model rather than on a direct action of ELF-EMF on some steps of cell cycle progression. As previously demonstrated by Ross in the 90's, markedly different effects, ranging from inhibition to stimulation of proliferation, were obtained, depending on the signal parameters (amplitude and frequency of ELF-EMF) as well as the types of utilized cell substrate (Ross SM, 1994). This fact is also supported by somewhat unclear results on the effect of the ELF-EMF on stromal stem cell proliferation (CFU-f); in fact, CFU-f from female mice showed a reduction, while CFU-f from male mice no decrease in cell proliferation (Van Den Heuvel et al., 2001).

More recently Wolf et al (2005) showed that the stimulation of proliferation, as well as the presence of DNA damage, was noted in HL-60 leukemia cells, Rat-1 fibroblasts and WI-38 diploid fibroblasts exposed for 24-72 h to 0.5-1.0-mT ELF-EMF. These effects were prevented by pre-treatment of cells with an antioxidant like alpha-tocopherol, suggesting that redox reactions were involved. Accordingly, the cells after exposure to 1.0 mT ELF-EMF exhibited a significant increase in ROS accumulation which was decreased by addition in the culture medium of an adequate scavenger (Wolf et al., 2005). Also under our experimental condition it was possible to note a significant increase of ROS production in all the tested cell lines even with a different qualitative and quantitative time-course. Moreover, also "in vivo" experiments seem to confirm that the chronic exposure to ELF-EMF is able to generate a stress oxidative status (Regoli et al., 2005; Harakawa et al., 2005; Yokus et al., 2005). In addition, the presence of an increase of ROS production is also indirectly demonstrated by the analysis of the enzymatic pathways involved in the catalytic removal of reactive oxygen species accumulated as an effect of ELF-EMF exposure. The "in vitro" experiments reported here, as well as the results derived from "in vivo" techniques (Lee et al., 2004) in mouse, show that the presence of ELF-EMF can induce a variable and specie-specific alteration of the stress oxidative pathway.

Summary

In vitro experiments performed in excitable cell lines: SY-SY5Y, GL15, PC12 and C2C12, seem to indicate that the biological response (proliferation rate) to ELF-EMF (0.1- 1.0 mT) exposure strictly depends on cell model than on the utilized ELF-EMF intensity or time of exposure. However, in both neuronal-like and glial-like cell lines, a significant increase of ROS production, with a different time-course in each cell line, was detected. This caused the enzymatic detoxification pathway involvement. In conclusion, even if further studies are necessary to identify the kind of ROS produced by the exposure to ELF-EMF, we propose that this biochemical substrate could be the candidate as the cellular "primum movens" of ELF-EMF induced effect on biological systems.

Acknowledgments

This study was supported by grants from MATT (5379/2002/SIAR; DSA/2004/0026774)

References

1. Blackman CF, Benane SG, House DE Evidence for direct effect of magnetic fields on neurite outgrowth FASEB J. 7(9):801-6; 1993.
2. Czyz J, Nikolova T, Schuderer J, Kuster N, Wobus AM. Non-thermal effects of power-line magnetic fields (50 Hz) on gene expression levels of pluripotent embryonic stem cells-the role of tumour suppressor p53. Mutat Res. 557(1):63-74; 2004.
3. Foster KR Mechanisms of interaction of extremely low frequency electric fields and biological systems. Radiat Prot Dosimetry. 106(4):301-10; 2003.
4. Frahm J, Lantow M, Lupke M, Weiss DG, Simko M. Alteration in cellular functions in mouse macrophages after exposure to 50 Hz magnetic fields. J Cell Biochem. Apr 5; 2006.
5. Harakawa S, Inoue N, Hori T, Tochio K, Kariya T, Takahashi K, Doge F, Suzuki H, Nagasawa H. Effects of a 50 Hz electric field on plasma lipid peroxide level and antioxidant activity in rats. Bioelectromagnetics. 26(7):589-94; 2005.
6. Jenrow KA, Zhang X, Renehan WE, Liboff AR. Weak ELF magnetic field effects on hippocampal rhythmic slow activity. Exp Neurol. 153(2):328-34; 1998.
7. Kavet R, Stuchly MA, Bailey WH, Bracken TD. Evaluation of biological effects, dosimetric models, and exposure assessment related to ELF electric- and magnetic-field guidelines. Appl Occup Environ Hyg. 16(12):1118-38; 2001.
8. Lee BC, Johng HM, Lim JK, Jeong JH, Baik KY, Nam TJ, Lee JH, Kim J, Sohn UD, Yoon G, Shin S, Soh KS. Effects of extremely low frequency magnetic field on the antioxidant defense system in mouse brain: a chemiluminescence study. J Photochem Photobiol B.73(1-2):43-8; 2004.
9. McFarlane EH, Dawe GS, Marks M, Campbell IC. Changes in neurite outgrowth but not in cell division induced by low EMF exposure: influence of field strength and culture conditions on responses in rat PC12 pheochromocytoma cells. Bioelectrochemistry. 52(1):23-8; 2000.
10. Nikolova T, Czyz J, Rolletschek A, Blyszczuk P, Fuchs J, Jovtchev G, Schuderer J, Kuster N, Wobus AM. Electromagnetic fields affect transcript levels of apoptosis-related genes in embryonic stem cell-derived neural progenitor cells. FASEB J. 19(12):1686-8; 2005.
11. Preece AW, Hand JW, Clarke RN, Stewart A. Power frequency electromagnetic fields and health. Where's the evidence? Phys Med Biol. 45(9):R139-54; 2000.
12. Regoli F, Gorbi S, Machella N, Tedesco S, Benedetti M, Bocchetti R, Notti A, Fattorini D, Piva F, Principato G. Pro-oxidant effects of extremely low frequency electromagnetic fields in the land snail Helix aspersa. Free Radic Biol Med. 39(12):1620-8; 2005
13. Repacholi MH, Greenebaum B. Interaction of static and extremely low frequency electric and magnetic fields with living systems: health effects and research needs. Bioelectromagnetics. 20(3):133-60; 1999.
14. Repacholi MH. WHO's health risk assessment of ELF fields. Radiat Prot Dosimetry.106(4):297-9; 2003.
15. Ross SM. Combined DC and ELF magnetic fields can alter cell proliferation. Bioelectromagnetics. 15(5):493; 1994.
16. Sieron A, Labus L, Nowak P, Cieslar G, Brus H, Durczok A, Zagzil T, Kostrzewa RM, Brus R. Alternating extremely low frequency magnetic field increases turnover of dopamine and serotonin in rat frontal cortex. Bioelectromagnetics. 25(6):426-30; 2004.
17. Simko M, Mattsson MO. Extremely low frequency electromagnetic fields as effectors of cellular responses in vitro: possible immune cell activation. J Cell Biochem. 93(1):83-92; 2004.
18. Stronati L, Testa A, Villani P, Marino C, Lovisolo GA, Conti D, Russo F, Fresegna AM, Cordelli E. Absence of genotoxicity in human blood cells exposed to 50 Hz magnetic fields as assessed by comet assay, chromosome aberration, micronucleus, and sister chromatid exchange analyses. Bioelectromagnetics. 25(1):41-8; 2004.
19. Van Den Heuvel R, Leppens H, Nemethova G, Verschaeve L. Haemopoietic cell proliferation in murine bone marrow cells exposed to extreme low frequency (ELF) electromagnetic fields. Toxicol In Vitro. 15(4-5):351-5; 2001.
20. Villarini M, Moretti M, Scassellati-Sforzolini G, Boccioli B, Pasquini R. Effects of co-exposure to extremely low frequency (50 Hz) magnetic fields and xenobiotics determined in vitro by the alkaline comet assay. Sci Total Environ. 361(1-3):208-19; 2006.
21. Wolf FI, Torsello A, Tedesco B, Fasanella S, Boninsegna A, D'Ascenzo M, Grassi C, Azzena GB, Cittadini A. 50-Hz extremely low frequency electromagnetic fields enhance cell proliferation and DNA damage: possible involvement of a redox mechanism. Biochim Biophys Acta. 1743(1-2):120-9; 2005.
22. Yokus B, Cakir DU, Akdag MZ, Sert C, Mete N. Oxidative DNA damage in rats exposed to extremely low frequency electro magnetic fields. Free Radic Res. 39(3):317-23; 2005.

Appendix

Instrumentation. The 50Hz ELF-EMF were generated by two different devices: a solenoid and a pair of

Helmholtz coils. These devices were planned and built to deliver variable, homogeneous, sine-wave alternate current magnetic fields with 50 Hz frequency and intensities ranging between 0.1-1.0 mT±2%. The horizontal cylindrical solenoid (length=340mm, diameter=113mm), on a supporting base, was supplied by a power supply Elgar Electronics (mod. CW-801P). The solenoid was used in an incubator (5% CO_2 and 37°C) for continuous long time cells exposures during which the solenoid's eventual added temperature was negligible. The pair of Helmholtz coils (r=445mm, distance between coils=400mm), producing homogeneous magnetic field over the specified volume-under-test corresponding to the cell chamber , were located in the working zone of a confocal microscope and connected to a power supply Elgar Electronics (mod. CW-1251P).

Cell culture. C2C12 and PC12 (American Culture Collection) and GL15 (functionally characterized in our lab, Mariggiò et al BMC Physiology 1:4, 2001) were cultured as exponentially growing cells in growth medium (GM). The GM for C2C12, SH-SY5Y and GL15 contains Dulbecco's modified Eagle's medium (DMEM), 10-20% foetal calf serum (FCS), 2-4 mM L-glutamine and 100 UI mL^{-1}-100 μg mL^{-1} Penicillin-Streptomycin. The GM for PC12 cells contains RPMI 1640 with 5% FCS and 10% horse serum, glutamine and antibiotics as mentioned above. Reagents for cellular culture were purchased from Gibco (Paisley, Scotland, UK). The cells were seeded on Petri dishes in GM and sub-cultured every 3 days (C2C12 and GL15) or weekly (SH-SY5Y and PC12) (Mariggiò et al, BMC Physiology 1:4, 2001; Guarnieri et al, Neuroscience 128:697–712, 2004; Pietrangelo et al., J Physiol.572(3):721-733, 2006). We exposed cell cultures to 50Hz ELF-EMF (0-1mT) generated by a solenoid or Helmholtz coils for different times according to the experimental plane.

Cellular proliferation was tested during 7 days in C2C12 and 4 culture days in the other cell lines, using the colorimetric assay of 3-[4,5-dimethylthiazol-2-yl]-2,5 diphenyltetrazolium bromide (MTT) as described by Pietrangelo et al. (J Physiol.572.3:721-733, 2006).

Mitochondrial membrane potential measurements. These were determined using a carbocyanine dye JC-1 (Molecular Probes, Eugene, Oregon, USA) which is taken up by the mitochondria. When the transmembrane potential is high, like in normal cells, JC-1 forms red fluorescence dimers (J-aggregate), while when it is low the red fluorescence disappears and green fluorescence emission appears (monomer). Briefly, the cells on coverslips were incubated in growth medium containing 5 mM of JC-1 for 10 min. After being rinsed three times with PBS, each coverslip was observed and images were recorded with or without the ELF-EMF generated by Helmholtz coils applied to a confocal microscope (excitation was fixed at 488 nm and emission was set to either 522 nm, for green monomer, or 605 nm, for red J-aggregate, using a bandpass filter). To estimate the modification of fluorescence in mitochondria, the change in green and red areas was calculated for the whole image using Scion Image ver. beta 3b (Scion Corporation, Frederick, Maryland, USA). The red/green area ratio, resulting from each single image of the experiment was plotted against time (Castellano et al., Arch. Pharm. Pharm. Med. Chem. 333:373–380; 2000).

ROS production. After different exposure times (10′, 20′, 30′, 60′) at different ELF-EMF intensities (0,1, 0,5 e 1mT), the cells, plated on 96 multiwell, were incubated at 37°C with dichlorodihydrofluorescin-diacetate (H_2DCF-DA) for 30'. After incubation the cells were washed and the ROS production was revealed by the fluorescence emission of oxidized 2',7'-dichlorofluorescein (DCF) read on a multiwell fluorimeter (excitation at 485 nm and emission at 530 nm).

Antioxidant enzyme activities. The enzymatic activities were measured on cell extracts using spectrophotometric assays according to Sun and Zigman (Anal. Biochem. 90: 81-89; 1978) for SOD1; Aebi HE (Methods in enzymatic analysis. New York: Academic Press; pp.:673-684; 1974) for CAT; Paglia and Valentine (J. Lab. Clin. Med. 70:158-169; 1967) for GSH-Px Se^{+}; Habig and Jacoby (Methods Enzymol. 77:398-405; 1981) for GSSG-Rx; Di Ilio et al. (Bioch. Med. 29:143-148; 1983) for GST; Volohonsky et al. (Chem. Biol. Interact. 140:49-65; 2002) for γ-GCS. The extracts were obtained through homogenization of $1x10^7$ cells and centrifugation at 12,000 rpm for 45 min.

GSH total levels. The total glutathione levels were determined using a kinetic assay in which catalytic amounts of GSH or GSSG derived from the continuous reduction of 5'5'-dithiobis (2-nitrobenzoic acid) (DTNB) by NADPH. The reaction rate is directly related to the concentration of glutathione at values up to about 2 mM. The formation of 5-thio-2-nitrobenzoate (TNB) was measured spectrophotometrically at 405 or 414 nm.

A ROLE OF ERK SIGNALING IN THE PROLIFERATIVE EFFECTS OF 50 Hz MAGNETIC FIELDS ON HUMAN NEUROBLASTOMA CELLS

M. A. MARTÍNEZ, M. A. CID, A. ÚBEDA, V. J. GARCÍA, J. LEAL, AND M.A. TRILLO

DEPT. INVESTIGACIÓN-BEM, HOSPITAL RAMÓN Y CAJAL, 28034-MADRID, SPAIN (m.antonia.martínez@hrc.es)

ABSTRACT

OBJECTIVE. We have reported before that 42 or 63 h intermittent exposure to 50 Hz, 100 μT magnetic field (MF) can induce cell proliferation in the NB69 line, from a human neuroblastoma (REFLEX Project, Final Report 2004). Evidence exist that mitogen-activated protein kinases can be involved in the MF- induced bioeffects. We have used a MAPK-specific inhibitor (PD98059) to investigate whether the activation of extracellular signal-regulated kinase (ERK1/2) is involved in the proliferative response elicited by MF.
METHODS. The growth response was analyzed through haemocytometer counting after 63 h of exposure to four conditions: control; PD98059 (20 μM); MF alone and MF + PD98059. In short-term studies, the expression of phosphoryled MAPK/ERK (p-ERK1/2) was analyzed (Immunocytochemistry - Image analysis) at 15, 30, 60 and 120 min of exposure.
RESULTS AND CONCLUSIONS. The results confirm that a 63 h, intermittent exposure to 50 Hz, 100 μT increases the growth rate of NB69 cells. This effect was blocked by the MAPK-specific inhibitor PD98059. In the short term, the MF induced a transitory significant increase of p-ERK1/2 expression peaking at 30 min (63.4%; p= 0.0010), such an effect was also negated by the inhibitor. These results indicate that the proliferative effects induced by the MF-exposure in NB69 cells could be mediated by a repeated (intermittent) transitory activation of the MAPK/ERK pathway.

INTRODUCTION

A number of epidemiological data have raised concerns about the relationship between exposure to power frequency magnetic fields (MF) and cancer promotion (Ahlbom *et al.* 2001) and on the potential contribution of the occupational exposure to power frequency fields to the pathogenesis of neurodegenerative diseases such as Alzheimer's or Parkinson's diseases (Feychting *et al.* 2003; Park *et al* 2005). Cellular studies are needed to reveal the cellular and molecular mechanisms underlying the biological effects and possible health implications of the exposure to power frequency MF.

In previous studies on NB69 human neuroblastoma cell line, we have reported that power frequency fields at 10 or 100 μT increase proliferation through activation of DNA synthesis (Trillo *et* al 2003; REFLEX-Project, Final Report 2004). Numerous studies have investigated the influence of power frequency magnetic fields with magnetic flux densities (MFD) in the mT range on cell proliferation (Katsir and Parola 1998; Wei *et al.* 2000; Wolf *et al.* 2005). However, there is limited evidence on the effects of MFD ≤ 100 μT, which corresponds to the ICNIRP recommended threshold for short-term exposure of the general public to 50-Hz MF. Since it is unlike that EMF can induce DNA damage directly, most studies have examined EMF effects at the cell membrane level, on general and specific gene expression, and on signal transduction pathways. Among the cellular processes proposed as implicated in the MF growth-promoting activity, signaling and regulatory cycle proteins have been reported altered, though this effect did not result in apparent changes in routine physiological processes such as cell growth or division (Korzh-Sleptsova *et al.* 1995; Richard *et al.* 2002; Lange *et al.* 2004). However, the type, the age and the state of the cell as well as the physical parameters of ELF-MF can affect in a different degree the reported MF bioresponses.

The aim of the present work is to explore the signaling and the regulatory proteins involved in the proliferative action exerted by a 50 Hz, 100 μT MF on the NB69 human neuroblastoma cell line, investigating whether mitogen-activated protein kinases (MAPK) could be involved in such a proliferative response. MAPK kinase pathways are signaling pathways that enable cells to respond to external stressors and stimuli (Kolch, 2000) and play a key role in a variety of cellular responses including proliferation, differentiation, and death. MAPK have been implicated in the cellular responses to magnetic fields (Jin *et al* 2000, Nie and Henderson,

2003). The MAPK family includes the extracellular signal–regulated kinases (ERK1/2). This ERK signaling pathway, also called the MEK-ERK cascade, is one of the principal cytoplasmic signal transduction systems that regulate processes of proliferation and survival in eukaryotic cells. Besides, up-regulation of ERK1/2 has been proposed to be implicated in tumor progression and metastasis in different cancer types (de Melo *et al.* 2006; Suthiphongchai *et al.* 2006; Cuevas *et al.* 2006). In the nervous system ERK1/2 has been connected to neuronal responses both, to functional (modulating neuronal survival, neuronal differentiation, and plasticity) and pathologic stimuli (such as Alzheimer or Parkinson disease, Chu *et al.* 2004; Webster *et al.* 2006). The results of the present study indicate that the activation of the extracellular, signal-regulated kinase, ERK1/2, is involved in the proliferative response of NB69 cells to the exposure to 50 Hz 100 μT MF.

MATERIAL AND METHODS

Cell growth assays. NB69 human neuroblastoma cells were maintained in Dulbecco's Minimum Essential Medium (D-MEM, Biowhittaker) supplemented with 15% heat inactivated fetal bovine serum, 4 mM L-Glutamine and 100 U/ml penicillin and 100U/ml streptomycin (Gibco BRL, Invitrogen, Spain). Cells were cultured at 37 ºC in a humidified incubator under an atmosphere of 5% CO_2. Cells were seeded, at a density of 4.5 x 10^4 cells/ml, into 60 mm Ø plastic Petri dishes (Nunc) or on circular 12 mm Ø coverslips placed into the Petri dishes, and cultured under standard conditions for three days. When needed, media were supplemented with the ERK1/2 kinase inhibitor, PD98059 (2'-amino-3'-methoxyflavone, Biosource). PD98059 was dissolved in dimethyl sulfoxide (DMSO). An equal dose of DMSO was added to the control dishes. The final concentration of DMSO in the medium was 0.1%. The mean value of the number of cells in controls with or without the vehicle, DMSO, was 649.0 ± 114.9 (x 10^4) and 647.2 ± 83.2 (x 10^4), respectively.

Magnetic field exposure. NB69 cells were exposed to a 50 Hz, sinus wave, linearly polarized magnetic field, at 100 μT. The MF was generated by a wave generator Newtronic Model 200MSTPC connected to a pair of coils set in a Helmholtz configuration. Currents in the coils were monitored using a multimeter (Hewlett Packart, model 974A, Loveland, CO) and measured with fluxgate magnetometers (EFA-3, Model BN 2245/90.20 Wandel and Goltermann S.A, EMDEX II, Enertech Consultants, Campbell CA). Two pairs of coils were placed inside two magnetically shielded chambers (co-netic metal; Amuneal Corp., Philadelphia, PA) kept in identical CO_2 incubators (Forma Scientific) with a 5% CO_2, 37 ºC and 100% humidity atmosphere. The background MF inside the shielded chambers was AC: 0.04 ± 0.03 μT; DC: 0.05 ± 0.04. In each experiment only one set of coils was energized. The samples in the unenergized set were considered sham-exposed controls. Both incubators were used, in a random sequence, alternatively for MF exposure and sham-exposure.

Study of the growth response at the end of a 63-hour lapse of intermittent exposure in the presence or absence of the MAPK inhibitor PD98059. NB69 cells were cultured under standard conditions for three days. At this time medium was renewed and 20 μM PD98059 was added to the culture media 60 min prior to the MF exposure. Ten Petri dishes, 5 with and 5 without PD98059 were placed in each exposure set up inside the incubators. The exposed group was treated intermittently, 3h On/3h Off, to 50 Hz MF at a 100 μT magnetic flux density for 63 h. The cells were subjected to: a) no treatment: controls, b) treatment with PD98059, c) exposure to MF, and d) MF exposure imposed upon PD98059 treatment. At the end of the exposure and or treatment, on day 6 post-plating (pp), the cellular viability and growth were determined through Trypan blue exclusion. All assays and analysis were performed in the blind for experimental condition.

Studies of the phosphoryled ERK1/2 expression in response to short-term MF exposure or PD98059 treatment. NB69 cells were exposed for 15, 30, 60 and 120 min at day 4 pp. The percent of phosphoryled ERK1/2 (p-ERK1/2) positive cells was analyzed by immunocytochemistry. At the end of the magnetic field exposure, the cells were fixed with 4% paraformaldehyde for 20 min at 4 ºC and permeabilized with 5% ethanol/acetic acid. The non-reactive sites were blocked (10% goat serum in PBS) for 1 hour at room temperature. Immunostaining was performed by incubating cells overnight at 4 ºC with primary antibody antiphospho –specific ERK1/2 (1:100) rabbit polyclonal antibody (44 -480G, Biosource) and a secondary, goat antirabbit IgG, antibody (1:500) conjugated with the fluorophore Alexa Fluor 488 (Molecular Probes) for 1 hour at room temperature. Hoechst 33342 (Bisbenzimide, Sigma) was included in the mounting medium as a counterstain for nuclei and was visualized and evaluated by photomicroscope. In each experiment 3 coverslips were studied per experimental group (Control; Inhibitor; MF; Inhibitor + MF). In each coverslip 15 random microscope-fields were analyzed and in each microscope-field the total nuclei (Hoechst fluorescent dye) and the percent of p-ERK1/2 positive cells were recorded. A total of about 4500-5000 cells per experimental group was evaluated. The statistical study applied the ANOVA test followed by the Student's T test.

RESULTS

1. Growth response at the end of a 63-hour lapse of intermittent exposure in the presence or absence of the MAPK inhibitor PD98059. The effects of 100 μT MF on the cell growth in the presence or absence of PD98059 at 20 μM are represented in Figure 1. The exposure to the MF induced a significant increase in the number of cells (9.1% over controls, $p< 0.01$), which confirms previously reported observations by our group (Trillo *et al*., 2003; REFLEX-Project, Final Report 2004). In contrast to that, the treatment with PD98059 provoked equivalent, significant decreases in the number of cells of MF-exposed (16.7% below controls, $p< 0.001$) or unexposed samples (16.7 % below controls; $p< 0.001$). The latest indicates that the MAPK inhibitor PD98059 inhibits cell growth in the NB69 line and blocks the MF-induced growing effect on these cells.

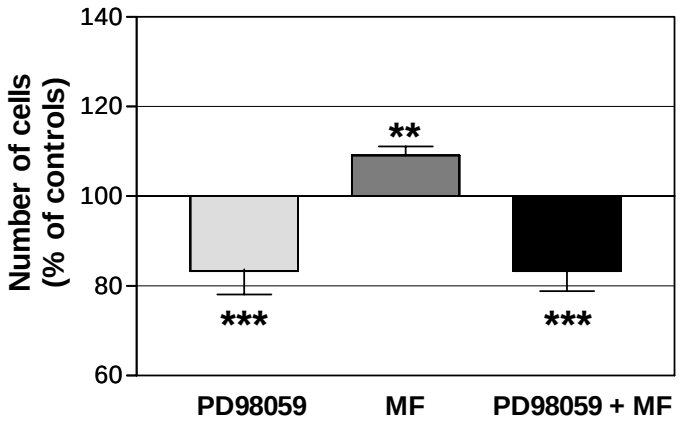


Figure 1. Effects of a 63 hours exposure to 100 μT MF and/or of treatment to 20 μM PD98059 on the number of cells. Data from 4 experimental replicates normalized with respect to controls (Mean ± SEM). **: $p< 0.01$; ***: $p< 0.001$ (ANOVA followed by Student's T-test.)

2. Phosphoryled ERK1/2 expression in response to short-term MF exposure or PD98059 treatment. Figure 2 shows the results of short-term treatment with MF or MAPK inhibitor on day 4 pp. The MF exposure provoked a transitory increase in the percent of cells that express p-ERK1/2, peaking at 30 min of exposure (63.4% over controls $p< 0.01$), the effect being prevented by PD98059. However, at 120 min of exposure a significant decrease in the p-ERK 1/2 expression (19.0% below controls; $p< 0.001$) was obtained. This response was similar to that induced by the inhibitor alone and by the combined treatment (27.6%; $p< 0.05$ and 28.8%, $p< 0.05$ below controls, respectively). As can be observed, the MAPK inhibitor PD98059 only provoked a significant reduction in ERK1/2 activation after 120 min of treatment, although it was able to prevent the MF induced ERK1/2 expression at 30 and 60 min of treatment. Taken together, these results indicate that the MF can induce transitory activation of the MAPK/ERK pathway in NB69 cells and suggest that the proliferative response induced by the exposure to 50 Hz 100 μT MF could be mediated by this transitory activation of MAPK, ERK1/2 transduction pathway, in each of the 3-hour On periods of the intermittent exposure cycle.

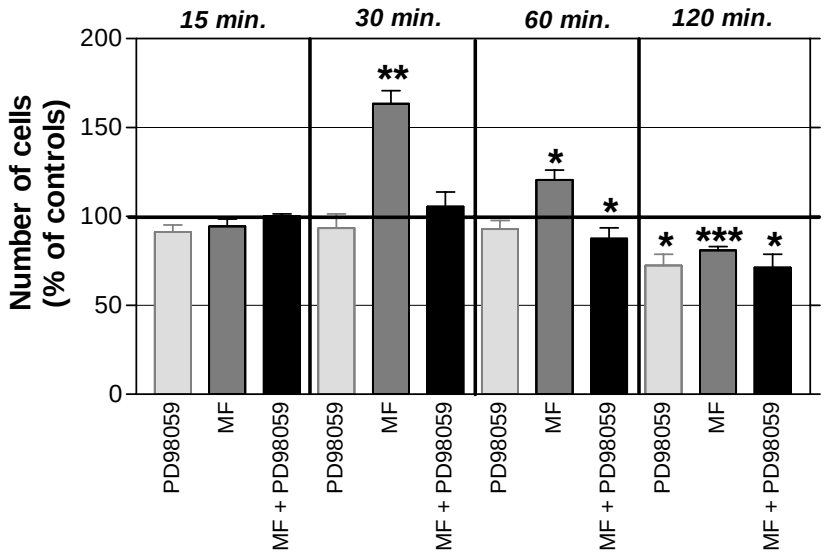


Figure 2. p-ERK 1/2 expression in response to short-term MF exposure or PD98059 treatment. Transitory effect of the MF exposure, peaking at 30 min. The MAPK-specific inhibitor, PD98059, blocks the MF effect. N = 4 independent replicates, data normalized with respect to controls (Mean ± SEM). *: $p< 0.05$; **: $p< 0.01$; ***: $p< 0.001$, Student's T- test.

DISCUSSION:

The effect of the MAPK-specific inhibitor PD98059 on MF-induced cell growth and on ERK1/2 phosphorylation was examined to determine whether ERK1/2 is involved in the proliferative effects of 50 Hz MF on NB69 human neuroblastoma cells. The ERK1/2 signaling pathway is a major determinant in the control of diverse cellular processes such as proliferation, survival, differentiation and motility. This pathway is often up regulated in human tumors (de Melo *et al.* 2006; Kohno and Pouyssegur 2006), and play an essential role in cell cycle progression, through induction of cell cycle regulatory proteins and transcription factors (Chang *et al.* 2003).

The present data confirm that a 63-hour intermittent exposure to 50 Hz, sinus wave MF at 100 μT promotes cell growth in the NB69 cell line. This increased growth was prevented when the specific inhibitor of the ERK1/2 activation, PD98059, was present. Besides, the field provoked a transitory increase in the activated, extracellular signal regulated kinase, p-ERK1/2, peaking at 30 min of exposure. The presence of PD98059 blocked this transitory activation of ERK1/2. At 120 min of MF exposure a significant decline in the expression of p-ERK1/2 occurred, both in the presence or in the absence of PD98059. Three other human cell lines (HTB 124, MCF7 and HL60), known to respond to MF with a 2 - 3-fold induction of HSP70 expression (Goodman *et al.* 1998), have also been reported to be responsive to a 30 min MF exposure (60 Hz, 8.0 and 80 μT) and induce ERK1/2 phosphorylation (Jin *et al.* 2000). The level of MAPK activation in MCF7 and HL60 cells exposed to the MF (60 Hz, 100 μT) was approximately equivalent to that in cells treated with 0.1 - 0.5 ng/ml of 12-O-tetradecanoylphorbal-13-acetate, TPA, (Nie and Henderson, 2003). Moreover, a cooperative effect on PKC activity has been observed when exposure to TPA and MF (50 Hz, 1 mT) were applied simultaneously on human amniotic cells (Richard *et al.* 2002), which is suggestive of a role for protein kinase C in the process leading to MAPK activation in MF exposed cells. It is currently believed that power frequency fields initiate the activation of the stress response when the signal affect receptors in the plasma membrane and that this subsequently triggers the specific signal transduction pathway that regulates different cell processes. In our study, the question whether the MF-activation of EKR1/2 in NB69 cells is a consequence of the conventional extracellular stress-activated signaling to the nucleus remains unanswered. However, like in the work by Jin *et al.* (2000), in the present study a MF activation of ERK1/2 was obtained, this activation being associated to the MF-induced promotion of proliferation in NB69 cells.

Different authors have reported effects of power frequency MF on cell proliferation in neuroblastoma lines; however, the molecular regulatory mechanisms underlying these MF-induced bioeffects remain unidentified. Namely, proliferation induction was obtained in neuroblastoma cells (LAN-5) after seven days of

continuous exposure to 50 Hz, 1 mT; this effect being associated to transitory increases of the proto-oncogen B-myb (Pirozzoli *et al.* 2003). Also, Tonini *et al.* (2001) reported inhibition of proliferation in NG108-15 cells treated with the differentiating agent BT2cAMP. This chemically-induced inhibition of cell proliferation was relieved by exposure to a 50 Hz MF at 120 or 240 μT. Our present results suggest that the proliferative response induced by the exposure to 50 Hz 100 μT magnetic fields could be mediated by a repeated transitory activation of MAPK, ERK1/2 transduction pathway, in each of the 3-hour On periods of the intermittent exposure cycle. Recently Ebisuya *et al* (2005) have reported that differences in the duration, magnitude and compartmentalization of ERK activity can generate variations in the signaling output that determine the cellular outcome. Furthermore, in the study by Ebisuya and coworkers several molecules have been identified as spatial, temporal or strength-controlling regulators of ERK activity. Consistent with that, a potential induced modulation by the MF exposure of these regulators of ERK activity could represent one of the mechanisms implicated in the MF-induced proliferation observed by us in NB69 cells.

SUMMARY

The purpose of the present work is to determine whether the mitogen-activated protein kinases MAPK, ERK1/2 is potentially involved in previously reported effects of the intermittent exposure to a 50 Hz, 10 or 100 μT magnetic field on the proliferation of the NB69 human neuroblastoma cell line. The influence of the MAPK-specific inhibitor PD98059 on MF-induced effects on cell growth and on ERK1/2 phosphorylation was examined. The obtained results show that the MF-induced growth response is prevented when the ERK1/2 activation was chemically inhibited. Besides, the MF provoked a time course significant, transitory increase in the p-ERK1/2 expression, peaking at 30 min of exposure. That transitory effect was also prevented by the MAPK specific inhibitor. Taken together, the present data indicate that the increase in cell proliferation induced by a 50 Hz, 100 μT MF in the NB69 line could be the result of a consecutive, transitory activation of the MAPK, ERK1/2 transduction pathway, during the On periods of intermittent exposure to the field.

Supported by EU Commission REFLEX-Project QLK4-1999-01574, FISS-03/0806 and Project I+T under agreement MOU EUROPA, ERG 101.013.

REFERENCES

Ahlbom A, Cardis E, Green A, Linet M, Savitz D, Swerdlow A. 2001. Review of the epidemiologic literature on EMF and Health. Environ. Health Perspect. 109: 911-933.

Chu CT, Levinthal DJ, Kulich SM, Chalovic EM, DeFranco DB. 2004. Oxidative neuronal injury. The dark side of ERK1/2. Eur.J.Biochem. 271: 2060-2066.

Chang F, Steelman LS, Shelton JG, Lee JT, Navolanic PM, Blalock WL,Franklin R, McCubrey JA. 2003. Regulation of cell cycle progression and apoptosis by Ras/Raf/MEK/ERK pathway (Review). Int. J. Oncol. 22:469-480.

Cuevas P, Diaz-Gonzalez D, Garcia-Martin-Cordova C, Sanchez I, Lozano RM, Gimenez-Gallego G, Dujovny M. 2006. Dobesilate diminishes activation of the mitogen-activated protein kinase ERK1/2 in glioma cells. J. Cell. Mol. Med. 10: 225-230.

de Melo M, Gerbasse MW, Curran J, Pache JC. 2006. Phosphorilated extracellular signal-regulated kinases are significantly increased in malignant mesothelioma. J. Histochem. Cytochem. Available: http://www.jhc.org/cgi/

Ebisuya M, Kondoh K, Nishida E. 2005. The duration, magnitude and compartmentalization of ERK MAP kinase activity: mechanisms for providing signal specificity. J. Cell. Sci. 118: 2997-3002.

Feychting M, Jonsson F, Pedersen NL, Ahlbom A. 2003. Occupational magnetic field exposure and neurodegenerative disease. Epidemiology 14(4):413-419.

Goodman R, Blank M. 1998. Magnetic field stress induces expression of hsp70. Cell Stress Chaperones, 3 : 79-88.

Jin M, Blank M, Goodman R. 2000. ERK1/2 phosphorylation, induced by electromagnetic fields, dismishes during neoplastic transformation. J. Cell. Biochem., 78 : 371-379.

Katsir G, Parola AH. 1998. Enhanced proliferation caused by a low frequency weak magnetic field in chick embryo fibroblasts is suppressed by radical scavengers. Biochem. Biophys. Res. Commun. 252 :753-756.

Kohno M, Pouyssegur J. 2006. Targeting the ERK signaling pathway in cancer therapy. Ann. Med. 38 : 200-211.

Kolch W. 2000. Meaningful relationships: the regulation of ras/raf/MEK/ERK pathway by protein interactions. Biochem J. 351: 289-305.

Korzh-Sleptsova IL, Lindstrom E, Mild KH, Berglund A, Lundgren E. 1995. Low frequency MFs increased inositol 1,4,5-trisphosphate levels in the Jurkat cell line. FEBS Lett. 359 : 151-154.

Lange S, Viergutz T, Simkó M. 2004. Modifications in cell cycle kinetics and in expression of G1 phase-regulating proteins in human amniotic cells after exposure to electromagnetic fields and ionizing radiation. Cell Prolif 37: 337-349

Nie K, Henderson A. 2003. MAP Kinase activation in cells exposed to a 60 Hz electromagnetic fields. J. Cell. Biochem. 90: 1197-1206.

Park RM, Schulte PA, Bowman JD, Walker JT, Bondy SC, Yost MG, Touchstone JA, Dosimeci M. 2005. Potential occupational risk for neurodegenerative diseases. Am J Ind Med 48: 63-77

Pirozzoli MC, Marino C, Lovisolo GA, Laconi C, Mosiello L, Negroni A. 2003. Effects of 50 Hz electromagnetic field exposure on apoptotic and differentiation in a Neuroblastoma cell line. Bioelectromagnetics 24 : 510-516.

REFLEX-Project 2004. Risk evaluation of potential environmental hazards from low energy electromagnetic field exposure using sensitive in vitro methods. Report Final, pp 274.
Available: http://www.verum-foundation.de/apopis

Richard D, Lange S, Viergutz T, Kriehuber R, Weiss DG and Simko M. 2002. Influence of 50 Hz electromagnetic fields in combination with a tumor promoting phorbol ester on protein Kinase C and cell cycle in human cells. Mol. Cell. Biochem. 232 (1-2): 133-141.

Suthiphongchai T, Phimsen S, Sakulkhu U, Tohtong R. 2006. PD98059-inhibited invasion of Dunning rat prostate cancer cells involves suppression of motility but not MMP-2 or uPA secretion. Oncol. Rep. 15: 1605-1610.

Tonini R Baroni MD, Masala E, Micheletti M, Ferroni A and Mazzanti M. 2001. Calcium protects differentiating neuroblastoma cells during 50 Hz electromagnetic Radiation. Biophys. J. 81 :2580-2589.

Trillo MA, Martínez MA, Cid MA, García VJ, Ubeda, A and Leal, J. 2003. Action of 50 Hz magnetic fields on the growth of human neuroblastoma cells., 25th BEMS Meeting, Maui, Hawaii, Abstract Book: 287

Wei M, Guizzetti M, Yost M, Costa LG. 2000. Exposure to 60-Hz magnetic fields and proliferation of human astrocytoma cells in vitro. Toxicol Appl Pharmacol. 162(3):166-176.

Webster B, Hansen L, Adame A, Crews L, Torrance M, Thal L, Masliah E. 2006. Astroglial activation of extracellular-regulated kinase in early stages of Alzheimer disease. J. Neuropathol. Exp. Neurol. 65: 142-151.

Wolf FI, Torsello A, Tedesco B, Fasanella S, Boninsegna A, Ascenzo MD, Grassi C, Azzena GB, Cittadini A. 2005. 50-Hz extremely low frequency electromagnetic fields enhance cell proliferation and DNA damage: Possible involvement of a redox mechanism. Biochim Biophys Acta 1743: 120-129.

GUIDELINES COMPLIANCE IN HUMAN EXPOSURE TO ELECTROMAGNETIC FIELDS FROM WLAN DEVICES

MERCEDES MARTÍNEZ-BÚRDALO, AGUSTÍN MARTÍN,
VÍCTOR PIZARRO, RAIMUNDO VILLAR

INSTITUTO DE FÍSICA APLICADA. CONSEJO SUPERIOR DE INVESTIGACIONES CIENTÍFICAS (CSIC)
C/ SERRANO 144. 28006 - MADRID. SPAIN

Abstract

Human exposure to electromagnetic fields from mobile communications (base-stations and mobile phones) has been widely studied in the last years. Nevertheless, the increasing use of wireless technology for short range data transfer (DECT, Bluetooth and WLAN) in home and office has enhanced the social concern about potential adverse health effects of electromagnetic fields from those technologies. Moreover, epidemiological studies and assessments of electromagnetic environments make necessary to know the influence that the electromagnetic field from a certain new technology source has in the total exposure level of a person.

The aim of this work is to assess, by using the finite-difference time-domain method (FDTD), the human exposure to electromagnetic fields from the antennas of wireless devices such as those of wireless local area networks (WLAN) access points. Several geometrical configurations are considered to simulate the exposure of the head of a person, as a worst case, to the fields from a WiFi antenna operating at 2400 MHz in home or office environments, calculating both, field values to be compared with reference levels and maximum specific absorption rate (SAR) values to be compared with basic restrictions. The situation of short-distance exposure to the bluetooth antenna of a personal digital assistant (PDA) in front of the eye of the user is also studied by calculating the SAR. Results are presented.

Introduction

In the last years, there has been a social concern about the possible harmful effects on the human health derived from people exposure to radiofrequency electromagnetic fields, specially those produced by mobile telephony (base-station antennas and mobile phones). Nevertheless, the rapid introduction in home and office environments of new emerging wireless technologies, such as the wireless local area networks (WLAN of WiFi) and Bluetooth, is motivating the users to worry about possible negative effects on their health caused by these technologies.

The human exposure to radiofrequency electromagnetic fields is regulated by national and international guidelines [1,2] which limit the exposure of general public to those fields, based on the guidelines from the International Commission on Non Ionizing Radiation Protection [3]. In the same way, the European Union has defined a specific directive for the protection of workers from the exposure to those fields [4].

Measurements of the WLAN signals in different environments have been made by several authors considering access points only, with client card enabled, uploading or downloading large files [5], or access points and mobile terminals with a maximum power of 100 mW [6], having found a strong dependence with distance and measured values far below the limits of the international guidelines. Measurements of the electric field near a WiFi 802.11b router so as numerical simulations of the electric field surrounding a wireless laptop computer with two hands over the keyboard have been made in [7], with a theoretical estimation of the channel occupation as a means of knowing the real emitted power of the system and an experimental assessment of compliance with safety limits of several short-range wireless devices used in home and office environments has been made in [8], by means of E-fields measurements in a semi-anechoic chamber and SAR measurements in a body-emulating phantom, concluding that, in the very near future, the background exposure in everyday life situations will exceed exposures from base stations and broadcast stations, so that it is necessary to assess the simultaneous exposure of people to multiple sources in its surrounding environment.

In this work the FDTD technique, which has demonstrated to be very useful for dosimetry studies of human exposure to electromagnetic fields, is used to analyze the field distribution in the vicinity of a person during the use of several radiofrequency devices. Two different situations will be considered, trying to simulate actual operating conditions in exposure to wireless access points antennas (based on the standard IEEE802.11b) in home or office environments and use of a WiFi or bluetooth PDA at several distances in front of the user's eye. In all cases, the SAR in the head of the user will be calculated to be compared with basic restrictions from the guidelines.

Models and Results

A. Exposure to wireless access points antennas.

Several situations of possible exposure to the antenna of a wireless access point in a domestic or office environment have been studied. In the simulations, brick walls and metalic cabinets are included to consider the influence of the environment in the SAR calculated in the head of the exposed person. Figure 1 shows the schematic geometries of four studied configurations: (a) a person working in a table where a desktop antenna in located, near the brick walls of the room, at a distance of 40 cm of the person head; (b) the worst-case of a person with the antenna in front of its eyes at a distance of 20 cm, with a reflecting plate behind the antenna at a distance of 4 cm; (c) a person in front of an antenna which is on the opposite side of a 12 cm thick brick wall, the antenna-eye distance being 20 cm or (d) a person exposed to the radiation of two desktop antennas at 15 and 20 cm from the head, respectively, with metalic cabinets behind the antennas at 15 and 25 cm (fig. 1d).

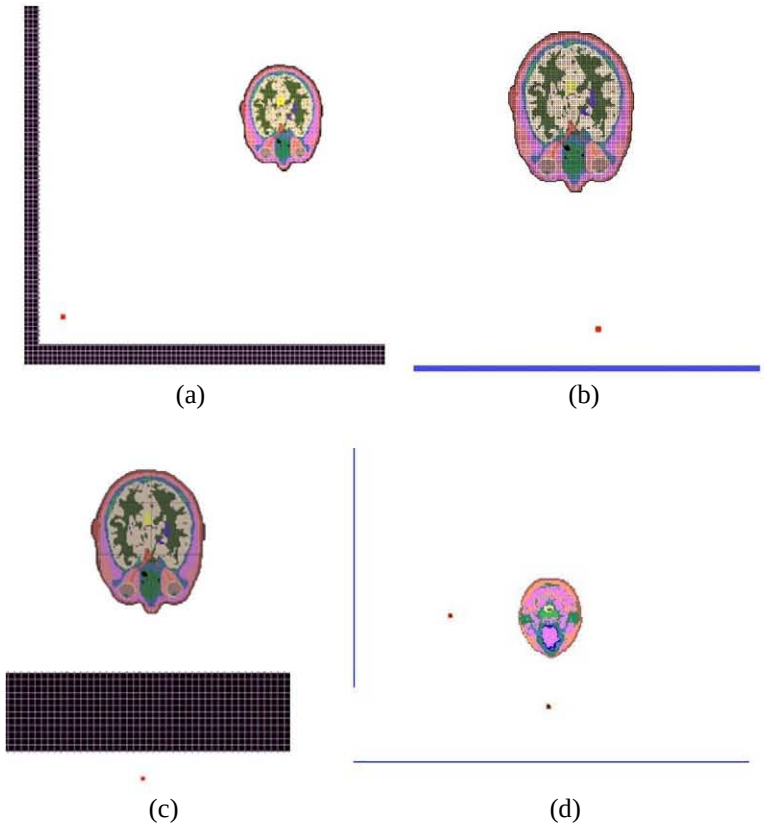


Figure 1. Schematic view of the analyzed exposure situations: (a) Head at 40 cm from the antenna which is at 4 cm of both walls. (b) Head at 20 cm from the antenna and at 24 cm of a metalic wall. (c) Head at 20 cm from the antenna, which is 4 cm on the opposite side of the brick wall. (d) Head in presence of two antennas, surrounded by metalic cabinets.

The antennas have been simulated, in all cases, as half-wavelength dipoles, operating at a frequency of 2400 MHz with a radiated power of 100 mW. To simulate the user, a high-resolution head and shoulders mesh,

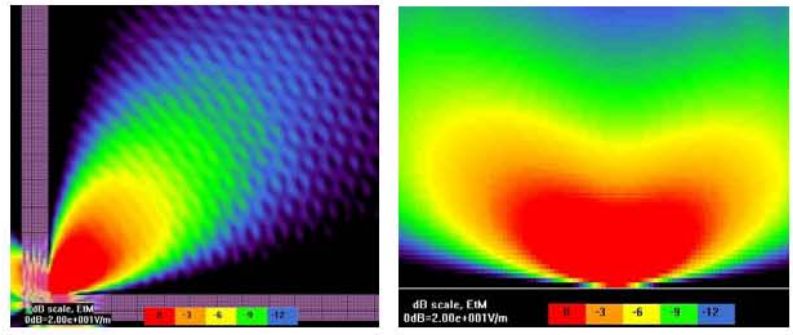
developed from nuclear magnetic resonance by REMCOM Inc. and the Hershey Medical Center, Hershey, PA, USA, has been used. The model has 2 x 2 x 2,5 mm cells and includes 17 different biological tissues which corresponding densities and dielectric characteristics at the operating frequency (2400 MHz) are sumarized in table 1 [9].

The walls have been modeled by rectangular plates with a width of 12 cm, by using a material which simulates the dielectric characteristics of brick, with a relative permitivity of $\varepsilon_r = 5.1$ and a conductivity of $\sigma = 0.028$ S/m, assumming they are similar to those corresponding to 1800 and 2140 MHz [10].

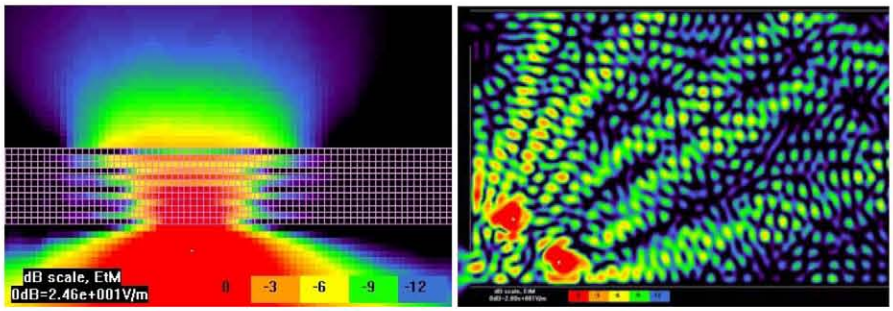
Tissue	ε_r (S/m)	σ (S/m)	ρ (kg/m^3)
Skin	37.63	1.29	1125
Tendon	44.03	1.80	1151
Fat, yellow marrow	4.4	0.08	943
Cortical bone	11.67	0.41	1850
Cancellous bone	17.47	0.60	1080
Blood	53.31	2.68	1057
Muscle	55.84	2.32	1059
Grey matter	46.47	2.10	1035.5
White matter	35.80	1.36	1027.4
Cerebro-spinal-fluid	66.87	3.22	1000
Sclera/cornea	51.77	2.11	1151
Vitreous humor	66.80	2.48	1000
Nerve	31.61	1.10	1112
Cartilage	37.18	1.57	1171
Tongue, thyroid	53.14	2.05	1059
Cerebellum	47.31	1.79	1035.5
Esophagus	36.10	1.47	1126

Table 1. Relative permitivities, conductivities and densities of the tissues in the head model for 2400 MHz.

By using the FDTD method, we have calculated the electric field values in the proximity of the antennas when there is no exposed person, to be compared with the limits stablished in the exposure guidelines (reference levels). Moreover, the SAR values inside the human head model have been calculated to be compared with basic restrictions. Figure 2 shows contour plots of the calculated fields in absence of the head model for, respectively, the four exposure situations described in the first paragraph.



(a) (b)



(c) (d)

Figure 2. Contour plots of the calculated fields in absence of the head model for the four exposure situations shown in figure 1.

In all the studied configurations, it can be observed that local field values in the position where the person is to be located are below the reference level for this frequency (61 V/m for the electric field). Spatially averaged values are obviously lower. As it is well known, guidelines compliance based on reference levels ensures the fullfilment of guidelines based on basic restrictions. Nevertheless, in exposure situations at short distances from the antennas, it is interesting the assessment of the SAR. The calculated values of SAR averaged over the whole exposed object (SAR_{wb}), so as the maximum local SAR values, averaged over 10 grams of contiguous tissue (SAR_{10g}), are shown in table 2.

	Geometry (a)	Geometry (b)	Geometry (c)	Geometry (d)
SAR_{wb} (W/kg)	0.00044	0.00054	0.00012	0.0006
SAR_{10g} (W/kg)	0.008	0.019	0.008	0.027

Table 2. SAR_{wb} and SAR_{10g} for the four simulated exposure situations.

It can be appreciated that SAR_{wb} and SAR_{10g} values are far below the corresponding basic restrictions for all geometries.

B. Use of a PDA device close to the user's face.

The study of the SAR produced by the use of PDA devices is interesting because, due to the reduced screen size, the distance from the antenna to the eye of the person (which is known to be a critical organ) can be very short. For that reason, we have modeled a 2400 MHz antenna in front of the eye of the head and shoulders model at several distances, from 5 to 30 cm, trying to simulate a worst-case exposure situation. The electrical and geometrical models of the antenna and the person are the same than those used in the previous section. Results for the calculated maximum SAR_{10g} as a function of the antenna-aye distance are presented in figure 3 for different antenna radiated powers.

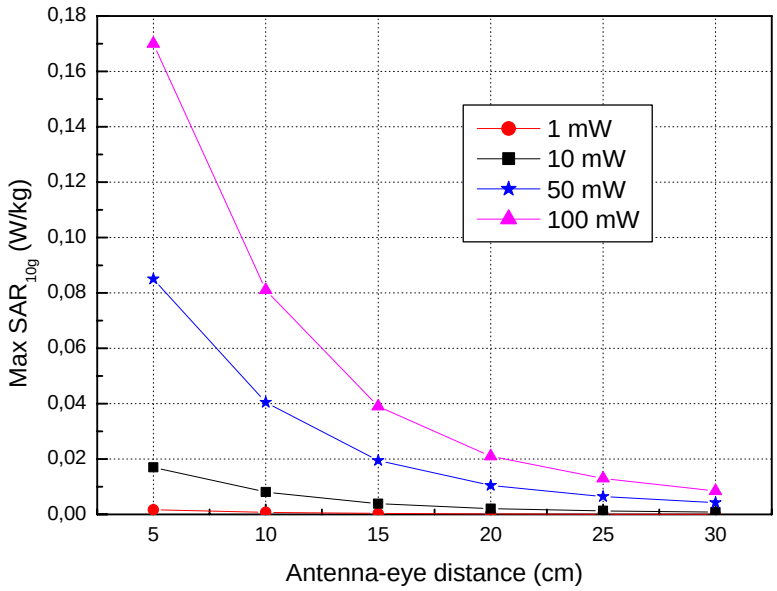


Figure 3.- Maximum SAR_{10g} as a function of antenna-eye distance for different radiated powers.

It can be seen that SAR values increase strongly as the antenna-eye distance becomes shorter, although the maximum value of 0.18 W/kg, obtained for the lowest (unusual) considered distance, corresponding to a radiated power of 100 mW (the maximum expected with WiFi or Bluetooth standards), clearly fulfills safety guidelines.

Conclusions

In this work, the human exposure to the electromagnetic fields from the antennas of wireless devices such as those of WLAN access points or WiFi or bluetooth personal digital assistants has been analyzed by using the FDTD method. Several exposure situations have been considered, assessing field levels and SAR in the exposure to access point antennas, to be compared with reference levels and basic restrictions, respectively, or max SAR_{10g} in short-distance exposure to a PDA device.

Results show that the exposure levels, even in worst case situations, as can be the case of WiFi access point or blueooth antennas at a short distance in front of the eye of a person, are lower than those obtained when analyzing the exposure to mobile phones, the SAR_{10g} values being far below the basic restrictions from the guidelines.

Acknowledgements

This work has been supported by the PN I+D+I of the Spanish Ministry of Science and Education, State Secretariat for Universities and Research, project TIC 2003-00130.

References

[1] Real Decreto 1066/2001, de 28 de septiembre, por el que aprueba el Reglamento que establece condiciones de protección del dominio público radioeléctrico, restricciones a las emisiones radioeléctricas y medidas de protección sanitaria frente a emisiones radioeléctricas, B.O.E. de 29 de septiembre de 2001.

[2] European Commission 1999 Council Recommendation (1999/519/EC) of 12 July 1999 on the Limitation of Exposure of the General Public to Electromagnetic Fields (0 Hz to 300 GHz). *Official Journal of the European Communities* **L199** 59-70.

[3] ICNIRP (International Commission on Non-ionizing Radiation Protection) Guidelines for limiting exposure to time-varying electric, magnetic and electromagnetic fields (up to 300 GHz) Health Phys 74 pp 494-522, 1998.

[4] European Union 2004 DIRECTIVE 2004/40/EC of the European Parliament and of the Council of 29 April 2004 on the minimum health and safety requirements regarding the exposure of workers to the risks arising from physical agents (electromagnetic fields) *Official Journal of the European Communities* **L 159** 47 1-26.

[5] K. R. Foster, "Dosimetric Studies on Wireless LANs," COST 281 Workshop, Graz, Austria, April 20-21, 2006.

[6] Chr. Bornkessel and M. Wuschek, "Exposure Measurements in Different WLAN-Scenarios," COST 281 Workshop, Graz, Austria, April 20-21, 2006.

[7] A. Cortel-Carrasco, A. Gati, M- Wong and J. Wiart, "WiFi Exposure Assessment", Abstracts of the XXVIII Annual Meeting of the Bioelectromagnetics Society (BEMS' 03), Cancun, Mexico, pp 49-51, June 2006.

[8] S. Kuehn, A. Kramer, U. Lott and N. Kuster, "Assessment Methods for Demonstrating Compliance with Safety Limits of Wireless Devices Used in Home and Office Environments," CD Proceedings of the XXVIIIth General Assembly of the International Union of Radio Science (URSI), New Delhi (India), October 2005.

[9] C Gabriel C. Gabriel and S. Gabriel, Compilation of the dielectric properties of body tissues at RF and microwave frequencies, *Technical Report* AL/OE-TR-1996-0037, King's College, Physics Department, London, 1996, available http://www.brooks.af.mil/AFRL/HED/hedr/reports/dielectric/home.html.

[10] P. Bernardi, M. Cavagnaro, R. Cicchetti, S. Pisa, E. Piuzzi and O. Testa, "A UTD/FDTD Investigation on Procedures to Assess Compliance of Cellular Base-Station Antennas With Human-Exposure Limits in a Realistic Urban Environment," IEEE Trans. Microwave Theory Tech., vol. 51, pp. 2409-2417, December 2003.

ELECTROMAGNETIC FIELD PREVISION AND EXPERIMENTAL VALIDATIONS IN INDOOR ENVIRONMENTS

MARINA BARBIROLI[1], MARIA LUCIA CALABRESE[2], GABRIELE FALCIASECCA[1], RITA MASSA[2]

[1]DEIS, UNIVERSITY OF BOLOGNA, ITALY
VIALE RISORGIMENTO, 2 - 40136 – BOLOGNA, ITALY
GFALCIASECCA@DEIS.UNIBO.IT
[2] DIET, UNIVERSITY OF NAPLES FEDRICO II, ITALY
VIA CLAUDIO, 21 - 80125 – NAPOLI, ITALY
MASSA@UNINA.IT

Abstract
The aim of this study was to provide an optimization procedure in order to experimentally evaluate RF exposure levels due to wireless devices, other than phones, used in home and office environments. To this end, several measurements were carried out at UMTS and Wi-Fi frequencies and the results were then compared with simulations provided by the ray tracing prediction model ARMONICA. The comparison between measurement and numerical results showed a satisfactory agreement and suggest that, in order to avoid time consuming measurements for monitoring the electromagnetic field levels due to wireless communications in indoor environments, the use of a ray tracing prevision model is a valid support allowing to perform experimental validations only in that points where the simulator has shown some critical aspect.

Introduction
In the last years the enormous growth of mobile telecommunications leads to the necessity of developing effective and accurate techniques to calculate and measure the electromagnetic field (EMF) levels in indoor environments. To determine the EMF levels and to assure population against excesive exposure according to the international standards [1], [2], that have specified the exposure limits, measurements must be done in the place under test, using appropriated procedures for the new types of radio communications signals. However, the use of experimental valuations in order to determine the EM fields levels in indoor settings could give rise to high costs and long times; for this reason an EMF prevision software could represent an advantageous opportunity to reach the purpose. The computation of electromagnetic field propagation in real environments is a complex problem for the difficulty to describe with sufficient precision the antenna system, the geometry, the electromagnetic properties of present objects, the morphology and the ground characteristics.
Besides, the zone interested by the field computation could be extremely extensive compared with the wave lengths of the typical mobile communication frequencies, so that the computation resources could become an excessive load. It is for these reasons, that the classical numerical techniques for the resolution of Maxwell equations such as the finite elements method (FEM) or the finite difference time domain technique (FDTD) are inapplicable. So many studies were carried out about this argument and empiric and semiempiric models were developed to solve the problem [3-6], but in the two last decade the ray tracing techniques [7-9] were applied to the EMF prediction since it is proved the more appropriate, although there are still some unsolved questions.
The aim of this study is to provide a methodology for characterizing realistic electric-field exposures in home, office and occupational settings and suggests an approach for evaluating compliance with guideline limits in such settings. To this end, several measurements were carried out at UMTS and Wi-Fi frequencies and the results were then compared with simulations provided by a ray tracing prediction model.
Materials and methods.
Simulations. The program used for the EMF prevision was ARMONICA; it was developed by DEIS (Dipartimento di Elettronica, Informatica e Sistemistica) at the University of Bologna in a joint work with A.R.P.A. Emilia Romagna (Italy). In particular, we used the "mray" module; it calculates the EM field in the analysis point as the vectorial sum of all contributions corresponding to all main rays that reach the receiving

point after a number of interactions with the possible obstacles. The adopted program implements a three dimensional spatial ray tracing model involving both reflection and rifraction contributions but negleting the diffraction ones. The program requires in input 5 files in order to:

- describe the radiative characteristics of the trasmitting antenna;
- describe the geometrical characteristics of environment:
- specify the electromagnetics properties of the materials;
- set up opportune boolean values in order to have an output file with the description of the various rays which contribute to the electromagnetic field value in each analysis point;
- define the irradiated signal frequency, the maximum number of reflected rays, positioning and orientation of the transmitting antenna, power supply, analysis domain and the type of output quantity.

The program provides in output:

- the amplitude of the electric field components: |Ex| [V/m]; |Ey| [V/m]; |Ez| [V/m];
- the amplitude of the electric field |E| [V/m];
- the received power [dB].

Measurements. A large number of measurements were carried out in different environments and configurations. Several analysis domains were considered: the microwave laboratory room (fig. 1), an office room (fig. 2) and a hall way out of the DIET (Department of Electronic and Telecommunication Engeneering at the University of Naples Federico II). The WiFi or UMTS signal was transmitted by either a WLAN antenna (Cisco Aironet Yagi 1949) or a ridged horn (Schwarzbeck BBHA 9120D). The measurements were performed using either a spectrum analyzer (R&S FSH3) connected to the receiving antenna (precision conical dipole PCD 8250, Austrian Research Centers, Seibersdorf), or a vector network analyzer (Anritsu 37247C) connected to the receiving (PCD 8250) and transmitting antennas. In the latter, several positions of the transmitting antenna, working at 2.0 GHz frequency, were adopted, while the receiving antenna was mounted on an automated planar scanning system (fig.3). In this way a planar distribution of the electric field was obtained [10] as shown in fig. 4. Then we analyzed the predictive potentality of the ray tracing technique in indoor environments by comparing the numerical results with those observed in the several measurements carried out in different settings.

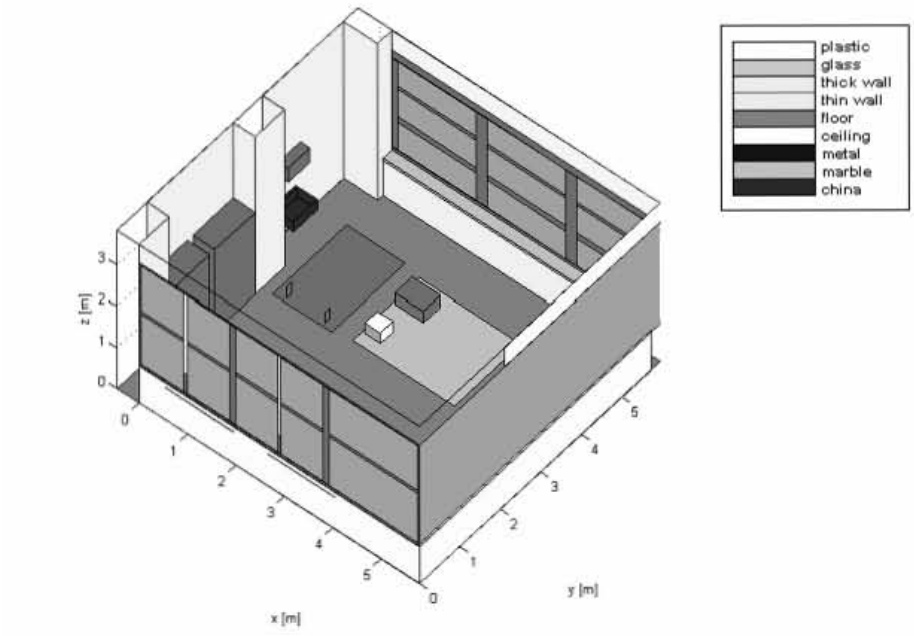


Fig. 1. Matlab three-dimensional reconstruction of the microwave laboratory at DIET, Un.of Naples Federico II.

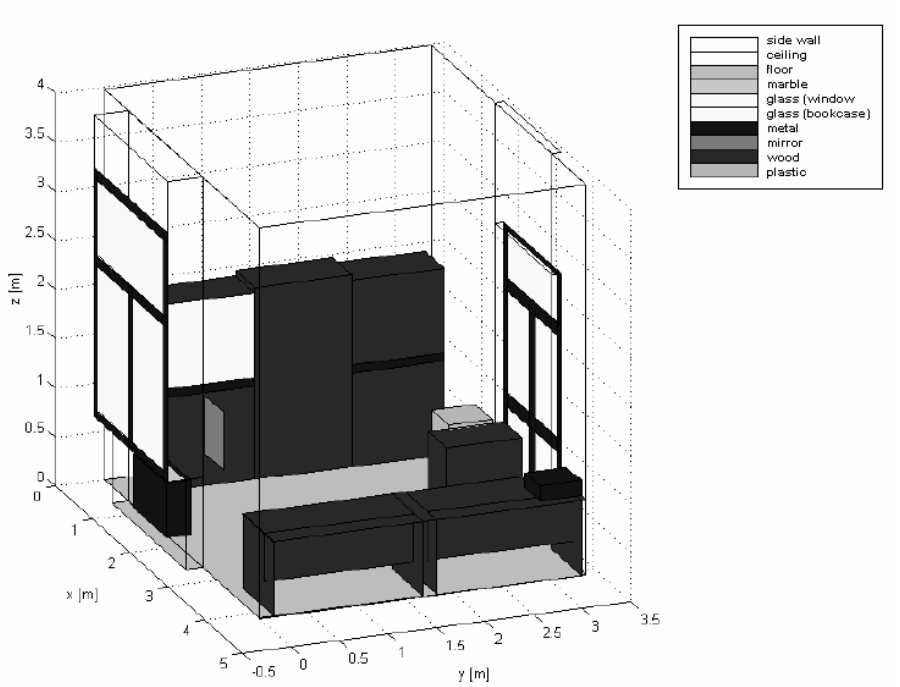


Fig. 2. Matlab three-dimensional reconstruction of the office room at DIET, Un.of Naples Federico II.

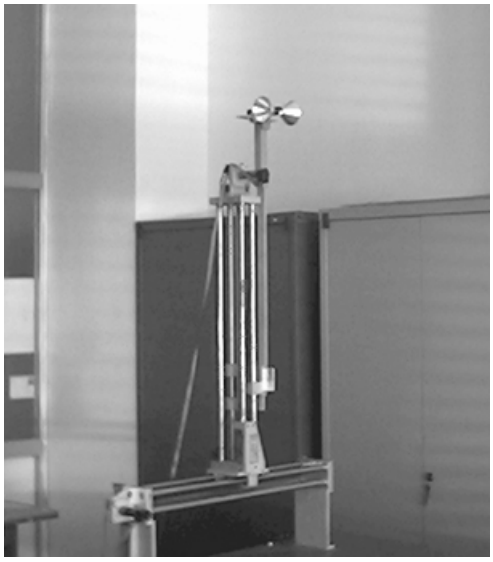
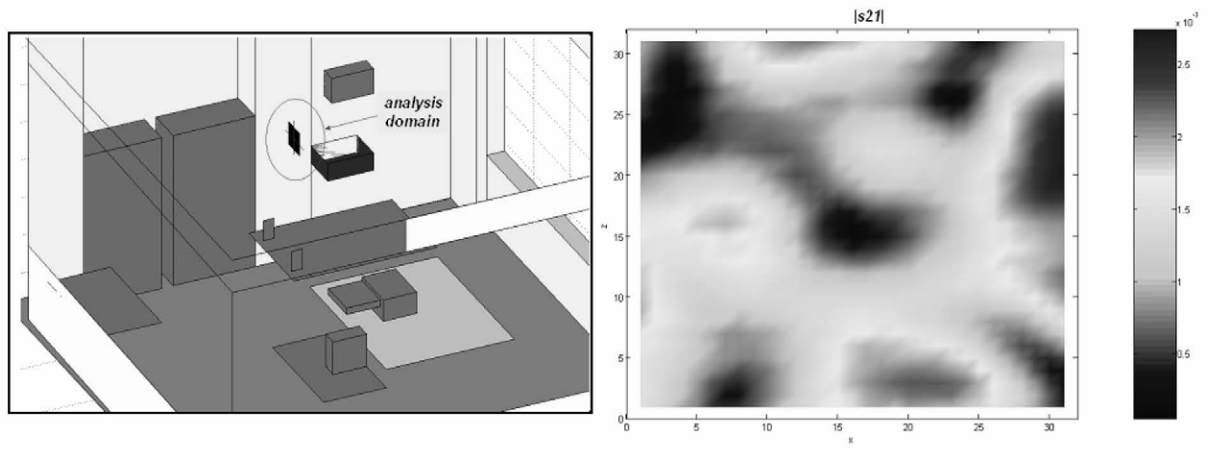


Fig. 3. Precision conical dipole receiving antenna mountated on planar scanning system.



a) b)

Fig.4.a) Microwave laboratory. Analysis domain; b) planar distribution (0.3 x 0.3 m^2) of the measured |s21| values.

Results. The comparison between measurement and numerical results showed a satisfactory agreement (figg. 5, 6). Although, due to the complexity of the analysis domain, some critical aspects were evidentiated: a not accurate geometric description of the environment can strongly affect the prevision model results; the addition of diffraction contributes can improve the numerical results; in indoor environments it isn't always simple to guarantee the far field conditions at the wireless working frequencies; a very accurate technical decription of the instrumentation is necessary.

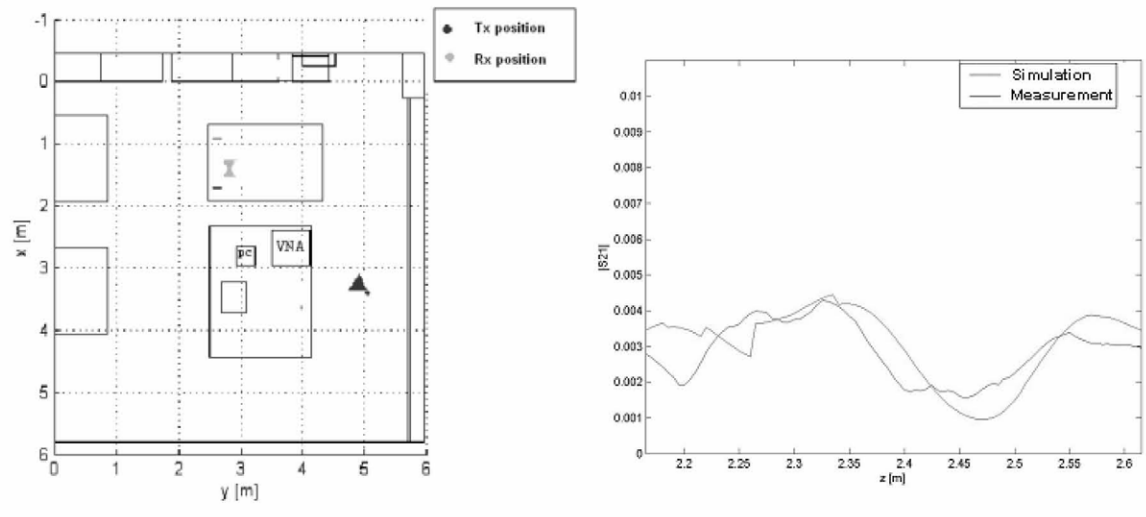


Fig. 5. Measured and calculated |s21| values and the corresponding scenario

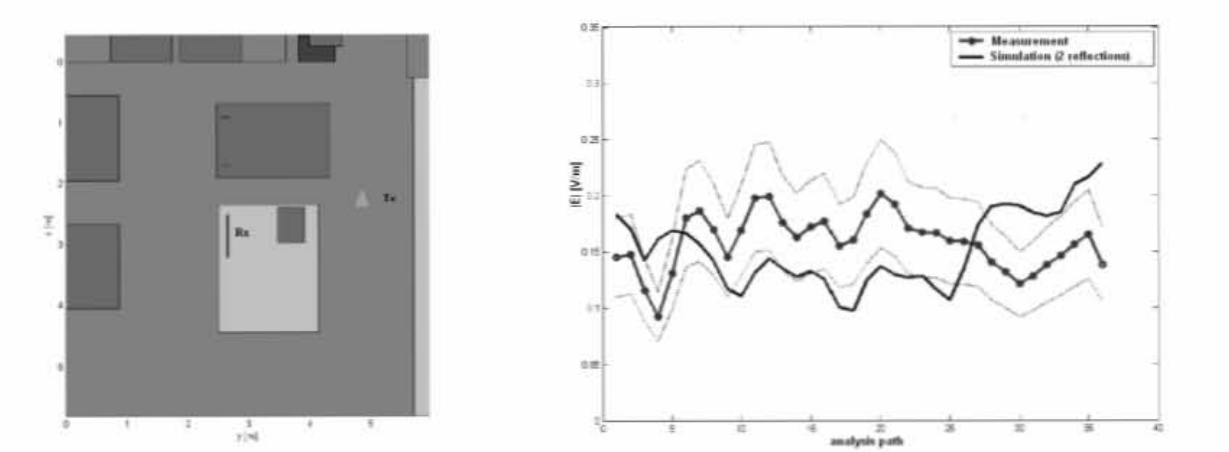


Fig. 6. Calculated and measured electric field levels, with estimated uncertainity, and the corresponding scenario.

SUMMARY

The aim of this study was to provide an optimization procedure for evaluating RF exposure levels due to wireless devices other than phones used in home and office environments. To this end several measurements were carried out in different settings; the results were then compared with those calculated by means of a ray tracing prediction model.

A satisfactory agreement between the experimental and calculated results suggest that, in order to avoid time consuming measurements for monitoring the electromagnetic field levels due to wireless communications in indoor environments, the use of a ray tracing prevision model is a valid support allowing to perform experimental validations only in that points where the simulator has shown some critical aspect.

AKNOWLEDGMENTS

The authors would like to remember professor Guglielmo d'Ambrosio for his constructive and helpful suggestions. The work was supported by CdC-ICT Campania Region Italy.

REFERENCES

[1] International Commission on Non-Ionizing Radiation Protection (ICNIRP), *Guidelines for Limiting Exposure to Time-Varying Electric, Magnetic, and Electromagnetic Fields (up to 300 GHz)*, Health Physics, no. 4, vol. 74, pp. 494-522, April 1998;

[2] American National Standards Institute (ANSI), *IEEE C95.1-1991: IEEE Standard for safety Levels with Respect to Human Exposure to Radio Frequency Electromagnetic Fields, 3kHz to 300 GHz*, IEEE Inc., 345 East 47 Street, New York, NY 10017-2394, USA;

[3] M. Barbiroli, C. Carciofi, M. Frullone, P. Grazioso, *A measurement-based methodology for the identification of validity domains of prediction models in urban environmen*t, IEEE Trans. Vehicular Tech., Vol 49, No. 5, pp. 1508-1515, Sept. 2000;

[4] M. Hata, *Empirical Formula for Propagation Loss in Land Mobile Services*, IEEE Trans. Vehicular. Tech., Vol. 29, No. 3, Aug. 1980;

[5] J. Walfish, H. Bertoni, *A theoretical model of UHF propagation in urban environments*, IEEE Trans. Ant. and Prop., Vol. 36, No. 12, pp. 1788-1796, Dec. 1988;

[6] H. H. Xia, H. Bertoni *et al.*, *Radio Propagation Characteristics for Lineof- Sight Microcellular and Personal Communication*, IEEE Trans. Ant. And Prop., Vol. 41, No. 10, pp. 1439-1446, Oct. 1993;

[7] Vittorio Degli-Esposti, Giancarlo Lombardi, Cristiano Passerini, and Guido Riva, *Wide-Band Measurement and Ray-Tracing Simulation of the 1900-MHz Indoor Propagation Channel: Comparison Criteria and Results,*

IEEE Transactions on Antennas and Propagation, vol. 49, no. 7, july 2001;
[8] G.E. Athanasiadou, A.R. Nix, *A Novel 3-D Indoor Ray-Tracing Propagation Model:The Path Generator and Evaluation of Narrow-Band and Wide-Band Predictions,* IEEE Transactions on Vehicular Technology, Vol. 49, no. 4, july 2000;
[9] M. Barbiroli, C.Carciofi, V. Degli-Esposti, G. Falciasecca, *Evaluation of Exposure Levels Generated by Cellular Systems: Methodology and Results*, IEEE Transactions on Vehicular Technology, vol. 51, no. 6, november 2002;
[10] M. Barbiroli, M. L. Calabrese, G. Falciasecca, R. Massa, *Electromagnetic Field Measurements and Simulations at UMTS and Wi-Fi Frequencies in Indoor Settings*, The Bioelectromagnetics Society 28th Annual Meeting, June 11-15, 2006, Cancun, Mexico.

A FAMILY OF RF EXPOSURE SISTEMS FOR MONITORING CONFORMATIONAL CHANGES OF BIOMOLECULES INDUCED BY ELECTROMAGNETIC FIELDS

Enrico M. Bucci[1], Ovidio M. Bucci[2,3], Maria Lucia Calabrese[2], Rita Massa[2]

[1] *IBB, CNR- NAPLES*
VIA MEZZOCANNONE 16, NAPOLI, ITALY
bucci@chemistry.unina.it
[2] *DIET, UNIVERSITY OF NAPLES FEDRICO II, ITALY*
VIA CLAUDIO, 21 - 80125 – NAPOLI, ITALY
MASSA@UNINA.IT
[3] *IREA, CNR-NAPLES*
VIA DIOCLEZIANO 328, NAPOLI, ITALY
bucci@unina.it

Abstract.
A set of different devices for "*in vitro*" exposures of biological samples (DNA, proteins) to electromagnetic field (300 MHz – 2.45 GHz) and the contemporary control of conformational changes of the exposed biostructure was designed and tested. To this end all the RF applicators were provided of a non perturbative optical apparatus, which allows the continuous monitoring, during the exposure, either the absorption spectra or the absorbance at a given wavelenght in order to observe reversible effects induced by the electromagnetic field.

Introduction

In vitro studies performed on simple but fundamental components of biological systems, i.e., biomolecules, in particular proteins and nucleic acid and artificial or isolated fragments of membranes, can provide important insights into fundamental mechanisms for biological effects due to electromagnetic field action. Proteins possess usually a net charge at pH corresponding to the native condition; moreover a large number of charge aminoacid residues are distributed in their structure. Protein structures are intrinsically flexible structures and can assume multiple conformations (in some cases called "open" and "closed"forms). During the course of their biological function, proteins undergo different types of structural rearrangements ranging from local to large-scale conformational changes. Since protein machines are flexible structures having own electric charges, such motions involved in many basic functions such as catalysis, regulation, transportation, and aggregation could be triggered by their interactions with electromagnetic field.

Since many years our research group is involved in the study of interaction mechanisms between the electromagnetic fields and biomolecules. An irreversible time dependent inactivation was observed in thermophilic enzymes exposed at 10.4 GHz. The percentage of deactivation depended on the temperature (60 – 90°C) , SAR (0.8 – 3.1 W/g), and microenvironment (enzyme concentration or influence of salts). Conformational changes detected by fluorescence and circular dichroism techniques suggested that microwaves induced in this cases protein structural rearrangements not related to temperature [1,2,3]. Non thermal effects induced by exposure to 1.95 GHz, a typical frequency used in mobile communication, have been observed on the kinetic of reconstitution of the heme binding site from acidic tuna myoglobin solution [4]. More recently our attention was focussed on the possibility that electromagnetic field can remotely control these nano-biomachines [5,6].

The possibility of evidencing possible reverse effects (effects that fade away when the field is turn off)

is particularly attractive, to this end a family of applicator working in the 300 MHz – 2.45 GHz frequency band was designed and tested in order to expose macromolecules to microwaves and contemporary control the conformational change of the structure during the exposure. In all the devices is possible to insert two fibre optics connected, from one end, to the spectophotometer Lambda 25 (Perkin Helmer, Wellesley, USA) while the other end was in contact with the quartz cuvette containing the sample.

Device design

At low frequencies (300 MHz – 900 MHz) the applicator was a coil similar to that used in [7]. It consisted of 35 turns with a cross section of ~1 cm^2 and with an open structure in the middle in order to allow the insertion, perpendicularly to the axis coil, of two teflon cilinders that facilitate accurate placement of the fibre optics for absorbance measurements (fig.1). The sample, a DNA solution, was contained in a 3mm x 3mm x 22 mm quartz cuvette axially inserted into the coil. Being the coil an open structure it was possible to follow both the increase of temperature and the temperature distribution on the sample surface by means of an infrared thermocamera (ThermoVision A40M, Flir System, North Billerica, Boston, USA).

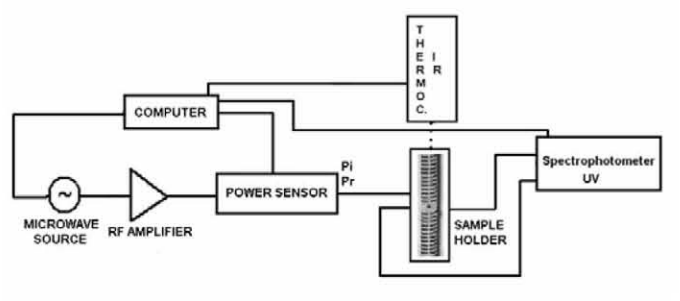


Fig.1 Exposure setup at 300 MHz and 900 MHz

Another applicator was designed in order to expose samples at 1.95 GHz, which is an up-link frequency of universal mobile telecommunication systems (UMTS). It was a rectangular thermostated waveguide (WR 430: 109.2 mm x 54.6 mm). The feeding end of the waveguide was a coax waveguide adapter Maury Microwave R213A2 (VSWR < 1.05) while on the other side a fixed short circuit (SC) termination was adopted. The sample was positioned in a maximum of the unperturbed field and inserted into a teflon support which allowed the fibre optics (fig.2) insertion.

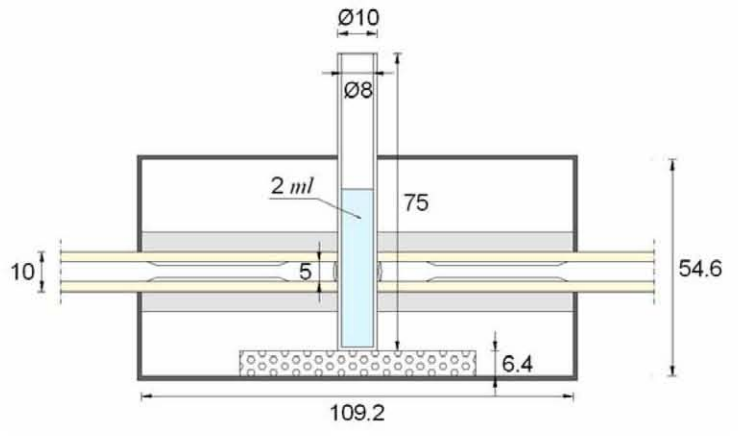


Fig.2 Cuvette inserted into a WR430 waveguide and fibre optics holder

Finally a thermostated rectangular waveguide cavity (72 mm x 33.8 mm x 340 mm), coupled to the coax-adapter waveguide by means an inductive diaphragm and excited by a 2.47 GHz radiation (fig.3), allowed the exposure of the samples to the only magnetic field. In fact, sample size (35 mm x 10 mm x 1 mm) and position (in contact with the short circuit) ensured a minimum interaction with the electric field and a satisfactory homogeneity of the magnetic field.

Dosimetry

Numerical and experimenatal dosimetry was carried out in order to assess efficiency and field uniformity into the sample. The efficiency of the system (the ratio between the absorbed power, P_a,and the incident power, P_0 , $\eta = P_a/P_0$) and the absorbed power distribution inside the samples were numerically and experimentally evaluated.

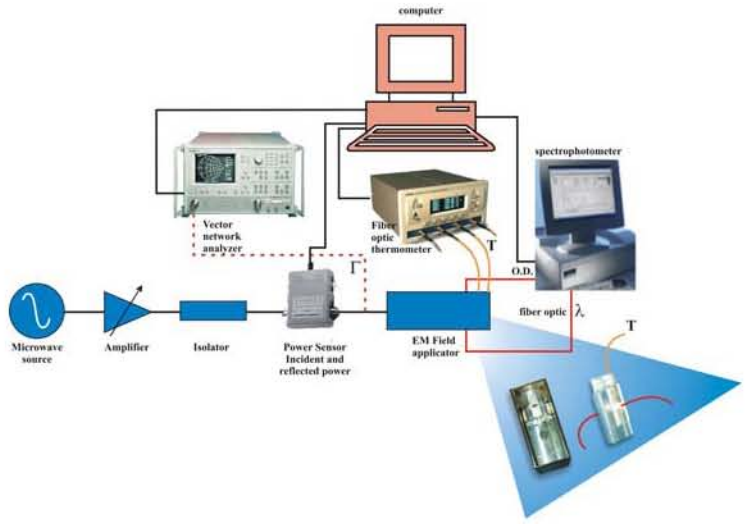


Fig.3 Exposure setup at 2.47 Ghz for magnetic field sample exposures.

In particular the following parameters were calculated [8]:

- $|E^1(x,y,z)|$: the local electric field amplitude per unit incident power [(V/m)/W]. This was evaluated at each node of the computing domain.
- $SAR^1(x,y,z) = \sigma |E^1|^2 / 2\rho$: the local absorbed power per unit mass and per unit incident power [(W/kg)/W]. This is also the local specific efficiency, and it is zero outside the sample ($\sigma = 0$).
- AV^1: the average $SAR^1(x,y,z)$ over the sample [(W/kg)/W].
- SD^1: the standard deviation of $SAR^1(x,y,z)$ values
- $CV = SD^1/AV^1$: the coefficient of variation [9] is usually taken [10] as the "nonuniformity degree"of the SAR^1 (P_0 = 1 W) values. The SAR (any P_0) nonuniformity degree, SD/AV, is the same as $CV = SD^1/AV^1$.

The local SAR values were calculated from the slope of the heating curves [11], T(t), at t = 0, as: $SAR = c\, dT/dt|_{t=0}$ (c being the sample specific heat; t=0 is the starting time of radiofrequency radiation).

The efficiency, $\eta = P_a/P_0$, was evaluated by measuring the reflection coefficient (s_{11}) [12] of the exposure chamber loaded by the samples by means of a microwave vector network analyzer (Wiltron-Anritsu 37269B, Japan) over the working band, being $\eta = 1 - s_{11}^{\ 2}$. In the case of the cavity the power absorbed by the samples was calculated by means of the measurements of the unloaded and loaded Quality factor [12].

Results

The efficiency simulated was successfully verified through measurements of the scattering parameters; as well as the nonuniformity degree was checked and confirmed by means of local temperature measurements using both the infrared thermocamera and the fibre optic thermometer.
The possibility of following the conformational change of the molecule was obtained. In particular we observed as [7] that a DNA double helix, with a gold nanocrystal covalently attached, was opened up and closed back upon exposition to an oscillating RF signal (~1 GHz), i.e., the electromagnetic field denaturated and renaturated the double-helical DNA. The extreme simplicity of assembly and operation of our devices, which resulted to be low cost and with an optical equipment that is commonly used in bio-chemical laboratory, makes them easily available and particularly interesting for studies about interaction mechanisms between biological structures and electromagnetic fields.

References

[1] La Cara F., Scarfì M.R., D'Auria S., Massa R., d'Ambrosio G., Franceschetti G., Rossi M., De Rosa M.: "Different effects of microwave energy and conventional heat on the activity of a thermophilic β-Galactosidase from *Bacillus acidocaldarius*", Bioelectromagnetics, 20, N.3, pag.172-176, 1999

[2] La Cara F., Scarfì M.R., D'Auria S., Zeni O., Massa R., d'Ambrosio G., Franceschetti G., De Rosa M., Rossi M.: "Microwave exposure effect on a thermophilic alcohol dehydrogenase", in press on Protein and Polipeptide Letters.

[3] Porcelli M., Cacciapuoti G., Fusco S., Massa R., d'Ambrosio G., Bertoldo C., De Rosa M., Zappia V.: "Non-thermal effects of microwaves on proteins: thermophilic enzymes as model system", FEBS Letters 402 (1997) 102-106.

[4] F. Mancinelli, M. Canaglia, A. Abbruzzese, G. d'Ambrosio, R. Massa, E. Bismuto: "Non thermal effects of electromagnetic fields at mobile phone frequency on the refolding of an intracellular protein: myoglobin" J. of Cellular Biochemistry, 93, pp.188-196, 2004.

[5] E.M. Bucci, O.M. Bucci, M.L. Calabrese, G. d'Ambrosio, R. Massa, A. Messere, G. Milano, D. Musumeci, G. Petraglia, G. Roviello, "Preliminary Report on a Radiofrequency Controlled Biosensor", The Bioelectromagnetics Society 27th Annual Meeting, June 19-24, 2005, Dublin, Ireland.

[6] E.M. Bucci, G. Bellizzi, O.M. Bucci, M.L. Calabrese, A. Capozzoli, A. Messere, G. Milano, D. Musumeci, G. Petraglia, G. Roviello and R. Massa: "Remote Control of Biomolecules by Radiofrequency: a test study". The Bioelectromagnetics Society 28th Annual Meeting, June 19-24, 2006, Cancun, Mexico.

[7] K. Hamad-Schifferli, J.J. Schwartz, A.T. Santos., S. Zhang, and J.M. Jacobson: " Remote electronic control of DNA hybridization through inductive coupling to an attached metal nanocrystal antenna". *Nature*, 415, 152-155, 2002.

[8] M.L. Calabrese, G. d'Ambrosio, R. Massa, G. Petraglia: "A High-Efficiency Waveguide Applicator for In Vitro Exposure of Mammalian Cells at 1.95 GHz", IEEE Trans. Microwave Theory and Techniques vol. 54,no. 5, pp. 2256-2264, May 2006.

[9] R. R. Sokal, F. J. Rohlf, "Biometry", 1st ed., San Francisco, California, USA: W. H. Freeman and Co., 1969, Chapter 4, pp. 50-63.

[10] N.Kuster, F. Schonbörn, "Recommended minimal requirements and development guidelines for exposure setups of bio-experiments addressing the health risk concern of wireless communications", *Bioelectromagnetics*, vol. 21, issue 7, pp. 508-514, 2000.

[11] J.W. Allis, C.F. Blackman, M.L. Fromme, S.G. Benane, “Measurement of microwave radiation absorbed by biological systems. Analysis of heating and cooling data”, Radio Sci., vol. 12, issue 6(s), pp. 1-8, 1977.

[12] D. M. Pozar, “Microwave Engineering”, 1st ed., New York, USA: Addison-Wesley Publising Co. Inc., 1993.

EFFECTS OF 915 MHZ ELECTROMAGNETIC FIELD IRRADIATED IN TEM-CELL ON BLOOD-BRAIN BARRIER AND NEURONS IN THE RAT BRAIN.

MASUDA H. [1], USHIYAMA A. [1], TAKAHASHI M. [1], WANG J. [2], FUJIWARA O. [3], HIKAGE T. [4], NOJIMA T. [4], FUJITA K. [5], KUDO M. [5] AND OHKUBO C. [6]

[1]Dept. of Environmental Health, National Institute of Public Health, 2-3-6 Minami, Wako-shi, Saitama 351-0197, Japan. [2]Dept. of Computer Science and Engineering, Graduate School of Engineering, Nagoya Institute of Technology, Gokiso-cho, Showa-ku, Nagoya 466-8555, Japan. [3]Dept. of Electrical and Computer Engineering, Nagoya Institute of Technology, Gokiso-Cho, Showa-ku, Nagoya 466-8555, Japan. [4]Graduate School of Information Science and Technology, Hokkaido University, Kita-ku, Sapporo, 060-0814, Japan. [5]Dept. of Pathology, Tokyo Medical University, 6-1-1 Shinjuku, Shinjuku-ku, Tokyo 160-8402, Japan. 6RAD, World Health Organization, Geneva CH1211, Switzerland.

Abstract

This study was carried out to evaluate whether or not albumin leakage and degenerated dark neurons were indeed present in rat brains of 50 days after a single 2 hour-exposure to 915MHz electromagnetic field (EMF) as reported earlier by Salford et al. Thirty two male F344 rats (12 weeks old) were used in the present study and they were exposed to 915MHz EMF at 0, 0.02, 0.2 and 2.0 W/Kg of whole body averaged SAR in a TEM cell for two hours as protocols described by Salford et al. The rats were killed 50 days later by a trans-cardiac perfusion technique with 4% PFA fixative solution under a deep anesthetic condition. The brains were examined histologically and immunohistochemically. As results, degenerated dark neurons, which were studied by Cresyl violet, HE and Fluoro Jade B stainings were only rarely present in small numbers with no statistically significant difference between exposed and sham exposed animals. In addition, no albumin immunoreactivity was observed anywhere even in any exposed groups. We must conclude thus that the data reported by Salford et al can not be confirmed by the present confirmation study.

Introduction

Since Salford et al. found that albumin leakage sites and increase in appearance of degenerated neurons presented in the rat brain 50 days after a single 2 hours-exposure to radiofrequency electromagnetic field (RF-EMF), many research groups have tried to confirm Salford's results. However, there were few confirmation studies performed using the same exposure system, endpoints, and experimental schedule. Therefore, the aim of present study was to confirm their reported results using a similar experimental design they used.

Thirty two male F344 rats (12 weeks old) were used in the present study. The rat placed in an acrylic box was set only on the upper side of the TEM-cell (Fig. 1) and was exposed to 915MHz EMF at 0, 0.02, 0.2 and 2.0 W/Kg of whole body averaged SAR for two hours as protocols described by Salford et al.. To know the whole body averaged SAR value that actually irradiated to the rat, we measured input, output, and reflected power using a power meter.

The rats were killed 50 days later by a trans-cardiac perfusion technique with 4% PFA fixative solution under a deep anesthetic condition. In the three selected sections of the brain (Fig. 2), albumin leakage sites were examined using immunohistochemistry of albumin. Furthermore, the appearance of degenerated neurons was evaluated using Cresyl violet, HE and Fluoro Jade B staining. We used a cold injury method for making positive control. A piece of dry ice was put on the skull of the rat for 5 min. Brown stained area was observed in positive control.

Degenerated dark neurons, which were studied by Cresyl violet, HE and Fluoro Jade B staining were only

rarely present in small numbers with no statistically significant difference between exposed and sham exposed animals. In addition, no albumin immunoreactivity was observed anywhere even in any exposed groups (Fig. 3).

Summary

We must conclude thus that the data reported by Salford et al can not be confirmed by the present confirmation study.

Acknowledgments

This study was financially supported by Association of Radio Industries and Businesses in Japan. We would like to thank Patrick A. Mason, PhD and Air Force Research Laboratory, Human Effectiveness Directorate, Directed Energy Bioeffects Division, Radio Frequency Radiation Branch, for lending us the TEM-cell.



Fig. 1. Exposure system (A)TEM-cell was used in the present experiment. Input, output, and reflected power were measured by a power meter through RF exposure. Whole body averaged SAR values were calculated these measured powers and rat body weights. (B)Rat placed in an acrylic box was set only on the upper side of the TEM-cell.

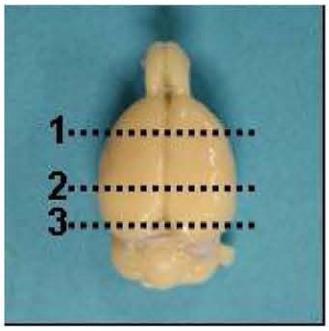


Fig. 2. Evaluated brain section. Three regions of the brain were selected for histological evaluation. Section 1, 2, and 3 are typical region including third ventricule, hippocampus, and pineal body, respectively.

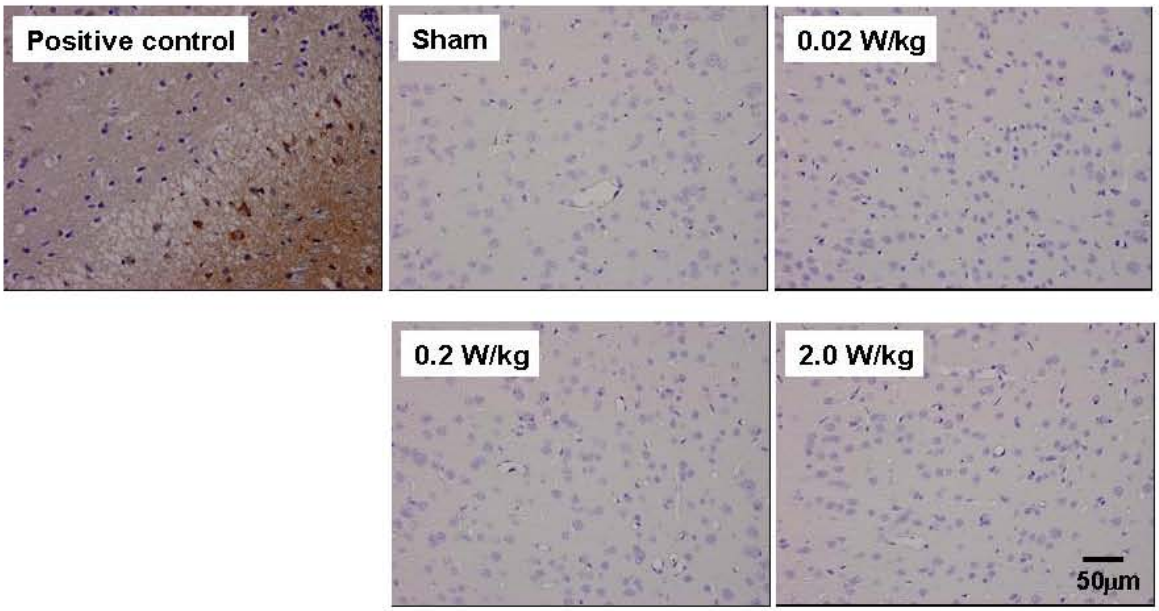


Fig. 3. Typical photographs of albumin immunohistochemistry. Albumin leakage sites were examined using anti-albumin antibody in the brain 50 days after RF exposure. Positive control was made by a cold injury method. A piece of dry ice was put on the skull of the rat for 5 min. Brown stained area was observed in Positive control. On the other hand, no stained area was seen in any exposed groups.

ASPECTS REGARDING RADIOFREQUENCY RADIATION EXPOSURE OF POPULATION IN ROMANIA

MICLAUS SIMONA[1], BECHET PAUL[2]

LAND FORCES ACADEMY, 3-5 REVOLUTIEI ST., 550170 – SIBIU, ROMANIA
miclaus@armyacademy.ro
COMMUNICATION AND INFORMATICS CENTER, 1-3 V. MILEA ST., 550325 – SIBIU, ROMANIA

Abstract
On the background of an accentuated risk perception of Romanian citizens to the radiofrequency (RF) radiation emitted by GSM base station antennas, we present the general situation in our country and results of a little scale measurement campaign we made for RF exposure assessment. The frequency selective method was used, the refinement of the methodology is discussed and results are presented and commented. All measurements showed that urban outdoor and indoor RF exposure is low comparative to the limits given in the ICNIRP guidelines that are applied in our country. We suggest for good quality exposure assessment and the need for a possibility to select between different RF sources radiation contribution in connection to further health impact studies.

Keywords: RF exposure, frequency selective method, measurement methodology, risk assessment

Introduction

Passed years in bioelectromagnetics research show that scientists cannot yet exclude the possibility that electromagnetic fields (EMFs), especially radiofrequency (RF) and microwaves (MW) can cause health problems, even for exposure levels lower than the ones stipulated in present exposure standards. One of the challenges of RF bioelectromagnetics remains the clear demonstration of the existence of athermal or nonthermal effects of RF/MW, since safety standards consider only the thermal biological effects as hazardous, when they give the basic restrictions and the reference levels in conformity [1], [2].

Exposure standards harmonization is not yet accomplished at international level, as with the efforts supported by the International EMF Project of World Health Organization. In the two most known regulations, i.e. ICNIRP guidelines [1] and IEEE standard C95.1-2005 [2], the establishment of the maximum permissible exposure limits is given in different ways: IEEE limits are based on spatial averaging of the incident field over the standing person's projection area, while ICNIRP refers to peak-field limits instead. A sensible aspect is that standard recommendations are based on short-term exposure. Of a special interest in present standardization are the problems concerning mobile and wireless communication systems, due to the rapid and huge spreading of this kind of RF radiation sources in the environment. In Europe there are countries that didn't adopted the ICNIRP reference levels for human exposure, but more stricter ones, as for example Italy and Switzerland, with specific rules for the base station transceivers (BTS) in mobile telephony systems. China and Russia are similar examples, which didn't adopted international guidelines, but due to a different rationale of the limits calculation. A debate is still going on from years, in many countries, on the application of the precautionary principle [3], regarding the sensitive problem of BTS sitting and only some local authorities in Italy, Switzerland and Belgium really apply it. Coming to citizens and media level, the situation is even more complicated, since, for example, neither can people be involved in BTS sitting decision, nor have they the right to be informed of the (expected) EMF exposure.

In Romania, the adopted limits for human exposure are those given in the ICNIRP guidelines [1]. European regulations [4],[5], were applied starting with 2002. That year the Romanian Health Ministry issued the Order no. 1007/13.12.2002 referring to the regulations on admissible exposure limits and the measurement

methodology, order that follows the European Directive no. 199/519/EC. General norms for work safety no. 880/06.12.2002 offer supplementary rules on working places in electromagnetic environment.

In the present, in Romania there are four public mobile communication operators: Vodafone (GSM 900MHz and 3G-UMTS 2GHz), Orange (GSM 900MHz and 3G-EDGE 2GHz), Telemobil - Zapp (CDMA and EV-DO 450 MHz) and Cosmote (DCS 1800MHz). 3G UMTS services were recently launched in Romania by Vodafone – April 2006 and Orange – June 2006. The present number of mobile telephone users in Romania is about 12 million, for a total population of 22 million people (approx. 55% of the population).

Mobile phone BTS antennas debate have become of unprecedented intense public health concern in Romania in the last period, starting with the end of 2005. Numerous journals at central and local level published articles on the issue under the pressure of citizens [6]. Numerous population complaints were received at Local Consumer Protection Agencies, Environmental Agencies and Guards. As a result, some local authorities adopted decisions for national budget financial support of EMF measurements campaigns in 2006 (first one in Cluj county, March 2006 [7]). Most of the newspaper articles and media news were published/broadcasted starting with January 2006 and focused on reported health state impair (even cancer-related cases – one in Oradea city, the second in Sibiu city) and complaints on BTS sitting on the blocks and private gardens (population protests in 2 counties: Sibiu and Zalau). At least 2 titles in newspapers refer to BTS antennas as a second "Tchernobil", by comparison to the nuclear threat. Two private judicial processes are mentioned in media, won by the complaining persons against mobile telephony operators. One hospital (County Hospital Salaj) cancelled its contract to a mobile phone operator in order to renounce to the antenna mounted on the hospital's roof. The National Consumers Protection Agency, which received tens of protests and complaints in 2006, decided to demand the Town (Local) Councils in the country to adopt decisions that forbid further BTS sitting on residential buildings. The Agency is preparing a well documented file on the issue. On the other hand, Romanian Government recognised the potential hazard of BTS antenna sitting (even mounted on its own building), by issuing the Ordinance no. 2/12.01.2006, on supplementary financial rights for hazardous workplace conditions (specific RF emissions) of public functionary, in a quote of 10% from the base salary. The authorised institutions for measurements of EMF emissions in Romania are: the Public Health Direction with its local institutions, Ministry of Defence Health Direction and Ministry of Transportation Health Direction. Measurements made till the end of 2005 in our country were done in the majority by using wideband survey meters type EMR-300 and Narda-8718. Relevant information on GSM topic is available to the public via the ACER Bulletin and ACER website (ACER is the Romanian Electromagnetic Compatibility Association - http://www.acero.ro), GSM Magazine, mobile telephony company websites and the press (which features related international press reports).

On this background, our study aimed to prepare for a reliable measurement campaign of residential exposure. This is needed from at least two essential perspectives: a) compliance testing of BTS antennas and other RF emission sources and in situ measurements, according to present methodology [5], [8] and standards; b) accurate assessment of frequency-selective RF exposure, that should be considered from the view of the finding that biological effects depend on the carrier frequency, as recently proved in the mobile communication band [9].

We had two principal objectives: a) refinement of the measurement methodology in accordance to the aim of the measurement; b) exposure assessment due to RF sources, especially GSM BTS antennas and comparison between quotients afferent to different sources.

The measurements were made by using the frequency-selective method (spectrum analyser with isotropic antenna) in a number of outdoor and indoor locations, urban and extra-urban places, for different settings of the measurement system.

Materials and methods

As for ICNIRP guidelines requirements, the principal need is that the measurement system be a frequency selective one. The equipment must also be sensitive enough, must allow averaging the values over any 6 minutes in time and averaging in space, considering the volume of the human body respectively the interesting areas of it. It is essential to use procedures that allow measurements with low uncertainty and good reproducibility [10], [11].

The equipment we used for most of the measurements was the TS-EMF system by Rohde & Schwarz, Germany. At some point we also used the Field Nose System by Austrian Research Centre in Seibersdorf, which

also helped in comparison of the same measurement results during one session. The TS-EMF system is composed by the R&S FSH3 spectrum analyser, an isotropic sensor (30MHz to 3GHz) and the computer software R&S RFEX for data acquisition and settings management. The tri-axis sensor has got an isotropic characteristic so the measurement is done independent from direction or polarization of the emitter. This makes measurements easier. In contrast to directional antennas, it is no longer necessary to move the antenna for covering all directions and polarization. The Field Nose System uses the proven Add3D technique to conduct precise measurements and is composed by an Anritsu M2711D spectrum analyzer with a broadband omnidirectional precision conical dipole PCD8250 as measurement antenna (80MHz to 2.5GHz), driven by Nose Basic software. The antenna is consecutively positioned in three orthogonal directions during the measurement, by a software-driven rotor. A picture of the two measurement systems is presented in fig.1.



Figure 1 –TS-EMF system by Rohde&Schwarz (left, “spherical antenna”) and Field Nose System by ARCS Seibersdorf, (right, “biconical dipole”).

Reproducible time averaging method with well known uncertainty estimation can be performed on one single point in the area of interest. Different measurement modes were possible and applied: a) single measurement; b) average and peak (e.g. 6 minutes average); c) long term (e.g. determination of time variations of the signals). The most used was the average & peak measurements. To increase the sensitivity of the TS-EMF system, the function Threshold-Calibration can be introduced, and in all measurements this was applied.

The measurement protocol took into account the objectives of the research which was either compliance verification, or in situ measurements [10]-[12]. We followed the measurement methods described in [5] and [8]. No a-priori knowledge was available regarding sources emissions or the environment. The general scheme for compliance verification was not completely followed, since no simulation was made prior to measurements and no measurement with broadband field probe was prior made. The measurements were executed by means of the frequency-selective system, in urban and extra-urban locations, either outdoor or indoor. The choice of measurement points (location and number of points) was in accordance with the general considerations in [5]. Refinement of the measurements by settings modification was made in most locations, in order to consider the “worst case” exposure. Processing of measured data and final report followed each measurement.

For the major services, the TS-EMF system offers pre-defined measurement packets. This should insure optimum settings for evaluation according to single frequencies, complete services and total emission. However, at least in the case of GSM measurements, personally defined packets/settings were also prepared, since we need to refine the measurements. Comparison between results obtained with different settings will be presented and discussed. Data presentation of the measured emissions (field strength, power density or exposure ratio - ‰ of

ICNIRP limit) was possible as a sum value and can be split into frequency bands if necessary. Detected signal spectrum and histograms may be represented.
All measurements were made fully-automatic using the R&S software RFEX and they were performed inside macrocells and mostly outdoor. The ten locations chosen for measurements were situated in intra-urban highly populated areas, and only in two cases it was situated remote from the city. All were positioned in the vicinity of the transmitter sites, the distance between the measurement system and the base stations being from 40 to 500m.

Results and Discussion

A. Refinement of the measurement methodology:
Residential exposure assessment, if highly accurate, is a complex task. It should take into account:

- position of the spot measurement;
- signal characteristics and variations in time and space;
- environment impact thru physical influences (fast fading, etc.)

However, since in the great majority the population partial exposure quotients due to various RF signals proved to be much lower than that stipulated in standards (for example, for BTS antennas generally the measured power density levels are <<10% from the reference levels, [13]), the question of optimum settings of a measurement system may be not so important. But if one is more sceptical regarding fundaments that conducted to present "safe" reference levels in standards, than he might always keep in mind that:

- not only RF/MW heating may be responsible for health hazards, but also athermal/nonthermal mechanisms of interaction could trigger a biological response;
- long term exposure was not the basis of standard value considerations;
- "frequency windows" were proved to exist in connection to specific biological responses,

and then the optimum settings of a system may crucially influence the results of the exposure assessments and further epidemiological findings.

In this respect, it is of big importance to correctly set the resolution bandwidth (RBW), sweep rate (SR) and detector type (DT) [14], in function of the measured signal. Secondary, in the case of GSM signal for example, the resolution of adjacent channels and the effect of number of active time slots should be attentively considered. We made measurements to compare results, while modifying different setting parameters. As an example, we show here the consequences of modification of "Trace mode" (TM) and "Detector type" (DT) on the results obtained in the case of a GSM 900MHz signal measured in one indoor location, with conserving all the interior environmental conditions the same, and all other system settings. The results are showed in table I and were obtained for a series of 10 consecutively measurements for each setting. For these measurements, the commune settings of TS-EMF system were: RBW=200kHz; Span=30MHz; Reference level=91 dBµV; Dwell time=5s.

Table I : Influence of trace mode (TM) and detector type (DT) of the measurement settings on the results

	TM = Clear/Write DT = RMS		**TM = Max hold DT = Positive peak**		**TM = Max hold DT = RMS**	
	Average	***Peak***	***Average***	***Peak***	***Average***	***Peak***
Total field strength, RMS, (V/m)	**0.141** ± 0.005	**0.190** ± 0.004	**0.510** ± 0.004	**0.720** ± 0.003	**0.091** ± 0.003	**0.110** ± 0.006
Max single value (V/m)	**0.050** ± 0.003	**0.050** ± 0.002	**0.082** ± 0.002	**0.111** ± 0.003	**0.051** ± 0.002	**0.050** ± 0.004

"Max hold" setting is generally used for worst case when time variations of the signal are present. "Positive peak detector" represents also a worst case, but it may give over-rated values. "RMS" detector is usually used for non-sinusoidal signals to correctly derive the average signal power (it is especially used for UMTS mobile signals). As one can observe in the table above, the combination "Max hold" + "Positive peak detector" will give the worst case assessment possible. The values in this case are approximately 5 times larger in the case of total field strength then the ones obtained with the setting "Max hold" + "RMS detector" and about 3.5 times higher than the ones with the setting "Clear/Write" + "RMS detector". However, these values may be overestimated. The results repeated as well for measurements on GSM 1800 signals. We could then conclude about the "worst case" settings. Due to these observations, most of the compliance testing or in situ measurements made by us for GSM900 and GSM1800 signals were done by using the intermediary setting, "Clear/Write" + "RMS detector".

Moreover, we were able to observe that a lower RBW, for example one of 30kHz, is a better choice for "worst case" measurement. This setting should be completed by a sufficiently low sweep rate (long dwell time, thousands of milliseconds), or even better, multiple sweeps, so that the independence of the result upon the instantaneous traffic on a GSM signal to be assured.

As a result of lots of GSM measurement sessions, we were able to conclude that it is practically impossible to predict positions in space where hot spots of field distribution will appear, either outdoor or indoor. Time evolution of the field level is only predictable on the basis of traffic diminution in the late time hours, but otherwise is low-predictable also. Special aspects for further refinement of measurement methodology should focus on frequency hopping and power control of BTS.

B. Compliance testing and in situ measurement results:

Peak values measured in some outdoor locations for GSM900 signals are given bellow. Locations 1 and 2 are urban locations, while location 3 is extra-urban. In figure 2 – a,b,c one can visualise these locations. The settings of the TS-EMF system were: Trace Mode:Clear/Write; Detector: RMS; RBW=200kHz, span=30 MHz, Dwell time=5000ms. Power density (S) peak values measured in the 3 locations exampled in fig. 2 are:

$S_1^{peak}=(9.66 \pm 2.73)x10^{-5}$ W/m^2

$S_2^{peak}=(23.00 \pm 5.51)x10^{-5}$ W/m^2

$S_3^{peak}=(62.00 \pm 13.54)x10^{-5}$ W/m^2



a – Loc. 1



b – Loc. 2



c – Loc. 3

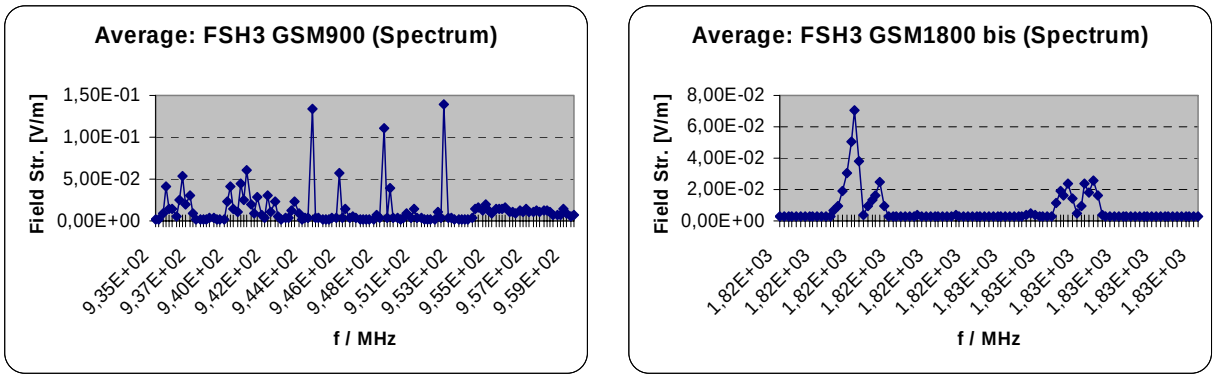
Figure 2 – Locations of outdoor measurements for GSM900 signals

The maximum peak value measured outdoor during the campaign either for GSM 900 or for GSM 1800, was $S_{max}^{peak}= 100x10^{-5}$ W/m^2, which is also far beyond ICNIRP reference levels. The reference levels are: for

GSM900, S_{ref}=4.5 W/m^2 and for GSM1800, S_{ref}=9 W/m^2. They are equivalent, for the E-field RMS value, to E_{ref}=42 V/m for GSM900 and E_{ref}=58 V/m for GSM1800.
Average values for GSM packets measured in location 2 (fig.1), at a later date, are given in table II. The location of the measurement is very central in the city. In table II, ER is the exposure ratio (=E^2/L^2 where L is the E-field limit given in standard). The values were obtained by "peak/average" menu of RFEX software, the averaging being made on 6 minutes of continuous scan. The scans alternatively changed from packet GSM900 to packet GSM1800. One can see from table II that the field levels are very low comparative to the reference levels. In figure 3 – a,b, a sample of the spectrum of measured GSM signals is given. Figure 4a shows a comparison of the prevalence of the two RF signals measured in location no. 2 as average exposure quotients (‰ of ICNIRP limits). In figure 4b, exposure quotients are represented for all significant RF signals present in the environment at the position of location no. 2. We used the prefigured packets with afferent settings offered by RFEX software itself for the measured bands. From fig. 4 one can outline that GSM 900 contribution is not much higher than "UKW" band or than "All 200M" band. In fact "UKW band" and "All 200M" band are the same, but have different analysis settings. "UKW band" covers frequencies between 87.6 – 106.3 MHz, with the following settings: Trace Mode / Detector: Max Hold / RMS, RBW=100kHz, Span=7.5 MHz, Dwell time=1000ms, while "All 200M" band covers emissions in the 88-106 MHz band, with the following settings: Trace Mode / Detector: Max Hold / RMS, RBW=300kHz, Span=45MHz, Dwell time=250ms. From histograms corresponding to the two similar packets, it is obvious how important the settings are, concerning field level assessment.

Table II: Values of average E-field RMS values for GSM signals in location no.2 from fig.1 and afferent exposure ratios:

Packet	Total Field (RMS) [V/m]	Total ER * 1000 [‰]
FSH3 GSM1800 bis	0,1224	0,0044
FSH3 GSM900	0,2815	0,0443
Sum	0,3070	0,0486

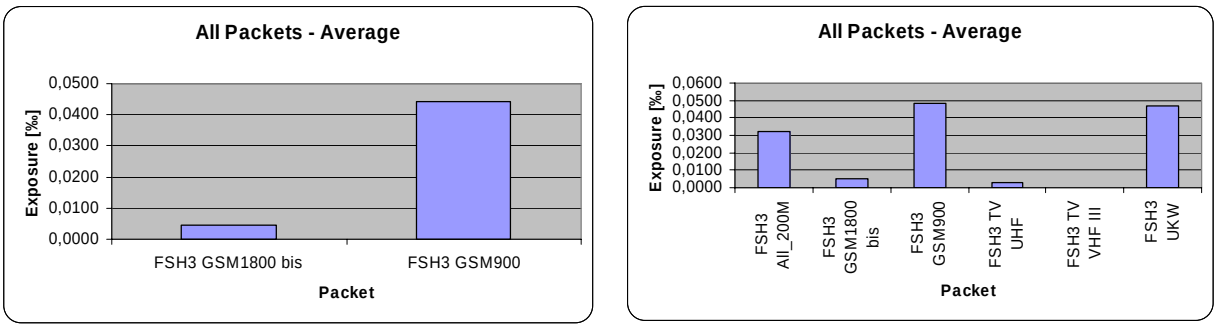


a) GSM 900 b) GSM 1800

Figure 3 – Spectrum of averaged values of GSM signals measured in location no. 2

Average values of total field and total exposure ratios for measured packets from above are given in table III. Here one observes a significant difference of the values corresponding to first and last line of the table respectively, which is solely due to system settings, and once more outlines the findings presented in part A of current section of the paper.

Generally, the existence of a large number of scatterers and absorbing objects around leads to a highly non-uniform field distribution in the environment of BTS antennas, due to shadowing and fast fading effects. Houses, trees, cars and other objects lead to field variations that can only be determined by very large measurement campaigns. The buildings cause a strong shadowing effect so the field distribution is very heterogeneous [15] – [17].



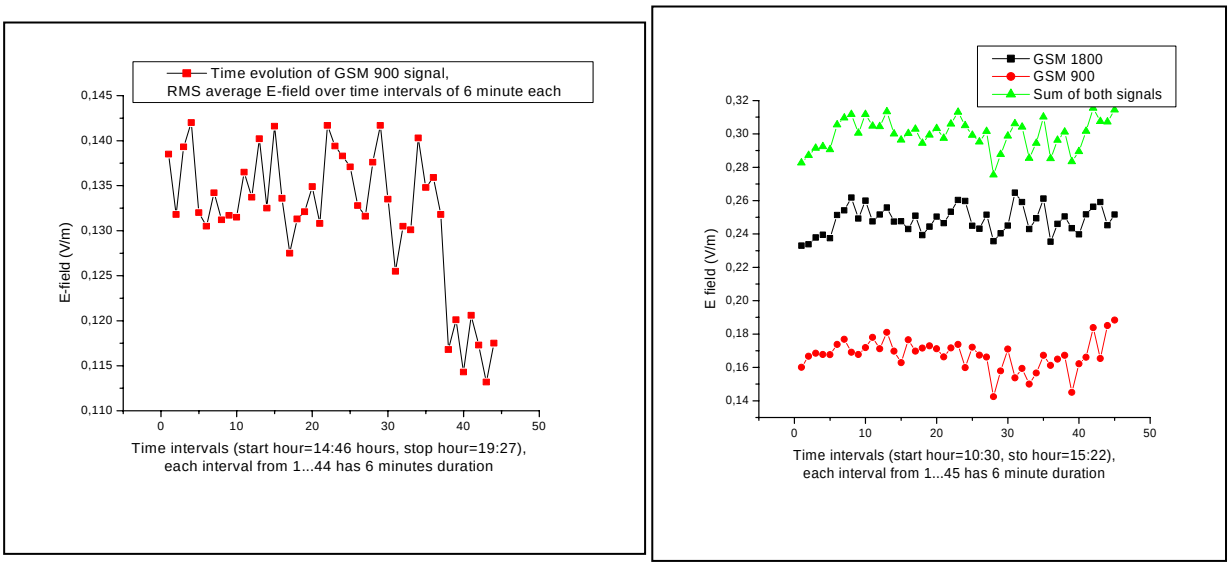
a) GSM bands comparison b) all RF signals comparison

Figure 4 – Histogram with exposure quotients (‰ of ICNIRP limits) corresponding to different RF signals measured in location no. 2

Table III: Values of average E-field RMS values for various RF signals measured in location no.2 and afferent exposure ratios:

Packet	Total Field (RMS) [V/m]	Total ER * 1000 [‰]
FSH3 All_200M	0,1568	0,0325
FSH3 GSM1800 bis	0,1309	0,0050
FSH3 GSM900	0,2941	0,0483
FSH3 TV UHF	0,0615	0,0028
FSH3 TV VHF III	0,0000	0,0000
FSH3 UKW	0,1876	0,0466
Sum	0,4089	0,1351

Time evolution of radiated GSM signals was also studied (long term measurements). Two examples are illustrated in figure 5 a,b, where traffic variations and trend in daytime, as a function of hour, can be seen for two indoor sites, situated between 300-500m distance from BTS antennas. For fig. 4a, the measuring location was location no. 2 from fig. 1. The field values are again far beyond ICNIRP references.



a) GSM 900 signal trend during afternoon hours; b) GSM 900 and 1800 signal trends during morning hours

Figure 5 – Time evolution of GSM signals: a) GSM900, measured between hours 14:46 and 19:27 in one indoor location; b) GSM900, GSM1800 and sum of them, measured between hours 10:30-15:22, in a second indoor location

Other indoor measurements were made in some sensitive sites, for both GSM signals and also for other RF signals in the environment. In indoor conditions (inside buildings), the field distribution is even more complicated. It may happen that inside a room volume, the E-field strength of a GSM broadcast channel (BCCH) alone, which operates permanently and on the same power, to vary from point to point inside the room as much as +8 to – 10 dB from the average value. So a single measurement is completely non-representative for the exposure scenario. Field variations versus time caused by changes of the power of traffic channels, the stability of BCCH's or moving scatterers have to be taken into account in order to determine their contribution to the uncertainty of exposure assessment [18]. The search for maximum field level is a very crucial point, because of the need of comparison to the limits given in exposure standards. The reproducibility of identified maxima is one of the largest problems, due to field variations in time and space. In this context it is important to say that the selection of the location for performing measurements is very important.

A challenging vista with regard to human exposure is nowadays the wireless devices technologies used in homes and offices. Several new wireless connectivity standards and technologies, e.g., DECT, Bluetooth, IEEE 802.11, may be interesting to be evaluated from human safety point of view. In present paper we assessed a DWL-2100AP 2.4GHz (802.11g) Wireless Access Point connected to the ANT24-1201 Outdoor antenna (figure 6). The antenna is mounted on the window frame of an educational institution, as seen in figure 6 and has a peak output power of 100mW. We measured the field level in the far field of the antenna, indoor, starting at a distance of 2 m of it. As in other cases, a non-predictable distribution of the E-field was achieved inside the classroom, all the values complying with the ICNIRP reference levels. At distance d=2m from antenna, average field value over 12 minutes was E=0.21V/m, representing an ER=0.01‰. A measurement sample spectrum for the antenna is presented in figure 7, in a position at a distance d=3m. The settings for these measurements were: Trace Mode / Detector: Max Hold / Max peak, RBW=1000kHz, Span=150 MHz, Dwell time=1000ms. Total field strength for the single measurement in fig. 7 was 0.29V/m, and ER=0.02 ‰.



ANT24-1201 Outdoor antenna,
12dBi , H50/V50, 2.4 GHz



DWL-2100AP High Speed
2.4GHz (802.11g) Wireless 108Mbps
Access Point



Figure 6 – Measurement of indoor field emitted by a 8011.g technology wireless access point antenna type ANT 24-1201.

A local radio broadcasting antenna radiation, placed in a residential zone, was measured in the neighbourhood zone, as seen in figure 8a. The Field Nose system was used this time. FM broadcasting antenna was placed on a tower at about 30m above the ground. The emitted frequency was f=103.2 MHz. The system settings were: frequency band=80 to 120 MHz; max peak detector; RBW = 100KHz; sweep rate= 40MHz/s; reference level=-20 dBm. Measurements were made at 2 different heights above the ground, at 1.7 and 1.2 m respectively, at a distance of about 50m from broadcasting antenna. E-field strength value for the two positions were: E_1=2.2 V/m and E_2=2.6 V/m respectively. Spectrum of the total field at 1.7 m height is represented in fig. 8b. The reference

level in ICNIRP guideline for this frequency is E=28V/m. In these conditions ER ≈ 10% and we can conlude that this case represents one of the highest exposures measured during present session. Cumulating with other RF sources emissions could conduct to non-neglijible exposure but still considerably under ICNIRP limits.

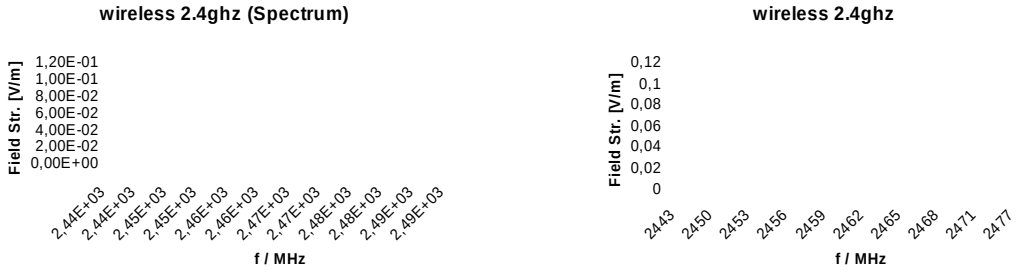
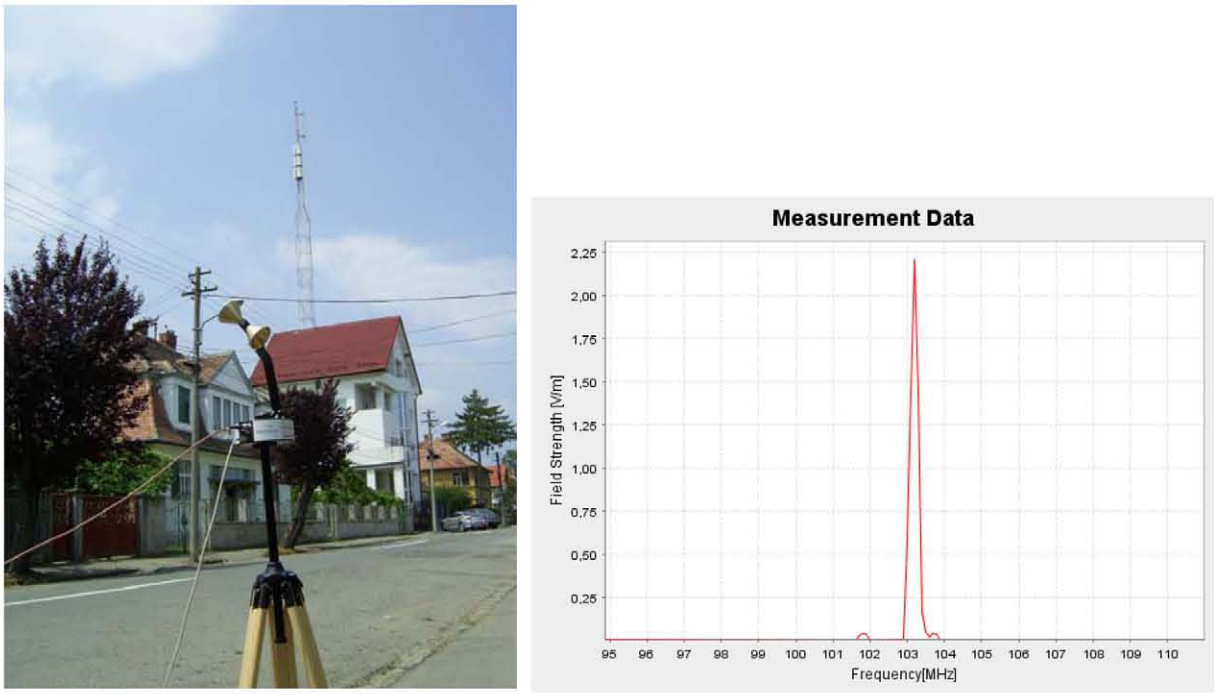


Figure 7 – Spectrum and histogram of E-field strength for wireless point outdoor antenna



(a) (b)

Figure 8 – RF broadcasting antenna measured by Field nose system: a) position in respect to emissive antenna; b) total E-field spectrum in a position at approx. d=50m, and at 1.7 m above the ground.

Conclusion

Risk perception accentuated in the last period in Romania in connection to RF sources emissions, and especially to BTS antennas. We consider that perceived risk differs from the assessed risk, in that it may more readily be manipulated. On this basis, at the level of accredited institutions it became obvious the need for measurement campaigns. Systematic studies to evaluate individual exposure of different parts of the population are needed. In this regard, at the level of each county, specific measures were taken, starting with financial support of measurement campaigns and ending to risk communication. However, fears exist that precautionary measures may undermine the scientific basis for the established exposure limits. In this view, precautionary measures for EMFs should be adopted only with great care. The national Agency for Consumer's Protection demanded all Local Town Councils to refuse further sitting of BTS antennas on blocks or residential roofs. The same agency prepares a well documented file on the issue and the Public Health Direction and Institutes were designated to apply specific measures for exposure assessment and reduction.

Results of present study showed the importance of a refined measurement methodology from the perspective that frequency and/or signal specific exposure recently turned out to be relevant, so exposure due to base stations might be important. Biological relevant exposure circumstances are of great interest in our opinion. Contributions from other RF sources have also to be taken into account. The reduce-scale campaign we developed in and around one single town in Romania, showed that RF exposure of citizens is reduced reported to regulations limits. A key concern across the epidemiological or health-related studies should be the quality of assessment of RF exposure. Despite the ubiquity of new technologies using RF, little is known about population exposure from RF sources and even less about the relative importance of different sources.

Acknowledgement: Present research was funded by the Romanian Ministry of Education and Research by the CEEX Programme 2005 / CERES, under the Contract CEx 05-D11-54/10.10.2005 with Land Forces Academy, Sibiu, Romania.

References

[1] ICNIRP, Guidelines for limiting exposure to time-varying electric, magnetic, and electromagnetic fields (up to 300 GHz), Health Physics 74 (4), pp. 494 – 522, 1998.
[2]. IEEE Standard for Safety Levels with Respect to Human Exposure to RF Electromagnetic Fields, 3kHz to 300GHz, IEEE Std. C95.1-2005.
[3] Wiedemann P.M., SchützH., The Precautionary Principle and Risk Perception: Experimental Studies in the EMF Area, Environmental Health Perspectives VOLUME 113 | NUMBER 4, 402-405, April 2005
4] EUR-OP: Council Recommendation of 12 July 1999 on the limitation of exposure of the general public to electromagnetic fields (0 Hz to 300 GHz) 1999/519/EC, Official J. European Communities, Luxembourg, 1999.
[5] ECC RECOMMENDATION (02)04 revised, Measuring non-ionising electromagnetic radiation (9kHz-300GHz), October 2003.
[6] Personal collection of newspapers articles (in Romanian): "Ziua" newspaper (issue 30 May 2006, issue 31 May 2006, issue 5 June 2006, issue 8 June 2006, issue 20 July 2006), "Jurnalul National" (issue 8 June 2006, issue 20 July 2006), "Ziarul" (issue 8 June 2006, issue 22 July 2006), "Tribuna Sibiului" (issue 18 January 2006, issue 20 July 2006, issue 21 July 2006).
[7] Hotararea nr. 234 din 28 martie 2006 a Consiliului Local Cluj Napoca (in romanian)
[8] Agence Nationale de Frequences, Protocole de mesure in situ, Visant à vérifier pour les stations émettrices fixes, le respect des limitations, en terme de niveaux de référence, de l'exposition du public aux champs électromagnétiques prévues par le décret n° 2002-775 du 3 mai 2002.
[9] Markova E., Hillert E., Malmgren L., Persson B.R.R., Belyaev I.Y., Microwaves from GSM Mobile Telephones Affect 53BP1 and -H2AX Foci in Human Lymphocytes from Hypersensitive and Healthy Persons, Environmental Health Perspectives VOLUME 113 | NUMBER 9 , 1172 -1177, September 2005
[10] Mann S.M., Cooper T.G., Allen S.G., Blackwell R.P., Lowe A.J.: Exposure to Radio Waves near Mobile Phone Base Stations, Chilton, Natl. Rad. Protect. Board Report-321, 2000.
[11] G. Neubauer, D. Papameletiou, T. Samaras, Y. Hamnerius, J. Wiart,K. Lamedschwandner, Methods to assess exposure of the population next to mobile communication base stations, 27th triennial General Assembly of the International Union of Radio Science, Maastricht, 2002.
[12] Müllner W., Neubauer G., Haider H., Add3D, a new technique for precise power flux density measurements at mobile communications base stations, 10th Internat. Fachmesse und Kongress für EMV, Düsseldorf, pp 305–312. 2002.
[13] Miclaus S., Bechet P., Goiceanu C., Olariu O.V., Demeter S., Practical issues concerning cellular base station emissions and population exposure in Romania, 3rd European Medical & Biological Engineering Conference, Prague, Czech Republic, 20-25 Nov. 2005, IFMBE Proceedings 11 (1), 2005.
[14] C. Olivier, L. Martens, Optimal Settings for Narrow-Band Signal Measurements Used for Exposure Assessment Around GSM Base Stations IEEE Trans. on Instrumentation and Measurement, vol. 54, No. 1, pp.311-317, Febr. 2005.
[15] Preiner P., Überbacher R., Kaczmarczyk A., Neubauer G.: Evaluation of Electromagnetic Field Distributions near Mobile Communication Base Stations, Proc. COST 281 Workshop: STM Base Station Monitoring, Vienna, 26-27 August 2003.
[16] C. Olivier, L. Martens, EMF measurements around base stations: Some issues, COST 281-STM Base Station Monitoring Workshop, Vienna, 26-27 Aug. 2003.
[17] G. Neubauer, H. Haider, K. Lamedschwandner, M. Riederer, R. Coray, Measurement Methods and Legal Requirements for Exposure Assessment Next to GSM Base Stations, International Zürich Symposium on EMC, pp 143 – 147, February 2003.
[18] H. Lehmann, B. Eicher, P. Fritschi, Indoor measurements of the electrical field close to mobile phone base stations, 27th triennial General Assembly of the International Union of Radio Science, Maastricht, 2002.

LOW POWER MICROWAVE RADIATION EFFECTS ON MAIZE SEEDS

RĂCUCIU MIHAELA[1*], MICLĂUŞ SIMONA[2]

[1] "Lucian Blaga" University, Faculty of Sciences, Dr. I. Ratiu Street, No.5-7, 550012, Sibiu, Romania, mracuciu@yahoo.com
[2] Land Forces Academy "N. Balcescu", 3-5 Revolutiei Street, 550170, Sibiu, Romania

Abstract
In this study young plantlets, obtained from the control and microwave irradiated seeds, were studied in laboratory experiments. The electromagnetic radiation with the frequency of 10.8GHz was generated by a microwave generator, based on a rectangular waveguide. The effective incident power was measured to be of 5.2mW. The *maize* seeds with uniform genophond were irradiated one at a time inside the irradiation waveguide, by means a Teflon cuvette, with different exposure times. After germination the young plantlets growing was conducted in the same controlled laboratory conditions and the culture medium of young plantlets was daily the same amount of deionized water. The length of the 12 days plantlets was measured as well and statistical analysis was performed on the data. Assimilatory pigments and average nucleic acid level were assayed of 12 days old plantlets, by spectrophotometric methods and using a Perkin - Elmer UV-VIS spectrophotometer. The data provided by the chlorophylls ratio (chlorophyll **a** / chlorophyll **b**) measurement offered the main insight into the photosynthesis complex processes since they revealed the response of the LHC II system (Light Harvesting Complex II), associated to the photosynthetic system II from the tylakoidal membranes, to the external stress. For chlorophylls ratio a slight stimulatory effect was noticed for shorter time exposures, suggesting putative stimulation of photosynthesis process. The same effect was registered to average nucleic acid level.

Keywords: low power microwave, *maize*, plants growth, photoassimilatory pigments, nucleic acids.

Introduction

The effect of electromagnetic microwave irradiation on agricultural crops has scarcely been studied yet. For decades a great variety of living beings have been used by researchers in order to detect possible changes in ecosystems. Thirty years ago two Canadian researchers observed a deterioration that was unpredictable on the plants subjected to microwaves (Tanner and Romero-Sierra) [1].

Some studies on the effect of microwave irradiation (2.45 GHz) on seeds were conducted and detected an enhanced rate of germination [2-4]. Bhaskara Reddy *et al*. [3-4] used the microwave range (2.45 GHz) on seeds of charlock, wheat, soybeans, peas and rice with the aim of pre-storage destroying. Yoshida *et al.* [5-7] used microwave radiations (2.45 GHz) on soybean, peanut and sunflower seeds for improving the triglycerides distribution in the seed. Studies on the effect of electromagnetic irradiation of the microwave range on seeds have also been conducted by Aladjadjiyan *et.al.* [8] and Kalinin *et.al.* [9].

Recent experiments have shown that exposure to radiation emitted from a global system for mobile communication (GSM) telephone followed by calcium deprivation, leads to meristem production in flax seedlings [10]. To investigate the possibility that plants may be affected by exposure to a frequency in this range some investigators used radiation with 105 GHz frequency at non-thermal levels by a Gunn oscillator [11].

[*] Corresponding author: E-mail: mracuciu@yahoo.com

As well known, photosynthesis is a very complex phenomenon resulting in the transformation of solar electromagnetic energy into chemical energy, stored in organic compounds, synthesized from inorganic carbon and water. The study of assimilatory pigments from plant green tissue is able to provide information upon the capacity of solar energy conversion at the level of chloroplast membranes, during photosynthesis.

In this paper the authors present some quantitative observations of microwave radiations exposure influence of seeds on the growth of *Zea mays* (*maize*) agrotechnical plants.

Materials and methods

Young plants, obtained from the control and microwave irradiated seeds, were studied in laboratory experiments. The electromagnetic radiation was generated by a microwave generator, based on a rectangular short-ended waveguide. The microwaves were generated as 10.8 GHz continuous waves modulated by rectangular pulses with a duty factor of ½ at a repetition frequency of 1.75 kHz. The effective incident power was measured to be of 5.2 mW. The absorbed microwave power inside the cuvette was estimated at 0.20 mW, corresponding to an average specific absorption rate of 1.33 W/kg. The *maize* seeds (plant species with major role in people life) with uniform genophond were irradiated one at a time inside the irradiation waveguide, by means a Teflon cuvette, with different exposure times. Batches of 30 seeds were irradiated for 5, 10, 15, 20, 40, 60 and 120 minutes. The irradiated seeds germinated in deionized water on porous paper support, in darkness and closed Petri dishes. After germination the young plantlets growing was conducted in the same controlled laboratory conditions (temperature (24^{o}C), illumination (10 h: 14 h light/dark cycle) and 90% humidity) and the culture medium of all young plantlets groups was daily the same amount (10ml) of deionized water.

The length of the 12 days plantlets was measured with 0.1 cm precision as well and statistical analysis was performed on the data.

After 12 days of plantlets growth, spectrophotometric assays were accomplished: the content of chlorophyll a and chlorophyll b and total carotenoid pigments (Meyer-Berthenrath's method modified by Ştirban [12]) and the average content of nucleic acids (Spirin's method [13]). The spectral device was a Perkin-Elmer spectrophotometer UV-VIS provided with quartz cells.

Green tissue harvested, from each exposed and control sample (mixture of green tissue picked up from all the 30 plantlets), was weighted, crushed and mixed with the same volumes, of 85% acetone in deionized water for the assimilatory pigments extraction [12] and 6% perchloric acid for nucleic acid extraction [13], being further quantitatively transferred into quoted glass tubes.

The levels of chlorophyll a, chlorophyll b and total carotenoid pigments may be calculated with the next formulae according to [12]:

$$\text{chla} = \frac{12{,}3\cdot \text{A}(663) - 0{,}86\cdot \text{A}(645)}{1000\cdot \text{d}\cdot \text{w}}\cdot \text{V},$$

$$\text{chlb} = \frac{19{,}3\cdot \text{A}(645) - 3{,}6\cdot \text{A}(663)}{1000\cdot \text{d}\cdot \text{w}}\cdot \text{V},$$

$$\text{t.c.} = \frac{10\cdot \text{A}(472)}{2485\cdot \text{d}\cdot \text{w}}\cdot \text{V},$$

while the average content of DNA and RNA is given by the relation [13]:

$$[\text{AN}] = \frac{\text{E}(270) - \text{E}(290)}{0.19}\frac{\text{V}}{\text{w}}$$

where: w-the fresh vegetal sample mass, V-the extract volume; A(λ)-the light absorption to the wavelength λ; d-the quartz cell width.

Three repetitions of each spectrophotometric assay have been accomplished. Statistic analysis was accomplished by means of average values, standard deviations and *t*-test (two tails, pair type) considering the significance criterion of 0.05.

Results and discussions

The average lengths and the standard deviations were calculated for each batch of test seeds. The confidence interval was calculated for every batch of plantlets using the Student test, for the confidence level P = 90%. In Fig. 1 average plantlets length for control and microwave exposure samples is presented.

The average values of plants length are enhanced proportionally to the microwave exposure time – a linear regression curve with correlation coefficients R^2 about 0.9561 was found.

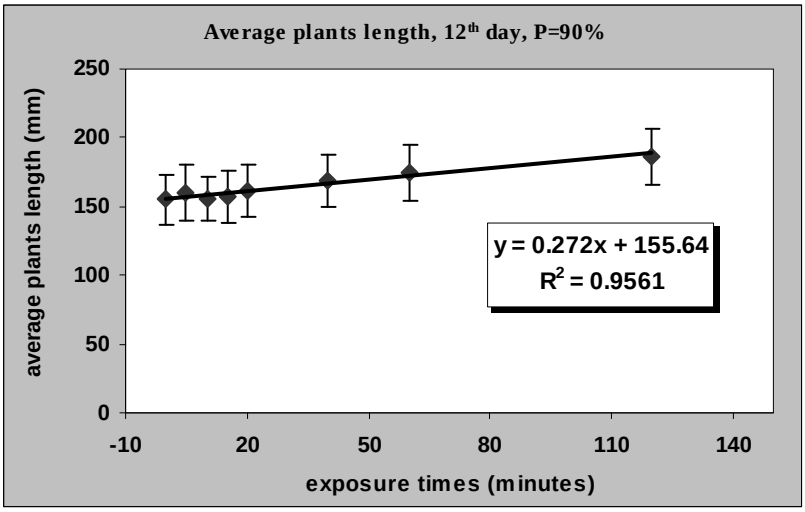


Fig.1. The average length versus microwave exposure time

The contents of photosynthesis pigments (**a** and **b** chlorophylls and total carotenoids) in the green tissue of young maize plantlets (aged of 12 days) for experimental samples in Fig.2 are presented. For all exposure times all three pigments present averaged values ranging around control values, i.e. small enhancements or small diminutions, with statistical significance for short exposure times (5; 10 and 15 minutes) while for longer exposure times (15; 20; 40; 60 and 120 minutes) the statistical analysis no revealed statistic significance. Similar response at microwave irradiation of seeds was get for the all three assimilatory pigments analyzed.

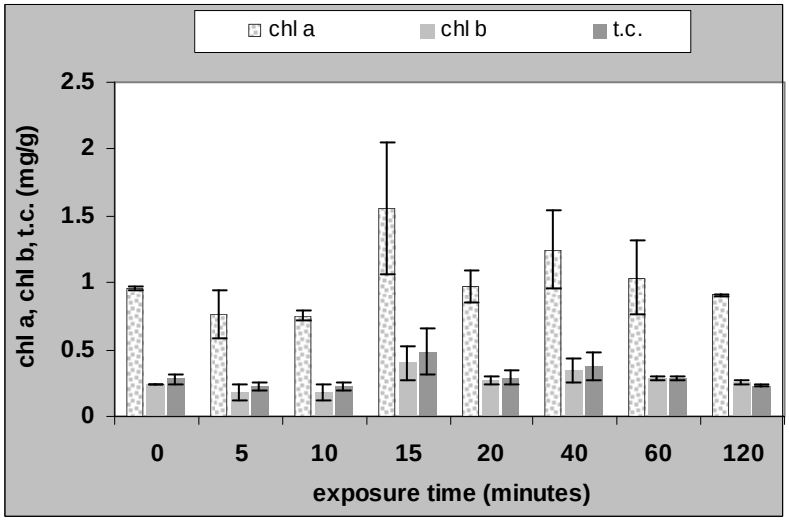


Fig.2. Assimilatory pigments level in *maize* plantlets versus microwave exposure time
(chl a –the content of chlorophyll a, chl b-the content of chlorophyll b,
t.c.-the content of total carotenoid pigments)

The total assimilatory pigments contents have the same variation to the increase of the microwave exposure time that was observed for chlorophyll **a** level. Very good linear correlations were revealed between pairs of pigments level (Fig.3). These results can be taken as an indication upon the correlated influences of microwave radiation in the all: chlorophyll **a**, chlorophyll **b** and the secondary carotenoids like pigments. As known chlorophyll **a** molecules represent the main photosynthesis pigment, able to control directly the solar energy conversion into chemical form while carotenoids are playing very important role in the sustaining of photosynthesis efficiency, by indirect energetic transfer of the absorbed energy to chlorophyll **a** molecules. Concluding on these results, all analyzed assimilatory pigments had similar variations versus microwave irradiation times.

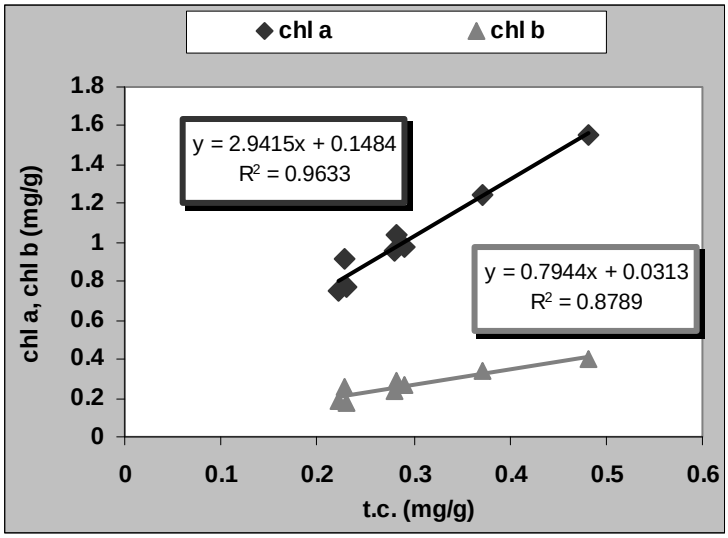


Fig.3. Linear correlation between chlorophyll a, chlorophyll b and total carotenoid pigments levels
(chl a –the content of chlorophyll a, chl b-the content of chlorophyll b,
t.c.-the content of total carotenoid pigments)

The best indicator upon the photosynthesis process efficiency is considered the chlorophylls ratio (chlorophyll **a** / chlorophyll **b**) [14] which provides indirect information on the enzymatic aggregates of the **L**ight **H**arvesting **C**omplex II (**LHC II**) from the photosynthetic system II located in the chloroplasts membranes. In Fig.4 a slight stimulatory effect can be seen for shorter microwave exposure time to photosynthesis process, as suggested by chlorophyll **a** and **b** ratio; inhibitory effect is obvious for the highest microwave exposure time. The ratio chlorophyll **a** / chlorophyll **b** was enhanced with 6% for shorter microwave exposure time sample and diminished with 15% for higher microwave exposure time.

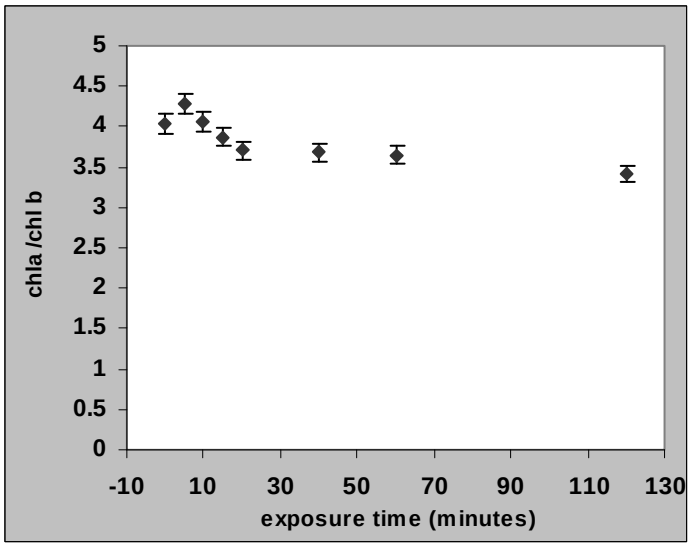


Fig.4. The effects of microwave exposure of seeds on chlorophylls ratio in 12 days old plantlets

The average content of nucleic acids (DNA and RNA) in young *maize* plantlets provided by microwave irradiated seeds, after 12 days of grown is presented in Fig.5. A stimulatory influence of microwave exposure on the biosynthesis of nucleic acids was revealed for low exposure times (to 14% for 20 minutes microwave exposure sample) while for the higher microwave exposure time an inhibitory effect (35%) than control was observed. Applying the *t*-test to compare control and test sample, data for the average nucleic acid level have revealed statistic significance ($p<0.05$) for all exposed samples.

Thermal as well as non-thermal effects of microwaves interaction with seeds are supposed to underlay these modifications.

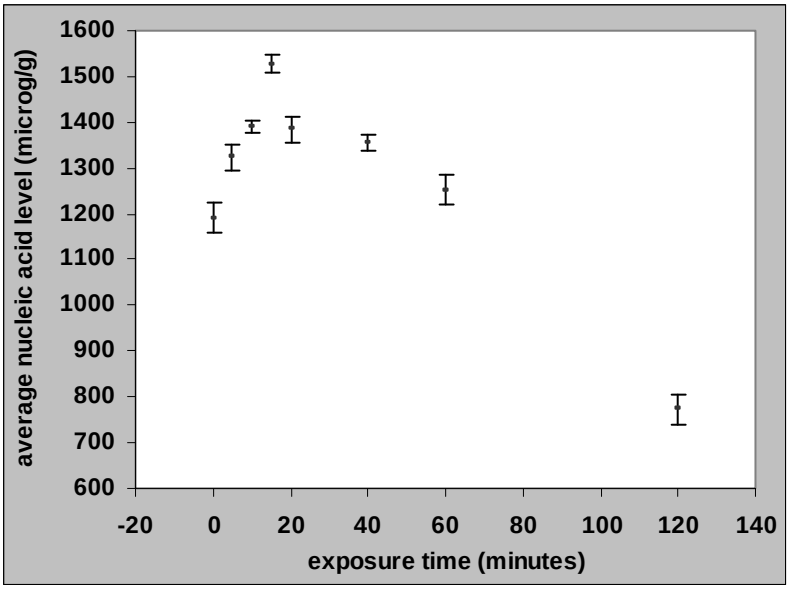


Fig.5. The average nucleic acid levels in *maize* plantlets provided by irradiated seeds

The electromagnetic energy of the microwave absorbed photon is six orders of magnitude lower than that of chemical or even hydrogen bonds needed to break down. So, the absorption of a microwave photon cannot break these bonds [15]. But, more complex indirect phenomena, possible within cellular complex structures may occur, that finally can lead to the plants growth disturbing. Maybe the accumulation of oxygen radicals is the primary cause, as they are suspected for dissociating the covalent bonds of DNA [16] when water molecules are adsorbed on the surface of large bio-molecules within cellular medium.

Summary

In summary, in this experimental study regarding microwave radiation with 10.8 GHz frequency influences upon maize seeds, observed on the 12 days old plantlets derived by irradiated seeds, a very slight stimulation of the photosynthesis process was revealed by means of chlorophylls ratio (to 6% increasing) in the case of shorter microwave exposure time. For the higher microwave exposure time the chlorophylls ratio was diminished with 15% than control. Also, a stimulatory influence of microwave exposure on the biosynthesis of nucleic acids was revealed for low exposure times (to 14%) while for the higher microwave exposure time an inhibitory effect (to 35%) than control was evidenced. The low power microwave treatment of seeds has revealed that *maize* young plantlets development may be slightly affected during their first twelve days of growth.

In fact the complexity of plant growth phenomena can not be evaluated only by means of the chlorophylls and carotenoids or nucleic acids behavior but also by considering the enzymes activity, the capacity of water accumulation and so on. It is designed that our further experimental projects to be focused on the diversification of the investigation methods able to provide data regarding the plant electromagnetic sensitivity in the range of microwave exposure parameters tested inhere.

Based on the fact that such microwave exposure can often occur in natural plant populations but no phenotypic changes are reported regarding the perturbation of the main biological patterns, the presumption that the recover mechanisms are also activated following the microwave exposure is a challenging issue.

References

[1] J.A. Tanner, C. Remero-Sierra, Beneficial and harmful growth induced by the action of nonionizing radiation, Annals of the New York Academy of Sciences, 238: 171-175 (1974).
[2] V. Nguyen Tran, Effects of Microwave Energy on the Strophiole, Seed Coat and Germination of Acacia Seeds, Australian Journal of Plant Physiology, 6(3): 277 - 287 (1979).

[3] M.V. Bhaskara Reddy, A.C. Kushalappa, G.S.V. Raghavan, M.M.P. Stevenson, Eradication of seedborne Diaporthe phaseolorum in soybean by microwave treatment, 66th Annual meeting of the Canadian Phytopathological Society, June 25-28, Toronto, (1995).
[4] M.V. Bhaskara Reddy, G.S.V. Raghavan, A.C. Kushalappa, T.C. Paulitz, Effect of microwave treatment on quality of wheat seeds infected with *Fusarium graminearum*, Journal of Agric.Engin.Res., 71:2 (1998).
[5]H. Yoshida, S. Takagi, Y. Hirakawa, Molecular species of triacylglycerols in the seed coats of soybeans following microwave treatment, Food Chemistry, 70:63-69 (2000).
[6] H. Yoshida, Y. Hirakawa, Y. Tomiyamaa, Y. Mizushina, Effects of microwave treatment on the oxidative stability of peanut (*Arachis hypogaea*) oils and the molecular species of their triacylglycerols, European Journal of Lipid Science and Technology, 105(7): 351 – 358 (2003).
[7] H. Yoshida, Y. Hirakawa, Y. Mizushina, T. Tanaka, Molecular species of triacylglycerols in the hulls of sunflower seeds (*Helianthus annuus L.*) following microwave treatment, European Journal of Lipid Science and Technology, 104(6): 347 – 352 (2002).
[8] A. Aladjadjian, D. Svetleva, Influence of Magnetron Irradiation on Common Bean (Phaseolus vulgaris L.) Seeds, Bulg. J. Agr. Science, 3: 741-747 (1997).
[9] L. G. Kalinin, I. L. Boshkova, G. I. Panchenko, S. G. Kolomiichuk, Influence of Low-Frequency and Microwave Electromagnetic Fields on Seeds, Biophysics, 50(2): 334-337 (2005).
[10] M. Tafforeau, M.C. Verdus, V. Norris, G. White, M. Demarty, M. Thellier, C. Ripoll, SIMS study of the calcium-deprivation step related to epidermal meristem production induced in flax by cold shock or radiation from a GSM telephone, J Trace Microprobe Techn., 20: 611–623 (2002).
[11] M. Tafforeau, M.C. Verdus, V. Norris, G. J. White, M. Cole, M. Demarty, M. Thellier, C. Ripoll, Plant sensitivity to low intensity 105 GHz electromagnetic radiation, Bioelectromagnetics, 00: 1-5 (2003).
[12] M. Stirban, *Procese primare în fotosinteza*, Ed. did. si ped., Bucharest, 1985, 229.
[13] A. Spirin, *Biochimia*, Ed. Mir , Moscow, 1958, 656.
[14] D. Ort, J. Whitmarsh, *Photosynthesis.Encyclopedia of Life, Sciences*, Macmillan, London, 2001.
[15] H. Fujikawa, H. Ushioda, Y. Kudo, Kinetics of Escherichia coli destruction by microwave irradiation, Applied and Environ. Microbiol., 58: 920-924 (1992).
[16] Y. Kakita, M. Funatso, F. Miake, K. Watanabe, Effects of microwave irradiation on bacteria attached to the hospiral white coats, International J. of Occup. Med. & Environ. Health, 12(2): 123-126 (1999).
[17] C. Polk, E. Postow, *Handbook of Biological Effects of Electromagnetic Fields*, CRC Press Ltd., Boca Raton, New York (1996).

PRELIMINARY DOSE-FINDING EXPERIMENT FOR THE STUDY OF THE PROMOTIONAL EFFECTS OF POWER FREQUENCY MAGNETIC FIELDS ON RAT LEUKEMIA

T. NEGISHI[1], I. NISHIMURA[1], K. SHIBUYA[2], M. ITABASHI[2] AND S. IMAI[1]

[1]Biological Environment Sector (Risk Assessment Group), Environmental Research Laboratory
Central Research Institute of Electric Power Industry
1646 Abiko, Abiko, Chiba 270-1194, Japan.
[2]Contract Testing Department, Nippon Institute for Biological Science
2221-1 Shin-machi 9, Ome, Tokyo 198-0024, Japan.

Abstract

A total of 200 female Donryu rats at 11 weeks of age were randomly divided into 10 groups of 20 rats. Animals in 8 groups were given 0 (olive oil: vehicle only), 10, 20, 30, 40, 50, 60 or 70 mg/kg body weight of 1-propyl-1-nitrosourea (PNU) by oral administration, 5 days a week for 5 weeks. Animals in other 2 groups were given 300 or 350 mg/kg body weight of PNU, once a week for 5 weeks. They were observed for 30 weeks after PNU administration. Except for dead animals due to acute PNU toxicity during PNU injection period and the first 2 weeks of observation period, the cumulative proportions of dead animals and animals with leukemia in 0, 10, 20, 30, 40, 50, 60, 70, 300 or 350 mg/kg of PNU-injected groups were 0.0, 0.0, 0.0, 10.5, 40.0, 47.4, 73.7, 80.0, 22.2, 27.8% and 0.0, 0.0, 5.0, 10.5, 10.0, 21.1, 63.2, 80.0, 27.8, 27.8%, respectively. Main cause of death was erythrocytic leukemia. The incidence of myelocytic leukemia, which we intended to induce mainly, was low and 5.0, 16.7, 22.2% in 20, 300 and 350 mg/kg of PNU-injected groups, respectively. Body weight gain during observation period showed that PNU toxicity was lower in 300 mg/kg group than 350 mg/kg group. Based on these results, administration of 300 mg/kg body weight of PNU, once a week for 5 weeks was selected for initiation method. 50Hz magnetic field exposure study of up to 350μTrms is now in progress.

INFLUENCE OF LOW-FREQUENCY MAGNETIC FIELD ON ENZYME ACTIVITIES OF STREPTOZOTOCIN-INDUCED DIABETIC RATS

Işıl Öcal[1], Gülen Atilla[2] and İsmail Günay[1]

[1]Cukurova University, Medical Faculty, Department of Biophysics, 01330 Balcalı/Adana, TURKIYE

[2]Cukurova University, Medical Faculty, Department of Biochemistry, 01330 Balcalı/Adana, TURKIYE

Tel:+90-322-3386060/3472

iocal@cu.edu.tr

The effects of magnetic fields seem to depend on their respective codes (frequency, intensity, and waveform). The aim of the present study is to examine the effects of magnetic field on changes of glucose, lipid levels and activations of alpha-amylase and lipase enzymes in diabetic rats that were different exposed durations to magnetic field. The rats were first divided into two groups. The first group (30 rats) was made up diabetic control group ((D_I, D_{VII} and D_{XIV}), the second group was comprised of rats described as diabetic-exposed to magnetic field groups (DMF_I, DMF_{VII} and DMF_{XIV}). Diabetic (D) and diabetic-exposed to magnetic field (DMF) groups were made up adult male Wistar Albino rats (60 rats). DMF groups (30 rats) were exposed to magnetic field for thirty minutes per one, seven and fourteen days. The combinations: of alternating modulated magnetic fields were set up 5 mT intensity, 50 Hz frequency and oriented north-south direction. Also, diabetic groups of adult male Wistar Albino rats (30 rats) were treated in identical fashion to the exposed rats, except that the magnetic field was switched off.

The end of first, seventh and fourteen days, blood of rats in diabetic-exposed to magnetic field and diabetic groups was collected under ether anesthesia for biochemical parameters, activations of enzymes and ion concentrations. The end of 1 st day that in diabetic-exposed to alternative magnetic field groups, while serum glucose and lipid levels were changed, changes of ion concentrations were changed end of seventh and fourteen day; increased serum K^+ and decreased serum Ca^{2+} concentrations.. In addition, activations of enzymes were no changed in diabetic rats exposed to 14 days magnetic field. Data are significantly ($p<0.05$). The effects of magnetic field in diabetic rats depend on exposed-duration to magnetic field. The changes of activations of enzymes of ion concentrations were depended on combinations of magnetic fields as exposure duration, intensity and directions. We observed different affected activations of enzymes and ion concentrations in diabetic-exposed to magnetic field according to exposed duration of magnetic field. The results indicate that an alternative magnetic field may positively affect diabetic rats in respect of blood serum parameters, depending on exposed duration of magnetic field

Key Words: Diabetic rats, alpha-amylase enzyme, Magnetic field, exposure duration to magnetic field.

Introduction

Numerous experimental findings suggest that exposure to extremely low-frequency (ELF) magnetic fields (MFs) affects various cell functions via actions exerted on intracellular and membrane proteins; including ion channels, membrane receptors and enzymes (1,2).

Diabetes has profound effects on the metabolism of various tissues, including vascular smooth muscle. Both glycolysis and glucose oxidation are decreased in diabetic animals and there is an overall decrease in ATP production (3). One mechanism that may contribute to this disturbance in tissue metabolism is the elevation of long-chain fatty acid levels (4,5). Recent investigations revealing that after exposure to magnetic fields, insulin release and glycogen levels are increased in diabetic rats and the blood glucose level is decreased provided the stimulus for the current studies. (6,7). Similar results were recorded in other studies (8-10). Goodman et al has been suggested that an electromagnetic field affects the movement of Ca^{2+} ions across membranes and has

effects at the gene level, but the mechanism of the MF effect is not yet clear (11,12). A recent study revealed ultrastuctural changes in β cells, with indications of extension of the rough endoplasmatic reticulum and significant expansion of the Golgi apparatus, in a group of rats exposed to a magnetic field (13). The rats used in this research had body weights of 284.4 ± 12.6 g: 35 were put into a sinusoidal magnetic field with frequency 10 Hz and intensity 1.8-3.8 mT; 35 were put into a sinusoidal magnetic field with frequency 40 Hz and intensity 1.3-2.7 mT for 30 minutes per day for 1, 3, 6, 9 and 14 days. It was thought that the expansion of the Golgi apparatus might relate to storage of increased amount of proinsulin in the form of small vesicles (14). The special granules around the site might indicate insulin storage by the β cells; they are affected by the magnetic field. On the other hand, electron-transparent vesicles in the β cells may indicate an intensification of hormone secretion after the oscillation of the insulin granules (13, 14). Finally, the reversible structural changes in β cells that occur depending on the magnetic parameters may increase insulin oscillation and synthesis.
A low intensity magnetic field has been used to treat late complications of diabetes such as diabetic retinopathy, diabetic angioplasty and peripheral neuropathy (15). In almost all the patients receiving this treatment, complaints of intestinal motor activities and pain disappeared and laboratory markers were normalized; magnetic therapy was further suggested for the treatment of juvenile diabetes (16,17). These studies on the effects of electromagnetic fields on living systems led us to investigate whether such fields may be used for treatment. For these reasons, we undertook this study to determine the effects of exposure to alternating modulated magnetic fields on blood parameters and activation of enzymes in diabetic rats.

Material and Method

Experiments were conducted on 60 male Wistar albino rats aged 5 months, weighing 245-300g. The experimental protocol was approved by the Animal Ethics Committee at Cukurova University. Firstly, animals were divided into two groups: control diabetic (D_I, D_{VII} and D_{XIV}) and diabetic-exposed to magnetic field groups ($D\text{-}MF_I$, $D\text{-}MF_{VII}$ and $D\text{-}MF_{XIV}$). We injected 45 mg/kg streptozotocin (STZ) in citrate buffer (CB) (pH 4.5) into the tail veins to induce diabetes (D group). A similar volume of CB solution without STZ was injected into control rats (S group). Then, animals were exposed to magnetic field between 09:00 and 09:30 or 13:00 and 13:30 h for one, seven and fourteen days to control for possible circadian variations in response. Rats in the D-MF groups were exposed for thirty minutes per day to alternating modulated magnetic fields of frequency 50 Hz, intensity 5 mT

Rats in the control or sham diabetic groups were treated in exactly the same fashion as the exposed rats, except that the magnetic field was switched off. The rats in each group were allowed to roam freely in the cage irrespective of exposure to the MF. They were fed a standard rat chow and tap water *ad libitum* and kept in an environmentally controlled room at 21-23°C, relative humidity 40-60%, with a light/dark cycle of 12/12 h.

The end of exposure period of one, seven and fourteen days, serum glucose and lipid levels were determined to indicate any relationship with diabetes mellitus. The serum was used to determine levels of glucose and lipids K^+ and Ca^{2+} concentrations, activations of alpha-amylase and lipase enzymes.

All values were expressed as means ± SEM. Levels of glucose, K^+ and Ca^{2+} ion concentrations and activations of enzymes were compared between diabetic and diabetic-exposed to magnetic field groups by 2-way ANOVA. Statistical significance was assumed at $p< 0.05$.

Results

The mean values of serum glucose and lipid levels of rats in three groups were significantly decreased after diabetic rats were exposed to magnetic field during one, seven and fourteen days, compared to those of the rats (glucose: D_I 259.8±5.1 mg/dl, DMF_I 257.2±7,1 mg/dl, D_{VII} 240.6 ±10,1, DMF_{VII} 190.2 ± 2.7 mg/dl, D_{XIV} 239.4± 3.8 mg/dl; DMF_{XIV} 176.6 ± 1.2 mg/dl) The mean values ± SEM of the other lipid levels were shown in Table1. When K^+ and Ca^{2+} ion concentration in serum of rats in diabetic-exposed to magnetic field groups were compared to control diabetic rats, we were measured decreased Ca^{2+} ion concentration in end of the fourteen days and increased K^+ ion concentration in end of the seven days according to intensity or density of diabetic (Table 2, Fig1,2).
There were no significant difference activations of α-amylase or lipase enzymes of rats between diabetic and diabetic-exposed to the magnetic field groups. (Table 2, Fig3,4).

Table 1. Serum parameters (glucose, cholesterol, triglyceride, HDL and LDL (mg/dl)) of rats were measured by enzymatic techniques in diabetic and diabetic-exposed to magnetic field groups (mean ± SEM).

	Groups					
Serum Parameters	**D_I**	**D-MF_I**	**D_{VII}**	**D-MF_{VII}**	**D_{XIV}**	**D-MF_{XIV}**
Glucose (mg/dL)	259.8±5.1	257.2±7.1	240.6±10.1	190.2±2.7	239.4 ± 3.8	176.6 ± 1.2
Cholesterol (mg/dL)	67.6±3.0	43.4±1.8	66.2±1.2	41.4±2.0	76.4±1.4	47.8±2.3
Trygliceride (mg/dL)	86±1.1	73.6±1.7	115.4±4.6	76.4±9.9	141,8±2.5	73.0±5.7
LDL (mg/dL)	1.2±0.2	1.2±0.1	1.4±0.4	1.2±0.4	2.7±0.6	1.3±0.9
HDL (mg/dL)	34.4±1.0	44.8±2.7	36.2±0.9	44.8±1.5	32.6±0.5	44.6±1.3

Table 2. Ion concentrations (K^+ and Ca^{2+}) and activations of enzymes (alpha-amylase and lipase) of rats were measured in diabetic and diabetic-exposed to magnetic field groups (mean ± SEM).

	Groups					
Serum Parameters	**D_I**	**D-MF_I**	**D_{VII}**	**D-MF_{VII}**	**D_{XIV}**	**D-MF_{XIV}**
Lipase (U/L)	13.2±0.6	12.6±0.8	12.0±0.8	11.6±0.7	13.0 ± 0.7	14.2 ± 0.9
α-amylase (U/L)	2107.4 ± 26.7	2077.8 ± 34.4	2232 ± 31.6	2229.8 ± 26.6	2111.0 ± 38.7	2111.8 ± 40.3
Ca2+ (mg/dL)	11.6±0.7	11.6±1.3	11.7±0.8	11.7±1.02	13.2±0.4	12.4 ± 0.9
K+ (mmol/L)	4.5±0.7	4.8±0.5	4.5±1.2	5.5±1.6	4.6±0.4	6.4 ± 1.2

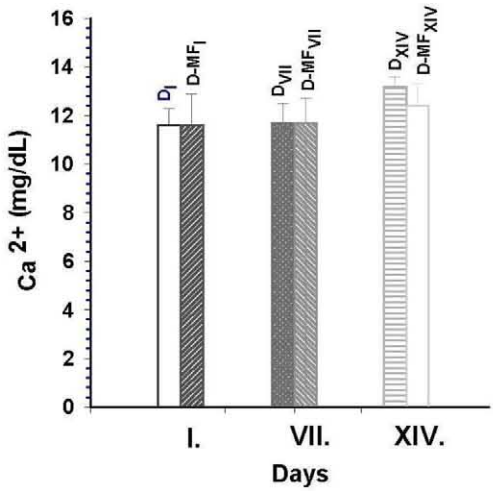


Fig1. Serum Ca^{2+} concentration of rats in D and DMF groups.

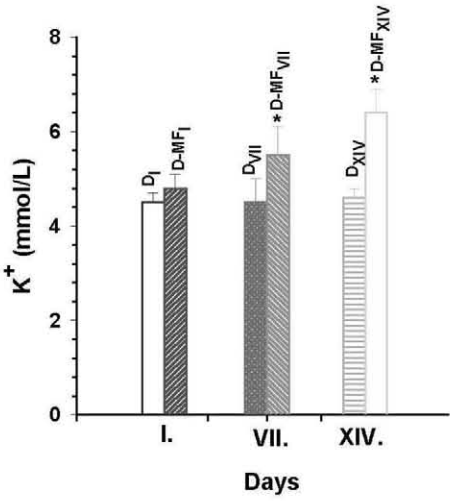


Fig2.Serum K^+ concentrations of rats in D and DMF groups

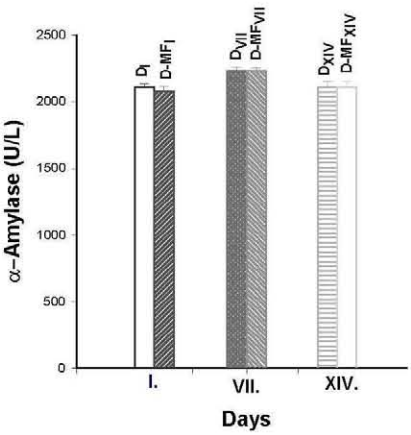


Fig3. Activation of serum α-amylase enzyme of rats in D and DMF groups

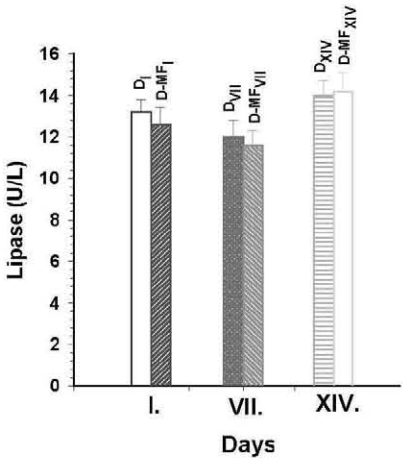


Fig4. Activation of serum lipase enzyme of rats in D and DMF groups

Discussion

Data from this study show that exposure duration of magnetic field can interact. In diabetic-exposed magnetic field one day, no significant change in blood parameters was observed in glucose, lipid and enzymes activities. The plasma glucose, lipid and cholesterol levels were slightly decreased in the D-MF group compared with the D group. These results might indicate a transiently healthy response by rats to the alternating modulated magnetic field. The decrease in plasma glucose was statistically significant ($p<0.05$). The MF may cause an increased synthesis and oscillation of insulin. Therefore, MF is expected to decrease the glucose level and increase the glycogen level (7,18-21) Oroza et al. 1987 found similar results. They suggested that the magnetic field slowed down the fat metabolism of the rats and so decreased the levels of glucose and lipid. If the magnetic field increases the synthesis and oscillation of insulin, as Laiti-Kobierska et al. 2002 suggested, then there may be a decrease in the blood glucose level in the diabetic rats. Epidemiological studies have indicated that MFs can also induce adverse health effects. Other studies have yielded important clues to the interaction between MF and cellular systems, particularly at the molecular level. Laiti-Kobierska et al. 2002 identified granules in the β cells of rats exposed or not exposed to a magnetic field; these granules were called special granules. On the other hand, there were inflated mitochondria and expanded endoplasmic tubules in the pancreatic acinar cells. These authors suggested that the observed changes occurred because of the magnetic field and were related to increased

synthesis and oscillation of insulin (13). If the special granules stimulate insulin synthesis, then decreased lipid and glucose levels are to be expected.
Chernysheva suggested that if the rats were exposed to an alternating magnetic field for 5 hours a day, the concentrations of cholesterol esters, triglycerides and free fatty acids decreased, so there was an increase in lipid catabolism and energy production (10). In addition, they observed that magnetic fields change the velocity, flow and direction of particles in biological systems, with impacts on the transport/charge system depending on shape, frequency, intensity and exposed duration (10). The decrease in plasma glucose, total cholesterol and triglyceride levels may be attributed to the retardation of lipid metabolism as suggested by Hefco et al , or to the increased synthesis and oscillation of insulin in the β cells as Laiti-Kobierska et al. 2002 suggested (13,22). Byus et al. and Blank et al. realized that there was an increase in the concentration of Na^{+}-K^{+}ATPase, effected through changes in intracellular Ca^{2+}. One of the most obvious candidates is the calcium ion. Changes in calcium concentration may influence the interaction with calmodulin, activate the protein kinase C, or act directly on the activity of intracellular enzymes. Other signal transductive candidates may membrane receptors whose interactions with G-proteins are modified by MF stimulation or ligand-gated channels that are acted upon by the fields. These findings might be attributed to complicated mechanisms. Further studies are required to show the effect of MF on intracellular Ca^{2+} ions and their movements, and on enzyme levels. Diabetes affects many mechanisms causing different complications at different stages of the disease. The apparently healthy response of the exposed rats might be consequent on a temporary recovery in hormonal regulation caused by the magnetic field, which may be a stress-generating factor. Therefore, we need to identify the mechanisms affected by the diabetes and the magnetic field and further studies are needed for this purpose. The mechanism of action of alternating magnetic fields on biological systems at the cellular level is under investigation.

References

1. C. Polk, E. Postow, Handbook of Biological Effects of Electromagnetic Fields, CRC Press, New York, 1996.

2. A. Lacy-Hulbert, J.C. Metcalfe, R. Hesketh, Biological responses to electromagnetic fields, FASEB J. 12 (1998) 395–420.

3. Behari J and Mathur R (1997). Exposure effects of static magnetic field on some physiological parameters of developing rats**.** *Indian Journal of Experimental Biology*, **35:**894-897.

4. Chen G, Suzuki H and Weston AH (1988). Acetylcholine releases endothelium-derived hyperpolarizing factor and EDRF from rat blood vessels. *Br J Pharmacol*, **95:**1165-1174.

5. Mayhan WG. Idvire SD, Sharpe GM (1999). Constrictor responses of resistance arterioles during diabetes mellitus. *Diabetes Research and Clinical Practice*), **44:**147-156.

6. Byus CV, Kartun K, Pieper S, Adey WR (1988). Increased ornithine decarboxylase activity in cultured cells exposed to low energy modulated microwave fields and phorbol ester tumor promoters. *Cancer Res*, 48:4222–4226.

7. Blank M, Soo I (1998). Enhancement of cytochrome oxidase activity in 60 Hz magnetic fields. *Bioelectrochem Bioenerg*, 45:253–259.

8. Beisher DE, Brehl RJ. (1975) Search for effects of 45 Hz magnetic field on liver triglycerides in mice. *Res Rep NU NAMRL*,1197.

9. Beisher DE, Grisett JD, Mitchell RE (1972). Exposure of man to magnetic fields alternating at extremely low frequency. *Naval Aerospace Medical Research Laboratory*,

10. Cherysheva ON (1987). Effect of alternating magnetic field of industrial frequency on the lipid composition of the rat liver. *Ukrainskii Biokhmicheskii Zhurnal*, 59:91-4.

11. Goodman EM, Greenebaum B, Marron MT (1993). Altered protein synthesis in a cell-free system exposed to a sinusoidal magnetic field. *Biochim Biophys Acta*, 1202:107–112.

12. Goodman EM, Greenebaum B, Marron MT (1995). Effects of electromagnetic fields on molecules and cells. *Int Rev Cytol*, 158:238–279.

13. Laiti-Kobierska A, Cieslar G, Sieron A and Grzybek H (2002). Influence of alternating extremely low frequency ELF magnetic field on structure and function of pancreas in rats. *Bioelectromagnetics*, 23;49-58.

14. Tartakoff AM (1980). The Golgi complex: crossroads for vesicular traffic. *Int Rev Exp Pathol*, 22:227-251.

15. Bassett C (1993). Beneficial effects of electromagnetic fields. *Cell Biochem,* 51(4):387-93.

16. Bassett C (1989). Fundamental and practical aspects of therapeutic uses of pulsed electromagnetic fields (PEMFs). [Review] [330 refs]. *Crit Rev Biomed Eng*, 17(5):451-529.

17. Navratil L, Hlavaty V, Landsingerova E (1993). Possible therapeutic applications of pulsed magnetic fields. *Cas Lek Cesk*, 132(19):11 PP. 590-4.

18. Iwasaka M, Miyakoshi J and Ueno S (2003). Magnetic field effects on assembly pattern of smooth cells. *In vitro Cell Dev Biol Anım,* **Mar;** 39(3):120-123.

19. Blank M, Goodman R (2001). Electromagnetic initiation of transcription at specific DNA sites. *J Cell Biochem,* 81:689–692.

20. Ovenchkina ZA, Martyniuk VS, Martyniuk SB and Kuchina NB (2001). Effects of the variable magnetic field of the extremely low frequency on metabolic processes in the liver of animals with various individual and typological characteristics. *Biofizika,* Sep-Oct**;** 46(5):915-

21. Oroza MA, Calcice L, Sanchez-Fkanco F, Rivas L (1987). Hormonal, hematological and serum chemistry effects of weak pulsed electromagnetic fields on rats. *Journal of Bioelectricity***;** 6(2):139-151.

22. Hefco V, Hefco E, Birca C (1969). Influence of the magnetic field on glycemia, pyruvic acid and lactic acid in white rat blood. *Rev Roum Biol-Zoologie,* 14:79-85.

CHANGES IN MEMBRANE POTENTIALS OF AORTA IN STREPTOZOTOCIN-INDUCED RATS EXPOSED TO LOW FREQUENCY MAGNETIC FIELD

Işıl Öcal[1], Mustafa Emre[1], Ufuk Mete[2] and İsmail Günay[1]

[1]Cukurova University, Medical Faculty, Department of Biophysics 01330 Balcalı/Adana, TURKIYE

[2]Cukurova University, Medical Faculty, Department of Histology 01330 Balcalı/Adana, TURKIYE

Tel:+90-322-3386060/3472

iocal@cu.edu.tr

Abstract

Endothelium-dependent and independent derived responses are diminish in some diseases, including hypertension, preclampsia and some models of diabetes. A study of the effects of weak, modulated sinusoidal low frequency electromagnetic field stimulation in changes in membrane potentials of the rat aorta in diabetes was carried out. Forty rats (n=40, Wistar albino spp) weighing between 220-300g were used in this study. The rats were first divided into four groups. The first group was made up of the citrated rats or sham (S, n=10), the second group was comprised of rats described as sham or citrated+magnetic field group (S-MF, n=10), third group contained experimental diabetic rats (D, n=10), and the fourth group was comprised of both experimental diabetic+magnetic field group (D-MF, n=10). Magnetic fields of 5 mT intensity and 50 Hz frequency oriented in the north-south direction was applied to the S-MF and D-MF groups for 2 hours and 45 minutes at each day during one month.

After one month, Rats were killed by decapitation. After the thoracic aorta preparation isolated, excess fats and/or connective tissues were removed. For measurement of smooth muscle membrane potential, arter was cut open longitudinally and pinned to the bottom, endothelial surface uppermost. Tissues were maintained at 37 °C and constantly perfused with Krebs buffer at a rate of 2 ml min^{-1}. Measurements of membrane potential were made sharp glass microelectrodes, back-filled with 3 M KCl and with resistances of 60-100 M Ω. All data were recorded through a Nihon Kohden instruments.

The negative of membrane potential of aorta in diabetes was significantly increased compared to control animals. One of the most obvious candidates is the calcium ion. Changes in calcium concentration may influence the interaction with calmodulin, activate the protein kinase C, or act directly on the activity of intracellular enzymes. Other signal transductive candidates are membrane receptors whose interactions with G-proteins are modified by EMF stimulation or ligand-gated channels that are acted upon by the fields. This knowledge could provide the basis of novel therapeutic inventions in the amelioration or prevention of vascular complications of these diseases.

Key words: Magnetic field, diabetes rat, rat aorta, resting membrane potential

Introduction

Macro and microvascular disease are currently the principal causes of morbidity and mortality in patients with type I and type II diabetes mellitus. Loss of the modulatory role of the endothelium may be a critical and initiating factor in the development of diabetic vascular disease. Microvascular disease is the main cause of morbidity and mortality in patients with diabetes Mellitus (DM). Endothelial dysfunction may be a critical and initiating factor to develop diabetic vascular disease (1). Mechanisms that participate in the reduced vasodilatory

responses in endothelial dysfunction include reduced nitric oxide generation, oxidative excess, and reduced production of hyperpolarizing factor.
Vascular smooth muscle relaxation in response to a signal initiated by stimulation of overlying endothelium is known as endothelium-dependent relaxation and involves the release of at least endothelium-derived relaxing factor /EDRF). There appear to be several important EDRFs the most well understood of these being NO and prostacyclin. It is now well established that endothelium-dependent vascular relaxation is often accompanied by K^+ channel-meditated hyperpolarization of the vascular smooth muscle. Because both NO and prostacyclin are known to be able to elicit vascular relaxation, at least in part, through activation of K^+ channels, endothelium-dependent hyperpolarization may often simply reflect part of the mechanism of relaxation produced by NO and prostacyclin.
An important function of all cells is their ability to regulate the movement of ions and macromolecules between the cell interior and its environment using membrane bound protein channels. If (K^+) channel opens in the vascular smooth muscle cell membrane, K^+ efflux increases, causing membrane potential hyperpolarization, closure of voltage-activated calcium (Ca^{2+}) channels, decreased Ca^{2+} entry, and vasodilatation. Biological effects of magnetic fields can be mobility or movement or induce variety of ions of effects in cells and tissues. These biological effects include nerve regeneration, influences on cell calcium levels and bone healing.
The release of endothelium-derived NO by agonists, such as acetylcholine (ACh), is dependent on a rise in intracellular calcium levels ([Ca^{2+}]i) within endothelial cells and activation of NO synthase (NOS). The entry of Ca^{2+} from the extracellular space is required to maintain production of NO (2,3) and several lines of evidence indicate that endothelial cell membrane potential plays a critical role in the regulation of Ca^{2+} entry (4). Ca $^{2+}$ entry is not dependent on voltage-gated Ca^{2+} channel activity, rather it occurs via a nonselective cation pathway and is dependent on membrane hyperpolarization to provide an inwardly directed electrochemical driving force for Ca^{2+} movement (4-7) Ocal et al magnetic field was supported to cause the changing movement of Ca^{2+} ions and direction in aorta rings of diabetic rats (8).
In the present study, we attempted to combine the beneficial properties of MF, which have been proved to be ion flows according to measure resting and 10^{-7} M phenylephrine (PE), 10^{-6}M acetylcholine (ACh) and 10^{-6} M sodiumnitroprusside (SNP)-induced membrane potentials.

Material and Methods

Approval for this study was obtained from local Institution's Animal Care and Ethics Committee. Forty adult white Wistar rats weighing 220 to 300 g were used in this study. The rats were first divided into four groups. The first group was made up of the citrated or sham rats (S, n=10), the second group was comprised of rats described as sham or citrated+magnetic field group (S-MF, n=10), third group contained experimental diabetic rats (D, n=10), and the fourth group was comprised of both experimental diabetic + magnetic field group (D-MF, n=10).
We injected 45 mg/kg streptozotocin (STZ) in citrate buffer (CB) (pH 4.5) into the tail veins to induce diabetes (D group). A similar volume of CB solution without STZ was injected into control rats (S group). Then, magnetic fields of 5 mT intensity and 50 Hz frequency oriented in the north-south direction was applied to the S-MF and D-MF groups for 2 hours and 45 minutes at each day during one month.
After the one-month study period, the rats under ether anesthesia before rats were killed by decapitation. After the thoracic aorta preparation isolated, excess fats and/or connective tissues were removed. For measurement of smooth muscle membrane potential, arter was cut open longitudinally and pinned to the bottom, endothelial surface uppermost. Tissues were maintained at 37°C and constantly perfused with Krebs buffer at a rate of 2 ml min^{-1}. Measurements of membrane potential were made sharp glass microelectrodes, back-filled with 3 M KCl and with resistances of 60-100 M Ω. A vessel sample was pinned to the bottom of the recording chamber. Modified Krebs solution had the following composition (mM): 119,: NaCl, 4.6 KCl, 1.5 $CaCl_2$, 1.2 $MgCl_2$ 15 $NaHCO_3$, 1.2 $NaHPO_4$ and 11 Glucose. All data were recorded through a Nihon Kohden instruments.
After the resting membrane potentials of rat aorta in each group were measured, ACh, PE and SNP-induced membrane potentials of aorta preparations were.measured. ACh, PE and SNP-induced membrane potentials were recorded though a Nihon Kohden instruments.
The negative of membrane potential of aorta in D group was significantly decreased compared to S group. While 10^{-7} M PE-induced negative of membrane potential were decreased in each group, 10^{-6} M-induced membrane potential in D-MF group was enclosed resting membrane potential of D group. Results were significantly ($p<0.05$).

Ultrastructure of thoracic aorta preparation

For histopathology of thoracic aorta preparations of rats, of citrated or sham, sham-exposed to magnetic field, diabetic and diabetic-exposed to magnetic field groups were examined. After opening the abdominal cavity,

samples of the thoracic aorta were taken, and after appropriate fixation and preparation were examined ultrastructurally in an electron microscope.

Solutions and chemicals

All drugs were obtained from Sigma Chemical Co. (St. Louis, MO,USA). Stock solutions of phenylephrine hydrochloride (PE), acetylcholine bromide (ACh) and sodium nitroprusside (SNP) were dissolved in distilled water. Streptozotocin was freshly dissolved in 0.1 M citrate buffer (pH 4.5) immediately before use at a concentration of 45 mg/kg; all drugs were obtained from Sigma Chemical Co.

Statistics

All data were expressed as means ± S.E.M. The statistical significance of all differences between mean values was calculated using Student's paired *t* test or repeated measures ANOVA followed by Tukeys *post hoc* test. A level of $P<0.05$ was considered to be statistically significant.

Results

Table 1. The mean ± SEM of 10^{-7} M phenylephrine (PE), 10^{-6} M acetylcholine (ACh) and 10^{-6} M sodium nitroprusside (SNP)-induced membrane potentials.

Experimental Groups	Membrane Potential (mV)			
	Resting	**10^{-7} M PE**	**10^{-6} M ACh**	**10^{-6} M SNP**
S	-56,2 ± 1,0	-51,1 ± 0,9	-59,2 ± 0,9	-56,1 ± 1,2
S-MF	-53,6 ± 0.6	-48 ± 0,6*	-57,8 ± 0,9	-51,8 ± 0,6
D	-47,5 ± 0,6*	-42,8 ±0,8*	-43,1 ± 1,7	-46,7 ± 0,8
D-MF)	-43,4 ± 0,7	-36 ± 0,3*	-43,7 ± 0,7	-44,4 ± 0,4

The mean values of negative of resting membrane potential of aorta preparations were significantly decreased in both groups of rats after sham-exposed and diabetic-exposed to the alternating modulated magnetic field groups for four weeks, compared to those of sham and diabetic groups (Table 1, Fig 1). The negative of 10^{-7} M PE-induced membrane potential of aorta in S, S-MF, D and D-MF groups were decreased (Table 1, Fig 2), while negative of the 10^{-6} M ACh-induced membrane potential in S, S-MF, D and D-MF groups were increased (Fig 3). Data were significant ($p<0.05$).

There was no significant difference between the membrane potentials of aorta preparation of rats in D or S and in SMF or DMF groups that the aorta induced by 10^{-6} M sodium nitroprusside (Fig 4).
Electron micrographs of the thoracic aorta preparations from the S-MF group showed only minimal ultrastructural changes (Fig 5,6). In the D-MF group, however, a decreased density of elastic tissues compared to the D group was apparent after 30 days (Fig 7,8).

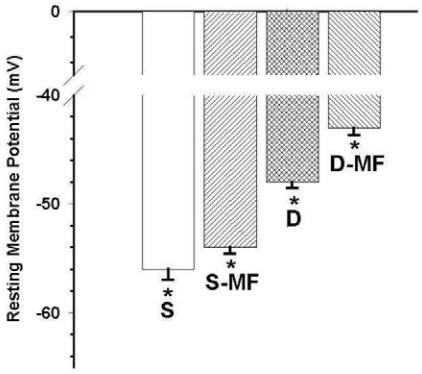


Fig1. Resting membrane potentials of aorta preparation of rats in citrated (S), citrated-magnetic field, diabetic and diabetic-magnetic field groups

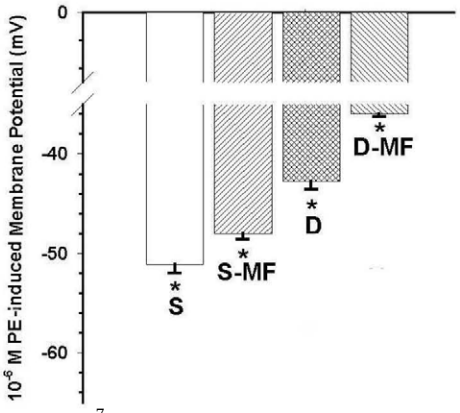


Fig2. 10^{-7} M PE-induced membrane potentials of aorta preparation of rats in citrated (S), citrated-magnetic field, diabetic and diabetic-magnetic field groups

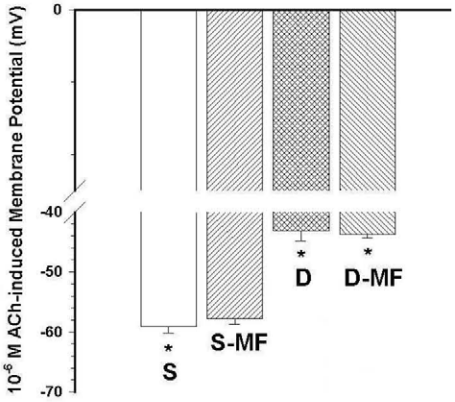


Fig3. 10^{-6} M ACh-induced membrane potentials of aorta preparation of rats in citrated (S), sitrated-magnetic field, diabetic and diabetic-magnetic field groups

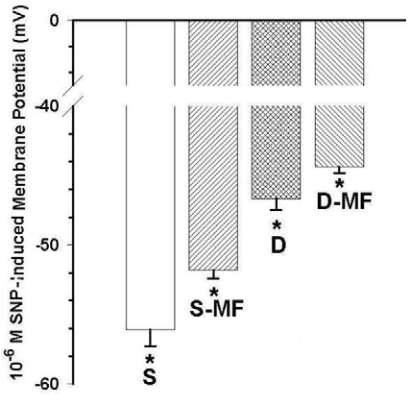


Fig4. 10^{-6}M SNP-induced membrane potentials of aorta of rats in citrated (S), citrated-magnetic field, diabetic and diabetic-magnetic field groups.



Fig 5. Electron micrograph of thoracic aorta from rats in the S group; el-elastic fibers, sm-smooth muscle.

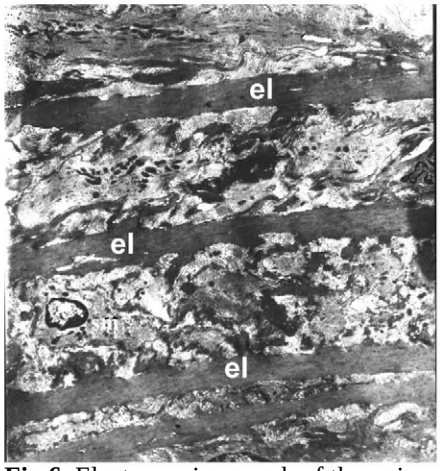


Fig 6. Electron micrograph of thoracic aorta from rats in the S-MF group; el-elastic fibers, sm-smooth muscle.

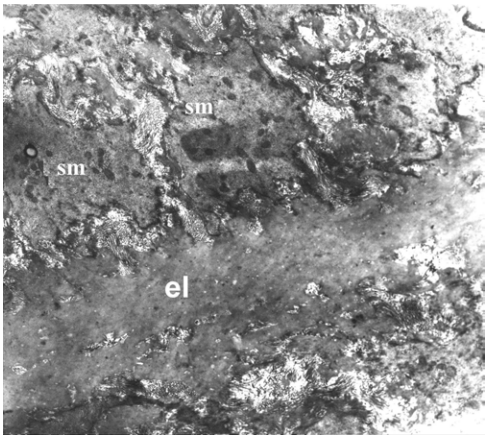


Fig 7. Electron micrograph of thoracic aorta from rats in D group; el-elastic fibers, sm-smooth muscle.

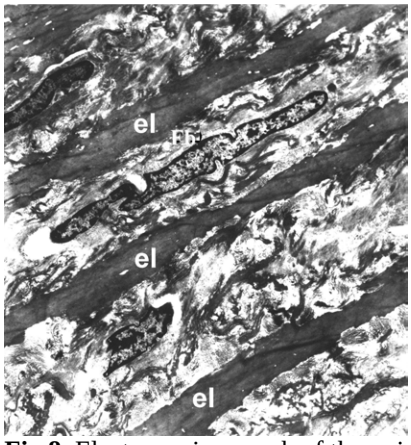


Fig 8..Electron micrograph of thoracic aorta from rats in the D-MF group; el-elastic fibers, sm-smooth muscle.

Discussion

Changes in EDRF in diabetes have been studied in most detail in streptozotocin (STZ)-induced diabetes in rats. In the rat aorta vessel, negative of resting membrane potentials were significantly diminished compared with membrane potentials of aorta preparations of rats in S group. The mechanisms underlying disease-associated impairment of EDHF-attributed hyper polarization and relaxation are far from clear and require further studies to determine whether the dysfunction arises in the smooth muscle cells and/or the endothelial cells and/or myoendothelial communication. This knowledge could provide the basis of novel therapeutic inventions in the amelioration or prevention of vascular complications of these diseases.

In the resting membrane potential of the rat aorta, negative of resting membrane potential in S group was decreased from-56.2 ±1.0 mV to -53.6± 0.6 mV compared with resting membrane potential of S-MF group. But there was no significant difference between the S and S-MF groups. When the resting membrane potentials of rat aorta in S group (-56.2 ± 1.0 mV) were compared with D groups (-47.5 ± 0.6 mV), negative of resting membrane potentials were increased (Table 1). Data were significantly. Also, negative of resting membrane potentials in D-MF groups were decreased from -47.5 ± 0.6 mV to 43.4 ± 0.7 mV too. Ocal et al were observed the positive effects of low frequency magnetic field on mechanical activities in diabetic rats (8). Magnetic fields may affect movement ions and directions in biological tissues. K^+ channels are critical in maintaining the normal resting membrane potential in a variety of excitable cells. But mechanism of relaxation is no only affected K^+ ion or K^+ ion movements.

In this study, we observed only minimal ultrastructural changes in electron micrographs of thoracic aorta preparations from rats in the S-MF group (Fig 5, 6). However, by the end of the 30th day, ultrastructural changes related to decreased elastic tissue density were seen in the D-MF group compared to the D group (Fig 7,8). Laiti-Kobierska et al. 2002 identified granules in the β cells of rats exposed or not exposed to a magnetic field; these granules were called special granules. On the other hand, there were inflated mitochondria and expanded endoplasmic tubules in the pancreatic acinar cells. These authors suggested that the observed changes occurred because of the magnetic field and were related to increased synthesis and oscillation of insulin (Laiti-Kobierska et al. 2002). Numerous experimental findings suggest that exposure to extremely low-frequency (ELF) magnetic fields (MFs) affects various cell functions via actions exerted on intracellular and membrane proteins, including ion channels, membrane receptors and enzymes (9,10).For these reason, enzymes activities and membrane receptors and as Ca^{2+} the other ions have to examine. One of the most obvious candidates is the calcium ion. Changes in calcium concentration may influence the interaction with calmodulin, activate the protein kinase C, or act directly on the activity of intracellular enzymes. Other signal transductive candidates may membrane receptors whose interactions with G-proteins are modified by MF stimulation or ligand-gated channels that are acted upon by the fields.

References

1- Pomilio M, Mohn A, Verrotti A, Chiarelli F (2002). Endothelial dysfunction in children with type 1 diabetes mellitus. J Pediatr Endocrinol Metab; 15: 343-61.

2. Lückhoff, A., Pohl, U., Mülsch, A. & Busse, R. (1988). Differential role of extra- and intracellular calcium in the release of EDRF and prostacyclin from cultured endothelial cells. *British Journal of Pharmacology* **95**, 189–196.

3. Kruse, H. J., Grunberg, B., Sıess, W. & Weber, P. C. (1994). Formation of biologically active autacoids is regulated by calcium influx in endothelial cells. *Arteriosclerosis Thrombosis* **14**, 1821–1828.

4. Nılıus, B. & Droogmans, G. (2001). Ion channels and their functional role in vascular endothelium. *Physiological Reviews* **81**, 1415–1459.

5. Busse, R., Fıchtner, H., Lückhoff, A. & Kohlhardt, M. (1988). Hyperpolarization and increased free calcium in acetylcholinestimulated endothelial cells. *American Journal of Physiology* **255**, H965–969.

6. Lückhoff, A. & Busse, R. (1990*a*). Activators of potassium channels enhance calcium influx into endothelial cells as a consequence of potassium currents. *Naunyn-Schmiedebergs Archives of Pharmacology* **342**, 94–99.

7. Kamouchı, M., Droogmans, G. & Nılıus, B. (1999). Membrane potential as a modulator of the free intracellular Ca2+ concentration in agonist-activated endothelial cells. *General Physiology and Biophysics* **18**, 199–208.

8. Öcal I, Günay İ: The effects of chronic ac magnetic field on contraction and relaxation of isolated thoracic aorta rings of healthy and diabetic rats. Brazilian Archives of Biology and Technology, 47(5), 2004.

9 C. Polk, E. Postow, Handbook of Biological Effects of Electromagnetic Fields, CRC Press, New York, 1996.

10 A. Lacy-Hulbert, J.C. Metcalfe, R. Hesketh, Biological responses to electromagnetic fields, FASEB J. 12 (1998) 395–420.

Temperature Increase and SAR in a Phantom Model of the Human Head Exposed to 1800 MHz Non-Ionizing Radiation

[1]Şükrü Özen, [1]Selçuk Helhel, [2]Ömer H.Çolak

[1]Akdeniz University, Department of Electrical and Electronics Engineering, Antalya, Turkey
[2]Akdeniz University, TBMYO, Department of Biomedical, Antalya, Turkey

sukruozen@akdeniz.edu.tr, selcukhelhel@akdeniz.edu.tr, omercol@akdeniz.edu.tr

Abstract

In this study, temperature rise and Specific Absorption Rate (SAR) induced by 1800MHz microwave (MW) frequency non-ionizing radiation in human brain tissue has been investigated by using brain equivalent liquid. Brain equivalent tissue was exposed to MW radiation of 1800MHz for various time duration within a system allowed positions. As a radiation source, 1800MHz MW generator was used. The brain tissue phantom model was placed in a near field of half wave dipole antenna. A temperature rise in a brain tissue which's equivalent model was exposed to 1800 MHz was measured for investigating a SAR absorbed in brain tissue of human head.

Keywords: MW, Cellular Phone, Brain-equivalent phantom, Temperature Rise, SAR.

INTRODUCTION

During the last years, wireless data and phone networks have become widely used. And especially, adverse health effects of cellular phones and base stations have been discussed. Many international organizations have defined safety limits for exposure to these type communication devices. Adverse health effects of the cellular phones used close to the human body have been especially interested, because of complexity of interaction of RF (Radio Frequency) radiation and human body, and EM (Electromagnetic) fields induced in human head difficulty determinations. Recently, it is possible to find a lot of investigations on this subject in the literature. Whole body SAR (Specific Absorption Rate) limit of 4 W/kg is recommended by international organizations [1]. After applying the safety standards, maximum SAR limits are 0.4 W/kg and 0.08 W/kg for controlled and uncontrolled environment, respectively. European standard of ENV50166-2 is determined SAR limit of 2 W/kg for 10g tissue and 6 minute period in a controlled environment [2]. Heat transfer mechanisms of human body are limited temperature rise for the SAR limit. For general public in Turkey, power density limits of f/200 W/m^2, 10 W/m^2 and $6.67x10^{-5}f$ are approved in the frequency ranges 0.4-2 GHz, 2-150 GHz and 150-300 GHz, respectively [3].

While theories on the biological effects of EM fields have not been exactly established, there are still insufficient treatments have not been exactly understood, yet. The interdisciplinary investigations have been continued. One of the known basic experimental method was used to investigate thermal effects of EM radiation in tissue equivalent liquids[4]. In this study, the temperature rise in human brain and SAR are investigated by using an equivalent model.

SPECIFIC ABSORPTION RATE (SAR)

SAR is an important quantity in dosimetry which indicates the temperature rise and the absorbed energy by tissue, and other biological events that occur in the tissue depended on internal fields. SAR varies depending on frequency and tissue properties. The effects in the biological tissues depend on the penetrated fields not to the external fields. To determine the SAR in human body and laboratory animals is so important to explain biological effects. There are two basic methods are used to evaluate SAR. They are calculation and measurement of absorbed energy in phantom models. Experimentally, SAR is determined measuring electric field $\left|\vec{E}\right|$ induced in tissue or temperature rise $\partial T/\partial t$.

$$SAR = \frac{\sigma}{2\rho}\left|\vec{E}\right| = C\frac{\partial T}{\partial t} \qquad (1)$$

Where; σ (S/m) is tissue conductivity, ρ (kg/m^3) is tissue density, *C* (j/kg°C) is the heat capacity of tissue (or phantom material) and E (V/m) is the rms value of intensity of the electric field induced in tissue. If the heating time is sufficiently short so that the effect of thermal conduction in the phantom can be neglected, the SAR can be derived form the measured temperature rise as follows[5]. If the temperature rise in tissue is measured, (1) can be arranged as

$$SAR = C\frac{\Delta T}{\Delta t} \quad [\text{W/kg}] \qquad (2)$$

Where; ΔT is the temperature rise in °C for Δt second period and *C* (j/kg°C) is the heat capacity of tissue (or phantom material). From the above, it is found that a temperature rise sufficient for SAR observation can be obtained by low power illumination for a short time if the specific heat of the phantom is small to a certain degree to an advantage in the measurement[6].

MEASUREMENTS

In this study, the brain equivalent tissue suggested by [7, 8] has been prepared and used. The human brain tissue equivalent mixture contains water of 54.90%, salt of 0.18% and Glycol (Diethylene Glycol Butyl Ether) of 44.92%. Electrical parameters of the equivalent tissue have been measured as ε_r=40.3 and σ=1.35(S/m) using HP4194A Impedance/Gain-Phase Analyzer. The measurement set-up of the temperature rise is shown in Figure 1. Prepared brain tissue equivalent liquid has been put into a spherical pyrex glass bowl that has an outer diameter of 224 ± 0.5 mm and glass thickness 5 ± 0.5 mm. Glycol provides a big easiness to prepare brain equivalent tissue. Evaporation of phantom liquid has been prevented from taking precautions in the measurement period and the measurements have been completed in one week.

The expected temperature rises in the liquid have been measured depending on the parameters of antenna-tissue distance, deepness, exposure time and signal generator output power and logged on a computer. PT-104 Platinum Resistance Thermometer Data Logger measurement system has been used. The system has sensitivity of 0.001^{0}C and accuracy of 0.01 ^{0}C. RF signal generator has adjustable output power level in the range of 0-2W and frequency in the range of 1800-1900MHz. 1800MHz half-wave dipole antennas has been used in the measurements. The liquid level was equal to 160 mm during all measurement.

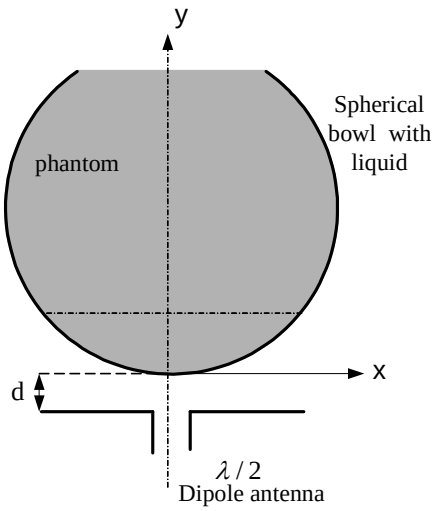


Figure 1. The measurement set-up of the temperature rise in the brain equivalent tissue

Measurements have been realized in the isolated box where the change in temperature approaches to zero. The temperature variation in the box has been continuously measured, and it has been logged when its value is approximately 22^{0}C±0.2^{0}C. Considering the radiation characteristics of the half wave dipole antenna, maximum field intensity is expected on the feed point direction. Because of this, temperature rise in the tissue that is on the feed point direction has been measured considering various exposure probabilities.

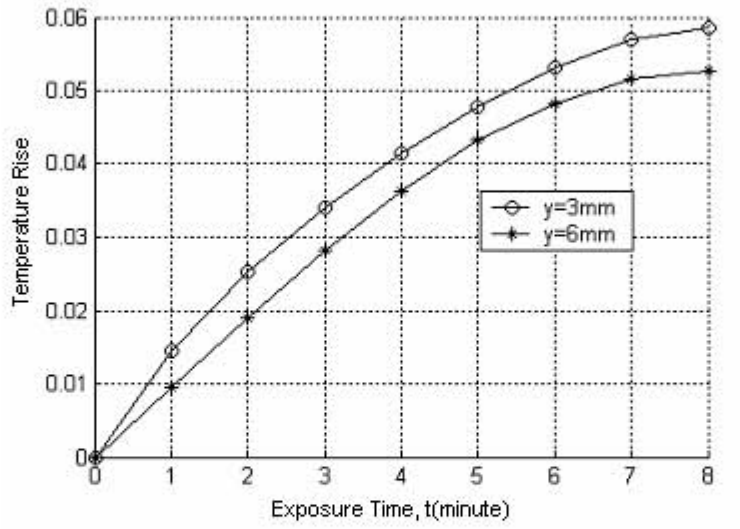


Figure 2. Varying in the temperature rise (^{o}C) in the brain equivalent liquid at 1800MHz depending on the exposure time period and deepness (d=13mm and p=1.5w)

The distance to the tissue surface has been adjusted to d=13mm and the temperature rise generated in the tissue at the distances of y=3mm and y=6mm has been measured depending on the exposure time period, as shown in Figure 2. The temperature rise decreases depending on the deepness.

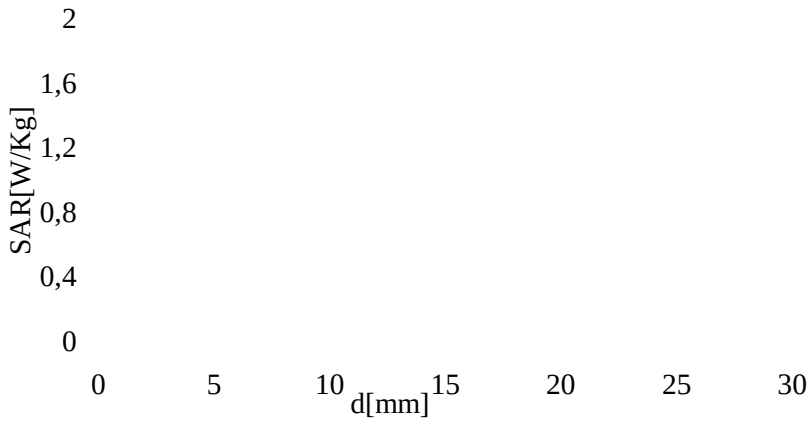


Figure 3. Changing in SAR depending on the distance between the antenna and the tissue at 1800 MHz (y=1mm, p=1.5w, Δt=120sn)

Absorbed SAR has been calculated by Equation 2. with the measured temperature rises in the brain equivalent tissue. The SAR calculated at the deepness of y=1mm at 1800MHz versus the distance between the dipole and the tissue is shown in Figure 3. The specific heat capacity has been chosen as C=4000 (W sec/kg °C) for the SAR calculation. As shown in Figure 3, the SAR absorbed by tissue decreases depending on the distance between the dipole and the tissue like the change of the temperature rise. The temperature rises depending on the various distances, d and exposure time at 1800MHz is shown in Figure 4.

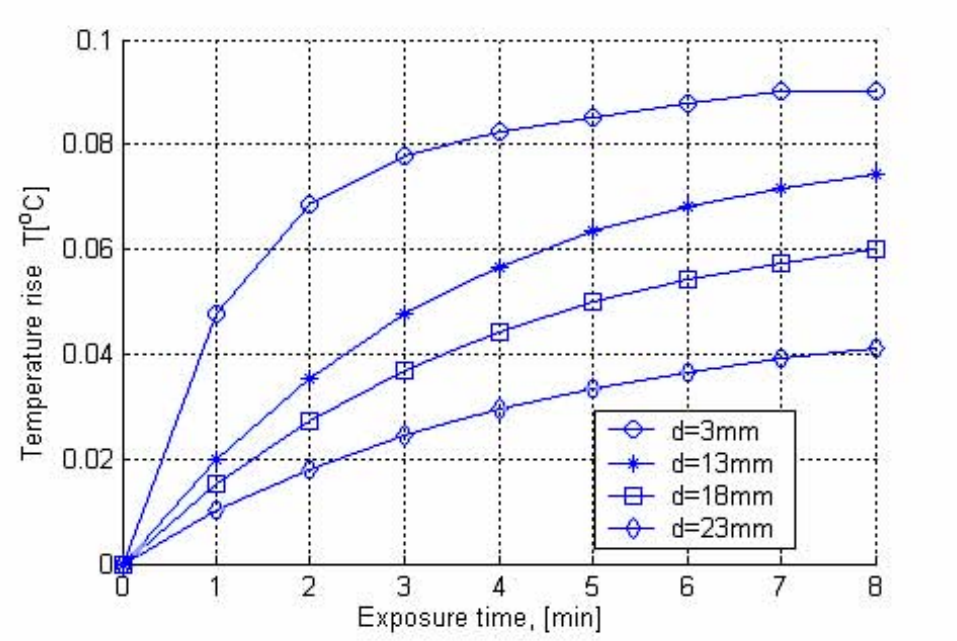


Figure 4. Shows the temperature rises depending on the various distances, d and exposure time at 1800MHz (y=1mm and p=2w)

CONCLUSIONS

The temperature rise generated in the brain tissue does not exceed 0.1 °C at 1800 MHz cellular phone frequency. The cellular phones operated at 1800 MHz cause the temperature rise less than the lower limit value 1°C. The temperature rise curves formed using measurement data are exponential function of the exposure time period. The SAR estimation has also been done depending on the temperature rise in the equivalent tissue using the model in this study. The cellular phones used in close body situation especially the head close usage causes absorbing the high level SAR. An investigations with laboratory animals present an indirect data for human being, and it is clear that the experimental investigations realized using biologic tissue equivalent phantom models provide big easiness. Further investigations on the other biological effects of the cellular phones are required considering thermal effects. Since the knowledge of biological structure and dielectric properties of children have not been exactly revealed, further investigations need to be focused on children.

REFERENCES

[1] IEEE Standard Board, IEEE-C95.1, Safety Levels With Respect to Human Exposure to Radio Frequency Electromagnetic Field, 3 kHz to 300 GHz, IEEE Standard Department, Piscataway, New Jersey, 1991.

[2] European Communities Prestandard, ENV 50166-2, Human Exposure to Electromagnetic Fields High Frequency (10 kHz to 300 GHz), 1995.

[3] TS ENV 50116 Türk Standardı, İnsanların Elektromagnetik Alanlara Maruz Kalması–Yüksek Frekanslar (10kHz-300GHz), TS ENV 50116 – 2, 1996.

[4] Ozen, S., Onural A.Ş., Çömlekçi S., Çerezci O., "Experimental Determination of Heat Rise and SAR Occurred by 900 MHz EM Radiation on Human Brain by Using Brain Phantom Model", G.U Journal of Science. 17(3):127-132, 2004

[5] Guy AW, Analyses of electromagnetic fields induced in biological tissues by thermographic studies on equivalent phantom models IEEE Trans MTT 1971; 19:205-214

[6] Koichi I., Katsumi F., Yoshinobu O., and Lira H., "Development and Characteristics of a Biological Tissue-equivalent Phantom for Microwave, Electronics and Communications in Japan, Part 1, Vol. 84, No.4, 2001

[7] Ozen S., Theoretical and Experimental Study on Thermal Analysis in Biological Tissue Which Under Exposure of MW Frequency EM Radiation, PhD, Thesis, Sakarya University, Science Institute, 2003.

[8] Ozen S., Köylü H., " Phantom Model Of Human Brain Tissue For Cellular Phone Frequencies in Electromagnetic Field Radiation Absorption Studies", G.U Journal of Science. 18(2):193-200, 2005

Acknowledgments- This study was supported by Scientific Research Projects Department of Akdeniz University

NO EFFECT OF 1800 MHZ RFR TO COLLAGEN SYNTHESIS TO GUINEA PIG LIVER TISSUE

ELCIN OZGUR, GOKNUR GULER

BIOPHYSICS DEPARTMENT, GAZI UNIVERSITY MEDICAL FACULTY
GAZI UNIVERSITESI TIP FAKULTESI BIYOFIZIK ANABILIM DALI
06510 BESEVLER ANKARA TURKEY
elcinozgur@gazi.edu.tr, gozturk@gazi.edu.tr

Abstract
RF radiation values generated Nokia 3210 mobile phone operating 1800 MHz frequency band measured by Electromagnetic (EM) radiation meter during experiment. Male Guinea pigs were exposed to operating mobile phone for 10 minute-periods in 7 days of a week. Average external Electric (E) field measured during exposure was 11.2 V/m. Effects of whole body exposure of 11.2 V/m to collagen synthesis in liver tissue were determined by using three different hydroxyproline level designation methods named H. Stegemann-K. Stalder, I.S. Jamall, V.N. Finell and ISO 3496.
It was observed that the increment found hydroxyproline level due to mobile phone radiation in liver was statistically insignificant. It was detected statistically that the hydroxyproline level designation methods of ISO 3496 is the most accurate way of measuring hydroxyproline level in between the methods used in this research.

Introduction
Since time began until about hundred years ago living beings had to deal with naturally occurring radiation, which somehow was balanced or life was shielded from detrimental parts of that radiation such as certain cosmic radiation. When people began to harness electricity, generate and transport it over long distances a different kind of energy was introduced to our life: AC (Alternating Current) electric, AC magnetic fields and radiofrequency radiation. The superimposition of electromagnetic fields caused by all kinds of electromagnetic radiation that arise in the human environment is known as electromagnetic pollution. Not only is electromagnetic pollution responsible for interference between electrical devices, but it is also affects the human body. The organism reacts to the electrical, magnetic and electromagnetic fields around it. The biological effects depend on the type, frequency and strength of these fields. The boom in the use of the cellular phone has led to a very evident increase in this kind of stress.
Many in vivo and in vitro studies have been performed to investigate the biological consequences and to assess health risks of RFR (Radio Frequency Radiation) generated from cellular phones. Relation between RFR and protein synthesis is still unclear mechanism continuing to investigate.
The connective tissue protein, collagen, is the most abundant protein in higher animals . Collagen also provides the framework for parenchymal organs such as the liver, kidney, and spleen, either in its fibrous form or organized in basement membranes. The rate of hydroxyproline formation is therefore considered to be a good indication of the rate of collagen biosynthesis. The collagen content of a tissue is determined by measuring the content of protein bound hydroxyproline. Hydroxyproline is necessary for collagen helix formation, and in its absence collagen is unable to be properly secreted from fibroblasts (Irvin, 1981; Craig et al, 1975; Takahashi and Lee, 1987).
The connective tissue protein, collagen, is not only abundant but also significant protein in higher animals since it is charged molecule tend to be directed trough electric field applied.. In this research, effects of RFR generated by mobile phones on liver tissue collagen examined by using tree different hydroxyproline detection methods.

Material and Method
In this investigation, 3 month-old guinea pigs were exposed to RFR radiated from Nokia 3210 mobile phone operated in GSM DCS 1800 MHz. During the exposure of every Guinea pig, external E fields were measured by NARDA EMR 300 and type 8.3 probe. Measurements were taken for duration of 10 minutes per 2 seconds and the data saved to the computer connected to device via fiber optic cable. The whole data were averaged before statistical analysis.
Guinea pigs were exposed to RFR averaged as 11.2 V/m for 10 minutes a day during 7 days and analyzed for the effects on liver tissue collagen level. Changes of collagen level were analyzed biochemically by three different

hydroxyproline determination method named as “H. Stegemann-K. Stalder”(Stegemann, 1958; Stegemann et al, 1963; Stegemann et al, 1964; Stegemann and Stalder, 1967a; Stegemann and Stalder, 1967b), “I.S. Jamall-V.N. Finell” (Jamall et al, 1981) and “ISO 3496” (TS 6236 ISO 3496, 1997). Also, histological analyzes were accomplished.

Result

The outcome of the biochemical analysis pointed out that hydroxyproline level increased with respect to control but this increase was not statistically significant for all methods ($p>0.05$). On the contrary, histological analyses showed that RF exposure makes fibrosis in liver tissue increase significantly. In addition to this, difference in hydroxyproline determination accuracy of ISO 3496 method with respect to other two methods was found as statistically significant ($p<0.05$) (Table 1- Figure 1).

Discussion

In this study, effects of RFR generated by mobile phones on liver tissue collagen examined by using hydroxyproline detection methods. Hydroxyproline is characteristic amino acid whose tissue level is used to determine the tissue collagen level (Dahl and Persson, 1963; Edwards and O’brien, 1980; Bondjers and Bjorkerud, 1973; James et al, 1990; Neuman and Logan, 1963; Stegemann, 1958; Stegemann et al, 1963; Stegemann et al, 1964; Stegemann and Stalder, 1967a; Stegemann and Stalder, 1967b; Mommersteeg etal, 1993; Reddy and Enwemeka, 1996; Switzer and Summer, 1971; Wood et al, 1990).

Biological effect mechanisms of RFR were analysed as thermally and non-thermally also the cumulative effects which are not clear yet. Increase of the molecular activities when matter interactions with EMF can cause thermal effects’ arises. Electrically charged particles as ion, molecular dipole and colloidal particles are always in motion in the unstable fields. Electromagnetic fields affect collagen since it is charged particle. If a low current is applied to the collagen solution in acid solvent, a concave band is formed around cathode which shows that collagen behaves like cation under the effect of electric field. Effects of electric field on hydroxyproline can be explained as collagen consists of hydroxyproline with the ratio of 1/10(Gustavson, 1956; Ramachandran, 1967a; Ramachandran, 1967b). The physical phenomenon which states that low frequency RFR can penetrate into more internal tissues than high frequency RFR can be active mechanism on which can explain why RF radiation is non-effective on liver tissue collagen. Also, wavelength changes with respect to electrical qualifications of the medium. Certain systems with ionic conductivity can have high dielectric constant in the range of several thousands. For this reason, it is considered that macro molecules can have comparable dimensions with the wavelength of microwaves which express spatial resonances. But, if the frequency increases, resonance of the large dipolar molecules like proteins gets harder with the field. Resonance frequency matching may be the reason why 1800 MHz RFR is not effective on collagen in liver tissue. Besides this study, the evidences in the earlier studies expressed that static and extremely low frequency (ELF) 50 Hz electric fields and magnetic fields applied in different direction and strength affected the hydroxyproline level in liver and some other tissues like kidney, lung, skin and wound (Güler, etal, 1996; Güler and Atalay Seyhan, 1996; Güler and Seyhan , 2001; Canseven and Seyhan, 2005; Canseven and Atalay Seyhan, 1995; Canseven and Atalay Seyhan, 1996; Canseven and Seyhan, 2000, Seyhan et al, 2006)

It is possible to determine the collagen level in tissue by applying hydroxyproline determination methods which should be very accurate since liver tissue collagen level is less than other tissues like skin or bone. In this study, “H. Stegemann-K. Stalder”, “I.S. Jamall-V.N. Finell” and “ISO 3496” were chosen as biochemical methods of liver tissue hydroxyproline level determination after literature search. In each of tree methods, tissue hydrolysis hydroxyproline measured by spectrometry after adding Cloramin-T reactive which stains the solution. The wavelength for measuring optic density of solution for “H. Stegemann-K. Stalder” and “I.S. Jamall-V.N. Finell” is 560 nm, but for the method called “ISO 3496” is 558 nm. One of the method named as “ISO 3496” was found as the most accurate method with respect to the other two ($p<0.05$). This method is nowadays used for determining the absolute value of hydroxyproline in the meat and meat product industry which should be very little collagen content in order to be fine product.

RFR radiated by mobile phones which are daily components of our daily lives, exposed to male guinea pigs 10 minutes daily for 7 days and the increase of hydroxyproline level in liver tissue was found as statistically insignificant with respect to controls. However, although not significant, this increase make a question be asked that what the consequence will be if the exposure period is prolonged because people use their mobile phones more than 1 week and also may use them more than 10 minutes daily.

For this reason, prolonged researches should be done in order to determine the biological effects of RFR.

Table 1: Comparison of liver tissue hydroxyproline level measured by tree different methods of 10 minutes exposure group with controls

H. Stegemann-K. Stalder		**I.S. Jamall-V.N. Finell**		**ISO 3496**	
Control –HP level	**Exposure- HP level**	**Control –HP level**	**Exposure- HP level**	**Control –HP level**	**Exposure- HP level**
0.2686	0.3260	0.1845	0.2902	0.2851	0.3419
0.3045	0.3003	0.2706	0.2882	0.2914	0.3302
0.2479	0.2418	0.3198	0.2872	0.2987	0.3158
0.2606	0.2551	0.3690	0.2671	0.3041	0.2849
0.3225	0.2710	0.2706	0.2730	0.3057	0.2861
0.2985	0.2911	0.3075	0.3171	0.3117	0.3044
0.2427	0.2729	0.3321	0.3029	0.3209	0.3006
0.2460	0.2913	0.2828	0.2652	0.3301	0.2910
0.2553	0.2692	0.3819	0.3152	0.3012	0.2994
0.2433	0.2547	0.2706	0.3006	0.3034	0.3037
0.2979		0.1968	-	0.3075	-
0.2716 ± 0.0289	**0.2773 ± 0.0251**	**0.2897±0.0622**	**0.2907±0.0185**	**0.3054 ± 0,0125**	**0.3058 ± 0.0186**

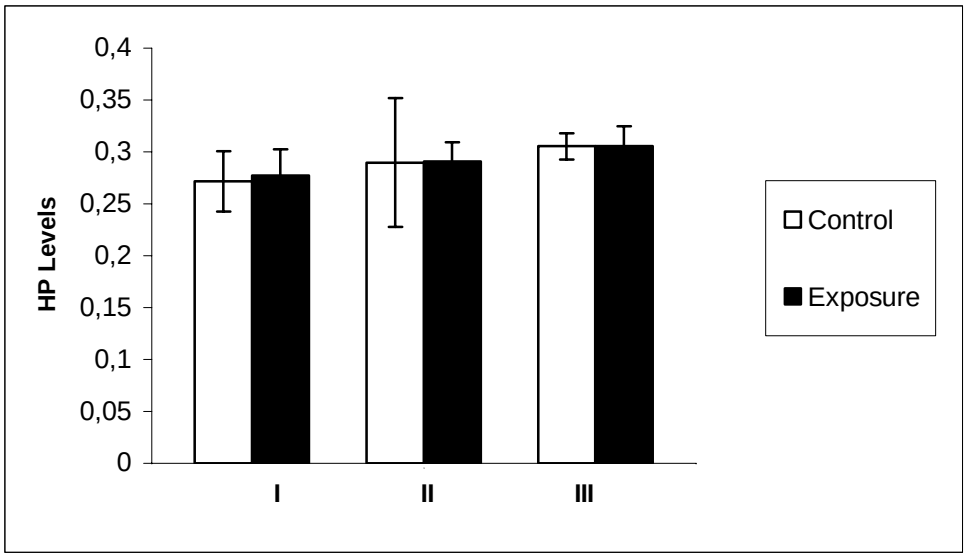


Figure 1: Liver tissue hydroxyproline level determination by using tree different biochemical methods I: H. Stegemann-K. Stalder's method, II: I.S. Jamall-V.N. Finell's method and III: Method of ISO 3496.

References

Bondjers G., Bjorkerud S. (1973). Spectrophotometric Determination of Hydroxyproline in Connective Tissue on the Nanogram Level, *Anal. Biochem*, 52, 496-504,.

Canseven, A.G., Atalay Seyhan, N. (1995). Electric Current – Collagen Synthesis Interaction in Wound Healing I. *Turkish Med J* 2:71-77 (Turkish)

Canseven, A.G., Atalay Seyhan, N. (1996). Is It Possible to Trigger the Collagen Synthesis by Electric Current in Skin Wounds?. *Indian J Biochem. Biophys* 33: 223-227.

Canseven, A.G., Seyhan, N. (2000). Changes in Skin Hydroxyproline Levels Under the Effect of Magnetic Fields. World Congress on Medical Physics and Biomedical Engineering. 23-28 July 2000, Navy Pier, Chicago (from CD/TU-B205-04)

Canseven, A.G., Seyhan, N. (2005). Effects of Ambient ELF Magnetic Fields: Variations in Collagen Synthesis of Guinea Pigs' Skin and Scaling From Animals to Human. *Gazi Medical Journal* 16:160-165 (Turkish)

Craig, RDP, Schofield, JD, Jackson, D. (1975).Collagen biosynthesis in normal and hypertrophic scars and keloid as a function of the duration of the scar. *Br. J. Surg*. 62 : 741-744.

Dahl, O., Persson, K (1963). Hydroxyproline, Methodological Studies of Analysis, *Act. Chem. Sc*., 17, 2499-2503,

Edwards C.A., O'brien W.D. Jr. (1980). Modified Assay for Determination of Hydroxyproline in a Tissue Hydrolyzate, *Clin Chim Acta*, 7: 104, 161

Güler G., Seyhan Atalay N., Özoğul C., Erdoğan D. (1996). Biochemical and structural approach to collagen synthesis under electric fields. *Gen. Physiol. Biophys*. 15: 429-440.

Güler, G., Atalay Seyhan, N. (1996). Changes in Hydroxyproline Levels in Electric Field Tissue Interaction. *Indian Journal of Biochemistry and Biophysics* 33: 531-533.

Guler, G.; Seyhan, N. (2001). The effects of electric fields on biological systems. Engineering in Medicine and Biology Society, 2001. Proceedings of the 23rd Annual International Conference of the IEEE , Volume 2, 25-28 Oct. 2001 Page(s):1023 - 1025 vol.2

Gustavson K.H. (1956). *The Chemistry and Reactivity of Collagen*, Academic Pres Inc., Publishers, New York.

Hutterer, F. , Singer, E.J. (1960). A Modified Method for Hydroxyproline Determination, *Anal. Chem.*, 32: 556-558

Irvin, T. (1981): *Wound Healing Principles and Practice*. Cambrige: Chapman and Hall Ltd., pp 2-6.

Jamall I.S., Finelli V.N., Que Hee S.S. (1981 Mar 15). A simple method to determine nanogram levels of 4-hydroxyproline in biological tissues, *Anal Biochem*. 112(1):70-75

James J., Bosch K.S., Aronson D.C., Houkooper J.M. (1990). Sirius Red Histophometry and Spectrophoometry of Sections in the Assessment of the Collagen Content of Liver Tissue and its Application in Growing Rat Liver, *Liver*,10: 1-5.

Mommersteeg T.J.A., Kauer J.M.G., Huiskes R.,Blankevoort L. (1993). Method to Determine Collagen Density Distributions in Fibrous Tissues, *Journal of Orthopaedic Reseach*, 11: 612-616.

Neuman, R.E., Logan, M. (1963). The Determination of Hydroxyproline, *J. Biol. Chem*., 184, 299-306.

Ramachandran G.N. (1967a).*Treatise on Collagen*, Volume 1, Chemistry of Collagen, Academic Pres, London and New York.

Ramachandran G.N. (1967b). *Treatise on Collagen*, Volume 2, Biology of Collagen, Academic Pres, London and New York.

Reddy G.K., Enwemeka C.S. (1996). A Simplified method fort he Analysis of Hydroxyproline in Biological Tissues, *Clinical Biochemistry*, 29: 225-229.

Seyhan, N., Canseven, A., Güler, G. (2006). Animal Studies on the Effects of ELF and Static EMF, in Bioelectromagnetics Current Concepts, The Mechanisms of the Biological Effect of Extremely High Power Pulses (Ayrapetyan S.N., Markov M.S., eds), NATO Security through Science Series B: Physics and Biophysics, Vol. 5, Springer Press, the Netherlands, pp: 195-212 ISBN: 1-4020-4277-9

Stegemann, H., Fuchs, G., Eger, W. Der Transplantierte Knochenspan und Seine Qualitat Nach Partieller und Vollstandiger Enteiweibung Bei Erhaltener Anorganischer Substanz, Arch., Klin. Chir., 303,240-60.

Stegemann, H., Stalder K., Bernhard, G. (1964). Über die Isomerisierung von Hydroxyprolin, *Hoppe- Seyler's Z. Physiol. Chem*., 337: 179-185.

Stegemann, H., Stalder K. (1967a). Determination of Hydroxyproline, *Clin. Chim. Acta*., 18: 267-273.

Stegemann, H., Stalder K. (1967b). Zur Ausscheidung von Hydroxyprolin im Harn, *Hoppe- Seyler's Z. Physiol. Chem.*, 348: ,242-3.

Stegemann, H. (1958). Mikrobestimmung von Hydroxyprolin Mit Chloramin- T und p-Dimethylaminobenzaldehyd, *Hoppe-Seyler's Z. Physiol. Chem*.,311: 41-5,

Switzer B.R., Summer G.K. (1971). Improved Method for Hydroxyproline Analysis in Tissue Hydrolyzates, *Anal. Biochem*, 39: 487-491,

Takahashi, S., Lee, J. (1987). Quantitative study of tissue collagen metabolism. *Ana l Biochem* 162: 553-561.

TS 6236 ISO 3496 , (April, 1997). Meat and meat products -- Determination of hydroxyproline content, Turkish Standards Institude, First Publication, ANKARA

Wood, D.D., Mclaurin J., Moscarello M.A. (1990). A Hydroxyproline- contining Protein from Shark Brain that is Related to Myelin Basic Protein, *Journal of Neurochemistry*, 55: 1697-702.

CELLULAR AND INTRACELLULAR RESPONSE TO ELECTROMAGNETIC FIELD OF ULTRA HIGH FREQUENCY RADIATION

IVAN PAVICIC
IVANCICA TROSIC

INSTITUTE FOR MEDICAL RESEARCH AND OCCUPATIONAL HEALTH
KSAVERSKA CESTA 2. POB 291. HR-10001 ZAGREB, CROATIA
e-mail: ipavicic@imi.hr, phone: ++ (385 1) 4673 188

Abstract

The aim of this study was to evaluate whether low-level, ultra high frequency (UHF) irradiation of 935 MHz influences the cytoskeleton and the cell growth of V79 cells. UHF field was generated inside a Gigahertz Transversal Electromagnetic Mode cell (GTEM-cell) equipped with a Hewlett Packard signal generator. The electric field strength was 8.2±0.3 V/cm, and the average specific absorption rate (SAR) was calculated to be 0.12 W/kg. Cell samples were cultivated in a humid atmosphere at 37 °C in 5% CO_2. Prepared cell samples were exposed to the 935 MHz continuous wave frequency field for 1, 2 and 3 hours. The structure of microtubule proteins was determined using the immunocytochemical method. Cell growth was determined by counting cells for each hour of exposure during five post-exposure days. The experimental procedure included exposed V79 and unexposed control cells. In comparison to the control cells, the microtubule structure of the exposed cells significantly altered after 3 hours of irradiation ($p<0.05$). Cell growth of the cells exposed for three hours significant dropped 72 hours after exposure ($p<0.05$). It could be concluded that the 935 MHz low-level UHF radiation affected microtubule proteins, consequently influencing the cell growth.

Introduction

Common concern about biological effects of ultra high frequency (UHF) electromagnetic (EM) fields in the range from 300 MHz to 3 GHz grows with development of telecommunications systems. So far, many reported biological effects of UHF are considered to be simply indeterminate with respect to their significance to health [1]. Therefore, it is important that biological effects of UHF fields be understood at least on cellular level. Numerous *in vitro* biological effects caused by low-level UHF irradiation have been reported, and a number of studies conducted to assess changes at the cellular level reported adverse effects on cell proliferation and cell membrane structure [2, 3]. It was also suggested that UHF could interact with different apoptosis pathways [4]. No other effects have been observed on the cell cycle, enzyme activity, gene expression or DNA and chromosome damage [5-12]. A wide range of studies *in vivo* showed that rat blood-forming system could be affected by low-level UHF fields [13, 14, 15]. In addition, a number of biological effects were observed in animals during non-thermal exposure to the UHF field [16, 17, 18]. It is apparent that studies of mobile phone frequencies often present conflicting results. Accordingly, there is a permanent need for independent and objective research of the UHF biological potency. In addition, Repacholi in 1998, has recommended that the time course of effects should be investigated to determine if they are chronic, acute, or whether the effects disappear after cessation of exposure [19].
The aim of this study was to evaluate whether low-level UHF of 935 MHz frequency field affects the cytoskeleton microtubule structure and cell growth in the continuous line of V79 cells after 1, 2 and 3 hours of exposure.

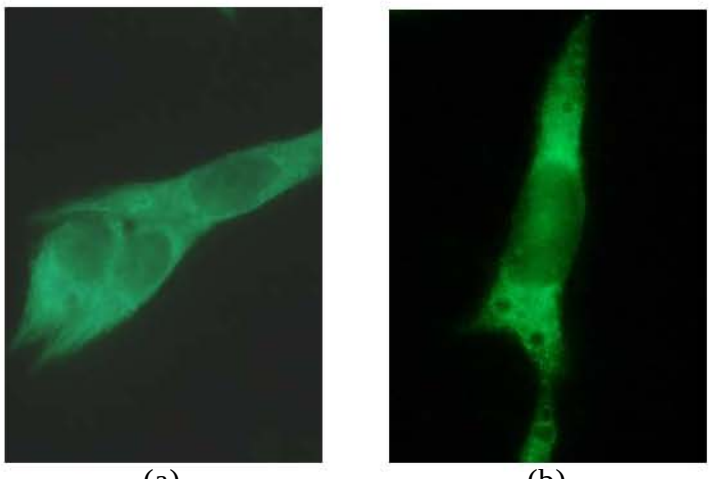
Material and methods

A continuous cell line of Chinese hamster V79 lung fibroblasts was routinely grown in nutrient medium supplemented with antibiotics and fetal calf serum, (RPMI 1640, SIGMA Chemical CO, St. Louis, USA). The cells were maintained in a humid atmosphere at 37 ^{0}C in 5% CO_2, and incubated for 24 hour prior to the beginning of the assay. Electromagnetic field frequency of 935 MHz was generated by a certified Gigahertz Transversal Electromagnetic Mode Cell (GTEM-cell) equipped with a signal generator (Mod. 5402, ETS^{TM}

Lindgren, USA and Hewlett Packard HP8657, Pablo Alto, USA) [20]. Cell samples were exposed to UHF EM radiation in triplicate for one, two and three hours. Control cells were kept in the same experimental conditions, but were not exposed to UHF EM radiation. Positive control cells treated with 0.1 mM colchicine (SIGMA Chemical CO, St. Louis, USA) were also included into the study. The specific absorption rate (SAR) was averaged to be 0.12 W kg^{-1} for a single cell. SAR was calculated by averaging the individual parameters of the cell substance in accordance with their volume fraction in the live cell according to the Steffensen's mathematical model [21, 22]. Temperature inside the GTEM-cell was measured at 10-minute intervals in order to preserve steady temperature of 37 ^{0}C during irradiation. Indirect immunocytochemical method was used to determine microtubule proteins in irradiated and control cells [23]. Cell culture samples were initially seeded in total volume of 5 ml in Permanox Lab-Tek Chamber Slides (Nunc, Roskilde, Denmark) at a concentration of $2.5x10^4$ cells/ml. After irradiation the cell culture samples were washed in 0.5% triton X-100 and permeabilized with calf albumin (Imunološki zavod, Zagreb, Croatia). Subsequently, cells were fixed in a 4% paraformaldehyde. Microtubule proteins were marked by a primary antibody (IgG anti-β-tubulin, SIGMA Chemical CO, St. Louis, USA). The secondary antibody was represented by a conjugate of anti-mouse IgG and fluorescein isothiocyanate (FITC, Imunološki zavod, Zagreb, Croatia). The smears of cells were mounted on a fluorescent medium. To determine cell proliferation, V79 cells were plated in the concentration of $1x10^4$cells/ml in 24-well plates (TPP, Switzerland). For each hour of exposure, cell proliferation was determined microscopically by cell counts on post-exposure hours 24, 48, 72, 96 and 120 [24]. Collected data were analyzed using Statistica 7.0 (StatSoft Inc., USA). Results were presented as mean values and standard deviations or errors (SD/SE). Pairwise comparisons between groups of data were performed using the analysis of variance ANOVA/MANOVA. Statistical difference was determined at $p<0.05$.

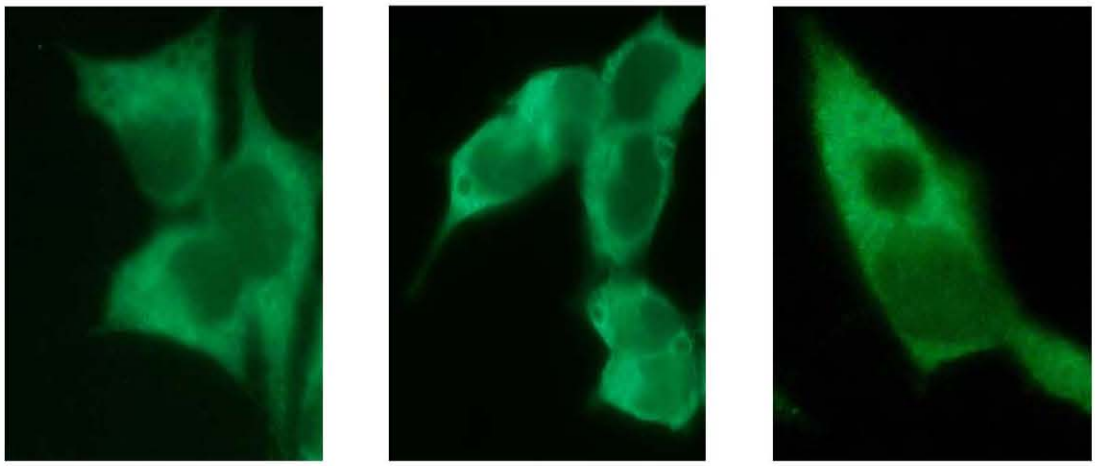
Results

Figures 1a and 1b show marked microtubule proteins in control and positive control samples V79 cells. Compared to controls, the exposed V79 cells showed time-dependent susceptibility to UHF irradiation associated with microtubule activity. Irregularities were also observed in cell morphology and microtubule protein structure. The observed phenotype changes in irradiated cells were characterized by cytoplasm membrane knobs and cytoplasm bubbles. After one and two hours of exposure, most microtubules were normally developed and their features did not essentially differ from control samples (Figure 2a, 2b). The structure of mitotic spindle remained regular (Figure 3). After the three-hour UHF exposure, the microtubule proteins started to significantly differ from matched control samples ($p<0.05$). After three irradiation hours cellular microtubule structure changed to more grainy (Figure 2c). Irregularity in microtubule structure was defined by distinct grainy clusters of proteins. These findings suggested that microtubule fiber organization could be acutely dissipated by the 935 MHz UHF irradiation. Figures 4, 5 and 6 show the growth of V79 cells after one, two and three hours of 935 MHz microwave irradiation and the growth of control cells. In comparison to control cells, cells exposed for three hours showed a significant drop ($p<0.05$) in cell growth 72 hours after irradiation (Fig. 6). The fall in the cell number on the fifth day (120 hours) after exposure seems to be the consequence of cell culture confluence and depletion of medium ingredients, which is confirmed by a decrease in the cell number of matched controls. Each data point at the curves represents the mean value obtained from six separate cell samples.



(a) (b)

Figure 1. Appearance of microtubules structure in control cells (a) and positive control cells (b)



(a) (b) (c)

Figure 2. Appearance of microtubules structure in V79 cells after 1(a), 2(b) and 3(c) hours of UHF exposure

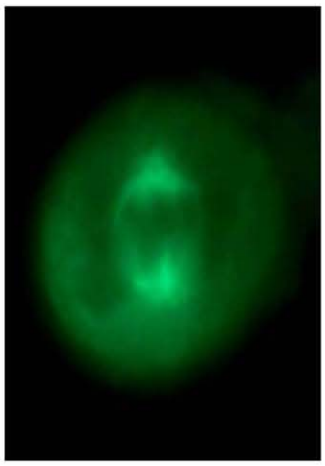


Figure 3. Mitotic spindle structure in V79 cell after two hours of UHF exposure

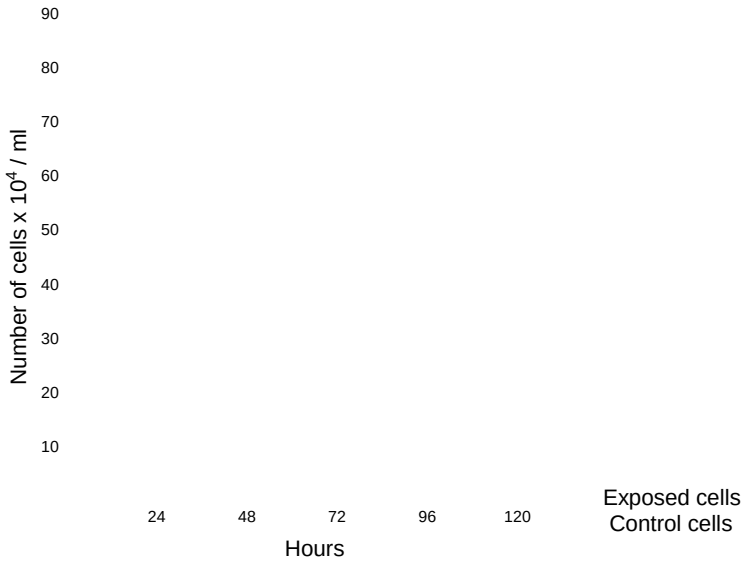


Figure 4. Growth of V79 cell culture after one-hour of UHF exposure and of matched control culture

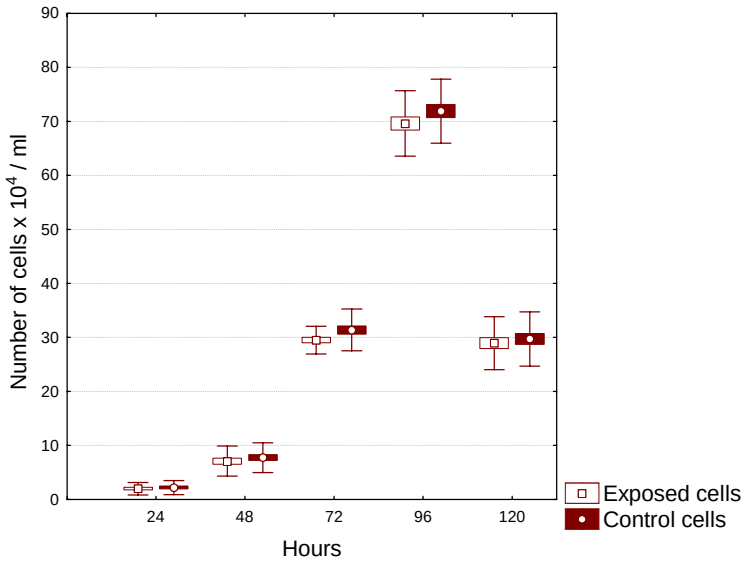


Figure 5. Growth of V79 cell culture after two-hour of UHF exposure and of matched control culture

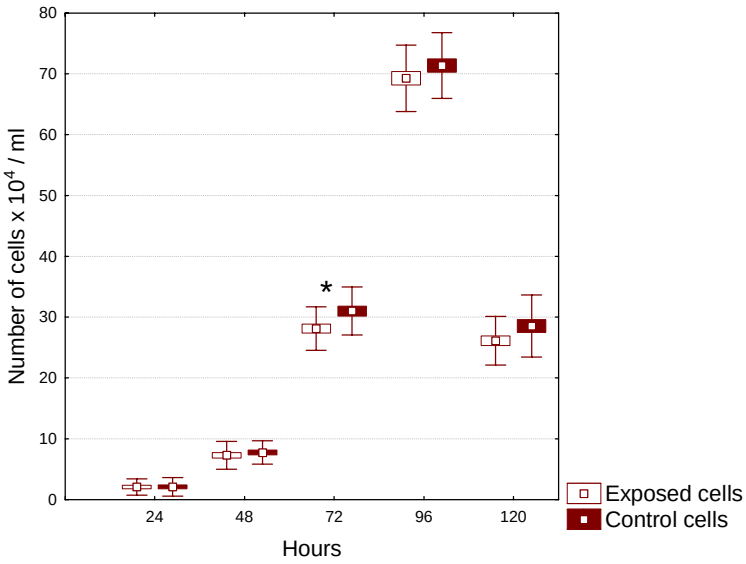


Figure 6. Growth of V79 cell culture after three-hours of UHF exposure and of matched control culture (* significance $p<0.05$)

Discussion

An experiment with whole-body exposure of rats showed that UHF EM irradiation had an effect on the proliferation and maturation of heamotopoietic cells [14]. Although the authors propose a reasonable explanation of the UHF EM action *in vivo*, we believe that a precise insight into the mechanism requires an *in vitro* approach to the problem. Microtubule protein fibers are extremely dynamical structures whose function depends on dynamic instability, i.e. on continuous binding of free tubulin proteins in microtubules and their degradation to basic protein units. It is believed that internal electrostatic forces and microtubule dynamic instability can be disturbed by outside electrostatic forces. Depending on the dipole momentum, an external electric field could affect the dynamic instability of microtubules and increase the number of free tubulin proteins in cytoplasm [25]. In our study the 935 MHz UHF exposure seems to have led to time-dependent increases of visible fluorescent grain structures or free cytoplasmatic tubulin proteins. The observed grain

structures revealed noticeable destruction of microtubule fibers. Pacini et al., demonstrated that exposure of cultured human cells to cellular phone radiofrequencies caused massive morphological and functional changes. After one hour of exposure to 902.4 MHz frequency field with the SAR of 0.6 W/kg, a significant increase was reported in gene expression related to the stress response proteins, cell cycle regulators, nuclear receptors, cytoskeleton and proteins of extracellular matrix [26]. The alteration of cytoskletetal actin protein structure in human astrocytoma cell line caused by 835 MHz irradiation and field power density of 40 mW/cm^2 was reported as well. In the same frequency field an alteration of cell proliferation was observed at 8.1 mW/cm^2 [27]. Neither Stagg's no Higashikubo's group observed any other changes through the G1, G2 and S phase, and cell division, immediately after exposure up to modulated 835.62 MHz frequency wave, SAR 0.6 W/kg [28, 29] for 100 hours. According Bohr & Bohr, UHF field affects the kinetics of conformational changes of the protein β-lactoglobulin. Exposure accelerates changes towards the equilibrium state by excitation of collective intrinsic modes in the protein [30]. Electric dipole momentum of microtubule proteins complies with the basic condition for vibration excitation and creation of internal oscillated electric field [31]. It becomes clear that internal oscillated electric field might interfere with outside electromagnetic forces which could finally lead to a measurable biological effect. It could be concluded that under the applied conditions, 935 MHz low-level UHF radiation affects microtubule protein structure, followed by disturbances in cell growth kinetics in a time-dependent manner.

Acknowledgements

Research described in this paper was supported by the Ministry of Science, Education and Sports, Republic of Croatia, Grant No. 0022005.

References

[1] Elwood, J.M. Epidemiological studies of radio frequency exposures and human cancer. Bioelectromagnetics. S6: 63-73(2003)

[2] Grundler,W., Keilmann F. Nonthermal effects of millimeter microwaves on yeast growth. Z. Naturforsch. 33(1-2):15-22(1978)

[3] Phelan, A.M. Lange, D.G. Kues, H.A. Lutty, G.A. Modification of fluidity in melanin-containing cells by low level microwave radiations. Bioelectromagnetics. 12: 131-146. (1992)

[4] Peinnequin, A., Piriou, A., Matheiu, J., Dabouis, V., Sdebbah, C., Malabiau, F., Debouzy, J.C. Non-thermal effects of continuous 2.45 GHz microwave on Fas-induced apoptosis in human Jurkat T-cell line. Bioelectrochemistry. 51: 157-161(2000)

[5] Cleary, S.F., Cao G.H., Liu L.M. Effect of isothermal 2.45 GHz microwave radiation on the mammalian cell cycle: comparison with effects of isothermal 27 MHz radiofrequency radiation exposure. Bioelectrochem. Bioenerg. 39: 167-173 (1996)

[6] Dutta, S.K., Das, K., Gosh, B., Blackman, C.F. Dose dependence of acetylcholinesterase activity in neuroblastoma cells exposed to modulated radio-frequency electromagnetic radiation. Bioelectromagnetics. 13(4): 317-322(1992)

[7] Pentafield L.M, Litovitz T, Krause D, Desta A, Mullins JM.. Role of modulation on the effect of microwaves on ornithine decarboxylase activity in L929 cells. Bioelectromagnetics. 18: 132-41.

[8] Fritze, K., Wiessner, C., Kuster, N., Sommer, C., Gass, P., Hermann, D.M., Klessing, M., Hossmann, K.A. 1997. Effect of GSM microwave exposure on the genomic response of the rat brain. Neuroscience. 81: 627-639(1997)

[9] Goswami, P.C., Albee L.D., Parsian, A.J., Baty, J.D., Moros, E.G., Pickard W.F., Roti Roti, J.L., Hunt, C.R. Proto-oncogene mRNA levels and activities of multiple transcription factors in C3H 10 T ½ murine embryonic fibroblasts exposed to 835.62 and 847.74 MHz cellular phone communication frequency radiation. Radiat Res. 151(3): 300-309(1999)

[10] Malyapa, R.S., Ahern, E.W., Straube, W.L., Moros, E.G.,Pickard W.F., Roti Roti J.L., Measurement of DNA damage after exposure to electromagnetic radiation in the cellular phone communication frequency band (835.62 and 847.74 MHz). Radiat Res. 148: 618-627(1997)

[11] Zeni, O., Chiavoni, A.S., Sannino, A., Antolini, A., Forgio, D., Bersani, F. Lack of genotoxic effects (micronucleus induction) in human lymphocytes exposed *In vitro* to 900 MHz electromagnetic fields. Radiat Res. 160: 152-158(2003)

[12] Bisht, K.S., Moros, E.G., Straube W.l., Baty J.D., Roti Roti j.l. The Effect of 835.62 MHz FDMA or 847.74 MHz CDMA Modulated radiofrequency radiation on the induction of Micronuclei in C3H $10T^1/_2$ Cells. Radiat Res. 157: 506-515(2002)

[13] Trosic, I., Busljeta, I., Kasuba, V., Rozgaj, R. Micronucleus induction after whole-body microwave irradiation of rats. Mutat Res. 521: 73-79(2002)
[14] Trosic, I., Busljeta, I., Modlic, B. Investigation of the genotoxic effect of microwave irradiation in rat bone marrow cells: *in vivo* exposure. Mutagenesis. 19(5): 361-364(2004)
[15] Trosic, I., Busljeta, I., Pavicic I. Blood-forming system in rats after whole-body microwave exposure; reference to the lymphocytes. Toxicol Lett. 154(1-2): 125-132(2004)
[16] Repacholi M.H., Basten, A., Gebski, V., Noonan, D., Finnie, J., Harris A.W. Lymphomas in Eμ-*Pim1* transgenic mice exposed to pulsed 900 MHz electromagnetic fields. Radiat Res. 147: 631-640(1997)
[17] Busljeta, I., Trosic, I., Milkovic-Kraus, S.. Erythropoietic changes in rats after 2.45 GHz nonthermal irradiation. Intl J Hyg Env Health. 207: 549-554(2004)
[18] Trosic, I. Multinucleated giant cell appearance after whole body microwave irradiation of rats. Int J Hyg Environ Health. 204: 133-138(2001)
[19] Repacholi M.H.. Low-level exposure to radiofrequency electromagnetic fields: health effects and research needs. Bioelectromagnetics. 19(1): 1-19(1998)
[20] Operating manual Gigazertz Transverse Electromagnetic cell (GTEM). Model 5400 Series. ETS test systems , LP. –ESCO Company EMCO. Austin, SAD (1999)
[21] Steffensen, K.V., Raskmark, P., Penersen, G.F. FDTD calculations of the EM-field distribution in a microtiter suspension well, COST 244: Biomedical Effects of Electromagnetic fields. Kuopio. 80-87(1995)
[22] World health organization. Electromagnetic Fields (300 Hz to 300 GHz), Environmental Health Criteria 137, World Health Organization, Geneva, pp.79. (1993)
[23] Bell PB, Safiejko-Mroczka B. Improved methods for preserving macromolecular structures and visualizing them by fluorescence and scaning elektron microcroscopy. Scanning Microscopy;9 (3):843-60(1995)
[24] Freshney, R.I. Culture of animal cells, A manual of basic technique.4th Ed. Wiley-Liss Publication, New York, 329 pp. (2000)
[25] Ortner MJ, Galvin MJ, Irwin RD. The effect of 2450-Mhz Microwave radiation during microtubular polymerization in Vitro. Radiation Res;93:353-63 (1983)
[26] Pacini, S., Ruggiero, M., Iacopo, S., Aterini, S., Gulisano, F., Gulisano, M. Exposure to global system for mobile communication (GSM) cellular phone radiofrequency alters gene expression, proliferation, and morphology of human skin fibroblasts. Oncol. Res./Anticancer Drug Des. 13: 19-24(2002)
[27] French, P.W., Donnellan, M., McKenzie, D.R. Electromagnetic radiation at 835 MHz changes morphology and inhibits proliferation of a human astrocytoma cell line. Bioelectrochem. Bioenerg. 43: 13-18(1997)
[28] Stagg, R.B., Thomas, W.J., Jones, R.A., Adey, W.R. DNA synthesis and cell proliferation in C6 glioma and primary glial cells exposed to a 836.55 MHz modulated radiofrequency field. Bioelectromagnetics. 18: 230-236(1997)
[29] Higashikubo, R., Ragouzis, M., Moros,EG, Straube, WL., Roti Roti, JL. Radiofrequency electromagnetic fields do not alter the cell cycle progression of C3H 10T1/2 and U87MG cells. Radiat Res. 156: 786-795(2000)
[30] Bohr, H., Bohr, J. Microwave enhanced kinetics observed in ORD studies of a protein. Bioelectromagnetics. 21: 68-72R(2000)
[31] Pokorný J, Jelínek F, Trkal V, Šrobár F. Vibration in microtubules. In: Bersam F, Ed. Electricity and magnetism in biology and medicine; Bologna; Kluwer Academic/Plenum Publishers; 967-70(1999)

INNOVATIVE MICROWAVE SYSTEM FOR THE CYTOLOGY DIAGNOSIS

G. BONGALLINO, M. BOZZETTI, G. CALO', A. D'ORAZIO, M. DE SARIO, L. MESCIA, V. PETRUZZELLI, F. PRUDENZANO*, F. TRISOLINI**

DEE – DIPARTIMENTO DI ELETTROTECNICA ED ELETTRONICA - POLITECNICO DI BARI

Via Re David, 200 – 70125 – Bari - Italy

***DIASS - DIPARTIMENTO DI INGEGNERIA DELL'AMBIENTE E PER LO SVILUPPO SOSTENIBILE – II FACOLTA' DI INGEGNERIA**

Viale del Turismo, 8 – 74100 – Taranto - Italy

****HOSPITEX DIAGOSTICS**

Via Provinciale Lucchese, 145 – Sesto Fiorentino (Florence) – Italy

Abstract

This paper proposes an innovative microwave system for the preparation of cytological slides. The system exploits an electromagnetic field to allow the cellular deposition thus reducing the use of the centrifuge. The analysis of the electromagnetic field effects on the cells in solution is of primary importance. In fact, to perform a uniform cell deposition, the generated electric field must not induce deformation of the cell structure and, in particular, the sizes of its nucleus.

A new version of GTEM cell able to generate a uniform and well controlled electromagnetic field has been designed. The cellular solution is inserted inside the GTEM cell by using a container, on the bottom of which the slide is placed. The electric and magnetic field strengths, that best fit the process requirements, have been evaluated by using a commercial computer code able to model the electromagnetic propagation inside the GTEM cell together with the cytological sample. The distribution of the electric and magnetic field modulus has been evaluated to verify the electromagnetic uniformity conditions.

Introduction

The conventional technique for the cytological tests is manual and based on the smear of vaginal cells (PAP TEST). The transfer of the material, captured by a small brush, on the glass is a complex practice. In most cases the smeared cells are not representative of the entire population of captured cells. In fact, all species must be present in reasonable quantities such to be able to represents the whole sample. Moreover, the cellular overlap and the casual disposition of mucus make difficult the PAP TEST preparation.

The most important parameter which is needed to evaluate the cell malignancy is the ratio between its total volume and the volume of its nucleus. In tumoral cells the nucleus, compared with the cell dimensions in its complex, appears enlarged. It is possible to distinguish two types of intraepithelial lesions: HSIL (High Grade Squamous Intraepithelial Lesion) and LSIL (Low Grade Squamous Intraepithelial Lesion). Therefore, the fixing effect can affect the correct interpretation of the cytological solution. In order to overcome this problem, that can compromise the diagnosis, the cytology market evolves in the direction of monolayer-based technologies [1-3]. At present, these technologies are not much spread, because of the required complex techniques, such as filtration and centrifuge steps, for cellular deposition on slide. In fact, because of the filtration step [4] some species, such as bacterium and little particles, could be not present on the slide. On the other hand, because of the centrifuge step, strong forces are involved, that might change the cellular nucleus sizes.

In this paper an innovative system for the preparation of the cytological slides is proposed. This system exploits the electromagnetic (EM) field in order to facilitate the cellular deposition thus reducing or avoiding the

centrifuge step.
Because of to the innovativeness of this technology, the analysis of the electromagnetic field effects on the cells in solutions is of primary importance. We propose a new version of the GTEM (Gigahertz Transverse Electro-Magnetic) cell to be used for the cytology slide preparation able to generate a uniform and well controlled electromagnetic field. The electric field polarization and strength, that best fit the process requirements, have been evaluated. In fact, to perform a uniform cell deposition and to increase the cell mobility, the electric field must not deform the cell structure and, in particular, the nucleus sizes. It is important to assure the uniformity of EM field in the sample. Therefore, the design of the GTEM cell has been aimed to achieve a uniform distribution of electromagnetic field in the test region. For this purpose, the requirement of the 50 Ω impedance matching condition along the propagation direction and at the terminal sections, must be satisfied.

GTEM cell prototype design

The GTEM cell is a tapered coaxial waveguide commonly used in Electromagnetic Compatibility (EMC) tests to simulate free-space radiation conditions in a shielded and restricted, environment. Accurate and repeatable measures can be performed for operating frequencies up to a few GHz. Additionally, a uniform EM field distribution can be guaranteed in the test region of the shielded overall volume. In absence of resonance and reflection phenomena inside the GTEM cell, a good EM field uniformity can be reached. This implies that the impedance matching condition must be satisfied both along the propagation direction and at the terminal sections by an appropriate design of the GTEM cell as regards its sizes and the absorbing load.
A GTEM cell can actually be considered as a tapered stripline with an offset inner conductor, here referred to as septum, that allows the only TEM mode propagates. Such a cell behaves as a transmission line with an associated characteristic impedance depending on the geometrical parameters of the structure. These have been chosen in order to maximize the test volume [5]: cell length L = 45 cm (pyramid height), aspect ratio $(b+d)/a$ = 2/3 (in the terminal section we have a = 24 cm, b = 4 cm and d = 12 cm), angles $\theta = 5°$, $\gamma = 10°$ and $\alpha = 15°$. These parameters are shown in Fig. 1. The characteristic impedance of the GTEM cell have been evaluated with the use of a code based on the singular integral technique [6]. A 50 Ω characteristic impedance occurs in the case of the septum width w to the cell width a ratio equal to $w/a = 0.7$. This impedance is constant because the tapered shape of the GTEM cell allows to hold the same aspect ratio throughout the propagation direction. In Fig.2 the fabricated GTEM cell prototype is shown.
The GTEM cell has been designed by using a full-wave commercially computer code (CST MW Studio), based on the Finite Integration Technique (FIT). Figs. 3 and 4 illustrate the used CST model of the GTEM cell without and with the sample, respectively. A few simplifications are introduced in order to reduce its complexity and the related computation time. The SMA connector, where the signal generator is connected, together with its transition to the GTEM cell septum, have been neglected. According to the CST specifications, a waveguide port has been defined by cutting the GTEM cell pyramidal shape in correspondence of the SMA-connector to the septum transition. A second waveguide port has similarly been defined at the terminal section of the GTEM cell, thus allowing an optimal impedance matching condition at both the input/output load sections.

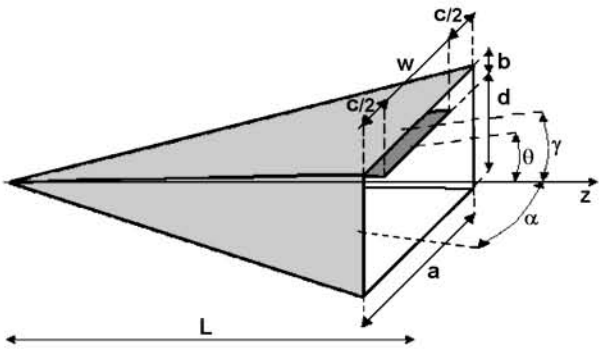


Fig. 1: Geometric parameters of the GTEM cell.

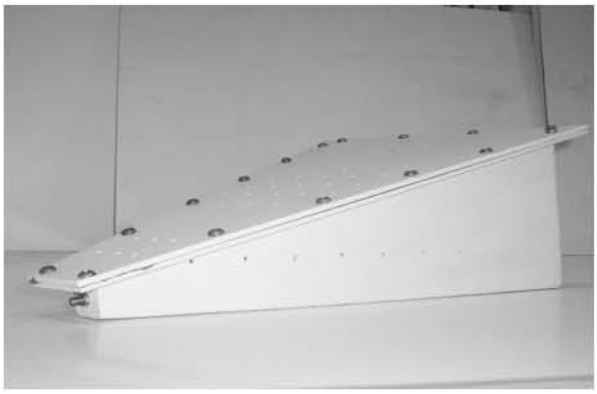


Fig. 2: Photo of the GTEM cell prototype.

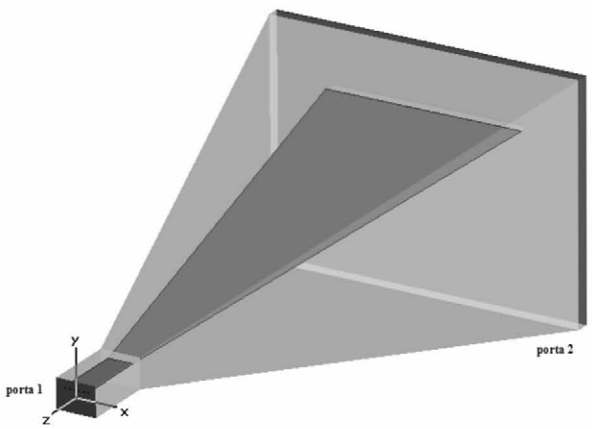


Fig. 3: CST model of the GTEM cell without sample.

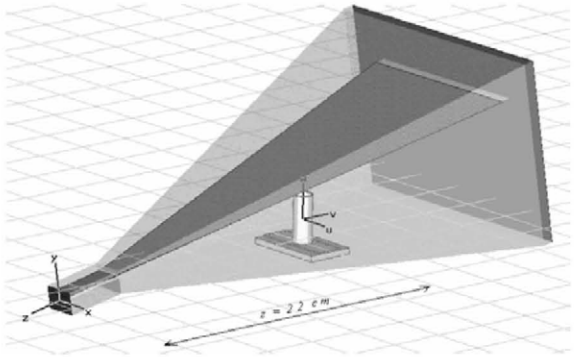


Fig. 4: CST model of the GTEM cell with the chamber.

Electromagnetic analysis

The electromagnetic analysis in the transversal section of the GTEM cell has been carried out by means of a home-made computer code based on the Transverse Resonance Diffraction (TRD) method [7]. In the region under the septum the E-field exhibits an almost uniform pattern along the propagation direction z. However, the tapered shape of the GTEM cell allows the propagation of a few higher-order modes. They can be originated only in correspondence of the larger sections and are responsible for a possible perturbation of the electromagnetic field distribution and uniformity. Further modes can be originated either by cross-sectional discontinuities or by the presence of the biological sample, that introduces inhomogeneous conditions along the propagation direction. These higher-order modes can be neglected, due to their low associated power. Moreover, the contribution of higher-order modes to the whole electromagnetic field can be minimized by suitably choosing the position of the sample in the GTEM cell. Therefore, the optimal position of the cytologic sample must be chosen in order to reduce the number of propagating modes and the induced electromagnetic field perturbation. In fact, the presence of higher-order modes reduces the extension of the test region in the GTEM cell. By means of the TRD method we have verified that for the frequency f = 0.9 GHz the monomodality is ensured from z = 0 m to z = 0.30 m. In fact, the first higher-order mode starts to propagate exactly from z = 0.295 m. On the other hand, for f = 1.8 GHz the monomodality is ensured only for z < 0.150 m. Therefore the best operating frequency is f = 0.9 GHz, for which two modes appear at the end section of the GTEM cell, that are the TEM and the TE_{p1} modes. The latter can be neglected , it being excited at the bottom of the GTEM cell and the energy exchange between the two modes being very low. Then, we can consider the only TEM mode without an valuable error. In order to confirm this result, the scattering parameters have been calculated. Fig. 5 reports the S_{11} and S_{21} parameters as a function of the frequency in the range from 0 Hz and 3 GHz. In particular, the S_{11} parameter is everywhere low, thus putting in evidence that the signal reflection is low. On the other hand, the S_{21} parameter assumes unitary value that is equivalent to total power transfer at the terminal section.
Moreover, the scattering parameters assume an almost flat behaviour for the frequencies around 1 GHz. Vice versa, for f > 1 GHz the scattering parameters assume an oscillating trend, with peaks more and more increasing. In conclusion, for f < 900 MHz the reflection phenomena inside the simulated GTEM cell model can be neglected.
The described ideal behaviour modifies by the introduction of the sample into the GTEM cell. To this aim the cellular solution is inserted into the GTEM cell by using a suitably designed holder, shown in Fig. 6, on the bottom of which the slide, devoted to collect the cells, is placed.
The holder has the following geometric parameters: basement of sizes 7.5 cm x 4.4 cm x 0.5 cm; slide of sizes 7.5 cm x 2.5 cm x 0.1 cm; cylinder extern diameter 1.8 cm; cylinder internal diameter 1.6 cm; cylinder height 4 cm. The basement and the cylinder, made of plastic, are characterized by the following electromagnetic parameters: $\varepsilon_r = 2.55$ and $\mu_r = 1$; the slide, made of Glass Pyrex by $\varepsilon_r = 4.82$ and $\mu_r = 1$. The cylinder has been simulated by considering the presence of cells in watery solution. This solution fills for half height the cylinder and is identified by $\varepsilon_r = 49.779$, $\mu_r = 1$ and dielectric tangent $\delta = 0.38$.
Figs. 7 and 8 show the S_{11} and S_{21} parameters as a function of the frequency in the range from 0 Hz to 3 GHz, calculated in the presence of the sample. Fig. 7 shows that the S_{11} parameter assumes low values, while Fig. 8 shows the S_{21} values equal to about 1 for f < 900 MHz.

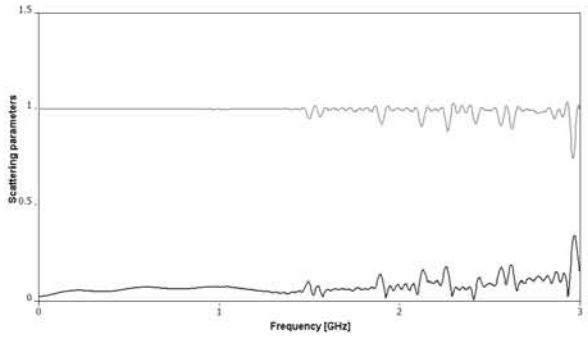


Fig. 5: Scattering parameters vs frequency for the GTEM cell without sample: S_{11} (red line) and S_{21} (green line).

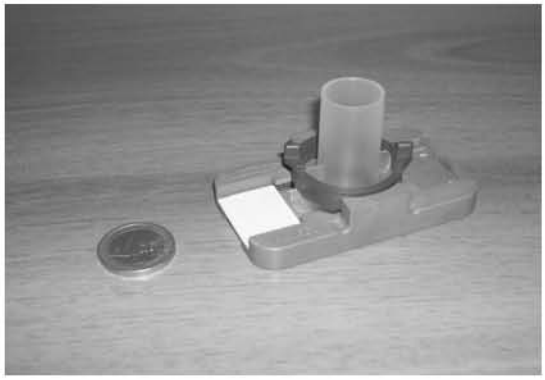


Fig. 6: Chamber for cytological vaginal samples.

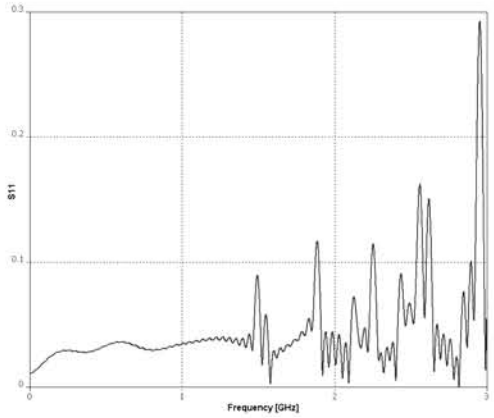


Fig. 7: S_{11} parameter vs frequency for the GTEM cell in presence of the cytological sample.

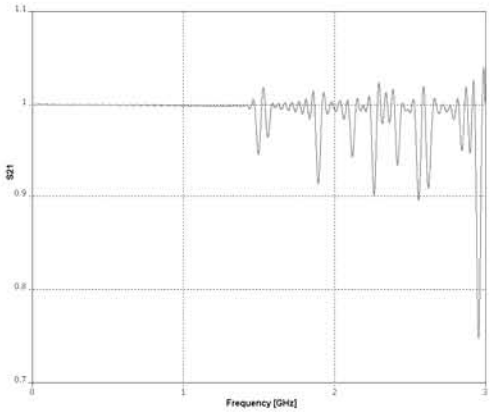


Fig. 8: S_{21} parameter vs frequency for the GTEM cell in presence of the cytological sample.

Electromagnetic field evaluation

Several simulations of the EM field have been carried out by changing the position of the holder in the GTEM cell. The monomodality is ensured from z = 0 m to z = 0.30 m, but the geometrical sizes of the holder do not allow to place the sample anywhere in the GTEM cell, owing to the presence of the septum. The sample has been placed in seven positions: z = 0.172 m, z = 0.182 m, z = 0.204 cm, z = 0.220 m, z = 0.236 m, z = 0.252 m, z = 0.262 m. The distance between two adjacent positions is 1.6 cm, equal to the diameter of the cylinder. For each position the average strength of the electric field components has been calculated in a circular section of the sample placed at a height of 1.5 cm from the bottom of the GTEM cell, having a thickness equal to 1 mm. Fig. 9 reports the average strength of the three E_x, E_y, E_z components of the electric field as a function of the seven positions. The most important electric field component for the cell deposition on the slide is E_y. In fact, in order to deposit the cells on slide without deforming its nucleus, the E_x and E_z components must be negligible with respect to E_y to avoid the deposition of the cells on the walls of the holder. Fig. 10 shows the variance V_E of the average components of the electric field. We can see that the dominant E_y component assumes an almost constant variance in dependence of the z position.

The same analysis has been carried out for the magnetic field and the results are shown in Figs. 11 and 12. The strength of the magnetic field must be very low in order to not give a rotational moment to the cells. On the basis of the obtained results, the sample inside the GTEM cell must be inserted in correspondence of the region within z = 0.23 m and z = 0.25 m.

In Figs. 13 and 14 the distribution of the electric and the magnetic field modulus is shown in the case of sample placed inside the GTEM cell at z = 0.236 m, where the best uniformity condition takes place.

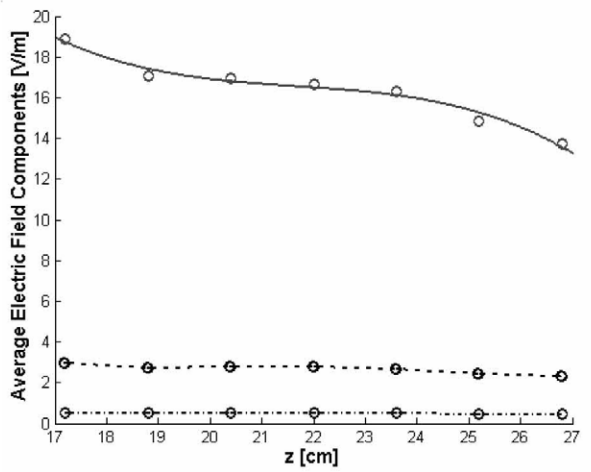


Fig. 9: Average electric field components vs z position: E_x (dash-dot curve); E_y (solid curve); E_z (dashed curve).

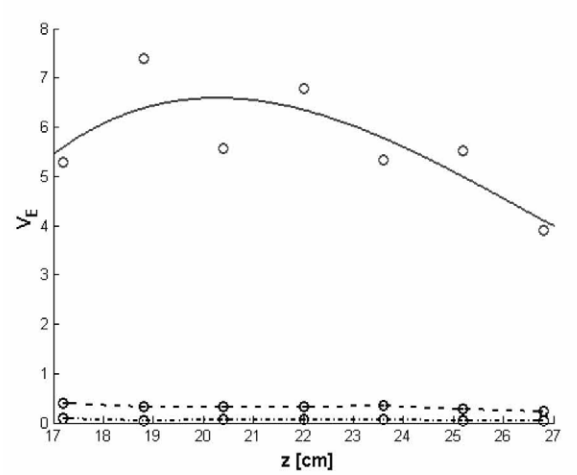


Fig. 10: Variance V_E of the average electric field components vs z position: E_x (dashed curve); E_y (solid curve); E_z (dash-dot curve).

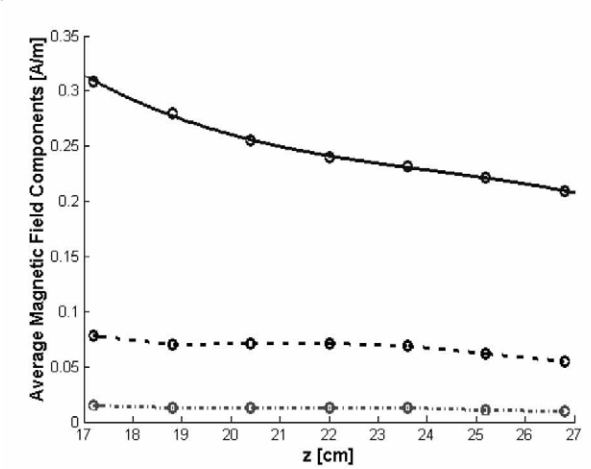


Fig. 11: Average magnetic field components vs z position: H_x (solid curve); H_y (dash-dot curve); H_z (dashed curve).

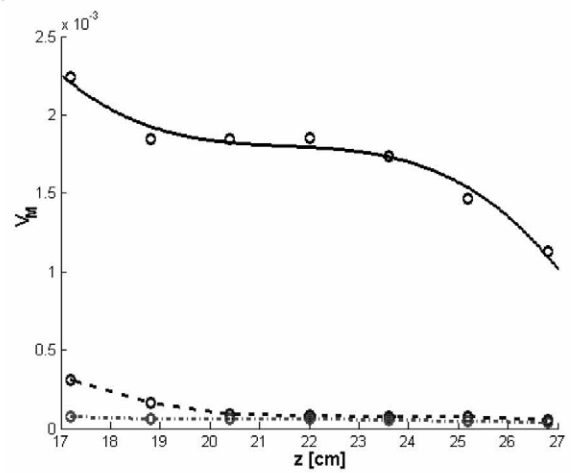


Fig. 12: Variance V_M of the average magnetic field components vs z position: H_x (dashed curve); H_y (dash-dot curve); H_z (solid curve).

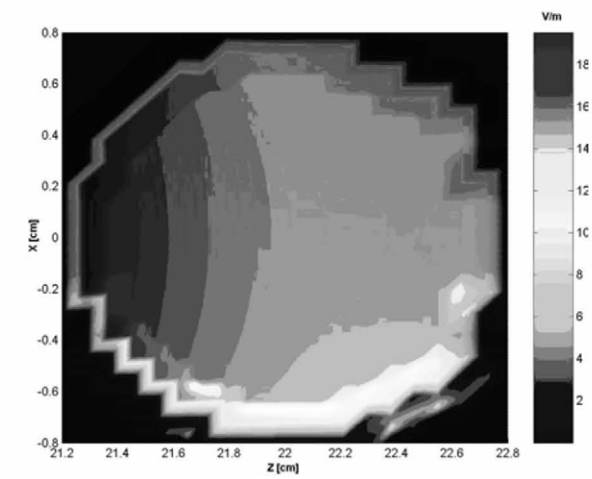


Fig. 13: Distribution of the electric field modulus with the sample positioned at z = 0.236 m.

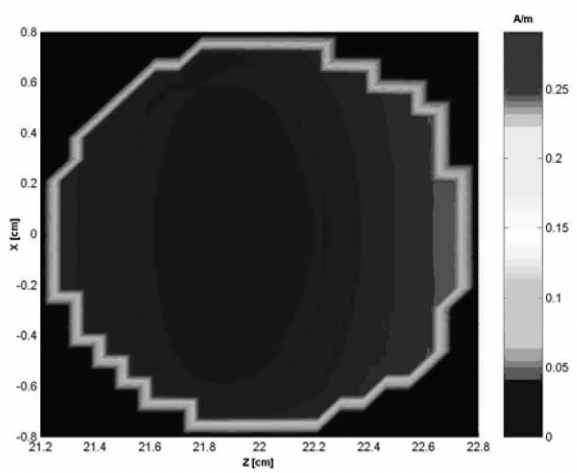


Fig. 14: Distribution of the magnetic field modulus with the sample positioned at z = 0.236 m.

Conclusions

An innovative system for the preparation of cytological slides has been studied. It exploits the electromagnetic field in order to allow the cellular deposition on slides. A new version of GTEM cell, able to generate a uniform and well controlled electromagnetic field, has been proposed and designed. A prototype has been realized by taking into account special test requirements. 50 Ω characteristic impedance has been found by adequately choosing the geometrical parameters. The electromagnetic analysis has been carried out by a Transverse Resonance Diffraction method and by a commercial computer code (CST MWS). The cellular solution has been inserted inside the GTEM cell by using an apposite holder, on the bottom of which the slide has been placed. At the best operating frequency f = 0.9 GHz, two modes propagate along the GTEM cell: the TEM and the TE_{p1} modes. This latter can be neglected because the energy exchange between the two modes is practically null.
By considering the average electric field at different positions along the GTEM cell, we have evaluated that the best position where the sample must be placed during the deposition is in the region within z = 0.23 m and z = 0.25 m. In fact, in those section both the electric and magnetic fields are uniform.

References

[1] Venancio Avancini Ferreira Alves, Marluce Bibbo, Fernando Carlos Landèr Schmitt, Fernanda Milanezi, and Adhemar Longatto Filho, M.Sc: “Comparison of Manual and Automated Methods of Liquid-Based Cytology: A Morphologic Study”, Acta Cytol 2004; 48:187-193.

[2] Maurice Fremont-Smith, James Marino, Bryan Griffin, Lynn Spencer, David Bolick: “Comparison of SurePath™ Liquid-Based Papanicolau Smear with the Conventional Papanicolau Smear in a Multisite Direct-to-Vial Study”, Cancer Cytopathology, Volume 102, No. 5, October 2004.

[3] Sandra M. Sulik, Karin Kroeger, Jennifer K. Schultz, Jennie L. Brown, Lorne A. Becker William D. Grant:: “Are Fluid-Based Cytologies Superior to the Conventional Papanicolaou Test? A Systematic Review”, The Journal of Family Practice, Vol. 50, No. 12, December 2001.

[4] P.Trempat, R.C. Zenou, P. Brousset: “Evaluation de la Conservation de l’AND et de l’ARN Dans Les Milieux de cytology Liquides”, Molecular Pathology, vol 55, No. 2, p. 125, April 2002.

[5] M. Bozzetti, G. Calò, A. D’Orazio, M. De Sario, L. Mescia, V. Petruzzelli, F. Prudenzano, G. Cibelli, R. Zefferino : “A Novel GTEM Cell for in vitro Dosimetric Experiments” , 3rd International Workshop on Biological Effects of ElectroMagnetic Fields, Kos, Greece, ISBN 960-233-151-8, vol. I, pp. 11-17, October 2004.

[6] J. Tippet, D. Chang : “Characteristic impedance of a rectangular coaxial line with offset inner conductor”, IEEE Trans. on Microwave Theory and Technique, vol. MTT-26, pp. 876-883, November 1976.

[7] R. De Leo, T. Rozzi, C. Svara, L. Zappelli, “Rigorous Analysis of the GTEM Cell”, IEEE Transaction on Microwave Theory and Technique, vol. MTT-39, n. 3, pp 488-499, 1991.

HANDS FREE KITS DOSIMETRY PROTOCOL AND RESULTS

D. PICARD
DRE - SUPELEC - 3 RUE JOLIOT CURIE - 91192 GIF SUR YVETTE CEDEX - FRANCE
TEL : 33 1 69 85 15 55 - dominique.picard@supelec.fr

Abstract
This study is the analysis of Hands Free Kits SAR measurement results corresponding to 124 different mobile phones. The mobile phones are measured following EN50361 protocol and the Hands Free Kits following a new specific protocol. The comparison between phone SAR and Hands Free Kits SAR is made and we introduce the SAR reduction factor, which is the ratio of the phone and the Hands Free Kits SAR values. The mean value of the SAR reduction factor is about 11 for GSM900 frequency band and 18 for DCS1800, which are very consistent values. The lower values of SAR reduction factor correspond to lower values of phone SAR. Finally, the use of Hands Free Kits decreases statically significantly the SAR value in the user head but the obtained SAR values are not absolutely negligible and it is necessary to study Hands Free Kits SAR.

Introduction
Since a few years the use of Hands Free Kits (HFK) with mobile phones is increasing. The distance between the phone antenna and the user head is larger with HFK and one can think that the RF power deposited in the user head is significantly reduced. However the wire of HFK is metallic and the RF currents induced on this wire can be the sources of power deposition is the user head [1] Supélec carries out dosimetry measurements for HFK since a few years, by the mean of its high sensitivity own dosimetry measurement system [2] (figure 1), and a large data base has been constituted from 2002 to 2004. 124 different mobile phones and HFK, corresponding to 20 different marks, have been tested, 100 of which are classical phones, 21 are clamshells and 3 are PDA. The number of monopole antenna handsets is 37 and the number of integrated antennas is 87.

Measurement protocols
The 124 different mobile phones and their HFK have been measured following EN50361 protocol for the handset and the following described protocol for HFK. There are 6 different measurements for each frequency band, corresponding to 2 different HFK wire configurations and 3 different frequencies: lower, center and upper frequencies. The 2 different wire configurations are 1) tensed wire (figure 2.a), 2) wire with two three cm diameter loops near the phone antenna (figure 2.b), the exact position of which corresponding to an obtained maximum SAR value at the center frequency. The tensed wire configuration corresponds to a ‘’natural’’ situation and the wire with loops to a worst case. The end of the wire near the earpiece is applied to the SAM phantom head surface close to the ear. The wire length in contact with the phantom is 2cm. The HFK Specific Absorption Rate (SAR) in each frequency band is the maximum obtained value for the 6 measurements.

Measurement results analysis
Phone and HFK SAR
The results of these measurements are shown in figure 3.a for GSM900 frequency band and b for DCS1800 band. The SAR values are very smaller in the case of HFK than for mobile phones for the two frequency band.



Figure 1: Supélec dosimetry facility.



Figure 2.a: Tensed HFK wire configuration.



Figure 2.b: Two loops HFK wire configuration.

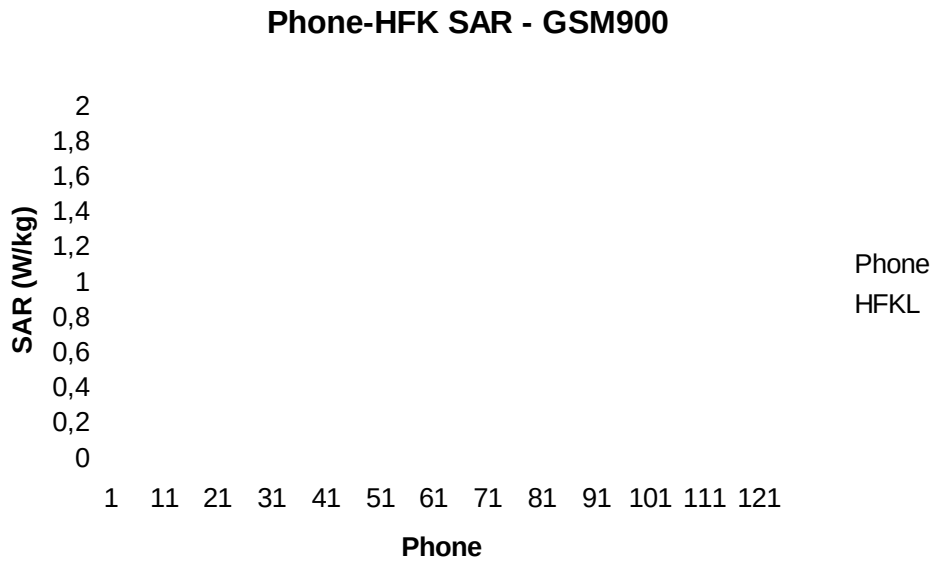


Figure 3.a: Maximum SAR values obtained in GSM900 frequency band function of mobile phone number.

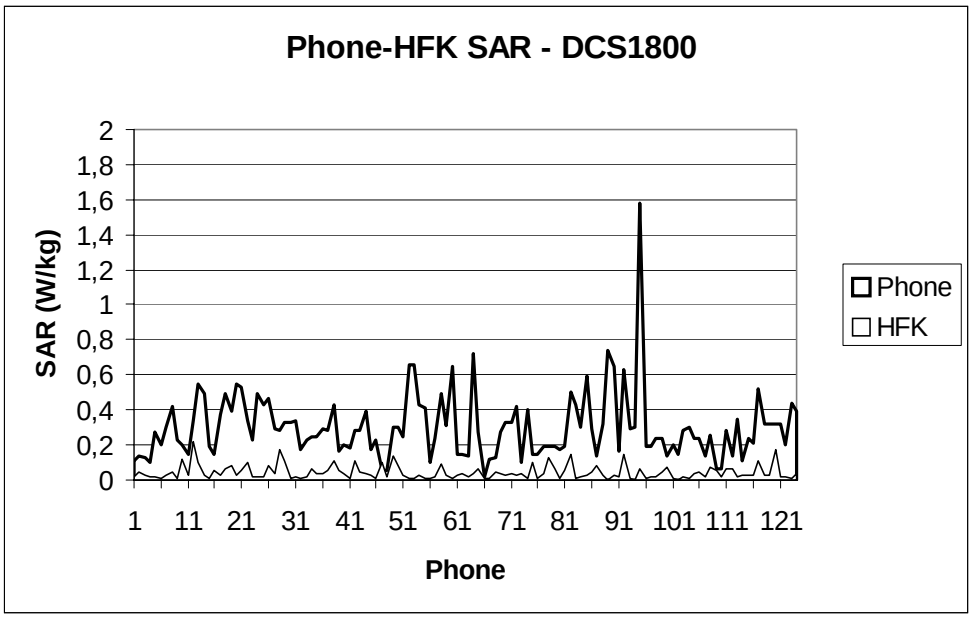


Figure 3.b: Maximum SAR values obtained in DCS1800 frequency band function of mobile phone number.

The measurement results have been analysed. Table 1 and fig 4.a and b show the repartition of the SAR values obtained for GSM900 and DCS1800 frequency bands.

	Handset		HFK	
Freq.band	GSM900	DCS1800	GSM900	DCS1800
Mean value	0.62	0.30	0.12	0.044
Standard deviation	0.23	0.19	0.088	0.041
Max.value	1.2	1.6	0.43	0.22
Min.value	0.17	0.018	0.006	0.001

Table 1: Maximum, minimum and mean value for SAR measurement results (W/kg). These values are taken on the different mobile phones.

For the handset SAR, GSM900 frequency band values are larger than DCS1800 frequency band values, in about a 2 to 1 ratio (the emitted power ratio). Phone SAR values are hardly larger than HFK SAR values with a ratio larger than 10.
The table 2 presents the phone proportion giving the maximum phone or HFK SAR value in the GSM900 or DCS1800 frequency band.

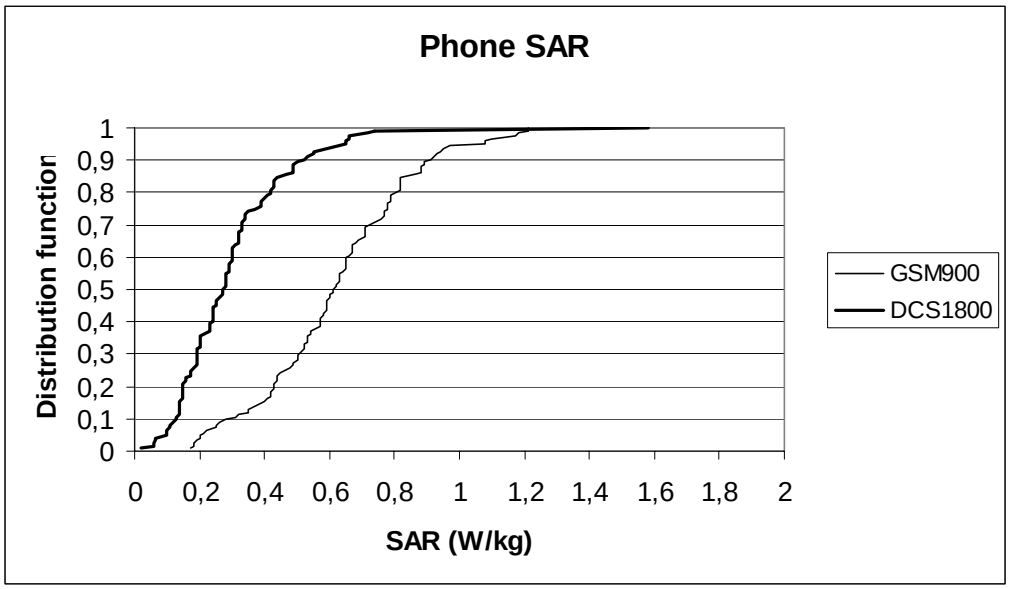


Fig. 4.a. Mobile phones SAR distribution function.

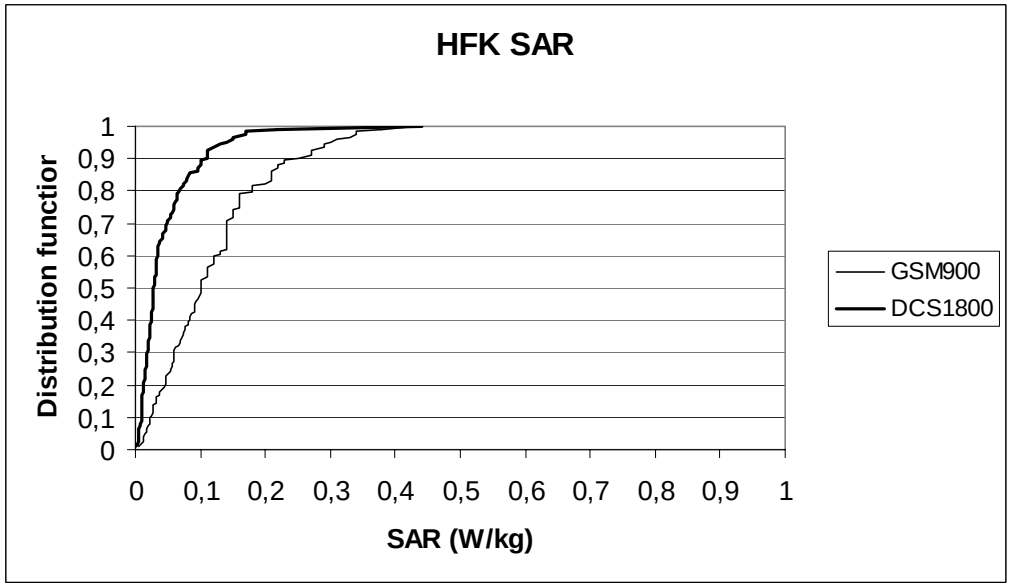


Figure 4.b: HFK SAR distribution function.

Freq. band	GSM900	DCS1800
Max. phone SAR	96%	4%
Max.HFK SAR	84%	16%

Table 2: Phones and HFK percentage giving the maximum phone or HFK SAR value in the corresponding frequency band.

A large majority of phones have their maximum phone and HFK SAR values for the GSM900 band, due to the two time higher emitted power.

SAR Reduction factor due to HFK

To evaluate the impact of HFK use on user head exposition, we have calculated the SAR reduction factor, which is the ratio of the handset SAR value and the HFK SAR value for a given frequency band. Table 3 and figure 5 present the SAR reduction factor value repartition obtained from the measurements.

The SAR reduction factor is very significant: the mean value is 11.2 for GSM900 frequency band and 17.4 for DCS1800 band. It can reach 103 and 300 respectively for GSM900 and DCS1800. For one handset, a PDA one, there is no SAR reduction and the SAR reduction factor is 0.63 for GSM900 and 0.36 for DCS1800.

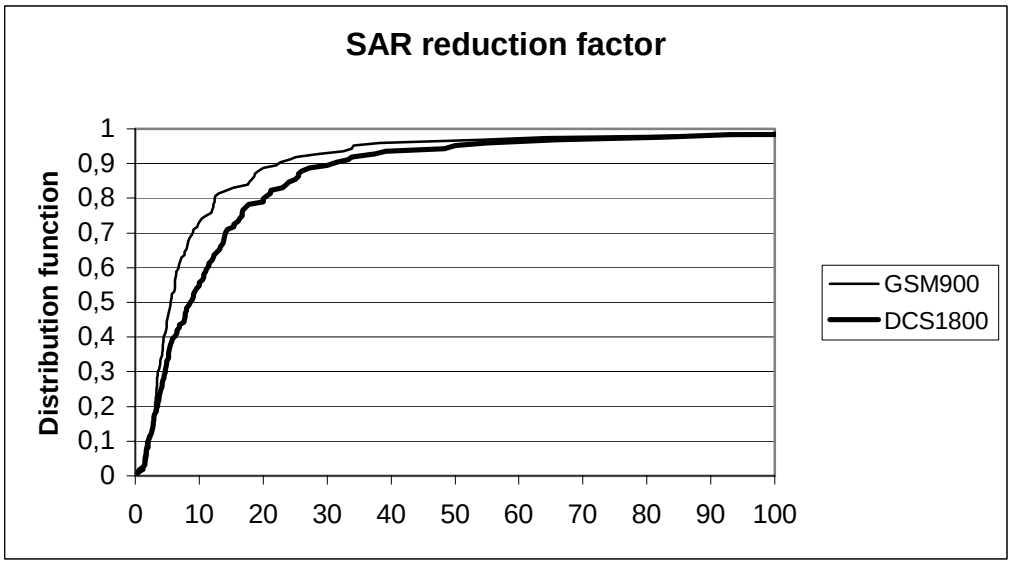


Figure 5: SAR reduction factor distribution function.

Freq. band	GSM900	DCS1800
Mean value	11.2	17.5
Standard deviation	17.2	36.2
Max. value	102	300
Min. value	0.63	0.57

Table 4: Maximum, minimum and mean value for SAR reduction factor. These values are taken on the different mobile phones.

Relation between Handset SAR and HFK SAR

For HFK SAR interpretation we have compared handset and HFK SAR values for each mobile phone. This comparison is done in figures 6.a and b.

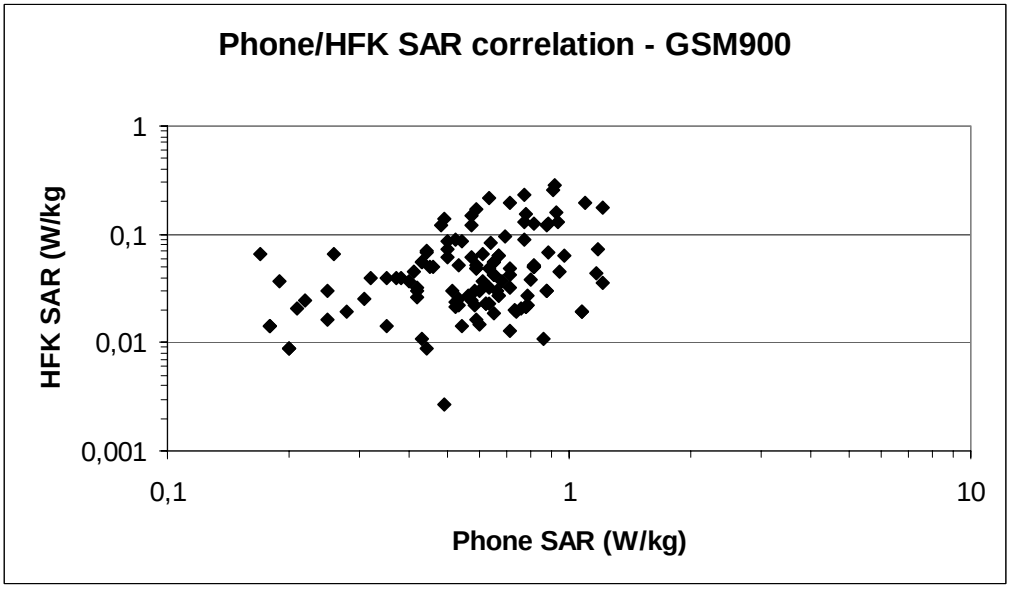


Fig. 6.a. Correlation between phone and HFK SAR values for GSM900 frequency band.

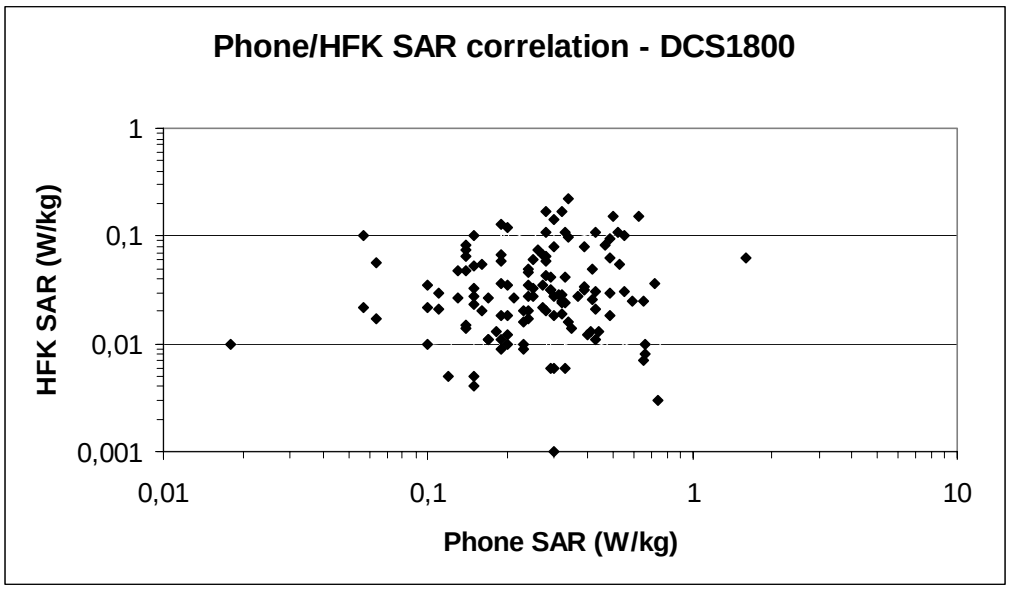


Fig. 6.b. Correlation between phone and HFK SAR values for DCS1800 frequency band.

The correlation between phone and HFK SAR values are low, especially for DCS1800 frequency band.

Relation between Handset SAR and SAR reduction factor

The same method has been applied to handset and HFK SAR reduction factor comparison. The figures 7a and b show this comparison.

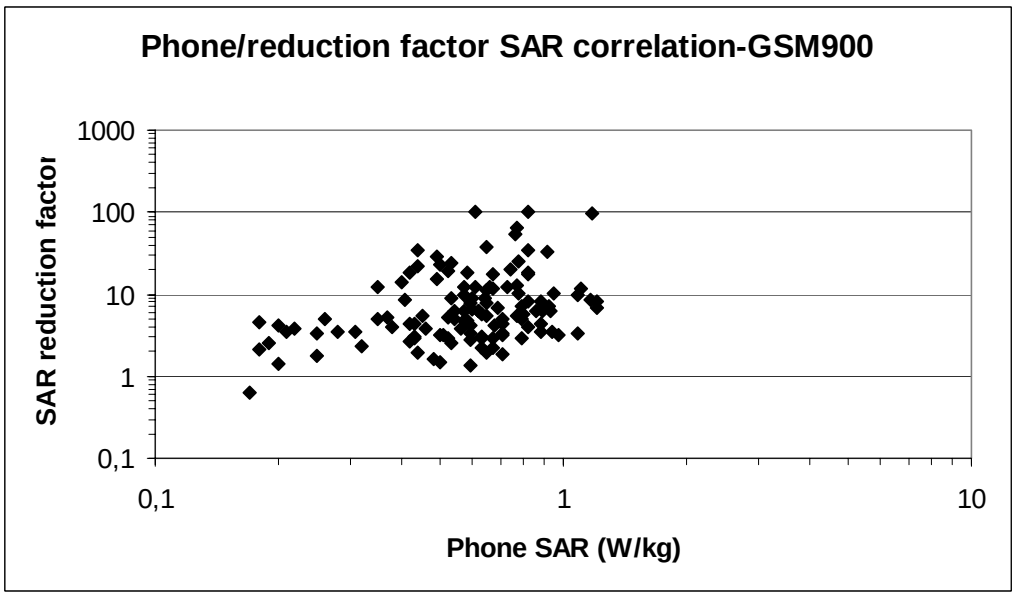


Figure 7a: Correlation between phone SAR and SAR reduction factor values for GSM900 frequency band.

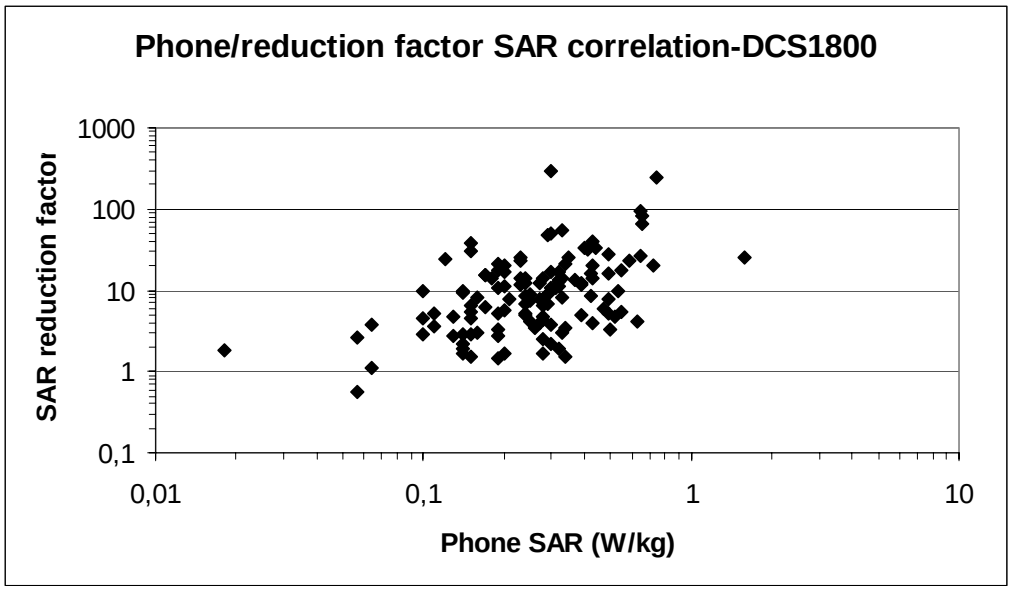


Figure 7b: Correlation between phone SAR and SAR reduction factor values for DCS1800 frequency band.

SAR reduction factor and phone SAR are also moderately correlated, but the lower values of SAR reduction factor corresponds to lower value of SAR phone values and higher values of SAR reduction factor corresponds to higher value of SAR phone values.

Conclusion

The use of HFK decreases significantly the phone user head exposition with a factor larger than 11 for GSM900 frequency band and 17 for DCS1800. There is quite no correlation between the phone SAR and the HFK SAR. HFK SAR are relatively low but not absolutely negligible. Consequently, it is interesting to measure systematically HFK SAR and to study it. We are now working to a new HFK dosimetry protocol in the french RNRT research program Adonis. Mobile phones manufacturers have also to consider this problem for HFK SAR reduction.

This research was sponsored by the french operator Bouygues Telecom.

References

1. S. E. Troulis, W. G. Scanlon, N. E. Evans, 2003, 'Effect of a hands-free wire on SAR for a waist-mounted 1.8GHz cellular telephone handset', Phys. Med. Biol., Vol.48, pp1675-1684.
2. D. Picard, A. Ziyyat, J. Ch. Bolomey, September 2001, 'Improvement of SAR measurement sensitivity on TDMA phones with detected E-field probes', 5th EBEA Conferences, Helsinki Finland.

SARMETER: AN EFFICIENT TOOL FOR MOBILE PHONE REAL EXPOSURE OF THE USER HEAD EVALUATION

D. PICARD[(1)] , S. CHAUVIN[(2)]

(1) DRE - SUPELEC- 3 RUE JOLIOT CURIE - 91192 GIF SUR YVETTE - FRANCE - dominique.picard@supelec.fr

(2) DIRECTION FREQUENCES ET PROTECTION - BOUYGUES TELECOM - 1, PLACE ABEL GANCE - 92640 BOULOGNE BILLANCOURT - FRANCE - sechauvi@bouyguestelecom.fr

Abstract

The real exposure to the RF radiation of a given mobile phone depends upon several parameters: emitted power level, TDMA pulses density, position of the handset, frequency bandwidth... The normative value for the SAR corresponds only to a given configuration at maximum power. The emitted power of a mobile phone can vary over a 30dB dynamic range due to Power Control (PWC). For GSM, when no information has to be transmitted, the TDMA pulses density can decrease with a factor 10 or more. The result of this is the potential variation of the mean emitted power of a mobile phone over a dynamic range larger than 40dB. Then the real SAR value can be significantly lower than the normative value.

The SAR meter performs real time in situ measurements of mobile phone radiated power, allowing the evaluation of the real exposure of the user head. This set up is portable and consists of a sensor, a receiver and a laptop microcomputer which performs data acquisition, signal processing and results visualization. A lot of measurements have been made and the order of magnitude of the real emitted power of mobile phones has been evaluated.

Introduction

The real exposure to the RF radiation of a given mobile phone depends upon several parameters: emitted power, TDMA pulses density, position of the handset, frequency bandwidth... The normative value for the SAR (EN50361) corresponds only to a given configuration at maximum power. The emitted power of a mobile phone can vary over a 30dB dynamic range due to Power Control (PWC). For GSM when no information has to be transmitted, the TDMA pulses density can decrease with a factor 10 or more. The result of this is the potential variation of mean emitted power of a mobile phone over a dynamic range larger than 40dB.

Real exposure

This paper describes a device allowing the evaluation of real mobile phones exposure of the user head. The principle of this device is to analyse the signal transmitted by the phone antenna by the mean of a low perturbing reception antenna. The received power is proportional to the phone emitted power. At the beginning of the communication the power is maximum (P_{max}), and we can use this value to normalize the emitted power (P) at a given time. Then, we obtain a reduction coefficient on the emitted power (C_{rp}).

$$C_{rp} = P/P_{max}$$

When all the TDMA pulses are present, their frequency is F_{max}=209Hz. This value allows the normalisation of the real frequency (F) of the TDMA pulses leading to the density (D) of the TDMA pulses.

$$D = F/F_{max}$$

In these conditions the mean emitted power (P_m) is decreased with a factor C_{rmp} in comparison with the maximum mean emitted power (P_{mmax})

$$C_{rmp} = P_m/P_{mmax} = C_{rp}\, D$$

The SAR is proportional to the mean emitted power and C_{rmp} is also the reduction coefficient on the SAR.

The device

The device consists in the low perturbation antenna, a specific receiver and a laptop micro computer [1]. The weight of the receiver and the antenna is about 1kg. The receiver uses 4 different channels: one wideband channel and 3 selective channels corresponding to GSM900, DCS1800 and UMTS frequency bands (figure 1). Each channel uses a detector followed by a low noise and high stability amplifier. The receiver dynamic range is

larger than 45dB. The antenna is a resistive loaded dipole. The sensitivity variation of this antenna in function of frequency is about 3dB. The figure 2 shows the antenna output signal corresponding to 11 different mobile phones emitting at the maximum power level in the GSM900 and DCS1800 frequency bands. The power variation of this signal in function of mobile phones is less than 10dB for each frequency band and less than 15dB for the two frequency bands.

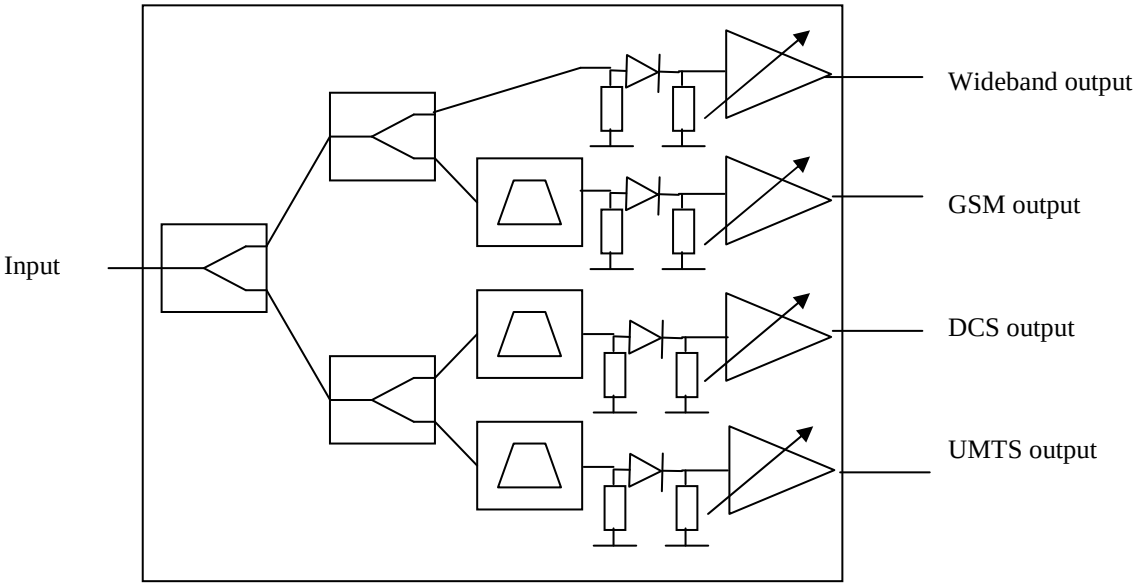


Figure 1: Receiver: overview with its four ways..

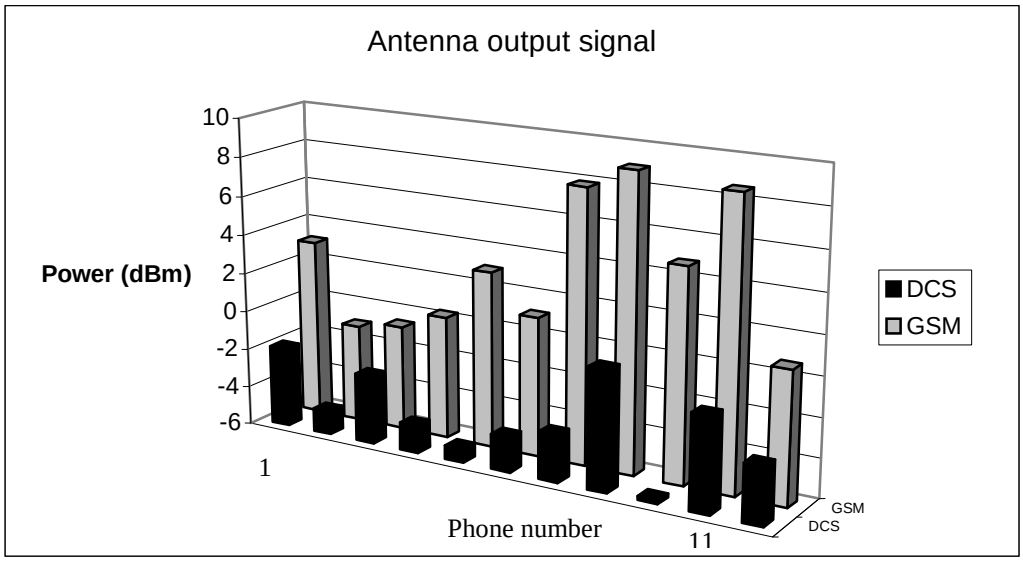


Figure 2: Antenna output signal corresponding to 11 different mobile phones for the GSM900 and DCS1800 frequency bands.

The laptop micro computer performs data acquisition and processing, with a specific software which has been developed with National Instrument Labview development system (figure 3). The power is measured on the broadband channel. Then, the reduction coefficient on the emitted power, the pulse density and the reduction coefficient on the mean emitted power, for a given duration are calculated. These three coefficients are displayed in real time during the measurement. The comparison between the different selective channels signals allows the determination of the used frequency band. The measured power and the frequency band are written in a file for each TDMA period for all the measurement duration. The figure 4 presents the entire SARmeter.

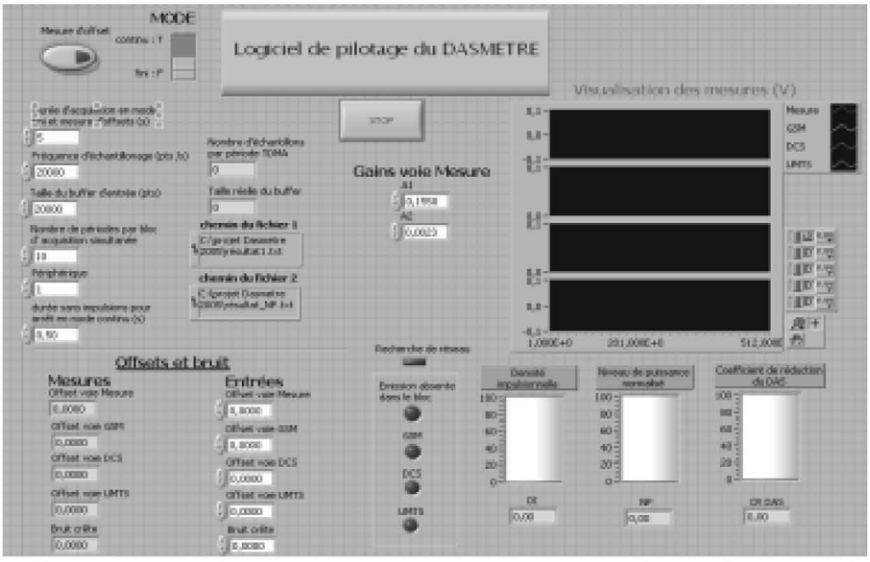


Figure 3 : Window of the SARmeter software.

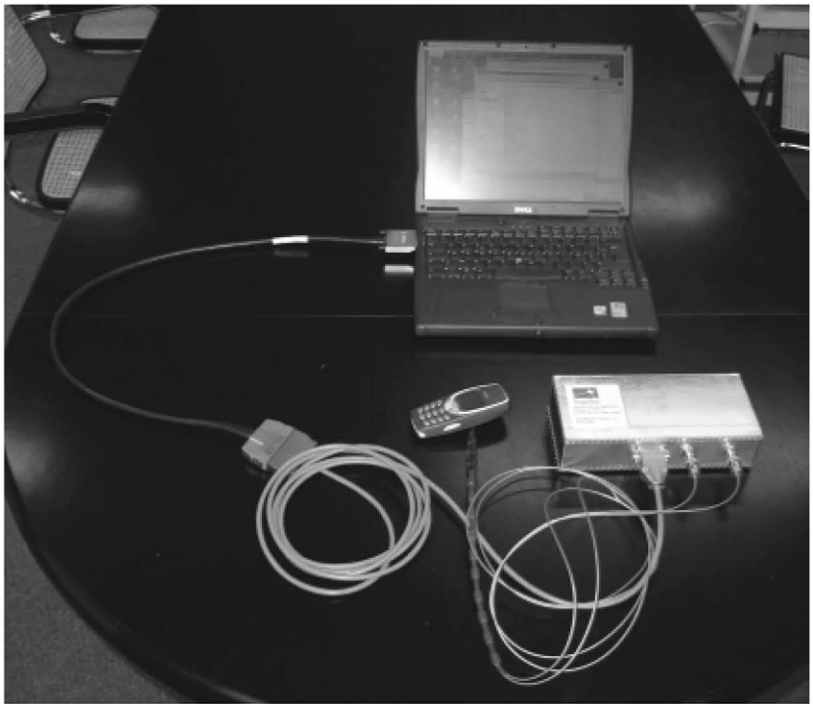


Figure 4: The SARmeter.

Result example

The figure 5 shows the variation of the emitted power in function of time for a pedestrian user on the Montparnasse Street in Paris [2]. The dynamic range of the emitted power is about 30dB and it is possible to see the different used power levels.

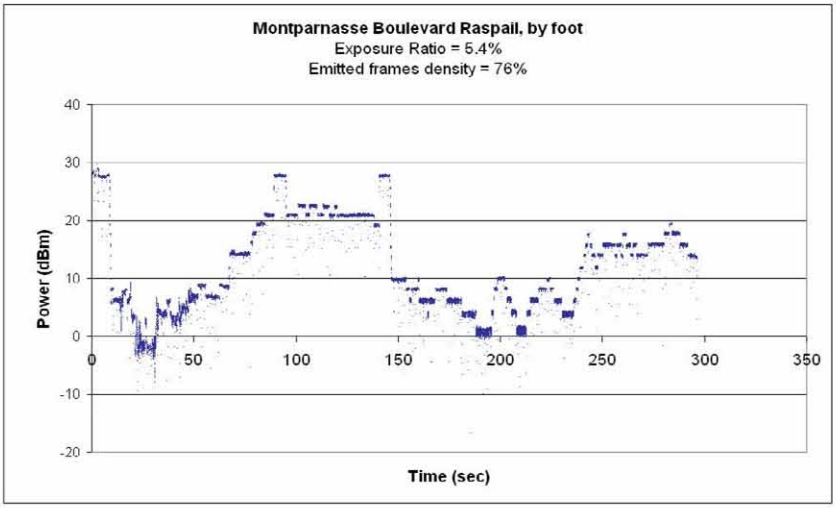


Figure 5: Example of measurement result: variation of emitted power in function of time.

Conclusion

Real exposure to RF radiation of mobile phone may hardly differ from normative SAR value. The SARmeter constitutes an efficient portable tool to determine in situ real exposure. Its use allows especially the real exposure comparison between several different networks or mobiles phones.

This research was sponsored by the french operator Bouygues Telecom.

References

[1] R. Veysset, D. Picard, S. Chauvin, 'Dispositif de determination des variations du DAS (Débit d'Absorption Spécifique) d'un mobile en communication', European Patent n°04292037.1-2411, 11.08.2004

[2] P. Le Duigou, S. Chauvin, D. Picard, R. Veysset, 'Assessment of user's exposure to GSM mobile phones emissions with the SARmeter, *BEMS 2005*, Bioelectromagnetics Society, Dublin, June 2005.

ELECTROMAGNETIC COMPATIBILITY BETWEEN SIMULATED GSM BASE STATION AT 1800 MHZ AND EEG SIGNALS.

PRAGIATIS LAZAROS[1], SOTIRIOU APOSTOLOS[1], NANOU ELENA[1], KAPARELIOTIS EVANGELOS[1], TSIAFAKIS VASILEIOS[1], PAPAGEORGIOU CHARALABOS[2], CAPSALIS CHRISTOS[1]

[1] NATIONAL TECHNICAL UNIVERSITY OF ATHENS, DEPARTMENT OF ELECTRICAL ENGINEERING, DIVISION OF INFORMATION TRANSMISSION SYSTEMS AND MATERIAL TECHNOLOGY, GREECE

[2] DEPARTMENT OF PSYCHIATRY, EGINITION HOSPITAL, UNIVERSITY OF ATHENS, GREECE

9 IROON POLYTECNEIOY STR., ATHENS, GREECE, 15773, Tel: ++30210-7722574, Fax: ++30210-7723520, email:laz_pra@mail.ntua.gr

Abstract

The current experiment studies the EMC issue that occurs when a simulated GSM base station is situated in the area where an electroencefalographer is functioning.

The experimental setup was situated in an anechoic chamber so that no electromagnetic interference would affect the measurements. The amplifier room, outside the anechoic room, situated the other part of the experimental apparatus. 32 electrodes entered a low-pass filter placed at the boundary wall of the Faraday screen room. The signal was amplified, before entering a 32-bit analogue to digital converter. The recording frequency was at 1 kHz.

The simulated GSM base station operated at the frequency of 1800 MHz emitting a GSM signal at the EIRP of 17dbm. The used piece of equipment is generally called DAS (Distributed Antenna Signal) and is used to simulate the signal emitted by one of the antennas of a GSM base station or for indoor coverage.

The results showed that the measured signals are significantly different both in frequency and in energy context.

Introduction

Issues regarding electromagnetic interference and medical devices continue to be popular topics in the technical world of electromagnetic interference. Reports of medical device failure from electromagnetic interference have increased [1, 2, 3]. This is due to the increasing number of electronically controlled medical devices in hospitals as well as the increasing number of the radiofrequency (RF) sources of radiation. The modern instruments are often more sensitive to electromagnetic interference (EMI) because they incorporate low power integrated electronic circuitry that can be much more sensitive to electromagnetic fields than their electrical and electromechanical predecessors. Digital wireless communications systems often utilize pulsed amplitude modulation, a type of modulation that can enhance the potential for EMI.

The European Union has gotten much of attention with regard to the regulation of electromagnetic compatibility (EMC) and medical electronics. Today, most medical EMC regulations originate within the International Electro technical Commission (IEC). The standard EN60601-1-2 [4] defines limits for emissions and levels of immunity and was updated to encompass the frequencies used by mobile. The IEC standard states that electronic medical equipment must operate normally in electric field intensity of 3 V/m and at a 10 V/m threshold for life – sustaining equipment.

The Electroencephalograph (EEG) is a recording equipment of brain signals with typical voltage of 100 μV and frequency range (EEG bands) beginning from 0.5 Hz up to several hundreds Hz. The EEG is connected directly to the patient in order to detect these small physiological signals which are then amplified. The EEG is known to be very sensitive to EMI due to the fact that the pulsed RF signals maybe demodulated by non-linear elements in amplifier circuits. [5].

The most recent problems of electromagnetic interference (EMI) with medical equipment arise from the widespread use of GSM signals in the hospitals [6]. Global System for Mobile communications (GSM) is an open, digital cellular technology used for transmitting mobile voice and data services in the 900MHz (890 MHz - 960 MHz) and 1.8GHz bands in Europe and Asia and the 1.9GHz PCS (Personal Communications Services) band in the US[7]. GSM uses digital technology and time division multiple access transmission methods (TDMA), which utilize schemes that produce 100% amplitude modulated pulses of the RF carrier at frequencies within the EEG frequency range. Recently, warnings have been published concerning the use of wireless communications equipment in the clinical environment. Morrisey et al. reported distortion of EEG bands throughout the 0-70 Hz range during full power exposure to CDMA and GSM signals for both frequencies of 1.800 and 1900 MHz at distances of between 0.25 to 0.5 m. [8]. Also a study by Tri et al. of Mayo Clinic revealed increase of the noise of the EEG waveform measured in the presence of a GSM signal [9].

Taking into account the above considerations, in our current work, we study the EMC status that involves the usage of an electroencephalograph in an environment infested with electromagnetic radiation produced by a GSM base station. The purpose is to observe the effects of the GSM signal on the EEG signal.

Materials and Methods

The experimental setup (Fig 1) was situated in a Faraday chamber so that no electromagnetic interference would affect the measurements. A head phantom was placed in the chamber and the signals were recorded from thirty two electrodes (Fp1, Fp2, Fpz, AFz, F2, F3, F4, F7, F8, FC1, FC2, FC5, FC6, C2, C3, C4, A1, A2, CP1, CP2, CP5, CP6, P3, P4, Pz, T3, T4, T5, T6, O1, O2,Oz) with a surface of Ag/ AgCl, which were placed on the scalp of the model-head. The electrodes were positioned according to the International 10-20 system of electroencephalography [10]. The measured magnitude was the voltage at the edges of a 2 kΩ resistance placed between each electrode and a common ground. The total electrode impedances were below 5 kΩ. The amplifier room, outside the Faraday room, situated the other part of the experimental apparatus. The electrodes entered a low-pass filter placed at the boundary wall of the Faraday screen room. The filter cut frequencies over 35 Hz so that the signal of the power supply network which is at 50 Hz would not interfere with the signal. The signal was amplified by a Braintronics DIFF/ISO-1032 amplifier, before entering a 32- bit analogue to digital converter which has a GPIB output. The digitized signal comprises an input for a Data Acquisition Card. The PC with the DAQ Card ran a LabView program for the recording of the signals, which can be monitored by an on-screen graphical representation. The recording frequency was at 1 kHz. Another PC, connected with the one described above, ran a program which triggered the other PC to save the brain signals

whenever the user wanted .The recording time was 1.5 sec so the saved signal consisted of 1500 values. The total task consisted of 55 repetitions.

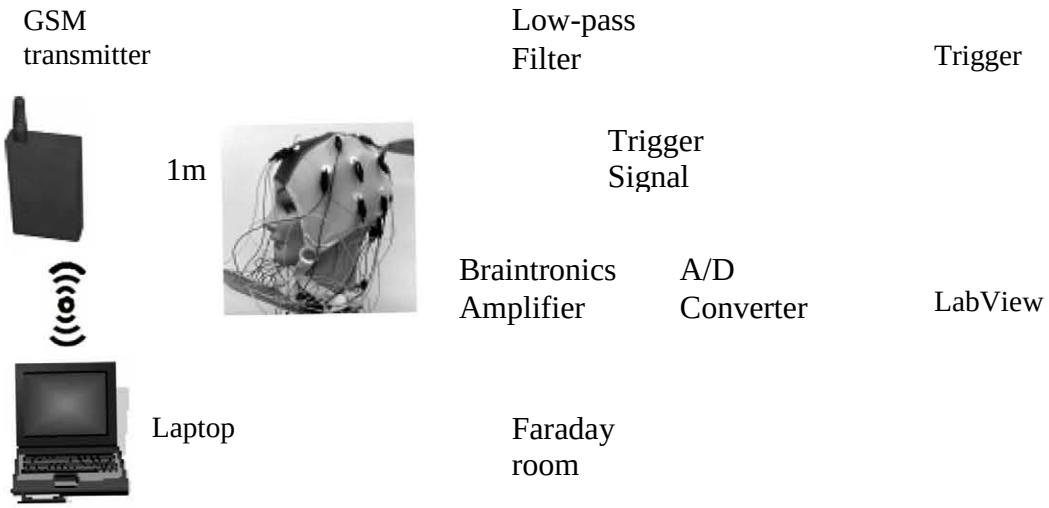


Figure 1. Experimental setup

A GSM TEMS Transmitter was placed at a distance of 1m from the head phantom. The GSM TEMS Transmitter was used to simulate the indoor coverage of a GSM base station within a cellular network. The GSM TEMS Transmitter sends out Frequency Correction Channel (FCCH), Synchronisation Channel (SCH) and optionally Broadcast Control Channel (BCCH) and Paging Channel (PCH) signaling, on a GSM carrier of human voice (900 MHz or 1800 MHz band). Prior to taking a measurement, the instrument was calibrated and adjusted. Scanning of the radio spectrum was performed in order to find a channel suitable for transmission. The Transmitter was equipped with four attenuators (3dB, 6dB, 10dB and 20 dB) suitable to connect between the Transmitter and an external antenna used with it. By combining the attenuators in all possible ways, output power levels from 17 dBm down to -22 dBm can be achieved. At the experiment the power level of 17dBm and frequency 1812,8 MHz (Absolute Radio Frequency Channel Number 550) was applied.

The electromagnetic field strength at the point where the head phantom was situated was 1,6 V/m.

The experimental procedure was done twice. The first time the GSM base station was off and practically the noise of the device was measured and the second time the GSM base station was functioning.

Finally in order to optimize the signal to noise ratio (SNR) the grand average across the 55 repetitions for each channel was calculated according to the following equation:

$$V_t = \frac{1}{55} * \sum_{j=1}^{55} V_{jt}$$

Where Vjt is the value that results after the subtraction of the amplification and the average referencing and corresponds at the time t of the trial j .This SNR optimization procedure is considered a standard practice when it comes to brain signal measurements, which are generally considered to be quite noisy [11].

The final data for analysis for each radiation condition consisted of 1500 amplitude values for each electrode, expressed in μVolts corresponding to the 1500 msec of the time period as described above.
For each electrode, the following magnitudes were also calculated:

- the energy E of the recorded signals ($E=V_t^2$)
- the amplitude in the frequency domain by using the Fourier Transform (FFT).

Statistical analysis

The amplitudes at the thirty two electrodes were subjected to Independent Samples t-test for the two radiation conditions (GSM off – GSM on). The mean values of the amplitudes for each electrode and radiation condition were also calculated. Statistical significance was set at 0.05.

Results

The data analysis showed that the energy of the recorded signals was significantly increased when the GSM Transmitter was operating. Figure 2 shows this increase at all electrodes except the C3 electrode. The white bars denote the calculated energy in the absence of the GSM signal while the black bars denote the signal energy in the presence of the GSM signal.

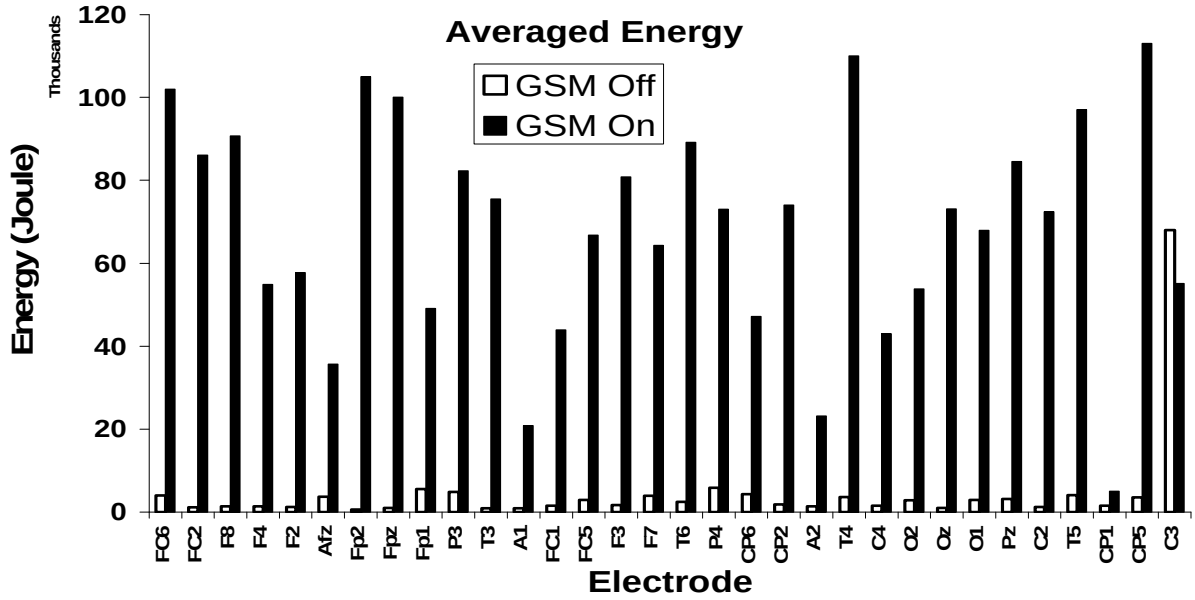


Figure 2. Averaged Energy at each electrode and each radiation condition. . The white bars denote the calculated energy in the absence of the GSM signal while the black bars denote the signal energy in the presence of the GSM signal.

The statistical analysis revealed that the presence of the GSM signal had significant effect on the amplitudes of the signals at the thirty two leads. Table 1 is quite helpful in explaining this effect, showing the mean values of the recorded signals at each electrode for the two radiation conditions.

Electrodes		**Mean Values**	
Number	**Name**	**GSM off**	**GSM on**
1	FC6	-1.61	8.25
2	FC2	-0.85	7.57
3	F8	-0.95	7.77
4	F4	-0.95	6.05
5	F2	-0.90	6.20
6	AFz	-1.55	4.87
7	Fp2	-0.59	8.38
8	Fpz	-0.78	8.18
9	Fp1	-1.90	5.72
10	P3	-1.78	7.41
11	T3	-0.76	7.09
12	A1	-0.77	3.72
13	FC1	-0.99	5.41
14	FC5	-1.36	6.67
15	F3	-1.03	7.34
16	F7	-1.59	6.55
17	T6	-1.27	7.71
18	P4	-1.94	6.97
19	CP6	-1.68	5.60
20	CP2	-1.07	7.02
21	A2	-0.95	3.92

22	T4	-1.54	8.57
23	C4	-0.99	5.35
24	O2	-1.35	5.99
25	Oz	-0.79	6.98
26	O1	-1.38	6.73
27	Pz	-1.42	7.50
28	C2	-0.89	6.95
29	T5	-1.63	8.04
30	CP1	-0.99	-1.73
31	CP5	-1.50	8.69
32	C3	-6.72	6.06

Table 1. Mean values of the amplitudes of the recorded signals for each electrode for the two radiation conditions.

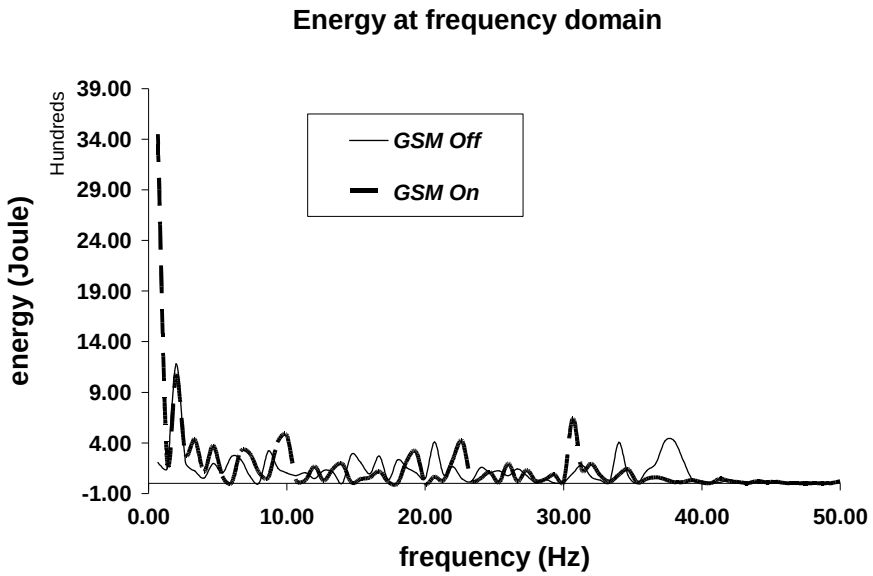


Figure 3. Calculated Energy of F8 electrode at frequency domain. The thin continuous black line denotes the calculated energy in the absence of the GSM signal while the discontinuous denotes the signal energy in the presence of the GSM signal.

Except the regarded increase of the amplitudes of the recorded signals in the time domain, the FFT calculation revealed that there was also a change in the frequency domain. A spike of the energy at the span of 1-2 Hz is observed in all electrodes. Figure 3 shows indicatory this fact at one of the 32 electrodes

Discussion

In the present study we focused on the electromagnetic interference of a GSM base station might on an electroencephalograph. The results of this study revealed that in the presence of radiation of the GSM transmitter the energy of the recorded signals was in average 38 times higher than the energy calculated in the absence of radiation. Also an alteration at the frequency domain was observed at the presence of GSM signal.

These effects are very important in view of the fact that the EEG energy as well as the frequency bands are magnitudes evaluated by doctors and related to brain activity [12, 13, 14, 15] so it is absolutely necessary to be measured accurately in order to achieve the right diagnosis.

These findings are similar to those reported by Morrisey et al [8] where distortion of EEG bands was observed. Also the studies of Sibakov and Appelqvist (1998) [16], Barbaro et al. (2000) [17], and Hietanen et al. (2000) [18] referred device sensitivity. However these findings were observed at the presence of GSM signals with higher power and at closer distance than this applied to our experiment. This is rather worrying, because EMI problems occurred even with less electromagnetic field strength.

It should be noted that although the testing was performed in a shielded environment, this doesn't exclude the influence of the measurements by some factors, such as coupling between electrodes and the presence of radiation reflecting or absorbing objects in the neighbouring area.

Moreover the source of radiation had constantly 17dBm power. This factor has to be taken into account in studies about EMI of GSM signals on Medical Equipment because most studies refer to GSM cell phones which are designed to quickly reduce their power when the channel paging stops.

According to our findings it seems that the distance of 1m and the 17dBm signal power are not sufficient to protect an electroencephalograph from EMI of GSM signals. The indoor GSM base stations are necessary inside buildings as relay stations. However before installing such a communication system an EMI study is essential in order to ensure the immunity of the medical equipment. The efficient distances of the base stations from the devices must be kept so that the electromagnetic field (EMF) power and field levels would be under the recommended values [19]. Technology does exist to protect or "harden" medical devices from radiation emissions including shielding, grounding, and filtering. These modifications are not always costly and are even less problematic if incorporated by the manufacturer during assembly.

EMC is a concern not just for manufacturers, but also for those who install, use, modify or maintain medical equipment. The existence of directives and standards has encouraged good EMC design practices, but should not be relied on to prevent EMI problems owing to the nature of the hospital electromagnetic environment. Mobile telecommunication systems are very convenient and useful to doctors, nurses and patients and studies must be done to promote awareness of EMI and its underlying coupling mechanisms.

References

1. Silberberg JL: Performance degradation of electronic medical devices due to electromagnetic interference. Compliance Eng 10(5):25-39, 1993.

2. Joyner K, Anderson V, Wood M: Interference and energy deposition rates from digital mobile phones. In: Abstracts Annual Meeting of the Bioelectromagnetics Society 16:67-68, 1994

3. Silberberg JL: Medical device electromagnetic interference issues, problem reports, standards, and recommendations. In: Proc Health Canada Medical Devices Bureau Round-Table Discussion on Electromagnetic Compatibility in Health Care, Ottawa, Canada, pp. 11-20, 1994.

4. International Electrotechnical Commission, "IEC 60601-1-2, Medical Electrical Equipment Part 1: General Requirements for Safety, Amendment No. 2. Collateral Standard: Electromagnetic Compatibility—Requirements and Tests," 1st ed., Geneva, 1993.

5. M P Robinson, D Bozec and C A Marshman, "Healthcare Engineering and Electromagnetic Compatibility", Healthcare Engineering: Latest Developments and Applications; I Mech E, London, 25-26 Nov 2003

6. Kok-Swang Tan Hinberg, "I.Radiofrequency susceptibility tests on medical equipment. Engineering in Medicine and Biology Society", 1994.

7. Wireless Intelligence 06/07/06. Also available at http://www.gsmworld.com/technology/what.shtml

8. Morrissey, Joseph James; Swicord, Mays; Balzano, Quirino, "CHARACTERIZATION OF ELECTROMAGNETIC INTERFERENCE OF MEDICAL DEVICES IN THE HOSPITAL DUE TO CELL PHONES", Health Physics. 82(1):45-51, January 2002

9. Jeffrey L. Tri, Rodney P. Severson, Allen R. Firl, David L. Hayes, and John P. Abenstein, "Cellular telephone interference with medical equipment" mayo clinic proceedings, October 005;80(10):1286-1290, 2005

10. Jasper H. The ten-twenty electrode system of the international federation. Electroencephalogr Clin

Neurophysiol, 1958

11. Roth, W.T., Ford, J.M., Pfefferbaum, A. and Elbert, T.R. Methodological issues in event-related potential and magnetic field studies. Chapter 78 in Psychopharmacology: The Fourth Generation of Progress, F.E. Bloom and D.J. Kupfer (Eds.), pp. 895-910. New York, NY: Raven Press, 1995

12. Chang PF, Arendt-Nielsen L and Chen AC. "Dynamic changes and spatial correlation of EEG activities during cold pressor test in man." Brain Res Bull 57:667–675, 2002

13. Fisch B.J.: "Fisch & Spehlmann's EEG Primer", Elsevier, 148pp, 1999

14. Epstein C.M.: "Introduction to EEG and Evoked Potentials", Lippincot Williams & Wilkins, 1983

15. Hughes J.R.: "EEG in Clinical Practise", Butterworth-Heinemann, Newton,15pp, 1994

16. Sibakov, V.; Appelqvist, M. "Immunity of medical electronic devices to electromagnetic field of cellular mobile hones."Helsinki, Finland: VTT Technical Research Center; VTT Tiedotteit Research Bulletin; 1998.

17. Barbaro, V.; Bartolini, P.; Benassi, M.; Di Nallo, A. M.; Reali, L.; Valsecchi, S. "Electromagnetic interference by GSM cellular phones and UHF radios with intensive care and operating room ventilators." Biomedical Instrum. Tech. 34:361–369; 2000.

18. Hietanen, M.; Sibakov, V.; Hallfors, S.; von Nandelstadh, P. "Safe use of mobile phones in hospitals." Health Phys. 79(Suppl. 2):S77–S84; 2000.

19. D Davis, B Segal, and T Pavlasek, "Can Minimum Separation Ensure Electromagnetic Compatibility in Hospitals? An Experimental Study," Biomedical Instrumentation and Technology/Association for the Advancement of Medical Instrumentation 33, no. 5: 411- 416, 1999

NUMERICAL DETERMINATION OF TRANSMEMBRANE VOLTAGE INDUCED ON IRREGULARLY SHAPED CELLS

GORAZD PUCIHAR, TADEJ KOTNIK, BLAŽ VALIČ, DAMIJAN MIKLAVČIČ

Faculty of Electrical Engineering, University of Ljubljana, Tržaška 25, SI-1000, Ljubljana, Slovenia.

e-mail: gorazd.pucihar@fe.uni-lj.si, tadej.kotnik@fe.uni-lj.si, blaz.valic@fe.uni-lj.si, damijan.miklavcic@fe.uni-lj.si

Abstract

The paper presents an approach that reduces several difficulties related to the determination of induced transmembrane voltage (ITV) on irregularly shaped cells. We first describe a method for constructing realistic models of irregularly shaped cells based on microscopic imaging. This provides a possibility to determine the ITV on the same cells on which an experiment is carried out, and can be of considerable importance in understanding and interpretation of the data. We also show how the finite-thickness, nonzero-conductivity membrane can be replaced by a boundary condition in which a specific surface conductivity is assigned to the interface between the cell interior (the cytoplasm) and the exterior. We verify the results obtained using this method by a comparison with the analytical solution for an isolated spherical cell, obtaining a very good agreement. In addition, we compare the ITV computed for a model of an irregularly shaped CHO cell with the ITV measured on the same cell by means of a potentiometric fluorescent dye. Finally we confirm that electropermeabilization occurs in those areas of cell membrane, where the absolute value of ITV is the highest.

1. Introduction

Induced transmembrane voltage (ITV) forms on the cell membrane when the cell is exposed to the external electric field [1-3]. The ITV is proportional to the amplitude of electric field and with a sufficiently strong field, a sudden increase in membrane permeability occurs, a phenomenon termed electropermeabilization. During the state of high permeability it is possible to deliver membrane impermeant ions and molecules into the cell.

In many applications of electropermeabilization an efficient and at the same time reversible permeabilization is essential (e.g. DNA electrotransfer [4-6]). Thus, a careful planning of the experiment, which involves the estimation of the amplitude of ITV leading to cell permeabilization, is required. It was demonstrated experimentally that ITV determines the regions of the membrane where electropermeabilization occurs [1, 2]. Namely, increased permeability is observed only in regions of the membrane where ITV exceeds a critical value. As already stated ITV is proportional to the electric field, varies with the position on the cell membrane, and is influenced by cell geometry and physiological characteristics of the medium surrounding the cell [3, 7-10]. For an isolated cell of simple shape, such as a cylinder, a sphere, or an ellipsoid, ITV can be described analytically [3, 8, 11 – 14]. However, when cell geometry is more complicated (e.g. cells in tissues) an analytical description is in general not attainable and ITV can be determined either experimentally [15-20] or numerically [21-28].

Usually, numerical models are constructed using simple geometrical shapes, e.g. hemi-spheres, hemi-ellipsoids or combination of simple shapes [22, 23, 28, 29]. These models can be realistic for cells in suspensions, but cells growing in a dish or in tissues typically have profoundly irregular shapes, and combinations of several simple geometrical objects are not usable anymore. In this study, we present a method for construction of more realistic models of irregularly shaped cells from their cross-section images. We also present a method to replace a cell membrane in the model with a boundary condition. We then calculate the ITV on the model of an irregularly shaped cell and compare it to the ITV determined experimentally by means of fluorescent dye. In addition, the course of permeabilization of this cell is monitored and regions of membrane where permeabilization occurred are determined.

2. Methods

2.1 Construction of a three-dimensional model of a cell

Three-dimensional models of irregularly shaped cells were constructed from a sequence of microscopic fluorescence images representing cross-sections of a cell attached to the cover glass. The models presented in the study were built from CHO cells, but the method can also be applied to other cell types. Fluorescence images were obtained by staining the cell with a fluorescent dye di-8-ANEPPS. The dye emits a strong fluorescence when it binds to the membrane, therefore making the cell edges visible. The cross-sections were obtained by shifting the focus on a fluorescence microscope (Zeiss AxioVert 200, objective ×100, oil immersion, Zeiss, Germany) in constant steps of 2 μm from the bottom to the top of the cell (Figure 1A). The images were acquired using a cooled CCD camera (VisiCam 1280, Visitron, Germany) and MetaMorph 5.0 software (Visitron, Germany), and converted from grayscale (8 bit) to black and white (1 bit, Figure 1B) in Corel PhotoPaint 11.0 (Corel Corp., Ottawa, Canada). Using FEMLAB 3.1 package (COMSOL Inc., Burlington, MA, USA) with MATLAB 6.5 (MathWorks Inc., Natick, MA, USA), the contours of the cell were detected using *flim2curve* (Figure 1C), transformed to solid planes with 35 edges with *solid2*, and the planes were connected into a 3D object using *loft* to obtain the model of the cell. This model was then imported to the FEMLAB workspace, where it was positioned to the bottom of a rectangular block, thereby mimicking the cell attached with its bottom to the cover glass (Figure 1D). To construct a model of several cells, or a cell cluster, this procedure is repeated for each cell separately [30]. In case of a cell cluster, individual cells are, after they are imported to FEMLAB, merged together to form a cluster.

2.2 Modeling the cell membrane

Direct incorporation of a realistic cell membrane (i.e. a layer of very small, yet non-zero thickness surrounding the cell) into the model is technically very problematic. Unless the distribution of the electric field, current density, and/or electric potential within the membrane is of interest, this can be avoided. Namely, the effect of the membrane on these electric quantities in the cell interior and exterior is equivalent to the effect of a corresponding surface conductivity assigned to the interface between the interior and the exterior. More precisely, as the specific conductivity of the membrane – typically about 5×10^{-7} S/m [31] – is at least five orders of magnitude lower than the specific conductivities of the media surrounding it, the current flows through the membrane practically orthogonally to its surface. Consequently, in the membrane the total current density is virtually equal to its normal component alone (J), which is given by:

$$J = \frac{\sigma_m (V_o - V_i)}{d}, \tag{1}$$

where σ_m is the specific membrane conductivity, d is the membrane thickness and V_o, V_i are the electric potentials at the outer and inner surface of the membrane, respectively. Here J, V_o, and V_i are functions varying with the position on the membrane, while σ_m and d are constants. For the purpose of determining ITV, the events inside the membrane layer are not relevant, and the ratio σ_m/d can be treated as a single entity — the specific surface conductivity, $\kappa_m = \sigma_m/d$. The interface between the cell interior (the cytoplasm) and the cell exterior is then characterized by

$$J = \kappa_m (V_o - V_i). \tag{2}$$

Despite the membrane as such being absent from the model, the drop of electric potential at such an interface is equivalent to ITV on a membrane with a specific conductivity σ_m and thickness d. In models constructed in this way, the mesh of finite elements is generated without difficulty, as very small elements corresponding to the membrane itself are avoided [30].

2.3 Settings of the model and subsequent computations of induced transmembrane voltage

The computation of the functions J, V_o and V_i was performed in FEMLAB by introducing two application modes, the cell exterior (extracellular medium) being active in the first, and the cell interior (cytoplasm) in the second mode. Both application modes were of a static current density type. For models containing several cells, an additional application mode active in the cytoplasm of each cell must be introduced, and the functions J_1, J_2, ... and V_o, V_{i1}, V_{i2}, ... are then computed.

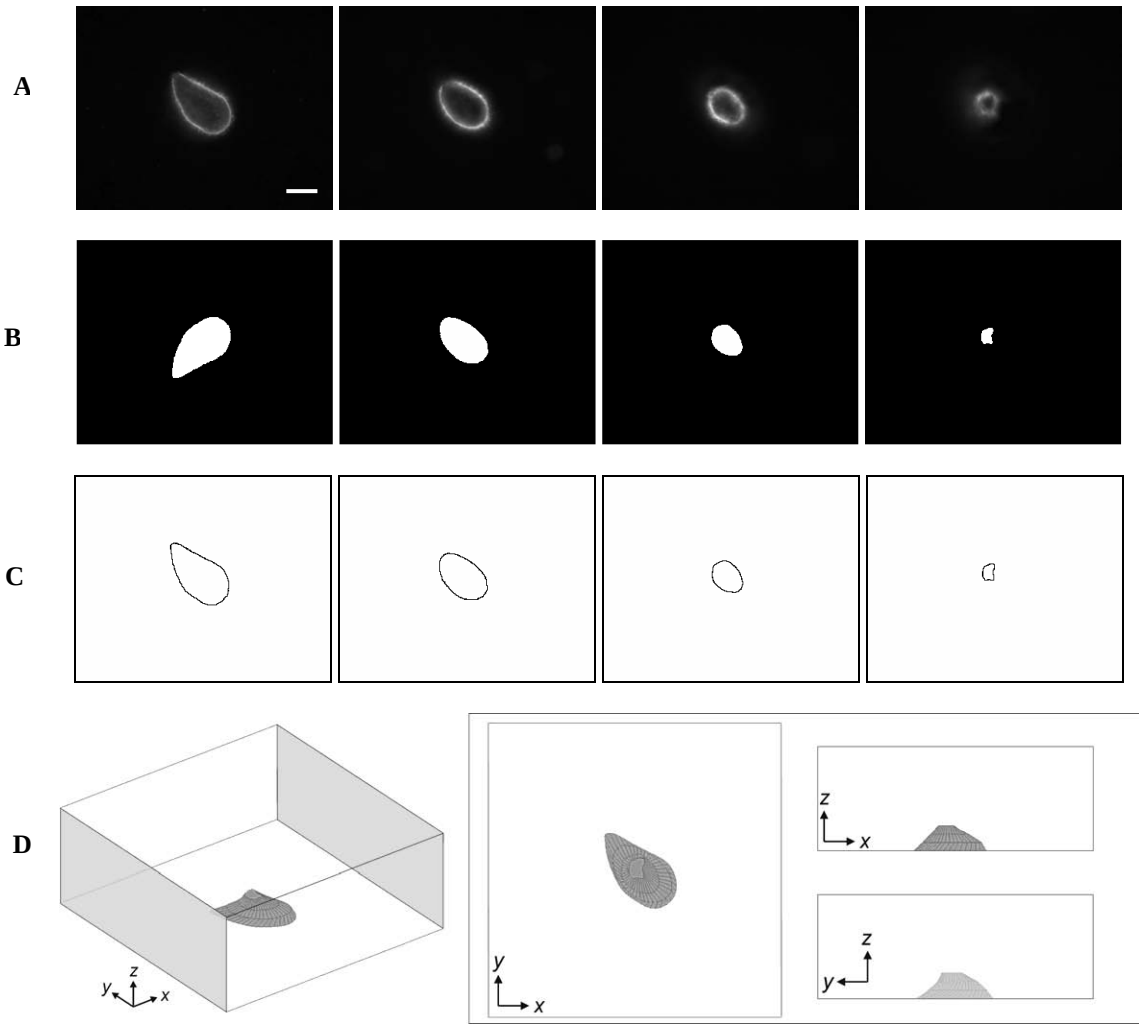


Figure 1. Construction of a 3D model of an irregularly shaped CHO cell. (A) Fluorescence images (8 bit) of an irregularly shaped CHO cell stained with di-8-ANEPPS. The images represent four cross-sections of the cell, acquired from bottom to the top of the cell in 2 µm steps. Bar represents 10 µm. (B) Black and white (1 bit) images. (C) The corresponding contour of the cell edge for a given cross-section. (D) The three-dimensional geometry of the cell model constructed from the cross-sections. The interior of the rectangular block represents the extracellular medium, the grey-shaded faces are the electrodes, and the other four faces are insulating.

The specific conductivity of the cell interior was set to 0.3 S/m [32], and the specific conductivity of the rest of the block (the cell exterior) to 0.14 S/m [33]. Two of the opposite vertical faces of the block were modeled as electrodes, which was done by assigning fixed electric potentials to both electrodes (one was usually set to ground) to obtain the voltage-to-distance ratio of 100 V/cm. The remaining four faces of the block were modeled as insulating surfaces, the bottom one representing the cover glass. At the boundary surface between the cell interior and exterior, the normal component of the current density was set corresponding to Eq. 2 with a negative sign (-*J*) in the mode corresponding to the cell exterior, and with a positive sign in the mode corresponding to the cytoplasm (or, with several cells, in all such modes). The specific surface conductivity was set at κ_m = 100 S/m^2, which is the ratio between a specific membrane conductivity of 5×10^{-7} S/m and a membrane thickness of 5 nm [34].

After the mesh was generated, the electric potential was computed using finite elements method with FEMLAB's stationary nonlinear Conjugate gradients solver with Algebraic multigrid preconditioner. ITV was calculated as the difference between electric potentials on the two sides of the boundary surface separating the inside and outside of the cell, i.e. as ITV = V_i - V_o. ITV was then plotted as a function of relative arc length.

2.4 Measurements of induced transmembrane voltage

To experimentally determine ITV we used di-8-ANEPPS, a fast potentiometric fluorescent dye. The dye binds to the cell membrane, which causes a considerable increase in its fluorescence. With the change in ITV, the fluorescence of the dye then varies linearly [15-17]. CHO K1 cells were grown on cover glasses in culture medium. Six to eight hours latter the culture medium was replaced with SMEM medium containing 30 µM of di-8-ANEPPS and 0.05% of Pluronic. After staining for 12 min at 4°C, the cells were washed thoroughly with pure SMEM to remove the excess dye. Before the experiments, SMEM was replaced with an isoosmotic pulsing buffer (10 mM K_2HPO_4/KH_2PO_4, 250 mM sucrose, 1 mM $MgCl_2$, [33]). Cells were then exposed to a voltage of 40 V applied for duration of 100 ms on two parallel wire electrodes with a 4 mm distance between them (voltage-to-distance ratio 100 V/cm). Before and during the pulse, the fluorescence image of the lowermost level of a cell or a cell cluster was acquired, with excitation at 490 nm and emission detected at 605 nm. The procedure was repeated five times, with a 2 s delay between pulses. The control image was then subtracted from the corresponding pulse image and the corrected images were averaged to increase the signal-to-noise ratio. The changes in fluorescence of the dye in the membrane were quantified by measurements of grey levels along the region of interest, which was a 5 pixel wide line encircling the cell at the site of the membrane. Using a calibration curve obtained in a separate experiment (6% of fluorescence change per 100 mV, not shown [30]), fluorescence changes were transformed to the values of ITV, which were plotted on a graph as a function of the normalized arc length. The images were acquired using the same imaging system as described in Section 2.1.

2.5. Monitoring the course of electropermeabilization

Cells (CHO K1) were grown and prepared as described in Section 2.4. Prior to experiments, the culture medium was replaced with pulsing buffer, which contained 100 µM of fluorescent dye Propidium Iodide (PI, Sigma, Saint Louis, USA). The dye is essentially membrane impermeant, but can enter the electropermeabilized cells, where its fluorescence increases significantly, making it suitable to detect electropermeabilization of cells. The electrodes were positioned to the bottom of cover glass. A 400 V, 200 µs pulse was delivered to the electrodes, and fluorescence from cells was monitored in 100 ms time steps. The imaging system was the same as described in Section 2.1.

3. Results and discussion

3.1 Validation of the model by comparison with analytical solution for a spherical cell

The method introduced in Section 2.1 was first verified by comparing the calculations of ITV on a model of a spherical cell with the analytically derived ITV for the same cell. Under physiological conditions, the ITV induced by an electric field E on a spherical cell with outer radius R is given by Schwan's equation [3]:

$$ITV = f_s E R \cos\varphi \tag{3}$$

where φ is the angle between the direction of the field and the line connecting the center of the cell to the point of interest and f_s is a function reflecting the electric and dimensional properties of the cell and the surrounding medium [8]:

$$f_s = \frac{3\lambda_o\left[3dR^2\lambda_i + \left(3d^2R - d^3\right)\left(\lambda_m - \lambda_i\right)\right]}{2R^3\left(\lambda_m + 2\lambda_o\right)\left(\lambda_m + \frac{1}{2}\lambda_i\right) - 2\left(R-d\right)^3\left(\lambda_o - \lambda_m\right)\left(\lambda_i - \lambda_m\right)} \tag{4}$$

In Eq. 4, λ_o, λ_i, and λ_m are the specific conductivities of the extracellular medium, cytoplasm and the membrane, respectively, and d is the thickness of the membrane. Schwan's equation provides a precise description of the ITV on a single spherical cell, and was as such used as the first test of the method of numerical determination of the ITV described in this paper. Figure 2B shows the ITV computed using this method and Figure 2C shows the error with respect to Schwan's equation (note that the y-scale is much smaller than in 2B). On the basis of these results we can conclude that the numerical computation of ITV using our method is sufficiently accurate for any practical purpose. Both the analytical and the numerical solution were determined for a spherical cell with R = 10 µm, λ_o = 1 S/m, λ_i = 0.2 S/m, $\lambda_m = 5 \times 10^{-7}$ S/m, and d = 5 nm. The cell was exposed to an electric field of 100 V/cm, which was, in the numerical solution, generated by applying 1 V to a pair of rectangular parallel plate electrodes 0.01 cm apart.

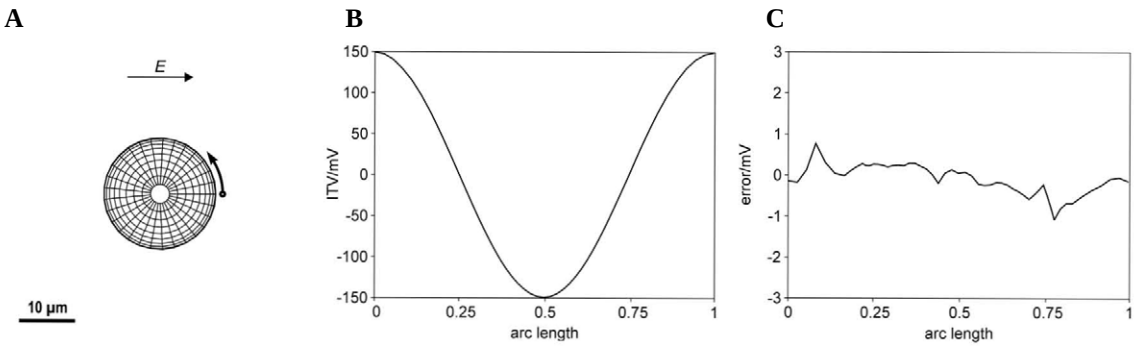


Figure 2. (A) Geometry of a spherical cell. The arrow denotes the start and the direction of the path along which the normalized arc length is measured. (B) Computed ITV for a spherical cell with a membrane modeled as a boundary condition. (C) The difference between the computed and analytically derived ITV. The calculations were performed for a spherical cell with R = 10 µm, λ_o = 1 S/m, λ_i = 0.2 S/m, $\lambda_m = 5 \times 10^{-7}$ S/m, d = 5 nm, and E = 100 V/cm.

The main advantage of replacing the cell membrane with a boundary condition is that the mesh elements corresponding to the membrane are avoided. This efficiently reduces the time for mesh generation and time needed to solve the problem. If the membrane is instead modeled explicitly, its thickness must typically be exaggerated by an order of magnitude or more, otherwise the number of mesh elements is far too large to be handled by a computer. To compensate for this, the membrane can be assigned a correspondingly higher specific conductivity [30].

3.2 Comparison with fluorescence measurements

The model of an irregularly shaped cell was constructed from four cross-sections of the cell photographed under a microscope, as described in detail in Section 2 (Figures 1A-1D). The distribution of electric potential was first computed (Figure 4A) and the ITV was than calculated as the difference between the electric potential in the cell interior and exterior. The results are, for the lowermost layer of the cell, shown in Figure 3C with dashed curve. Figure 4B shows the areas of the cell where the absolute value of ITV is the highest (within arbitrarily chosen range of 15% of the maximal value). The calculations of ITV were then compared with measurements of ITV on the same cell using a potentiometric fluorescent dye di-8-ANEPPS. The changes in fluorescence of dye upon exposure of cell to the electric field are presented in Figure 3A and are hardly noticeable. They become visible after subtraction from the control image (without electric field) as shown in Figure 3B. In this figure, the side of the cell colored in white represents an increase in fluorescence, and the side of the cell colored in black, a decrease in fluorescence. Fluorescence changes were transformed to ITV using a calibration curve (see Materials and Methods) and are presented with solid curve in Figure 3C as a function of the normalized arc length. The results are shown for two opposing orientations of external electric field (100 V/cm). For the investigated cell, ITV changes along the cell membrane between approximately 75 mV and -65 mV for electric field directed from left to right and between -80 mV and 55 mV for the opposite direction of the field (Figure 3C) and is in qualitative agreement with the calculated ITV. Small differences between the amplitudes could be attributed to the variations of the slope of calibration curve between different cells, the differences between the actual and implemented parameters of the model (especially the membrane permeability), and the experimental setup.

3.3 Monitoring the course of electropermeabilization

In the presence of the membrane-impermeant fluorescent dye Propidium Iodide, the same cell was then exposed to a single unipolar rectangular 400 V pulse (1000 V/cm) with 200 µs duration. The changes in fluorescence of the cell were observed 100 ms after the pulse application on both sides of the membrane, denoting the regions where permeabilization occurred. With time, cell interior becomes more fluorescent indicating continuous dye uptake into cell after permeabilization. The fluorescence regions of the membrane on the first image (100 ms) were compared with calculations of ITV (shown in Figure 4B). A good agreement between the observed fluorescence increase and the regions where the absolute value of ITV was the highest was obtained (cf. Figure 4B and Figure 5A).

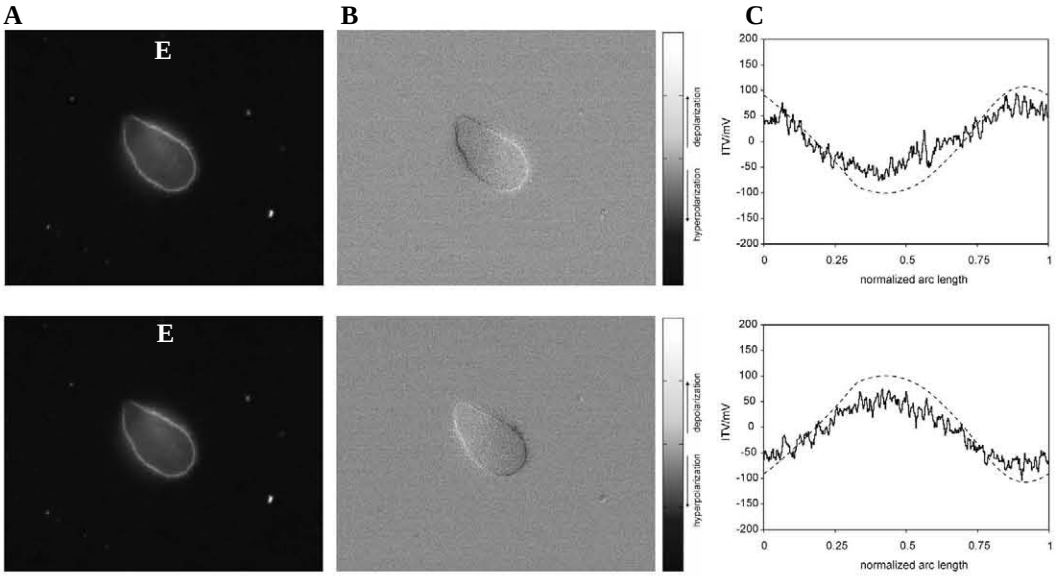


Figure 3. Measurements of ITV on an irregularly shaped CHO cell. First row shows the results for the electric field *E* directed to the right and the second row for the opposite direction. (A) The 8-bit fluorescence images of a cell stained with di-8-ANEPPS and acquired during the exposure to 40 V (100 V/cm), 100 ms rectangular pulse. Bar represents 10 µm. (B) Changes in fluorescence of cell obtained by subtracting the control image (not shown) from the image with pulse and shifting the grayscale range by 50%. White arrow shows the path along which ITV was measured. (C) ITV as a function of normalized arc length. Solid curve – measured values, dashed curve – numerically calculated values. The changes in fluorescence were transformed to ITV by using a 6%/100mV calibration curve.

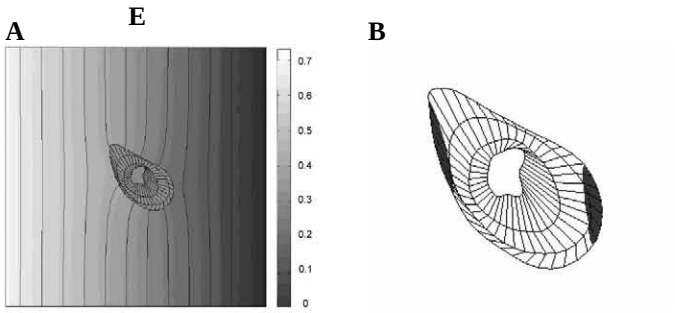


Figure 4. (A) The calculated distribution of the electric potential around and inside the cell in the lowermost x-y plane of the cell. The black curves represent the equipotentials and the arrow marks the path along which the potential was measured. The scale is in volts. (B) Regions of the membrane where the absolute value of ITV, calculated as a difference between the potentials on both sides of the membrane ($ITV = V_i - V_o$), is the highest (within arbitrarily chosen range of 15% of the maximal value).

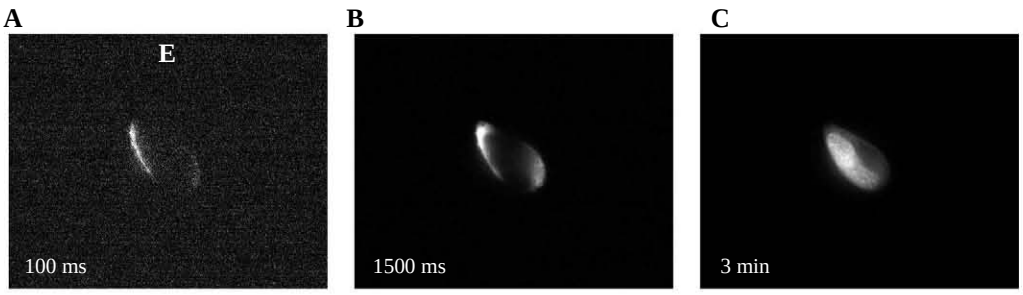


Figure 5. Monitoring of cell electropermeabilization. (A) Fluorescence of the cell 100 ms, (B) 1500 ms, and (C) 3 min after pulse delivery. The images were corrected for the background fluorescence and the brightness was automatically enhanced. The cell was exposed to a 1×400V, 200 µs (1000 V/cm) rectangular pulse. Propidium Iodide was added to suspension before the pulse was applied to visualize the permeabilized regions. Bar represents 10 µm.

4. Summary

We demonstrated how to construct realistic models of irregularly shaped cells from their cross-section images. This allows determination of the ITV on the same cells on which the experiment is carried out, and can be of considerable importance in understanding and interpretation of the data. We also presented a method to replace a cell membrane in the model with a boundary condition. Such replacement efficiently eliminates the number of elements of the mesh and consequently time needed to solve the problem. To validate the method, the computed ITV for a spherical cell was compared with the analytical expression describing the ITV for the same cell, showing a very good agreement between both solutions. This can be considered as the evidence that this method is a reliable and accurate one. We then showed that the ITV computed for a model of an irregularly shaped cell is comparable to the ITV measured on the same cell. Finally, we confirmed that electropermeabilization occurs in those areas of cell membrane, where the absolute value of ITV is the highest. The presented methods of model construction from cross-section images and replacement of the membrane by a boundary condition can also be used to study more complicated cell geometries, such as several cells in contact, which represent a simple model of a tissue.

5. Acknowledgements

This work was supported by the Ministry of Higher Education, Science and Technology of the Republic of Slovenia. The authors wish to thank dr. Marko Puc for building the switcher device for delivery of electric pulses in the experiments.

6. References

1. Hibino M., et al. *Biophys. J.* 59:209-220, 1991.
2. Hibino M., et al. *Biophys. J.* 64:1789-1800, 1993.
3. Schwan H. P. *Adv. Biol. Med. Phys.* 5:147-209, 1957.
4. Golzio M., et al. *Gene Therapy.* 12: 246-251, 2005.
5. Somiari S., et al. *Mol. Ther.* 2:178-187, 2000.
6. Šatkauskas S., et al. *Mol. Ther.* 5:133-140, 2002.
7. Gabriel B. and Teissié J. *Eur. Biophys. J.* 27:291-298, 1998.
8. Kotnik T., et al. *Bioelectrochem. Bioenerg.* 43:285-291, 1997.
9. Lojewska Z., et al. *Biophys. J.* 56:121-128, 1989.
10. Pucihar G., et al. *Bioelectrochemistry* 54:107-115, 2001.
11. Kotnik T. and Miklavčič D. *Biophys. J.* 79:670-679, 2000a.
12. Kotnik, T. and Miklavčič D. *IEEE T. Bio- Med. Eng.* 47:1074-1081, 2000b.
13. Gimsa J. and Wachner D. *Biophys. J.* 81:1888-1896, 2001.
14. Gimsa J. and Wachner D. *Eur. Biophys. J.* 30:463-466, 2001.
15. Gross D., et al. *Biophys. J.* 50:339-348, 1986.
16. Montana V., et al. *Biochemistry* 28:4536-4539, 1989.
17. Loew L. M. *Bioelectromagnetics.* 1:179-189, 1992.
18. Knisley S. B., et al. *Circ. Res.* 72:255-268, 1993.
19. Bedlack R. S., et al. *Neuron.* 13:1187-1193, 1994.
20. Hassan N., et al. *IEEE T. Plasma Sci.* 30:1516-1524, 2002.
21. Miller C. E. and Henriquez C. S. *IEEE T. Bio-Med. Eng.* 35:712-718, 1988.
22. Fear E. C. and Stuchly M. A. *IEEE T. Bio-Med. Eng.* 45:856-866, 1998a.
23. Fear E. C. and Stuchly M. A. *IEEE T. Bio-Med. Eng.* 45:1259-1271, 1998b.
24. Susil R., et al. *Electro. Magnetobiol.* 17:391-399, 1998.
25. Pavlin M., et al. *IEEE T. Bio-Med. Eng.* 49:605-612, 2002.
26. Valič B., et al. *Bioelectrochem.* 63:311-315, 2004.
27. Gowrishankar T. R. and Weaver J. C. *Proc. Natl. Acad. Sci. USA.* 100:3203-3208, 2003.
28. Buitenweg J. R., et al. *IEEE Trans. Biomed. Eng.* 50:501-509, 2003.
29. Valič B., et al. *Eur. Biophys. J.* 32:519-528, 2003.
30. Pucihar G., et al. *Ann. Biomed. Eng.*, 34:642-652, 2006.
31. Gascoyne P. R. C., et al. *Biochim. Biophys. Acta.* 1146:119-126, 1993.
32. Harris C. M. and Kell D. B. *Bioelectrochem. Bioenerg.* 11:15-28, 1983.
33. Rols M. P., et al. *Eur. J. Biochem.* 254:382-388, 1998.
34. Alberts B., et al. Biology of the Cell, 3rd ed., Garland Publishing, New York, 1994.

MODULATION OF *IN VITRO* EMF-INDUCED EFFECTS ON HUMAN KERATINOCYTES (HaCaT) BY Ca^{2+}-DEPLETION

(††)DURANTI G., (*)BARTOLETTI C., (††)ERDEMBILEG T., (**)FALSAPERLA R., (††)FAZIO G., (††)PAGNOTTA S., (††)ROSATO N., (††)ROSSI A., (**)ROSSI P., (*)SACERDOTI G., (†)SUPINO R.

(*)University of Rome "La Sapienza" – Italy;
(**)National Institute of Occupational Safety and Prevention (ISPESL) – Rome – Italy;
(††)University of Rome "Tor Vergata" – Rome – Italy; (†)Istituto Nazionale Tumori – Milano – Italy.

Abstract

Effects of 900 MHz CW on human immortalized keratinocytes (HaCaT) were investigated. Cells kept in a CO_2 independent medium were exposed inside a cell-culture incubator at 37 °C. Sham samples were in the same environmental conditions. Exposure durations ranged from 2 up to 18 hours, and dose-response investigation was performed at average SAR levels of 0.7 mW/kg and 3 mW/kg.

The inhibition of proliferation and viability reached its maximum for exposures of 2^h15^m duration (21% at lower SAR level and 12% at highest one), and for exposures of 18^h duration (40% at lower SAR level and 20% at highest one). Less marked effects were observed with exposures of 4 and 9 hours to the SAR level of 3 mW/kg.

To test the dependence on calcium of the effect, experiments were performed in Ca-depleted medium (KCl 1mM was added to keep the right ionic strength). Exposure to EMF for 18 hours in these experimental conditions caused a further 10% increase in cell growth inhibition, regardless SAR levels.

Moreover we studied the effect of EMF on the structure of tissue Transglutaminase (tTG), a calcium-dependent enzyme involved in wound healing and epithelial differentiation. Indeed, after 2 hours exposure at the SAR level of 0.7 mW/kg, the fluorescence spectrum of tTG (excited at 293 nm) was differentially modulated in comparison to sham samples. EMF treatment seems to induce a conformational change similar to that observed during its activation which occurs upon calcium addition.

Introduction

Several authors reported about the alteration of cell membrane surface charges exposed to low frequency electromagnetic fields (EMF) and conflicting results have been reported on the probably consequent mobilization of intracellular calcium. However only little studies have been reported on the effects of radiofrequencies (900 MHz) on calcium metabolism in normal human cells. The role of calcium ions in several biological pathways has been supported. In the case of EMF it could be hypothetized that EMF exposure, by disturbing intracellular calcium availability and fluxes, can interfere with biological cellular pathways. Additional mechanism of interaction of EMF with biological tissue could be traced to the different permeability of certain ions, like calcium, through the canals of the membranes that permit the passage of salts (called ionic canals); today of fundamental importance for the study of brain cells and of other neurological diseases (Marchionni et al., 2006). Moreover, exposure to EMF is able to change *in vitro* protein conformation and enzyme activity suggesting a great influence in cellular metabolism (Barteri et al., 2005). It has been reported also that 900 MHz do not modulate the signal transmission in the peripheral nervous system, whereas 50/60 Hz are effective. Moreover biphasic actions depending on frequencies and intensities have been reported (Marchionni *et al.*, 2006).

Following the previuos results assessing that exposure to 900 MHz could trigger a differentiation program in HaCaT cells (Duranti et al, 2004; Duranti et al., 2005), in the present work, we investigated *in vitro* the EMF-induced effects in relation to calcium concentration. We choose a human normal immortalized keratinocytes cell line (HaCaT), since keratinocytes are naturally exposed to both mechanical and thermal stimuli, and skin is usually exposed to electromagnetic radiation at considered frequency more than inner tissues. We examined the cell proliferation at different times of EMF exposure in the presence or absence of calcium and at different SAR exposures. Moreover we observed, by spectrophotometric determination, a modification in the structure of tissue transglutaminase (tTG) a calcium-dependent enzyme involved in wound healing and epithelial differentiation.

Altogether, our results suggest an involvement of the intracellular Ca^{2+} availability in the cell response to 900 MHz EMF exposure.

Materials and Methods

Reagents

Cell culture media (Dulbecco's MEM mix F-12 and CO_2-independent media) were obtained from Invitrogen, Carlsbad, CA, USA; heat-inactivated fetal bovine serum FBS and trypsin were obtained from HyClone, Oud-Beijerland, Holland. Tris (hydroxymethyl)-aminomethane, HCl, were obtained from Fluka (Buchs, Switzerland), Calcium-free keratinocyte growth medium from Cambrex-Clonetics (Baltimore USA). Primary and secondary antibodies were obtained from Santa Cruz (Santa Cruz, CA USA). All the other reagents, unless otherwise specified, were from Sigma Chemical (St. Louis, MO, USA).

SAR determination

Computational simulations have been carried out by employing the electromagnetic commercial simulator Microwave Studio (MWS) by CST-Germany, based on the Finite Integration Technique (FIT). This numerical method, developed by Weiland in 1977, provides a discrete reformulation of Maxwell's equations in their integral form suitable for computers and it allows simulating real-world EMF problems with complex geometry. In order to numerically solve Maxwell's equations, a finite calculation domain is defined. By creating a suitable mesh system, this domain is splitted up into small cubes, so-called grid cells. In combination with the FIT, MWS employs the Perfect Boundary Approximation (PBA) for the spatial discretization of the simulated structure that allows an accurate modelling of bend-shaped structures.

In order to simulate in vitro tests, the exposure set up was represented as two parallel metallic plates of (80 x 99) mm size, at 27 mm of distance and 4 Petri dishes or 2 flasks were inserted between the plates. In simulation for exposure to 900 MHz EMF, the plexiglas dishes were of 35 mm of diameter, height of 8 mm and 1 mm of thickness. Each culture medium was then parameterized as dish of 33 mm of diameter and 3.5 mm of height for a total liquid volume of 3 ml. In the simulation of exposure to 1.8 GHz EMF the flasks were represented by means of a plexiglas parallelepiped of (35 x 35 x 20) mm size and of 1 mm thickness for each wall. Consequently each culture medium was parameterized as a parallelepiped of (33 x 33 x 3.7) mm size, for a total liquid volume of 5 ml.

Cell cultures and EMF exposure

Human keratinocytes (HaCaT) were grown in T25 cell colture flask (SARSTEDT) in a 1:1 mixture of minimal essential medium (Dulbecco's MEM) and Ham's F-12 medium supplemented with 10% (v/v) heat-inactivated foetal calf serum, 1% non-essential amino acids, at 37°C with 5% CO2 in a humidified atmosphere. No antibiotics were used. Cells were split 1:6 twice weekly and fed 24 hours before each experiment.

Cells were seeded (8.000 cells/cm^2) in culture medium and allowed to recover physiological growth conditions in a 5% CO_2 atmosphere at 37°C for 24h. Then medium was replaced with calcium-free keratinocyte growth medium and KCl (1mM) was added to keep the right ionic strength, then samples were transferred in a 37°C incubator without CO_2 and exposed to EMF for different times.

Shame samples prepared exactly as the exposed were in the same incubator out of radiation field. All samples were in duplicate. All the results are the mean with standard deviation of at least 3 independent experiments.

Cell proliferation

HaCaT cells, were exposed to an EMF of 900 MHz with different intensities ranging between 1.5 and 12V/m for different times (2h-72h). To assess HaCaT viability and proliferation, cells were counted at 72h after EMF exposure by a Burker chamber and viability was evaluated by trypan blue exclusion assay. Briefly, cells were trypsinized, collected in 1 ml PBS and mixed 1:1 with trypan blue solution (0.8 mM in PBS). Viable cells exclude trypan blue while dead cells stain blue due to trypan blue uptake.

Spectroscopic Assays

tTG from guinea pig liver was dissolved in Tris-HCl 50 mM buffer, pH 7.5, containing 5 mM EDTA. Steady-state fluorescence was measured with a ISS-K2 fluorometer (ISS, Champaign, IL) thermostating the sample at 20°C by an external bath circulator. The emission spectra was detected through a WG 305 cut-off filter to suppress scattered light.

Protein expression level

10-20 µg of cellular proteins (in 25 mM Tris-HCl pH 8, 0.5% SDS, 0.05% mercaptoethanol, 2.5% glycerol and 0.001% bromephenol blue) were denaturated at 100°C for 5 minutes, subjected to SDS-PAGE on a 10% polyacrylamide gel and then electroblotted onto a PVDF membrane at 130 V for 1 hour. Blots were blocked with 5% non-fat dry milk (Biorad, Hercules, CA) and then incubated with specific primary antibodies, p-ERK (Santa Cruz CA USA) and β-tubulin (Santa Cruz CA USA). After washing and incubation with the horseradish peroxidase-conjugated secondary antibody, detection was carried out with ECL (Amersham).

Results and Discussion

Effects of 900 MHz CW on HaCaT cells were investigated. Exposure for 18 h to 900 MHz at different intensities in a range between 1.5 and 12 V/m corresponding to a maximal SAR of 3 mW/kg caused a cell growth inhibition not directly related to the intensity (Table 1).

Table 1. HaCaT proliferation after exposure for 18 h to 900 MHz at different intensities

	V/m (SAR:mW/kg)			
	1.5	3	6 (0.7)	12 (3)
Sham	1	1	1	1
Exposed	0.95±0.04	1.0±0.1	0.73±0.04	0.82±0.08

The antiproliferative effect of EMF was evaluated at 72h after different times of exposure ranging from 2 up to 72 hours. As shown in table 2, maximal effects were found for short exposure times, whereas at 72h of exposure, no cell growth inhibition could be detected.

Table 2. HaCaT proliferation after exposure to 900 MHz for different times

	Time of exposure (hours)					
	2.15	4.30	9	18	24	72
Sham	1	1	1	1	1	1
Exposed (0.7 mW/kg)	0.79±0.12	n.d.	n.d.	0.80±0.1	n.d.	n.d.
Exposed (3 mW/kg)	0.74±0.1	0.86±0.03	1.05±0.04	0.82±0.08	0.84	0.97

The inhibition of proliferation and viability reached its maximum for exposures of 2h15m duration (21% at the lower SAR level and 26% at the highest one), and for exposures of 18h duration (20% at the lower SAR level and 18% at the highest one) (Table 2). Less marked effects were observed with exposures of 4 and 9 hours to the SAR level of 3 mW/kg (Table 2).

Since it has been reported an involvement of ion channels in the effects of EMF exposure on biological materials, we investigated the dependence on calcium of the effects of EMF at SAR level of 3 mW/kg as above reported. Thus we performed some experiments in Ca-depleted medium. Exposure to EMF for 18 hours in these experimental conditions caused a further 10% increase in cell growth inhibition (Table 3).

Table 3. Cell proliferation after exposure to 900 MHz EMF (3 mW/kg) for 18h in the presence or absence of Ca^{2+}. Cell number was determined at 72h after the end of exposure.

	Cell number x 10^3	
	+ Ca^{2+}	- Ca^{2+}
Sham	520±26	407±32
Exposed	467±28	313±19

This result suggests that a modification of intracellular calcium concentration would affect the antiproliferative activity of 900 MHz EMF. Ca^{2+} modulates several signaling pathways. In epidermal growth factor receptor stimulation, calcium is required for the activation of the extracellular signal-regulated kinases (ERK) (Pusl *et al*., 2002). ERKs, in turn, phosphorylate the transcription factor Elk-1 which becomes active. Activation of Elk-1 leads to the transcription of growth-related genes (Sharrocks, 2001) (Fig.1). We therefore examined the level of phospho-ERK expression by western blot analysis. A barely detectable decrease of phospho-ERK expression was found immediately after EMF exposure with respect to the control sham cells. This effect was more evident for exposures performed in the absence of Ca^{2+} , supporting a role for calcium in keratinocytes proliferation and differentiation. After 72h recovery, p-ERK expression in exposed cells rise to sham level suggesting that the decrease in ERK phosphorylation was due to the presence of the EMF (Fig. 2). Additional experiments are required to determine the role of EMF in such process.

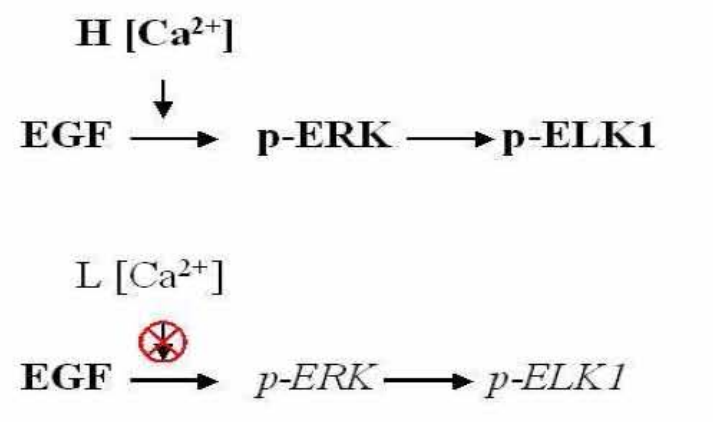


Fig.1 Effect of High (H) and Low (L) calcium concentration on ERK phosphorylation.

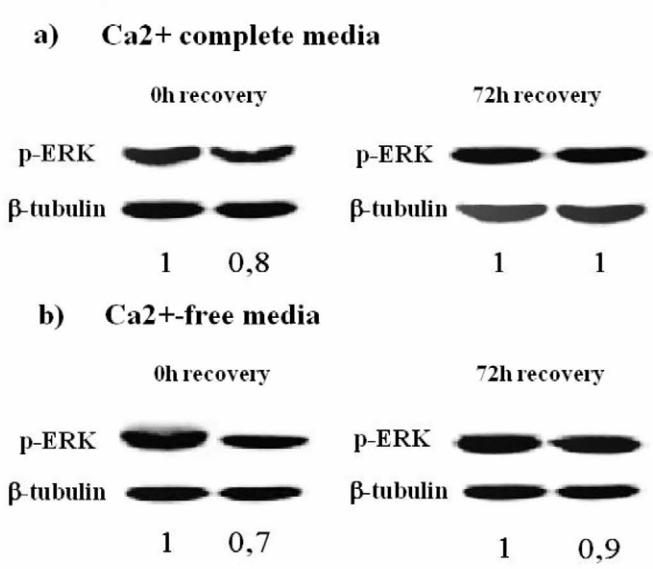


Fig. 2 – Phospho-ERK expression after exposure to 900 MHz EMF for 18h in the presence or absence of Ca^{2+}. Western blot analysis was performed immediately after exposure and 72h after exposure in Ca^{2+} complete medium (a) or in Ca^{2+} free medium (b). Tubulin is reported as control of loading. Numbers indicate the normalization of p-ERK band in exposed samples versus sham samples.

Transglutaminases are a class of enzymes that induce cross-link between proteins by catalyzing the formation of an isopeptidyl bond. They are involved in processes like apoptosis, differentiation, wound healing. Tissue transglutaminase (tTG) is activated by a conformational change induced by calcium which is necessary for its activation (Folk *et al*., 1967). It has been reported that calcium binding to tTG can be monitored because it alters the steady-state protein fluorescence spectra (Di Venere *et al*., 2000). We found that after 2 hours exposure at the SAR level of 0.7 mW/kg, the fluorescence spectra of tTG was altered in comparison to sham samples in a way resembling calcium binding to the enzyme. Therefore EMF treatment seems to induce a conformational protein change similar to that observed during its activation. It is interesting to note that EMF could exerts this effect in absence of calcium. Further studies are needed to clarify the mechanism and the effects on cell metabolism.

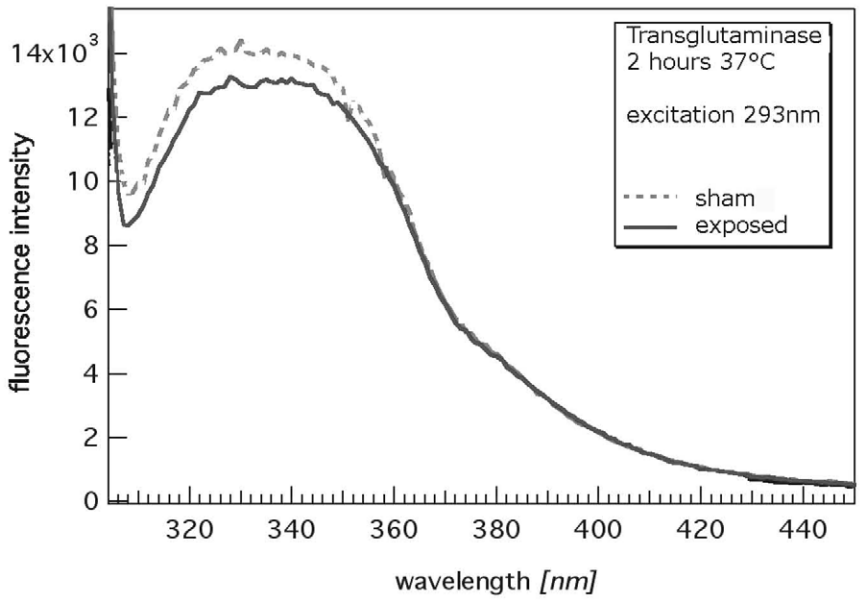


Fig. 3 – Steady state fluorescence spectra of tTG exposed at 900 MHz EMF for two hours (solid line) compared to sham (dotted line). Excitation wavelenght at 293 nm.

Altogether, our results suggest that the cellular response to EMF could be mediated by intracellular Ca^{2+} availability.

References

Barteri M., Pala A., Rotella S. Structural and kinetic effects of mobile phone microwaves on acetylcholinesterase activity. Biophys Chem. 2005 Mar 1;113(3):245-53.

Duranti G, Rossi A, Rosato N, Fazio G, Sacerdoti G, Rossi P, Supino R. In vitro evaluation of biological effects on human keratinocytes exposed to 900 MHZ electromagnetic field. Proceedings of the 3rd International Workshop Biological Effects of EMFS, Kos, Greece 4-8 october, 2004.

Duranti G, Rossi A, Rosato N, Fazio G, Sacerdoti G, Rossi P, Falsaperla R, Cannelli V, Supino R. In vitro evaluation of biological effects on human keratinocytes exposed to 900 MHz electromagnetic field. The Environmentalist 2005; 25:113-119.

Di Venere, A., Rossi, A., De Matteis, F., Rosato, N., Finazzi Agro', A. and Mei, G.: 2000,'Opposite effects of Ca(2+) and GTP binding on tissue transglutaminase tertiary structure' *J. Biol. Chem.* **275**, 3915-3921.

Folk, J.E., Mullooly, J.P. and Cole, P.W.: 1967, 'Mechanism of action of guinea pig transglutaminase. II. The role of metal ion in enzyme activation' *J. Biol. Chem.* **242**, 1838-1844

Marchionni, I., Paffi, A., Pellegrino, M., Liberti, M., Apollonio, F., Abeti, R., Fontana, F., D'Inzeo, G. and Mazzanti, M.: 2006, 'Comparison between low-level 50 Hz and 900 Mhz electromagnetic stimulation on single channel ionic currents and on firing frequency in dorsal root ganglion isolated neurons' *Biochim. Biophys. Acta* **1758**, 597-605.

Pusl, T., Wu, J.J., Zimmermann, T.L., Zhang, L., Ehrlich, B.E., Berchtold, M.W., Hoek, J.B., Karpen, S.J., Nathanson, M.H. and Bennett, A.M.: 2002, 'Epidermal Growth Factor-mediated Activation of the ETS Domain Transcription Factor Elk-1 Requires Nuclear Calcium' *J. Biol. Chem.* **277**, 27517-27527.

Sharrocks, A.D.: 2001, 'The ETS-domain transcription factor family' *Nat. Rev. Mol. Cell. Biol.* **2**, 827-837.

HIGH FREQUENCY EMFs ON HUMAN KERATINOCYTES IN VITRO: DIFFERENT TIME EXPOSURE EFFECTS

[†]SUPINO R., [*]BARTOLETTI C., [*]CAPUTO G., [††]DURANTI G., [#]ESPOSITO G. ,[**]FALSAPERLA R., [†]FAVINI E., [††]ROSATO N., [**]ROSSI P., [*] SACERDOTI G., [†]ZUNINO F.

[†]Istituto Nazionale Tumori – Milano – Italy; e.mail rosanna.supino@istitutotumori.mi.it
[*]University of Rome "La Sapienza" – Italy
[**]National Institute of Occupational Safety and Prevention (ISPESL) – Rome – Italy
[††]University of Rome "Tor Vergata" – Italy
[#] Politecnico di Milano - Italy

Abstract

The effects of ultra high frequency EMFs with biological systems were investigated by *in vitro* studies in human immortalized keratinocytes (HaCaT). Cells were exposed to 900 MHz CW at average SAR level of about 1-5 mW/kg, and 1.8 GHz CW at average SAR level of about 10 mW/kg, for different periods of time. Exposures to 900 MHz CW, at durations of 2^h15^m and 18^h caused a reduction in the cell growth, whereas same duration exposures to 1.8 GHz CW caused an increase of cell proliferation. Cell cycle perturbations were observed in both cases, with a decrease of G1 phase after 18^h exposure. Longer exposure durations (72^h) were ineffective, suggesting a cellular adaptation to these stress conditions.
Preliminary studies showed that the effects of 900 MHz exposure were independent of temperature (34°C or 38°C), but dependent on calcium concentration in the medium. The effects of exposure on the redox balance were examined. Short time (2^h15^m) 900 MHz exposure evidenced a decrease of Total Antioxidant Status (TAS) values, whereas 1.8 GHz was ineffective, regardless the higher SAR level. Our results suggest that exposure to different frequencies and SAR levels caused different effects on biological systems. Cell cycle perturbations and oxido-reductive response seem to be involved.

Introduction

Electromagnetic field (EMF) exposure from sources such as power lines, mobile phones, TV and radio transmitters, and from new and emerging technologies, is frequently seen as a potential source of risk for people and environment. While significant EMF research has been conducted over the past years, technological changes have been so rapid that science has been unable to sufficiently assess potential health risks in a timely manner [1]. The effect of extremely low-frequency electromagnetic field (ELF/EMF) exposure on human health has been widely debated. A number of epidemiological studies have pointed to a slight increase in malignant diseases in populations exposed to electromagnetic fields through the vicinity of power lines. A significant positive association was observed between childhood leukemia and exposure of children to magnetic fields during the night [2-4]. Our previous studies showed a low but reproducible antiproliferative effect of 50 Hz magnetic field on human leukemia cells [5] while no long term effects were found in human breast carcinoma cells [6]. The increasing number of epidemiological observations prompted us to a study on the impact of electromagnetic fields on biological parameters of a human normal keratinocytes cell line, to verify whether there exist significant effects induced by the exposure to high frequency EMF in a controlled and reproducible experimental condition (biological and physical). HaCaT (human keratinocytes) cell line has been chosen as an excellent model to study the biological effect of radiations since they are cells which receive, in the first line, the energy associated to radiations. We already reported that exposure to 900 MHz could trigger a differentiation program in HaCaT cells [7,8]. We examined the eventual effects of two different high frequencies (900 MHz and 1.8 GHz) on cell proliferation, cell cycle progression and oxidative response of these cells after different times and intensities exposures. The aim was to examine the biological effects of exposures to a wide range of SAR values. Thus, we started the study by exposing cells to very low levels of SAR such as 1mW/kg at 900 MHz and 10mW/kg at 1.8 GHz.

Interestingly we observed an increase in cell growth after exposures to 1.8 GHz and an inhibition of cell growth after exposures to 900 MHz. Exposures till 24 h caused differences in the considered biological parameters whereas after longer times of exposure a kind of adaptation and a decrease of the effects, which revert to control values, was found. The involvement of temperature and of calcium concentration was also examined.

Materials and Methods

SAR determination

Computational simulations have been carried out by employing the electromagnetic commercial simulator Microwave Studio (MWS) by CST-Germany [9], based on the Finite Integration Technique (FIT) [10]. This numerical method, developed by Weiland in 1977, provides a discrete reformulation of Maxwell's equations in their integral form suitable for computers and it allows simulating real-world EMF problems with complex geometry. In order to numerically solve Maxwell's equations, a finite calculation domain is defined. By creating a suitable mesh system, this domain is splitted up into small cubes, so-called grid cells. In combination with the FIT, MWS employs the Perfect Boundary Approximation (PBA) for the spatial discretization of the simulated structure that allows an accurate modelling of bend-shaped structures [11].

In order to simulate *in vitro* tests, the exposure set up was simplified. In fact in the numerical model only the exposure zone of the two set up was modelled, presuming that the detailed description of the adaptive section was not relevant for SAR evaluation purposes. Each exposure set up was then represented as two parallel metallic plates of (80 × 99) mm size, at 27 mm of distance and Petri dishes or flasks were inserted between the plates. In simulation for exposure to 900 MHz EMF we have four plexiglas dishes of 35 mm of diameter, height of 8 mm and 1 mm of thickness. Each culture medium was then parameterized as dish of 33 mm of diameter and 3.5mm of height for a total liquid volume of 3 ml. In the simulation of exposure to 1.8 GHz electromagnetic field we have two polystyrene flasks. Each flask was represented by means of a plexiglas parallelepiped of (35 x 35 x 20) mm size and of 1 mm thickness for each wall. Consequently each culture medium was parameterized as a parallelepiped of (33 x 33 x 3.7) mm size, for a total liquid volume of 5 ml.

Cell cultures and EMF exposure

Human keratinocytes (HaCaT) were grown in D-MEM/F-12 medium (Invitrogen, Carlsbad, CA, USA), supplemented with 10% (v/v) heat-inactivated foetal calf serum (HyClone, Oud-Beijerland, Holland) and non-essential aminoacids 1%, at 37°C in a 5% CO_2 humidified atmosphere. No antibiotics were used. Cells were seeded (8.000 cells/cm^2) in culture medium and allowed to grow in physiological conditions in a 5% CO_2 atmosphere at 37°C for 24 h. Then medium was replaced with CO_2-independent medium (Invitrogen) to maintain the correct pH and samples were transferred in a 37°C incubator without CO_2 and exposed to EMF for different times.

Sham samples, prepared exactly as the exposed, were in the same incubator out of radiation field. All samples were in duplicate. The results are the mean with standard deviation of at least 3 independent experiments.

Cell proliferation and Cell cycle analysis

HaCaT cells, were exposed to an electromagnetic field of 900 MHz with different intensities ranging between 1.5 and 12 V/m or 1.8 GHz at 25 V/m for different times (2 h-72 h).

Cell proliferation was evaluated at 72 h after EMF exposure by counting, in a Burker chamber, trypan blu excluding cells (alive cells).

For cell cycle analysis, samples were washed in PBS (phosphate buffered solution) and stained with a solution of propidium iodide (PI) (20 µg/ml) (Sigma-Aldrich, St. Louis, MO, USA) e RNase (Sigma) 1 mg/ml in PBS. Cell cycle distribution was analyzed by a FACScan cytofluorimeter equipped with an argon laser for fluorescence excitation at 488 nm (Becton Dickinson, Mountain View, CA, USA) after 30-60 min of incubation. Analysis of the percentage of cells in each phase of the cell cycle was performed by means of Cellfit software (Becton Dickinson).

Total Antoxidant Status

Total antioxidant status (TAS), including enzymatic and non-enzymatic cellular systems, was measured in cells homogenates as Trolox Equivalent Antioxidant Capacity (TEAC), with the modification of ABTS-cation radical method [12].

After exposure, cells were trypsinized, centrifuged, and the cell pellets were resuspended in 100 µl PBS with 1 mM PMSF. After sonication, 10 µl of cellular homogenates was immediately tested.

Briefly, 300 µl ABTS (500 µM), 36 µl metamyoglobin (70 µM), 487 µl PBS, 10 µl sample (0.6 mg of proteins) were mixed and then the reaction was started by adding 167 µl H_2O_2 (450 µM). This method is based on the reactivity of intracellular antioxidant compounds relative to a 1 mM Trolox (vitamin E analogue) standard. A Trolox-calibration

curve by three concentrations was performed during each esperiment. The reaction was followed specrophotometrically at 734 nm for 15 minutes. All compounds were from Sigma-Aldrich.

Protein level expression

10-20 µg of cellular proteins (in 25 mM Tris-HCl pH 8, 0.5% SDS, 0.05% mercaptoethanol, 2.5 % glycerol and 0.001 % bromephenol blue) were denaturated at 100°C for 5 minutes, subjected to SDS-PAGE on a 10% polyacrylamide gel and then electroblotted onto a PVDF membrane at 130 V for 1 hour. Blots were blocked with 5% non-fat dry milk (Biorad, Hercules, CA) and then incubated with specific primary antibodies, HSP-70 (Chemicon International) and β-tubulin (Abcam plc, Cambridge,UK). After washing and incubation with the horseradish peroxidase-conjugated secondary antibody, detection was carried out with ECL (Amersham-GE Healthcare).

Results and discussion

SAR determination

By applying the above reported computational simulation for SAR determination, we verified that with an EMF at 900 MHz with an electric field between 1.5 and 12 V/m, the mean value of SAR in our samples was between 1 and 5 mW/kg. In samples exposed to 1.8 GHz at an electric field of 25 V/m, the mean value of SAR was 10 mW/kg.

Cell growth

HaCaT cell growth was determined by cell counting at 72 h after different times of EMF exposure. As shown in Fig. 1 (panel A) exposures to 900 MHz caused a reduction in cell growth at least till 24 h, whereas exposures to 1.8 GHz caused an increase of cell proliferation. In both cases longer times of exposition to EMF were ineffective on cell proliferation. Moreover (Fig.1, panel B), exposures to 900 MHz to different intensities were ineffective till 3 V/m, whereas 6 and 12 V/m caused a marked decrease in cell growth.

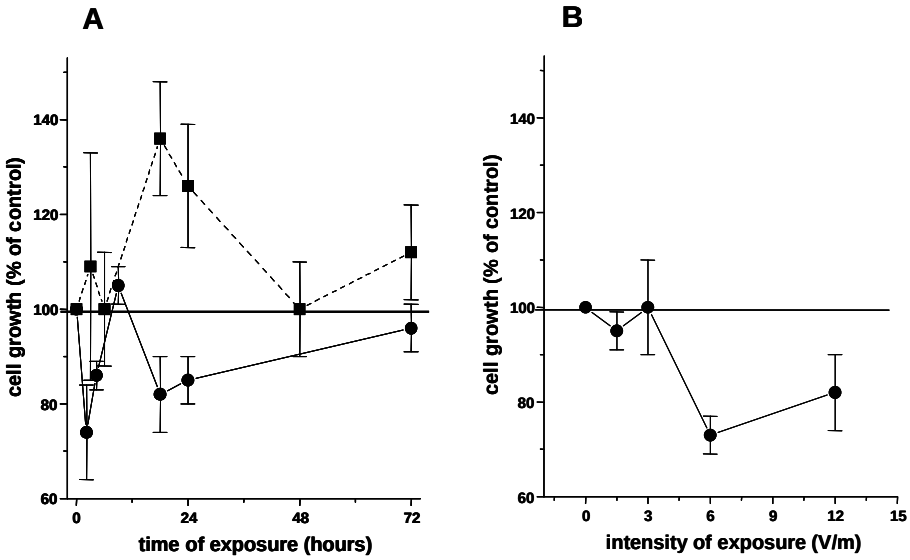


Fig. 1 HaCaT cell growth at different times of exposure to EMF 1.8 GHz 25 V/m (dotted line) or 900 MHz 12 V/m (solid line) (panel A), or 900 MHz and different intensities for 18 h (panel B).

Thus next experiments were performed after short time exposures (2.15 or 18 h) and at 12 V/m (SAR = 5 mW/kg) of intensity for 900 MHz and 24h of exposure to 25 V/m (SAR = 10 mW/kg) for 1.8 GHz.

As shown in table 1, exposure to EMFs of 900 MHz or 1.8 GHz caused a modification in S phase, immediately after exposure to 900 MHz for 18 h. The decrease in S phase after 900 MHz exposition and increase in the same phase after

1.8 GHz are in agreement with the respective decrease and increase in cell proliferation. At longer times of exposure (not shown) or of recovery after a 18 h exposure, values similar to sham control samples were found in all experimental conditions.

Table 1. Effect of 18 h EMF exposure on cell cycle distribution after different times of recovery. The percentage of cells in each phase is reported.

	0 h of recovery			24 h of recovery			48 h of recovery		
	G1	S	G2	G1	S	G2	G1	S	G2
Sham	44	41	15	44	41	14	48	40	12
900 MHz (5mW/kg)	50	31	19	46	42	14	49	40	11
1.8 GHz (10mW/kg)	38	46	16	43	42	15			

Since modification of temperature induced by EMFs could be involved in the observed modification in cell proliferation and cell cycle progression, cell growth after incubation for 18 h at 34°C or 38°C was evaluated. As shown in table 2, no modifications in cell cycle distribution were observed nor at 34°C nor at 38°C, indicating that the EMF effects were not related to the temperature.

Table 2. Effect of EMF on cell cycle distribution at different times of recovery after 18 h of exposure to different temperatures. The percentage of cells in each phase is reported.

		% of cells		
		G1	S	G2
0 h of recovery	37°C	44	41	15
	34°C	38	43	19
	38°C	40	41	19
24 h of recovery	37°C	44	41	14
	34°C	45	40	15
48 h of recovery	37°C	48	40	12
	34°C	44	43	13

Results are from one of two independent experiments.

A dependence of EMF antiproliferative effect on Ca^{++} was found. Indeed in the absence of Calcium (replaced by K^{+}) a higher reduction of cell growth in comparison to that of cells exposed in normal culture conditions was observed (Fig 2). This result suggests that an inhibition of calcium-dependent enzymes could synergize with the antiproliferative effect of EMF.

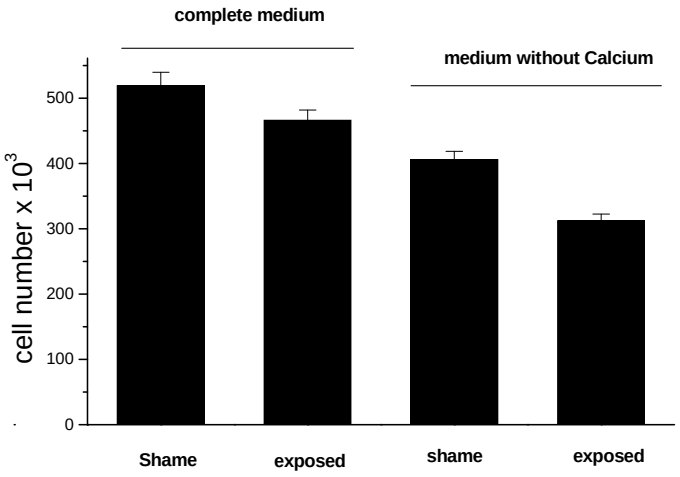


Fig. 2 – Cell proliferation after exposure to 900 MHz EMF for 18 h in the presence or absence of Ca^{++}. Cell number was determined at 72 h after exposure.

To deeply understand the mechanism of the induction of the cellular response observed in EMF exposed cells, we examined the redox balance after 2.15 h and 18 h of 900 MHz exposure. As shown in Fig. 3 a decrease in the total antioxidant status was found mainly after 2.15 h of exposure. At longer times (18 h of exposure) a less marked reduction was observed.

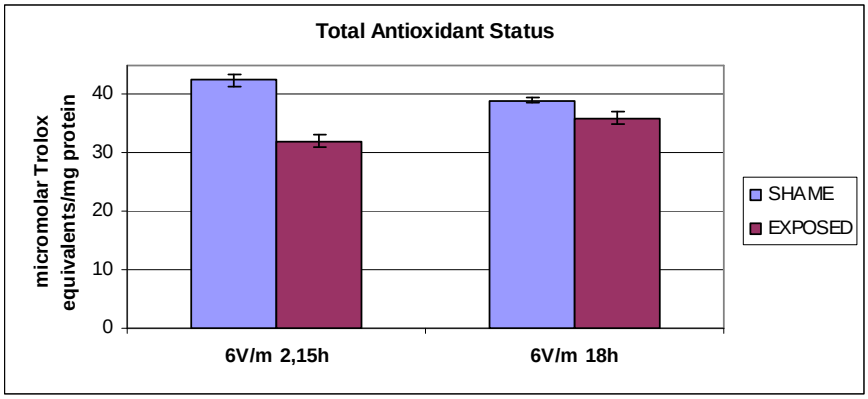


Fig. 3 – Total Antioxidant Status of HaCaT cells after exposure to 900 MHz EMF for 2.15 h or 18 h.

Then the expression level of HSP-70, a stress induced protein, was detected. In agreement with the above reported results an increase in HSP-70 expression was found in cells exposed for 2.15 h to 900 MHz (Fig. 4). Again, after 18 h of cell exposure to EMFs, the expression level of this protein was similar to sham samples.

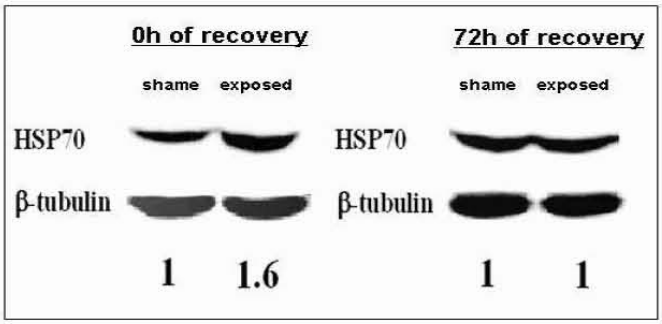


Fig. 4 – HSP-70 protein expression. Protein level was determined at 0 h and 72 h after 18 h of EMF exposure. Tubulin is reported as control of loading. Numbers indicate the normalization of HSP-70 band in exposed samples versus sham samples.

In conclusion the biological effects of the two different high frequencies (900 MHz and 1.8 GHz) examined in the human normal cell line HaCaT after exposures for different times and to different intensities were quite different. Indeed, we observed an increase in cell growth after exposures to 1.8 GHz and an inhibition of cell growth after exposures to 900 MHz. These modulations were reduced (10-25 %) but reproducible. Temperature, often reported as the cause of biological effects of EMF [13] was ineffective, in range between 34°C and 38°C on this cell system suggesting the lack of its involvement in the response of HaCaT cells. On the contrary, an increase EMF antiproliferative effect was found in the absence of calcium, suggesting a dependence of biological effects of EMF on calcium concentration.

Moreover the inhibition observed after 900 MHz exposure was related to an increase in the expression of HSP-70 a protein related to the cellular stress and to the antioxidant status of the cell. The observation that these parameters reverted to control levels after longer times of exposure or of recovery after exposure to EMFs support the hypothesis of other authors of an “adaptation” of cells to the effects produced by electromagnetic energy on the biological matter.

From this study it emerges that an interaction between EMF and cell systems exists even at very low levels of exposure. Moreover they confirm that frequency, intensity, and time of EMF exposure are parameters markedly affecting the biological response for which is not easy to find a model of correlation.

References

1. Repacholi MH. WHO's health risk assessment of ELF fields. Radiat Prot Dosimetry. 2003; 106(4):297-9.
2. Dockerty JD, Elwood JM, Skegg DC, Herbison GP. Electromagnetic field exposures and childhood leukaemia in New Zealand. Lancet 1999; 354:1967-8.
3. Hocking B. Pulsed electromagnetic fields and cancer. Occup Environ Med. 1998; 55:288.
4. Repacholi MH, Ahlbom A.Link between electromagnetic fields and childhood cancer unresolved. Lancet 1999 Dec 4; 354:1918-9.
5. Supino R, Dal Bo L, Favini E, Zunino F, Bartoletti C, Sacerdoti G, Rossi P, Caputo G, Rosato N. In vitro evaluation of biological effects on human cell lines exposed to elf and static electric and magnetic fields. Proceedings of the 3rd International Workshop Biological Effects of EMFS, Kos, Greece 4-8 october, 2004.
6. Supino R, Bottone MG, Pellicciari C, Caserini C, Bottiroli G, Belleri M, Veicsteinas A. Sinusoidal 50 Hz magnetic fields do not affect structural morphology and proliferation of human cells in vitro. Histol Histopathol. 2001; 16(3): 719-26.
7. Duranti G, Rossi A, Rosato N, Fazio G, Sacerdoti G, Rossi P, Supino R. In vitro evaluation of biological effects on human keratinocytes exposed to 900 MHZ electromagnetic field. Proceedings of the 3rd International Workshop Biological Effects of EMFS, Kos, Greece 4-8 october, 2004.

8. Duranti G, Rossi A, Rosato N, Fazio G, Sacerdoti G, Rossi P, Falsaperla R, Cannelli V, Supino R. In vitro evaluation of biological effects on human keratinocytes exposed to 900 MHz electromagnetic field. The Environmentalist 2005; 25:113-119.

9. Microwave Studio, User's Manuals 5.02 2004, CST Computer Simulation Technology, D-64289 Darmstadt, Germany.

10. T. Weiland T. A discretization method for the solution of Maxwell's equations for six-component field, Electronics and Communications AEÜ 1977, 31:116-20.

11. Krietenstein B, Schuhmann R, Thoma P, Weiland T. The Perfect Boundary Approximation technique facing the challenge of high precision field computation. Proc. of the XIX International Linear Accelerator Conference (LINAC '98), 1998, Chicago, USA, pp. 860-862.

12. Miller NJ, Rice-Evans C, Davies MJ, Gopinathan V, Milner A. A novel method for measuring antioxidant capacity and its application to monitoring the antioxidant status in premature neonates. Clin Sci (Lond). 1993 Apr;84(4):407-12.

13. Sukhotina I, Streckert JR, Bitz AK, Hansen VW, Lerchi A. 1800 mHz electromagnetic field effects on melatonin release from isolated pineal glands. J. Pineal Res. 2006, 40:86-91.

\

MODELLING SURFACE ROUGHNESS EFFECTS IN THE INTERACTION OF EM FIELDS WITH BIOLOGICAL CELLS

A. SANCHIS

G. MARTÍNEZ

M. SANCHO

J.L. SEBASTIÁN

S. MUÑOZ

DPT. DE FÍSICA APLICADA III, FACULTAD DE CIENCIAS FÍSICAS
UNIVERSIDAD COMPLUTENSE, 28040 MADRID, SPAIN

Abstract

Standard models of cells for studying their interaction with electromagnetic fields are based on shelled spheres or ellipsoids with characteristic electrical parameters –permittivity and conductivity– for each homogeneous region. However, many biological cells present a complex surface structure with microvilli, blebs, folds, etc., that make these models inadequate to correctly describe the field effects.

In this work we examine the dielectric response of 2D dielectric particle models with surface roughness in quasi-static approximation, using a BEM method based on the integral formulation for the induced polarization charges on the interfaces. Different mathematical surface morphologies are considered: sinusoidal or fractal corrugations, characterized by their corresponding height and correlation length. Results are interpreted by comparing with the standard BEM approach for the electrostatic potential.

Introduction

The dielectric behavior of materials depends sensitively on the characteristics of their surfaces. These characteristics have influence on important phenomena and applications, such as the dielectric breakdown of insulating materials, the development of capacitors with very high capacitance using fractal surfaces or the electrorheological response of particle suspensions [Klingenberg and Cooper 1995]. On the other hand, it is well established that most examples of surfaces exhibit certain degree of roughness. The inclusion of the surface structure in the models that describe the electrical response of colloidal suspensions, can be of help in the characterization of particles using dielectric spectroscopy or electrokinetic measurements, as well as for designing purposes in the development of new applications in these or related fields. In the high frequency range, scattering by rough surfaces have been extensively investigated using Kirchhoff theory, based on a local application of Fresnel laws, using the tangent plane approximation [Caron et al. 2002]. At lower frequencies, where the roughness size is comparable or greater than the field wavelength, the incorporation of the detailed morphology of surfaces in the numerical treatment of the electromagnetic field at dielectric interfaces poses a great challenge for the capability of existing computational methods. This is probably the main reason behind the fact that there are very few studies that consider realistic rough surfaces in the dielectric modeling of particles in spite of its obvious interest.

Methods

In order to investigate the dielectric response of particles with complex surface structure, we have applied two approaches with complementary characteristics. They consist of boundary element (BE) formulations that give information on the potential and charge density distributions. For the sake of clarity, a brief account of the basis of these methods is given below. The interested reader is referred to publications for more details.

i) BEM for the quasi-static potential

This method is based on the following integral equation [Poljak and Brebbia 2005]

$$\frac{\varepsilon_i+\varepsilon_j}{2}\phi(\boldsymbol{r}) = \phi_0(\boldsymbol{r}) + \left(\varepsilon_i-\varepsilon_j\right)\int_L \phi(\boldsymbol{r}')\frac{\partial G(\boldsymbol{r},\boldsymbol{r}')}{\partial n'}dl' \tag{1}$$

where ϕ is the electric potential at a point of a dielectric interface between media of complex permittivities ε_i and ε_j, immersed in an external potential ϕ_0 and the integral extends to the interface contour. $G(\boldsymbol{r},\boldsymbol{r}')$ is the Green's function, defined by $\nabla^2 G = \delta(\boldsymbol{r},\boldsymbol{r}')$. For a 2D problem, $G(\boldsymbol{r},\boldsymbol{r}') = \ln\left|\boldsymbol{r}-\boldsymbol{r}'\right|/2\pi$. The singularity in the integrand when $\boldsymbol{r} = \boldsymbol{r}'$ has been integrated and the integral in the r.h.s. of (1) is to be interpreted in the sense of Cauchy principal part. The formulation can be easily extended to the case of several dielectric interfaces.

The problem is discretized by dividing the contour into N sub-elements of length Δ and equation (1) correspondingly converted to an algebraic equation. The coefficients A_{ij} have a simple analytical expression,

$$A_{ij} = \int_\Delta \frac{d}{dn}(\ln|\boldsymbol{r}-\boldsymbol{r}'|) = \int_\Delta \frac{\cos\theta}{|\boldsymbol{r}-\boldsymbol{r}'|}dl' = \varphi \tag{2}$$

where φ is the angle subtended by the element j from the center of the element i. The algebraic system of equations for the potentials at the N points on the contour is solved by a triangulation method.

ii) BEM for the charge density on the interfaces

For certain types of applications, especially those related to ponderomotive effects produced by electromagnetic fields, we have shown that a BEM formulation based on the charge density induced by the external field can be advantageous. The corresponding integral equation is in that case [Sancho et al. 2003]

$$\frac{\varepsilon_i+\varepsilon_j}{2}\sigma(\boldsymbol{r}) = \left(\varepsilon_i-\varepsilon_j\right)\sigma^0(\boldsymbol{r}) + \left(\varepsilon_i-\varepsilon_j\right)\int_L \sigma(\boldsymbol{r}')\frac{\partial G(\boldsymbol{r},\boldsymbol{r}')}{\partial n}dl' \tag{3}$$

where $\sigma(\boldsymbol{r})$ is the complex charge density at the point $\boldsymbol{r}$ of a dielectric interface and $\sigma^0(\boldsymbol{r}) = \varepsilon_0 E_{ij}^0(\boldsymbol{r})$, $E_{ij}^0(\boldsymbol{r})$ is the normal component of the electric field, pointing from medium i to medium j. The complex character of the permittivity of each medium, depending on the magnitudes of their real permittivity and conductivity, gives rise to complex charge densities, phase shifted with respect to the applied field. As in equation (1), the integral in (2) is interpreted in the sense of the Cauchy principal value.

Results

A measure of the response of a dielectric particle to an external electric field is given by its complex polarizability $\tilde{\alpha}$. This property is related to the dipole moment induced on the particle by means of the expression:

$$\tilde{\boldsymbol{p}}_{eff} = \tilde{\alpha}(\omega)\,\tilde{\boldsymbol{E}} \tag{4}$$

where $\tilde{\boldsymbol{p}}_{eff}$ is the effective dipole moment of the particle, $\tilde{\boldsymbol{E}} = \boldsymbol{E}_0 e^{-i\omega t}$ is the external electric field applied and $\boldsymbol{\omega}$ the angular frequency of the field. These magnitudes are frequency dependent, so they are complex quantities. In this work we deal with the response of a particle to a field strength of 1V/m at a fixed frequency of 10^5 Hz, in order to pay attention to the effects of surface roughness, a question hardly taken into account in previous studies about dielectric particles under electric fields.

The polarizability of 2D circular dielectric objects in an external field is representative of very long dielectric circular cylinders with the electric field applied perpendicularly to the cylinder axis.

As a first approach to this problem, we have investigated how the polarizability of the particle is dependent on the depth of a sinusoidal roughness all around the cylinder surface. We have first considered the case of a lossless particle with a permittivity $\varepsilon_1 = 10\varepsilon_0$ immersed in the vacuum. As indicated in the cross section of the

schematic draw in Figure 1, the particle is characterized by a radius $a = 1$ μm and a roughness extent given by the parameter h. The figure also shows the results of the transverse polarizability of the cylindrical particle when two different numbers of undulations are considered. We can observe that when the roughness is getting smaller with respect to the radius, the results are becoming similar in both cases, and tend to the value for a circular particle.

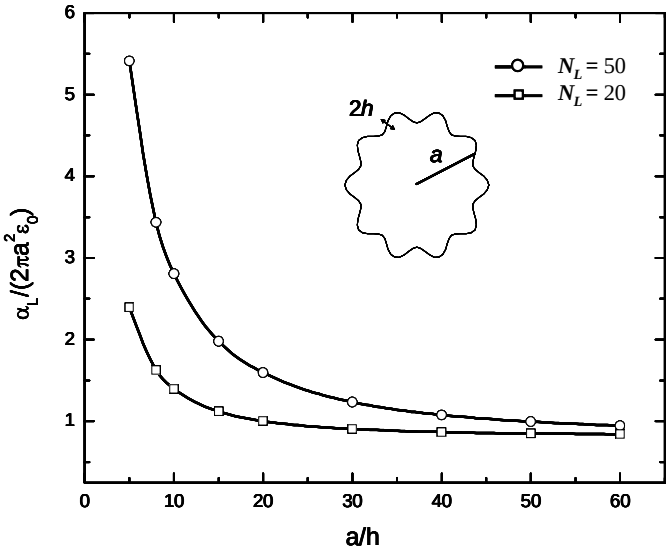


Figure 1. Transverse polarizability of a dielectric circular cylinder with sinusoidal surface roughness. Cylinder permittivity ε =10ε$_o$; N_L is the number of undulations.

For the sake of comparison, we have analyzed the induced superficial charge and potential over both a soft and a rough surface of the particle. The results are given in Figure 2(a) and (b), respectively.

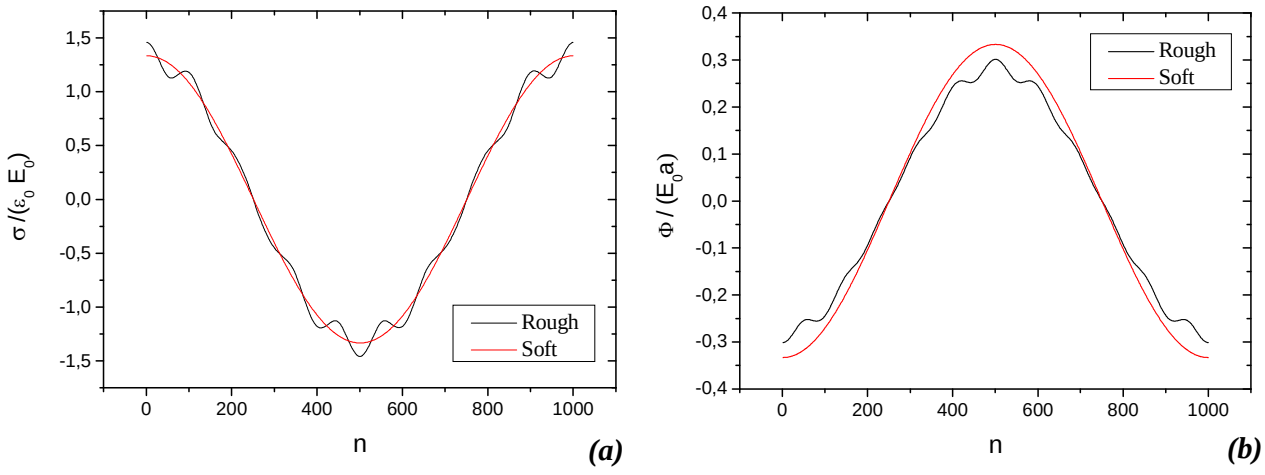


Figure 2. Induced surface charge (a) and induced potential (b) along the surface points by an electric field of 1V/m on both soft and rough dielectric surfaces; the number of undulations is N_L = 10, the total number of points N = *1000* and the ratio a/h = 20.

The next step for the 2D analysis of the roughness surface effects consists on the study of the polarizability of a layered particle, as a typical biological cell. The cell has been modeled as a particle of 1 μm of radius

surrounded by an undulating shell –the membrane– with 10 nm of thickness. This characterization of the cell membrane as a roughness surface is a first improvement in the approach to the reality of the complex cell envelope. The cell is considered immersed in an external continuous medium formed by electrolytes in free water with the dielectric properties of physiological saline. All the results presented in this work have been obtained by using typical values for the electric properties of the internal layer, membrane and external medium. These values are based on interpolations of impedance measurements on tissues and theoretical calculations [Gabriel et al. 1996]. Table 1 shows the electrical parameters for the non conductive membrane and the highly polarizable internal layer considered for the cell as well as those for the external medium. In Figure 3 the obtained polarizability of a particle as a function of the roughness relative height, *a/h*, is shown.

Layer	Parameter	Value
Internal Layer	**ε**	50
	σ	0.5
Membrane Uniform shell d = 10 nm	**ε**	10
	σ	$1x10^{-6}$
External Medium	**ε**	80
	σ	$1.5x10^{-3}$

Table 1. Electrical parameters for the different layers of the cell model: relative permittivity ε and conductivity σ (S m^{-1}).

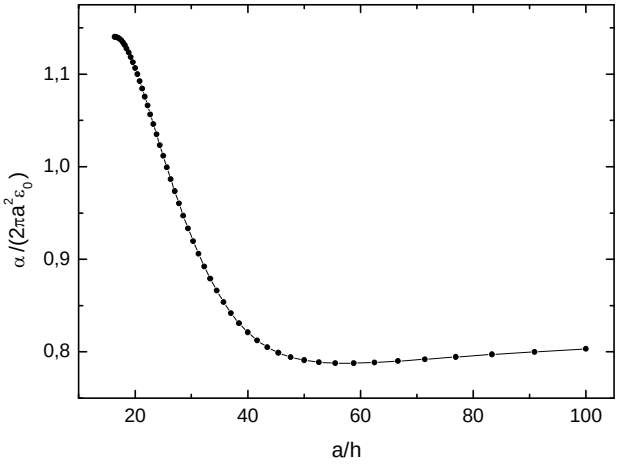


Figure 3. Variation of the polarizability of a shelled particle with sinusoidal undulated membrane as a function of *a/h*; the number of undulations is $N_L = 80$.

Further improvement in the approach to the real, highly irregular surface of a cell with different protrusions and microvilli, has been realized by means of a different morphology based on fractal surfaces. The fractal description provides a very general, scale-invariant, characterization of the electrical response of a biological membrane. It has been applied to the analysis of impedance measurements of human lymphocytes by Bordi et al. [1990]. A fractal surface topography can be generated using a modified (truncated) Weierstrass-Mandelbrot function that can be written as [Yan and Komvopoulus 1998]

$$f(r) = \sum_{n=-n_{\max}}^{n_{\max}} b^{-n(2-D)}[1 - k\cos(b^n r + \varphi)] \tag{5}$$

In this equation *f(r)* is the rough profile, *b* is a frequency multiplier factor (with a typical value between 1.1 and 3), φ is a randomly generated phase, *D* is the fractal dimension (it has a non integer value between 1 and 2), and *k* is a form factor used to modify the profile.

The dielectric response of a cell with fractal surface has been analyzed using the BEM for surface charge. Average results, obtained using five different random phases, for typical membrane topography are shown in figure 4.Variable *h* is the square mean value of the roughness height.

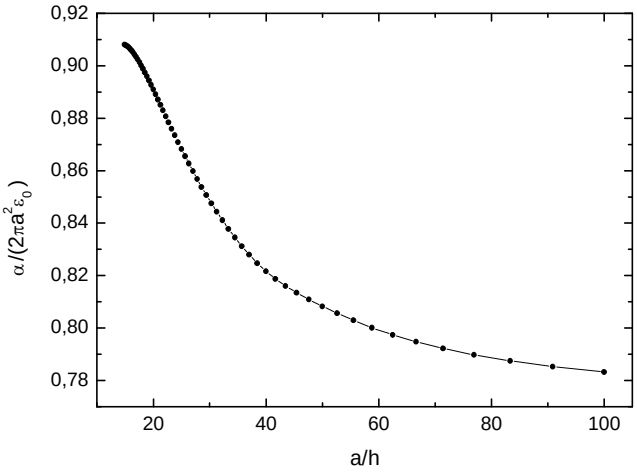


Figure 4. Variation of the polarizability of a shelled particle with a fractal membrane of fractal dimension D = 1.5 as a function of *a/h*. Form factor *k* = 1.9.

Discussion and Summary

We have analyzed the electrical response of plain and coated particles characterized by a rough surface using a superficial 2D model. Sinusoidal and fractal surfaces have been generated and their electrical characteristics have been studied using BE methods. We have found that both the potential and the induced charge experience changes following the surface topography. As a consequence, the polarizability is in general markedly enhanced as the roughness height increases. The trends for sinusoidal and fractal topography are similar, except in the region of intermediate roughness height, where the polarizability for the sinusoidal case is lower, probably due to correlations in the induced charges on neighbor undulations. Although the results have been obtained for 2D models, similar conclusions can be expected for globular cells such as lymphocytes or spiculated red blood cells. In fact, it has commonly been obtained that the specific capacitance of these cells derived from electrorotation (ER) data, is greater than the typical cell membrane value of 1 mF/m^2. Work on full 3D models that allows to interpret these ER studies is in progress.

References

Bordi F., Cametti C. and Di Biasio A., Determination of cell membrane passive electrical properties using domain dielectric spectroscopy technique. A new approach, BBA-BIOMEMBRANES 1028 (1990): 201-204.

Caron J., Lafait J. and Andraud C., Scalar Kirchoff´s model for light scattering from dielectric random rough surfaces, Optics Communications 207 (2002): 17-28.

Gabriel S., Lau R.W. and Gabriel C., The dielectric properties of biological tissues: III. Parametric models for the dielectric spectrum of tissues, Phys. Med. Biol. **41 (**1996): 2271-2293.

Klingenberg D.J. and Cooper S.L, Electrostatics at Rough Interfaces, J. Electrostatics, **35** (1995): 339-348.

Poljak D. and Brebbia C.A., Boundary Element Methods for Electrical Engineers (WitPress, Southampton, Boston, 2005)

Sancho M., Martínez G. and Martín C., Accurate modelling of shelled particles and cells, J. Electrostatics 57 (2003): 143-156.

Yan W. and Komvopoulus K., Contact analysis of elastic-plastic fractal surfaces, J. Appl. Phys. 84 (1998): 3617-3624.

ACUTE EXPOSURE TO WEAK, 800 HZ MAGNETIC FIELD DOES NOT ALTER SKIN MICROCIRCULATION OR PRESSURE PAIN THRESHOLD IN HEALTHY VOLUNTEERS

VEIT SCHNABEL AND LARS ARENDT-NIELSEN

DEPARTMENT OF HEALTH SCIENCE AND TECHNOLOGY,
AALBORG UNIVERSITY, FREDRIK BAJERSVEJ 7 D3, 9220 AALBORG, DENMARK
EMAIL VS@HST.AAU.DK

Abstract

The therapeutic application of weak electromagnetic fields (EMF) is often targeted at improving circulation or alleviating pain. This double-blind, cross-over study was aimed at quantifying the effects of acute exposure to a weak EMF in healthy volunteers.

20 healthy volunteers participated in the experiment in two sessions (at one week interval). Two coils, 4 cm in diameter, where placed laterally on both ankles (device manufacturer Actera A/S, Denmark). The frequency was 800 Hz (monopolar, triangular waveform). The flux density ranged from 0.2 mT, at the center between the coils, to 6 mT directly underneath the coils (RMS values). There were three placebo devices and one active device. The subjects were treated with two devices (one at each ankle) in each session, and the order and position of the devices was randomised. Pain thresholds to pressure were determined before and after 30 minutes exposure. Cutaneous microcirculation was monitored with thermography and laser-Doppler-flowmetry.

The repeated measures ANOVA test showed no effect of the device treatment factor for either pain thresholds or cutaneous microcirculation.

This study demonstrates that, in healthy volunteers, acute exposure to a weak (below 6 mT), 800 Hz magnetic field has no effect on cutaneous microcirculation or pressure pain thresholds.

Introduction

The therapeutic application of magnetic or electromagnetic fields is gaining in popularity and the range of treated ailments is increasing (Shupak et al., 2003). By the year 2004, more than 2 million patients had been treated worldwide for a large variety of injuries, pathologies and diseases, with an 80% success rate and practically absent side effects (Markov, 2004). Despite this high success rate, electromagnetic therapy is still not fully accepted as standard clinical practice. This is partly because some of the clinical trials are based on small sample sizes or have methodological shortcomings (Podd et al., 1998; Cullum et al., 2001), and partly because there is no consensus as to which biophysical or biochemical mechanisms are involved (Polk et al., 1996; Stavroulakis, 2003; Swanson et al., 2006). It has been shown theoretically and experimentally that strong magnetic fields (over about 1.5 T) can have direct cardiovascular effects in humans (Jauchem, 1997). For magnetohydrodynamic interactions, even stronger fields are required, about 5 to 10 T (Kinouchi et al., 1996). Exposure to an electromagnetic field, that induces currents in the body that are about 25 to 40 times stronger than those used in the present study, evokes a pain sensation with muscle contraction, accompanied by a reduction in skin blood flow in the fingertips (Ueno et al., 1986).

The beneficial effects of electromagnetic therapy are often explained by improving blood circulation, thereby reducing pain and inflammation, and enhancing soft tissue repair (McMeeken, 1992). This study seeks to quantify, in healthy volunteers, the acute effects of a weak (below 6 mT) magnetic field.

Methods

Study Design. The study was performed as a double-blind, randomised, placebo controlled trial with cross-over. The experiment had been approved by the local ethics committee "Den Videnskabsetiske Komité for Viborg og Nordjyllands Amter", case number VN 2005/62.

a) b)

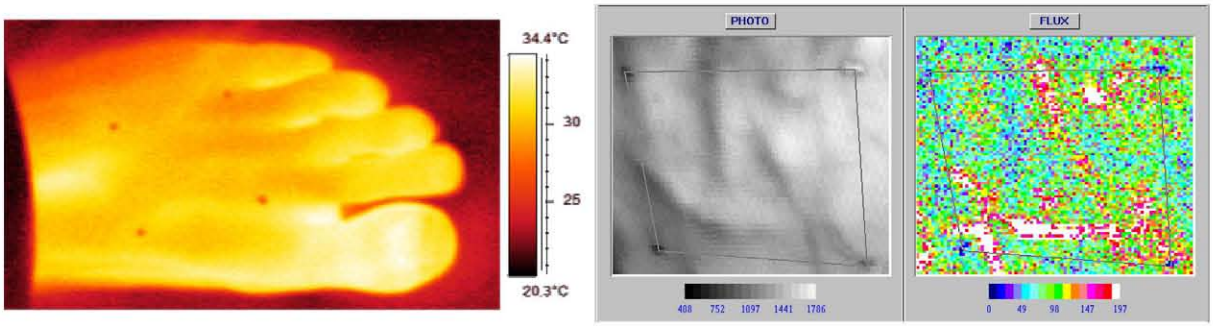


Fig. 1 Examples of pictures as recorded with thermography, a), and laser-Doppler-flowmetry, b). The corners of a 4×4 cm square were marked with a silver pen, visible on both pictures. Mean values of temperature and blood perfusion over this area were calculated and stored for analysis. The cork shield, used for covering the coils, is visible on the left side of a).

Subjects. 20 healthy volunteers (14 male, 6 female) were recruited through on-campus advertisements. The mean age was 24 years (range 22–30 years), mean BMI was 22.2 ± 2.9 kg/m². Subjects were only admitted to the experiment if they were healthy, not pregnant, and not taking any form of medication. None of the participants had tried any form of magnetic or electromagnetic therapy before. None of the participants were heavy smokers or had excessive use of tea/coffe/alcohol. The subjects were instructed not to drink tea/coffee/alcohol, nor to smoke, for a period of 2 hours prior to the experiment. All subjects gave signed written informed consent before conducting the study. All subjects received a compensation (600 DKK) for their participation in the experiment.

Magnetic Field Exposure Condition. The devices used for this study were Actera ELMS-3 stimulators (Actera A/S, Aalborg, Denmark). These devices consist of two applicator coils, approximately 4 cm in diameter, and a control unit. The positions "high" intensity, 800 Hz frequency, and 30 min duration were chosen, resulting in a non-uniform magnetic field with flux densities ranging from 0.2 mT, at the centre between the coils, to 6 mT directly underneath the coils (RMS values). The produced magnetic field was monopolar (about 20% static offset) and had an asymmetric, saw-tooth like waveform repeated at 800 Hz (duty cycle 100%). There was one active device and three placebo devices, with labels A–D. The placebo devices looked and behaved exactly like the active device, but did not produce any magnetic field. It was not possible to see, hear, feel, or sense in any other way which of the devices was active or placebo. The devices were provided by Actera A/S, and only their Chief Technology Officer knew which of the devices the active one was. The blinding was maintained until after the experiment had been concluded and the statistical analyses had been completed.

Assessment of Blood Flow. Skin temperature and cutaneous microcirculation were measured with thermography (Thermovision, Scanner 900 SW-TE, AGEMA Infrared System, Sweden) and laser-Doppler-flowmetry (LDI, Moor Instruments, Devon, UK), respectively, on a predefined area (4×4 cm), proximal and centred to the base of the middle toe. The thermography camera records the infrared emission of the skin as a measure of the skin temperature, which is affected by both cutaneous and deeper lying (muscular) structures as a result of blood perfusion and metabolic processes. A temperature-coded colour picture of the foot was taken, and the mean temperature over the predefined area was calculated and stored. Cork shields were used to cover the magnetic coils when taking the thermographic pictures, because the electrical current flowing through the active device slightly heats up the coils (by about 2°C after 30 minutes), which could not be felt by the subjects but might have unveiled the active device on the thermographic pictures. Laser-Doppler-flowmetry uses a low power laser beam to scan the skin in a raster pattern. Moving blood in the microvasculature causes a Doppler shift in the laser beam, which is processed to build up a colour coded image of blood flow in relative perfusion units (PU). Laser-Doppler-flowmetry measures the cutaneous microcirculation in the superficial layers of the skin within a depth of a few hundred of microns, as a product of number and velocity of the erythrocytes. The mean perfusion value over the predefined area was calculated and stored. Both measurements were non-contact at about 40 cm distance. In Fig. 1, examples of pictures as recorded with thermography and laser-Doppler-flowmetry are shown.

Assessment of Pressure Pain Threshold (PPT). PPT measurements were performed with a hand-held electronic algometer (Somedic AB, Stockholm, Sweden) mounted with a 1-cm diameter circular rubber probe calibrated in kilopascals. To assess the PPT, the probe was held perpendicularly and pressure increased at a constant rate of 30 kPa/s. The PPT, defined as the value where the subject felt the first change from pressure sensation to pain, was recorded. When PPT was reached the volunteers were instructed to press a button that froze the actual pressure on a digital display. The median of three measurements on each point was recorded as

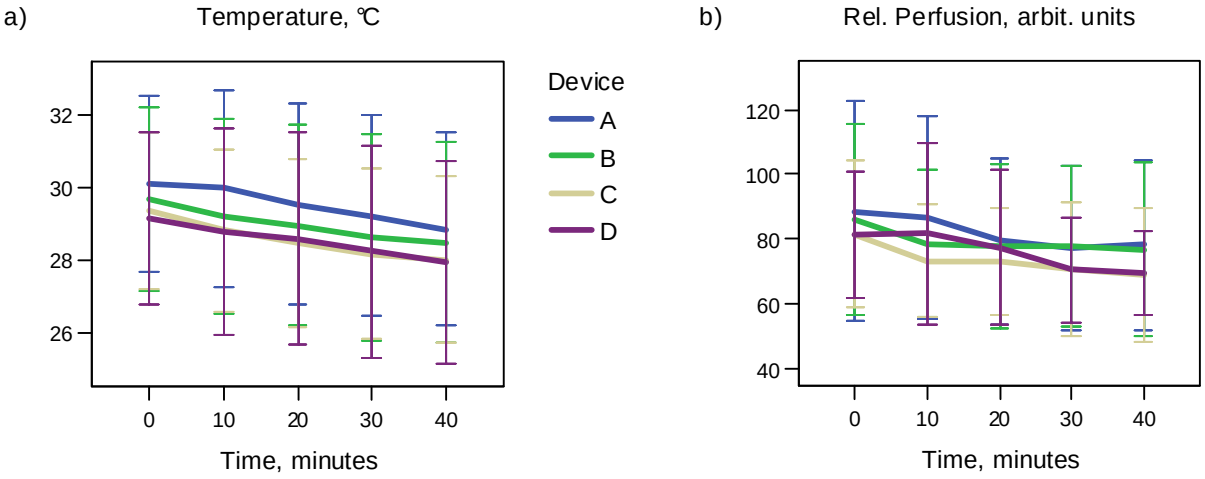


Fig. 2 Profiles of skin temperature and blood perfusion in the dorsum of the foot, at baseline (0 min), 10 and 20 min after start of stimulation, at the end of stimulation (30 min), and 10 minutes post-stimulation (40 min). Values are means ± standard deviation (n = 20).

threshold value. PPT values were measured on the top of both feet (mostly skin and bone) and on the centres of the tibialis anterior muscles.

Assessment of Vaso-Motoric Reaction to Mild Heat. A small (approximately 1 cm^2) metal plate was heated up to 41°C (computer-controlled) and was applied to the skin for 30 seconds, 4 cm medial to the centre of the tibia. Cutaneous microcirculation was measured in a predefined area (4×4 cm) around the heat stimulation site, both before and after the heat impulse, with thermography and laser-Doppler-flowmetry (see above). The heat impulse resulted in vasodilatation in the superficial layers of the skin, increasing the blood perfusion. The increase of the mean temperature and flux profiles due to the heat impulse was recorded (difference post-pre impulse).

Experimental Procedures. Each subject participated in two sessions with one week interval (on the same time of the day). In each session, the subjects received stimulation (active and/or placebo) from two devices, one for each ankle. The order and position of the four devices was randomised according to a random permutation table, prepared with a computer programme (MATLAB 7, The MathWorks Inc., Natick, MA, USA). The room temperature in the laboratory ranged from 21 to 23°C, and all experiments were performed under normal illumination conditions (fluorescent light). The subjects were in supine position, with bare legs and feet, throughout the experiment. The vaso-motoric reaction to mild heat was measured on the right and left leg, followed by determination of the PPT on right foot, right leg, left foot, and left leg. After a 10 minute rest period, the coils were placed laterally on both ankles, and baseline values for the blood flow (temperature and blood perfusion) in the right and left foot were determined. Then, the electromagnetic therapy devices were switched on. After 10, 20, 30 (end of stimulation), and 40 minutes (10 minutes post-exposure), temperature and blood perfusion were measured in the right and left foot. Finally, vaso-motoric reaction to mild heat and PPT were determined as mentioned before. One experimental session lasted in total between 1.5 to 2 hours.

Statistical analysis. The results were expressed as means and standard deviation (means ± SD) in the text and figures. The statistical procedures performed, for the analysis of the blood flow, were multivariate (skin temperature and blood perfusion) repeated measures ANOVA, with within-subject factors “device” (4 levels) and “time” (5 levels). For the analysis of PPT values and vaso-motoric reaction to mild heat, multivariate (foot PPT, leg PPT, increase in skin temperature, and increase in blood perfusion) repeated measures ANOVA was applied, with within-subject factors “device” (4 levels) and “time” (2 levels).
The software used for the statistical analysis was SPSS 14.0 (SPSS Inc., Chicago, IL, USA). A value of $P < 0.05$ was considered as significant.

Results and Discussion

There were no drop-outs in this study, and complete measurement sets were obtained for all 20 subjects. No side effects were observed in this study. None of the participants felt any discomfort, paresthesia, or pain during or after the magnetic field exposure. Only three participants felt warmth in one of the legs after the exposure, but the indicated leg was receiving placebo stimulation in all three cases. None of the participants guessed the active

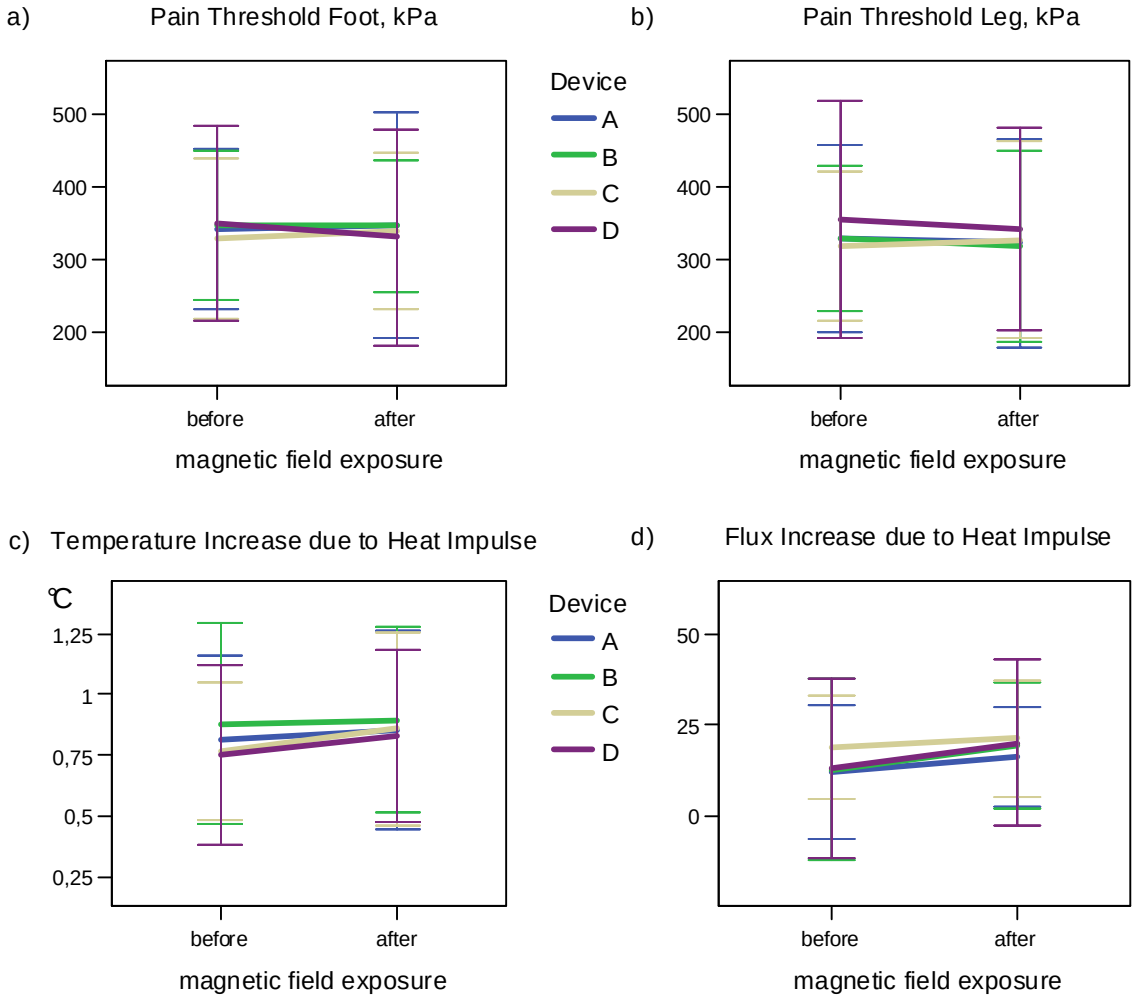


Fig. 3 Profiles of pain thresholds: on dorsum of foot, a), and on the centre of the tibialis anterior muscle, b). Profiles of vaso-motoric reaction to mild heat: temperature and blood perfusion increase caused by a 41°C heat impulse, c) and d). Measurements were done 15 minutes before and 15 minutes after magnetic field exposure. Values are means ± standard deviation (n = 20).

device correctly (only three of the participants tried to identify the active device). A few of the participants became sleepy, and four of them fell asleep during the experiment.

Skin Temperature and Blood Microcirculation (Fig. 2). At baseline, the mean value (averaged over all four devices and all 20 subjects) of the foot temperature was 29.6 ± 2.3°C (mean ± SD, n = 80), and the mean value of the foot blood perfusion was 84.3 ± 26.6 arbitrary units. At the end of the experiment, the mean values decreased to 28.3 ± 2.6°C and 73.4 ± 22.4, respectively. Profiles of the mean values for the four devices at each time point are shown in Fig. 2. The multivariate (dependent variables temperature and blood perfusion) within-subject repeated measures (factors time and device) ANOVA test showed a statistically significant effect for the time factor ($p < 10^{-8}$; partial $\eta^2 = 0.36$), but failed to reach statistical significance for the device factor ($p = 0.40$; partial $\eta^2 = 0.053$; observed power = 0.40) and the time×device interaction ($p = 0.44$; partial $\eta^2 = 0.051$; observed power = 0.82). The univariate tests confirmed the statistically significant effect ($p < 0.001$) of the time factor on both dependent variables, temperature (partial $\eta^2 = 0.56$) and blood perfusion (partial $\eta^2 = 0.36$).

Pain Thresholds and Reaction to Mild Heat (Fig. 3). Before magnetic field exposure, the mean value (averaged over all four devices and all 20 subjects) of the pain threshold in the foot was 342 ± 112 kPa (mean ± SD, n = 80), mean pain thresholds in the leg was 332 ± 124 kPa, mean temperature increase due to mild heat stimulation was 0.80 ± 0.35°C, and mean blood perfusion increase due to mild heat stimulation was 14.25 ± 20.74 arbitrary units. The post-exposure values of the means were 342 ± 126 kPa, 327 ± 135 kPa, 0.86 ± 0.38°C, and 19.24 ± 17.57 arbitrary units, respectively. The corresponding mean values for the four devices are shown in Fig. 3. The multivariate (dependent variables foot PPT, leg PPT, temperature increase, and

increase in blood perfusion) within-subject repeated measures (factors time and device) ANOVA test did not reach statistical significance, neither for the factors time ($p = 0.22$; partial $\eta^2 = 0.29$; observed power = 0.39) or device ($p = 0.30$; partial $\eta^2 = 0.08$; observed power = 0.66), nor for the time×device interaction ($p = 0.89$; partial $\eta^2 = 0.04$; observed power = 0.30).

Unblinding. Device A was the active device.

Discussion. The only statistically significant effect in this study was observed for the time factor. This means, that over time both the temperature and the blood perfusion changed. Since the subjects were in a passive supine position for 40 minutes with bare legs and feet, it was expected that the temperature would decrease over time. The results show that this was indeed what happened (see Fig. 2). This is consistent with other studies (Schuhfried et al., 2005). There are other forms of application of electromagnetic fields where either the intensity or the frequency is high enough to heat body tissue due to eddy currents (Ueno et al., 1986; Alekseev et al., 2005). But the magnetic field used in the present study is too weak to evoke eddy currents in the body of the required amplitude. Direct heating of the skin with the magnetic field device might also occur due to ohmic heating of the applicator coils (McMeeken, 1992). McMeeken (1992) observed a temperature increase of the applicator coil of 3.7°C after 15 minutes of operation, which led to a temperature increase of 0.5°C in the skin underneath the applicator (due to infrared radiation), without affecting the blood flow. In the present study, we observed a temperature increase of the applicator of 2°C after 30 minutes of operation.
There was no statistically significant effect of the device factor in the present study. If there were an effect of the device factor, then baseline values would have to be different for the different devices (different intercepts in Fig. 2 and 3). However, this is not a reasonable assumption.
It would be reasonable to assume different slopes of the profiles, e.g. if the leg treated with the active device cooled less than the leg treated with the placebo device. This is tested by the time×device interaction, which did not reach statistical significance. The observed power of this test was 82%. Therefore it is concluded that a magnetic field (only present in the active device) of strength and frequency as used in the present study does not change temperature and blood flow in healthy volunteers. This is consistent with other studies (McMeeken, 1992; Schuhfried et al., 2005; Wenzel et al., 2005).

Summary

This study shows that, in healthy volunteers, acute exposure to a weak (below 6mT) magnetic field with a specific waveform, repeated at 800 Hz, does not change skin blood flow and temperature, nor pressure pain thresholds.
Acute exposure of healthy volunteers was chosen in this study in order to detect (and quantify) a possible basic, direct effect of magnetic fields. Prolonged or repeated exposure might show different effects. Patients receiving the magnetic field stimulation might show different effects, because the biological response to electromagnetic field exposure depends on the state of the biological target tissue (Mayrovitz et al., 2001). It was shown that patients react differently than healthy people to electromagnetic therapy (Giordano et al., 2000).
The results of the present study do not allow drawing conclusions about the possible effects of electromagnetic therapy in patients. Therefore, this study can not answer the question whether enhanced microcirculation might or might not be an effect of electromagnetic therapy in patients. However, this study shows that there is no direct (acute) effect of exposure to a magnetic field, of strength and frequency as used in this study, on microcirculation in healthy subjects.

Acknowledgements

This project was financially supported by Actera A/S, Denmark, and the Faculty of Engineering, Science and Medicine, Aalborg University. The authors thank Parisa Gazerani for her kind help in the preparation of the experiment.

References

Alekseev SI, Radzievsky AA, Szabo I, Ziskin MC. 2005. Local heating of human skin by millimeter waves: effect of blood flow. *Bioelectromagnetics* 26(6):489–501.

Cullum N, Nelson EA, Flemming K, Sheldon T. 2001. Systematic reviews of wound care management: (5) beds; (6) compression; (7) laser therapy, therapeutic ultrasound, electrotherapy and electromagnetic therapy. *Health Technology Assessment* 5:1-221.

Giordano N, Battisti E, Geraci S, Santacroce C, Lucani B, Fortunato M, Mattii G, Gennari C. 2000. Analgesic-antiinflammatory effect of a 100 Hz variable magnetic field in RA. *Clin Exp Rheumatol* 18(2):263.

Jauchem JR. 1997. Exposure to extremely-low-frequency electromagnetic fields and radiofrequency radiation: cardiovascular effects in humans. *Int Arch Occup Environ Health* 70:9–21.

Kinouchi Y, Yamaguchi H, Tenforde TS. 1996. Theoretical analysis of magnetic field interactions with aortic blood flow. *Bioelectromagnetics* 17(1):21–32.

Markov MS. 2004. Magnetic and electromagnetic field therapy: Basic principles of application for pain relief. In: Rosch PJ, Markov MS, editors. *Bioelectromagnetic Medicine*. Marcel Dekker, p 251–264.

Mayrovitz HN, Groseclose EE, Markov M, Pilla AA. 2001. Effects of permanent magnets on resting skin blood perfusion in healthy persons assessed by laser Doppler flowmetry and imaging. *Bioelectromagnetics* 22(7):494–502.

McMeeken JM. 1992. Magnetic fields: effects on blood flow in human subjects. *Physiotherapy Theory and Practice* 8:3–9.

Podd J, Page W, Rapley B, Beale I. 1998. Bioelectromagnetic research and statistical power. *Proceedings of the 2nd International Conference on Bioelectromagnetism*, p 197-198.

Polk C, Postow E. 1996. *Handbook of biological effects of electromagnetic fields*. 2nd edition, CRC Press, Boca Raton, New York, London, Tokyo.

Schuhfried O, Vacariu G, Rochowanski H, Serek M, Fialka-Moser V. 2005. The effects of low-dosed and high-dosed low-frequency electromagnetic fields on microcirculation and skin temperature in healthy subjects. *Int J Sports Med* 26(10):886–90.

Shupak NM, Prato FS, Thomas AW. 2003. Therapeutic uses of pulsed magnetic-field exposure: A review. *The Radio Science Bulletin* 307:9–32. www.ursi.org/RSBissues/RSBdecember2003.pdf (retrieved June 2006).

Stavroulakis P. 2003. *Biological effects of electromagnetic fields*. Springer, Germany.

Swanson J, Kheifets L. 2006. Biophysical mechanisms: a component in the weight of evidence for health effects of power-frequency electric and magnetic fields. *Radiat Res* 165(4):470-8.

Ueno S, Lövsund P, Öberg PÅ. 1986. Effects of alternating magnetic fields and low-frequency electric currents on human skin blood flow. *Med Biol Eng Comput* 24(1):57–61.

Wenzel F, Reissenweber J, David E. 2005. Cutaneous microcirculation is not altered by a weak 50 Hz magnetic field. *Biomed Tech (Berl)* 50(1-2):14-8.

INFLUENCE OF MICROWAVE RADIATION ON SERUM ALKALINE PHOSPHATASE IN RAT

M.SEDEHI ESFAHANI, S.KHADIVI F.RASHID NAJAFI, J.GOODARZI , A.KOHBODI

Biological research center of institute of standard and industrial research Of Iran. P.o.box:31585-163

Email address:mansoureh_sedehi@yahoo.com

Abstract

The level of serum alkaline phosphatase(alp),as a a possible promoter of bone or tumor disease was studied in 80 rats exposed to microwave radiation(2450 mh with power density of 1 and 10mw/cm²), for a period of one year.
The animals were devided to 5 groups of 16 each(8males and 8 females), 4 for treatment and one for control group. First two treated groups were exposed to microwave radiation at power density of 1mw/cm² in different period (30 minutes for one group and 5 minutes for another one), daily. Next two treated groups were exposed to microwave radiation at power density of 10 mw/cm² in different period (30 minutes for one and 5 minutes for another group), daily. Control group were kept under the normal condition without any microwave exposure.
Animals were observed daily and body weight and food and water consumption was assessed weekly too.
In the end of study the blood sample were taken from the heart of animals under ether anesthesia and alp analysis was performed on blood serum of animals.
According to the test result and statistical analysis the level of alp in groups exposed To microwave radiation at power density of 10 mw/cm² was significantly increased ($p<0/011$), but in other treated groups,the statistical resuts has not been significant in comparison with control group.

Introduction :

Alkaline phosphatase is a group of enzymes found primarily in the liver and in bone.It also is produced by the placenta and to a lesser extent by the intestines and kidney.
In this study, the gole of measuring alkaline phosphatase is to check the possibility of bone or liver disease in rat after a period of one year exposure to 2450 mh microwave radiation at incident power densities of 1and 10 mw/cm2 for 5 and 30 minutes daily.

Method of study :

Animals

80 sprague Dawley rats with 5 week age were used in this investigation for a period of one year. The animals were housed individually in polycarbonate cages under standard conditions with free access to tap water and standard food (1,2,3,4,5). the rats were devided to 5 group , each containing 16 rats (8 male and 8 females) , as follows :

Group D and E : exposed to microwave radiation with power density of 1 mw/cm2 for 30 minutes daily for group D and 5 minutes daily for group E .

Group F and G : exposed to microwave radiation with power density of 10 mw/cm2 for 30 minutes daily for group F and 5 minutes daily for group G .

Group H : as a control group were kept under the same condition without any microwave exposure .

Records and Control :

The rats were weighed before experiment and weekly and recorded. Any clinical abnormality were noted and recorded .

Food and water consumption were controlled weekly too .

Method of ALP Measurment :

In the and of study the blood sample were taken from the heart of animals after 12 howrs fasting under ether anesthesia .

The level of alp was measured by enzymatic method. the enzyme splits off the phosphate group from 4-NPP to form free 4-mitrophenol. Thus the rate of formation of 4-NP by the action of the enzyme on 4-NPP at 37oC can be monitored with a recording spectrophotometer(6,7,8):

4-nitrophenylphosphate+h2o---ALP-------→-phosphate+4-nithrophenol

Statistical analysis :

Statistical evaluation of data for comparison of treated and control group were made by using one way analysis of variance (anova) technique , followed by a multiple comparison , the one way anova was applied using the F distribution to assess significance at the level of 0/05

Results and discussion :

Clinical observation :there was one death related to group E.

Body weight and food and water consumption : according to the results , the percentage of body weight and food consumption was reduced in treated groups in comparison with control(9), but the *percentage of* water intake was increased in treated groups especially in group F in comparison with control.

Serum ALP Level :

As illustrated in fig 1-3 , the level of ALP in group male of G and mixed group male and female of G that were exposed to microwave radiation at power density of 10 mw/cm2 for 5 minutes daily was significantly increased ($P < 0/01$) , but as statistical analysis is showed in table1-3 increasing of ALP in other treated groups was not significant in the level of 0/05 , in which microwave exposure at 10 mw/cm2 is suspected as a possible promoter of bone or tumor disease that should be considered (6,10,11,12)

Fig 1- Mean content of ALP in male groups

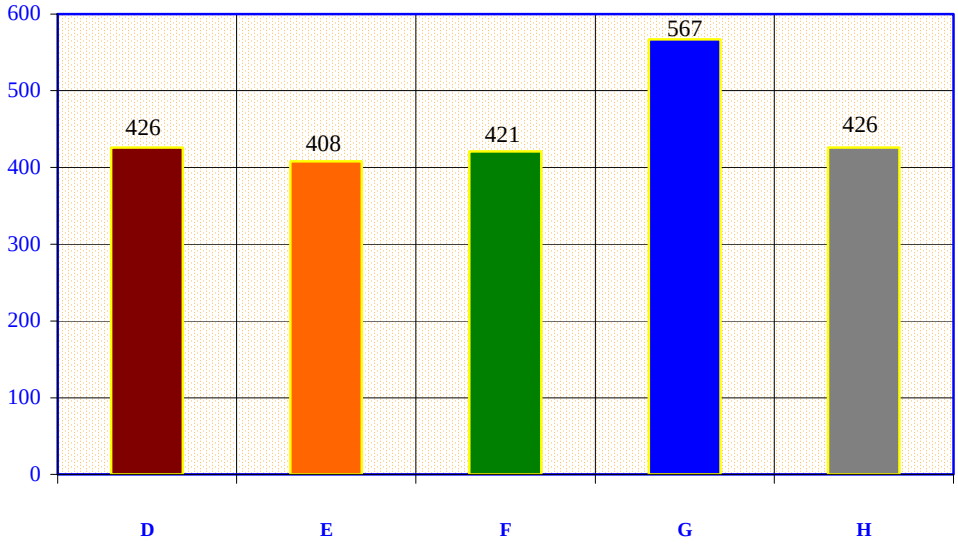


Fig 2- Mean content of ALP in female groups

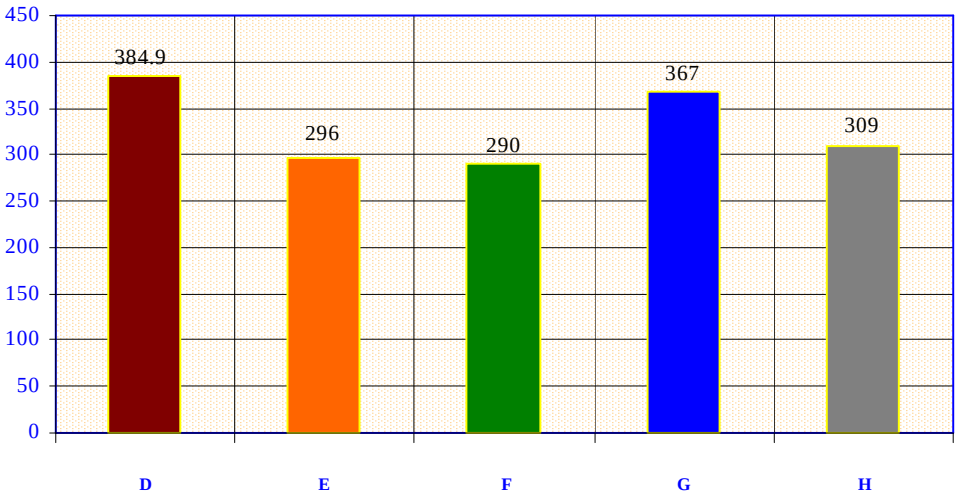


Fig 3- Mean content of ALP in Mixed groups (males and females)

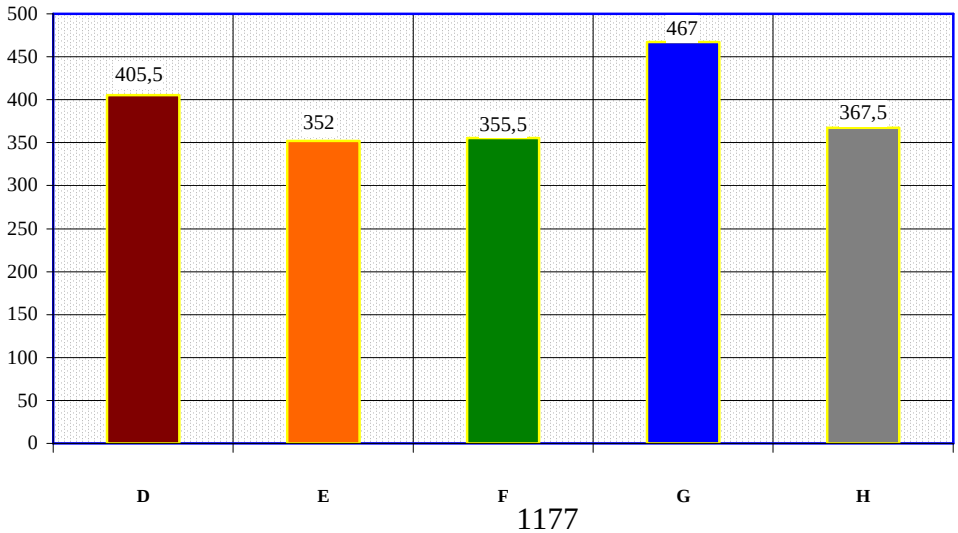


Table 1- Comparison of Statistical analysis of ALP in treated female groups with control group

Dependent Variable	(I) V14	(J) V14	Mean Difference (I-J)	Std. Error	Sig.	95% Confidence Interval	
						Lower Bound	Upper Bound
ALP	H	D	-75.13	41.41	075	-158.08	7.83
		E	13.50	41.41	.746	-69.45	96.45
		F	19.50	41.41	.640	-63.45	102.45
		G	-70.25*	41.41	095	-153.20	12.70

*. The mean difference is significant at the 05 level .

Table 2- Comparison of Statistical analysis of ALP in treated male groups with control group

Dependent Variable	(I) V14	(J) V14	Mean Difference (I-J)	Std. Error	Sig.	95% Confidence Interval	
						Lower Bound	Upper Bound
ALP	H	D	-17.00	53.55	.752	-124.28	90.28
		E	18.13	53.55	.736	-89.15	125.40
		F	5.38	53.55	.920	-101.90	112.65
		G	-141.38*	53.55	011	-248.65	-34.10

*. The mean difference is significant at the 05 level .

Table 3- Comparison of Statistical analysis of ALP in treated both male and female groups with control group

Dependent Variable	(I) V14	(J) V14	Mean Difference (I-J)	Std. Error	Sig.	95% Confidence Interval	
						Lower Bound	Upper Bound
ALP	H	D	-46.06	41.12	.265	-127.49	35.36
		E	15.81	41.12	.701	-65.61	97.24
		F	12.44	41.12	.763	-68.99	93.86
		G	-105.81*	41.12	011	-187.24	-24.39

*. The mean difference is significant at the 05 level .

Summary :

In conclusion , the results shown here confirm that , the level of ALP was increased in serum of rats exposed to microwave radiation at power density of 10 mw/cm2 is suspected as a possible promoter of bone or tumor disease , that should be considered. our data also indicate that the measure of ALP in other treated groups has not been significantly increased in the level of 0/05 in comparison with control group .

Acknowledgment :

We wish to thank to miss T.Niavarani for technical assistance and also grateful to Mr Sh. Kasgeh for statistical analysis of data, and research center of pars azmoon for supporting this work .

References :

1- Presented pursuant to act Eliz “code of practice for the housing and care of animals used in scientific procedures” , C.14 section 21 , 1986 .

2- Clarke , HE. Coates Meeva . JK, Ford “Dietary standards for laboratory animals” report of the lac diets advisory committee. Lab.11 1-28 , 1977 .

3- Royal society / UFAW “Guidelines on the care of laboratory animals and their use for scientific purposes” , 1987 .

4- Ivan Bartosek et al “Animals in toxicological research” Raven press , 1981 .

5- Wallach , Boever “Diseases of animals, medical and surgical management” W.B saunders company 1983 , P 132-195 .

6- Carl A . Burtis Tiets textbook of chemical chemistry 2th , 1994 .

7- Weisshaar , D. Grossau , EU. Faderl B.med. welt 26 , 387-390 , 1975 .

8- Bowers , GM , JR , McComb , RB : A continuous spectrophotometric method for measuring the activity of serum alkaline phosphatase clin chem. , 12 : 70-89 , 1966 .

9- Ray 5 , Behari J “Physiological changes in rats after exposure to low level of microwaves” Radiat Res 123 (2) : 199-202 Aug 1990 .

10- Gorczynska E , wegrzynowicz R , “Effect of static magnetic field on some enzymes activities in rats” . J Hyg Epidemol Microbiol Immunol 33 (2) : 149-55 , 1989 .

11- Pashovkina Ms, Akoev IG.“Effect of low intensity pulse modulated electromagnetic radiation on activity of alkaline phosphatase in blood serum” , Radiats Biol Radioecol . 41 (1) : 62-6 , 2001 .

12- Schmitto, “The influence of the electromagnetic filed on the activity of alkaline phosphatase in immobilised children” . Arch orthop trauma surg 93 (1) : 21-4 , 1978 .

EFFECT OF MICROWAVE EXPOSURE ON SOME HEMATOLOGICAL PARAMETERS IN RAT

M.SEDEHI ESFAHANI,A.KOHBODI,S.KHADIVI,

Biological research center of institute of standard and industrial research of Iran.P.o.box:31585-163

Email address:mansoureh_sedehi@yahoo.com

Abstract

80 sprague Dawley rats were exposed to 2450 mhz microwave field for a period of one year. The experiment groups were devided to 5 groups,each 16(8 males and 8 female), 4 for treatment,and one,for control(D,E,F,G,H).

The incident power density of the first two experiment groups was 1mw/cm^2,and, for next two grours,was 10mw/cm^2.The daily exposure time,was5 minutes for groups F and G,and 30 minutes for groups,D and F. The animals in control group(H) were under normal condition without any microwave exposure.

In the end of the study the blood samples were taken from the heart of animals under ether anesthesia,and determination of blood parameters were performed by cell counter auto analyser.

Accrrding to the statistical results the level of RBC in male groups of F and G,and percentage of PCVin female and male groups of F,and content of HB,in female groups of F,in comparison with control group were significantly increased and variation of results in other groups were not significant.

Introduction :

The aim of this study was to investigate and check the possibility altration of some blood parameters in rats after a period of one year exposure to 2450 Mh microwave radiation at power density of 1 and 10 mw/cm^2 for 5 and 30 minutes daily and also to compare the treated groups with that of control group .

Method of study :

Animals

80 sprague dawley (SD) rats with 5 weeks age were used this study for a period of one year. The animals were housed individually in polycarbonate cages under standard condition with free access to tap water and standard food (1,2,3,4,5).the rats were devided into 5 groups (4 treated and 1 control) of eight male and eight female rats each .Two first experimental groups were exposed to 2450 mh microwave radiation with field powers density of 1mw/cm^2 for 30 minutes daily for group (D) and 5 minutes daily for group (E) .

Next two treated groups were exposed to 2450 mh microwave radiation with filed power density of 10 mw/cm^2 for 30 minutes for group (F) and 5 minutes for groups (G) daily.Control group(H) were under normal condition without any microwave radiation exposure.

Records and control :

The animals were weighed before experiment and weekly and recorded .

Any clinical abnormality were cared and recorded. Food and water consumption were also weekly controlled .

Blood analysis :

In the end of study the blood samples were taken from the heart of animals under ether anesthesia and the blood samples were mixed with ethylenediamine tetraacetic acid (EDTA) and then analysed by auto analyser of cell counter .

Statistical analysis :

The differences between groups were analysed using appropriate one way analysis of variance (anova) technique , followed by a multiple comparison .

The one way anova was applied using the F distribution to assess significance in the level of 0/05 .

Fig 1- mean difference of R B C in female groups

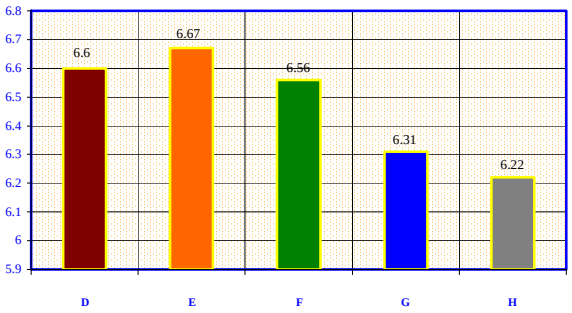


Fig 2- mean difference of R B C in male groups

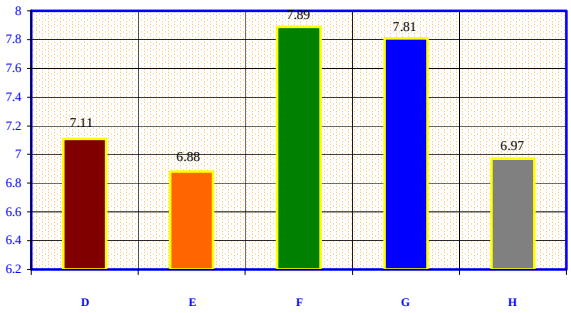


Fig 3- mean difference of P V C in female groups (%)

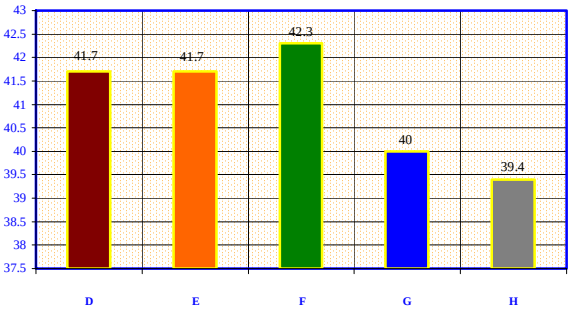


Fig 4- mean difference of P V C in male groups (%)

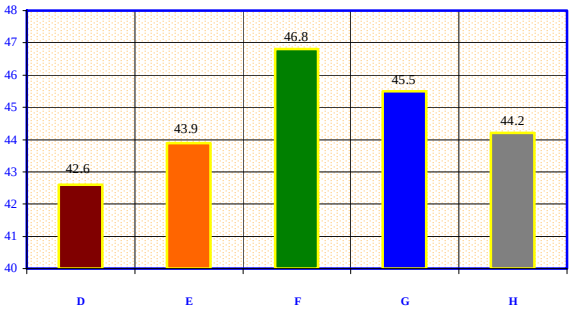


Fig 5- mean difference of Hb in male groups (g/dl)

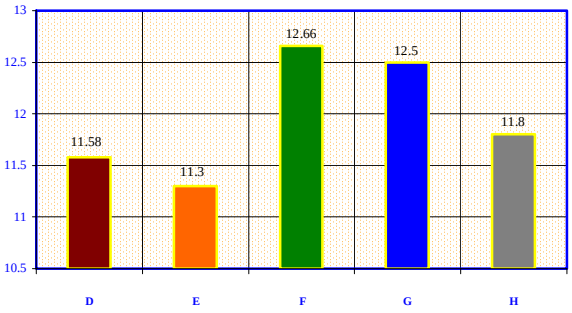
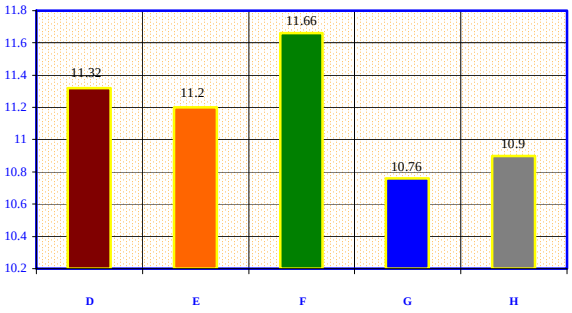


Fig 6- mean difference of Hb in female groups (g/dl)



Summary :

The data presented in this study indicate that there is increasing of blood parameters of RBC , PVC and Hb in treated groups exposed to microwave radiation at power density of 10 mw/cm^{2,} in

which microwave exposure in this field is a probable agent for stimulation of proliferation processes in red bone marrow,may be due to hypoxia and releasing of erythropoietin hormon, that can be considered. Our data also indicate that the test results of same blood parameters in treated rats exposed to microwave radiation at 1 mw/cm^2 powers density has not been significant in comparison with that of control group.

Acknowledgment :

We wish to thank to Dr Z. Maleki for her advice and comments, and also grateful to Miss T.Niavarani, Miss F.Najafi for technical assistance and Mr Sh.kasgeh for assistance with the data analysis and statistical evaluation.

References :

1- Clarke , HE. Coats , Meeva. JK , Ford "Dietary standards for laboratory animals" report of the lac diets advisory committee , lab .11 1-28 , 1977 .
2- Presented pursuant to act Eliz"code of practice for the housing and care of animals used in scientific procedures" C.14 section 21 , 1986 .
3- Royal society / UFAW "Guidelines on the care of laboratory animals and their use for scicntific purposes" , 1987 .
4- Ivan Bartosek et al "Animals in toxicological research" Raven press , 1981 .
5- Wallach , Boever "Diseases of animals,medical and surgical management" W.B saunders company p 132-195 , 1983 .
6- Ragan .HA, Phillips RD et al"Hematologic and immunologic effects on pulsed microwaves in mice" Bioelectromagnetics ; 4 (4) : 383-96, 1983.
7- Koveshnikova IV. Antipenke EN. "Changes in body weight of rats during irradiation with microwave of nonthermal intensity" Radiobiologiia . 28 (4) : 561-3 , 1988 .
8- D , Andrea JA , Gandhi op, et al "Physiological and behavioral effects of chronic exposure to 2450 Mh microwaves" J Micro power;14(4):351-62,1979
9- Human exposure to radio frequency radiation : A Comprehensive review pertinet to air force operations .
http://www.brooks.af.mil/AFRL/HED/hedr/reports/human_exosure/htmfile 13.html .
10-The associated bioelectromagnetics technologists http://emfbioeffects. Org, 4/15/04 .
11- Ray – S , Behari –J"Physiological changes in rats after exposure to low level of microwaves" Radiat – Res 123 (2) 199-202 , Aug 1990 .
12-cleary Sf et al"Effects of x-band microwave exposure on rabbit erythrocytes"Bioelectromagnetics;3(4):453-66,1982.
13-Alex O Sonnenwirth,Leonard Jarett"clinical laboratory methods and diagnosis"8th 1980.
14-Carl A,Burtis tiets"textbook of clinical chemistry",2th,1994.

EFFECT OF EXTREMELY LOW FREQUENCY ELECTROMAGNETIC FIELDS ON MOUSE THYMUS AND TESTIS

FUMIO SHIMAMOTO,
DEPARTMENT OF HEALTH AND SCIENCE, PREFECTURAL UNIVERSITY OF HIROSHIMA
e-mail:simamoto@pu-hiroshima.ac.jp

HANDAN TUNCEL,
DEPARTMENT OF BIOPHYSICS, CERRAHPASA MEDICAL FACULTY ISTANBUL UNIVERSITY

TAKASHI TAKATA, KOUEI SAI
DERPATMENT OF ORAL PATHOLOGY, HIROSHIMA UNIVERSITY

MASAAKI TATUKA,
DEPARTMENT OF MOLECULAR RADIOLOGY, RESEARCH INSUTITUTE FOR RADIATION BIOLOGY AND MEDICINE, HIROSHIMA UNIVERSITY

Abstract

PURPOSE: We examined the apoptotic effects of extremely low-frequency electromagnetic fields (EMFs) on murine thymus gland and testis after whole-body irradiation.

METHODS: Thymus gland and testis are highly susceptible to ionizing irradiation (IR). When suffered to apoposis by IR, the apoptosis-related signal molecules including nuclear transcription factors and cytoplasmic caspases are activated. Here, we measured the expression levels of nuclear transcription factors such as ATF-3 and p53 and a caspase-3-cleaved product LyGDI/GDI-D4/RhoGDI2/RhoGDIβ in thymus gland and testis after whole-body EMFs irradiation.

RESULT: Both transcription factors, ATF-3 and p53, were not up-regulated according to time course and dose-response of EMFs. The caspase-3-cleaved product, N-terminal deleted 21-kDa fragment of LyGDI (ΔN(1-19)LyGDI), was also not induced by EMFs. Besides, in immunoblotting of ΔN(1-19)LyGDI, we noticed an unexpected 55-kDa band which was disappeared by EMFs although this epitope has not been identified. CONCLUSION: Apoptotic signals mediated by DNA strand breaks are not generated in whole-body irradiation of EMFs. Instead of this, an unknown intracellular signalling may possibly be provoked in EMFs-irradiated thymic gland and testis.

Introduction

An association between residential extremely low-frequency electronic and magnetic fields (EMF) and childhood leukemia was first reported in 1979 by Wertheimer and Leeper[1)]. In Japan also epidemiologic studies recently showed that residential power-frequency magnetic fields levels above 0.4 micro T exposure was associated with a higher risk of childhood leukemia (acute lymphoblastic leukemia)[2)]. Experimentally, we found that the offspring mice coming from late pregnant mice exposed to a 500mG 50Hz developed chronic

myelogenic leukemia with chronic exposure[3]. Exposure to a 60-Hz magnetic field at 0.001mT for 24 hr was reported to cause a significant increase in DNA single-and double-strand breaks in the brain cells of rats[4].

As a general mechanism, apoptotic cell death is triggered by DNA strand breaks. When apoptotic signalling caused by ionizing radiation (IR) is generated in the cells, transcription factors such as ATF-3 and p53 are up-regulated. Subsequently, as post-mitochondrial signals, caspases are activated to execute apoptosis. LyGDI, also known as GDI-D4/RhoGDI2/RhoGDIβ, is a substrate of caspase-3 and is cleaved by activated forms of this during IR-induced thymic apoptosis[5]. Therefore, the cleaved product, N-terminal deleted ΔN(1-19)LyGDI, becomes a marker for the activation of caspase-3. To examine whether EMFs provoke such an apoptotic signalling, we measured the expression levels of either transcription factors and ΔN(1-19)LyGDI in thymic gland and testis from whole-body irradiation of EMFs. The presented data clearly indicate that EMFs do not induce the apoptotic signalling in both thymic gland and testis. Besides, an unidentified immunoblot band, which is reactive to N-terminus of ΔN(1-19)LyGDI, has been found to respond to EMFs in both organs.

Materials and Methods

Animal: C57BL/6NCrlCrlj male mice were purchased from Charles River Japan Inc. at 6 weeks of age.

EMF exposure: The exposure facility was produced by Chugoku electronics (Hiroshima, Japan). Magnetic fields were provided by electromagnet which has air gap of 10cm cubic and exciting coli of 1400 turns. Sixty Hz magnetic fields of 100mG, 500mG, 1G, 5G and 10G were generated for exposure. Animals in the air gap were kept under constant conditions of temperature(24±2℃) and humidity(50± 10%).

Experimental procedure:

1) To investigate expression of ΔN (1-19) LyGDI and full-length LyGDI in the exposed cells, mice were exposed to 60Hz field 5G for 6 hours. Then thymus and testis were aseptically taken out from sacrified mice.
2) Time-dependent p53 and ATF-3 were studied with 60Hz field of 10G, at 0, 3 and 6hr, respectively.
3) Dose-dependent p53 and ATF-3 were examined with 60Hz field of 0, 0.1, 0.5, 1, 5 and 10 G, respectively for 6hr.

Mouse thymus irradiated with 5 Gy was used as positive control in expression of ATF-3 and p53.

Antibodies:

Primary antibodies used in the present study is summarized in Table 1.

Table 1. Primary antibodies used in the present study

Recognized molelcule	antibody	Source	Type number
Full length LyGDI	goat polyclonal antibody	Santa Cruz	sc-6047G
N-terminal deleted form of LyGDI	monoclonal antibody	Active Motif	40941
p53	goat polyclonal antibody monoclonal antibody	Santa Cruz Cell Signaling	sc-6243G 2524
ATF-3	rabbit polyclonal antibody	Santa Cruz	sc-188
α-tubulin	monoclonal antibody	Cederlane	L9002T

Protein analysis:

To extract total protein, thymus and testis was homogenized with ice-cold sodium dodecyl sulfate(SDS) sample buffer (pH 6.8) consisting of 25mM Tris-HCl, 5% glycerol and 1% SDS. The homogenized solution was sonicated five times for 5 s on ice and centrifuged at 15,000 rpm for 1min at 4℃. The supernatant was then used for Western blot analysis. After extraction, the protein concentration was determined using a BioRad protein assay Kit. Then Protein of 20 micro gr per lane were applied to a 12% SDS-polyacrylamino gel, after which whole cell lysate and the fractionated samples were resolved by electrophoresis and transferred to Immobilon-P membrane. The gels were probed with primary antibodies, followed by secondary antibodies. Horseradish peroxidase-conjugated anti-goat rabbit antibody and horseradish peroxidase-conjugated anti-mouse or anti-rabbit donkey antibodies were used as secondary antibodies. Proteins were visualized on X-ray film using ECL Western Blotting Detection Reagent.

Results and discussion

To elucidate the apoptosis-inducing signal of exposed thymus and testis cells, we first investigated the cleavage of LyGDI. In mouse LyGDI, cleavage by caspase 3 and caspase 1 occurs after the Asp^{18} and Asp^{54} residues, respectively, resulting in the production of two truncated protein, 21-kDa and 17-kDa products. Thus the products of truncated LyGDI indicates which caspase are activated in exposed cells. But as Figure 1 shows, truncated LyDGI was not detected in both of thymus and testis with 5 G exposure for 6hr. Interestingly, unknown substance (55kDa) reactive antibody recognized the N-terminal amino acids of the deleted ΔN (1-19) LyGDI, was detected in thymus and testis cells and indicated decrease in exposed both the cells(Figure 1-B).

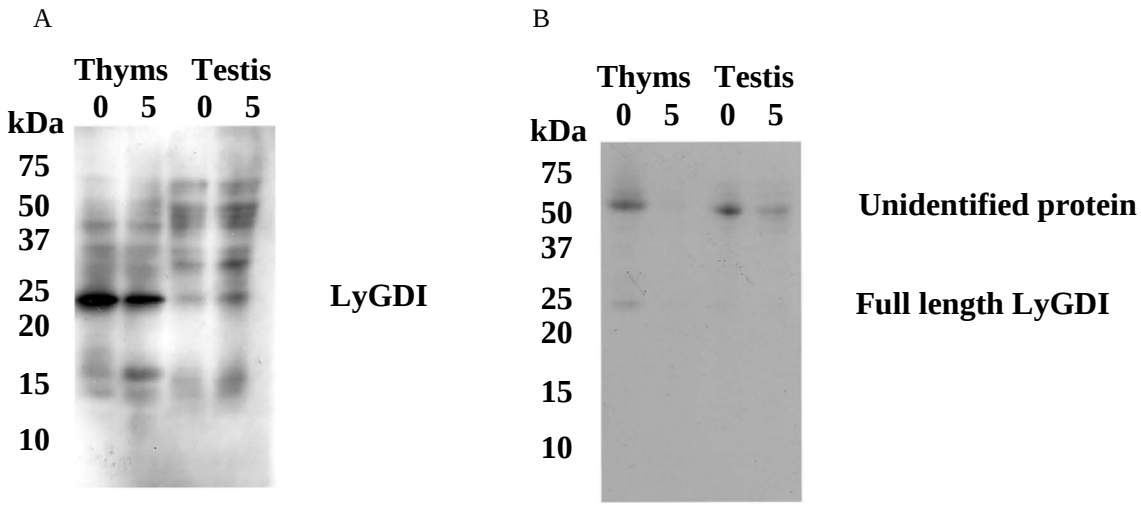


Figure1. Truncation of LyGDI and full-LyGDI after magnetic irradiation for 6hr. Panel A: Full-LyGDI was detected in both of thymus and testeis with 0 and 5 G. Panel B: Truncation of LyGDI was not found in both of thymus and testis with 0 and 5 G, respectively. Unknown substance was detected in about 55KDa with antibody of delta19-LyGDI.

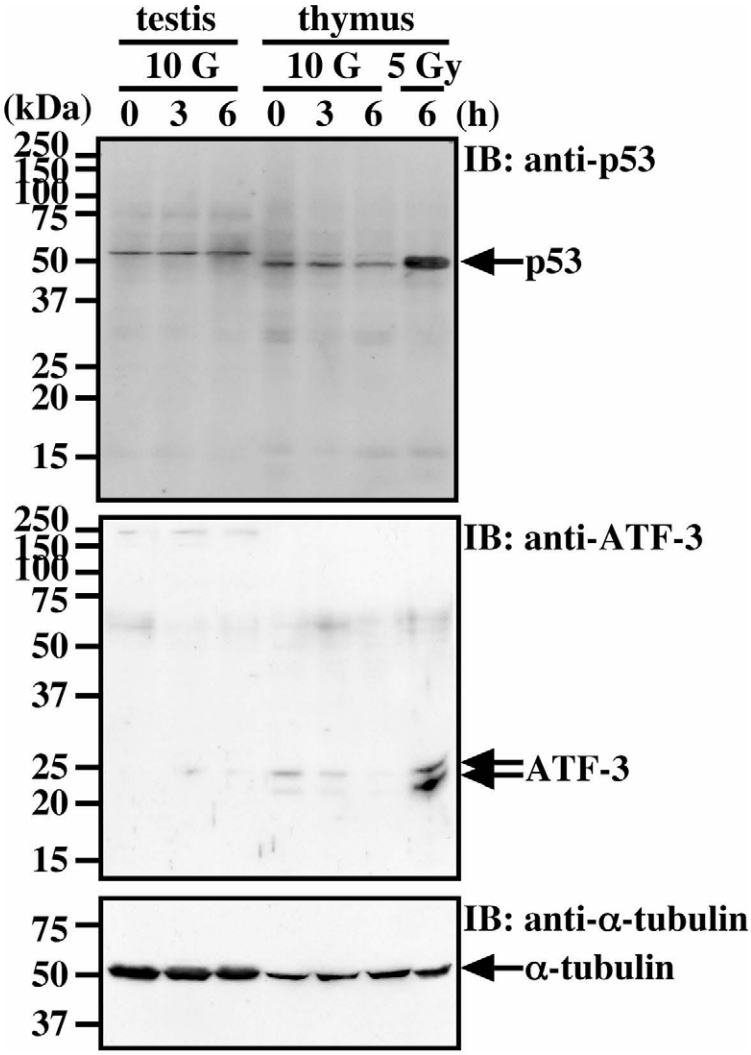


Figure 2. Variation in the protein level of p53 and ATF-3 in thymus and testis with time after exposure with 10 G.

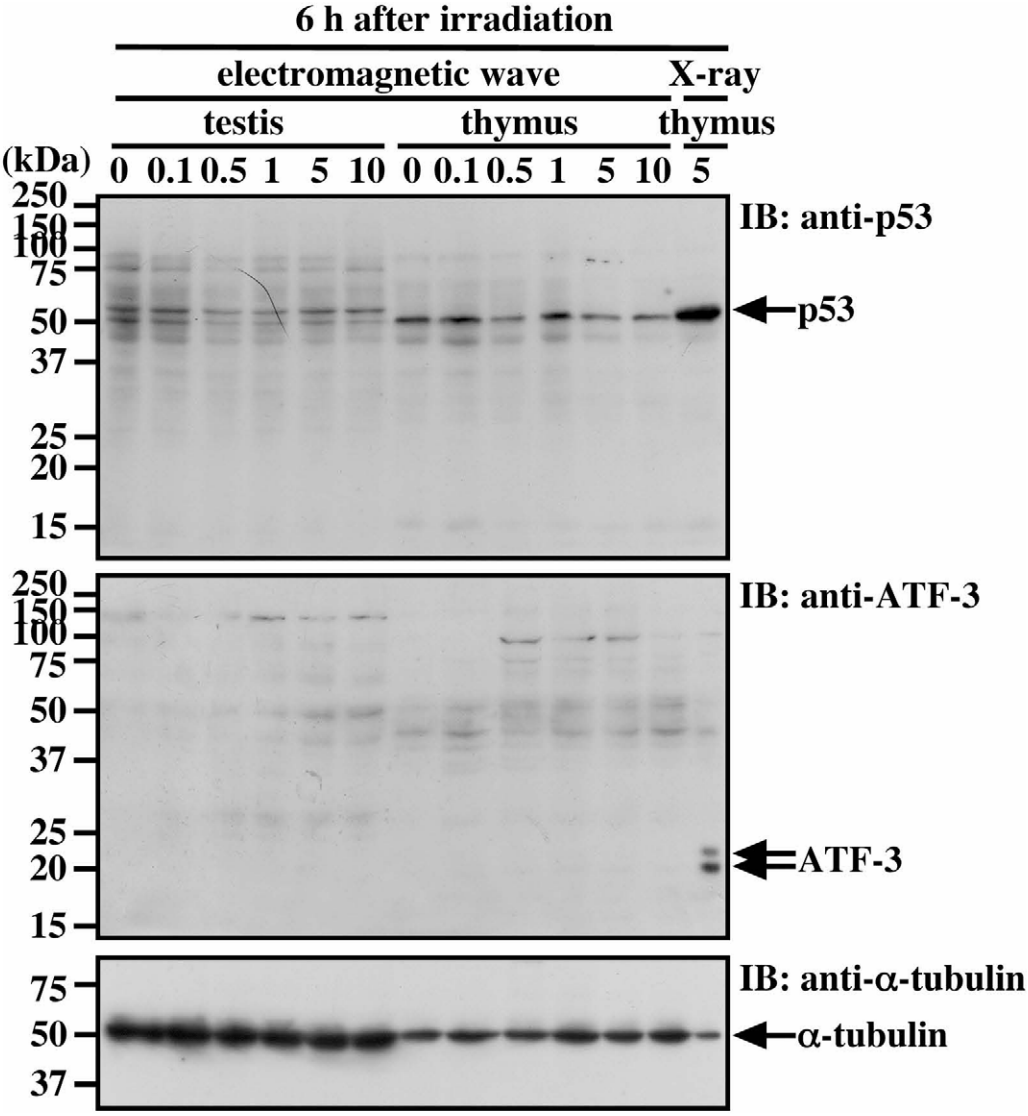


Figure 3. Effect of the exposed dose on activation of p53 and ATF-3 of thymus and testis in 6hr after exposure.

ATF3(activating transcription factor 3)is a member of the ATF/CREB subfamily of basic-region leucine zipper(bZIP) protein and is induced in response to endoplasmic reticulum stress or amino acid starvation[6]. ATF3 is a novel stress-activated regulator of p53 protein stability/function providing the cell with a means of responding to a wide range of environmental insult[7]. It is also reported that regulation of ATF3 induction after DNA damage utilizes both the p53-dependent and-independent pathways, and may also involve MAP kinase signalling pathway[8]. In this study we could not detected significant expression of AFT3 and p53 of thymus and testis in time- and dose-dependent variation. The important role of ions, particularly of Ca^{2+}, in the apoptotic process of the exposed cells is considered[9], and then there may be another p53-independent pathway in magnetic field action on apoptosis.

Those result indicated that that there may be another signaling pathway to produce the effects of EMF, although EMF-induced signaling cascade that mediates apoptosis was not found.

Acknowledgements

We would like to thank Emeritus Prof. S.Keitoku, Miss Sakiie and Miss Suto for help of animal experiment and molecular analysis. This work was supported by the Research Fund of Prefectural University of Hiroshima, H16(2003).

Reference

[1] Wertheimer N, Leeper E. Electrical wiring configurations and childhood cancer. Am J Epdemiol. 1979, 109: 273-84

[2] Kabuto M, Nitta H, Yamamoto S, Yamaguchi N, Akiba S, Honda Y, Hagihara J, Isaka K, Saito T, Ojima T, Nakamura Y, Mizoue T, Ito S, Eboshida A, Yamazaki S, Sokejima S, Kurokawa Y and Kubo O. Childhood leukemia and maginetic fields in Japan: A case-control study of childhood leukemia and residential power-frequency magnetic fields in Japan. Int J Cancer. 2006, 119: 643-650

[3] Shimamoto F, Tuncel H, Takada T, Aoki E, Sai K, Watanabe M, Keitoku S. Effect of extremely low frequency electromagnetic fields on pregnant mice. Biological effects of EMFs 3rd International Workshop Proceedings, 2004, 939-943

[4] Lai H and Singh NP. Magnetic-Field-Induced DNA strand breaks in brain cells of the rat. Environmental Health Perspectives. 2004,112,687-693

[5] Xinwen Zhou, Shiho Suto, Takahide Ota, and Masaaki Tatuka.: Nuclear Translocation of cleaved LyGDI dissociated from Rho and Rac during Trp53-dependent ionizing radiation-induced apoptosis of thymus cell in vitro. Radiation research 162,287-295(2004)

[6] Jiang Hy, Wek S A, MuGrath BC, LuD, Hai, Harding HP, Wang X, Ron D, Cavener DR.: Activating transcription factor 3 is integral to the eukaryotic initiation factor 2 kinase stress response. Mol Cell Biol. 2004 Feb;24(3):1365-77.

[7]Yan C, Lu D, Hai T, Boyd DD.: Activating transcription factor 3, a stress sensor, activates p53 by blocking its ubiquitination EMBO J. 2005 Jul 6;24(13):2425-35. Epub 2005 Jun 2.

[8] Fan F,Jin S, Amundson SA, Tong T, Fan W, Zhao H, Zhu X, et al.: ATF3 induction following DNA damage is regulated by distinct signaling pathways and over-expression of ATF3 protein suppresses cells growth. Oncogene. 2002 Oct 24;21(49):7488-96.

[9] Santini MT, Ferrante A, Rainaldi G, Indovina P, Indovina PL.:Extremely low frequency (ELF) magnetic fields and apoptosis. Int J Radiat Biol. 2005 Jan;81(1):1-11

EFFECTS OF RF ELECTROMAGNETIC FIELDS ON MICROORGANISMS

LUDĚK STRAŠÁK[1,3], LUKÁŠ FOJT[1,3], VÁCLAV ŽALUD[2], JAN NOVÁK[1], FRANTIŠEK VOŽEH[2], VLADIMÍR VETTERL[1,3]

1 INSTITUTE OF BIOPHYSICS, CZECH ACADEMY OF SCIENCES, KRÁLOVOPOLSKÁ 135, 612 65 BRNO, CZECH REPUBLIC
2 CHARLES UNIVERSITY IN PRAGUE, FACULTY OF MEDICINE IN PILSEN, DEPARTMENT OF PATOPHYSIOLOGY, LIDICKÁ 1, 301 66 PLZEŇ, CZECH REPUBLIC
3 DENTAL RESEARCH CENTER, MASARYK UNIVERSITY, VINAŘSKÁ 6, 603 00 BRNO, CZECH REPUBLIC

Abstract

We examined the viability of bacteria Escherichia coli and yeast Saccharomyces cerevisiae after their exposure to radio-frequency electromagnetic field. The frequency of the field was f=867 MHz, the maximal power was 10W and the maximal duration of irradiation was 48min. The exposure took place at laboratory temperature. We measured the viability using optical spectrography of microbial culture in broth and we also used the CFU (colony forming units) counting on agar plate. We observed the decrease of viability both for bacteria and yeasts. According to our previous results for ELF-EMF the electromagnetic field effect showed the saturation and the viability decrease of bacteria was bigger compared to decrease in viability of yeasts.

Introduction

High frequency electromagnetic fields (HF-EMF), very often called as radio-frequency (RF), are electromagnetic fields with frequency in the range of GHz. It consists of GSM range (0.9-2.1 Ghz) and microwaves (up to 3000 GHz) The wave length in vacuum is from 0.33m – 0.1 mm.
The effect of high frequency electromagnetic fields on living organisms is subjected to research. The importance of investigation growths with increasing use of different high-frequency devices, mainly cell phones, that produce potentially harmful radiation. Controversy and contradiction still surround the question whether HF-EMF cause any detectable biological effects. In spite of great deal of results it is necessary to observe that it is often difficult to obtain a good repeatability of data among different laboratories, thus generating conflicting results about possible effects. It is important to perform all experiments in well-defined experimental conditions. Searching in the databases we must have on mind that the results depend on the power of electromagnetic field, on the examined cells or tissue, on the duration of exposure and on the other parameters. We can bring in works showing the HF-EMF effects (1-3), or showing no EMF effect (4,5) on living organisms.

Electromagnetic fields can have negative effects on human. International Commission on Non-Ionizing Radiation Protection, part of WHO, estimated on the base of plenty scientific studies the exposure limit for HF-EMF SAR=0.4W/kg (6). There are not clear evidences whether long-term exposures under the limit are harmful for health. The mechanism of acting is not still clarified. The possible way to understand it could be experiments on microorganisms in vivo.

Microorganisms – bacteria and yeasts seem to be good biological objects to study electromagnetic fields effects. Bacteria, their life cycle and metabolic paths are well-examined and described. Short replication time enable us

to study more bacterial generations. Similar properties have also yeasts. They are the simplest eucaryotic organisms. Using microorganisms we study effects both on cell level and the reaction of the whole organisms. The EMF effects on bacteria has been studied for many years (7-10).

In our previous studies we applied low-frequency electromagnetic fields (50 Hz, Bm=10mT, duration of exposure till 1h) on different bacterial strains (for example *Escherichia coli, Leclercia adecarboxylata, Staphylococcus aureus...*) and on the yeasts (S*accharomyces cerevisiae*). We observed the decrease of viability of exposed bacteria and yeasts. The decrease was strain-dependent, the effect was higher for rod-like bacteria, spherical bacteria were more resistant to electromagnetic field exposure (11-15).

In this work we used HF-EMF on the same microorganisms. The electromagnetic field was the same as was for exposure of neurodefective C3H mices. The acute effect of HF EMF on the central nervous system excitation and inhibition and some histochemical (NADPH diaphorase) and immunohistochemical (c- Fos) characteristics were investigated. The acute exposure to HF EMF had no significant effect on these parameters but the long-term irradiation (3hours daily, 1-2 months, 880MHz) had. (16). The exposure induced the difference in NADPH-diaphorase activity in hippocampus in C57B1/7 mice and shifted spontaneous cortical and LTH hippocampal activities to lower frequencies (17).

Experimental

Bacteria

Bacteria *Escherichia coli* K12 Row, genotype 58-161 *metB1*rpsL 1^{+} F^{def}(P.Fredericq) from Department of biology of Faculty of Medicine of Masaryk University Brno (Czech Republic) were used. Bacteria were cultivated in TY broth (8 g tryptone, 5 g yeast extract – HiMedia Lab, Bombay; 5 g NaCl –Lachema Brno/ 1 l water). The growth in closed system took place in laboratory temperature (25°C)

Yeasts

The prototrophic tetraploid strain *α/A* of yeast *Saccharomyces .cerevisiae* CCY 21-4-59 (yeast collection, Institute of Chemistry, Slovak Academy of Science, Bratislava) was used. Yeast cultures were grown in Malt extract Broth (2% Malt extract broth – Fluka, 2% Glukose – Lachema Brno) laboratory temperature (25°C). Number of microorganisms was determined using spectrophotometry.

For all experiments fresh yeasts and bacteria cultures were used.

Spectrophotometry

Spectrophotometer Libra S 22(Biochrom) was used to measure optical density (OD) at the wavelenghts 570 and 620nm. As a reference sample the distilled water was used. The calibration curve was repeatedly measured by taking values of OD_{570} or OD_{620}. and counting of corresponding number of CFU (see bellow). The logarithmic calibration curves were calculated by the method of minimal squares from 36 measured data.

HF-EMF Exposure

Electromagnetic field was generated by HF generator with HF amplifier. Frequency of the field was 867 Hz (close to the frequencies used in mobile phones). The wave (TEM 111) was directed by a waveguide to the place of exposure). The power output was 10W. The system microorganisms in broth were exposed 4.5-5h since its inoculation to field with SAR=2W/kg. The density of cells during the exposure was approximately 10^6 cells/ml.

Statistics

The data are collected from 5 experiments. Each experiment consists of 3 measurements. The Student's statistics (P=0.95) and t-test were used to analyse.

Results and discussion

Bacteria *E.coli* were exposed to electromagnetic field for 12min, 24min and 48 min. Fig. 1 shows the growth curve of bacteria. The number of bacteria is expressed in units optical density (OD), it means relative absorbance of bacterial culture compared with the absorbance of reference (water). Time T=0 h marks the beginning of exposure. The decrease of number of bacteria in solution was observed for all exposed samples. The decrease of viability is adequate to duration of exposure.
Yeasts *S.cerrevisiae* were exposed to electromagnetic field by the same way as bacteria. The growth curves are presented on Fig. 2. Comparing growth curves *E.coli* and *S.cerevisiae* we can observe smaller effect of EMF on yeasts. The significant changes in growth curve were observed for 24 min and 48 min exposures.

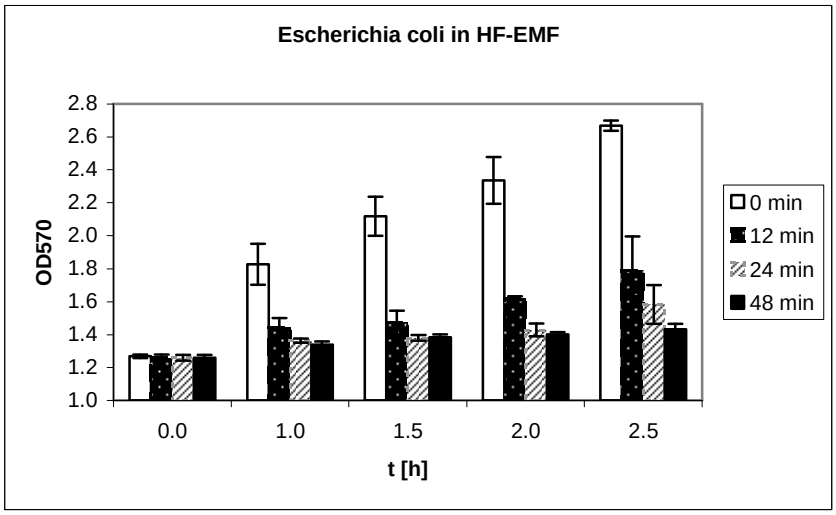


Fig.1. *Growth curves of bacteria E.coli after magnetic field exposures.*

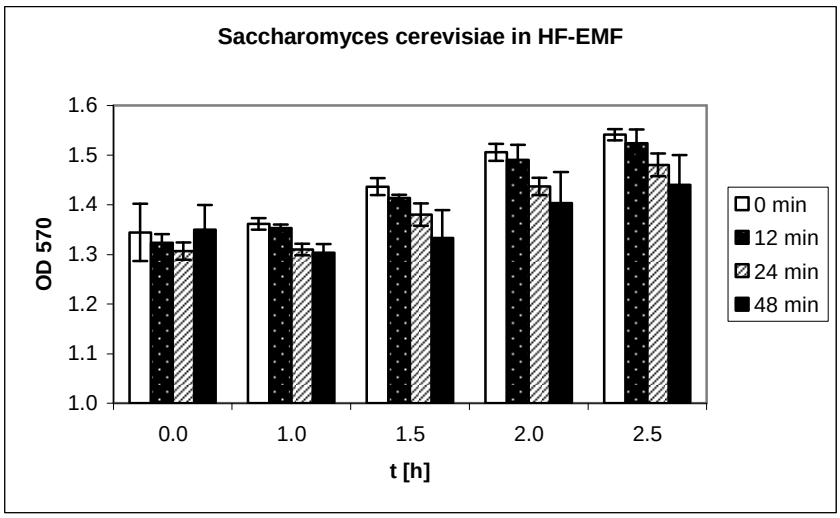


Fig.1. *Growth curves of yeast S.cerevisiae after magnetic field exposures.*

These results show that
a) EMF decreases the number of cells in broth.
b) EMF effect is stronger in bacteria cells
c) the decrease of the number of cells is apparent in the first serie of measurement after exposure.
d) the number of cells in affected cultures is growing with time, but the growth is slower than in control culture.
e) the effect of HF-EMF on the observed parameters is similar to the effect of ELF-EMF (11-13)

From the results it seems that EMF kill part of cells in broth. The growth of affected cultures is retarded by the smaller initial number of cells continuing to division process. The next progress of exposed cultures continues by the normal way, with the same rate of division.

It would be useful to perform the experiments measuring the number of cells during the EMF action.

References

1) M.H. Repacholi, A. Basten, V. Gebski, D. Noonan, J. Finnie and A.W. Harris, Lymphomas in Eμ-Pim1 transgenic mice exposed to pulsed 900 MHz electromagnetic fields, Radiat Res 147 (1997), 631–640.
2) B. Junkersdorf, H. Bauer and H.O. Gutzeit, Electromagnetic fields enhance the stress response at elevated temperatures in the nematode Caenorhabditis elegans, Bioelectromagnetics 21 (2000), 100–106.
3) T. Miyakawa, S. Yamada, S.-I. Harada, T. Ishimori, H. Yamamoto and R. Hosono, Exposure of Caenorhabditis elegans to extremely low frequency high magnetic fields induces stress responses, Bioelectromagnetics 22 (2001), 333–339.
4) T.D. Utteridge, V. Gebski, J.W. Finnie, B. Vernon-Roberts and T.R. Kuchel, Long-term exposure of Eμ-Pim1 transgenic mice to 898.4 MHz microwaves does not increase lymphoma incidence, Radiat Res 158 (2002), 357–364.
5) .D. Utteridge, V. Gebski, J.W. Finnie, B. Vernon-Roberts and T.R. Kuchel, Long-term exposure of Eμ-Pim1 transgenic mice to 898.4 MHz microwaves does not increase lymphoma incidence, Radiat Res 158 (2002), 357–364.
6) ICNIRP Guidelines, Guidelines for limitting exposure to time-varying electric, magnetic, and electromagnetic fields, ICNIRP, Health Physics, 74(1998), 494-522
7) Goldblith S.A., Wang D.I.C. Effect of microwaves on Escherichia coli and bacillus subtilis. Appl. Microbiol. 15(6) (1967), 1371-1375.
8) Belyaev Y., Alipov Y.D., Shcheglov V.S., Lystsov V.N. Resonance effect of microwaves on the genome conformational state of E.coli cells. Z. Naturforsch. 47C (1992), 621-627.
9) Atmaca S., Akdag Z., Dasdag S., Celik S. Effect of microwaves on survival of some bacterial strains. Acta Micr. Immun. Hungarica 43(4) (1996), 371-378.
10) Yeo C.B.A., Watson I.A., Stewart-Tull D.E.S., Koh V.H.H. Heat transfer of Staphylococcus aureus on stainless steel with microwave radiation. Journal of Applied Microbiology 87 (1999), 396-401.
11) Strašák L., Vetterl V., Šmarda J., Effects of low-frequency magnetic fields on bacteria Escherichia coli, Bioelectrochemistry and Bioenergetics 55(2002)161-164
12) Fojt L., Strašák L., Vetterl V., Šmarda J., Comparison of the low-frequency magnetic field effects on bacteria Escherichia coli, Leclercia adecarboxylata and Staphylococcus aureus, Bioelectrochemistry 63 (2004), 337-341
13) Strašák, L, Fojt L., Vetterl, V, Šmarda, J., Effects of low-frequency magnetic fields on the living organisms, Proceedings of Biological effects of EMFs, 3rd International workshop, Kos, Greece, 4.-.8.10.2004, Ed: P.Kostarakis, p.944-949.
14) Strašák L, Vetterl V, Fojt L., Effects of 50 Hz magnetic fields on the viability of different bacterial strains,ELECTROMAGNETIC BIOLOGY AND MEDICINE,24, 293-300, 2005
15) Novák J., Strašák L., Fojt L. , Slaninová I.Vetterl V.,Effects of low-frequency magnetic fields on the viability of yeast Saccharomyces cerevisiae, Bioelectromagnetic, in press 2006
16) Cendelín J., Schmidtmayerová B., Štenglová V., Vožeh F., CNS excitability in normal and neurodefective C3H mices exposed to high-frequency electromagnetic field, Proceedings of Biological effects of EMFs, 3rd International workshop, Kos, Greece, 4.-.8.10.2004, Ed. P.Kostarakis, p.866-871
17) Vožeh F., Barcal J., Cendelín J., Korelusová I., Štenglová V., Žalud V., The effect of high-frequency electromagnetic field on some brain function in healthy and neurodefective mice, Proceedings of Biological effects of EMFs, 3rd International workshop, Kos, Greece, 4.-.8.10.2004, Ed. P.Kostarakis, p.1113-1120

MAGNETIC FIELDS IN PUBLIC TRANSPORTATION IN CZECH REPUBLIC

JAN NOVÁK[1] , LUDĚK STRAŠÁK[1,2], LUKÁŠ FOJT[1,2], VLADIMÍR VETTERL[1,2]

1 INSTITUTE OF BIOPHYSICS, CZECH ACADEMY OF SCIENCES, KRÁLOVOPOLSKÁ 135, 612 65 BRNO, CZECH REPUBLIC
2 DENTAL RESEARCH CENTER, MASARYK UNIVERSITY, VINAŘSKÁ 6, 603 00 BRNO, CZECH REPUBLIC

Abstract

There is a lot of epidemiological studies showing possible effects of magnetic fields on the living systems. The ICNIRP limit for maximal magnetic field exposure was established by WHO to protect people before not-fully understood and not-fully proved harmful magnetic field effect on human. The public transportation is a place where we meet magnetic fields.

We measured magnetic fields in tramways, trolleys and buses in Brno city, tramways, trolley and buses in Ostrava city and subway and tramways in Prague. In addition the magnetic fields in intercity trains were measured.

Our results stated that the measured values do not exceed the ICNIRPs limit.

Introduction

Man-made low-frequency magnetic fields became an important part of our environment. They occur in our biosystem everywhere where low-frequency electric field is produced. Magnetic field exposure is in vicinity of electric equipments including electric engines in means of public transport. The passenger are exposed to magnetic fields. The ICNIRP (International Committee for Non Ionising Radiation Protection) limits of magnetic field exposure are highly protective and are based on all the available scientific evidence. For 50 Hz field is limit ICNIRP 100 μT (1).
The passenger's magnetic field exposures were studied in London *(2)* and in Toronto *(3)*. Our study shows the results from public transportation in three cities in Czech Republic to determine whether the ICNIRP limit is fulfilled and to compare magnetic fields in different means of transport.

Experimental

The EnviroMentor Magnetic Field Meter BMM-3000 (produced by EnviroMentor AB, Sweden) was used for used for measurement of magnetic induction.
The device is able to measure magnetic field in low-frequency range 5 - 2000 Hz and five induction ranges (200 nT-2 mT).

Tramways:

T3 (m=16 000 kg, P= 4 x 40 kW, capacity 110 passengers, 1961-1990, produced by Tatra ČKD Smíchov, Czech Republic, measured in Brno, line 1),

K2 (m=21 800 kg, P= 4 x 40 kW, capacity 157 passengers, 1966-1989, produced by Tatra ČKD Smíchov, Czech Republic, measured in Brno, line 1, 4),

KT8D5 (m=38 000 kg, P= 8 x 45 kW, capacity 231 passengers, 1999 –, produced by Tatra ČKD

Smíchov, Czech Republic, Brno, measured in line 1) and

Anitra (m=24 200 kg, P= 4 x 90 kW, capacity 155 passengers, 2000-present, produced by Škoda Plzeň, Czech Republic, measured in Brno, Ostrava, lines 1).

Trolleys:

14Tr and 14TrM (m= 10 000 kg, P= 2x100 kW, capacity 145 passengers, 1974-1984, produced by Škoda Ostrov, Czech Republic, measured in Brno, line 30),

15 Tr (m= 15 900 kg, P= 100 kW, capacity 80 passengers, 1983, produced by Škoda Ostrov, Czech Republic, measured in Brno line 26 and Ostrava line 104) and

22 Tr (m= 18 000 kg, P= 2x132 kW, capacity 140 passengers, 2002, produced by Škoda Ostrov, Czech Republic, measured in Brno line 26).

Metro trains:

81-717.1 (m= 33 500 kg, P= 4x110 kW, capacity 260 passengers, 1977-1990, produced by Mitishchinsky engineering factory, Soviet Union, measured in Prague lines A, B)

2MT (m= 31 000 kg, P= 110 kW, capacity 262 passengers, 1996-present, produced by Škoda Plzeň, Czech Republic, measured in Prague lines A, B)

M1 – Siemens (m= 27 900 kg, P= 141.5 kW, capacity 284 passengers, 2000-present, produced by Siemens AdTranz,, Czech Republic, measured in Prague line C)

Intercity train:

Pendolino 680 (m= 385 000 kg, P= 4000 kW, capacity 333 passengers, 2003, produced by Alstom Ferroviaria, Italy, route Prague – Děčín - Prague).

Results

Tramways

Totally 12 600 values, 3012 during stops, 9588 operating. The maximal value of magnetic induction was 7.23 μT (operating) or 1.16 μT (standing).

Trolleys

4369 data, 1030 – standing, 3339 – operating. The maximal value was 3.23 μT (operating) or 1.03 μT (standing).

Metro

10136 data, 2269 – standing, 7867 – operating. The maximal value was 8.17 μT (operating) or 0.09 μT (standing).

Train

6648 measured values. The maximal value was 0.14μT (operating) or 0.002 μT (standing).

The comparison of all used means of public transport is summarized in Fig.1. The maximum peak value was measured in metro (8.17 μT), then it decreased in order tramway>trolley>train (0.139 μT). The different order is if we take in the account average value. In that case trolleys have the biggest induction (3.18 μT) and than tramway>metro>train (0.002 μT).

The average values of different means of transportation differ depending on the type of tram, trolley or metro. It depends also on the external sources of magnetic fields, on the driver's style and on the profile of track. The engine draws maximal electric energy during acceleration or during breaking. In other cases the train uses inertia. The maximal values of magnetic induction are reached in a very short time just before changes in its velocity.

As for magnetic field exposure, the public transportation in Czech Republic is safe. All data are below ICNIRP limit, which is 100 μT for 50Hz fields.

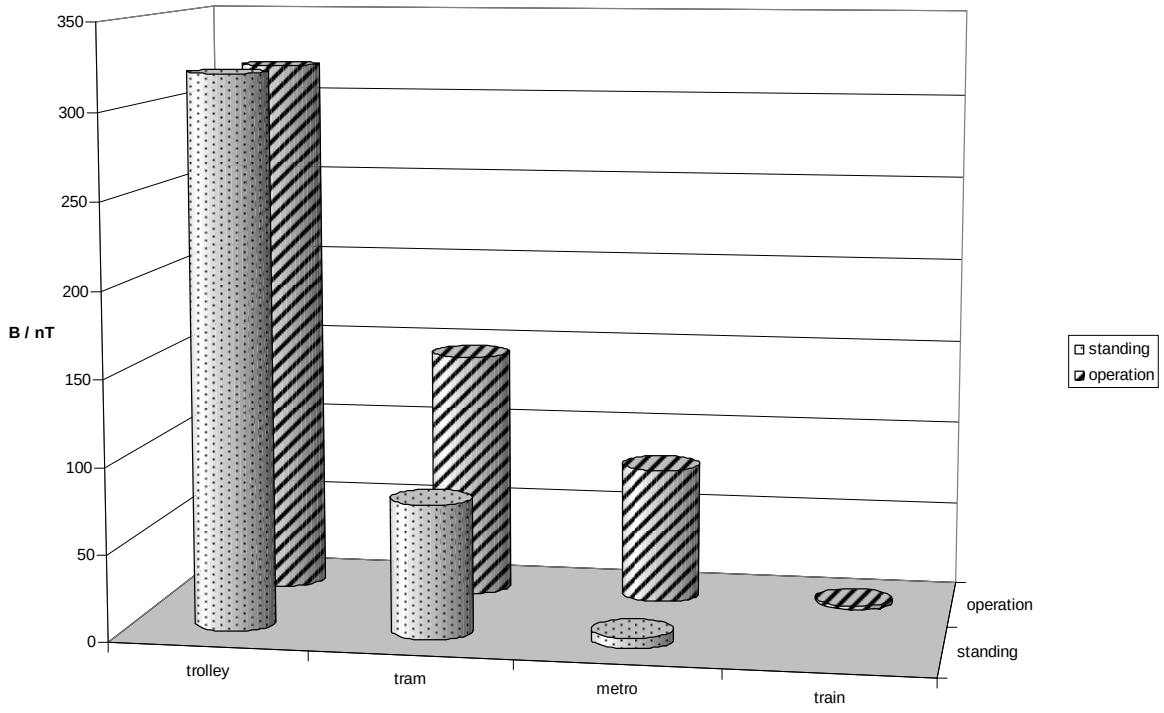


Fig.1 *Comparision of average values of magnetic induction in different means of public transport***.**

		Number of data	Max (nT)	Min (nT)	Median (nT)	Mode (nT)	Average (nT)	Stdev (nT)	Confidence (95%) (nT)
tram	stop	3012	1160	0	50.0	20.0	77.6	90.0	3.2
tram	operating	9588	7230	0	80.0	20.0	145.1	273.7	5.5
trolley	stop	1030	2230	0	220.0	0.0	319.6	334.7	20.4
trolley	operating	3339	3230	0	230.0	10.0	318.2	353.2	12.0
metro	stop	2269	90	0	2.0	0.0	6.4	11.1	0.5
metro	operating	7867	8170	0	20.0	10.0	80.1	242.6	5.4
trains	operating	6680	139	0	0.3	0.2	1.7	5.8	0.1

Tab.1:Review of all measurements. Mode = the most often measured value, Stdev= standard deviations, Confidence = The error of measurement (Student's distribution)

References

1) ICNIRP Guidelines, Guidelines for limitting exposure to time-varying electric, magnetic, and electromagnetic fields, ICNIRP, Health Physics, 74(1998), 494-522

2) Chadwick F., Lowes F., Magnetic fields on British Trains. Annual Hygienic Occupational 1998;42: 331-335

3) Havas M., Shum S., Dhalla R., Passenger exposure to magnetic fields on go-trains and on buses, streetcars, and subways run by the Toronto transit comission. In: Proceedings of Biological effects of EMFs, 3rd International workshop, Kos, Greece, 4.-.8.10.2004, Editor P.Kostarakis, p.1065-1071

TRANSIENT EFFECTS OF RF-EMF EXPOSURE ON THE BRAIN MICROCIRCULATION IN EITHER JUVENILE OR ADULT RATS.

TAKAHASHI M. [1], HIROTA S.[1], MASUDA H. [1], USHIYAMA A. [1], TANAKA S. [2], KAWAI H. [2], WAKE K. [2], WATANABE S. [2], TAKI M. [3] and OHKUBO C. [4]

[1]Dept. of Environmental Health, National Institute of Public Health, 2-3-6 Minimi, Wako-shi, Saitama 351-0197, Japan. [2] Electromagnetic compatibility group, applied electromagnetic research center, National Institute of Information and Communications Technology, 4-2-1 nukui-kitamachi, koganei, Tokyo 184-8795, Japan. [3]Dept. of Electrical and electronic Engineering, Tokyo Metropolitan University, 1-1 minami-osawa, hachioji, Tokyo 192-0397, Japan. [4]RAD, World Health Organization, Geneva CH1211, Switzerland.

Abstract

The aim of the present study is to investigate whether radio frequency electromagnetic fields (RF-EMF) exposure induces acute effects on brain microcirculation being transiently observed only during RF-EMF radiation period in juvenile rats. As a model of juvenile and adult rats, we used 4 and 8 weeks old male Sprague-Dawley rats, respectively. All rats were subjected to cranial window implantation prior to the experiments and intravital-microscopic observation under anesthesia. Rat's head in RF group was locally exposed to 1,457MHz electromagnetic near-field by an ‘‘8’’-shaped loop antenna. RF-EMF exposure intensity was maintained at an averaged SAR (2.0W/kg) in parietal targeted area. Three microcirculatory parameters (BBB-function, plasma velocities, and vessel diameters) in pial venules were measured every 10 min for 50min exposure period. In 4 weeks juvenile rats, no changes in any of the three microcirculatory parameters were elicited by the RF-EMF exposure. No statistical changes were recognized between those values obtained from RF group and sham exposed group. These negative effects in juvenile rats were also confirmed in adult rats. The results reveal that there were no RF-EMF exposure effects at least on our measured brain microcirculatory parameters in either juvenile or adult rats under the present exposure conditions.

Introduction

Possible adverse health effects of radiofrequency electromagnetic field (RF-EMF) exposure during mobile phone uses on the brain are one of the public health concerns, especially, the effects on the developing brain in the children. However, few studies have evaluated this possible effect using juvenile animals. Our previous studies focused on the brain microcirculation during RF-EMF exposure, and showed no noticeable change in parameters including blood-brain barrier function, vessel diameters or plasma velocities was found in adult rats. The aim of the present study is to investigate whether RF-EMF radiation affects the brain microcirculation in juveniles or not.

We used 4-week-old male Sprague-Dawley rats as juvenile animals. The rats were divided into two groups: RF group was exposed to RF-EMF and Sham group was not exposed to any RF-EMF. All rats were subjected to cranial window implantation prior to the exposure experiments and intravital-microscopic observation under anesthetic. To compare the results of juvenile animals with those of adult animals, we also performed the same preparation and experiments in 8-week-old SD rats.

Rat heads were locally exposed to 1,457MHz electromagnetic near-field TDMA (time division multiple access) signal for PDC (Personal Digital Cellular, Japanese cellular telephone standard) systems by the ‘‘8’’-shaped loop antenna placed 4 mm upward to the cranial window. RF-EMF exposure was maintained at 2.0 W/kg of the averaged SAR in parietal targeted area (Table 1).

Table 1 Averaged SAR (W/kg)

Age	Target area	Whole brain	Whole body
4-week-old	2.0	0.59	0.057
8-week-old	2.0	0.54	0.032

The pial microcirculation within cranial windows was observed using a fluorescent microscope equipped with an EBCCD camera. In order to measure four microcirculatory parameters, BBB function, plasma velocities, leukocyte behaviours, and arteriole vasomotion, we used rhodamine 6G for leukocyte behaviours and FITC-Dx (70k or 2000k) for the other three parameters.

We prepared two experimental protocols. Arteriole vasomotion was observed for 12 min experimental period including 3 min RF-EMF exposure. The other three microcirculatory parameters, BBB-function, plasma velocities, and leukocyte behaviours in pial venules were measured every 10 min during 80 min experimental period including 50 min RF-EMF exposure. The results were compared between RF and Sham group. The statistical analysis was performed by Student's t-test or ANOVA.

BBB permeability was evaluated by extravasation of FITC-Dx (70kDa) from pial microvessels. After intravenous injection of FITC-Dx, the fluorescence intensities of brain surface area (0.74 mm^2) were measured every 10 min during pre- and during RF exposure period. As a result, there was no significant difference in the intensity changes between sham and exposed group in either juvenile or adult rats (Figure 1).

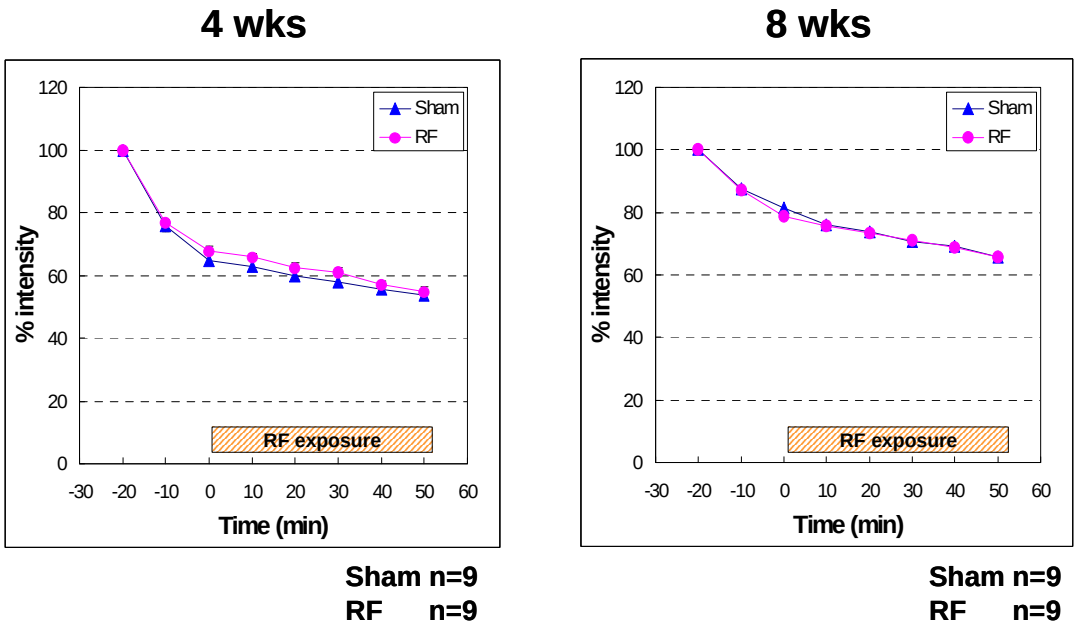


Figure 1 BBB permeability changes during RF-EMF exposure

The numbers of rolling and sticking leukocytes stained with rhodamine 6G were counted at 0, 10, 20, 40 min after RF exposure. As a result, no significant difference in these counts was found between sham and exposed group even in juvenile rats.

The velocities of plasma flowing in the pial venules were measured using Dual-Slit technique. We compared the velocities of each period with those of 20 min before RF exposure. But there was no significant difference in the plasma velocity between sham and exposed group even in juvenile rats.

The arteriolar vasomotion was monitored pre-, during, and post- RF exposure. As a index for dynamic changes in the vasomotion, we calculated the mean values of arteriolar diameter for each experimental period and showed them as a relative (%) diameter of pre-exposure. As a result, no significant difference in the arteriole diameter was found between two groups even in juvenile rats.

Conclusions

The results reveal that there were no effects of RF-EMF exposure on brain microcirculatory parameters, at least on BBB-function, leukocyte behaviours, blood flow or arteriolar vasomotion, in either juvenile or adult rats under present exposure conditions.

Acknowledgments

This study was financially supported by The Committee to Promote Research on the Possible Biological Effects of Electromagnetic Fields, Ministry of Internal Affairs and Communications, Japan.

INFLUENCE ON THE TRANSIENT EVOKED OTOACOUSTIC EMISSION BY GSM 915 MHZ ELECTROMAGNETIC FIELDS: COMPARATIVE ANALYSIS BETWEEN CONTROL AND EXPOSED GROUPS

MARTINES F.[(1)], MARTINES E.[(2)], TINE' G.[(3)], *Member IEEE*

(1), (2): UNIVERSITY OF PALERMO – DIPARTIMENTO DI BIOTECNOLOGIE MEDICHE E MEDICINA LEGALE – SEZ. DI AUDIOLOGIA, PIAZZALE DELLE CLINICHE 5 – 90126 PALERMO, ITALY
(3): COUNCIL NATIONAL RESEARCH (CNR), – ISTITUTO DI STUDI SUI SISTEMI INTELLIGENTI PER L'AUTOMAZIONE, VIA DANTE 12 – 90141 PALERMO, ITALY

Abstract
To evaluate the possible alterations of the human cochlear activity to the GSM 915 MHz electromagnetic fields (EMF) exposition in a significant statistically human subjects group, the transient evoked otoacoustic emissions (TEOAEs) have been measured.
130 volunteers took part in the experiment; they were randomly divided into two groups (group X, exposure to EMF consisting of 85 people; group Y, control consisting of 45 people) and underwent TEOAEs measurements two times. Participants were healthy young adults (18–40 years old) without any evidence of hearing or ear disorder. In group X the TEOAEs were recorded before and throughout 6 minutes EMF exposition (average power irradiated: 1Watt), while for group Y the TEOAEs were recorded for two consecutive intervals of six minutes without EMF.
The TEOAEs were measured in the time domain while the corresponding analysis have been carried out by the estimate of the density power spectrum relating to each waveform using the Welch's method. Comparing the results obtained in the case-control groups the variations of the density power spectrum found in the exposed subjects are not significant statistically respect to ones in the control group. Therefore the external hair cells activity is not modified by GSM cellular phones.

Introduction
The explosive increase in the use of mobile phones during the last years has aroused suspicions about their adverse effects on human health. Normally the cellular phone antenna is positioned near the human head and in particular close the ear causing a part of the electromagnetic energy emitted from the antenna to be absorbed by the auditory apparatus. Some authors studied the interaction between the electromagnetic fields (EMF) generated by cellular phone and inner ear, in particular the cochlear outer hair cells measuring the otoacoustic emission in humans [1], [2] [3]. Sometimes significant variations on the otoacoustic emission due to the presence of the electromagnetic fields have been reported while in other cases any variations has been noticed. In addition to these conflicting results must be considered that in the studies above reported the number of subjects examined was very low.
In this paper the study of the effects of the electromagnetic fields generated by 915 MHz GSM cellular phones on the otoacoustic emission in a statistically significant number of subjects is reported. The volunteers that took part at the study were divided randomly in two groups: control and exposed group. All the subjects underwent transient evoked otoacoustic emission (TEOAE) measurements. The TEOAE signals are generated by the movement of the outer hair cells on the Corti's organ when the auditory periphery is stimulated by an acoustic click. The TEOAEs are present in 100% of normal hearing subjects and constitute an expression of a normal cochlear functionality. To evaluate the alterations brought on by the EMF on the auditory responses the power spectral density (PSD) estimation of each TEOAE have been calculated. Since these signals are noise corrupted the classic FFT algorithm is not indicated for the PSD estimation but it is advisable to apply the periodogram method and in particular the Welch method. Finally in order to evaluate the presence of statistically significant variations in the exposed group respect to the control group the Chi square test has been carried out.

Experimental procedure and set-up

The OAE are stimulated by the application of a sound stimulus in the ear channel. A rectangular stimulus (click) has been chosen because it is very brief and has a broad-range frequency spectrum, so that a complete and simultaneous stimulation of the Corti's organ can be obtained down its entire length.
The experimental activity was performed using the ILO88 system by Otodynamics. It is composed of analog-to-digital converter, a preamplifier, an acoustic probe (microphone) and software to manage the stimulus and to collect and elaborate data. As the probe position can modify the stimulus' shape, checking the noise floor level, shape, spectrum and intensity level of the stimulus is compulsory. The probe fit was evaluated by measuring the adequacy of stimuli, i.e., flat acoustic spectrum across the frequency range of 0.5 – 5 kHz. The OAEs were obtained with stimuli consisting of clicks of 80 μs duration. The stimulus level in the outer ear was set at 80 ± 3 dB SPL. The click rate was 50 click per second and post-stimulus analysis was in the range of 2 to 20 ms. A total of 700 sweeps, corresponding about 6 minutes, was averaged above the noise rejection level of 47 dB.
The responses were filtered with the use of a II order high pass filter, with cutoff at 500 Hz, and a low pass IV order filter with cutoff at 5 kHz and sample rate of 25000 samples/s for a total of 512 samples. A response is valid if its amplitude is higher than noise floor level plus 3 dB.
The TEOAE was recorded in ASCII files and analysed later with a suitable Matlab® computer programme [4].
The exposition system was composed by: a vector signal generator SMIQ02B by Rohde&Schwarz for the generation of the TDMA mobile radio standard signals as GSM, GSM-EGDE etc., operating in the 300 kHz - 2.2 GHz frequency range; to amplifier the signal generated at the desired level a 5 W linear amplifier, operating in the frequency range 860 MHz – 960 MHz, it was cascade connected to the signal generator; to measure the transmission and reflection power from the antenna a mobile power measurement, with NRT sensor and PC card adapter NRT-Z4 by Rohde&Schwarz, it was interposed between the amplifier and the antenna; at the end of the generation and transmission chain a short dipole antenna to radiate the signal was connected. The positioning of the antenna near the ear was realized by a suitable plastic support mounted on an modified earphones.
The average power at the antenna input was fixed to 1 Watt and the exposition frequency at 915 MHz.

Subjects

130 subjects volunteers took part in the investigation; they were informed in detail about the purpose and procedures of the study and a written informed consent was obtained. Participants were healthy young adults (18–40 years old) without any evidence of hearing or ear disorder, corresponding to the ISO standard definition of otologically normal to exclude middle ear pathology that may impair OAE measurements.
The rationale was to test a group that was representative of the population of young otologically normal people. Absence of pre-existing hearing or ear disorder maximizes the sensitivity of the study to detect small changes that may occur. Acceptance as participants was based on otoscopy, audiometry by air conduction (0.5, 1, 2, 3, 4, 6, 8 kHz) and bone conduction (0.5, 1, 2 kHz), tympanometry and acoustic reflex testing, and a simple screening questionnaire concerning medical and otological history.
The subjects were randomly divided into two groups (group X, exposure to EMF consisting of 85 people; group Y, control consisting of 45 people) and underwent TEOAEs measurements twice. In group X the TEOAEs were recorded before and throughout 6 minutes EMF exposition (average power irradiated: 1Watt), while for group Y the TEOAEs were recorded for two consecutive intervals of six minutes .

Signal detection

To analyse TEOAEs, the signals revealed by the microphone are averaged by time-locking to the transient stimuli and alternatively storing them into two separate buffers (A and B). Thus each of the two waveform A and B (see Fig.1) corresponds to an average of 700 accumulated responses without any intervening time lag.
The two waveforms of each signal collected in separate buffers were cross correlated by means of a product moment correlation coefficient. The entity of correlation is considered as a measure of the response reliability and hence as a score of the functional efficiency of the auditory system. In the ILO88 test, an correlation index, called "Repro", between two waveforms of an OAE signal is considered. An index value > 70 % is considered as physiological, therefore if this condition should not occur the examination would not have considered.
In Fig. 1 two waveforms related to TEOAE response with "Repro"=90% is shown. Each waveform is composed by 512 points graphically interpolated and the differences among the waveforms A and B are due to the noise overlapped to the signals.

Power spectrum density estimation

In order to quantify the TEOAE response alterations the power spectral density (PSD) estimate associated with

each TEOAE has been calculated. There are several approaches to calculate PSD estimates; the most widely used PSD method analysis it is based on the application of the well know FFT algorithm while other use the periodogram method which is know as classic way to estimate PSD.
Widely, the PSD estimate of a time varying signal is obtained by computing first the frequency spectrum of the sampled data through the Discrete Fourier Transform (DFT) then the square module amplitude of the frequency spectrum. In case of signal corrupted by noise it is appropriate to compute power spectral density estimate of the signal using the Bartlett and Welch periodogram methods [5]. These methods make no assumption about how data was generated and, hence, are called nonparametric [6].

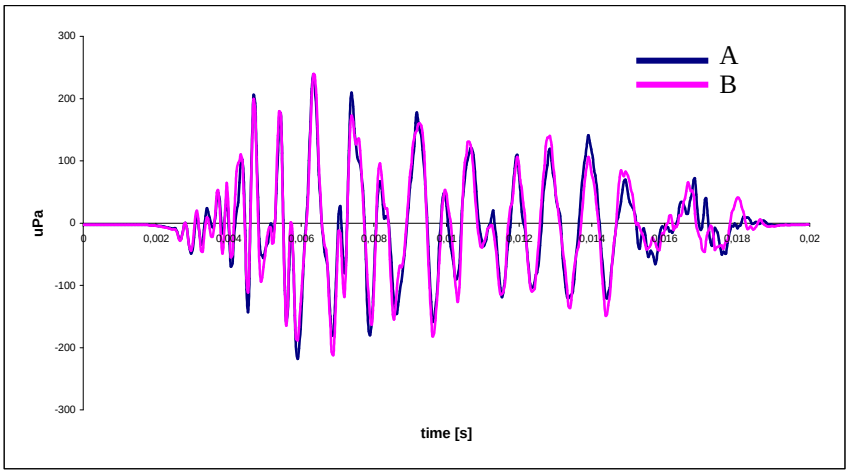


Fig. 1. Waveforms of a click evoked otoacoustic emission signal: A and B are two waveforms of a typical TEOAE signal recorded by the ILO88 system.

In the Bartlett method the N-point time domain sequence x(0), x(1), x(2),……, x(N-1) is divided into P no overlapping segments, where each segment has length D.
For each segment, the periodogram is computed and the Bartlett power spectral density estimate is obtained by averaging the periodograms for the P segments, as in the following formula:

$$S_B(f)=\frac{1}{P}\sum_{p=0}^{P-1}\frac{1}{DT}\left|T\sum_{n=0}^{D-1}x^{(p)}[n]\exp(-j2\pi fnT)\right|^2 \qquad (1)$$

By this averaging of the spectrum the variance of the spectrum estimation is reduced by a factor P, however at the expense of a reduction of the frequency resolution by a factor P.
Welch has modified Bartlett's method by using windowed data segments overlapping in time. The overlapping is used for further reducing the periodogram variance while the windowing is applied to reduce the spectral leakage associated with finite observation intervals. The frequency spectrum calculated by the Welch periodogram is given by:

$$S_w(f)=\frac{1}{P}\sum_{p=0}^{P-1}\frac{1}{UDT}\left|T\sum_{n=0}^{D-1}w[n]x^{(p)}[n]\exp(-j2\pi fnT)\right|^2 \qquad (2)$$

U is the discrete-time window energy of the used window function w[n] as defined as follow:

$$U=T\sum_{n=0}^{D-1}w^2[n] \qquad (3)$$

In our case the Welch method has been applied with a 50% overlapping and Hamming window selected.
In Fig.2 an example of PSD estimate computed by the Welch's method is shown. It has been calculated using a Matlab® software toolbox with A and B TEOAE signals as input data. The numerical computation output are two column vectors called [$P_x^{(A)}$ (f)] and [$P_x^{(B)}$ (f)] with dimension 256x1. The elements of [$P_x^{(A)}$ (f)] and [$P_x^{(B)}$ (f)] represent the power spectrum density estimates calculated for each frequency value of the column vector [f] of same dimension.

The example reported in Fig.2 shows the Power Spectrum Density (PSD) estimates in Watt/Hertz (W/Hz) vs. frequency (f) in Hertz (Hz) of the TEOAE signals reproduced in Fig.1.

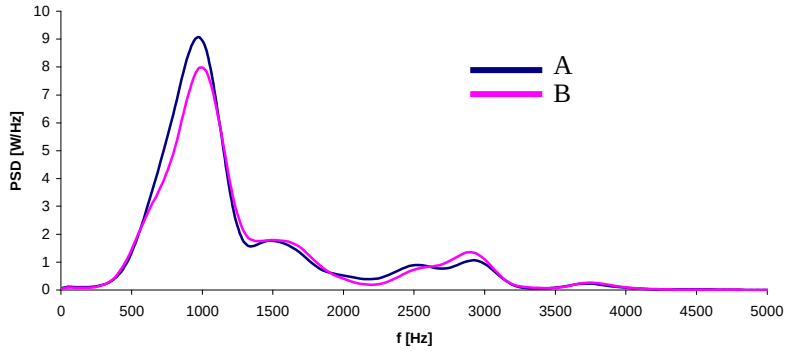


Fig.2. Example of Power Spectral Density estimate computed by Welch's method: these curves are relative to the TEOAE waveforms shown in Fig.1

Data analysis procedure

The data analysis for the exposed group has been carried out following the below procedure:

1. Estimation of the PSD using the Welch's function available on Matlab® software for the A and B TEOAE signals;
2. Evaluation of the average power associated to each signal by numerical integration of $[P_x^{(A)}(f)]$ and $[P_x^{(B)}(f)]$ above the frequency range 500 Hz – 5 kHz;
3. Calculation of the mean between the two power values determined in the previous step and evaluation of the mean relative deviation;
4. Repetition of the steps 1 – 3 considering the TEOAE registered in presence of electromagnetic fields;
5. Comparison between the means calculated with and without EMF;
6. The difference computed in the 5 step is defined "Significant" when its absolute value is greater than the addition of the relative deviations calculated in the two cases with and without EMF.

As regard the data analysis of the control group the procedure is the same of the exposed group with the only difference that the subjects are not exposed to EMF.

Results

In Tab.I an example of the numerical result obtained applying the first 5 steps of the above procedure is reported. In particular the average power for the two TEOAE signals relative to a single subject in both the exposition and no exposition conditions are calculated. Moreover the mean and the mean relative deviation it is also computed for both conditions. All the power values are expressed in decibel (dB).

Tab.I – Example of average power calculated for a single subject with and without EMF

Subject XXX	Average power signal A [dB]	Average power signal B [dB]	Mean [dB]	Mean relative deviation [dB]
No exposed	37,47	37,73	37,60	± 0,13
Exposed	37,98	37,72	37,85	± 0,13

In order to compare the results obtained in the two conditions the difference between the means has been calculated and the result is shown in Tab.II, where "Mean (NoEx)" indicates the mean of the average powers in the 'no exposed' condition while "Mean (Ex)" indicates the mean of the average powers in 'exposed' condition.

Tab.II – Difference of the means and "Significant" variation test

Subject XXX	Absolute value difference [dB]	"Significant" variation
Mean (NoEx) – Mean (Ex)	0,24	NO

In the same table the result of the "Significant" variation test is also reported. In the test, the absolute value of the

difference is compared with the addition of the relative deviations respect to the corresponding means obtained in the two condition above mentioned. The result of the test is a Boolean variable which value is "YES" when the difference absolute value is greater than the addition of the relative deviations. In the example shown in Tab.I the addition of the relative deviations is 0,26 dB while the difference absolute value is 0,24 dB, thus in this case the test response is "NO".
Repeating the procedure for all the subjects included in the exposed and control groups the results obtained are summarized in Tab.III and Tab.IV respectively.

Tab. III – Exposed group: summary sheet	
Subjects number	85
"Significant" differences number	58 (68,2%)
"No Significant" differences number	27 (31,8%)

Tab. IV – Control group: summary sheet	
Subjects number	45
"Significant" differences number	25 (55,6%)
"No Significant" differences number	20 (44,4%)

Analysing the above results an greater cases number with TEOAE response alterations in the exposed group (68%) respect to control group (55,6%) it has been obtained. Besides in the control group, in absence of EMF, more than 50% presents a "Significant difference" probably due to the random noise overlapped to the TEOAE signal.

Statistical analysis

The results do not clear up if the TEOAE alterations founded in the exposed group was really in correlation to the typical GSM electromagnetic field, so a statistical comparison of the results obtained in the two group it is necessary.
In our case the Chi square test is indicated. Chi square is a non-parametric test of statistical significance for bivariate tabular analysis. Any appropriately performed test of statistical significance lets us know the degree of confidence we can have in accepting or rejecting an hypothesis. Typically, the hypothesis tested with Chi square is the null hypothesis [7]. In our case it establish that the two groups (exposed and control groups) are not different enough respect to their behaviour in presence of EMF.
The first step in the building the Chi square test is the data summary in a table (as shown in Tab.V) where in the rows the independent variables and in the columns the dependent variables are reported. In this analysis the two groups are considered the independent variables while the results of the computation analysis on the TEOAE responses are considered the dependent variables

Tab.V – Data summary of the experimental results			
	"Significant" differences	No "Significant" differences	Total
Exposed group	58	27	85
Control group	25	20	45
Total	83	47	130

The expected frequencies for the above data are calculated multiplying the total number of each row for the total number of each column and dividing the result by the subjects total number. The results are shown in Tab. VI.

Tab.VI – Data summary of the experimental results			
	"Significant" differences	No "Significant" differences	Total
Exposed group (**observed**)	58	27	85
Exposed group (**expected**)	54,26	30,73	
Control group (**observed**)	25	20	45
Control group (**expected**)	28,73	16,26	
Total	83	47	130

Before to calculate the Chi square value it is necessary to determine the threshold of tolerance for error. For our purposes we set a probability of error threshold of 1 on 20, or $p < 0.05$. Applying the following formula (4) the Chi square value has been computed:

$$\chi^2 = \sum_{i=1}^{4} \frac{(O_i - E_i)^2}{E_i} \qquad (4)$$

where O_i represent the observed values while E_i the expected values. On the basis of the data reported in Tab.VI the Chi square value is:

$$\chi^2 = 0{,}257 + 0{,}452 + 0{,}484 + 0{,}86 = 2{,}05$$

For significance at the 0,05 level and degree of freedom equal to one, the Chi square should be greater than or equal to 3,84.
Therefore the distribution is not significant and the null hypothesis is not rejected. In other words, the difference between the two groups is not statistically significant respect to their TEOAE responses in presence or not of EMF, so the variations are not ascribable at the electromagnetic fields emitted by the GSM cellular phones but probably to the random noise overlapped to the TEOAE signals.

Summary

A study of the GSM 915 MHz electromagnetic fields effects on the auditory system has been carried out. For the first time the subjects number that taken part in a study of this matter has been statistically significant. 130 healthy young adults volunteers randomly divided into two groups have been considered: group (X) exposed to EMF consisting of 85 people and group (Y), control, consisting of 45 people.
All the subjects have been underwent TEOAEs measurements two times. In particular for the group (X) the TEOAEs were recorded before and throughout 6 minutes EMF exposition (average power irradiated: 1Watt), while for the group (Y) the TEOAEs were recorded for two consecutive intervals of six minutes without EMF.
The TEOAEs measured are composed by two slightly different signals in the time domain. The difference is due at the randomly overlapped noise to the signal. The analysis of the signals have been carried out by the density power spectrum estimate related to each waveform using the Welch periodogram method.
The results shown an greater cases number with TEOAE response alterations in the exposed group (68%) respect to control group (55,6%). Besides in the control group, in absence of EMF, more than 50% of the subjects present TEOAE response alterations probably due to the random noise overlapped at the TEOAE signal
Therefore a statistic analysis has been conducted in order to establish whether the alterations found in the exposed group are correlated with the EMF exposition. Applying the Chi square test the null hypothesis has been tested: the two groups, exposed and control, are not different in their behaviour in presence of EMF.
The test result indicates that the distribution is not significant and the null hypothesis is not rejected. In other words, the difference between the two groups is not statistically significant respect to their TEOAE responses in presence or not of EMF, so the variations are not ascribable at the electromagnetic fields emitted by the GSM cellular phones but probably to the random noise overlapped to the TEOAE signals

References

[1] Grisanti G., Parlapiano C., Tamburello C., Tinè G., Zanforlin L.: "Cellular phones effects on otoacoustic emissions", Microwave Symp. Digest IEEE MTT-S Int. 2, pp. 771-774, 1998.
[2] Ozturan O., Erdem T., Miman M.C., Kalcioglu M.T., Oncel S. : "Effects of electromagnetic field of mobile thelephones on hearing", Otolaryngology 122, pp. 289-293, 2002.
[3] Parazzini M., Bell S., Thuroczy G., Molnar F., Tognola G., Lutman M.E., Ravazzani P. : "Influence on the mechanisms of generation of distorsion product otoacoustic emision of mobile phone exposure", Hearing Research 208, pp. 68-78, 2005
[4] Matlab Editor, Version 7.0.0, The Mathworks, Inc.
[5] Marple S.L. : "Digital spectral analysis with applications", Prentice-Hall, ISBN 0-8493-7892-3, 1987.
[6] Proakis J.G., Manolakis D.G. :" Digital signal processing principles, algorithms and application", 3rd ed., New Delhi, India, Prentice-Hall, 2002.
[7] Papoulis A., Pillai U.S.: "Probability, random variables and stochastic processes", McGraw Hill, 2002.

EPIDEMIOLOGICAL STUDY TO ASSESS THE RISK OF RF-EMFS FROM MOBILE TELEPHONY

RAVINDRA TIWARI[1*], AHUJA YR[2], BHARGAVA SC[3], LAKSHMI NK[1]

[1] Bhavans New Science College, Narayanguda, Hyderabad, Andhra Pradesh, India.
[2] Director, Department of Genetics and Molecular Medicine, Vasavi Medical and Research Center, Khairthabad, Hyderabad, Andhra Pradesh, India.
[3] Head, Dept of Electrical and Electronic Engineering, MGIT, Gandipet, Hyderabad, Andhra Pradesh, India.
*** Corresponding Author**

Abstract

Modernization has led to increased proliferation of various electronic and electrical equipment in all fields of human life including domestic, industrial, the fast expanding information technology sector and above all wireless telecommunication. The increasing use of mobile telephony in our society has brought focus and great concern on the health effects of EMFs. A number of epidemiological, *in vitro*, *in vivo* studies have shown conflicting, inconclusive and controversial reports. Considering the scientific evidence from the current scenario, the objective of this epidemiological study was planned to assess the genotoxic potential of RF-EMF exposure from mobile telephony (800-900MHz). 100 subjects using mobile telephones for more than three years, were compared with 80 age and sex matched controls. The statistical data indicated in our study, involving Comet assay showed a lesser significance in exposed subjects compared to controls. The hormonal profile of melatonin is supportive to our study, possibly envisaging the role of the hormone in EMFs stress. Lipid Peroxidation assay also substantiated the DNA damage via oxidative stress. The comparatively lesser significance reported from our findings may have large implications with chronic exposure, emphasising the need for health concern, amidst the environmental hazard of this invisible electromagnetic pollution.

Introduction

The radiofrequency (RF) signals emitted from mobile phones are considered as a type of non-ionizing electromagnetic radiation and are perceived as health risk. More focus has been brought on the potential effect of RF-EMFs to elicit biological response, in association with its detrimental effects on widespread application and long-term induction. The biological effects as a result of RF exposure include changes in cell membrane function, metabolism, cellular signal communication, activation of protooncogenes and cell death. There are scientific evidences on the health hazards due to RF-EMFs, like neurodegenerative disorders, brain tumors and cancer. Most of these reports are inconclusive and no convincing data has been established on causal relation between RF and health risk.

Mobile phone has become the fastest selling consumer product with about 1.6 billion users worldwide and 76 million users in India, contributing to 8% of the population. To date, few epidemiological studies have directly examined the relationship of mobile phones to genomic instability. With a need to arrive at a scientific consensus, an attempt has been made to study the genomic instability on human subjects exposed to mobile phones operating at 800-900MHz.The subjects using mobile phones for more than 2 years were screened with age and sex matched controls with similar socioeconomic status (non-smokers, non-alcoholics). The frequency and duration of mobile phone use along with the model and type of phone with specific absorption rate (SAR) were taken into account.

The whole body exposure of mobile phone radiation is hypothesized to result in structural rearrangement of DNA and increase in number of single-strand and double strand DNA breaks. The DNA damage was observed using

single cell gel electrophoresis SCGE (comet assay) in which the leukocytes were isolated, placed on a microscope slide, lysed, eventually electrophoresed and silver stained. The DNA fragmentation was assessed from the DNA migration path length or comet tail length.

The potentially hazardous effects of electromagnetic fields on melatonin rhythm disturbances remain to be elucidated. The physiological relevance of melatonin could be important in the explanation of the RF-EMFs effect via oxidative stress. The RF fields may induce oxidative stress that has been implicated with increase in free radicals, which mainly enhance lipid peroxidation. To substantiate lipid peroxidation, the level of malonyl dialdehyde (MDA) in plasma and RBCs was measured.

Methodology

DNA Integrity

Single cell gel electrophoresis or Comet assay (Singh *et al*, 1998) was used to study DNA damage. Leukocytes suspended in low-melting agarose were embedded on to a pre-coated layer of normal melting agarose and layered again with low-melting agarose. The cells were treated in lysing solution for overnight and then incubated in alkaline electrophoresis buffer for 20 minutes to facilitate DNA unwinding and expression of alkali labile sites. Electrophoresis was carried out for 30minutes at 300mA at 0.67V/cm and then neutralized using Tris buffer. Silver stain technique was followed to visualize and measure migration path length. 200 cells per treatment was measured in duplicates. Mean$\pm$SD of DNA damage was calculated.

Melatonin Levels

Competitive enzyme immunoassay was performed for the quantitative determination of melatonin in plasma (IBL kit. Germany). The sealed ELISA plate consisting of equal proportion of sample (standard, subject and controls), melatonin-biotin and antiserum was incubated overnight at 2-8˚C. The plates washed thrice with assay buffer and enzyme conjugate was added (1:5) and incubated for 2 hours at room temperature. After incubation, washing step was repeated and substrate p-nitrophenyl phosphate (PNPP) added to incubate for 20 minutes. Stopping solution was then added to end the substrate reaction. Optical density was read at 405nm.

Lipid peroxidation assay

Lipid peroxidation was estimated by measuring the stable end product, malondialdehyde(MDA) in plasma (Lef'evre *et al*, 1998) and RBCs (Armstrong and Browne, 1994). The protein free plasma was treated with thiobarbituric acid that forms a 1:2 adduct measured at 535nm with spectrophotometer. Mean and ± SD or SE was established for the samples. The concentration of MDA equivalents in nmol/ml in samples were interpolated from the standard curve.

Results & Discussion

The findings from our epidemiological study show, some statistical significance in the DNA migration path lengths, of the exposed subjects when compared with the controls. The SCGE (Comet assay) demonstrated a mean of comet tail length for control group as 6.63 $\pm$ 0.120 and for the subjects as 8.26 $\pm$ 0.092. Phillips (1998) reported, DNA single strand breaks exposed to cellular telephone frequency at 813.5 MHz and 836.5 MHz. The protocol and findings for evaluating the DNA breaks is similar and supportive to the present study. Similarly, Gandhi and Anita (2005) employed SCGE assay for assessing genetic damage in mobile phone users being exposed to 800-2000 MHz and reported a significant increase in DNA tail length and micronuclei. The Swedish-Norwegian epidemiological study concluded a statistical significance between mobile phone users and prevalence of certain bioeffects (Mild *et al* 1998). The *in vitro* study performed by Diem *et al* 2006 indicated a stronger non-thermal DNA breakage effect, in intermittent exposure by mobile phone radiation at 1800MHz. A dose dependent increase in DNA strand breaks from microwave RF at low intensity levels as evaluated by Lai and Singh (1995, 1996) indicate a casual relationship between RF exposure and genetic damage. Many controversial findings report on non-cooperative action between the RF-EMF exposure and induced DNA damage (Annemarie *et al* 2006).

Few epidemiological studies reported an increased risk of brain tumors among analogue cellular phone users (Hardell *et al* 2003). Repacholi *et al* (1997), conducted mice studies using 900 MHz mobile phone frequency radiation and found a statistically significant 2.4 fold increase in lymphoma. On the contrary, Heynick's (2003) report on epidemiological studies showed no indication of *in vivo* and *in vitro* exposure of RF field and cancer.

Currently, there is insufficient evidence to assess an association between RF exposure and brain cancer, leukaemia, or lymphoma (ICNIRP, 2004).

The sleep disruption related to radiofrequency radiation hypothesized from our findings for melatonin relevance has been reported in several scientific studies (Lai and Singh 1998, Burch *et al* 2002). Mann *et al* (1996) and Loughran *et al* (2005) observed that a radiofrequency radiation, similar to digital mobile phones reduced sleep in humans altering the EEG (brain wave) signals.

The increase in free radical production for LPO activity shows a statistical significance (Table 1) in the exposed population compared to those unexposed. This observation is similar to the data published by Stopczyk *et al* 2005.

Despite both negative and positive findings about the biological effects of radiofrequencies, certain more long term studies, better conceived and supported by, *in vitro* experimentations would envisage the possible cumulative effects on general health. Further, the lag periods that have been examined are short, where if a longer lag period of about 10 years is required for a health effect to occur, it would not be possible in short exposures and the results will be difficult to interpret.

Table 1: RBC and Plasma markers of Oxidative stress for Lipid Peroxidation (MDA)

MDA (nm/mL)	Control Group	Exposed Population
RBC	0.20 ± 0.07	0.28 ± 0.10
Plasma	0.21 ± 0.1	0.42 ± 0.2

Data in terms of Mean $\pm$ SD; Significant * $P<0.001$

Summary

Mobile telephony, the integral unit of modern telecommunication and third generation wireless technology, relays information with RF signals. The extensive use of mobile telephones has given rise to public concern about the possible health effects that the whole-body exposure to RF signals may have. There is a wide spread conviction that electromagnetic emissions from mobile phones were capable of significant biological tissue interactions. The temperature increase is insignificant to cause direct effect but certain scientific reports document increase in DNA strand breaks and chromosomal damage in cells. The non-thermal resultant effects do include increased free radical production, cell stress and premature aging, changing in brain function, neurodegenerative conditions, reduction in melatonin secretion and cancer.

This epidemiological study, assesses the long-term human health risk from RF-EMF exposure for genomic instability. Some individuals have reported to experience certain non-specific symptoms such as sleeplessness, fatigue and headache. The levels of melatonin and the oxidative stress marker, MDA could substantiate in hypothesizing the correlation of non-specific symptoms and whole body exposure to mobile phones. The effects of the RF-EMFs on genomic instability determined by SCGE assay in our study showed lesser statistical significance from the control population. The results are expressed in terms of an estimate of relative risk, ie the multiplier by which risk is higher in people exposed to the RF-EMF of mobile telephony than in unexposed group. However, the findings and scientific interpretations drawn from this epidemiological study about the potential risk from mobile telephony might not be sufficient to arrive at a consensus. But possible implications on long term and chronic exposure to mobile phone use could be made.

Acknowledgement

The authors acknowledge the generosity of the UGC, New Delhi, India for the sanction of Major Project without which this attempt would not have been completed.

Reference

1. Annemarie Maes, Urbain Van Gorp and Luc Verschaeve. Cytogenetic investigation of subjects professionally exposed to radiofrequency radiation Mutagenesis. 2006, 21(2):139-142.
2. Armstrong, D. and Browne, R. The analysis of free radicals, lipid peroxidases, antioxidant enzymes and compounds related to oxidative stress as applied to the clinical chemistry laboratory. Free Radicals in Diagnostic Medicine, 1994, 366:46.
3. Burch JB, Reif JS, Noonan CW et al. Melatonin metabolite excretion among cellular telephone users. Int J Radiat Biol 2002, 78:1029–1036.
4. Diem E, Schwarz C, Adlkofer F, Jahn O, Rudiger H Non-thermal DNA breakage by mobile-phone radiation (1800 MHz) in human fibroblasts and in transformed GFSH-R17 rat granulosa cells in vitro. Mutat Res. 2006, 603(1):104 -106.
5. Gandhi Gursatej, Anita. Genetic damage in mobile phone users: some preliminary findings. Indian Journal of Human Genetics. 2005, 11 (2): 99-104.
6. Hardell L, Mild KH, Carlberg M. Further aspects on cellular and cordless telephones and brain tumors. Int J Oncol. 2003, 22: 399-407.
7. Heynick LN, Johnston SA, Patrick A, Mason PA. Radio frequency electromagnetic fields: Cancer, mutagenesis, genotoxicity. Bioelectromagnetic. 2003,24: 74-100.
8. ICNIRP Report. Epidemiology of health effects of radiofrequency. Environ Health Perspect. 2004, 112 (17): 1741-1754.
9. Lai H and Singh NP. Acute low intensity microwave exposure increases DNA single-strand breaks in rat brain cells. Bioelectromagnetics. 1995,16:207-210.
10. Lai H and Singh NP. Single-and double-strand DNA breaks in rat brain cells after acute exposure to radiofrequency electromagnetic radiation. International Journal of Radiation Biology. 1996, 69:513-521.
11. Lai H, Singh NP. Melatonin and a spin-trap compound block radiofrequency electromagnetic radiation-induced DNA strand breaks in rat brain cells. Bioelectromagnetics. 1998, 18(6): 446 – 454.
12. Lef'evre G., et.al. Evaluation of lipid peroxidation by measuring thiobarbituric acid reactive substances. Annals de Biologie Clinique. 1998, 56(3): 305-319.
13. Loughran, Sarah P, Wood, Andrew W., Barton, Julie M., Croft, Rodney J., Thompson, Bruce b, Stough, Con. The effect of electromagnetic fields emitted by mobile phones on human sleep. SLEEP Neuroreport. 2005, 16(17): 1973-1976.
14. Mann K and Roschke J. Effects of pulsed high-frequency electromagnetic fields on human sleep. Neuropsychobiology. 1996, 33: 41-47.
15. Mild KH Oftedal G Sandstrom M Wilen J Tynes T Haugsdal B and Hauger E, 1998. Comparison of symptoms experienced by users of analugue and digital mobile phones. A Swedish-Norwegian epidemiological study. National Institute for Working Life. 1998, 23. Umea, Sweden.
16. Oktem F, Ozguner F, Mollaoglu H, Koyu A, Uz E. Oxidative Damage in the Kidney Induced by 900-MHz-Emitted Mobile Phone: Protection by Melatonin. Arch Med Res. 2005, 36(4): 350-355.
17. Phillips J, Ivaschuk Ishida-Jones T, Jones R, Campbell-Beachler M, Haggren W. DNA damage in Molt-4 T-lymphoblastoid cells exposed to cellular telephone radiofrequency fields in vitro. Bioelectrochemistry and Bioenergetics. 1998, 45: 103-110.
18. Repacholi MH Basten A Gebski V Noonan D Finnie J and Harris AW. Lymphomas in Eμ-Pim 1 transgenic mice exposed to pulsed 900 MHz electromagnetic fields. Radiation Research. 1997, 147: 631-640.
19. Singh NT, Mc Coy NT, Tice RR, Schneider A. A simple technique for quantification of low levels of DNA in individual cells. Experimental cell research. 1998, 517: 184-191.
20. Stopczyk D, Gnitecki W, Buczynski A, Markuszewski L, Buczynski J.Effect of electromagnetic field produced by mobile phones on the activity of superoxide dismutase (SOD-1) and the level of malonyldialdehyde (MDA)--*in vitro* study Med Pr. 2002, 53(4): 311-314.

THE EFFECT OF RF FIELDS ON GERMINATION AND GROWTH OF *LACTUCA SATIVA, LYCOPERSICUM ESCULENTUM* AND *ALLIUM CEPA*

MIRTA TKALEC[1], KREŠIMIR MALARIĆ[2], ŽELJKA VIDAKOVIĆ-CIFREK[1], BRANKA PEVALEK-KOZLINA[1]

[1]UNIVERSITY OF ZAGREB, FACULTY OF SCIENCE, DEPARTMENT OF BIOLOGY, ROOSEVELTOV TRG 6, HR-10000 ZAGREB, CROATIA
[2]UNIVERSITY OF ZAGREB, FACULTY OF ELECTRICAL ENGINEERING AND COMPUTING, UNSKA 3, HR-10000 ZAGREB, CROATIA

Abstract

The effects of exposure to radiofrequency fields on germination and seedlings growth were investigated in lettuce (*Lactuca sativa* L.), tomato (*Lycopersicum esculentum* L.) and onion (*Allium cepa* L.). Seeds were exposed to continuous EMF (23 V m^{-1}) at 400 and 900 MHz for 2 and 4 h as well as to modulated field (80% AM 1 kHz sinus) for 2 h in GTEM-cell. At 400 MHz, inhibition of lettuce germination was noticed after 2 h of exposure to continuous RF-EMF while the growth of lettuce and tomato was decreased after 4 and 2 h of exposure, respectively. Contrary, the growth of onion was increased after 2 h of exposure to continuous RF-EMF. At 900 MHz, increased germination of tomato was observed after exposure to modulated field. At this frequency, the growth of lettuce increased after 4 h of exposure to continuous RF-EMF while the growth of onion increased also after exposure to modulated field. On the other hand, the growth of tomato decreased after 2 and 4 h of exposure to continuous RF-EMF. Results indicate that seedlings growth was more sensitive to RF-EMF exposure than germination and that the effects depended on field and exposure characteristics as well as plant species.

INTRODUCTION

Various kinds of radiofrequency electromagnetic fields (RF-EMF) from 30 kHz to 300 GHz are used to transmit information (TV, radio, mobile phones and satellite communications). Although classified as nonionizing, these fields can have various biological effects including changes in the cell membrane's permeability and interferences with ions and molecules like DNA and proteins (Kwee & Raskmark 1998, Kwee *et al.* 2001, Banik *et al.* 2003).
Germinating seeds and seedlings subjected to environmental stresses could failure to cope with the adverse effects which results in poor germination, disturbed seedling development, and eventually reduced crop yields. Only few investigations about effects of RF-EMF exposure on seed germination and early plant growth have been reported so far with various results (Jonas 1952, Nelson & Walker 1961).
In this work the effects of exposure to EMF at 400 and 900 MHz on germination of lettuce (*Lactuca sativa*), tomato (*Lycopersicum esculentum*) and onion (*Allium cepa*) seeds as well as some parameters of seedlings early growth were investigated.

Determination of germination and early growth

Seeds of *Lactuca sativa* L. ("Unicum"), *Lycopersicum esculentum* L. ("Marglobe") and *Allium cepa* L. ("Srebrnjak") were placed in plastic Petri dish on filter paper wetted with distilled water. The Petri dishes were maintained for 12 h at 24 ± 2 ºC in the darkness and then subjected to EMF. During exposure control was kept in the same growth conditions (24 ± 2 ºC, darkness) as seeds exposed to EMF but in the field-free environment. Three replicates of 15 seeds were used in each treatment. Protrusion of the radicle was the criterion used for germinated seed. After germination seedlings were watered every day and their root and shoot length as well as fresh weight was measured after four days (lettuce) or seven days (tomato and onion). All results were expressed as means followed by the

corresponding standard errors. Significant differences between means ($P \leq 0.05$) were established by one-way ANOVA followed by Duncan's multiple range test (STATISTICA 6.0) and presented in the Figures with asterisks (*).

Exposure to radiofrequencies fields

For generation of RF-EMFs Gigahertz Transversal Electromagnetic (GTEM) cell (Fig. 1.) was used (Tkalec *et al.* 2005). In GTEM-cell, electric and magnetic field exist at the same time and they are perpendicular to the wave propagation direction. Besides the GTEM-cell, a signal generator with continuous wave and an amplifier was also needed.
Seeds in plastic Petri dishes were exposed in GTEM cell to the continuous EMFs of 400 and 900 MHz at field strengths of 23 V m^{-1} for 2 and 4 hours as well as modulated EMF (80% AM 1 kHz sinus) for 2 h. Petri dishes were placed in parallel, perpendicular to the electric field, in the area where field was uniform with required field levels (Fig. 2).

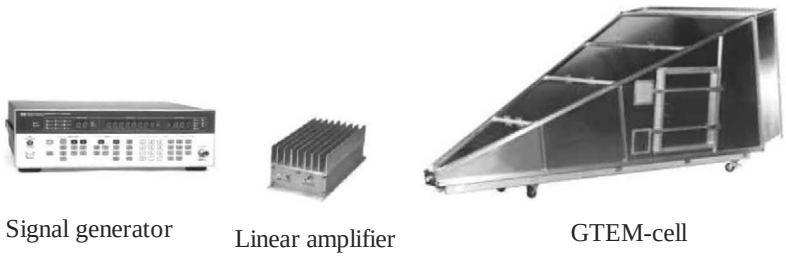


Figure 1. Instruments used for the exposure to RF-EMF: GTEM-cell, HP 8657A signal generator and 5 W MiniCircuits amplifier.

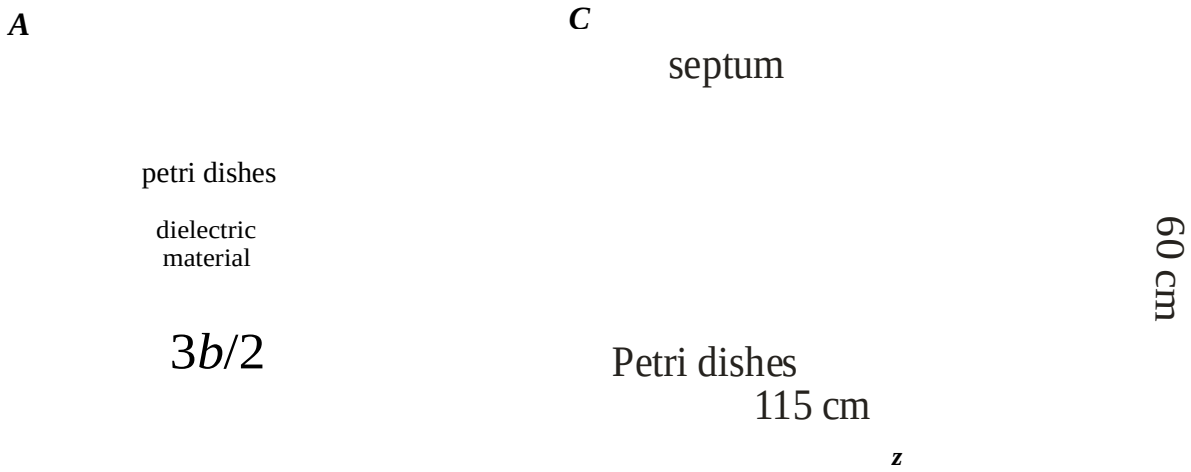


Figure 2. Position of Petri dishes (*d*=9 cm, *h*=1.5 cm) in GTEM-cell: below the septum (A), in respect to the direction of wave propagation, *z* (B).

RESULTS

Seed germination

The exposure of seeds to continuous EMF at field frequency of 400 MHz and strength of 23 V m^{-1} for 4 h as well as to modulated field at the same frequency and strength for 2 h did not have significant effect on germination of lettuce (*Lactuca sativa*), tomato (*Lycopersicum esculentum*) and onion (*Allium cepa*) seeds in comparison with non-exposed seeds. On the other hand, exposure to continuous field at 400 MHz and 23 V m^{-1} for 2 h inhibited lettuce germination (Figure 3A).

The exposure of seeds to continuous EMF at field frequency of 900 MHz and strength of 23 V m^{-1} for 4 h as well as to modulated field at the same frequency and strength for 2 h also did not have significant effect on germination of seeds. The exception was stimulation of tomato germination noticed after exposure to modulated field at 23 V m^{-1} for 2 h (Figure 3B).

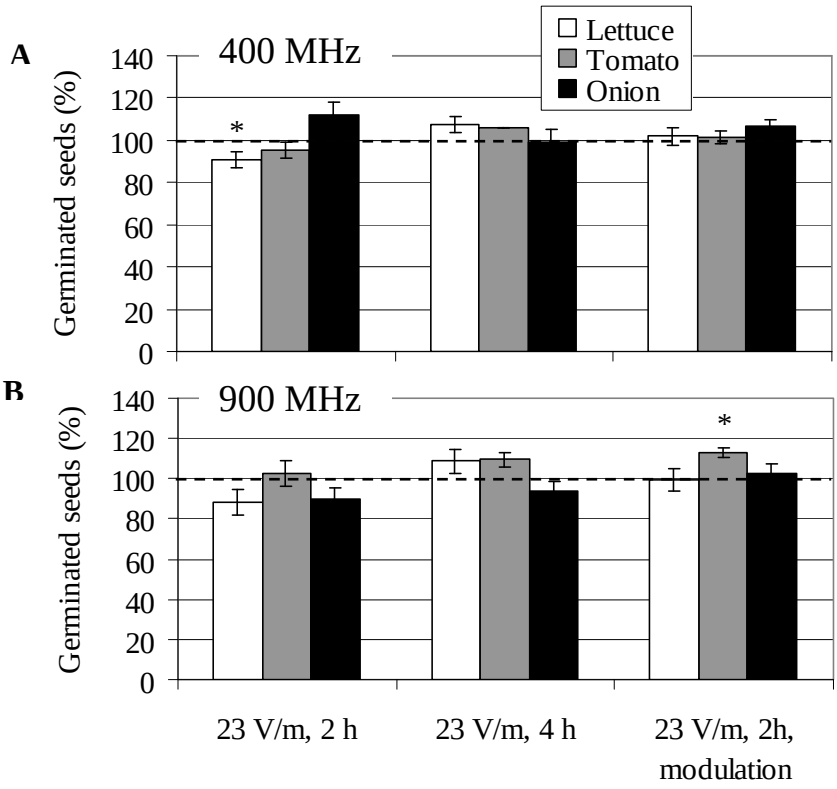


Figure 3. Germinated seeds (%) of lettuce (*Lactuca sativa*), tomato (*Lycopersicum esculentum*) and onion (*Allium cepa*) seeds after exposure at 400 and 900 MHz to continuous field at 23 V m^{-1} for 2 and 4 h and to modulated field for 2 h. Data represent means ± SE (n = 45). Control (non-exposed seeds) is expressed as 100 %. Significant differences between exposed and non-exposed seeds at $P \leq 0.05$ are marked with asterisk (*).

Early growth of seedlings

The growth of lettuce seedlings measured as root and shoots length and seedling fresh weight was neither affected by exposure for 2 h to continuous nor modulated EMF at 400 MHz and 23 V m^{-1}. But, lettuce root length and fresh weight decreased after exposure for 4 h to continuous EMF at the same frequency and strength (Fig 4A).

Root and shoot length and fresh weight of tomato seedlings decreased after exposure for 2 h to the continuous field at 400 MHz and 23 V m^{-1} while exposure to the modulated field and longer exposure to the continuous field at the same frequency and strength did not affect tomato growth significantly (Fig. 4B).

The growth of onion seedlings was not significantly impaired after exposure to EMFs at 400 MHz except increase of shoot length noticed after exposure for 2 h to the continuous field at 23 V m^{-1} (Fig. 4C).

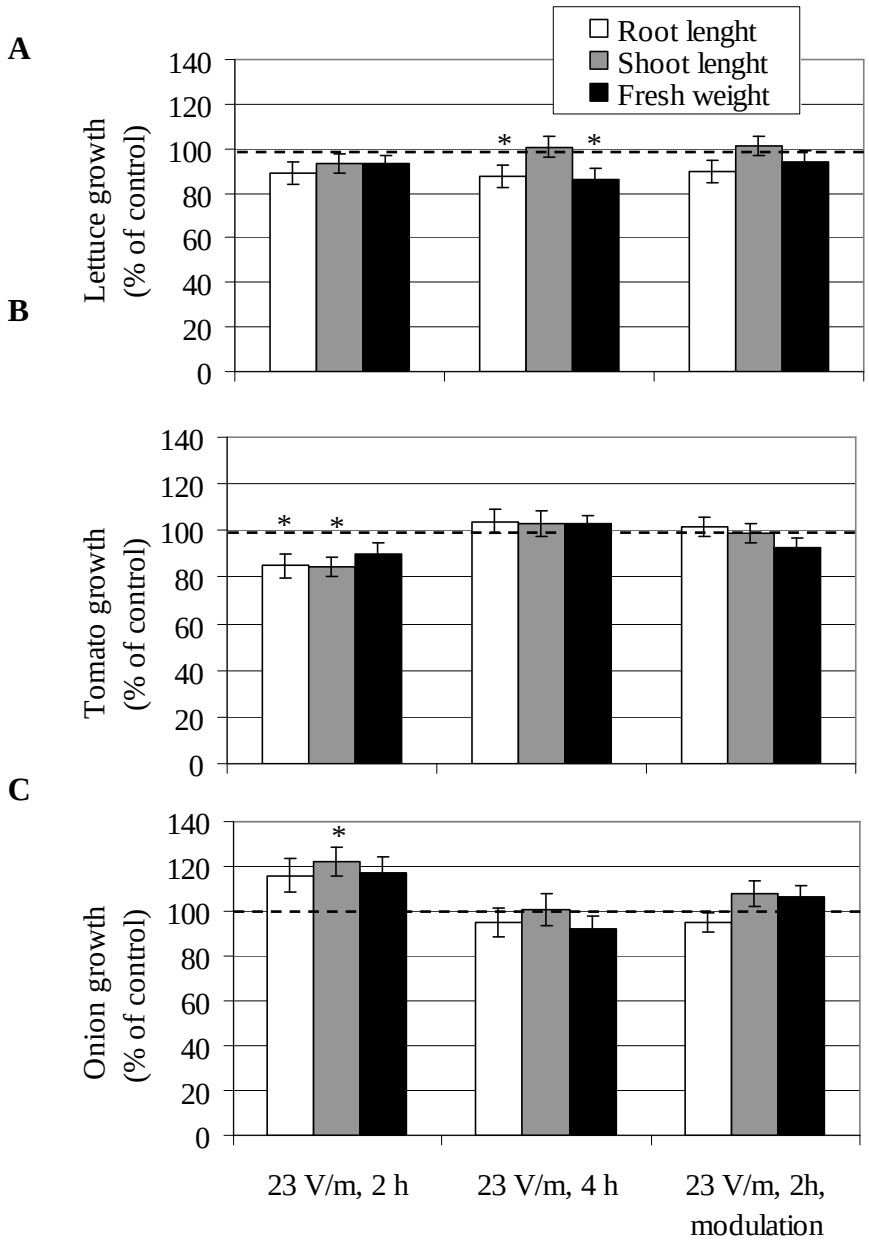


Figure 4. Root and shoot length as well as fresh weight of lettuce (A), tomato (B) and onion (C) seedlings after exposure at 400 MHz to continuous field at 23 V m^{-1} for 2 and 4 h and to modulated field for 2 h. Data represent means ± SE (n = 45). Control (non-exposed seeds) is expressed as 100 %. Significant differences between exposed and non-exposed seeds at $P \leq 0.05$ are marked with asterisk (*).

At 900 MHz the early growth of lettuce seedlings, similarly as at 400 MHz, was neither affected by exposure to continuous nor modulated field at 23 V m^{-1} for 2 h. However, at this frequency, lettuce shoot length and fresh weight significantly increased after exposure for 4 h to continuous EMF (Fig 5A).

The growth of tomato seedlings measured as fresh weight significantly decreased after exposure for 2 h to continuous field at 900 MHz and 23 V m^{-1}, similarly as after exposure at 400 MHz, but at this frequency longer exposure to the field had the same effect (Fig. 5B).

The growth of onion seedlings at 900 MHz, like lettuce growth, significantly increased after exposure for 4 h to the continuous field at 23 V m^{-1} as well as after exposure to modulated field (Fig. 5C).

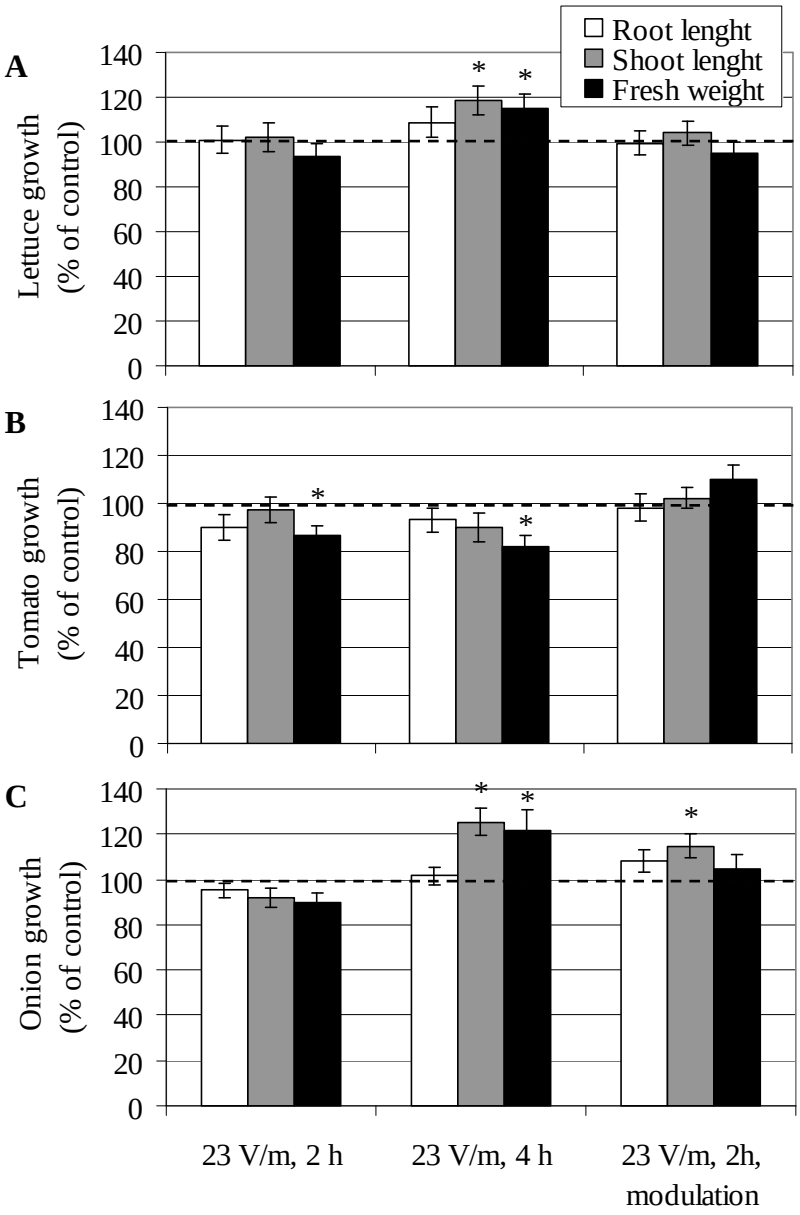


Figure 5. Root and shoot length as well as fresh weight of lettuce (A), tomato (B) and onion (C) seedlings after exposure at 900 MHz to continuous field at 23 V m^{-1} for 2 and 4 h and to modulated field for 2 h. Data represent means ± SE (n = 45). Control (non-exposed seeds) is expressed as 100 %. Significant differences between exposed and non-exposed seeds at $P \leq 0.05$ are marked with asterisk (*).

Summary

The effect of radiofrequency electromagnetic fields (RF-EMF) on seeds germination and early plant growth has been investigated. At 400 MHz, the exposure to continuous field at 23 V m^{-1} for 2 h inhibited the lettuce germination while longer exposure decreased the growth of lettuce seedlings. At this frequency after 2 h of exposure to the continuous field growth of tomato seedlings was decreased, but the growth of onion seedlings significantly increased. At 900 MHz, germination of tomato seeds was increased after exposure to modulated field at 23 V m^{-1} as well as the growth of onion seedlings. The growth of lettuce and onion seedlings significantly increased after 4 h of exposure to continuous field at this frequency while, on the other hand, the tomato growth decreased after 2 and 4 h of exposure. Obtained results indicated that seedlings growth was more sensitive to RF-EMF exposure than germination and that the effects of RF exposure on plant germination and growth could be positive as well as negative depending not only on field and exposure characteristics but on plant species as well.

References

Banik S, Bandyopadhyay S, Ganguly S. 2003. Bioeffects of microwave-a brief review. Bioresource Technol. 87:155-159.

Jonas H. 1952. Some effects of radio frequency irradiations on small oilbearing seeds. Physiol. Plant. 5:41-51.

Kwee S, Raskmark P. 1998. Changes in cell proliferation due to environmental non-ionizing radiation 2. Microwave radiation. Bioelectrochem. Bioenerg. 44:251-255.

Kwee S, Raskmark P, Velizarov S. 2001. Changes in cellular proteins due to environmental non ionizing radiation. I. Heat-shock proteins. Electro Magnetobiol. 20:141-152.

Nelson SO, Walker ER. 1961. Effects of radio-frequency electrical seed treatment. Agric. Eng. December:688-691.

Repacholi MH. 2001. Health risk from the use of mobile phones. Toxicol. Lett. 120:323-331.

Tkalec M, Malarić K, Pevalek-Kozlina B. 2005. Influence of 400, 900 and 1900 MHz electromagnetic fields on Lemna minor growth and peroxidase activity. Bioelectromagnetics 26:185-193.

ACUTE EFFECTS ON OXIDATIVE STRESS MARKERS OF HIGH FREQUENCY ELECTROMAGNETIC FIELD 900 AND 1800 MHz IN RATS- PRELIMINARY EXPERIMENTS

L.Traikov[1], G.Lawlor[3], A.Bocheva[2], V.Hajimitova[1], C.Shalamanova[4], M.Israel[4], H.Koshimizu[5], M.Markov[6]

1- Department of Medical Physics and Biophysics, Faculty of Medicine, Medical University-Sofia , Sofia-1431, Bulgaria

2- Dept. Pathophysiology, Faculty of Medicine, Medical University-Sofia, Sofia-1431, Bulgaria

3-Department of Environmental Health; National Institute of Public Health,

Tokyo-108-8638, Japan

4- Dept. Physical Factors, National Institute of Public Health, Sofia-1431, Bulgaria

5- Department of Human Living System Design, Kyushu University, Fukuoka-815-8540, Japan

6- Research International, Buffalo Office, 135 Arielle Court Apt E, Williamsville NY 14221, USA

Abstract

Over the past 3 decades the actions of Radio-frequency EMF (RF) on biological systems have been examined extensively, concurrently with investigations into the generation of free radicals and reactive oxygen species under stress conditions. Biological systems endure complex environments where countless interactions among myriad different factors are important to our understanding the pathophysiological mechanisms and events by which RF may induce the activation or suppression of natural occurring antioxidant systems.

A total of 75 rats were exposed to 2 frequencies of RF (SAR=0.5 W/kg): (n=25, sham exposure; n=25, 900 MHz; n=25, 1800 MHz). After a 30 min exposure period, blood plasma levels showed increased levels of both catalase (CAT) and superoxide dismutase (SOD) and total glutathione peroxidase (GSH-Px). After initiating RF exposures at 900 MHz and 1800 MHz, animals at each 5 min interval (5min (n=5); 10min (n=5); 15min(n=5); 20min (n=5); 25min (n=5)), showed increasing levels of malondialdehyde (MDA) (lipid peroxidation product). After 10-th minute from the beginning of exposure simultaneous increasing of SOD, CAT and GSH-Px concentrations in rat blood plasma appear. No statistically significant differences in these blood plasma products were observed between the 2 RF exposures used. Our results are in good agreement with previous investigations examining free radical generation in the early stages of EMF exposure. Radio-frequency EMF may affect biological systems by increasing the lifespan of reactive oxygen species.

Introduction

Studies of electromagnetic field promotion of free radical formation are provided widely and significant effects are obtained in low frequencies of electromagnetic field spectrum, which are predominant. According Bordiushkov,IuN, et al. 2000 low frequency EMF, increase 2 fold SOD activity. Katsir,G. and Parola,A.H. 2002 showed indirectly changes of catalase activity by low frequency EMF.

High frequency EMF may affect biological systems by increasing free radicals, which appear mainly to enhance lipid peroxidation, and by changing the antioxidase activities of human blood which leading to oxidative stress.

ACUTE EFFECTS ON OXIDATIVE STRESS MARKERS OF HIGH FREQUENCY ELECTROMAGNETIC FIELD 900 AND 1800 MHz IN RATS- PRELIMINARY EXPERIMENTS

Influence of high frequency EMF on Antioxidant enzymes activity at model systems in vitro correlative analysis of SOD activity and MDA concentration in human blood platelets at 900 MHz exposure for different time intervals have been investigated by Stopczyk,D. [Stopczyk,D. et al 2002; Stopczyk,D. et al. 2005], they obtained significant increase of both levels of MDA and SOD after 7 min exposure.
Again at in vitro experiments Hook,G.J et al. 2004 find out that the levels of activities of superoxide dismutase (SOD), total glutathione peroxidase (GSH-Px) are increased by 847.74 MHz (CDMA) RF EMF.
Other investigations of RF EMF action at systems in vivo with healthy volunteers showed that, after RF EMF exposure lipid peroxide and the activities of superoxide dismutase (SOD), total glutathione peroxidase (GSH-Px) and catalase levels are measured. The results obtained showed that the plasma level of lipid peroxide was significantly increased after 1, 2 and 4 h of exposure to RF EMF. Moreover, the activities of SOD and GSH-Px in human erythrocytes showed significant reduction while the activity of catalase in human erythrocytes did not decrease significantly. These results indicate that acute exposure to RF EMF of commercially available cellular phones may modulate the oxidative stress of free radicals by enhancing lipid peroxidation and reducing the activation of SOD and GSH-Px, which are free radical scavengers. Therefore, these results support the interaction of radiofrequency fields of cellular phones with biological systems [Moustafa,Y.M. et al 2001]

Free radical processes in living organism could be impact by exogenic way as follow:

- direct reducing of abnormal production of ROS by means of antioxidant molecules;
- by inactivation of already formed prooxidants;
- by means of phagocyte inhibitors or by COX inhibitors.

In our experiments we divided experimental animals by groups according time intervals each interval has a 5 min by three investigated groups (Sham, Exposed 900, Exposed 1800 MHz) and estimate four parameters MDA concentration and SOD, CAT, and GSH-Px enzyme activity.

Exposure Mean Enzyme activity Rel.U.	Sham exposed	900 [MHz]	1800 [MHz]
SOD	2.31±0.201	2.66±0.495	3.56±0.172
CAT	2.03±0.201	2.49±0.436	2.56±0.432
GSH-Px	2.42±0.201	2.19±0.695	2.48±0.373

Anti-oxidative activity
Fluorescent analysis were applied for investigation of concentrations of antioxidant enzymes (SOD, CAT, and total GSH) when their concentration where measured we calculated their activity per protein concentration and velocity of substrate catalysis.

TBARS-test (Thiobarbituric Acid Reactive Substances) was applied for in vivo registration of MDA derivates. The influence on the ROS formation in liposome suspensions was investigated by measurement of MDA (malondialdehyde), which is the final product of lipid peroxidation in the same model systems. The sensitivity of TBARS has made this assay the method of choice for screening and monitoring lipid peroxidation, a major indicator of oxidative stress [Armstrong, D. and Browne, R. 1994; Yagi, K, 1998]. Some modifications made possible the application of this rapid procedure at animal biological tissues [Janero, D. 1998]. Despite of some controversy regarding the specificity of TBARS toward compounds other than MDA, the test remains the most widely employed assay used to determine lipid peroxidation [Armstrong, D. and Browne, R. 1994].

According to TBARS-test, MDA is captured by thiobarbituric acid in a colored product comprising 532 nm chromophore by means of condensation presented in Figure 3:

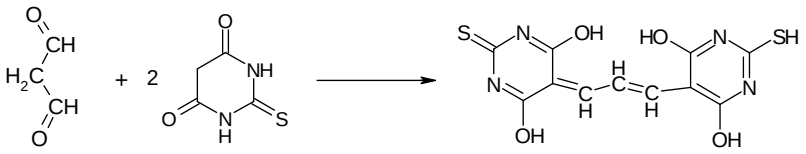


Figure 3. Condensation of TBA with MDA and creation of 532 nm chromophore

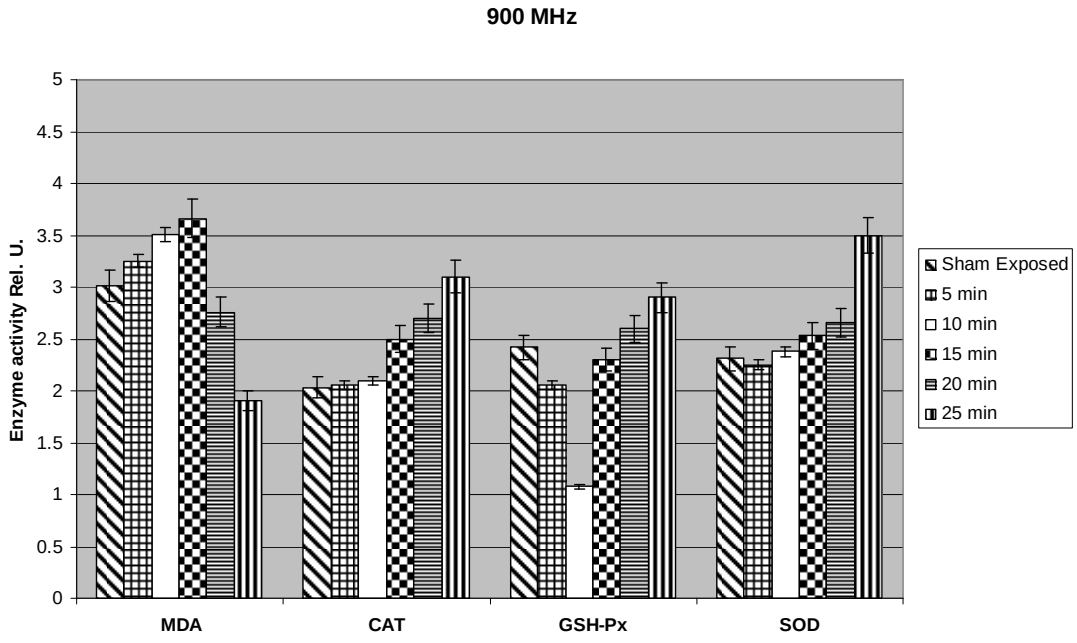
The concentration of MDA as a product of lipid peroxidation is calculated from the molar extinction coefficient (E) as specified below.

The samples were centrifuged at 3000 rpm for 10 min, the supernatant was taken off and 1.8 ml of 0.5% thiobarbituric acid was added to 2 ml of supernatant. The resulted solution was incubated at 90^{o}C for 40 min to obtain pink color with λ_{max} = 532 nm [Asakawa, T. and Matsushita, S. 1980]. The molar extinction coefficient (E) was measured at 532 nm with spectrophotometer (Cecile-3000) with polystyrene quvettes.

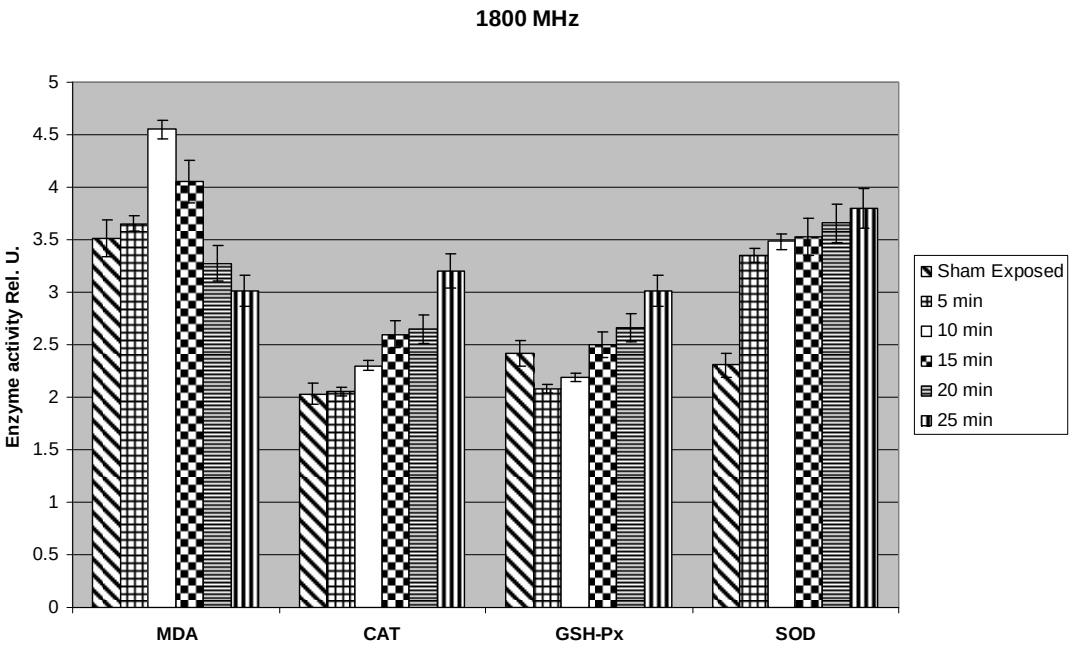
ANOVA statistical method for evaluation of significance of the present results were applied, Bonferoni test for statistical significance in the range P>0.05 were applied and results are presented as ±S.D.

Results

We obtained time dependence of high frequency EMF action at in vivo systems by means consequence measurements of concentration of oxidative stress marker (MDA) and antioxidant enzymes activity



For 900 MHz exposure we obtained significant changes at MDA concentration at 15 min. after beginning of exposure and for 25-th minutes we obtained maximum of SOD concentration.



For 1800 MHz exposure we obtained significant changes at MDA concentration at 10 min. after beginning of exposure and for 25-th minutes we obtained maximum of SOD concentration. Other enzymes CAT and GSH-Px, have smaller but also significant increase of their concentrations in comparison with sham exposed group. Between two exposed groups have no significant differences therefore we can claim for any frequency dependence of RF EMF action.
It have been measured tendency for increasing of life span of ROS formation and in parallel with that increasing of concentration of anti-oxidant enzymes, but with significant time-delay.

Summary

On the base of our results we can conclude that oxidative stress after exposure to RF EMF may be the reason for many adverse changes in cells and may cause a number of systemic disturbances in the human body

References

[1] Armstrong, D.; Browne, R. The analysis of free radicals, lipid peroxidases, antioxidant enzymes and compounds related to oxidative stress as applied to the clinical chemistry laboratory. Free Radic. Biol. Med. 366(1):43-58; 1994.

[2] Asakawa, T. and Matsushita S. Coloring conditions of thiobarbituric acid test for detecting lipid peroxides. Lipids 15[1], 137-140. 1-1-1980.
Ref Type: Magazine Article

[3] Bordiushkov, I.; Goroshinskaia, I. A.; Frantsiiants, E. M.; Tkacheva, G. N.; Gorlo, E. I.; Neskubina, I. V. [Structural-functional changes in lymphocyte ans erythrocyte membranes after exposure to alternating magnetic field]. *Vopr. Med Khim.* **46**:72-80; 2000.

[4] Bordiushkov, I.; Goroshinskaia, I. A.; Frantsiiants, E. M.; Tkacheva, G. N.; Gorlo, E. I.; Neskubina, I. V. [Structural-functional changes in lymphocyte ans erythrocyte membranes after exposure to alternating magnetic field]. *Vopr. Med Khim.* **46**:72-80; 2000.

[5] Cotgreave, I. A. Biological stress responses to radio frequency electromagnetic radiation: are mobile phones really so (heat) shocking? *Arch Biochem Biophys* **435**:227-240; 2005.

[6] Hook, G. J.; Spitz, D. R.; Sim, J. E.; Higashikubo, R.; Baty, J. D.; Moros, E. G.; Roti Roti, J. L. Evaluation of parameters of oxidative stress after in vitro exposure to. *Radiat Res* **162**:497-504; 2004.

[7] Janero, D. Malondialdehyde and thiobarbituric acid-reactivity as diagnostic indices of lipid peroxidation and peroxidative tissue injury. Free Radic. Biol. Med. 9(1): 515-540; 1998.

[8] Katsir, G.; Parola, A. H. Enhanced proliferation caused by a low frequency weak magnetic field in chick embryo fibroblasts is suppressed by radical scavengers. *Biochem Biophys Res Commun.* **252**:753-756; 1998.

[9] Moustafa, Y. M.; Moustafa, R. M.; Belacy, A.; Abou-El-Ela, S. H.; Ali, F. M. Effects of acute exposure to the radiofrequency fields of cellular phones on plasma lipid peroxide and antioxidase activities in human erythrocytes. *J Pharm. Biomed Anal.* **26**:605-608; 2001.

[10] Musaev, A. V.; Ismailova, L. F.; Shabanova, A. B.; Magerramov, A. A.; Iusifov, E. I.; Gadzhiev, A. M. [Pro- and antioxidant effect of electromagnetic fields of extremely high frequency (460 MHz) on brain tissues in experiment]. *Vopr. Kurortol. Fizioter. Lech. Fiz Kult.* 19-23; 2004.

[11] Yagi, K. Simple procedure for specific assay of lipid hydroperoxides in serum or plasma. Free Radical and Antioxidant Protocols 108(1):101-106; 1998.

URINARY 6-SULFATOXYMELATONIN EXCRETION IN RATS AFTER MICROWAVE IRRADIATION

IVANCICA TROSIC
IVANA BUSLJETA
IVAN PAVICIC
LJILJANA ZANINOVIC[1]
SANJA MILKOVIC-KRAUS

INSTITUTE FOR MEDICAL RESEARCH AND OCCUPATIONAL HEALTH
KSAVERSKA CESTA 2. POB 291. HR-10001 ZAGREB, CROATIA
e-mail: itrosic@imi.hr, phone: ++ (385 1) 4673 188
[1]ENDOCRINOLOGY LABORATORY, CLINICAL HOSPITAL CENTER, ZAGREB, CROATIA

Abstract

Aim of this study was to examine whether 2.45 GHz irradiation has effects on rats' nocturnal urinary 6-sulfatoxymelatonin (6SM) excretion. Urinalysis parameters after whole-body exposure of two hours per day, five days a week, throughout fifteen days lasting experiment was followed-up. The average specific absorption rate (SAR) was calculated to 1.25 (±0.36) W/kg. The concentration of 6SM in urine samples was determined by direct radioimmunoassay kit (Stockgrand Ltd., Guildford, UK). Urinary glucose, bilirubin, ketones, specific gravity, blood, pH, protein, urobilinogen, nitrite and leukocytes appearance has been accomplished by means of multiple reagent strips (N-Multistix® Bayer Diagnostic, UK). In comparison to the sham-exposed group, no significant changes in body temperature or food and water intake were observed. Delayed significant decline in 6SM of irradiated rats has been obtained between days eight and eleven. Until the end of experiment 6SM level remained low. The results of urinary pH, glucose, bilirubin, ketones, specific gravity, blood, protein, urobilinogen, nitrite, leukocyte appearance in the urine indicated no significant differences between treated and control group. In conclusion: it is likely that applied microwave field poses capacity to affect the hormone melatonin balance in rats after repeated exposure.

Introduction

Current scientific effort is based on the growing recognition that low-intensity radiofrequency microwave (RF/MW) exposure can be detected in living tissues and result in well-defined bioeffects. Because mechanisms involved into the complexity of RF/MW biological activity are multiple, animal studies play an important role in evaluating the complex reactions of various body systems. Systems like nervous, haematopoietic or immune are largely responsible for homeostasis – the essential maintenance of the internal environment. Co-coordinated, interdependent response of these systems when challenged by potentially damaging stimuli could be easier reproduced in contrast to a human study [1, 2]. One of straightforward approach with comprehensive output of possible elucidation how RF/MW affects living organisms, certainly could be covered by melatonin hypothesis [3]. Hypothesis that melatonin as oncostatic, or inhibitor of cancer cell growth or it is effect on immune system, along with the report that EMF could alter its oncostatic properties [4]. There are three postulates how EMF could be acting through the melatonin pathway. EMF could lower melatonin concentration, resulting in increased estrogen and prolactin levels, and consequently increase hormonally-mediated cancers. Further, lower melatonin levels, with melatonin acting as an antioxidant, could result in increased susceptibility to DNA damage. This may result in a general increase in risk for a variety of cancers. Finally, EMF may affect the effectiveness of melatonin for inhibiting cell proliferation. This mechanism could be relevant to cancer in general [3]. Several studies show that EMF across the spectrum from extremely low

frequencies (ELF) to RF/MW reduces melatonin in animals and people [5]. Light going through our eyes passes a message to the pineal glands in the brain which slows down the production of melatonin during the day time. At night the production of melatonin is speeded up. Melatonin is considered to scavenge cancer cells and impurities in our bodies and boost the immune system. Non-ionizing radiation is supposed to act on the pineal gland and suppress the night-time melatonin to daytime levels; hence the good work of the melatonin at night will be restricted leading to suppression of the immune system [6]. Otherwise, melatonin circadian profile was not been disrupted in 37 young male volunteers submitted to the EMFs of 900 and 1800 MHz frequency field [7]. Additionally, both continuous and/or pulsed 900 MHz field exposure for 15 min to 6 hours at day or night had no notable effect on pineal melatonin synthesis in rodents [8].

There has been insufficient research on the effects of RF/MW on melatonin excretion level, and the few existing studies do not provide clear information about such effects. As urinary 6-sulfatoxymelatonin (6SM) appears to be the main metabolic end product of pineal melatonin hormone, the aim of this investigation was to examine whether 2.45 GHz exposure has effects on rats' nocturnal urinary 6SM along with. Urinalysis parameters after exposure were also studied.

Materials and Methods

Male Wistar rats (13 week old, approximate body weight 450 g) had passed through a week accommodation period. Both sham-exposed control (n=10) and exposed animal group (n=10) were kept in steady-state microenvironment conditions (22 ^{o}C ± 1 ^{o}C), receiving standard laboratory food and water from 7:00 AM till 7:00 PM, with alternating 12-hours light and dark cycles. The animals were exposed to 2.45 GHz continuous waves two hours daily, five days a week every day between 8:00 AM and 10:00 AM. The animals were exposed to RF/MW source (modified Micro-Chef Moulinex generator, 900 W, 2.45 GHz) in individual Plexiglas cages. Rats were irradiated separately at the same time. The field power density within the cages was measured by EM Radiation Monitor, EMR-20 and 8.2, Wandel & Golterman GmbH & Co. Germany, at "average mode". The exposures were conducted with a field power density of 5-10 mW/cm^2. Specific absorption rate (SAR) was estimated according to radiation dosimetry handbook [9]. The average whole-body SAR value was calculated to be 1.25 (±0.36 SE) W/kg. According to recent literature calculated SAR of this range excludes thermal stress in rats [10]. The animals did not receive food or water during exposure sessions. The experiment lasted fifteen days. The rectal body temperature was measured by Thermo Scan thermometer (Braun GmbH, Germany) before and after the treatment. No significant changes in body temperature were observed. Control animals were handled as the treated ones, but without RF irradiation. In order to collect nocturnal urine, both, control and exposed animals were held individually in metabolic cages every night, from 7:00 PM till 7:00 AM next day. The volume of collected urine was measured. The concentration of 6SM in rat urine samples was determined by direct radioimmunoassay kit (Stockgrand Ltd., Guildford, UK). To get a quick overview into the urinary biochemical parameters, a rapid screening test has been performed. Nocturnal urinary glucose, bilirubin, ketones, specific gravity, blood, pH, protein, urobilinogen, nitrite and leucocyte manifestation has been accomplished by multiple reagent strips (N-Multistix® Bayer Diagnostic, UK). During or after exposure procedure no changes were observed neither in food/water intake or behavioral pattern. The results were statistically evaluated using Mann-Whitney and Kruskal-Wallis tests [11].

Results

When we conducted the 6SM test after 2.45 GHz rats' whole-body microwave irradiation, samples of urine were collected every morning at the same time during the fifteen days lasted experiment. The time-course of nocturnal 6SM in rat urine samples during the 2.45 GHz exposure of 2 hours a day, 5 days a week is presented at Figure 1. In comparison with sham-control animal group the significant decline in 6SM of irradiated rats has been obtained between experimental days eight and eleven ($p<0.05$). Reduced metabolic end product of melatonin appears to be consequence of cumulative RF/MW irradiation. The 6SM level in urine of exposed animal group remained low until the end of the experiment, but it has not significantly differed in comparison with the sham-control ones.

The semi-quantitative biochemical findings in nocturnal urine samples during the 2.45 GHz exposure of 2 hours a day, 5 days a week is presented at Figure 2. The results of urinary pH, glucose, bilirubin, ketones, specific gravity, blood, protein, urobilinogen, nitrite, leukocyte appearance in the nocturnal urine indicated no significant differences between treated and control animal group.

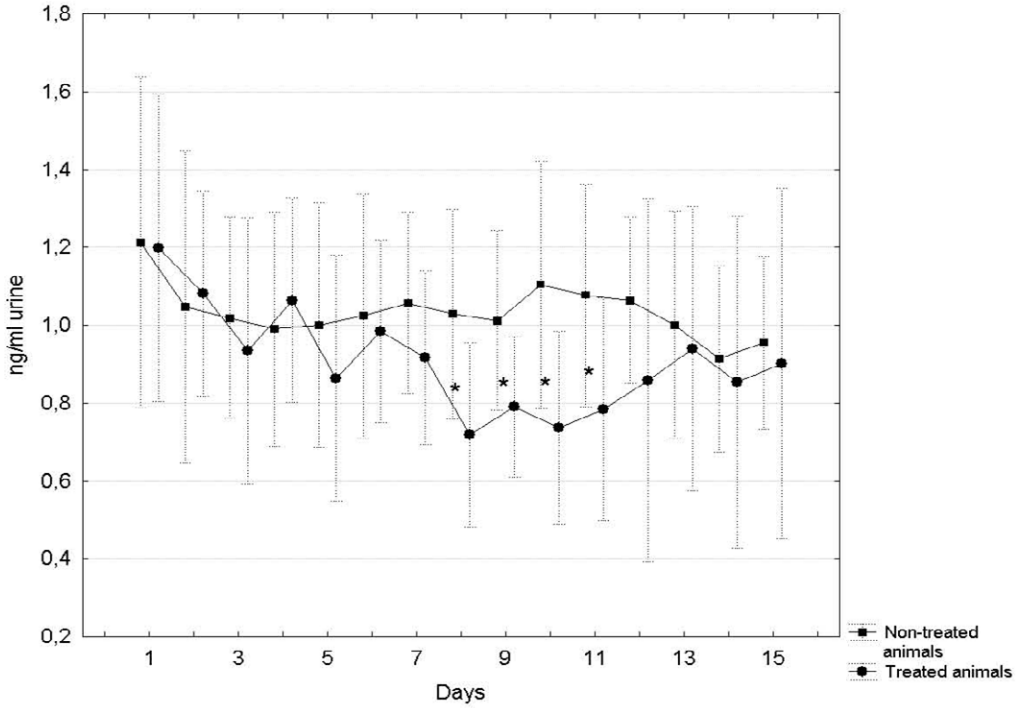


Figure 1. The time-course of nocturnal melatonin metabolite; 6-sulphaxymelatonin (6SM) in rat urine samples during the 2.45 GHz exposure and matched sham-controls (*significant difference $p<0.05$)

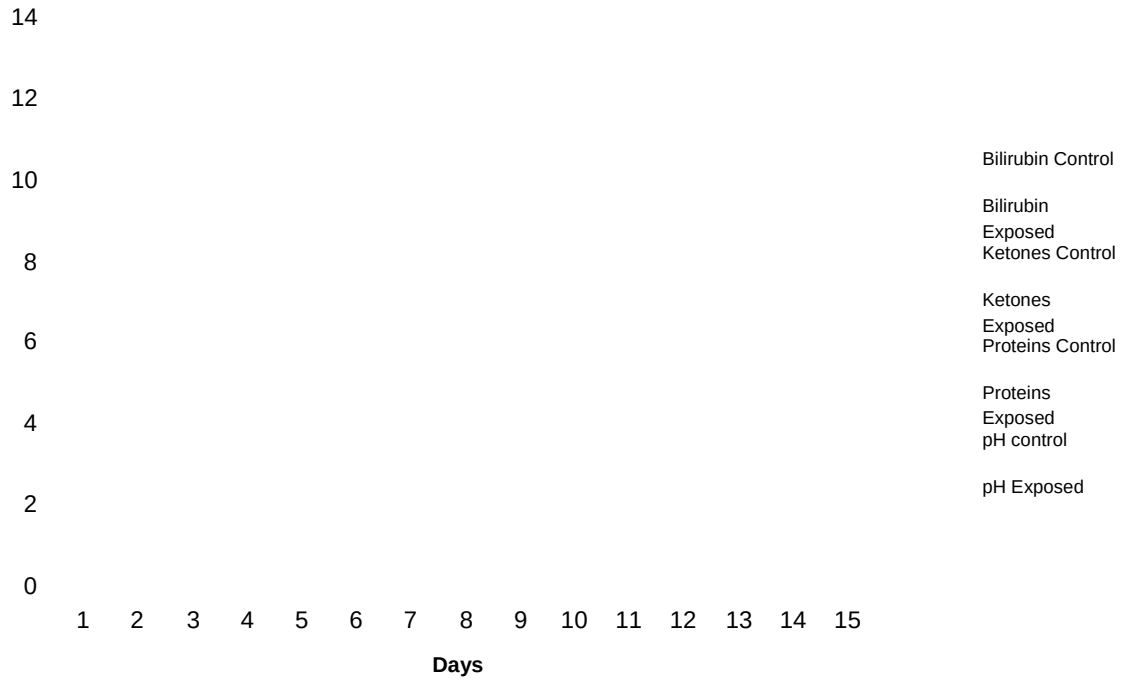


Figure 2. Semi-quantitative biochemical findings (urinary pH, bilirubin, ketones, protein) in nocturnal urine samples during the 2.45 GHz irradiated and sham-exposed control rats

Discussion

Interest in melatonin is that it could help explain results of some studies on unsafe EMF biological potency across the spectrum from ELF to RF/ MW by means of the reasonable underlying mechanisms of action. Melatonin has been reported to block RF/EM radiation-induced DNA strand breaks in rat brain cells and slow the growth of some preneoplastic lesions in rats in relation to the influence of EM exposure [12, 13]. Studies on small animals provide the strongest data supporting the hypothesis that EM field suppresses melatonin. It gives the impression that EMF suppresses different elements of melatonin biosynthesis, specifically secretion and metabolism [4, 14, 15, 16]. On the other hand, chronic exposure of lambs to the environmental electric and magnetic fields revealed that EMF does not affect the mechanism underlying the generation of the circadian pattern of melatonin secretion [17]. Additionally, Stärk et al., call attention to the absence of chronic RF exposure effect on salivary melatonin concentrations in cattle, along with Vollrath's group who found no short-term effect of high frequency RF exposure on the mammalian pineal gland and melatonin synthesis [18, 8]. Recent investigations suggest that short term exposure to 1439 MHz field does not alter melatonin synthesis in rats, and two hours daily exposure to the 900 and 1800 MHz during 14 day period achieve no effect on 6SM excretion in rats [19, 20]. We studied whether 2.45 GHz frequency field has demonstrable effects on nocturnal urinary 6SM level and urinalysis parameters in rats after exposure of two hours a day, five days a week exposure. The animals were not irradiated for two days on weekends. Major decline in 6SM excretion in microwave exposed rats has been obtained between experimental days eight and eleven ($p<0.05$). Reduction in melatonin metabolite levels seems to be consequence of increasing RF/MW irradiation over the time. Obtained effects appeared after repeated exposure, but apparently not leading into the irreparable damage. Recovery of 6SM urinary excretion is likely related to absence of irradiation on experimental day thirteen and fourteen. The findings reveal that urinary melatonin metabolite could be a sensitive marker of RF/MW biological potency (Figure 1). Accordingly, it is in agreement with Lai's statement that: "Existing results indicate changes in the response characteristics of the nervous system with repeated exposure suggesting that the effects are not "forgotten" after each episode of exposure" [21]. The semi-quantitative biochemical findings in nocturnal urine indicated that applied 2.45 GHz exposure does not influence glucose, bilirubin, ketones, blood, protein, urobilinogen, nitrite, leukocyte appearance as well as urinary pH and specific gravity (Figure 2). The behavioral pattern of the animals was not altered during the course of the experiment. It can be concluded that 2.45 GHz microwave field has a capacity to affect the hormone melatonin balance in rats after repeated exposure.

Acknowledgements

The research was supported by Ministry of Science, Education and Sports, Croatia, Grant No. 0022005.

References

[1] Trošić I, Mataušić-Pišl M, Radalj Ž, Prlić I. Animal study on Electromagnetic field biological potency. Arh. Hig. Rada Toksikol. 50: 5-11 (1999)

[2] Trosic I, Busljeta I, Modlic B. Investigation of the genotoxic effects of microwave irradiation in rat bone marrow cells: *in vivo* exposure. Mutagenesis 1:361-364 (2004)

[3] Stevens RG, Davis, S. The melatonin hypothesis: electric power and breast cancer. Environ. Health Perspect. 104: (Suppl 1), 135-140 (1996)

[4] Brainardet GC, Kavet R, Kheifets LI. The relationship between electromagnetic field and light exposure to melatonin and breast cancer risk: A review of the relevant literature. J. Pineal. Res. 26: 65-100 (1999)

[5] Cherry, N. EMR Reduces Melatonin in Animals and People. Available from: http://www.feb.se/EMFguru/Research/emf-emr.htm (2000a)

[6] Cherry N. Probable Health Effects Associated with Base Station in Communities: The Need for Health Surveys. In: Oberfeld G. (Ed.), Proceedings of International Conference on Cell Tower Sitting. Printing Office Salzburg, Austria, p.p. 192-233 (2000b)

[7] deSeze R, Ayoub J, Peray P, Miro L, Touitou Y. Evaluation in humans of the effects of radiocellular telephones on the circadian patterns of melatonin secretion, a chronobiological rhythm marker. J. Pineal. Res. 27: 237-242 (1999)

[8] Vollrath L, Spessert R, Kratzsch T, Keiner M, Hollmann H, No Short-Term Effects of High-Frequency Electromagnetic Fields on the Mammalian Pineal Gland. Bioelectromagnetics 18:376-387 (1997)

[9] Durney CH, Iskander MF, Massoudy H, Allen BS, Stewart J, Mitchell BS, John C. Radiofrequency Radiation Dosimetry Handbook, 3rd Ed, USAF School of Aerospace Medicine, Texas (1980)
[10] IEGMP (Independent Expert Group on Mobile Phones): Mobile phones and Health, Available from: http://www.iegmp.org.uk (2000)
[11] Willemsen EW. Understanding statistical reasoning. Freeman WH & Company, San Francisco (1974)
[12] Lai H, Singh NP. Melatonin and a Spin-Trap Compound Block Radiofrequency Electromagnetic Radiation-Induced DNA Strand Breaks in Rat Brain Cells. Bioelectromagnetics 18: 446-454 (1997)
[13] Imaida K, Hagiwara A, Yoshino H, Tamano S, Sano M, Futakuchi M, Ogawa K, Asamoto M, Shirai T. Inhibitory effects of low doses of melatonin on induction of preneoplastic liver lesions in a medium-term liver bioassay in F344 rats: relation to the influence of electromagnetic near field exposure. Cancer Letters 155:105-114 (2000)
[14] Brendel H, Niehaus M, Lerchl A. Direct suppressive effects of weak magnetic fields (50Hz and $16^{2/3}$ Hz) on melatonin synthesis in the pineal gland of Djungarian hamsters (*Phodopus sungorus*). J. Pineal. Res. 29:28-33 (2000)
[15] Fernie KJ, Bird DJ, Petitclerc D. Effects of Electromagnetic Fields on Photophasic Circulating Melatonin Levels In American Kestrels. Environ. Health Perspect. 107:901-904 (1999)
[16] Grota LJ, Reiter RJ, Keng P, Michaelson S. Electric field exposure alters serum melatonin but not pineal melatonin synthesis in male rats. Bioelectromagnetics 15:427-437 (1994)
[17] Lee JM, Stormshak F, Thompson JM, Thinesen P, Painter LJ, Olenchek EG, Hess DL, Forbes R, Foster DL. Melatonin Secretion and Puberty in Female Lambs Exposed to Environmental Electric and Magnetic Fields. Biology of Reproduction 49:857-864 (1993)
[18] Stärk KDC, Krebs T, Altpeter E, Manz B, Griot C, Abelin, T. Absence of chronic effect of exposure to short-wave radio broadcast signal on salivary melatonin concentrations in dairy cattle. J. Pineal. Res. 22:171-176 (1997)
[19] Hata K, Yamaguchi H, Tsurita G, Watanabe S, Wake K, Taki M, Ueno S, Nagawa H. Short Term Exposure to 1439 MHz Pulsed TDMA Field Does Not Alter Melatonin Synthesis in Rats. Bioelectromagnetics 26:49-53 (2005)
[20] Bakos J, Kubinyi G, Sinay H, Thuróczy G, GSM Modulated Radiofrequency Radiation Does Not Affect 6-Sulfatoxymelatonin Excretion of Rats. Bioelectromagnetics 24:531-34 (2003)
[21] Lai H. Neurological effects of radiofrequency electromagnetic radiation. Workshop on Possible Biological and Health Effects of RF Electromagnetic Fields Vienna, Austria p.p. 1-13 (1998)

THE EFFECT OF EMF ON THE EARLY COMPONENTS OF ERPS IS DEPENDENT ON THE KIND OF STIMULUS USED.

TSIAFAKIS VASILEIOS[1], NANOU ELENA[1], KAPARELIOTIS EVANGELOS[1], PRAGIATIS LAZAROS[1], PAPAGEORGIOU CHARALAMBOS[2], SOLDATOS KONSTANTINOS[2], RABAVILAS ANDREAS[3], CAPSALIS CHRISTOS[1]

[1] NATIONAL TECHNICAL UNIVERSITY OF ATHENS, DEPARTMENT OF ELECTRICAL ENGINEERING, DIVISION OF INFORMATION TRANSMISSION SYSTEMS AND MATERIAL TECHNOLOGY, GREECE

9 IROON POLYTECNEIOY STR., ATHENS ,GREECE, 15773, Tel: (+30)210 7722574, Fax: (+30)210 7723520, email:vtsiaf@mail.ntua.gr

[2] DEPARTMENT OF PSYCHIATRY, EGINITION HOSPITAL, UNIVERSITY OF ATHENS, GREECE
email: cpapage@eginitio.uoa.gr

[3] UNIVERSITY MENTAL HEALTH RESEARCH INSTITUTE, ATHENS, GREECE.

Abstract

Probable alterations of human cognitive functions, caused by electromagnetic fields (EMF) emitted by cellular phones, are still under investigation. The present study focused on the effect of a 900MHz signal on the early components of event related potentials (ERPs) recorded during an auditory memory task.

Nineteen normal subjects (10 women and 9 men) were examined with and without radiation in a random order. Measurements included the recording at 16 scalp electrodes of the P50 and N100 components which were evoked by two warning stimuli which differed in frequency (low=500 Hz, high=3000Hz).

Results showed that for the low frequency stimulus radiation caused a statistically significant positive shift on the waveform of the early components while for the high frequency stimulus there was a significant negative shift at the Fp1 electrode. The affected area of the left prefrontal cortex (Fp1 electrode site) plays a key role in working memory operation.

These findings provide further evidence that both the P50 and N100 components of the ERPs, which reflect pre-attentive and attentive information processing respectively, are modality specific. Furthermore the amplitudes of the two components for the two modalities are influenced by EMF in opposite ways.

Introduction

Cellular (GSM) telephones are widely used throughout the world. Although there is no clear evidence of possible effects of the electromagnetic field (EMF) on brain physiology, there is common concern about this matter. In this context, some reports suggested that the exposure to mobile phone (MP) EMF exerts facilitating effects on these brain operations [1, 2, 3, 4] while other studies did not find any changes in these functions in relation to the applied MP-EMF [5, 6]. Thus, it has been proposed that 'the inability to replicate previous findings could have been caused by lack of actual EMF effects or the magnitude of effects being at the sensitivity threshold of the test used. [5].

Event related potentials (ERPs) due to their high resolution properties can be of significant use in studying EMF effects on brain activity [7]. It should be noted that the earlier components of the ERPs are thought to represent the activity of the sensory pathways that transmit the signal generated at peripheral receptors to central processing systems. These components are 'modality specific', that is they are influenced primarily by the stimulus parameters such as intensity and frequency. In this respect, given that both attention and WM are associated with the P50 and N100 components of ERPs [8, 9, 10] it seems reasonable to review the effects of MP-EMF on these components taking also into account the kind of stimulus that provokes them.

The analysis of the patterns of N100 waveforms of ERPs during MP-EMF exposure revealed conflicting results. Urban et al., [11] did not find changes to the visual evoked N100 components of ERPs (amplitude and latency) following 5 min exposure to EMFs. A recent study by Maby et al. [12], based on the investigation of auditory evoked potentials recorded from healthy volunteers and epileptic patients revealed that the exposure to MP-EMF induced decreased N100 amplitude in both assessed groups, and decreased N100 latency for the healthy subjects. The authors drew the conclusion that these effects are attributable to the 'mild, localized heating' evoked by MP-EMF. It is possible that some of the inconsistencies just mentioned may be related to the different modalities involved (i.e. auditory versus visual) and complexity of the tasks employed

Taking into account the above considerations, we hypothesized that the electrophysiological brain activity as indexed by P50 and N100, in relation to WM operation, could be of value in detecting possible psychophysiological mechanisms underlying alterations evoked by MP-EMF. Thus, the present study was designed to assess the effect of the exposure of MP-EMF on the patterns of P50 and N100 ERP components elicited during a WMtest.

Methods

Participants

Nineteen healthy individuals (9 men and 10 women, mean age = 23.3 ± 2.23 years, mean education = 16.9 ± 1.82 years) participated in the experiment. The male and female subgroups were homogeneous with regards to age and educational level. All participants were right-handed and had no history of any hearing problem. Informed consent was obtained from all subjects.

Stimuli and procedure

The subjects were evaluated with the digit span Wechsler Auditory test [13, 14]. A warning stimulus of either high (3000 Hz) or low frequency (500 Hz) was presented through earphones to the subjects, who were asked to memorize the numbers that followed. The warning stimulus lasted 100msec. A one second interval followed the onset of the warning stimulus and then the numbers to be memorized were presented by a male voice. At the end of the number sequence presentation, the same signal tone was repeated. If the frequency of the signal tone was low the subjects had to recall the numbers in the same order with that presented, else, if the frequency was high, the subjects had to recall the numbers in the opposite order.

Before any ERPs' recording, practice trials were administered until the subjects could clearly discriminate the warning stimuli (tones). After completion of the above-mentioned process, a rest period of five minutes followed, before the recording of the ERPs.

The experimental setup included a Faraday room, which screened any electromagnetic interference that could affect the measurements. The subjects sat in an anatomical chair and a certified dipole antenna was fixed near their right ear. Care was taken so that the distance between telephone and ear (about 20 cm) was constant during the whole session. The antenna was driven by a signal generator, which could be switched on or off. In the on mode the antenna emitted a 900 MHz electromagnetic field with mean power at 64 mWatt [13].

ERPs were recorded during 1 sec between the onset of the warning stimulus and the onset of the first

administered number. The electrophysiological signals were recorded with Ag/AgCl electrodes. Electrode resistance was kept constantly below 5 kΩ. EEG activity was recorded from 15 scalp electrodes based on the International 10-20 system of Electroencephalography [15], referred to both earlobes. An electrode placed on the subject's forehead served as ground. The bandwidth of the amplifiers was set at 0.05 Hz to 35Hz. During the administration of stimuli, the subjects had their eyes closed in order to minimize eye movements and blinks. Eye movements were recorded through electro-oculogram (EOG) and recordings with EEG higher than 75mV were rejected. Warning stimuli, as well as learning material, i.e. the numbers to recall, were presented binaurally via earphones at an intensity of 65dB sound pressure level. The evoked biopotential signal was submitted to an analogue-to-digital conversion, at a sampling rate of 1 KHz, and was averaged by a computerized system. Each recording session consisted of 52 repetitions of the trial.

Because the P50 and N100 components are included in the array of early-endogenous ERPs components, which normally are modality specific, the ERPs induced by the two modal stimuli were averaged separately [7]. In particular, two varieties of waveforms for each component were obtained, one (low P50 and low N100) evoked by the low frequency modality (26 trials) for each lead in all subjects and another (high P50 and high N100) evoked by the high frequency modality (26 trials) for each lead in all subjects .

The following parameters were calculated. ERPs were recorded for each subject at EEG leads Fp1, Fp2, F3, F4, C3, C4, C5, C6, P3, P4, O1, O2, Pz, Cz, and Fz. Recordings with acceptable EEG level were averaged for each lead by a computerized system. An algorithm was used, which identified the P50 as the most positive peak in each averaged lead curve, between 30 and 80 msec and the N100 as the most negative peak in each averaged lead curve, between 70 and 150 msec, after the onset of the warning stimulus. Peak amplitudes were measured relative to the mean amplitude of the 100-msec prestimulus baseline period and latency measurements were computed relative to stimulus onset.

Statistical analysis

The values of the P50 and N100 amplitudes and latencies at the fifteen leads were subjected to multivariate analysis of variance with the two frequency tones and the two radiation conditions as the between subjects factors. The frequency X radiation interaction was also taken into consideration. Post-hoc pairwise comparisons (with the necessary corrections for multiple comparisons) were carried out between the two frequencies in the absence and presence of radiation, as well as between the two radiation conditions at the low and high frequencies for both components. Statistical significance was set at 0.05.

Results

The multivariate analysis revealed that neither frequency, nor radiation by themselves had any significant effect on P50 and N100 amplitudes of the entire group of subjects taken as a whole. There was, however, a significant frequency X radiation interaction effect (p value of Pillai's trace=0.013).

Figure 1 and figure 2 are quite helpful in explaining this interaction effect. In the absence of radiation the following findings were observed: The low frequency tone induces higher negative peak amplitude values of the N100 component than the high frequency one at all the fifteen leads under consideration. This difference achieves statistical significance at nine leads (Fp1, C3, Fp2, C6, O1, O2, P3, Pz, Fz). The high frequency tone induces higher positive peak amplitude values of the P50 component than the low frequency one at all the fifteen leads under consideration. This difference achieves statistical significance at eleven leads (Fp1, C5, C3, Fp2, C6, C4, O1, O2, P3, Pz, Fz).

The application of EMF radiation demotes these differences, since in the case of this application statistically significant differences of the P50 amplitudes for the two frequency tones are observed only in three leads while no statistically significant differences of the N100 amplitudes for the two frequency tones are observed.

This is accomplished by a slight increase of the negative values of the N100 amplitudes together with a slight decrease of the positive values of the P50 amplitudes at the high frequencies. These differences achieve statistical significance at lead Fp1 for both N100 and P50. Also a slight decrease of the N100 amplitudes together with a slight increase of the P50 amplitudes was observed at the low frequencies. In P50 the increase achieves statistical significance at two leads (Fp1 and O1) while in N100 the decrease achieves statistical significance at lead Fp1

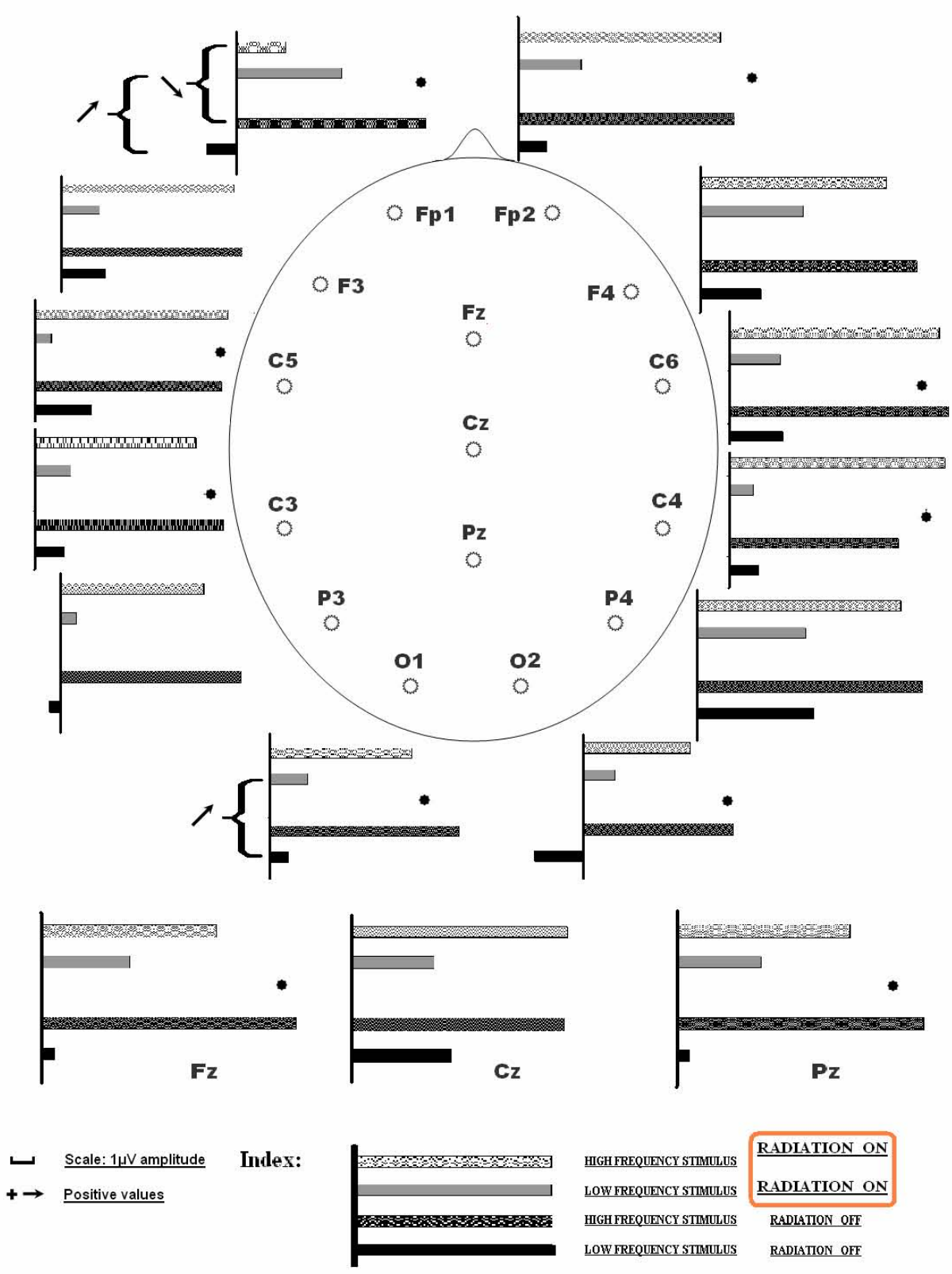


Figure1: P50 amplitudes at 15 leads for high and low frequency stimuli, with and without EMF exposure.

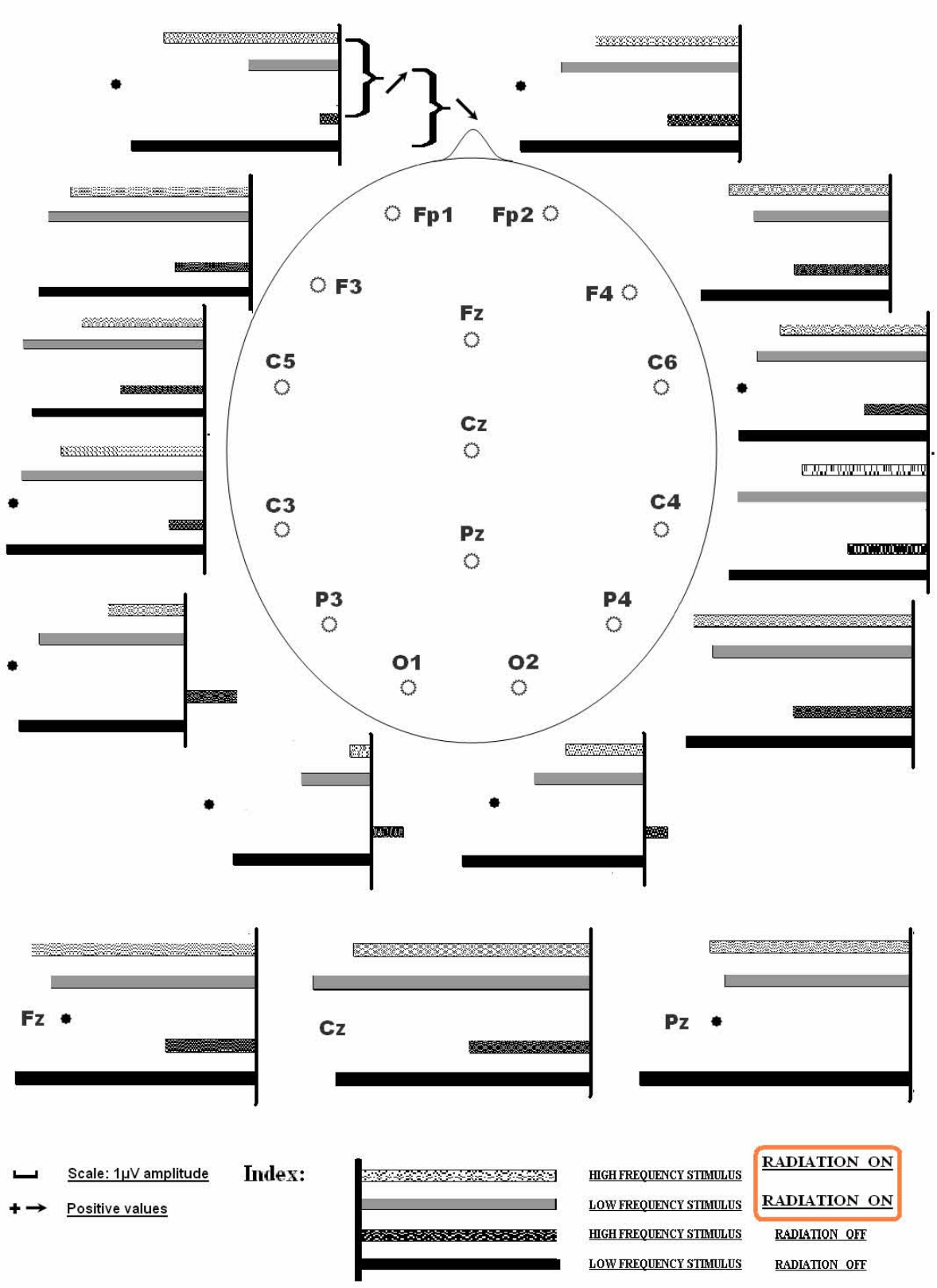


Figure2: N100 amplitudes at 15 lead for high and low frequency stimuli, with and without EMF exposure

The crossover effect of these changes results in the fact that Fp1 stands as the only lead, at which in the presence of radiation the N100 amplitudes are lower at the low frequency than at the high frequency tone while the P50 amplitudes are higher at the low frequency than at the high frequency tone. This is the main reason for the appearance of a significant overall frequency X radiation interaction effect.

Neither radiation, nor frequency, nor their interaction had any significant effect on the N100 and P50 latencies. Memory performance did not differ, in both cases, between the two frequency modalities (58.4±26.5 for the low frequency tone, and 54.9±24.6 for the high frequency tone, *t*-test, p=0.552). It also did not seem to depend on radiation, and sex.

Discussion

The findings of the present study indicate that MP-EMF may alter the patterns of the auditory P50 and N100 components of ERPs elicited in a working memory task. More precisely, the results showed that the presence of MP-EMFs, when high frequency stimulus was applied, induced statistically significant decrease in the amplitude of P50, while there was a statistically significant increase in the amplitude of N100 at Fp1 electrode site, as compared to themselves without MP-EMF exposure. In contrast, the exposure to EMF when low frequency stimulus was applied, revealed statistically significant increase of the amplitude of P50 at Fp1 and O1 electrode site while there was a statistically significant decrease of the amplitude of N100 at Fp1 only electrode site, as compared to themselves without EMF exposure. Also the amplitude of P50 without radiation appeared significantly higher in the high frequency warning stimulation as compared with those of low frequency stimulation while the opposite situation appeared for the N100 (smaller values of N100 for the high than these for low frequency stimulus)

The observed differences of the amplitudes of P50 and N100 without radiation may be explained considering the fact that these components belong to the earlier components of ERPs which are sensitive to physical parameters of the stimuli [7]. The dissociation observed for the P50 and N100 potentials with reference to the modality of the warning stimuli just mentioned, suggests that an alternative explanation must be considered in connection with the effects of EMF upon these peaks evoked by high frequency and the peaks evoked by low frequency warning stimuli.

In line with this point of view, the obtained changes concerning N100 waveforms evoked by low frequency warning stimuli seem to be in accordance with those reported by Maby et al.[12] and Hamblin et al.[11], as mentioned earlier. On the other hand, the patterns of results concerning the N100 evoked by the high frequency warning stimuli appears to be consistent to those reported by Koivisto et al.[3] who reported that the exposure to the EMF has a facilitating effect of attentive processing involving left frontal area during the manipulation of information in WM.

Taken together, the obtained results provide evidence that the EMF emitted by mobile phone affect differentially the attentive information processing, as it is reflected by the N100 component of ERPs. This differential effect might be explained considering that the N100 arises from multiple sources [17, 18]. An alternative explanation can be conceived in terms of attentional demands: Eulitz et al. [19] reported that 30 min EMF exposure altered the beta frequency band of the brain electrical response to acoustic stimuli in an oddball paradigm. More precisely, this effect appeared when subjects processed task-relevant target stimuli but it was not present for irrelevant standard stimuli. Another group of investigators observed reduced slow brain potentials as an effect of exposure to EMF during a demanding experimental condition, whereas they did not observe any alteration when the exposure occurred during a not demanding experimental condition [20]. Thus, a possible explanation of the finding concerning the N100 evoked by the high frequency warning stimuli may be due to the fact that in this condition the subjects had to recall the administered numbers in the opposite order (see experimental procedure), consequently, the subjects faced a rather demanding experimental condition.

The findings of P50 amplitudes in relation to the MP-EMF radiation cannot be compared with those of other studies, because to our knowledge there are no previous reports assessing this ERP component in relation to MP-EMF radiation. An exception appears to be the study by **Arai** et al. [21], which reported no effects on mid latency evoked brain potentials in 15 healthy controls using the Japanese mobile phone emitting 800MHz. But there are important differences in methodology that make a direct comparison difficult, for instance, in the present study the obtained findings would likely have occurred immediately upon presentation of the MP-EMF and lasted throughout its presence, whereas, in the study by Arai et al., [21] the reported effects referred to evoked brain response before and after using a mobile phone for 30 min. The main difference is that in the present study the evoked potentials were recorded during the presence of the radiation and without the presence of the radiation, while in the study of Arai the ERPs were studied before and after the expose to the MP-EMF. However, it may be easier to understand the importance of the pattens in P50 amplitude during MP-EMF radiation reported here in the light of psychophysiological indices concerning the meaning of the P50 potential on the one hand, and on the other considering the proposed influence of MP-EMF on brain function. The P50 potential is a subcomponent of the γ EEG activity reflecting the transient synchronization of thalamocortical

activity in response to sensory stimulation [22, 23]. In keeping with this suggestion, concerning the low frequency amplitude of P50 waveforms, the present findings, seem to be compatible with a recent study by Croft et al.,[24] focusing on the effects of mobile phone on EEG as a function of time, which show 'an increase in the γ response at midline frontal and lateral posterior sites'. Further, since the MP-EMF is observed to enhance the enzymatic activity of the cholinergic system [25, 26, 27], and on the other hand the augmentation in P50 amplitude is thought to reflect increased cholinergic activation during arousal [28, 29], thus it is reasonable to suppose that this mechanism could account for the observed increase in the amplitude of P50 evoked by the low frequency stimuli, in association with MP-EMF radiation. The obtained results provide evidence that the MP-EMF emitted by mobile phone affect pre-attentive information processing; however, the underlying mechanisms of such influence are still unclear, although several possibilities exist, calling for potential directions of future research. These highly complex physical and biological phenomena necessitate the development of new experimental, measuring and observation procedures.

A further point for discussion is the location of the observed changes with regard to the N100 amplitude. The affected area of the left prefrontal cortex (Fp1 electrode site) plays a key role in working memory operation [30, 31]. Moreover, comparable effects on this brain area after PM-EMF exposure has been reported by other researchers. Specifically, Huber et al. [32] using positron emission tomography scans showed that exposure to MP-EMF alters the cerebral blood flow of 12 healthy young men in the left dorsolateral brain region. In line with this, it is noteworthy that brain imaging studies suggest that attention and working memory generally engage left frontal areas of the brain cortex [33, 34].

In conclusion, the findings of the present study support the view that MP-EMF during the performance of a WM task, affect pre-attentive and attentive operation, possibly mediated by the left frontal brain networks. However, before drawing any final conclusions, the present results advocate the need for more follow-up studies in order to evaluate not only the short-term but also the long-term effects of MP-EMF use in pre-attentive, attentive and WM operation.

The findings of the present study indicate that MP-EMF may alter the patterns of the auditory P50 and N100 of ERPs elicited during a working memory task. More precisely, the results showed that the presence of MP-EMFs, when high frequency stimulus was applied, induced statistically significant decrease in the amplitude of P50, while there was a statistically significant increase in the amplitude of N100 at Fp1 electrode site, as compared to themselves without MP-EMF exposure. In contrast, the exposure to EMF when high frequency stimulus was applied, revealed statistically significant increase of the amplitude of P50 at Fp1 and O1 electrode site while there was a statistically significant decrease of the amplitude of N100 at Fp1 only electrode site, as compared to themselves without EMF exposure.

References

[1] N. Edelstyn , A. Oldershaw, The acute effects of exposure to the electromagnetic field emitted by mobile phones on human attention, Neuroreport 21;13(1) (2002) 119-21.
[2] M. Koivisto, A. Revonsuo, C. Krause, C. Haarala, L. Sillanmaki, M. Laine, H. Hamalainen, Effects of 902 MHz electromagnetic field emitted by cellular telephones on response times in humans, Neuroreport 11 (2000) 413-415.
[3] M. Koivisto, M.C. Krause, A.Revonsuo, M. Laine, H. Hamalainen, The effects of electromagnetic field emitted by GSM phones on working memory, Neuroreport 11 (2000) 1641-1643.
[4] T.M. Lee, P.K. Lam, L.T. Yee, C.C. Chan, The effect of the duration of exposure to the electromagnetic field emitted by mobile phones on human attention, Neuroreport 14(10) (2003)1361-4.
[5] C Haarala , M. Ek, L. Bjornberg, M. Laine, A. Revonsuo, M. Koivisto, H . Hamalainen, 902 MHz mobile phone does not affect short term memory in humans, Bioelectromagnetics 25(6) (2004) 452-6.
[6] M.C. Krause, C. Haarala, L. Sillanmaki, M. Koivisto, K. Alanko, A. Revonsuo, M. Laine, H. Hamalainen, Effects of electromagnetic field emitted by cellular phones on the EEG during an auditory memory task: a double blind replication study, Bioelectromagnetics 25(1) (2004) 33-40.
[7] M.Fabiani, G. Gratton, M. Coles, Event-related potentials: methods, theory, and applications. In: Cacioppo J, Tassinary L, Bernston G, eds. Handbook of psychophysiology, Cambridge University Press, New York, 2000, pp. 53–84.
[8] EM Conley , HJ Michalewski, A. Starr, The N100 auditory cortical evoked potential indexes scanning of auditory short-term memory, Clin Neurophysiol. 110(12) (1999) 2086-93.
[9] JT. Coull, Neural correlates of attention and arousal: insights from electrophysiology, functional neuroimaging and psychopharmacology, Prog Neurobiol 55(4) (1998) 343-61.
[10] E.J. Golob , A. Starr, Serial position effects in auditory event-related potentials during working memory retrieval, J Cogn Neurosci. 16(1) (2004) 40-52.
[11] P. Urban, E. Lukas, Z. Roth, Does acute exposure to the electromagnetic field emitted by a mobile phone influence visual evoked potentials? A pilot study, Eur J. Public Health 6(1998) 288-290.
[12] E.Maby , R. Le Bouquin Jeannes, C. Liegeois-Chauvel, B. Gourevitch, G. Faucon, Analysis of auditory evoked potential parameters in the presence of radiofrequency fields using a support vector machines method, Med Biol Eng Comput. 42(4) (2004) 562-8.
[13] C. Papageorgiou, E. Nanou, V. G. Tsiafakis, C. Capsalis, A. D. Rabavilas, Gender related differences on the EEG during a simulated mobile phone signal, Neuroreport, 15 (2004) 2557-2560.
[14] D. Wechsler, Manual for the Wechsler adult intelligence scale. New York: Psychological Corporation, 1955.
[15] H. Jasper, The ten-twenty electrode system of the international federation, Electroencephalogr Clin Neurophysiol. 10 (1958) 371–375.
[16] D.L. Hamblin, A.W. Wood, R.J. Croft, C. Stough, Examining the effects of electromagnetic fields emitted by GSM mobile phones on human event-related potentials and performance during an auditory task, Clin Neurophysiol. 115(1) (2004) 171-178.
[17] B.Godey , D. Schwartz , J.B. de Graaf , P. Chauvel , C. Liegeois-Chauvel, Neuromagnetic source localization of auditory evoked fields and intracerebral evoked potentials: a comparison of data in the same patients, Clin Neurophysiol. 112(10) (2001) 1850-1859.
[18] Yvert B, Fischer C, Bertrand O, Pernier J. Localization of human supratemporal auditory areas from intracerebral auditory evoked potentials using distributed source models. Neuroimage 28(1) (2005) 140-53.
[19] C. Eulitz, P. Ullsperger, G. Freude, T. Elbert, Mobile phones modulate response brain activity, Neuroreport 9 (1998) 3229-3232.
[20] G. Freude, P. Ullsperger, S. Eggert, I. Ruppe, Effects of microwaves emitted by cellular phones on human slow brain potentials, Bioelectromagnetics 19 (1998)384-387.
[21] N. Arai, H. Enomoto, S. Okabe, K. Yuasa, Y. Kamimura, Y. Ugawa, Thirty minutes mobile phone use has no short-term adverse effects on central auditory pathways, Clin. Neurophysiol. 114 (2003)1390-1394.
[22] A.B.Clementz, D.L. Blumenfeld, S. Cobb, The gamma band response may account for poor P50 suppression in schizophrenia. Neuroreport. 8(18) (1997)3889-3893.
[23] G. Zouridakis, N.N. Boutros, H.B. Jansen, A fuzzy clustering approach to study the auditory P50 component in schizophrenia. Psychiat. Res. 69 (1997) 169-181.
[24] R. J. Croft, J.S. Chandler, A.P.Burgess, R.J.Barry, J.D.Williams, A.R.Clarke, Acute mobile phone operation affects neural function in humans, Clin. Neurophysiol. 113(2002)1623-1632.
[25] M. Barteri, A. Pala, S. Rotella, Structural and kinetic effects of mobile phone microwaves on acetylcholinesterase activity, Biophys. Chem. 113 (2005) 245-253.
[26] H. Lai, A. Horita, A.-W. Guy, Acute low-level microwave exposure and central cholinergic activity: studies

on irradiation parameters. Bioelectromagnetics 9 (1988)355-362.
[27] H. Lai, M.-A. Carino, A. Horita, A.-W. Guy, Acute low-level microwave exposure and central cholinergic activity: a dose-response study. Bioelectromagnetics 10 (1989), 203-209.
[28] M. J. Griffth, E.J. O'Neill, F. Petty, D. Garver, D. Young, R. Freedman, Nicotinic receptor desensitization and sensory gating deficits in schizophrenia Biol Psychiat., 44(1998) 98-106.
[29] K.F. Stevens, J. Meltzer, G. M. Rose, Nicotinic cholinergic normalization of amphetamine-induced loss of auditory gating in freely moving rats, Psychopharmacology, 119(1995)163-170.
[30] L.A. Dade , R.J. Zatorre , A.C. Evans , M. Jones-Gotman, Working memory in another dimension: functional imaging of human olfactory working memory, Neuroimage 14(3) (2001) 650-60.
[31] A.D. Wagner , A. Maril , R.A. Bjork , D.L. Schacter, Prefrontal contributions to executive control: fMRI evidence for functional distinctions within lateral Prefrontal cortex, Neuroimage 14(6) (2001) 1337-1347.
[32] R. Huber, V. Treyer, J. Schuderer, T. Berthold, A. Buck, N. Kuster, H.P. Landolt, P. Achermann, Exposure to pulse-modulated radio frequency electromagnetic fields affects regional cerebral blood flow, Eur J Neurosci. 21(4) (2005) 1000-6.
[33] H.R.Naghavi, L. Nyberg, Common fronto-parietal activity in attention, memory, and consciousness: shared demands on integration? Conscious Cogn 14(2) (2005) 390-425.
[34] B.R. Postle, L.N. Brush, The neural bases of the effects of item-nonspecific proactive interference in working memory, Cogn Affect Behav Neurosci 4(3) (2004) 379-92.

P-SELECTIN EXPRESSION IN A COLON TUMOR MODEL EXPOSED BY SINUSOIDAL ELECTROMAGNETIC FIELDS

HANDAN TUNCEL, ASSOC.PROF.DR.,
ISTANBUL UNIVERSITY, CERRAHPAŞA MEDICAL FACULTY,
DEPARTMENT OF BIOPHYSICS, TÜRKİYE
handantun@superonline.com

FUMIO SHIMAMOTO, PROF.DR.,
PREFECTURAL UNIVERSITY OF HIROSHIMA, JAPAN
simamoto@pu-hiroshima.ac.jp

MEHMET ALI KORPINAR, PROF.DR.,
ISTANBUL UNIVERSITY, CERRAHPAŞA MEDICAL FACULTY,
DEPARTMENT OF BIOPHYSICS, TÜRKİYE
korpinar@istanbul.edu.tr

MUSTAFA TUNAYA KALKAN, PROF.DR.,
ISTANBUL UNIVERSITY, CERRAHPAŞA MEDICAL FACULTY,
DEPARTMENT OF BIOPHYSICS, TÜRKİYE
tunaya@istanbul.edu.tr

Abstract:

P-selectin plays roles mainly in the initial process of tumor cell adhesion to platelets. The object of present work was to determine the expression level of P-selectin in a colon tumor model that was affected by sinusoidal electromagnetic fields (SMF).

We used male Wistar albino rats 2-2.5 months age. Animals were divided into 4 groups: I (MNU), II (SMF+MNU), III (SMF) and IV (CONTROL). Rats were housed five per polycarbonate cage. 60 mg MNU was dissolved in 6 ml sterile 0.9% NaCl. Prepared solutions were given i.r. to the 1st and 3rd groups as 0.2 ml /per animal. The same procedure was applied to the 2nd and 4th groups but 0.2 ml /per animal sterile isotonic solution was administrated instead. This procedure was repeated once a week for 10 weeks. After administered at MNU, 2nd and 3rd groups were exposed to a sinusoidal magnetic field (SMF, 50 Hz, 5mT) for 6 hours/day for 8 months. The expression of P-Selectin in four groups of rat colon tissues by immunohistochemistry on paraffin sections. The labeled streptavidin biotin method was performed.

Fisher's exact test was used for differences between proportions. There was no statistically significant ($p>0.05$) change in expression level of P-selectin.

Keywords:
P-selectin, carcinogenesis, electromagnetic fields

P-SELECTIN EXPRESSION IN A COLON TUMOR MODEL EXPOSED BY SINUSOIDAL ELECTROMAGNTIC FIELDS

Introduction:

One of the major man-induced environmental changes, which occurred in the last century, is the continued use of oscillating electromagnetic fields (EMF). These fields are generated for communication (*via* radio, television, cellular telephones), as by products of the technology set up for the visualizing on computer and television screens, or from power lines. It has been long believed that electromagnetic radiation in this wavelength range were harmless, and for sure, their inconvenience as pollutants were extremely small when compared to the health dangers associated with, for instance, smog-generating fuel. Yet, now that the major sources of environmental pollution have been identified and are being taken care of, the question about the biological effects of these electromagnetic fields becomes relevant (1).

In fact, some investigators have seen variations in cell proliferation and apoptosis after exposure to ELF fields (2), while others have not observed such changes. Thus, from a careful examination of the literature in this field, it is apparent that further studies examining the role of ELF fields in cancer are necessary. Cancer cell proliferation, apoptosis, invasion, and metastasis are complex phenomena controlled by an even more complex series of pathways, which communicate with each other through a myriad of signaling cascades. In this scenario, a pivotal role is played by cell adhesion molecules (CAMs). CAMs and their receptors mediate cell–cell and cell–matrix interactions and also play a fundamental role in tumor growth, death, metastasis, and invasion. The CAMs principally involved in these processes are those directed against important components of the extracellularmatrix (ECM) such as fibronectin, collagen, laminin, hyaluronan, heparan sulfate, and elastin. Although the number of studies examining the effects of magnetic fields on cell adhesion is rather limited, nonetheless, several studies have provided important insights into this important question (3).

Stimulated endothelial cells and activated platelets express P-selectin (CD62P), a member of the selectin family of cell adhesion molecules, which interacts with P-selectin glycoprotein ligand-1 (PSGL-1, CD162) for leukocyte rolling on stimulated endothelial cells and heterotypic aggregation of activated platelets onto leukocytes. Cross-linking of PSGL-1 by P-selectin also primes leukocytes intracellularly for cytokine and chemoattractant-induced integrin activation for firm adhesion of leukocytes. Furthermore, P-selectin mediates heterotypic aggregation of activated platelets to cancer cells and adhesion of cancer cells to stimulated endothelial cells. There is an increasing body of *in vivo* experimental evidence indicating that P-selectin can play important roles in the growth and metastasis of cancers.In this regard, the elucidation of the molecular mechanisms responsible for the regulation of the expressions of these different P-selectin ligand molecules in various human cancer cells will be an important and very interesting future task (4).

The object of present work was to determine the expression level of P-selectin in a colon tumor model that was affected by sinusoidal electromagnetic fields (SMF).

Material and Methods:

Animals

Healthy male Wistar albino rats, 2-2.5 months age, were employed in the present study. A duration of one week before the experimental period was held for the compliance and controls of experimental animals. Animals were divided into 4 groups as shown in Table 1.

TABLE 1.

Experimental groups with number of animals.

1-MNU 7
2-SMF+MNU 7
3-SMF 9
4-Control 5

Rats were housed five per polycarbonate cage (cages standard for all groups were cleaned twice a week). Water and pelleted diet were available ad libitum. The animal room was checked for temperature, humidity and light status (12:12 light-dark cycle). Temperature was maintained between 23 and 25 °C and relative humidity between 35 and 65 %.

Carcinogen administration

60 mg MNU (N-Methyl-N-Nitrosurea) (Sigma Chemical Co., Dorset, England) was dissolved in 6 ml sterile isotonic solution (0.9% NaCl). Prepared solutions were given i.r. (intra-rectal) to the MNU and SMF+MNU

groups as 0.2 ml /per animal. In the procedure a number 8 feeding tube was inserted 6 cm into the rectum and solution was administered. The same procedure was applied to the SMF and Control groups but 0.2 ml /per animal sterile isotonic solution was administrated instead. This procedure was repeated once a week for 10 weeks.

Application of magnetic field

12 serially connected copper solenoid coils generated the magnetic fields, each having 560 turns. The cores of the coils were filled with soft iron rods and they were tightened to increase the magnetic flux intensity. Plastic cages were used so that the magnetic field strength and distribution would not be affected. The coils were placed vertically and the cages were held 1.2 cm above the coils to hinder them from probable vibration. To protect the cages from heat of the coils, 1 cm thick wooden plates were placed between the coils and the cages. The coils were connected to the 220 V 50 Hz sinusoidal city electric systems. When current passed through the coils, the magnetic flux intensities were measured at five different places inside the cages to be 5 mT. For measurement, we used a Leybold Heraeus 54050 model Hall effect teslameter.

Histological processing

The animals from all groups were killed 8 months after the first i.r. injections of MNU. Immediately after the sacrifice, colons were removed, cut open along its longitudinal axis, and fixed flat in 10% buffered formalin for 24 hours at room temperature. We photographed and/or checked the aberration of the surface of colon mucosa.

Immunohistochemistry and evaluation

For immunohistochemical analysis, the labeled streptavidin biotin method was performed using a Vectastain Universal Quick Kit (Vector Laboratories, Burlingame, CA, USA) with microwave accentuation. The paraffin-embedded sections were heated for 30 minutes at 65°C, deparaffinized in xylene, and rehydrated through graded alcohols at room temperature. A 0.05 M Tris-HCl buffer (pH 7.6) was used to prepare solutions and for washes between various steps. Incubations were performed in a humidified chamber. Four-µm-thick sections were treated for 20 minutes at room temperature with 5% BSA and incubated overnight at 4°C with primary antibodies against P-selectin (BD PharMingen, San Diego, CA, USA). For each case, negative controls were performed on serial sections. On the control section, incubation with the primary antibody was omitted. Horseradish peroxidase activity was visualized by treatment with H_2O_2 and diaminobenzidine for 5 minutes. At the last step, the sections were weakly counterstained with hematoxylin.

A semiquantitative analysis of the immunohistochemistry was performed to determine the approximate percentage of cells expressing P-selectin as follows: absent (-), 0% expression; slight (+), up to 20% of cells positive; moderate (++), 21% to 50% of cells positive; and strong (+++), more than 50% of cells positive.

Histopathological examination

Histological evaluation was performed by routine procedures with H&E staining. The stained sections were examined for grade of histological abnormality.

Results

No appreciable change in food consumption was observed among different groups of rats. Fisher's exact test was used for differences between proportions. There was no statistically significant ($p>0.05$) change in expression level of P-selectin.

Discussion:

Electric and magnetic fields associated with the production, transmission, and use of electricity are ubiquitous in industrialized society. These electric and magnetic fields are predominantly of low frequency (60 Hz in the US, 50 Hz in Europe and Japan) and generally of low intensity. Electric fields exist when there is electric potential in a line, while magnetic fields exist only when there is current flow (5). Since both electric and magnetic fields often occur together and are interactive, these fields have often been referred to as electric and magnetic fields or EMFs.

More recent research has focused on potential adverse biological effects of exposure to magnetic fields. The residential exposures in most homes are to magnetic field intensities of <2 milligauss (mG), which is equivalent to 0.2 microtesla (µT) although some areas in homes may exceed this field intensity. In certain industrial settings, mean workplace magnetic field exposure may exceed 10 mG (6).

Metastasis is a cascade of cellular events by which cancer cells establish new colonies at distant sites in the

body (7,8). It comprises multiple, consecutive steps. Several cell adhesion molecules are involved in the various stages of cancer metastasis (9). P-selectin has been shown to bind to several human cancers and human cancer-derived cell lines, such as colon cancer, lung cancer including small-cell lung cancer, breast cancer, malignant melanoma, gastric cancer, neuroblastoma, and adenoid cystic carcinoma of the salivary gland. There is an increasing body of *in vivo* experimental evidence indicating that P-selectin can play important roles in the growth and metastasis of cancers. In this regard, the elucidation of the molecular mechanisms responsible for the regulation of the expressions of these different P-selectin ligand molecules in various human cancer cells will be an important and very interesting future task (10,11,12).

The expression of P-selectin is regulated at both the transcriptional and cellular levels. At the transcriptional level, tumor necrosis factor-á induces P-selectin expression in mouse and bovine endothelial cells (13,14) whereas interleukin-4 and oncostatin M induce P-selectin expression in human umbilical vein endothelial cells, which can last up to 72 h (15).There is still a long way to go to elucidate the details regarding this pathway (12).

Immunohistochemical studies of P-selectin expression in this model demonstrated no statistically significant ($p>0.05$) differences between the groups. Our results suggest that this study needs confirmation by repetitive experiments, including new methods for P-selectin detection in-vivo and in-vitro. Further work is required to determine the relative effect of the magnetic fields on this molecule and relation with metastasis phenomena.

Acknowledgements

We thank thank Katsunari Ogawa and Miyo Oda for their excellent technical assistance.
This study was supported in part by Tsuchiya Hospital, Japan.
This study was supported by the Research Fund of the University of Istanbul.

References

1-Paolo U. Giacomoni,. & Glen Rein, 2001. Factors of skin ageing share common mechanisms Biogerontology 2: 219–229

2-Tofani,S., Barone, D., Cintorino, M., De Santi, M.M., Ferrara, A., Orlassino, R., Ossola, P.,Peroglio, F., Rolfo,K., and Ronchetto, F. 2001. Static and ELFMagnetic Fields InduceTumor Growth Inhibition and Apoptosis. Bioelectromagnetics 22:419-428.

3-Maria Teresa Santini, Gabriella Rainaldi, Antonella Ferrante, Pietro Luigi Indovina, Paolo Vecchia, and Gianfranco Donelli, 2003. Effects of a 50 Hz SinusoidalMagnetic Field on Cell Adhesion Molecule Expression in Two Human Osteosarcoma Cell Lines (MG-63 and Saos-2). Bioelectromagnetics 24:327-338.

4-Ming Chen and Jian-Guo Geng ,2006. P-selectin mediates adhesion of leukocytes, platelets, and cancer cells in inflammation, thrombosis, and cancer growth and metastasis.Arch. Immunol. Ther. Exp., 54, 75–84.

5-Miller,F.J. and Schroeer,D. (1987) College Physics. 6th edn. Harcourt Brace Jananovich, San Diego, CA.

6-Theriault,G., Goldberg,M., Miller,A.B., Armstrong,B., Guenel P., Deadman,J., Imbernon,E., To,T., Chevalier,A., Cyr,D. and Wall,C. (1994) Cancer risks associated with occupational exposure to magnetic fields among electric utility workers in Ontario and Quebec, Canada, and France: 1970–1989. Am. J. Epidemiol., 139, 550–572.[Abstract]

7- Albelda S. M. and Buck C. A. (1990): Integrins and other cell adhesion molecules. FASEB J., **4**, 2868–2880.

8-Miyasaka M. (1995): Cancer metastasis and adhesion molecules. Clin. Orthop. Relat. Res., **312**, 10–18.

9-Huang Y. W., Baluna R. and Vitetta E. S. (1997): Adhesion molecules as targets for cancer therapy. Histol. Histopathol., **12**, 467–477.

10-Aruffo A., Dietsch M. T., Wan H., Hellstrom K. E. And Hellstrom I. (1992): Granule membrane protein 140 (GMP140) binds to carcinomas and carcinoma-derived cell lines. Proc. Natl. Acad. Sci. USA, **89**, 2292–2296.

11-Mannori G., Crottet P., Cecconi O., Hanasaki K., Aruffo A., Nelson R. M., Varki A. and Bevilacqua M. P. (1995): Differential colon cancer cell adhesion to E, P, and L-selectin: role of mucin-type glycoproteins. Cancer Res., **55**, 4425–4431.

12-Ming Chen and Jian-Guo Geng, 2006. P-selectin mediates adhesion of leukocytes, platelets, and cancer cells in inflammation, thrombosis, and cancer growth and metastasisArch. Immunol. Ther. Exp., 54, 75–84

13-Hahne M., Jager U., Isenmann S., Hallmann R. And Vestweber D. (1993): Five TNF-inducible cell adhesion mechanism on the surface of mouse endothelioma cells mediate the binding of leukocytes. J. Cell. Biol., **121,** 655–664.,

14-Sanders W. E., Wilson R. W., Ballantyne C. M. And Beaudet A. L. (1992): Molecular cloning and analysis of *in vivo* expression of murine P-selectin. Blood, **80,** 795–800.

15-Yao L., Pan J., Setiadi H., Patel K. D. and McEver R. P. (1996): Interleukin 4 or oncostatin M induces a prolonged increase in P-selectin mRNA and protein in human endothelial cells. J. Exp. Med., **184**, 81–92.

BIOLOGICAL EFFECT ON BLOOD-CEREBROSPINAL FLUID BARRIER DUE TO RADIO FREQUENCY ELECTROMAGNETIC FIELDS EXPOSURE OF THE RAT BRAIN IN VIVO

USHIYAMA A.[1], MASUDA H.[1], HIROTA S.[1], KAWAI H.[2], TANAKA S.[2], WAKE K.[2], WATANABE S.[2], SUZUKI Y.[3], TAKI M.[3] and OHKUBO C.[4]

[1]Dept. of Environmental Health, National Institute of Public Health, 2-3-6 Minimi, Wako-shi, Saitama 351-0197, Japan. [2] Electromagnetic compatibility group, applied electromagnetic research center, National Institute of Information and Communications Technology, 4-2-1 nukui-kitamachi, koganei, Tokyo 184-8795, Japan. [3]Dept. of Electrical and electronic Engineering, Tokyo Metropolitan University, 1-1 minami-osawa, hachioji, Tokyo 192-0397, Japan. [4]RAD, World Health Organization, Geneva CH1211, Switzerland.

Abstract

In this study, we explored the subchronic effect of RF-EMF on blood-cerebrospinal fluid barrier (BCB) function, which defined as one of the blood-brain barrier functions. To attain the purpose, we used the micro-perfusion method, which makes it possible to quantify BCB function in vivo with high sensitivity, and evaluate the effect on barrier function during RF-EMF exposure to rat. Using a custom-made "8"-shaped loop antenna, which optimized for RF-EMF exposure to rat's head locally, we exposed 1.5 GHz RF-EMF with PDC modulation to the head of juvenile rats. A 30 minutes exposure was repeated everyday for 6 successive days, and on the 6th day, BCB function was quantified by using micro-perfusion method. The fluorescence intensity in collected cerebrospinal fluid did not increase indicating BCB did not affected by RF exposure at the brain average SARs of 0.5, 2.0 and 10 W/kg. These results suggest that the daily exposure of 1.5 GHz RF-EMF did not affect the BCB function in juvenile rats under our experimental conditions.

Introduction

Possible health effects of weak RF-EMF have been discussed worldwide. However, further scientific evidences are needed for better health risk assessment, particularly; the effects on the blood-brain barrier (BBB) which are still not clear due to the variety of experimental designs. One of the main problems on BBB study is that there are few methods which are able to monitor the barrier function on real time in vivo. In this study, we developed a real-time measuring system for blood-cerebrospinal fluid barrier (BCB) function which defined same as BBB in a broad sense. To collect CSF continuously, we employed micro-perfusion method to the measuring system. By using this method, we explored the subchronic effects on the BCB when RF-EMF was exposed to the head of animal.

Animals and surgical procedure We used male Sprague-Dawley rats (Tokyo Laboratory Animals Science Co., Japan) aged 5 weeks. Rats were anesthetized by i.m. injection of a cocktail of ketamine hydrochloride (90 mg/kg body weight, Sigma Chemical Co., St. Louis, MO) and xylazine hydrochloride (10 mg/ kg body weight, Sigma Chemical Co.), and a guide cannula (Eicom Co., Kyoto, Japan) was introduced to one of the lateral ventricles through the hole and secured to the skull with dental cement. Assembly of push-pull cannula including guide cannula was shown in Fig 1.

Exposure conditions Rats for exposure groups were divided into three groups. Each exposure condition was at 0.5, 2.0, 10W/kg (brain averaged SAR) for 30 minutes per day for 6 consecutive days. We applied RF-EMF (1,439 MHz) with PDC modulation which generated by an 8-shaped loop antenna (Fig.2). During exposure, the antenna was located at 4 mm above the rat head by using the stereotaxic apparatus. In the sham exposure group, rats were also anesthetized and kept on the stereotaxic apparatus without RF-EMF exposure. On the 6th day of exposure, a push pull cannula (Fig.1) was inserted into a guide cannula. The inlet and the outlet of the cannula

were connected to the push-pull micro perfusion pump unit (EP-70, Eicom Co.) which enabled the collection of CSF continuously. At the beginning of RF-EMF exposure, FITC-labeled albumin (FITC-albumin) was injected into caudal vein and CSF perfusion was started at a rate of 1 µl/min. Fluorescence intensity of FITC-albumin in perfusate was monitored by using spectrofluorometry under the condition of excitation /emission wave length at 490/515nm .Fluorescence intensity in perfusate was monitored for 180 minutes from the beginning of the exposure. Experimental setup was summarized in Fig. 3.
All experimental procedures are approved by the animal experiment committee in National Institute of Public Health.

Results No statistical difference on BCB function was detected among each exposure condition (Fig.4).

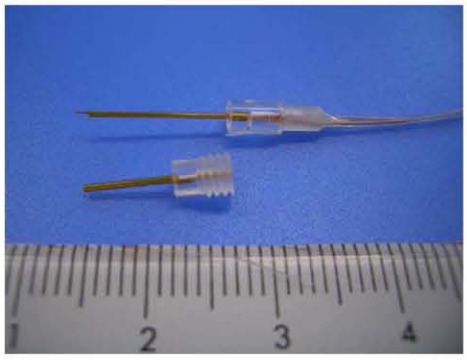


Fig 1 Assembly of push-pull cannula for rat
Upper is an inner cannula which includes in/out route and lower is a guide cannula

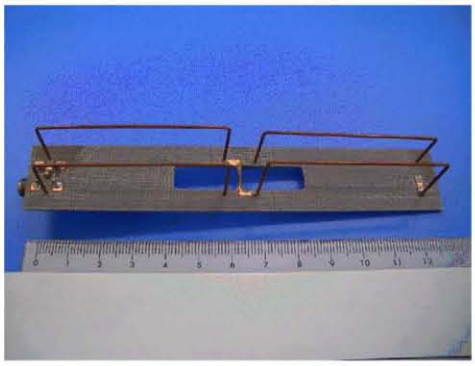


Fig 2 Overview of an "8-shaped" loop antenna for RF-EMF exposure

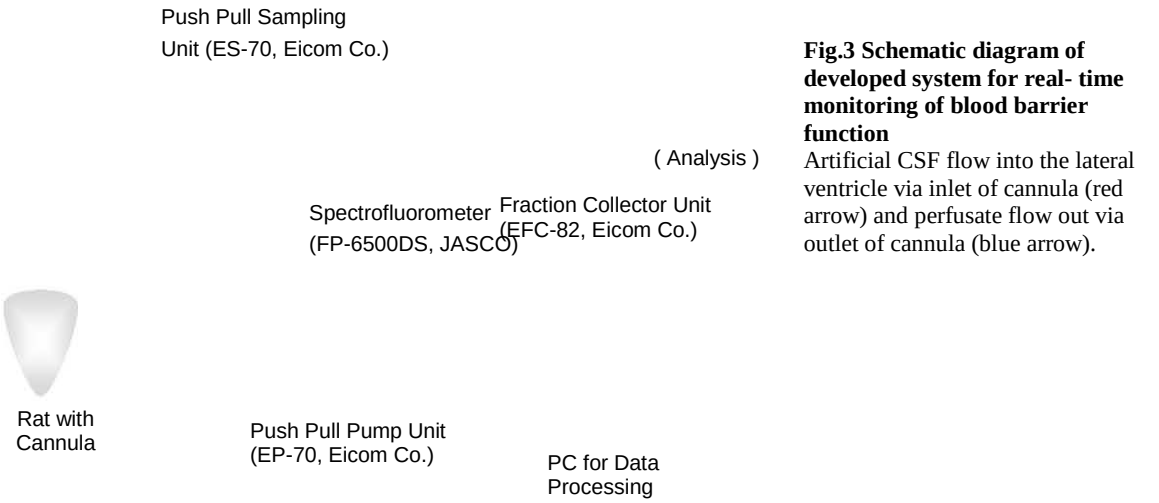


Fig.3 Schematic diagram of developed system for real- time monitoring of blood barrier function
Artificial CSF flow into the lateral ventricle via inlet of cannula (red arrow) and perfusate flow out via outlet of cannula (blue arrow).

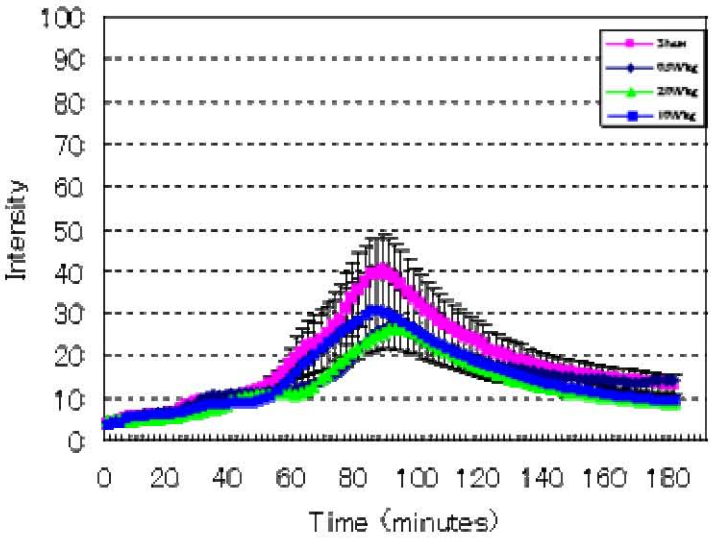


Fig.4 Fluorescent profiles of sham and RF-EMF exposed group
Fluorescence intensity was emitted by fluoro-spectrometer which connected to the outlet of the push-pull cannula. Due to the dead-volume of the connection tubes, changes of fluorescence intensity in cerebrospinal fluid were reflected to this profile with some time delay. There is no statistical difference among each group.

Summary

In the previous studies, we have already reported that acute exposure to RF-EMF does not induce the effect on the blood-cerebrospinal fluid barrier (BCB) [1, 2]. In this study, we explored the subchronic effect on BCB by RF-EMF exposure. To attain the purpose, we used the micro-perfusion method, which makes us possible to quantify the barrier function in vivo with high sensitivity, and can be applied during exposure. After 6 consecutive days exposure for 30 minutes/day to 1.5GHz RF-EMF using an "8"-shaped loop antenna, the fluorescence intensity in collected fluid did not increase in any group. These results indicate blood-cerebrospinal fluid barrier did not affected by the RF exposure. As a conclusion, sub-chronic RF-EMF exposure under this experimental condition was not affect blood-cerebrospinal fluid barrier function in rats.

Acknowledgements

This study was financially supported by the Ministry of Health, Labour and Welfare, Japan.

References

[1] Ushiyama A, Masuda H, Hirota. S, Watanabe. H, Wake K, Watanabe S, Yamanaka. Y, Taki M, Ohkubo C. Acute effects on blood barrier function by RF-EMF exposure to rat brain in vivo. In: Abstract book of the 28th General Assembly of International Union of Radio Science; 2005 Oct 23-29; New Delhi, India. 2005. KP.6(01436) in CD-ROM.

[2] Ushiyama A, Masuda H, Hirota S, Takahashi M, Kawai H, Tanaka S, Wake K, Watanabe S, Suzuki Y, Taki M, Ohkubo C. Blood-Cerebrospinal barrier in rats is not affected by 1.5 GHz RF-EMF exposure at non thermal level. In: Abstract Collection of the 28th Annual meeting of Bioelectromagnetics Society; 2006 Jun 11-15; Cancun, Mexico. 2006. p.384-385

THE EFFECT OF HIGH-FREQUENCY ELECTROMAGNETIC FIELD ON SOME SOMATIC AND NERVOUS CHARACTERISTICS IN HEALTHY AND NEURODEFECTIVE MICE

[1]FRANTIŠEK VOŽEH, [1]ANTONÍN DONĚK, [1]JAN CENDELÍN, [1]IVANA KORELUSOVÁ, [2]JAN VRBA

[1]CHARLES UNIVERSITY IN PRAGUE, FACULTY OF MEDICINE IN PILSEN, DEPARTMENT OF PATHOPHYSIOLOGY, LIDICKÁ 1, 301 66 PLZEŇ, CZECH REPUBLIC

[2]CZECH TECHNICAL UNIVERSITY IN PRAGUE, FACULTY OF ELECTRICAL ENGINEERING, DEPARTMENT OF ELECTROMAGNETIC FIELD, TECHNICKÁ 2, 166 27 PRAHA 6, CZECH REPUBLIC

e-mail: frantisek.vozeh@lfp.cuni.cz

Abstract

The effect of long-term exposure to high frequency electromagnetic field (HF EMF) on some somatic and neural characteristics was studied in neurodefective Lurcher mutant (+/Lc) and normal wild type mice (+/+). Both newborn and young adult (3 months) animals derived from two strains (C3H, C57Bl/7) were exposed to HF EMF (870 MHz) from 1st to 21st day or from 91st to 120th day respectively. In animals of both groups and controls we observed the development of body weight. Moreover, in the HF EMF exposed adult C57Bl/7 animals we studied spatial learning ability, motor functions and the CNS excitability. To investigate specific energy absorption rate (SAR) in experimental animals we have done the basic 3D calculations of the electromagnetic energy distribution in the simplified model of the mouse. The HF EMF exposed animals exhibited a mild increase of body weight with small strain differences. The long-term exposure to HF EMF did not significantly influence the ability to learn in the Morris water maze. However, lower swimming speed was found in the irradiated +/Lc as well as lower motor activity of +/+ in the open field when compared to controls. No significant differences were found between HF EMF irradiated animals and controls in examination of the CNS excitability and motor functions.

Introduction

Increasing use of different devices (mobile phones) and other ones (radars, radio transmitters) that emit potentially harmful radiofrequency (RF) radiation is the reason why the effect of high frequency electromagnetic field (HF EMF) on human (and/or animal) body and especially on the brain, is subjected to a concentrated research. Despite this effort there is e.g. no unambiguous evidence about broadly discussed promoting effect of RF EMF on the brain cancer growth. Some results have indicated increased risk (Repacholi et al., 1997; Hardell et al., 2002) while other studies have shown no effect (Salford et al., 1997a) or even decreased risk (Adey et al., 1999). On the other hand, the clear effect of RF radiation - including that from global system for mobile communication (GSM) microwaves (MWs) - increase in blood-brain barrier (BBB) permeability in rats for their own albumin has been found (Persson and Salford, 1996; Fritze et al., 1997; Persson et al., 1997; Malmgren, 1998; Salford et al., 2001; Töre et al., 2001). Furthermore, it was observed, that the albumin leakage over the BBB caused neuronal damage in both the cortex, the hippocampus and the basal ganglia in the brains of rats exposed acutely two hours to GSM mobile phone EMF of different strengths (Salford et al., 2003). Recently, rats exposed also for 2h to GSM MWs (915 MHz, SAR 0.4 mW/g) exhibited affected expression of genes in cerebellar cells (Belyaev 2006).

Behavioral experiments in animals showed performance deficits in spatial learning in rats (Lai, 1996; Lai et al., 1998) and in mice (Sienkiewicz et al., 1998) exposed to low-frequency EMF (50 and 60 Hz). Affected learning process was also described in rats exposed to HF EMF (2450 Hz) and examined in the radial and the

Morris water maze (Lai et al., 1994; Wang et al., 2000). On the contrary, no significant effect on spatial learning was described in rats influenced by head only exposure system emitting a 900-MHz GSM EMF (Dubreuil et al., 2002).

In human, changes of working memory and evoked potentials were found as a consequence of mobile phone use (Koivisto et al., 2000; Jech et al., 2001). Except for influence of EMF on membrane ion transport (Bawin, Adey, 1976; Blackman et al., 1982; Dutta et al., 1989; Liu et al., 1990; Cleary 1990a,b, 1995) and neurotransmitter system (Merritt et al., 1977; Modak, et al., 1981; Inaba et al., 1992) the reason of the effect can be also, that mobile phones broadcast specifically at frequencies at which the head serves as an antenna and brain tissue serves as a demodulating radio receiver (Weinberger and Richter, 2002).

In previous works we described the results of our research dealing with some functional and morphological characteristics of the brain in normal and neurodefective mice exposed to both acute and chronic influence of HF EMF (Vožeh et al. 2004, Cendelín et al. 2004). The aim of this work was to survey further results of experiments concentrated on somatic and neurobehavioral characteristic in the same types of mice chronically influenced by HF EMF in two phases of their life.

Animals and methods

Experimental animals we used were Lurcher mutant and wild type mice of both sexes derived from two strains (C3H, C57B1/7). Mice were kept on a 12:12 hour light:dark cycle with constant temperature (21± 1^{o} C) and humidity (60±10%). Water and food were available ad libitum. All these experiments have been done in full agreement with the law of the Czech Republic dealing with the right treatment of experimental animals.

The mutants suffer from genetically determined olivocerebellar degeneration due to mutation of the δ2 glutamate receptor gene. The δ2 glutamate receptor is especially expressed by cerebellar Purkinje cells (Zuo et al., 1997) and this is a reason why Lurcher mutants (heterozygotes, +/Lc) are characterized by complete progressive extinction (a type of excitotoxic apoptosis) of Purkinje cells and by a substantial decrease in number of cerebellar granule cells and inferior olive neurons (Caddy and Biscoe, 1979). The mutants exhibit signs of cerebellar ataxia, deterioration of cognitive function and higher sensitivity to some neurotoxic agents (Caddy and Vožeh, 1997; Vožeh et al., 1999). Their littermates - wild-type mice (homozygotes +/+) are healthy. One half of experimental animals (+/Lc and +/+) was subjected to chronic exposure to HF EMF, the unexposed animals of the second half were controls. The whole body exposition was performed using HF generator with HF amplifier and antenna. Frequency of HF EMF was 870 MHz (close to mobile phones frequency) and power output of the apparatus was 10 W. The radiation was directed by a wave guide to a plastic box with the animals placed just in front of it (Fig.1).

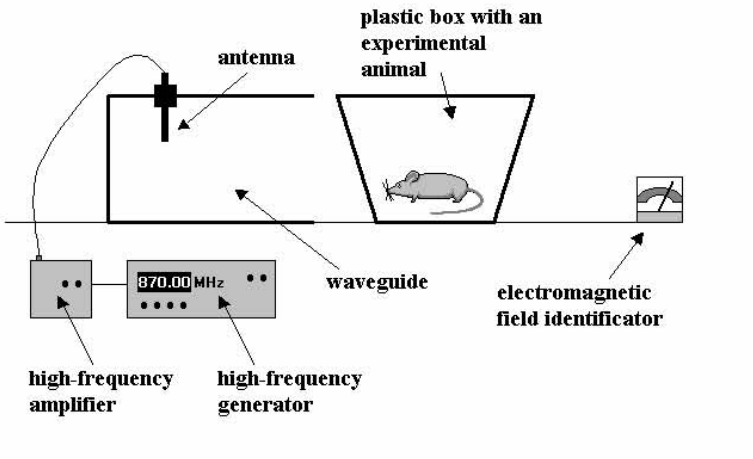


Fig. 1: Scheme of HF EMF exposure

The animals of two developmental periods were exposed to HF EMF:

1) newborns (irradiated from 1st to 21st day of life, 2.5 h daily, together 162 animals of both strains),

2) young adults (irradiated from 91st to 120^{ies} day of life, 3 h daily, together 94 animals of both strains).

To estimate SAR in experimental animals we have done basic 3D calculation of electromagnetic energy distribution in a simplified dielectric model of an adult mouse. The model consists of a homogenous lossy dielectric material mimicking muscle tissue and has shape of a cylinder (radius 3 cm and high 9 cm terminated to cone) with dielectric properties $e_r = 54$, conductivity s = 0.8 S/m, density r = 1000 kg/m^3 (Fig. 2).

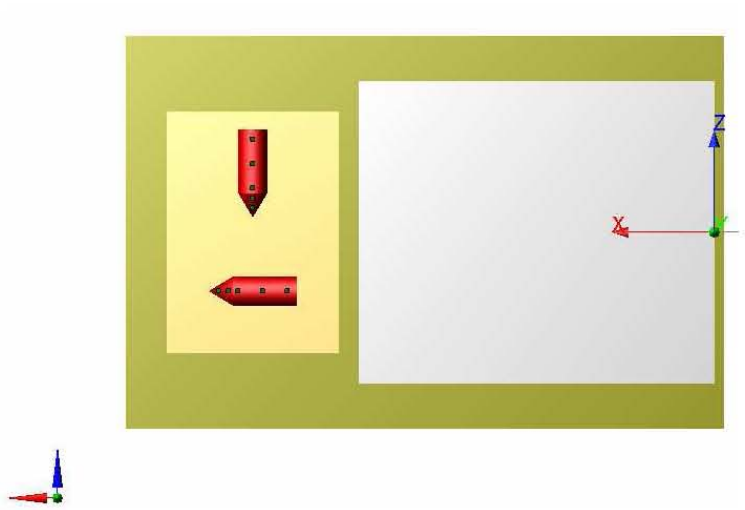


Fig. 2: Scheme of the simplified dielectric model of an adult mouse during SAR measurement (bird´s-eye view).

The calculations were done with the aid of 3D electromagnetic field simulator SEMCAD which used FDTD (Finite Different Time Domain). The method is based on the fact that original continuous function is replaced by the set of discrete function´s values. Maxwell's equations are discretized using a 2nd order finite-difference approximation both in space and in time in an equidistantly spaced mesh. Several simulations for different positions of mice were done. Input power during simulations was normalized to 1 watt.

Both HF EMF exposed and unexposed animals (C3H and C57B1/7 newborns and young adults) were subjected to examination of the body weight development during the irradiation periods. Spatial learning ability, passive avoidance learning, CNS excitability and behavioral activity as well as topical motor skills were tested in young adult C57B1/7 mice only.

The topical body weight in individual animals was investigated every day during the irradiation period. Data obtained in individual days we used for calculation of the relative body weight increase which represented the ratio of the values in individual days to the value received on the first day of the HF EMF exposure.

Spatial learning was tested using Morris water maze. It consists of round plastic pool with a small round platform hidden under the water surface, permanently at the same place. The mouse had to locate the platform only by its relationship to distant landmarks (window, laboratory furniture, tube lights). Four swimming trials daily were performed during 6 days long examination period (D1 – D5 and D8). If the mouse did not find platform within 60 s, it was placed there. The mouse stayed on the platform always for 30 s. Mean latencies of reaching platform, swimming speed and the length of trajectory were compared in HF EMF exposed animals and controls.

For examination of discriminative learning we used "step down" method of the passive avoidance inhibitory reaction. In this test the mouse is positioned on a small platform (bench), the size of which is dependent on the age of the animal, 5 mm above an electrified grid floor of the plastic box (200 x 250 x 200 mm high). The animal is trained until the chosen criterion (100 s on the bench without descent) is met. Four parameters are measured: latency to the first descent, number of descents, time to criterion and time of stay on the grid. The same procedure is repeated 24 hours later and evaluation of each parameter is obtained by dividing the values of the retention test by those obtained in the learning (1st day) test.

CNS excitability was tested with the audiogenic epilepsy method. The mouse was placed into a plastic box covered with a transparent lid. Inside the box was an electric doorbell which served as a source of a sound stimulus of intensity of 90 dB. The sound was switched on for 60 s and the reaction of the animal was observed. The reactions were divided into 5 degrees: 1. no reaction, or exploration, 2. running, 3. fast running and

jumping, 4. convulsions, 5. death of the animal as a consequence of the convulsions. Mean reaction degree was compared.

Behavioral and spontaneous motor activity were studied using the open-field test. The open-field chamber was rectangular plastic box (400 x 400 x 450 mm high), open at the top. The box was cleaned using dilute alcohol before each trial to eliminate odorous cues. Behavior of mice and their activity were coded by a simple computer program and time spent in the central zone or in individual corners of the box as well as the length of locomotion trajectory were evaluated.

The topical complex motor skills were tested using four methods:

1) Fall - releasing the mouse (the right hand grips the mouse tail, the left hand the skinfold behind) from the height of 30 cm and evaluation of the drop to the cushioned table either to four extremities or to the flank.
2) Wire suspension - evaluation of the mouse ability to hang on a horizontal wire (diameter 1 mm, 40 cm above a cushioned table) after its front paws were placed on it. The criterion for success: 1 min.
3) Slanting ladder - evaluation of the mouse ability to stay on or climb up the ladder (length 35cm, width 4 cm, distance of 1 cm, inclination from horizontal 60^{o}) after being positioned in the middle of it with head upwards.
4) Rotating cylinder - evaluation of the mouse ability to stay on a slowly rotating cylinder (diameter 15 cm, length 20 cm, after being positioned there with its head in the direction of the rotation.The criterion for success: 1 min.

Results

The animals exposed to HF EMF from 1^{st} to 21^{st} day exhibited body weight differences between them and controls only in C3H wild type mice females. They revealed statistically significant body weight increase mainly between 7^{th} and 18^{th} day of irradiation (Fig. 3).

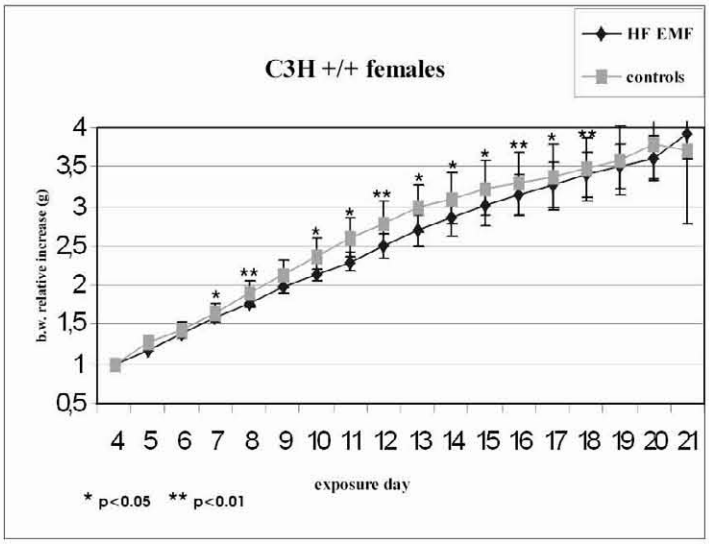


Fig. 3: Relative body weight (b.w.) increase (in grams) in C3H wild type HF EMF irradiated females and controls during the postnatal period 1 - 21 days.

The animals exposed to HF EMF between days 91 and 120 of their life exhibited most significant body weight differences also in females but in some cases in males too. In C3H neurodefective females the significant body weight increase was found 7 times during the 30 days irradiation period (Fig. 4).

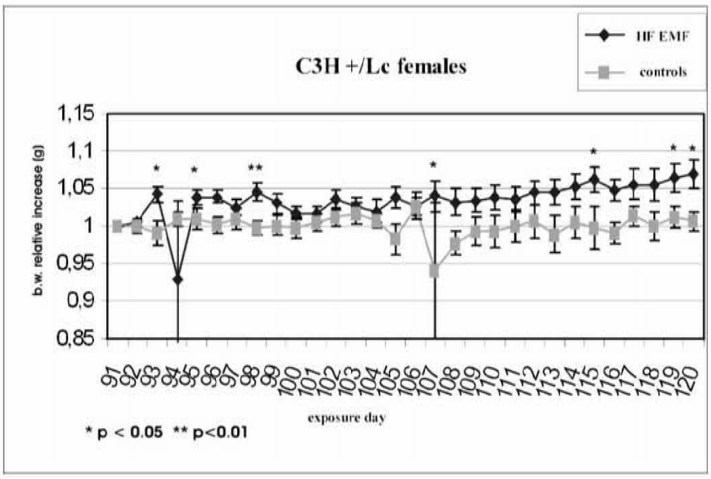


Fig. 4: Relative body weight (b.w.) increase (in grams) in C3H Lurcher mutant HF EMF irradiated females and controls during the postnatal period 91- 120 days.

In C57B1/7 neurodefective females were no significant differences between HF EMF exposed animals and controls while the HM EMF irradiated neurodefective males revealed significant body weight increase 3 times during the first half of the irradiation period (Fig. 5).

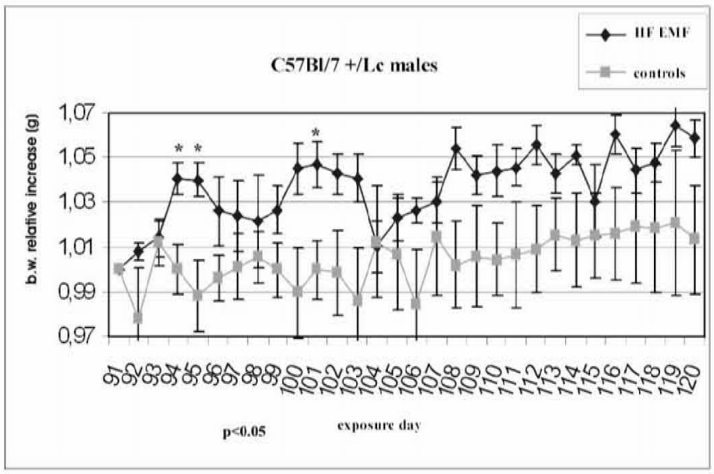


Fig. 5: Relative body weight (b.w.) increase (in grams) in C57Bl/7 Lurcher mutant HF EMF irradiated males and controls during the postnatal period 91- 120 days.

Investigation of spatial learning ability showed no statistically significant differences in latencies of climbing the platform and the lengths of trajectories between HM EMF exposed animals and unexposed controls of both types (+/+, +/Lc). However, HF EMF exposed Lurcher mutant mice revealed significantly lower swimming speed (in D1 and D2, $p<0.01$ and $p<0.02$ respectively) in comparison with controls (Fig. 6).

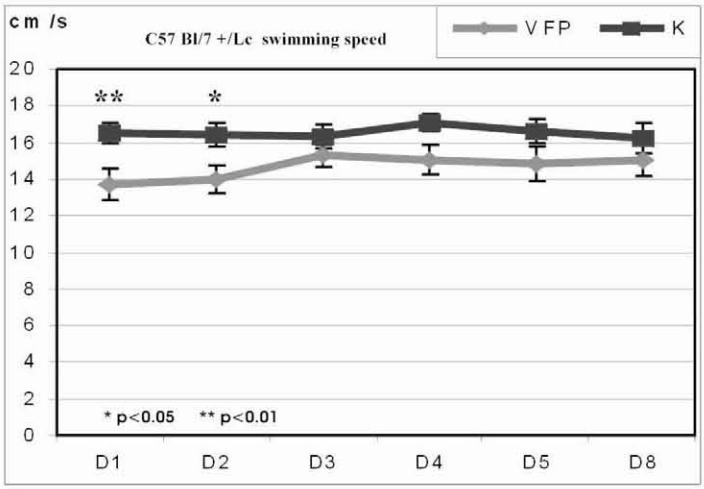


Fig. 6: Average swimming speed in C57Bl/7 HF EMF irradiated Lurcher mutants and controls in individual days of the spatial learning process examination.

Results of inhibitory reaction of passive avoidance learning showed no significant differences between HF EMF exposed animals and unexposed controls of both types (+/+, +/Lc). Any significant differences were found between experimental (irradiated) animals and controls neither in investigation of open field activity nor in the examination of CNS excitability by the method of audiogenic epilepsy. Nevertheless, HF EMF irradiated wild type mice exhibited mildly lower motor activity (on the margin of statistical significancy) in the open field testing when compared to controls.

Also tests of complex topical motor skills did not show any statistically significant differences between animals exposed to HF EMF and unexposed controls. On the other hand there are visible clear differences in the graphs between performances of healthy wild type mice a neurodefective Lurcher mutants (Figs. 7A, B).

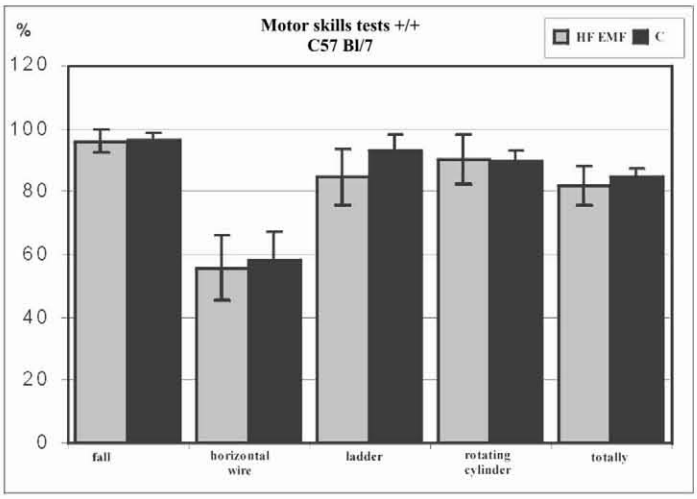


Fig. 7A: Meeting criteria in individual topical motor skills tests and in total expressed as percentage in C57Bl/7 HF EMF irradiated wild type mice and controls.

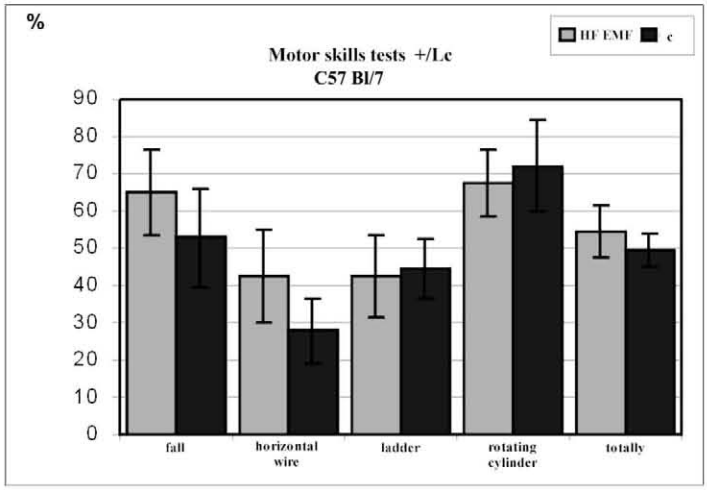


Fig. 7B: Meeting criteria in individual topical motor skills tests and in total expressed as percentage in C57Bl/7 HF EMF irradiated Lurcher mutant mice and controls.

Calculations of SAR performed in connection with the simulation of absorption electromagnetic energy by experimental animals using the artificial dielectric model showed the dependence of the absorption on the real topical position of the mouse against the waveguide and was in the range of 0.05 to 1.44 mW/g (Fig. 8).

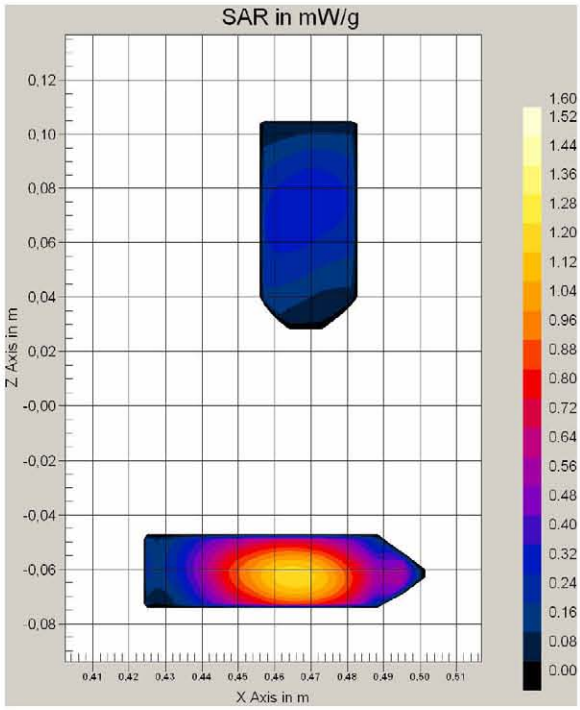


Fig. 8: SAR value (in mW/g) expressed as different hues in dependence on position of the dielectric mouse model.

Summary

Similarly as in our previous works the results were obtained in healthy and partly neurodefective mice in two developmental periods chronically exposed to HF EMF which corresponded to that used in GSM mobile phones.

Both healthy and partly neurodefective animals were used and some of experiments were realized in both types of mice derived from two different strains. The fact that the chronical exposure of mice to HF EMF was performed in their early ontogeny (during the first 3 weeks of life) which involved "the brain growth spurt" period and later (from 3 to 4 month of life) enabled us to investigate the effect of HF EMF in complex and more detailed way.

First of all, the results of our experiments showed the positive effect of chronic HF EMF exposure on gentle but in some cases significant body weight increase mainly in females of both strains. In addition, on days (D1, D2) HF EMF irradiated C57Bl/7 Lurcher mutants exhibited significantly lower swimming speed in the Morris water maze when compared with HF EMF unexposed animals.

Despite other examinations didn´t show any further significant differences between HF EMF irradiated animals and HF EMF unexposed controls it is possible to say: in agreement with our previous results the HF EMF revealed the indubitable effect on some somatic and neuro-behavioral characteristics in newborn and young adult animals. This is the reason why the problem of the biological effect of HF EMF on living beings needs to be further studied.

Acknowledgement

The work was supported by the Research Program Project MSM CR 021620816

References

1. Adey, W., Byus, C., Cain, C., Higgins, R., Jones, R., Kean, C. et al.: Spontaneous and Nitrosourea-induced Primary Tumors of the Central Nervous System in Fisher 344 rats exposed to 836 MHz Modulated Microwaves. Radiat Res. 152: 293-302, 1999.
2. Bawin, S.M., Adey, W.R.: Sensitivity of calcium binding in cerebral tissue to weak environmental electrical fields oscillating at low frequency. Proc. Natl. Acad. Sci., USA 73(6): 1999-2003, 1976.
3. Belyaev, I.Y., Koch, C.B., Terenius, O., Roxtrom- Lindquist, K., Malmgren, L.O., H. Sommer, W., Salford, L.G., Persson, B.R.: Exposure of rat brain to 915 MHz GSM microwawes induces changes in gene expressuion but not double stranded DNA breaks or effects on chromatin conformation.
4. Blackman, C.F., Benane, S.G., Rabinowitz, D.E., House, D.E., Joines, W.T.: Effects of ELF fields on calcium-ion efflux from brain tissue in vitro. Radiation Res. 92: 510-520, 1982.
5. Caddy, K.W.T., Biscoe, T.J.: Structural and quantitative studies on the normal C3H and Lurcher mutant mouse. Phil. Trans. Roy. So. Lond. B. 287: 167-201, 1979.
6. Caddy, K.W.T., Vožeh, F.: The effect of 3-acetylpyridine on the inferior olivary degeneration in the Lurcher mutant and wild type mice. Europ. J. Pharmacol. 330: 137-142, 1997.
7. Cendelín J., Schmidtmayerová B., Štenglová V., Vožeh F., CNS excitability in normal and neurodefective C3H mice exposed to high-frequency electromagnetic field, Proceedings of Biological effects of EMFs, 3rd International workshop, Kos, Greece, 4.-.8.10.2004, Ed. P.Kostarakis, p.866-871.
8. Cleary, S.F.: Cellular effects of radiofrequency electromagnetic fields. In: Biological Effects and Medical Applications of Electromagnetic Energy (O. P. Gandhi, Ed.). Engelewood Cliffs, New Jersey, Prentice-Hall, p 339, 1990a.
9. Cleary, S.F.: Biological effects of radiofrequency electromagnetic fields. In: Biological Effects and Medical Applications of Electromagnetic Energy (O.P. Gandhi, Ed.). Englewood Cliffs, New Jersey, Prentice-Hall, p 236, 1990b.
10. Cleary, S.F.: Effects of radiofrequency radiation on mammalian cells and biomolecules in vitro. In: Electromagnetic Fields: Biological Interactions and Mechanisms (M. Blank, Ed.). Washington, American Chemical Society, p 467, 1995.
11. Dubreuil, D., Jay, T., Edeline, J.M.: Does head-only exposure to GSM-900 electromagnetic fields affect the performance of rats in spatial learning tasks? Behav. Brain Res. 129: 203-210, 2002.
12. Dutta, S.K., Ghosh, B., Blackman, C.F.: Radiofrequency radiation-induced calcium-ion-effux enhancement from human and other neuroblastoma cells in culture. Bioelectromagnetics 10: 197-202, 1989.
13. Fritze, K., Sommer, C., Schmitz, B., Mies, G., Hossman, K., Kiessling, M. et al.: Effect of global system for mobile communication (GSM) microwave exposure on blood-brain barrier permeability in rat. Acta Neuropathol. (Berlín) 94: 465-470, 1997.
14. Hardell, L., Hallquist, A., Hansson, Mild, K., Carlberg, M., Pählson, A., Lilja, A.: Cellular and Cordless telephones and the risk for brain tumours. Europ. J. of Cancer Prevention 11: 377-386, 2002.
15. Inaba, R., Shishido, K., Okada, A., Moroji, T.: Effects of whole body microwave exposure on the rat brain contents of biogenic amines. Eur. J. Appl. Physiol. 65: 124, 1992.

16. Jech, R., Sonka, K., Ruzicka, E., Nebuzelsky, A., Bohm, J., Juklickova, M., Nevsimalova, S.: Electromagnetic field of mobile phones affects visual event related potential in patiens with narcolepsy. Bioelectromagnetics 22 (7): 519-28, 2001.
17. Koivisto, M., Krause, C.M., Revonsuo, A., Laine, M., Hamalainen, H.: The effects of electromagnetic field emitted by GSM phones on working memory. Neuroreport 11: 1641-3, 2000.
18. Lai, H., Horita, A., Guy, A.W.: Microwave irradiation affects radial-arm maze performance in the rat. Bioelectromagnetics 15: 95-104,1994.
19. Lai, H.: Spatial learning deficit in the rat after exposure to a 60 Hz magnetic field. Bioelectromagnetics 17: 494-496, 1996.
20. Lai, H., Carino, M.A., Ushijima, I.: Acute exposure to a 60 Hz magnetic field affects rats´ water- maze performance. Bioelectromagnetics 19: 117-122, 1998.
21. Liu, D.S., Astumian, R., Tsong, T.: Activation of Na^+ and K^+ pumping modes of NA/K-ATPase by an oscillating electric field. J. Biol. Chem. 265: 7260, 1990.
22. Malmgren, L.: Radio frequency systems for NMR-imaging-Coil development and studies of non-thermal biological Effects. Series of Licentiate and Doctoral These, No. 6, Department of Applied Electronics, Lund University, Lund, Sweden. 1998.
23. Merritt, J.H., Chamness, A.F., Hartzell, R.H., Allen, S.J.: Orientation effects on microwave-induced hyperthermia and neurochemical correlates. J. Microwave Power 12: 167, 1977.
24. Modak, A.T., Stavinoha, W.B., Dean, U.P.: Effect of short electromagnetic pulses on brain acetylcholine content and spontaneous motor activity in mice. Bioelectromagnetics 2: 89, 1981.
25. Persson, B., Salford, L.: Permeability of the blood-brain barrier in rats induced by continuous wave and pulse-modulated 915 MHz electromagnetic radiation exposure in TEM-cells. (Chiabrera A, Juutilainen J, eds). Brussel: EU DG XIII, 66-72, 1996.
26. Persson, B., Salford, L., Brun, A.: Blood- brain barrier permeability in rats exposed to electromagnetic fields used in wireless communication. Wireless Networks 3: 455-461, 1997.
27. Repacholi, M., Basten, A., Gebski, V., Noonan, D., Finni, J., Harris, A.W.: Lymphomas in Eμ-Pim 1 transgenic mice exposed to pulsed 900 MHz electromagnetic fields. Rad. Res. 147: 631-640, 1997.
28. Salford, L.G., Brun, A., Persson, B.: Brain tumour development in rats exposed to electromagnetic fields used in wireless communication. Wireless Networks 3: 463-469, 1997a.
29. Salford, L.G., Person, B., Malmgren, L., Brun, A.: Téléphonie Mobile et Barriére Sang-Cerveau. In: Téléphonie Mobile-Effets Potentiels sur la Santé des Ondes Électromagnétiques de Haute Fréquence. (Pietteur Marco, ed.) Embourg, Belgium, 141-152, 2001.
30. Salford, L.G., Brun, A.E., Eberhardt, J.L., Malmgren, L., Persso, B.R.: Nerve cell damage in mammalian brain after exposure to microwaves from GSM mobile phones. Environ Health Perspect 111 (7): 8813, 2003.
31. Sienkiewicz, Z.J., Haylock, R.G., Saunders, R.D.: Deficits in spatial learning after exposure of mice to a 50 Hz magnetic field. Bioelectromagnetics 19: 79-84, 1998.
32. Töre, F., Dulou, P.E., Haro, E., Veyret, B., Aubineau, P.: Two-hour Exposure to 2 W/kg, 900 MHz GSM microwaves induces Plasma Protein Extravasation in Rat Brain. In: Proceedings from the 5th International Congress of the European Bioelectromagnetics Association, 6 September 2001 (Hietanen, M, Jokela, K, Juutilainen, J, eds.). Finnish Institute of Occupational Health, Helsinki, 43-45, 2001.
33. Vožeh, F., Cendelín, J., Motáňová, A.: The development of different types of learning in cerebellar degeneration model. Homeostasis 39: 248-250, 1999.
34. Vožeh, F., Barcal, J., Cendelín, J., Korelusová, I., Štenglová, V., Žalud, V.: The effect of high-frequency electromagnetic field on some brain function in healthy and neurodefective mice, Proceedings of Biological effects of EMFs, 3rd International workshop, Kos, Greece, 4.-.8.10.2004, Ed. P.Kostarakis, p.1113-1120.
35. Wang, B., Lai, H.: Acute exposure to pulsed 2450-MHz microwaves affects water-maze performance of rats. Bioelectromagnetics 21: 52-56, 2000.
36. Weinberger, Z., Richter, E.D.: Cellular telephones and effects on the brain: The head as an antenna and brain tissue as a radio receiver. Med. Hypotheses 59: 703-705, 2002.
37. Zuo, J., De Jager, P.L., Takahasi, K.J., Jiang, E., Linden, D. J., Heintz, H.: Neurodegeneration in Lurcher mice caused by mutation of δ2 glutamate receptor gene. Nature 388: 769-773, 1997.

FAST MICRODOSIMETRY

Z. WANG, Y. ALFADHL, X. CHEN

DEPARTMENT OF ELECTRONIC ENGINEERING, QUEEN MARY, UNIVERSITY OF LONDON,
MILE END ROAD, LONDON, E1 4NS, UK

Abstract

Microdosimetry has emerged as an interesting area in the electromagnetic studies at cellular level. However, it is confronted with the difficulty of the treatment of the thin cell membrane, which often leads to extremely large memory usage and long running time in simulation. In this paper, we have introduced a technique for fast microdosimetry in the RF band. A simple double layer spherical cell model has been set up with given dielectric properties. Under the quasi-static approximation, the E field of the cell model can be evaluated by solving Laplace's equation. This simple cell model was solved by using Finite Element Method (FEM), verified with analytical solution and MIE theory. Next, the FEM with quasi-static approximation has been applied to evaluate the EM field interaction with the cells in various shapes, such as ellipsoidal, cylindrical and erythrocyte. It is demonstrated that, under the same meshing scheme, the FEM with quasi-static approximation runs much faster than the FEM solving full-wave Maxwell's equations.

I. Introduction

Recently, microdosimetry, i.e. the numerical study of EM fields interacting with the cellular and sub-cellular substances has received considerable interest. However, microdosimetry is confronted with a major difficulty, that is, the treatment of the thin cell membrane, which quite often leads to extremely large memory usage and long running time in simulation. In the previous work [1], FEM (Finite Element Method) with adaptive meshing has been used to solve the Maxwell's equations to evaluate the electric field distribution within cells. In the literature [2], quasi-static approximation was introduced to simplify the problem, i.e., the electric field distribution being approximately evaluated by solving Laplace's equation.

In this paper, a quantitative evaluation of the quasi-static approximation has been performed on a simple double layer spherical cell model at first. It is demonstrated that, under the same meshing scheme, the FEM with quasi-static approximation runs much faster than the FEM solving full-wave Maxwell's equations. The FEM with quasi-static approximation has been applied to evaluate the EM field interaction with the cells in various shapes, such as ellipsoid, cylinder and erythrocyte.

II. The models

The initial cell model in this study is a rigid particle rounded by a thin shell, representing a cell with membrane, with homogeneous, lossy and dispersive dielectric properties for each layer, as shown in figure 1. The cell radius is normally 10 μm and membrane thickness is 10 nm. The cell is exposed to a linear polarized plane wave with the electric field E_0 of 1V/m in the external medium. Due to the axial symmetry; a 2D model is adopted to evaluate the electric field distribution within the cell.

The frequency-dependent dielectric properties of the cytoplasm, membrane and external medium vary according to the Debye 1st order relaxation model, which will be further discussed in section 3.1. The values at 2.45GHz are listed in table 1.

	Cytoplasm (Ω_1)	Membrane (Ω_2)	External (Ω_3)
Permittivity (ε)	55.6	11.3	75.3
Conductivity (σ)	1.43	0	2.04

Table 1 Dielectric properties of cell compartments at 2.45 GHz